Technical Report NAVTRAEQUIPCEN 75-C-0009-13

AVIATION WIDE-ANGLE VISUAL SYSTEM TRAINER SUBSYSTEM DESIGN REPORT

SINGER - LINK DIVISION
Binghamtom, New York 13902

Final Report

May 1977

NAVAL TRAINING EQUIPMENT CENTER
ORLANDO, FLORIDA 32813

DISCLAIMER NOTICE

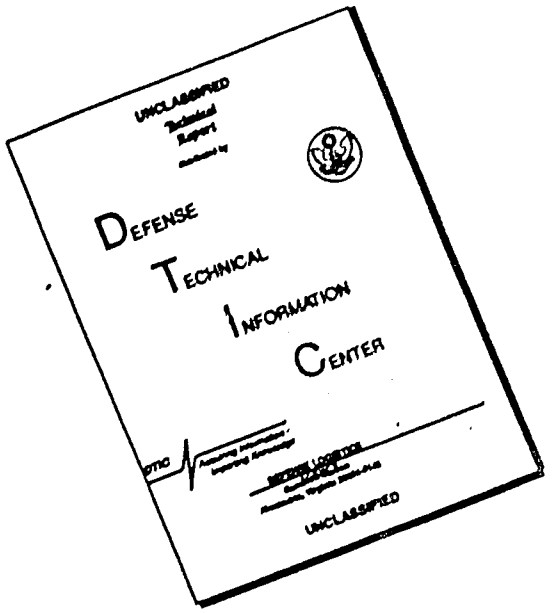

THIS DOCUMENT IS BEST QUALITY AVAILABLE. THE COPY FURNISHED TO DTIC CONTAINED A SIGNIFICANT NUMBER OF PAGES WHICH DO NOT REPRODUCE LEGIBLY.

SECURITY CLASSIFICATION OF THIS PAGE (When Data Entered)

REPORT DOCUMENTATION PAGE

READ INSTRUCTIONS BEFORE COMPLETING FORM

1. REPORT NUMBER: NAVTRAEQUIPCEN 75-C-0009-13
2. GOVT ACCESSION NO.
3. RECIPIENT'S CATALOG NUMBER

4. TITLE (and Subtitle): AVIATION WIDE-ANGLE VISUAL SYSTEM (AWAVS) TRAINER DESIGN REPORT • Subsystem Design Report •

5. TYPE OF REPORT & PERIOD COVERED: FINAL REPORT.

6. PERFORMING ORG. REPORT NUMBER: AWAVS-7

7. AUTHOR(s): Robert A. Fisher, Robert Lyons

8. CONTRACT OR GRANT NUMBER(s): N61339-75-C-0009

9. PERFORMING ORGANIZATION NAME AND ADDRESS: Singer-Link Division, Binghamton, New York 13902

10. PROGRAM ELEMENT, PROJECT, TASK AREA & WORK UNIT NUMBERS: Work Unit 4781, Program Element 63720N, Project W4308

11. CONTROLLING OFFICE NAME AND ADDRESS: Naval Training Equipment Center, Orlando, Florida 32813

12. REPORT DATE: May 1977

13. NUMBER OF PAGES: 392

14. MONITORING AGENCY NAME & ADDRESS (if different from Controlling Office): 396p.

15. SECURITY CLASS. (of this report): UNCLASSIFIED

15a. DECLASSIFICATION/DOWNGRADING SCHEDULE

16. DISTRIBUTION STATEMENT (of this Report): W4308

Approved for public release, distribution unlimited.

17. DISTRIBUTION STATEMENT (of the abstract entered in Block 20, if different from Report)

18. SUPPLEMENTARY NOTES

Related published contract report: NAVTRAEQUIPCEN 75-C-0009-1, AVIATION WIDE-ANGLE VISUAL SYSTEM (AWAVS) DESIGN ANALYSIS REPORT, APRIL 1975.

19. KEY WORDS (Continue on reverse side if necessary and identify by block number)

Model Board	Target Insetting
Optical Probe System	Target Image Generator (TIG)
Gantry	Background Image Generator (BIG)
Target Projection System	Wake Image Generator (WIG)

20. ABSTRACT (Continue on reverse side if necessary and identify by block number)

This Visual System Design Report is provided in response to Data Item A003 of Contract No. N61339-75-C-0009 for the Aviation Wide-Angle Visual System (AWAVS). The overall objective of the Design Report, together with the Configuration, Facilities, Math Model and Design Analysis Reports is to present a total

DD FORM 1 JAN 73 1473 EDITION OF 1 NOV 65 IS OBSOLETE S/N 0102-014-6601

UNCLASSIFIED

SECURITY CLASSIFICATION OF THIS PAGE (When Data Entered)

picture of the design and development engineering functions, and the implementation of these functions to achieve the characteristics and performance for the visual portion of the AWAVS/VTFS system as required by AWAVS NAVTRAEQUIPCEN Specification 212-102.

The primary purpose of the Visual Design Report is to provide, as clearly and concisely as possible, all required design information relative to AWAVS visual hardware systems, elements, and components. Each of the major areas shown in the Master Block Diagram, are treated separately in the various detail block diagrams. Each of the interfaces, e.g., electrical, mechanical, and optical, is defined in terms of its function, design features, and implementation. In this respect, the contents of DID S-0003, dated 6 October 1971, has been used as a guideline in generation of the material presented herein. An analysis of the design and development of each AWAVS subsystem has also been included in this report, however, only to the extent that such analysis differs from (or has evolved from) the one given in the Design Analysis Report NAVTRAEQUIPCEN 75-C-0009-A001.

This report covers the visual portion of the AWAVS/VTFS trainer only. A separate report (F002) has been generated to provide details of the OFT portion.

19. (CONT)

Zoom Perspective
FLOLS Tracker
FLOLS Image Generator
Scene Keying Generator
BIG/WIG
Horizon Generation

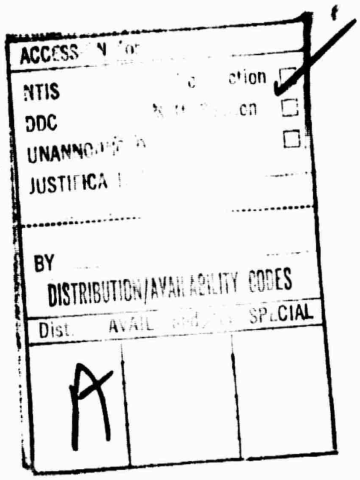

TABLE OF CONTENTS

TABLE OF CONTENTS (Contd)

TABLE OF CONTENTS (Contd)

LIST OF ILLUSTRATIONS

LIST OF ILLUSTRATIONS (Contd)

LIST OF ILLUSTRATIONS (Contd)

LIST OF ILLUSTRATIONS (Contd)

LIST OF ILLUSTRATIONS (Contd)

LIST OF ILLUSTRATIONS (Contd)

LIST OF ILLUSTRATIONS (Contd)

LIST OF TABLES

LIST OF TABLES (Contd)

LIST OF TABLES (Contd)

LIST OF TABLES (Contd)

SECTION I

1.0 GENERAL

This section provides details of the design considerations and assumptions contributing to the development of the Aviation Wide Angle Visual Systems (AWAVS). The overall system description, also given in this section, provides quantitative data relative to system parameters required by AWAVS NAVTRAEQUIPCEN Specification 212-102.

1.1 Design Considerations and Assumptions

The AWAVS visual system includes a target image system, a background image system, a wraparound spherical projection screen, and a digital computer. When combined with the VTFS (Visual Technology Flight Simulator), these systems provide the pilot with a realistic view of an external scene which responds to the simulated operation of the aircraft, and enable the following flight tasks to be accomplished:

a. Circling carrier traffic patterns under daylight, dusk, and night conditions.

b. Circling carrier arrested landing under daylight, dusk, and variable ceiling conditions.

c. Catapult takeoff and bolter under daylight, dusk, and variable ceiling conditions.

The visual system is designed in such a way that, without modification of the display system, additional image generation equipment can be added to simulate the following:

a. Shore traffic patterns under day, dusk, and night conditions.

b. Approaches to, landing on, and takeoff from a runway, under day, dusk, night and variable ceiling conditions.

c. Night tough-and-go landings on a runway under variable ceiling conditions.

d. Air-to-air combat.

e. Air-to-ground weapon delivery.

f. Formation flight.

The visual system shall be integrated with an existing flight simulator research tool, consisting of a cockpit, motion platform, and computer. The flight simulator is comprised of a T-2C cockpit, instruments, and controls. The AWAVS computer is a SEL 3250 series digital computer programmed for T-2C flight dynamics.

1.1.1 Applicable Specification Paragraph Numbers. The general design specification for the AWAVS visual system is NTEC Specification 212-102, dated 1 August 1973, and as modified by changes approved under Contract No. N61339-75-C-0009. Applicable paragraphs of this specification include:

a. Definition of general material and design requirements-paragraphs 3.1, 3.2.

b. Definition of reliability and maintainability requirements-paragraphs 3.3, 3.4.

c. Definition of functional performance requirements-paragraph 3.6.

d. Definition of testing requirements-paragraph 4.3.3.2.

1.1.2 Design and Test Criteria. The visual system design and test criteria will be in accordance with the specification references in paragraph 1.1.1 above. Insofar as is consistent with these criteria, the system design has been based on existing subsystems and operational components.

1.2 System Description

The AWAVS visual system presents a composite of two scenes projected onto the inside surface of 10-foot radius sphere. The target image system provides a high-brightness, monochrome television image of a high quality "area-of-interest" aircraft carrier and wake, combined with a high-brightness color FLOLS (Fresnal Lens Optical Landing System) image presentation. The background image system provides a bright, wide-angle monochrome television image of seascape, horizon, and sky presentation, in which the target image is inset. The high-resolution carrier, wake, and FLOLS image is moved about in position and orientation relative to the background scene in response to cockpit inputs, and in accordance with all simulator requirements.

The visual system consists of the individual target and background image generation and projection systems, a 10-foot radius spherical display screen, a modified Advanced Simulation Technology (AST) linkage, and various controls and monitors which are integrated with the VTFS. The major part of the linkage and all computer equipment therein is part of the VTFS. All communication between visual system controls which are part of the VTFS and visual system hardware is via the linkage. Distribution of power within AWAVS is controlled by circuitry on the VTFS. Section V of this report is related to the AWAVS power distribution system.

1.2.1 Target Image System. The Target Image System has three major subsystems. The camera model system, target projection system the FLOLS simulation system. The AWAVS computer (part of VTFS) controls the performance of these subsystems via the VTFS real-time interface or linkage. The camera model system generates a television picture of the carrier model and wake in concert with the target projection system, such that an image of proper size and perspective appears on the screen. The FLOLS image system employs a scaled model board of the FLOLS assembly. The model board image is optically coupled and combined with the target image at the input of the target projection, thus providing a FLOLS image of proper size and color, in the correct position and attitude with respect to the carrier.

The camera model system incorporates a 370:1 scale factor model of the CVA-59 Forrestal Class aircraft carrier. The model moves in respect to the model board surface under computer control in response to inputs from the instructor. Maximum limits are $\pm 5^{o}$ of pitch in a period of sixteen seconds, $\pm 12^{o}$ of roll in a period of sixteen seconds, and ± 30 ft in heave in a period of ten seconds. A full three hundred and sixty degree carrier heading and carrier speeds up to fifty knots are simulated by including these functions in the gantry position and velocity parameters. The carrier model also includes a scaled two thousand foot removable wake aft of the carrier model. The carrier model superstructure is easily detachable so as to not damage the optical probe during a crash condition. The model also has operational deck edge, runway edge, runways centerline(with strobe), and vertical drop lights. The lamp brightness and strobe rate is under instructor control.

The optical probe will operate in an area of interest mode such that the carrier model can be viewed by the probe for simulating every possible flight path. The probe is capable of a 60^{o} wide by 40^{o} high field of view, and is equipped with a 4:1 zoom capability, full 360^{o} roll and heading capability, and a $+45^{o}$ to -90^{o} pitch capability. The probe image is relayed to the two-inch intensified vidicon camera.

The vidicon camera raster is dynamically shaped in order to maintain image distortion to less than 5% due to the projector/observer geometry and lens mappings of the target system. Television resolution of over 700 TV lines horizontal by 500 TV lines vertical is achieved when the target system is operated at the designed 825 scan line 30 frame, 2:1 interlace system rate. The target system is also capable of operating at 1025 and 525 scan line, 30 frame, 2:1 interlace system rates. The target projection system employs a high brightness monochromatic light valve projector and optical system capable of dynamically placing the area of interest carrier model image anywhere with a $+150^{o}/-110^{o}$ horizontal by

+90°/-70° vertical observer field of view. The target projector optics employ a 10:1 zoom and a full 360° roll capability in addition to the azimuth and elevation capability delineated above. The projection system is capable of better than four foot candles peak output brightness.

The FLOLS image generator consists of a 40:1 scale model board of the carrier FLOLS lighting system. The horizontal datum lights, vertical wave-off lights, auxiliary wave-off lights, cut lights, and glide slope indicator lights are simulated. When viewed from the cockpit, FLOLS lights will appear in natural color, in correct size and position accurate to within 5% of the carrier width. A minimum of a 5:1 ratio in FLOLS brightness to carrier image brightness is achieved. Visibility of the FLOLS image, with respect to viewing angle, flight path, and weather conditions are simulated. The FLOLS projector relays the model board image to the target projection optics at the output of the target projector. The FLOLS projector is equipped with computer-controlled iris, zoom, zoom iris, roll, and X/Y translation servos to properly achieve FLOLS simulation.

1.2.2 Background Image System. The wide-angle background image is projected from the spherical screen center so as to present a 160° horizontal by 80° vertical observer field of view. Two projection positions are employed resulting in a +40°/-120° horizontal by +50°/-30° vertical field of view, or a ±80° horizontal by +50°/-30° vertical field of view.

The wide-angle projection lens employs an anamorphic element to convert the 3 x 4 inch light valve projector raster format into the required 160° by 80° field of view. The background image format consists of a constant light tone sky and horizon line, followed by a varying gray tone sea merge area that blends into waves in the image foreground.

Wave imagery is generated by the background image generator flying spot scanner film transparency. Two separate film transparencies at a 25,000:1 scale factor representative of a sea states two and three are employed. The flying spot scanner raster is dynamically shaped to present a proper perspective of the wave image as viewed on the display screen. The aircraft attitude (±90° pitch, 360° roll and heading), altitude (deck level to 760 feet), and velocity (up to 400 knots) are reflected in the flying spot scanner shape, size, and position, respectively. In addition, the static system distortions due to system geometry and lens mapping are taken into account, resulting in less than 4% image distortion. The waves imagery blends smoothly into the synthetic seamerge video at a ground range of 1870 feet.

Seamerge video, horizon and sky are created in the special effects generator using analog techniques. The effect of low visibility is generated by mixing synthetic haze with the video signal below the horizon, as a function of slant range to the ground plane, indicative of atmospheric scattering. The function of visibility to the horizon is under instructor control.

The background scene also contains a hole of the proper size, shape, and position into which the target image is projected. This insetting (scene keying) is accomplished by viewing the background field of view with a camera. When the camera detects the carrier image projected on the display screen, a hole is blanked into the background video. In order for the camera to discriminate between the target and the background scene, a red blocking optical filter is placed in the background projector light path. The result is a slightly bluish-green background image. A red-pass optical filter is placed in the lens of the camera, and thus the camera sees only the red spectrum projected by the target projector. The scene key camera video is detected at or above the eighth shade of gray of the target image under day conditions, and at or above the fifth shade of gray for dusk conditions. Under night conditions no scene keying will take place. In order to assure registration between the target image and the insetting hole, the scene keying camera raster must map into the background projector raster plane. This raster convergence is controlled by the scene key camera raster computer which properly shapes the camera raster.

The background image resolution is 1000 TV lines horizontal by 600 TV lines vertical when operated at the design scan rate of 825 scan lines, 30 fields at 2:1 interlace. The background image system is also capable of operation at 1025 and 525 scan lines, 30 frames at 2:1 interlace.

1.2.3 Display Screen. The ten-foot radius screen employs one sixteen inch thickness aluminum panels of proper radius riveted to a spherical super-structure. The seams in the panels are filled and sanded to the proper radius. The screen presents a homogeneous projection surface with a screen gain of at least 2.5. The screen structure is capable of withstanding 4 g's of acceleration, and is mounted rigidly to the motion platform. Access into the screen is through an enclosure on the back of the cockpit area. The enclosure is equipped with lighting and ventilation.

1.2.4 Linkage/Interface. The AWAVS system and digital computer interface equipment includes all input/output conversion equipment and discrete inputs and output circuits. On the AWAVS side there are three AST (Advance System Technology) subcontrollers linked back to the VTFS Master Controller. One subcontroller is located on the gantry Y carriage assembly which services the gantry servos, probe servos and TIG camera systems. Another subcontroller is located in the cockpit enclosure electronics rack which services the target projector servos, FLOLS projector servos and scene key camera system. The final subcontroller is located in the BIG/WIG

electronics cabinet which services the background image generator, lamp bank control, carrier model special effects generator and scene keyed insetting electronics systems.

1.2.5 Visual System Controls and Monitors. In addition to the automatic controls of the visual system exercised by the computer, there are certain controls which are manually operated. These fall into the categories of instructor controls and maintenance controls. Instructor controls are used to establish initial visual conditions and to modify conditions during the course of training exercises. Maintenance controls, on the other hand, will be used during intervals when the visual system is not being used for training.

The instructor station (Experimentor/Operator Station) is provided with facilities to control visual system parameters and initial conditions. Control and monitoring is exercised through discrete indicators and controls located on the EOS panels. Maintenance facilities provided with the visual system include manual test provisions. Manual testing is provided by means of servo maintenance control panels and video maintenance controls.

The servo maintenance control panels are located in the gantry cabinet and the cockpit enclosure. These panels provide facilities for disconnecting the probe, gantry, and projector servo systems and model lighting subsystems from the computer, and substituting manually controlled input signals. In addition to this ability to substitute signal sources, the gantry cabinet maintenance panel provides position readouts for each of the three gantry servos, whether in the normal or maintenance mode of operation.

The TIG cabinet and the BIG electronics cabinet (formerly known as the BIG/WIG cabinet) contain all the controls required for the daily setup and alignment of the video system. In addition to the camera control unit, waveform and picture monitors are included for quantitative and qualitative evaluation of the video signals. A test signal generator provides standard, calibrated signal inputs to video processing and display subsystems.

SECTION II

2.0 MASTER BLOCK DIAGRAM AND SYSTEM CHARACTERISTICS

The major functional hardware areas of the AWAVS visual system for the VTFS trainer are depicted in the master block diagram, Figure 1. The master block diagram is first divided into the two primary systems - target and background - which individually create and project on the display screen the two components of the visual scene. The remaining blocks, including the linkage/interface and Experimenter/Operator Station, are primarily part of the VTFS. They do, however, receive limited coverage herein, to the extent necessary to maintain continuity in the AWAVS descriptions. Distribution of power to and within the AWAVS system cabinets is covered in Section V of this report.

2.1 Target System

The three functional groups of the target system are the target image generator (TIG), the Fresnel Lens Optical Landing System (FLOLS) simulator, and the target projection system. Basically, the target image generator creates a monochromatic video signal of a model of a Forrestal class aircraft carrier. A gantry mounted optical probe pickup provides the illusion of a pilot "flying" around the carrier model. The FLOLS simulator uses a scale model of an actual FLOLS to optically create the three-color FLOLS image. The target projection system synthesizes the projected image from the TIG video signal, combines it with the optical imagery from the FLOLS simulator, and projects the composite target image.

2.1.1 Target Image Generator. A television camera model system is used as the target image generation subsystem. This subsystem consists of a Forrestal class aircraft carrier model, model illumination, optical probe, television camera, and gantry system. A 370:1 scale factor was chosen for the design. This scale factor provides for correct pupil placement for simulated ranges up to 2300 feet using a 24 x 24 foot model board. Simulation of ranges greater than 2300 feet is accomplished by a zoom lens in the optical probe. The analysis shows that perspective distortion of the canted deck for all simulated range will be less than 2 arc minutes.

The target image generator is comprised of five major functional entities which generate the basic monochromatic target video signal. These are:

a. A model board assembly containing the carrier model, with carrier deck lighting, driven to simulate pitch, roll, and heave motions; and having its own electronics cabinet.

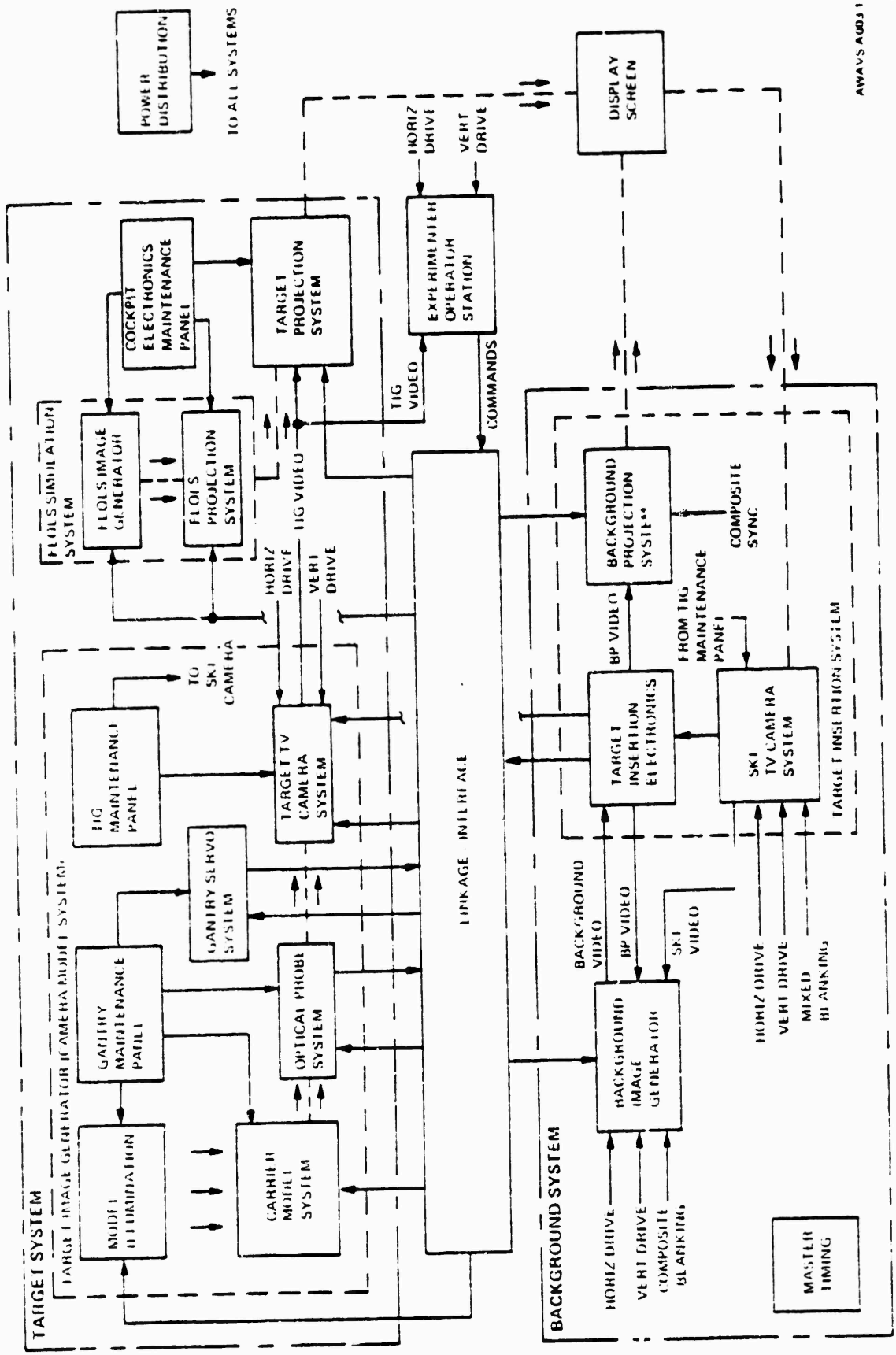

Figure 1. Visual System, Master Block Diagram

b. A flood lighting structure to provide the required ambient light levels for day, dusk, and night simulation.

c. An optical probe system consisting of: a probe pickup which "flys" around the target carrier and wake; a zoom lens for simulating long distances; and a closed-loop servo for precision pointing of the optics towards the FLOLS position on the carrier.

d. A monochromatic target television camera with associated drive and blanking circuitry mounted on the gantry, behind the optical probe; and with video processing and control circuitry and monitoring equipment housed in a separate electronics cabinet.

e. A three-axis gantry structure including rail and tower, which houses the probe and camera equipment; x, y and z translation servos; and the necessary power supply and control components; and, works in concert with its own electronics cabinet.

In order to minimize the registration error of the Fresnal Lens Optical Landing System on the projected video image of the carrier, it has been concluded that a closed loop probe pointing system must be employed.

Illumination of the model board is uniform over the area of the carrier and wake. Provision has been made in the lamp bank to add additional lamps without structural modification, to provide for future applications.

An analysis of the optical probe indicates that a conventional probe, by virtue of its simplicity and ability to resolve vertical surfaces, is the most desirable configuration for the AWAVS application.

A television camera employing a 2-inch intensified vidicon will provide the necessary resolving power and sensitivity. Distortions, resulting from target projection pointing, are compensated for by use of dynamic raster shaping. This shaping does affect camera performance in the areas of video flashing, lag characteristics, and modulation transfer function. Methods of compensating for these effects have been analyzed and, from this analysis, the effects have been found to be correctable.

Selectable television sweep rates of 525, 825, and 1025 lines are provided to allow for controlled variation of system resolution.

2.1.1.1 General Configuration

2.1.1.1.1 Model Board Assembly. The model board assembly consists of a carrier model with integral deck lighting, a painted wake, a servo operated motion system, and a welded steel support structure. The carrier model itself is a 370:1 scale model of the CVA-59 Forrestal Aircraft Carrier. The carrier deck lighting includes runway edge, centerline, and athwartships lights, deck edge lights, and vertical "dropline" lights. A strobe light effect is simulated for the runway centerline lights. Fiber optic bundles are used to simulate the runway lights, with subminiature incandescent "pin lights" used for the deck edge and dropline lights.

A simulated 2000-ft painted wake is attached to the model board structure, behind the carrier model. The wake is picked up by the target television camera and inset into the background scene along with the carrier image.

Roll, pitch, and heave servos are employed in the carrier model motion system. The model positioning servomechanisms are non-continuous type dc position servos, utilizing dc torque motors and follow-up potentiometers. DC tachometers are used to stabilize the loop. Antiback-lash gearing is used between the load and follow-up potentiometer.

Variable lighting functions such as brightness, on-off, and strobing of centerline lights are normally controlled by the AWAVS computer, as are the servo operated motions of the carrier model. For maintenance purposes, however, manual control of these functions is possible from the gantry cabinet maintenance panel, overriding the computer. Maintenance panel controls facilitate static positioning of each motion servo.

The model support structure consists of three trussed frames bolted to the floor of the facility and linked horizontally by a series of steel angle beams. When facing the model board from the light bank position, the three left bays form a 24 by 24 foot area covered by matte black panels, in the center of which is located the carrier model and wake. A circle of approximately 22-ft diameter around the carrier represents the operational range of the probe. The right hand bay is open and used for placement of the electronics cabinets. Overall dimensions of the model board structure are 32-ft long by 29.25 ft high. Spanning the top of the structure is the x-axis guide rail for the gantry.

2.1.1.1.2 Target Model Illumination. The function of the model illumination subsystem is to illuminate the carrier model and wake so that the probe has sufficient signal for adequate pickup. Primary illumination is from the light bank assembly which is located behind the gantry tower and aimed at the model board. Fill-in lighting is provided by four No. 2 reflector photoflood lamps mounted on the tower assembly. These eliminate the shadow of the gantry tower on the model board.

Primary power for the light bank assembly is provided directly from the 277/480 volt, 3-phase facility supply. Power control circuitry is an integral part of the light bank assembly.

A total of 32 lamps are currently used on the light bank assembly to light the carrier model and wake. The lamps used are 1000-watt metal hallide lamps in wide beam totally enclosed fixtures. The lamps are mounted in four horizontal rows of eight lamps each with a 4-foot vertical by 2-foot horizontal distance between lamps. The structure on which the lamps are mounted is the same size as the three left hand bays of the model board assembly. Light gray steel panels fill in the spaces between the lamp reflectors over a 24 by 24 foot area, corresponding to the black panel area of the model board structure. There are 50 additional holes around the perimeter of the lamp bank for mounting lamps for future applications.

Each lamp is supplied with its own ballast assembly, and each lamp-ballast combination draws 1080 watts. The starting current does not exceed running current of the ballasts, and they permit only a 10% change in lamp wattage for a 10% change in input voltage. Normal warm-up time for each lamp is five minutes. A time delay is incorporated in the power control circuitry to prevent immediate reignition of the lamps after initial turnoff, allowing sufficient time for lamps to cool.

Time of day simulation (day/dusk/night) is controlled by a 3-position switch on the Experimenter/Operator Station, with commands applied to the light bank power control circuitry via the linkage. Day is simulated by having all 32 lamps on; dusk by extinguishing alternate lamps leaving 16 on in a checkerboard pattern; and night by turning all lamps off.

For maintenance and test purposes, local control of lamp bank ignition and time-of-day simulation is possible from the maintenance panel in the gantry cabinet, bypassing the linkage and EOS selections.

2.1.1.1.3 Optical Probe System. The optical probe is the servo operated pick-up device for the target television camera. The probe system is comprised of a laser light source located on the carrier model, the optical probe assembly, and a closed loop servo probe positioning system known as the FLOLS tracker. The servo is required for precision pointing of the probe at the FLOLS position on the carrier, and is responsible for accurate registration of the FLOLS imagery on the projected carrier image. The loop consists of the FLOLS tracker optics and electronics, the computer linkage which is part of the VTFS, and the optical probe signal interface, electronics, and probe drive servos. In simple terms, the tracker optics separates the laser image from the carrier and wake image and relays it to the tracker electronics. The electronics form the X and Y correction terms used to modify the computer commands for probe positioning. The signal interface transforms the digital output from the computer into an analog drive signal which is used by the probe electronics to form the five dc motion commands for the servos. Stability is enhanced by a position feedback signal to the computer from each servo. The probe can also be operated manually from the gantry cabinet maintenance panel.

The optical probe simulates all possible flight paths to and landings on the aircraft carrier. The probe is comprised of a complete optical system, which corrects and transfers the slant range view to a focal plane with the entire field of view in focus. Aircraft attitude changes are achieved in the probe by servos that receive commands from the linkage/computer. The probe motion system operates on three servo driven main gimbal axes (pitch, roll and heading) which simulate the three degrees of freedom of the aircraft. To maintain proper focus, a servo driven focusing lens is positioned as a function of range as determined from computer inputs. A servo driven zoom lens is incorporated into the system. It provides the zoom capability of 1:1 to 4:1, changing the true field coverage of the camera from 60° to 16.4°. This servo also responds to computer inputs. A simple iris diaphragm servo comprised of a motor and potentiometers is also incorporated into the system.

2.1.1.1.4 Target TV Camera System. The target television camera system receives the optical image from the probe, and forms the processed TIG video signal. TIG video is a combination composite of camera video, horizontal and vertical drives, and visibility effects. Horizontal and vertical drives for the target camera are input from the master timing generator, which is considered as part of the background system.

A vidicon TV camera head with associated drive forming electronics and initial video processing circuitry is mounted on the Z-axis carriage of the gantry tower, immediately behind the probe assembly. A dynamic analog raster computer (DARC) is used to shape the horizontal and vertical deflection sweeps applied to the vidicon. Raster shaping is used to compensate for apparent loss of true perspective due to target projector pointing on the spherical screen. Camera shading and FOV blanking generators are used to reduce undesirable side effects inherent in vidicon camera systems. Initial video processing includes amplification of the camera signal dc restoration and addition of retrace blanking.

A high voltage power supply and camera control unit (CCU) in the TIG electronics cabinet generate most of the dc voltages for operation of the vidicon, and provide a means of adjustment of beam current and target and focus voltages. The CCU also provides for control of video gain and black level signal pedestal.

Processed video from the gantry TV camera is applied to the target special effects generator, wherein a single variable cloud level function is added to simulate restricted visibility. The degree of restricted visibility normally comes from a computer command via the linkage. At the special effects generator, any of four video test patterns from a test pattern generator in the target insertion electronics may be substituted for the camera video signal. Test patterns are used for setup and alignment of the target camera and projection systems.

The target video with visibility effects added (or the test pattern) is applied to an image enhancer to increase the apparent picture crispness by amplifying the white peaks. The same image enhancer has been successfully used by Singer in many previous visual systems. The output of the image enhancer is looped through a 17-inch TV monitor in the TIG cabinet and becomes the primary output of the target image generator. A secondary output is applied to an identical TV monitor in the EOS. An oscilloscope is also provided in the TIG cabinet for checking waveforms.

The target camera system has the capability of operating at three different horizontal scan rates: 525, 825 and 1025 lines. The camera head setup is accomplished by remote control from a line rate switch on the TIG maintenance panel. The TIG DARC is set up for various line rates by the installation of the proper waveform generator printed circuit card. The image enhancer is equipped with a line rate select switch that places the video boost for optimum crispness.

2.1.1.1.5 Gantry System. The optical probe, monochromatic camera, and associated electronic devices are rigidly mounted to the Z-axis carriage, the motion of which is perpendicular to the model plane. The Z-axis drive motor and shaft are mounted to the Y-carriage and effect translation of the Z-carriage by means of a linear actuator fastened thereto The Y-axis carriage is driven the height of the tower through the medium of a linear actuator translating along the drive shaft attached to the tower.

The tower is mounted to a trolley assembly having two wheel supports on the precision steel X-guide rail The X-guide rail is mounted solidly to a steel I-beam assembly which, in turn, is bolted and grouted to the facility floor. Static equilibrium is obtained through an extension to the upper part of the tower toward the upper X-guide rail and attached to the top of the model support structure,which incorporates guide rollers in contact with the rail. One trolley wheel forms an integral part of the X-drive assembly, and tower motion is imparted through friction between the wheel and the lower X-axis guide rail. Rotary optical encoders, together with rack and pinion action in all three axes, provide for position feedback.

The gantry electronics cabinet contains the drive control electronics and gantry maintenance panel. The X-, Y-, and Z- axis drive servos are of the noncontinuous dc velocity type. The maintenance panel provides a means to select between servo commands issued by the linkage computer and local manual control for test and setup. A position readout of the optical encoder feedback signal for each gantry axis is also featured on the maintenance panel. The position feedback to the linkage closes the servo loops.

Limit switches, shock absorbers, and hard stops are provided on the gantry structure to limit travel in each of the three axes. Overspeed cutouts are also provided for the velocity servos. Reset provisions provided on the maintenance panel are to be used in the event or limiting device is actuated. It should be noted that the motion limiting devices are primarily for emergency use. They are not designed to be used as operational stops.

2.1.1.2 Reliability Characteristics. (To be supplied.)

2.1.1.3 Maintainability Characteristics. (To be supplied.)

2.1.1.4 Human Factors Characteristics. There is no human interface with components of the target image generator.

2.1.2 FLOLS Simulator. The FLOLS must be simulated in such a way that when viewed from the cockpit, the lights appear in the correct position and attitude with respect to the carrier and present the correct size, color, and configuration for all altitudes and ranges.

A separate FLOLS image generator with high intensity light sources is optically coupled into the path of the target projector. The FLOLS simulator consists of a scaled model (about 40:1) of the FLOLS array, with the necessary optics for imaging and motion to project a high intensity image at the target zoom. The model board is fixed with respect to the target projector, thus eliminating errors due to differences between the target projector and the FLOLS projector.

The FLOLS and the carrier images are combined at the target projector optics and projected as a composite image.

The FLOLS range simulation is done completely with the FLOLS zoom. Range simulation of the FLOLS is determined by the relative powers of the FLOLS zoom and the target projection zoom. The projection zoom operates in conjunction with the probe zoom to provide a carrier image of proper angular subtent. The FLOLS image must change in size down to the limit of 500 ft where the simulated FLOLS image is no longer useful. Since the FLOLS zoom is used in conjunction with the projection zoom to display the FLOLS image, the product of their relative powers must equal the ratio of 500 ft to the simulated range.

The FLOLS are on whenever the pilot is within the meatball field of view. This occupies a 40°H x 1-1/2°V cone, referenced about the basic glideslope angle. When he is not within this cone, the FLOLS zoom iris servo is closed thus extinguishing the lights. The zoom is operated at f/12 to f/15, thus, just a few degrees rotation of the zoom iris barrel will extinguish the lights.

2.1.2.1 General Configuration

2.1.2.1.1 FLOLS Image Generator. The individual FLOLS lights are each modeled by a fiber and lens. The fiber conducts the light from an arc lamp and shutter system to a model board which appears just like the FLOLS system. Each lens on the model collimates the output end of its fiber and is cut to the size and shape of the particular FLOLS light. All the individual lights on the FLOLS are collimated and have their axis parallel to the system axis. This is so that when the zoom lens is at its greatest focal length the FLOLS field lens images or decollimates the pupil of the zoom through the fiber end and projects all onto the same surface. FLOLS image luminance is constant over the zoom range.

A 2 x 6 inch model board is the primary imaging device for the FLOLS simulation. It is comprised of 32 fixed lenses backed up by appropriately colored filters to simulate the datum, wave-off, auxiliary wave-off and cut lights, and one movable lens to simulate the FLOLS meatball. The vertical position of the meatball with respect to the datum lights defines the pilot's orientation relative to the glideslope. (On the actual carrier the meatball is positioned approximately 150 feet behind the datum lights, and the vertical orientation of the observer gives the impression of a movable meatball.) At its lowest level, a chopper with a red filter is imposed in front of the meatball to simulate the danger zone. Meatball motion is normally under control of the linkage computer. For test and maintenance, however, manual control may be substituted from the cockpit electronics test panel.

A shutter simulates on/off operation of the auxiliary wave-off lights; and a variable position mirror aims light from the arc lamps to either the wave-off or cut lamps, as selected from the EOS. Both lamps are never used at the same time in a landing operation. A chopper imposed in the path of the wave-off lights causes them to flash whenever on. The wave-off, auxiliary wave-off, and cut lights are normally controlled from the EOS via the linkage; no computer control is involved. For test purposes, they also may be operated from switches on the cockpit electronics test panel.

2.1.2.1.2 FLOLS Projector. The FLOLS projector relays the model board image to the point where it is combined with the target image, and provides correct orientation of the FLOLS with respect to the target optical axis and the aircraft roll axis. It also contains a zoom lens, which is the primary element for FLOLS range simulation, and two optical irises - one for on/off simulation and the other for FLOLS intensity control.

The linkage sends commands to the FLOLS servo electronics which, in turn, form the dc drive commands for the servos. There are six servos: zoom, zoom iris, roll, X-displacement, Y-displacement, and iris. For test purposes servos can be manually positioned from the cockpit enclosure test panel.

The zoom lens has a zoom range of 10:1. Zooming is controlled by a non-continuous position servo. The iris in the zoom lens is a full-closing type which is servo controlled to "turn off" the FLOLS when closed. It is also controlled by a non-continuous position servo. Neither the zoom or zoom iris servo has a limit stop, but both are equipped with friction clutches to prevent damage if run to the end of travel.

The roll servo operates a prism in the FLOLS optics, and provides the FLOLS with aircraft roll which is synchronized with probe roll. The X- and Y-displacement servos operate optical pitch wedges. These move the FLOLS image from the center of the target field as the probe point of interest varies from the FLOLS carrier position to the aircraft body axis. Servos move the pitch wedges to position the FLOLS image within the target FOV, as calculated by the linkage computer. Roll and pitch wedge servos are continuous rotation dc position servos.

The iris servo operates an optical iris independent of the zoom lens. This iris controls the intensity of the FLOLS image entering the combining optics in the target projection system. The aperature is controlled by the linkage computer and is a function of both visability and slant range from aircraft to target. This is a noncontinuous dc position servo with stops at both ends of travel. No reset is required if a travel limit is reached.

2.1.2.2 Reliability Characteristics. (To be supplied.)

2.1.2.3 Maintainability Characteristics. (To be supplied.)

2.1.2.4 Human Factors Characteristics. There is no human interface with components of the FLOLS simulation equipment.

2.1.3 Target Projection System. The target projection system is the portion of the target image system that functions to combine the FLOLS and camera video and display the composite carrier, wake, and FLOLS image within the required field of view.

2.1.3.1 General Configuration. The target projection system is comprised of a light valve TV projector which synthesizes the carrier and wake image, and a gimbal-mounted, servo-controlled optical chain that displays the image on the spherical screen within the projected background.

The linkage relays servo commands to the optical chain. These commands govern the attitude, size, and position of the projected target image. The attitude servos are dc position servos that rotate roll and pitch prismatic optical elements. The size of the image is controlled by a projection zoom lens and servo which are identical to those used in the FLOLS simulator. In the case of the target zoom lens, however, the iris is used for control of target luminance rather than merely as an on/off device. The target position servos are noncontinuous dc velocity servos, which govern the azimuth and elevation of the carrier image by physically pointing the zoom lens and several of the final optical elements. Limit stops are provided on the azimuth, and elevation servos. For test purposes, all target projection servos may be manually operated from the cockpit electronics test panel.

The target projection system receives timing signals in the form of composite sync from the master timing generator in the background image system. Sync and video signals are routed to the target projector via an electronic interface which provides the necessary signal isolation. Control of the video picture (contrast, brightness, etc.) may be accomplished using a remote control unit supplied with the projector. This accessory may be operated either from its normally mounted position on the cockpit electronics structure, or from within the aircraft cockpit via an umbilical cable.

2.1.3.2 Reliability Characteristics. (To be supplied.)

2.1.3.3 Maintainability Characteristics. (To be supplied.)

2.1.3.4 Human Factors Characteristics. There is no human interface with components of the target projection system.

2.2 Background System

The major functional groups comprising the background system are the background image generator (BIG), the background projection system, and the master timing generator. The background video produced by the BIG normally consists of a seascape image of unlimited expanse fading into the horizon, with a cloud overcast. Generation of the seascape image is accomplished using standard flying spot scanner techniques with a photographic transparency for the seascape model. The remaining effects, along with a variable total coverage cloud tone to simulate restricted visability, are electronically produced. The background video may also be an above cloud or in cloud presentation, or any of five internally generated test patterns. The background projector synthesizes the background scene and projects it onto the screen. When operating in the primary mode (as for simulated carrier landings) the remaining components of the background projection system blank out a "hole" in the projected scene, into which the target (carrier and wake) image is projected. This prevents the projected background scene from appearing superimposed with the projected target image. The master timing generator included as part of the background system generates and distributes all video timing signals used by both the target and background systems.

2.2.1 Background Image Generator. The background image is comprised of sky, horizon, seamerge and seascape imagery. Standard flying spot scanner (FSS) techniques are employed to generate seascape. The seascape image will appear in proper perspective for aircraft attitude, heading, velocity and altitude. This is accomplished by properly shaping the FSS sweep inputs to dynamically follow the aircraft attitude, altitude, velocity and heading parameters and the static perspective required by optical distortions, mapping and projection/screen geometry consideration.

Because of hardware limitations the seascape visual cues for velocity are limited to a maximum of 400 knots along the CRT deflection axis and to altitude from 40 to 760 ft. Outside these limits no further visual cue will be generated in the seascape imagery. The raster reset method used to provide the velocity cue does have the advantage of an unlimited gaming area.

2.2.1.1 General Configuration. Raster shaping in the background image generator is accomplished using a dynamic analog raster computer (DARC). The background DARC receives display timing information from the master timing generator and aircraft attitude information from the AWAVS digital computer (via the linkage). Artificial timing and attitude data may be input via the BIG/WIG maintenance panel for test and alignment purposes, bypassing the linkage. Two sets of outputs are provided by the DARC. Instantaneous direction cosines with respect to observer frame of reference are supplied to the special effects generator and the FSS sweep input waveforms are supplied to a flying spot scanner. The flying spot scanner converts film plate wave imagery, with the proper perspective, into video time base information (seascape video).

Seascape video is fed to the special effects generator where, under computer control via the linkage and as a function of position in the field of view, the clouds, horizon, seamerge and visibility range information are added to create the composite background video scene. Seamerge shading fills in the sea between the film plate image and the horizon, providing a gradual transition to the selected film plate seascape image. The transition to a definable seascape imagery varies as a function of the depression angle below the horizon, eventually becoming all seascape film plate video and continuing to the bottom of the projected scene. The horizon itself is formed by the relatively hard transition between the cloud level and the remainder of the video scene. Synthetically generated video is employed to simulate the remaining functions.

When above the clouds, an internally generated cloud shade fills the portion of the scene below the horizon, while a sky level fills the area above. In clouds, a constant cloud shade fills the entire picture. In either of these conditions, synthetically generated video is totally substituted for the FSS video. An effect of overall restricted visibility is simulated by combining the internally-generated cloud level with either seascape or sky video. The degree to which visibility is to be restricted may be controlled from the EOS. A thorough discussion of all environmental simulation techniques used herein is given in Section IV of this report.

Also contained within the background image generator are two monitors - one for video and another for waveforms. A video switching module in the BIG electronics cabinet selects the presentations for display on both monitors. Presentations which may be monitored include the seascape and special effects generator output from within the background image generator, as well as background projector and SKI video signals from other blocks of the background image system.

2.2.1.2 Reliability Characteristics. (To be supplied.)

2.2.1.3 Maintainability Characteristics. (To be supplied.)

2.2.1.4 Human Factors Characteristics. There is no human interface with components of the background image generator.

2.2.2 Background Projection System. The background projection system is a closed loop TV camera/projector system which serves the dual function of blanking out the "hole" into which the target carrier and wake will be projected and projecting the resultant video imagery on the spherical screen. Using extreme wide angle optics, the background image is projected over a 160° horizontal by 90° vertical field of view (FOV).

2.2.2.1 General Configuration. The method selected to blank the hole in the background image is called projected scene keying. A scene keying camera (SKC) scans the exact FOV projected by the background projector. This scene includes both the background scene and the superimposed target. By use of spectral coding of the background and target images, however, the SKC sees only the target carrier and wake. On each horizontal sweep of the background video, the scene keying electronics blanks the signal within the target area described by the scene keying camera. Blanking assures that the background image does not appear superimposed over the target image, creating the impression of sea waves on the deck of the carrier.

2.2.2.1.1 Scene Key Insetting (SKI) Electronics. Under normal conditions, the scene keying electronics accepts background video from the background image generator, blanks the hole for insertion of the target in response to SKC video, and redrives the video for transmission to the background projector. A secondary output returns the same video to the BIG TV monitor equipment covered in paragraph 2.2.1.1. It also responds to variations in target intensity due to screen position and time of day, and produces one component of the target visibility effects. Ancillary functions include control of the background projector optical filter, generation of test patterns for both the target and background projectors, and generation of test mode discretes for transmission to the linkage.

2.2.2.1.2 Background Projection Equipment. The background projection equipment consists of a light valve projector (supplied with remote control unit), the BP electronic interface, and the background projector optics. The background projector and its optics are fixed mounted with respect to the motion platform. The remote control unit supplied as part of the projector is housed in the cockpit electronics enclosure. It is accessible from the rear, but may be removed from its location and carried into the cockpit while still connected to the projector. Except for the optics, the background and target TV projectors and remote control units are fully identical.

The BP electronic interface relays the background video from the BIG electronics and composite sync from master timing to the projector. At this point, background video is the background SEG composite signal with the "hole" blanked for target insertion. The background projector transforms the electronic signal into a projected image. The wide angle optics display the image on the spherical screen with the required field of view, and add the spectral coding required for projected scene keying.

Spectral coding of the background video is implemented by placing a blue-green filter in the projector optics. This produces a projected image devoid of red light. Since the scene keying camera uses filtration which permits it to see red light only, it cannot detect the background scene. For calibration and setup, however, a test pattern projected by the background projector must be visible to the camera. This is facilitated by a signal from the linkage which electro-mechanically removes the blue-green filter during a calibration procedure.

2.2.2.1.3 Scene Keying Camera Subsystem. The primary components of the scene keying camera subsystem are the scene keying camera (SKC), the SKC optics, the camera control unit (CCU), and the dynamic analog raster computer (DARC). Basically, the SKC is aimed at the same area of the display screen as the background projector, and uses the same wide angle optics design as the projector (except for the filter). By virtue of its optical filtration, the camera detects only the white light aircraft carrier and wake. Vertical and horizontal deflection sweeps for the camera are developed by the DARC. These sweeps provide a camera raster which is conjugate with the raster of the background projector. All other electronics for camera operation and video processing, including dc power supplies and alignment and operating controls, are housed in the CCU. The primary output of the CCU is the SKI VIDEO used by the SKI electronics assembly to blank the "hole" in the background video. A secondary output is provided for video and waveform monitoring. The scene keying camera subsystem uses horizontal and vertical drive and composite blanking from the master timing generator.

2.2.2.2 Reliability Characteristics. (To be supplied.)

2.2.2.3 Maintainability Characteristics. (To be supplied.)

2.2.2.4 Human Factors Characteristics. There is no human interface with components of the background projection system.

2.2.3 Master Timing Generator. The master timing generator encompasses the circuitry which generates and distributes all system timing signals for AWAVS. These include vertical, horizontal, and composite sync; composite blanking; and vertical and horizontal drives. The foregoing signals are simultaneously generated at scan rates of 525, 825, and 1025 TV lines.

2.2.3.1 General Configuration. The hardware for development and distribution of timing signals is included in the scene keying electronics drawer, the sync generator drawer, and the sync generator distribution panel. High frequency signals are generated in the scene keying electronics drawer, since this is the only equipment which directly uses high frequency master clocks. The source for all AWAVS timing is a voltage-controlled oscillator which is phase locked to the 30Hz computer iteration rate from the linkage. The phase lock assures that all computer update information is provided during the vertical blanking period.

The VCO output is digitally divided down and applied as a main clock to the sync generator drawer, wherein all line rate timing is developed. Switching on the front panel of the sync generator drawer allows independent selection of TV line rates for the target and background systems.

Vertical and horizontal sync signals from the sync generator are applied directly to the SKI electronics drawer. All remaining timing signals are applied to the sync generator distribution panel assembly, wherein they are redriven and output to the AWAVS system.

2.2.3.2 Reliability Characteristics. (To be supplied.)

2.2.3.3 Maintainability Characteristics. (To be supplied.)

2.2.3.4 Human Factors Characteristics. There is no human interface with components of the master timing generator.

2.3 AWAVS Visual Display.

Coverage of the video display in this report will include both the design details of the spherical projection screen as well as analysis and descriptions of the projected imagery. In order to adequately describe the latter, a certain degree of redundancy with the projection equipment descriptions from previous paragraphs becomes necessary.

2.3.1 General Configuration. The background and target video images are projected onto the inside surface of 10-foot radius dome constructed of aluminum panels riveted to a spherical superstructure. Seams are filled and sanded to present a homogeneous projection surface. The dome is rigidly mounted to the motion platform with the apex of the dome approximately 17 feet above the platform floor. The equator of the dome when viewed from the polar axis subtends an arc of 360°, less the area taken up by an access door behind the T-3C simulated cockpit. The interior of the dome is dark when the door is closed. Lighting and ventilation provided inside the dome are considered to be part of the VTFS. The dome structure, as mounted on the motion platform, will withstand 4 G's of acceleration.

The exit pupil of the background projection lens is located at the geometric center of the dome. The projector is mounted to provide a declination angle in the projector optics of 2.5°. This moves the upper extremity of the background image directly over the head of the observer, when the projector is pointed straight ahead. (The observer's eye position is 6 inches forward of the polar axis.) The scene keying camera, which must scan the exact background image area, is mounted along side (to the right of) the background projector and aligned vertically. It is then pointed back 1.5° left to cover the background FOV. Both projector and camera are fixed mounted with respect to the motion platform. A common mounting permits the pair to be pointed laterally without affecting mechanical alignment. For the primary mission (simulation of carrier landings), the background projector is pointed 40° to the left of center. For future use, in situations such as formation flying or air-to-air combat, a straight ahead orientation is provided.

The target projector is fixed mounted atop the cockpit electronics structure to the left of the background projector. The target projection optics, however, are mounted on a two degree of freedom gimbal assembly. Servos point the target within the background FOV in response to commands from the linkage, and cause the target image to be projected exactly within the area blanked by the SKI electronics. The range of projection optics pointing is sufficient so that coverage includes both primary and secondary FOV's of the background projector.

2.3.2 Reliability Characteristics. (To be supplied.)

2.3.3 Maintainability Characteristics. (To be supplied.)

2.3.4 Human Factors Characteristics. (To be supplied.)

2.4 Linkage and VTFS Interface.

Linkage is comprised of the AWAVS digital computer, all input/output conversion equipment, the Visual Technology Flight Simulator (VTFS) master controller, and three Advanced Systems Technology (AST) subcontrollers. Only the subcontrollers are actually AWAVS components; the remaining items are part of the VTFS. The Experimenter/Operator Station (EOS), also a VTFS installation, includes certain AWAVS controls and indicators. These are covered in this report to the extent necessary to maintain continuity within the subsystem discussions. All communication to and from the EOS controls and indicators is via the VTFS linkage. Except for a remote target system TV monitor in the EOS, there is no direct communication between the EOS and AWAVS. Subparagraphs which follow apply to AWAVS subcontrollers only.

2.4.1 General Configuration. AWAVS linkage subcontrollers are located on the gantry Y-carriage assembly, the cockpit enclosure electronics rack, and in the BIG electronics cabinet. Each subcontroller processes both analog and digital input/output signals, and each is linked back to the VTFS master controller. The gantry subcontroller processes gantry servo, probe servo, and target TV camera subsystem signals. The cockpit electronics subcontroller processes target projector servo, FLOLS servo, and scene keying TV camera subsystem signals. The subcontroller in the BIG electronics cabinet processes I/O signals affecting the background image generator, lamp bank control circuitry, carrier model servos and lighting, special effects generators, and SKE electronics.

2.4.2 Reliability Characteristics. (To be supplied.)

2.4.3 Maintainability Characteristics. (To be supplied.)

2.4.4 Human Factors Characteristics. There is no human interface with any AWAVS linkage components. Those relative to the EOS are discussed in the VTFS Design Report.

SECTION III

3.0 DETAIL BLOCK DIAGRAMS

This section presents a detailed block diagram for each functional entity of the master block diagram given in Section II. Text supporting each detailed block diagram describes at a minimum each input signal, output signal, and functional entity illustrated. When considered necessary for clarity, additional subordinate diagrams or pictorial illustrations are provided. Analysis used in determination of the final design is incorporated in each discussion, where applicable. At the conclusion of each block diagram discussion, a paragraph entitled "Maintenance Panel Interface" describes all applicable manual controls.

3.1 Target Image Generator

Due to the complexity involved, the target image generator is subdivided into individual discussions as follows, with individual diagrams given for each: A pictorial sketch is given in Figure 2.

a. Model Board Assembly

b. Target Model Illumination

c. Optical Probe System (includes FLOLS tracker)

d. Target TV Camera System

e. Gantry System

A television camera model system is used as the target image generator. This system consists of a Forrestal class aircraft carrier model, model illumination, optical probe, television camera and gantry system. A 370:1 scale factor was chosen for the design. This scale factor provides for correct pupil placement for simulated range up to 2300 feet using a 24 x 24 foot model board. Simulation of ranges greater than 2300 feet is accomplished by a zoom lens in the optical probe. The analysis shows that perspective distortion of the canted deck for all simulated range will be less than 2 arc minutes.

In order to minimize the registration error of the Fresnel Lens Optical Landing System (FLOLS) on the projected video image of the carrier, it has been concluded that closed loop probe pointing system must be employed.

Illumination of the model board is uniform over the entire area to provide for future applications. However, some sections of lights can be extinguished to conserve power while still providing sufficient illumination on the carrier model to satisfy the signal requirements of the television camera.

An analysis of the optical probe indicates that a conventional probe, by virtue of its simplicity and ability to resolve vertical surfaces, is the most desirable configuration for the AWAVS application.

A television camera employing a 2-inch intensified vidicon will provide the necessary resolving power and sensitivity. Distortions, resulting from target projection pointing, are compensated for by use of dynamic raster shaping. This shaping does affect camera performance in the areas of video flashing, lag characteristics, and modulation transfer function. Methods of compensating for these effects have been analyzed and, from this analysis, the effects have been found to be correctable.

Selectable television sweep rates of 525, 825, and 1025 lines are provided to allow for controlled variation of system resolution.

3.1.1 Model Board Assembly. The model board assembly consists of a carrier model with integral deck lighting, a painted wake, a servo-operated motion system, and a welded steel support structure. The assembly is the basic source of imagery for the target image generator. A pictorial diagram, which also shows basic overall dimensions, is given in Figure 2. Figure 3 is a block diagram of the camera model system, which is essentially synonomous with the model board assembly, although it includes inputs from the maintenance panel and linkage. Note that both the model lights and servos may be operated either under program control via the linkage, or manually from the maintenance panel located in the gantry cabinet. The block diagram also shows the FLOLS tracker laser assembly, laser, and fiber optic relay to the carrier deck. Although physically located on the model board assembly, the discussion of the FLOLS tracker laser is included with the optical probe system, of which it forms a functional entity. (See paragraph 3.1.3.2.) Descriptions of the detail blocks of the camera model system are given in subsequent paragraphs.

Illumination of the model board assembly surface is primarily accomplished by a bank of thirty-two 1000-watt metallic hallide lamps mounted to a welded steel frame of triangular prismatic configuration. Fill in lighting is provided by smaller floodlights mounted on the Z-drive assembly of the gantry tower. A complete description of the lighting system is given in paragraph 3.1.2.

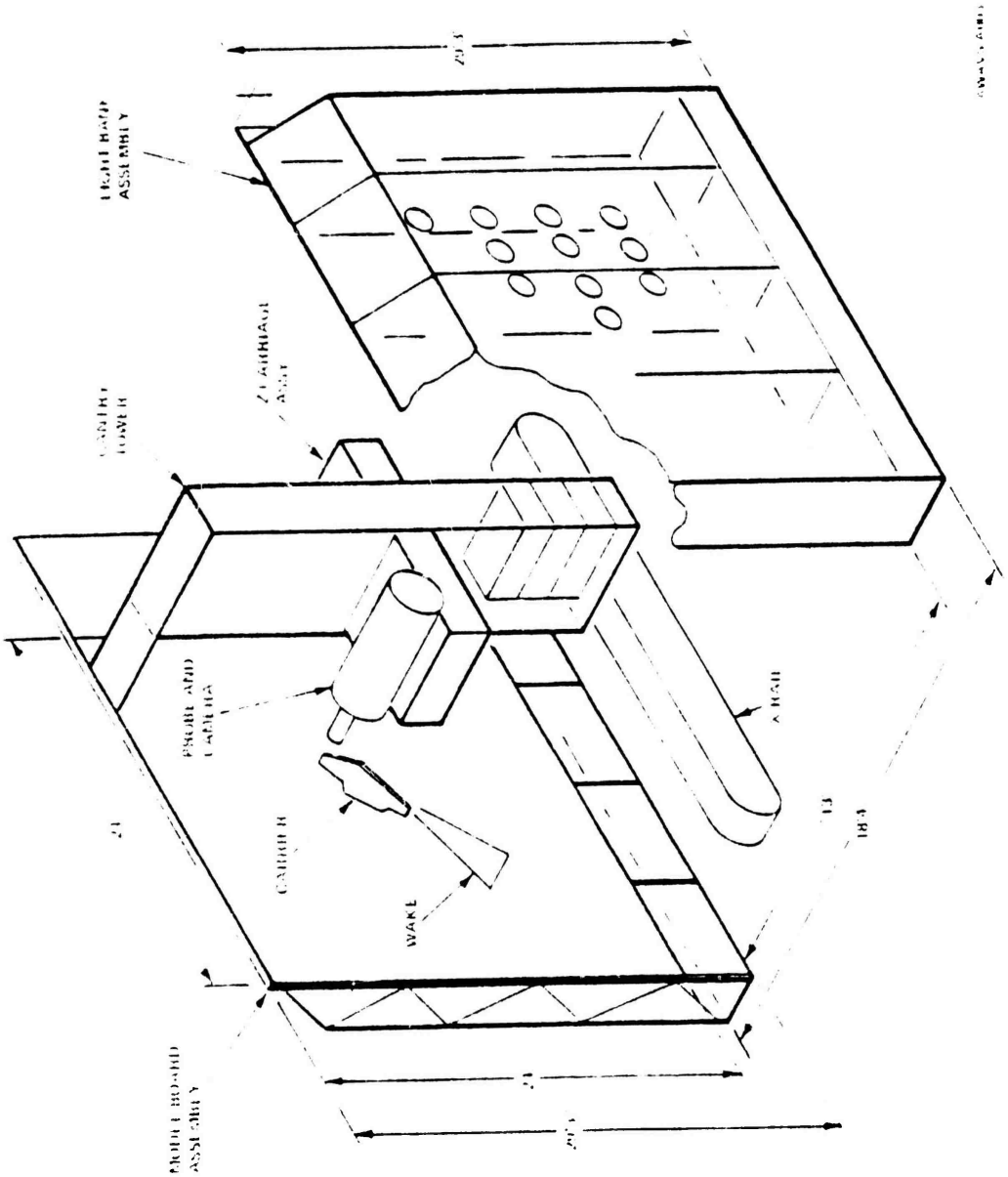

Figure 2. Target Image Generator, Pictorial Diagram

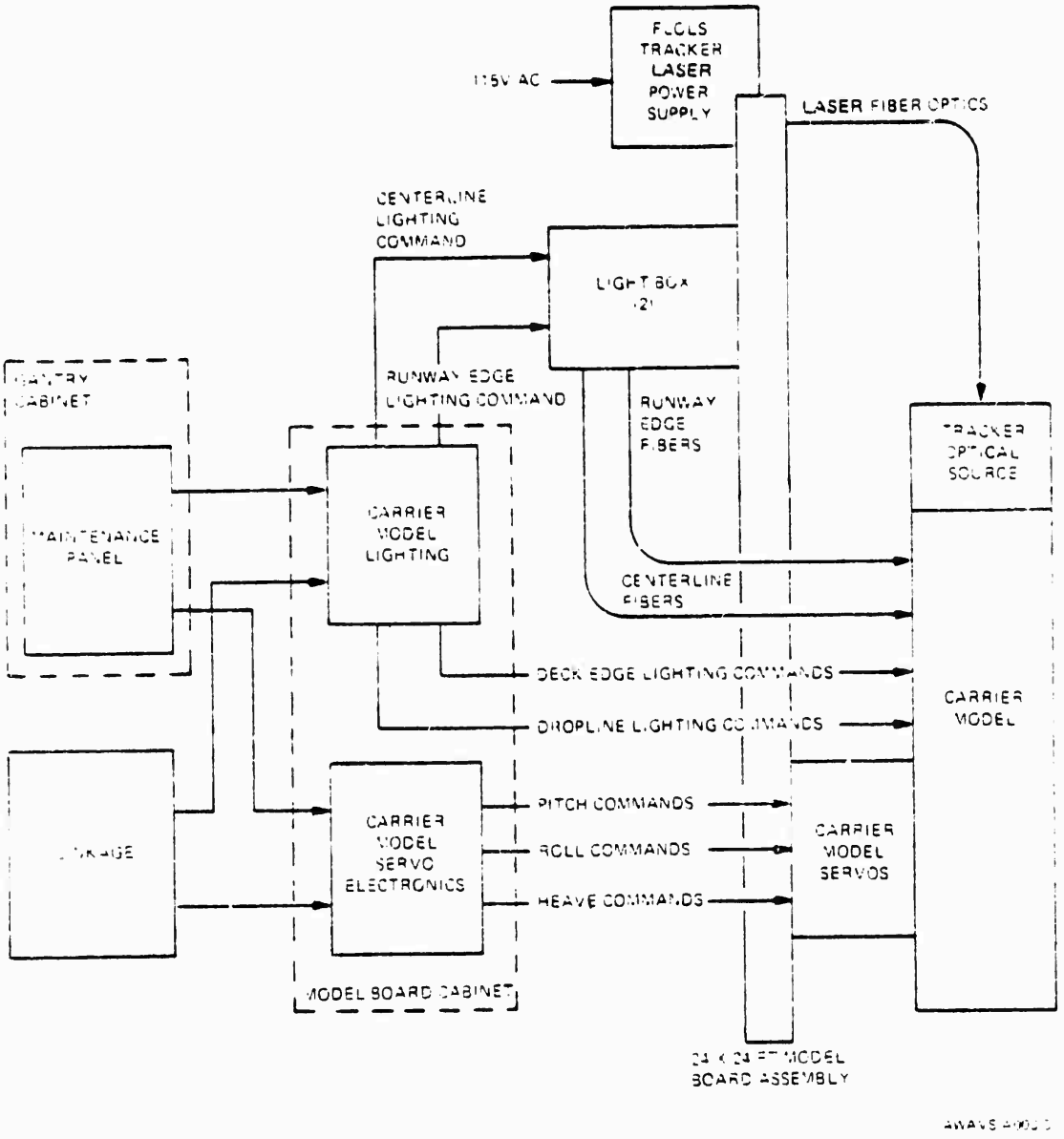

Figure 3. Carrier Model System, Block Diagram

3.1.1.1 Carrier Model. The general model layout is defined as a 370:1 scale model of the CVA-59 Forrestal Aircraft Carrier. The model layout drawing shows lighting locations, structural detail, and positioning of various features (light boxes, conning tower, runway lines, etc). Special detail was placed on the conning tower and runway to enhance realism. Groups of lights are positioned as they actually exist on the aircraft carrier. The carrier lighting has provision for discrete manual and computer control to vary the light luminance. The carrier deck is removable for easy servicing of the fiber optics and light cones.

3.1.1.1.1 Carrier Deck Lighting. Figure 4 is a plan view of the aircraft carrier showing the approximate location of all carrier deck lights. There are five types of deck lights, as follows:

a. Runway Edge Lights

b. Runway Centerline Lights

c. Runway Athwartship Lights

d. Deck Edge Lights

e. Vertical Dropline Lights

The following subparagraphs discuss the technique used to simulate each of the foregoing types of carrier deck lighting. Paragraph 3.1.1.1.2 provides a block diagram discussion of the technology for control of the deck lighting.

a. Runway Edge Lights. These lights define the lateral limits of the runway. They are located in two rows parallel to and equidistant from the runway centerline. The rows are 35 feet from the centerline, and form a runway width of 70 feet. Twenty-seven lights are located, so that a line perpendicular to the runway centerline and passing through a centerline light also passes through each of two edge lights. In this manner, a symmetrical, rectangular pattern is exhibited. The twenty-eighth light would fall outside the flight deck area. The lights are unidirectional, aligned with the beam facing aft and parallel to the angled deck centerline. Lighting for the runway edge lights originates at a light box assembly and is transmitted to the carrier deck via fiber optic bundles. The lights on the carrier are simulated by molded plexiglass cones imbedded in and bonded to the carrier deck as illustrated in Figure 5. Each cone projects a directional field with a vertical spread of approximately 5° and a horizontal spread of approximately 60°. Removal of the carrier deck (by unfastening the bottom thumb screws) makes the cones accessible for inspection and maintenance.

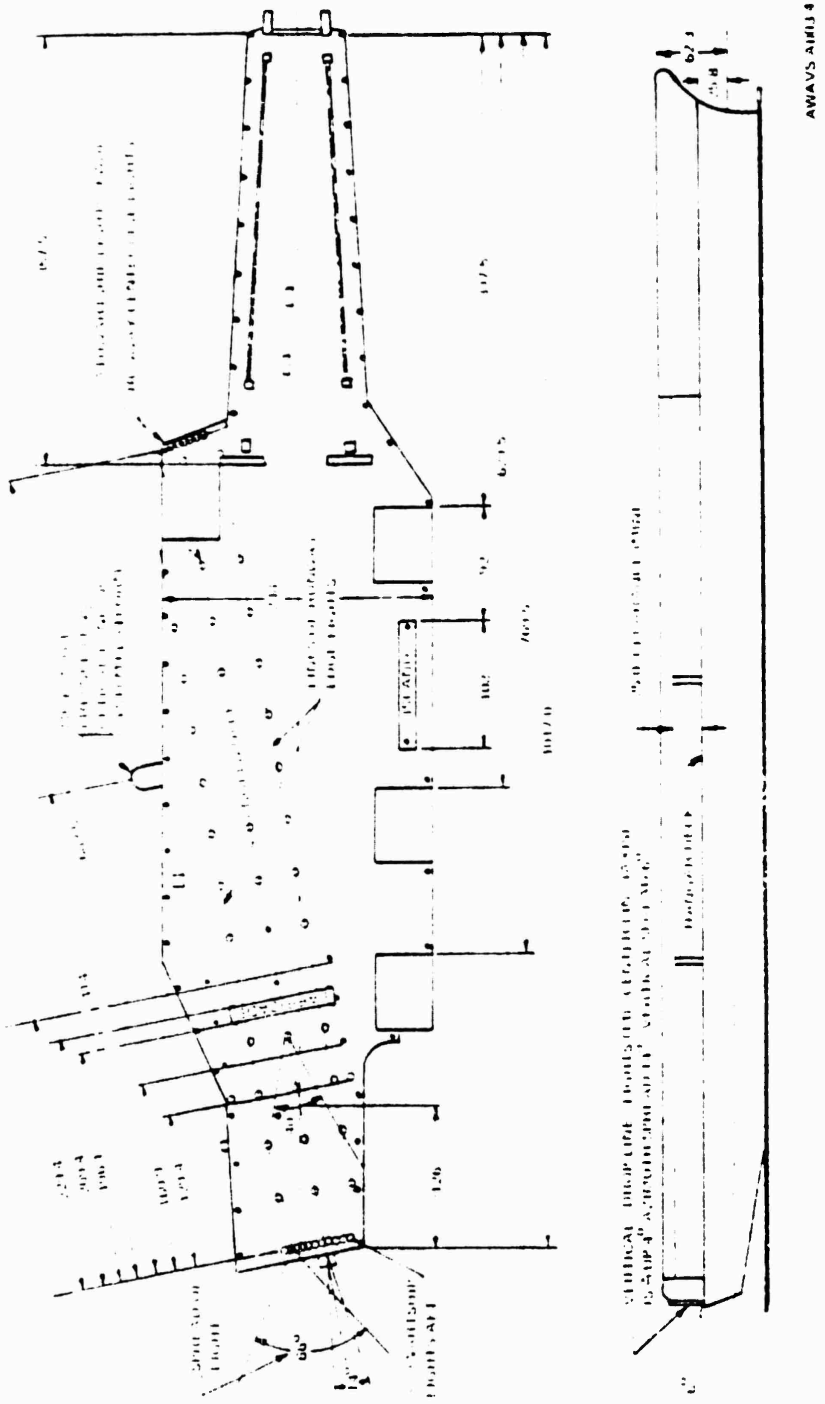

Figure 4. Plan View of Flight Deck with Required Lights

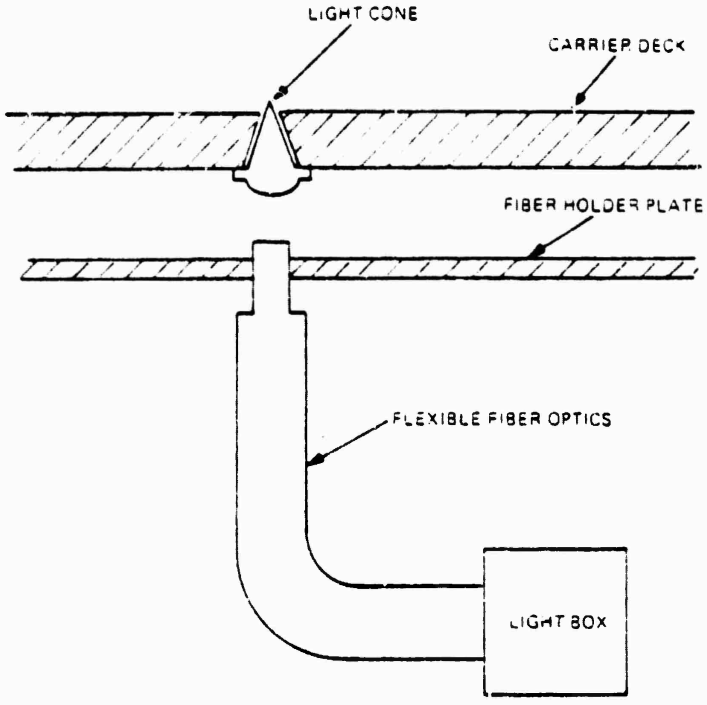

Figure 5. Runway Light Cones

b. Runway Centerline Lights. These lights provide primary information to incoming pilots. They are located on the centerline of the landing area (runway) on the angled deck at intervals of approximately 45 feet. There are no simulated lights within 10 ft aft of any arresting-gear wires. There are fourteen positions for directional fibers, located with the beam axis facing aft and parallel to the angle deck centerline to represent real-world configuration. The simulation technique utilizes the same light box, fiber optic relay, and optical cone configuration described above for the runway edge lights, except for the addition of a motor-driven disk assembly to provide the effect of a variable rate strobe.

c. Runway Athwartship Lights. The purpose of these lights is to define the longitudinal limits of the runway. They are placed on lines perpendicular to the runway centerline at the extremities of the landing area. The ramp lights are spaced at five-foot intervals outboard from the aft centerline light. The outermost athwartship lights in this line are five feet inboard of the runway edge lights. The forward athwartship lights are spaced at approximately 5-foot intervals outboard from the forward runway centerline light. The 12 lights for the ramp and seven lights for the forward will be unidirectional and aligned with the beam axis, facing aft, and parallel to the angled deck centerline. The same simulation technique described in paragraph a, above, for the runway edge lights is utilized herein, except that optical galss rods polished on both ends are imbedded into the carrier deck in place of the plexiglass cones.

d. Deck Edge Lights. The purpose of these lights is to outline the edge of the flight deck. The lights will be spaced at 40-foot intervals around the perimeter of the flight deck. The lights are omnidirectional and of low intensity. There are 44 deck edge lights on the model. The deck edge lights are simulated by subminiature incandescent "pin" lights powered by an external supply.

e. Vertical "Dropline" Lights. These lights are at the aft section, mounted in a vertical row, below the deck level at the ramp. To simulate the proper azimuthal and vertical spread angles, a prefabricated mask has been developed to contain the bundles within the angular boundaries. There are 14 of these lights assembled as a vertical "dropline" light assembly. The vertical dropline lights, like the deck edge lights, are simulated by incandescent "pin" lights powered from an external supply.

3.1.1.1.2 Deck Lighting Block Diagram Discussion. A functional block diagram of the carrier deck lighting is given in Figure 6. All simulated lights discussed in paragraph 3.1.1.1.1 are represented. The light box assembly shown represents either of two boxes — one for the centerline and the other for the athwartship and runway edge lights. The special function block represents the strobe disk and control (centerline lights only) as well as the provision for possible addition of color configurations. The fiber optic bundles distribute light to the optical cones or fibers used for simulation of runway lights as described in paragraph 3.1.1.1.1. The incandescent lights used for simulation of the dropline and deck edge lighting are powered by a separate supply. Variable functions such as brightness, on-off, and sequencing of centerline lights are normally under program control by the linkage. For maintenance purposes, however, control may be manually provided from the maintenance panel.

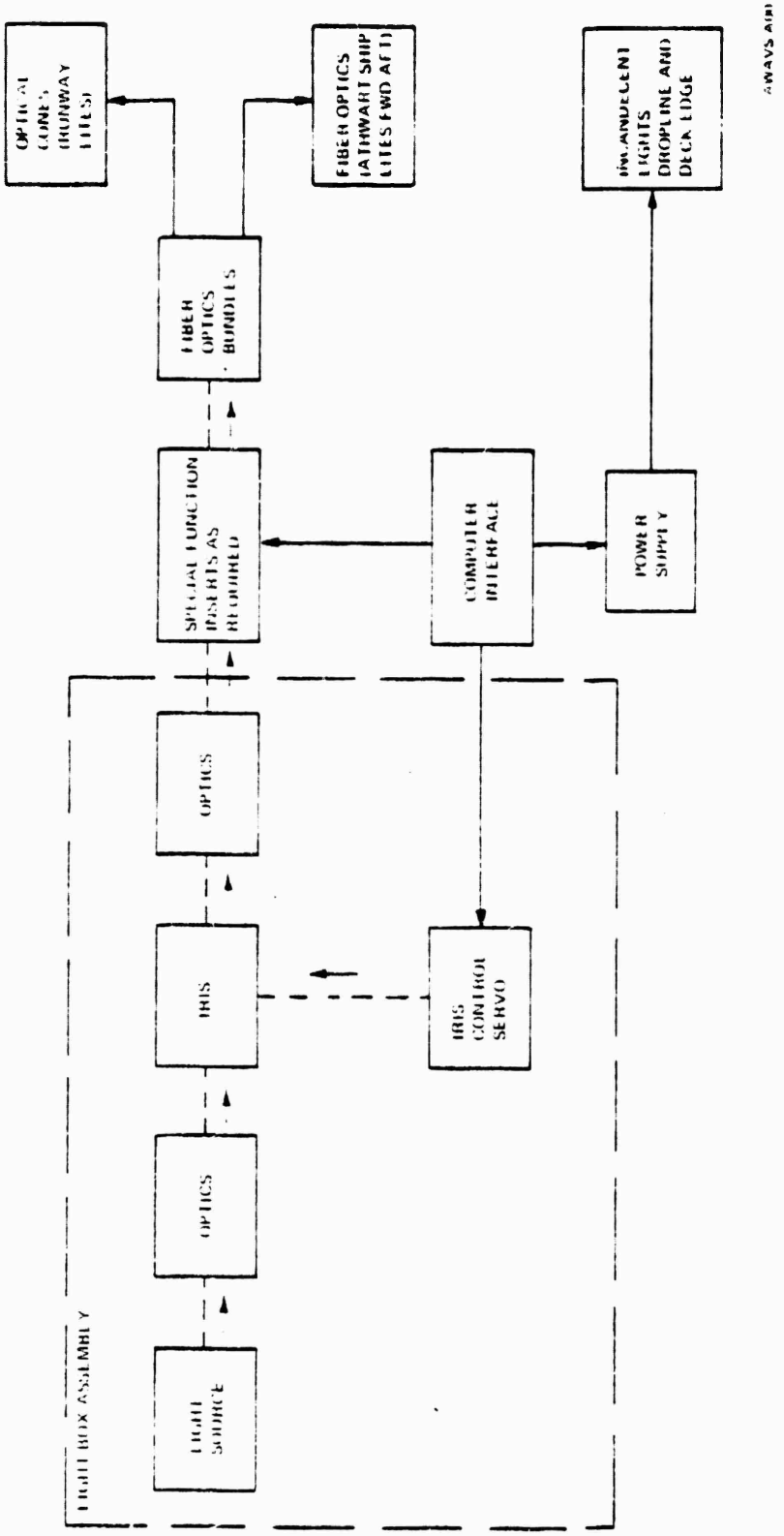

Figure 6. Carrier Lighting, Functional Block Diagram

The light boxes are mounted on support brackets which hold the carrier model servo assembly at a distance of about 13 inches from the back of the model panels. This mounting arrangement supports the light boxes in an upright position so that the bulb operates in its proper base-down attitude, and so that the light output is upward to the fiber optics. By adhering to this design, maximum accessibility is provided for replacing any fibers which may be broken and for replacing lamps. The fiber bundle is attached to a second supporting bar located immediately above the light box.

3.1.1.1.2.1 Fan and Light Source. The light source for the light boxes used is a 300-watt,120-volt projector lamp. This lamp was selected because it has the highest average life span (500 hours) available in this type lamp. In order to insure maximum life of the bulb, a 43 cfm fan is provided to maintain a base temperature of the bulb at less than 150°C, and the lamp is operated at a lower voltage. Lab tests show that the configuration described maintains base temperatures of approximately 105°C for the bulb.

3.1.1.1.2.2 Optics. The optical configuration employed by the light box is shown in Figure 7. The lenses are mounted in lens barrels with lenses 1 and 2 in one barrel, and lenses 3, 4, 5 in another. The lenses are adjustable as groups during set up and alignment to provide for compensation adjustment for manufacturing tolerances. This design forms an image of the light source at the iris by lenses 3, 4, 5. Lenses 1 and 2 serve to relay an image of the entrance pupil of lens group 3-4-5 onto the glass plate at the base of the fiber bundle. Thus, varying the size of the iris causes a proportional change in light output to the fibers while the pupil-imaging design maintains uniform light intensity across the entire 0.75-inch diameter fiber bundle.

3.1.1.1.2.3 Iris and Iris Control. The iris is a fully closing iris with a mechanical travel of 90° of the control arm. Positioning of the iris for the amount of light required is accomplished by a dc servo and servo amplifier driven by computer control.(See Figure 8 for servo amplifier, motor and follow-up potentiometer connections.) Actual iris position is fully closed with 0 volts on the D/A input. Fully open position of the iris occurs when +10 volts is placed on the D/A input. The general shape of the brightness control curve is illustrated in Figure 9. In addition to interface D/A input, an input for maintenance mode operation from the maintenance panel may be substituted.

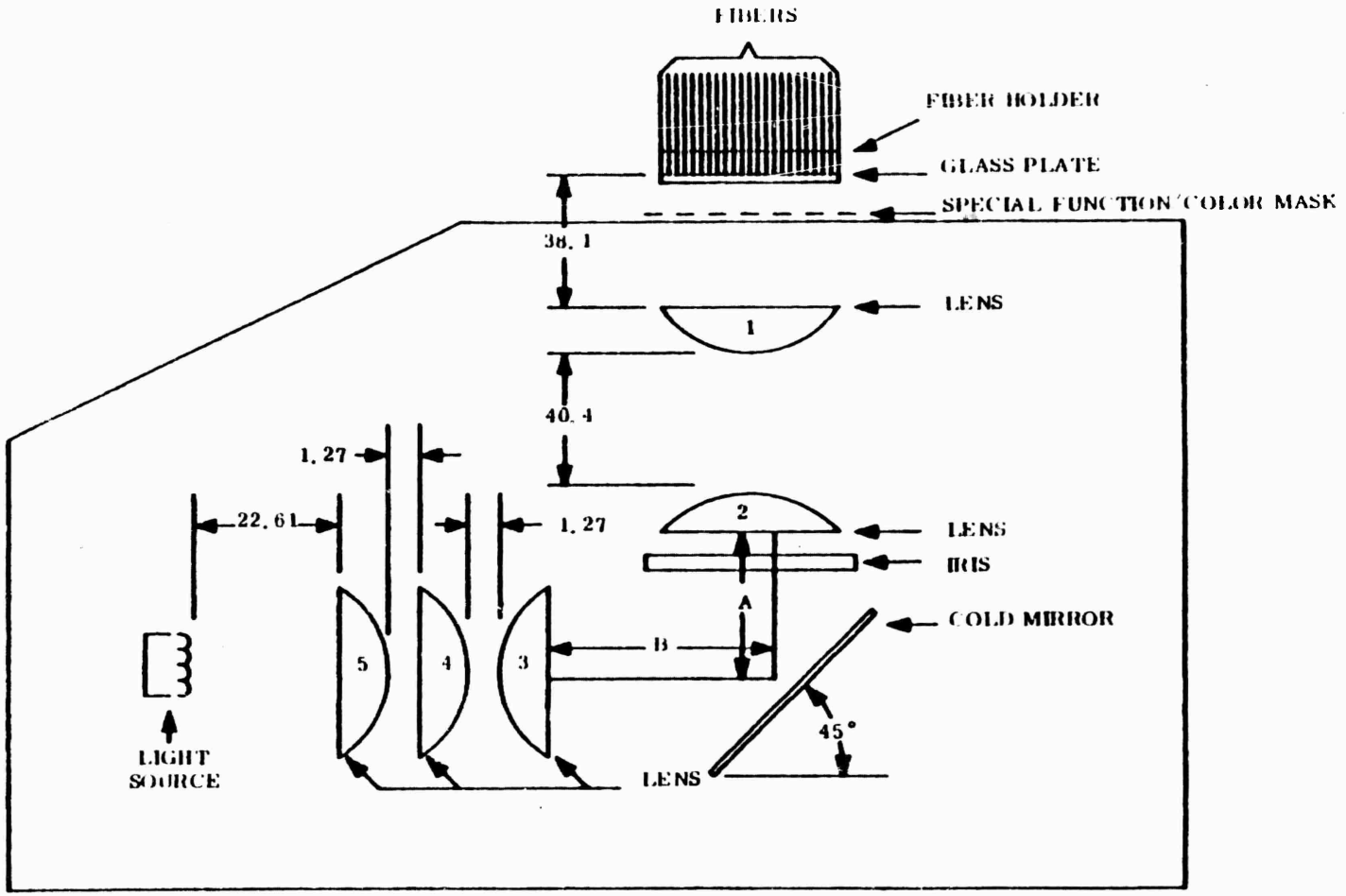

NOTE 1 Dimensions in millimeters

2 Dimensions A + B = 79.26 millimeters

AWAVS AIR17

Figure 7. Light Box, Optical Schematic Diagram

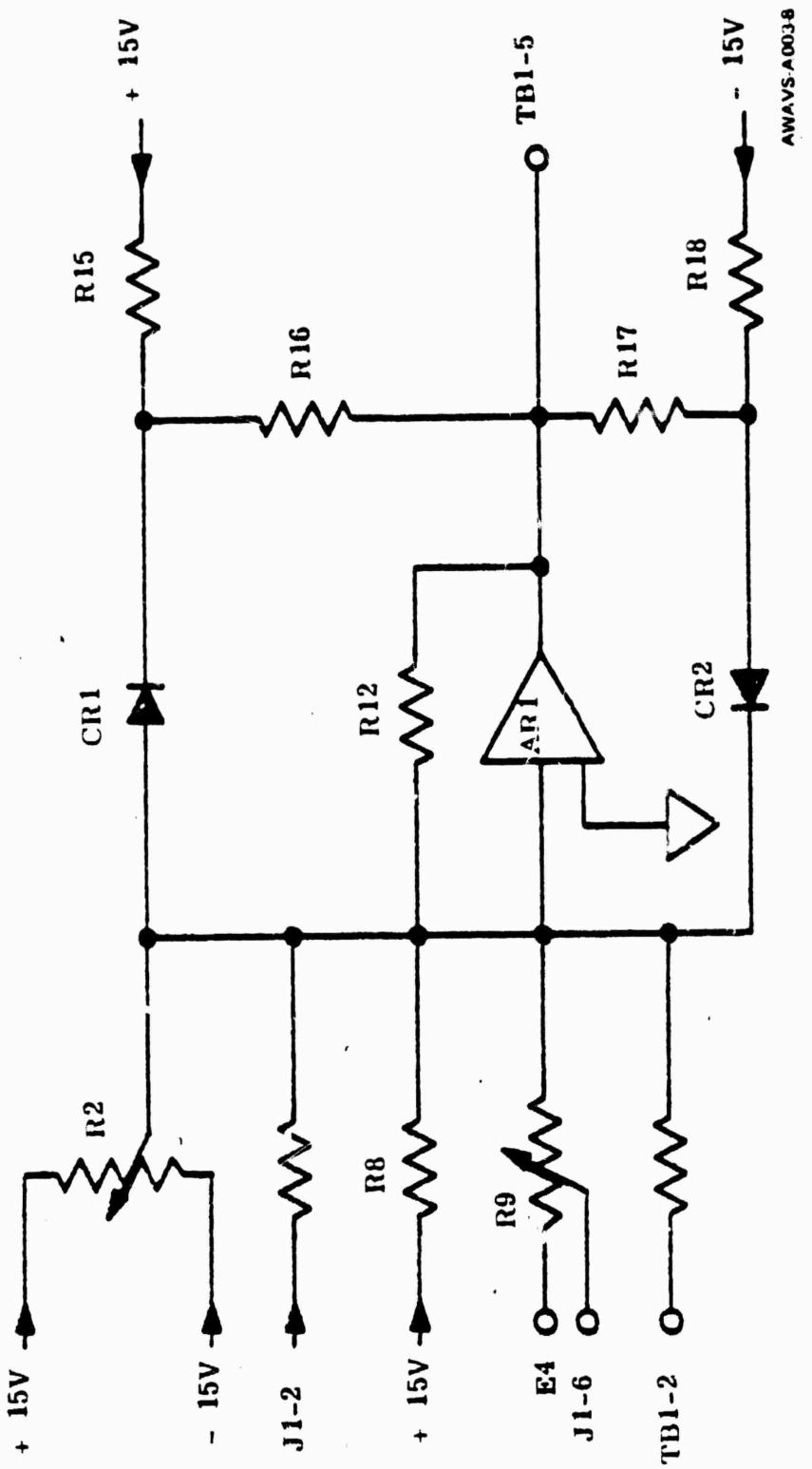

Figure 8. Light Box Servo Amplifier, Schematic Diagram

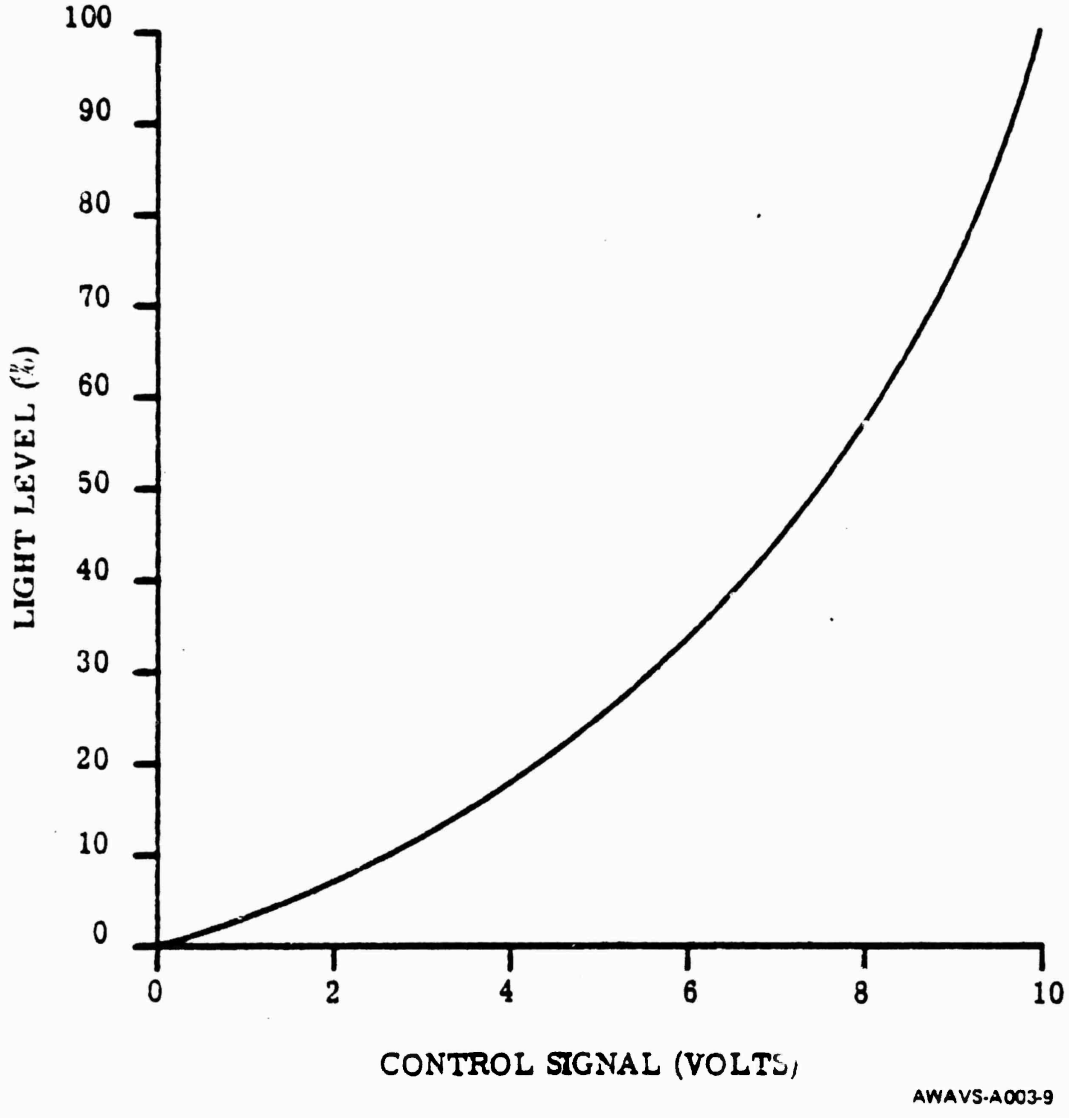

Figure 9. Voltage Control of Light Box Output

3.1.1.1.2.4 Servo Amplifier. A servo amplifier assembly is used to drive the iris servo to the desired brightness setting. The servo is a conventional closed-loop position servo (Figure 8) of the Class I type (i.e., position feedback without rate feedback). The control signal (from 0 to +10 volts) is applied at pin J1-6. The amplifier design is such as to provide a nominal gain of 10:

$$G \approx \frac{R12}{R8 + \frac{1}{2} R9} = \frac{330}{27.4 + 5} \approx 10.2$$

The value of R9 is adjusted so that the iris will be full open with full +10 volts input. Other adjustments and inputs provided are:

a. Zero adjust (R2) so that iris is just closed with zero volts input.

b. TB1-2 input for signal from feedback potentiometer.

c. J1-2 input for manual signal from maintenance panel.

d. TB1-5 output signal to iris drive motor. The voltage excursion on the output lead (TB1-5) is limited to ±6 volts to avoid overdriving (and possibly damaging) the drive motor. The clamping circuits are CR1, R15, R16 for the negative-going signal and CR2, R17, R18 for the positive.

3.1.1.2 Carrier Wake. A simulated 2000-ft painted wake is attached to the model board structure behind the carrier model. The wake is picked up by the target television camera and inset into the background scene along with the carrier image.

The following analysis shows the problem of wake cutoff by the limited field of view of the target system. The wake cutoff and field of view have been computed for four relative aircraft to carrier positions. In this analysis six points on the carrier wake are compared with the probe field of view for four aircraft locations in the turn to final approach.

A 2,000-ft wake length is used, with a width of 250 ft at the carrier stern and 500 ft at the aft end. The six wake points, in the wake frame offset to the FLOLS location, are (in feet):

1) stern port corner $= \begin{bmatrix} -407 \\ 15 \\ 62 \end{bmatrix} = \underline{a}_1$

2) stern center $= \begin{bmatrix} -407 \\ 140 \\ 62 \end{bmatrix} = \underline{a}_2$

3) stern starboard corner $= \begin{bmatrix} -407 \\ 265 \\ 62 \end{bmatrix} = \underline{a}_3$

4) aft port corner $= \begin{bmatrix} -2407 \\ -110 \\ 62 \end{bmatrix} = \underline{a}_4$

5) aft center $= \begin{bmatrix} -2407 \\ -140 \\ 62 \end{bmatrix} = \underline{a}_5$

6) aft starboard corner $= \begin{bmatrix} -2407 \\ 390 \\ 62 \end{bmatrix} = \underline{a}_6$

The four aircraft locations, in the wake frame offset to the FLOLS location are (in feet):

1) 90° turn point (R = 1.5 nm, h = 500 ft) $= \begin{bmatrix} -7380 \\ -5334 \\ 438 \end{bmatrix} = \underline{b}_1$

2) FLOLS entry (R = 1.3 nm, h = 450 ft) $= \begin{bmatrix} -7771 \\ -1370 \\ -388 \end{bmatrix} = \underline{b}_2$

3) Wake crossing
(R = 1.25 nm, h = 425 ft)

$$= \begin{bmatrix} -7587 \\ 140 \\ -363 \end{bmatrix} = \underline{b}_3$$

4) Line-up
(R = 1.0 nm, h = 400 ft)

$$= \begin{bmatrix} -5965 \\ 1105 \\ -338 \end{bmatrix} = \underline{b}_4$$

For each aircraft location, the transformation from the wake frame orientation to the area-of-interest frame orientation (FOV is centered about the FLOLS location) is:

$$\underline{T} = \begin{bmatrix} \cos\psi \cos\theta & \sin\psi \cos\theta & -\sin\theta \\ -\sin\psi & \cos\psi & 0 \\ \cos\psi \sin\theta & \sin\psi \sin\theta & \cos\theta \end{bmatrix} ;$$

where:

$$\psi = \tan^{-1} (b_y/b_x)$$

$$\theta = -\tan^{-1} (b_z/\sqrt{b_x^2 + b_y^2}).$$

Each carrier wake point, in the area-of-interest frame located at the pilot's eyepoint, is:

$$\underline{c} = \underline{T} (\underline{a} - \underline{b})$$

and, from the center of the field of view, the horizontal and vertical viewing angles are:

$$\alpha = \tan^{-1} (c_y/c_x)$$

$$\gamma = -\tan^{-1} (c_z/\sqrt{c_x^2 + c_y^2})$$

Table 1 shows the computed viewing angles for the six wake points for each of the four aircraft locations.

TABLE 1. CARRIER WAKE VIEWING ANGLES

A/C Location	Wake Point	α (Deg.)	γ (Deg.)
1	1	1.63	-0.50
1	2	2.27	-0.48
1	3	2.90	-0.45
1	4	10.53	-1.26
1	5	11.86	-1.17
1	6	13.13	-1.09
2	1	0.65	-0.62
2	2	1.59	-0.62
2	3	2.52	-0.60
2	4	3.21	-1.86
2	5	5.71	-1.82
2	6	8.14	-1.77
3	1	0.06	-0.65
3	2	1.06	-0.65
3	3	2.05	-0.65
3	4	-1.70	-1.95
3	5	1.05	-1.95
3	6	3.81	-1.95
4	1	-0.60	-0.85
4	2	0.64	-0.87
4	3	1.90	-0.88
4	4	-8.32	-2.92
4	5	-4.66	-3.01
4	6	-0.86	-3.10

The field of view half-angles are determined by probe zoom (Z_p). Probe zoom and display zoom (Z_D) are constrained such that total system zoom (Z_T) is:

$$Z_T = Z_P Z_D = \frac{Rp}{R}$$

where:

Rp = probe slant range (scale ft.)
R = simulated slant range (ft.)

In our simulation approach,

$Z_D = 1.0$ $\quad R < 1,000$ ft

$Z_D = \frac{1000}{R}$ $\quad 1,000$ ft. $< R < 10,000$ ft

$Z_D = 0.1$ $\quad R > 10,000$ ft

therefore, the probe zoom is:

$$Z_P = \frac{Z_T}{Z_D}$$

$Z_P = 1.0$ $\quad R < 1,000$ ft.

$Z_P = \frac{Rp}{1000}$ $\quad 1,000$ ft. $< R < 10,000$ ft

$Z_P = 10 \frac{Rp}{R} = \frac{10r_2}{R}$ $\quad R > 10,000$ ft

where, in our approach:

$Rp = R$ $\quad R < R_1$

$Rp = R - \left(\frac{R-R_1}{R_2-R_1}\right)^2 (R_2-r_2)$ $\quad R_1 < R < R_2$

$Rp = r_2$ $\quad R > R_2$

$R_1 = 2300$ ft

$R_2 = 5840$ ft

$r_2 = 4070$ ft

The distance subtended by the probe horizontal field of view half-angle, in the object plane, is:

$$d = \frac{Rp}{Zp} \tan 30^{o}.$$

At the eyepoint, this distance subtends a horizontal field of view half-angle of:

$$\alpha' = \tan^{-1} \frac{d}{R}$$

$$= \tan^{-1} \left(\frac{Rp}{Z_p R} \tan 30^{o} \right);$$

since:

$$Zp = \frac{Z_T}{Z_D} = \frac{Rp}{Z_D R}$$

$$\alpha = \tan^{-1} (Z_D \tan 30^{o});$$

and, by the same process, the vertical field of view half-angle, at the eyepoint, is:

$$\gamma' = \tan^{-1} (Z_D \tan 20^{o}).$$

For the four aircraft locations used:

$$Z_D = \frac{1000}{R} ;$$

and,

$$\alpha' = \tan^{-1} \left(\frac{1000}{R} \tan 30^{o} \right)$$

$$\gamma' = \tan^{-1} \left(\frac{1000}{R} \tan 20^{o} \right).$$

Table 2 shows the simulated slant ranges, probe slant ranges, display zoom ratios, and FOV half-angles (from the eyepoint) for the four aircraft locations used.

Figure 10 shows, for the four aircraft locations, the shape of the carrier wake together with the FOV limit frame. Perspective distortion is not included in this analysis.

TABLE 2. CARRIER WAKE FIELD OF VIEW

R (ft)	Rp (scale ft)	Z_D	α (deg)	γ (deg)
9120	4070	1/9.12	3.62	2.29
7904	4070	1/7.90	4.18	2.64
7600	4070	1/7.60	4.34	2.74
6080	4070	1/6.08	5.42	3.43

3.1.1.3 Carrier Model Servo Description. The roll, pitch, heave model positioning servomechanisms are dc position servos, utilizing high-resolution dc torque motors and follow-up potentiometers. DC tachometers are utilized to stabilize the loop. In order to provide accurate positioning, minimum gearing is utilized between load and follow-up potentiometer. All gearing used is anti-backlash gearing.

The maintenance control panel located on the gantry, probe, model control cabinet contains local manual-control potentiometers to position each axis independently. Control mode switches are located on this panel to select computer or local inputs. The roll, pitch and heave servos are limited rotation devices and include electrical switches and mechanical limit stops.

A simplified block diagram of a typical carrier model servo loop is shown in Figure 11. Figure 12 shows physical configuration details of the servo components for all axes as viewed from the top, starboard side, and aft end of the carrier model. These figures also give mounting data, rotational directions, and gear ratios, as applicable. Paragraph 3.1.1.4 provides an analysis of the servo design for the roll, pitch, and heave functions.

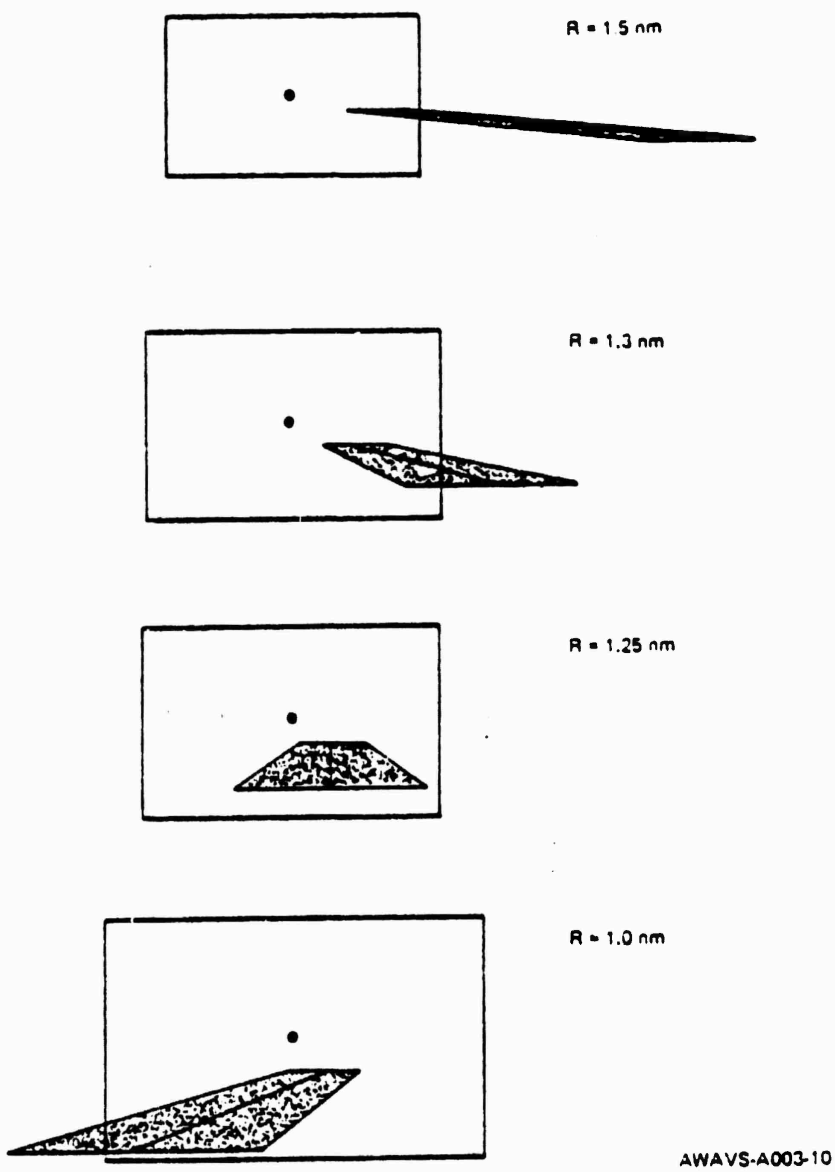

Figure 10. Carrier Wake and Field of View

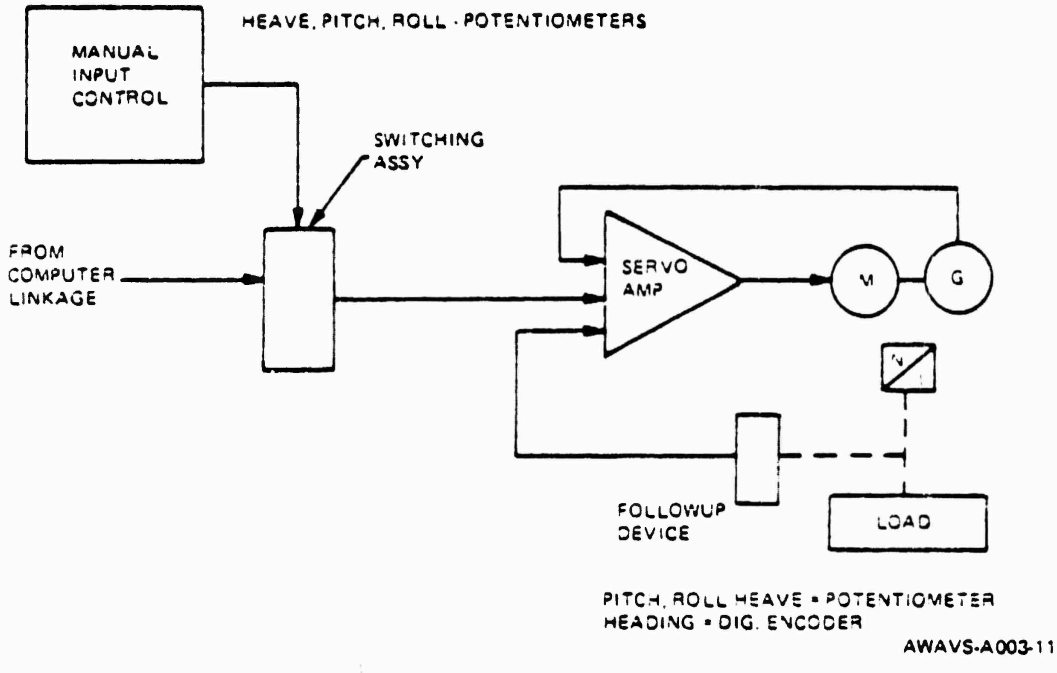

Figure 11. Typical Model Servo Signal Flow Diagram

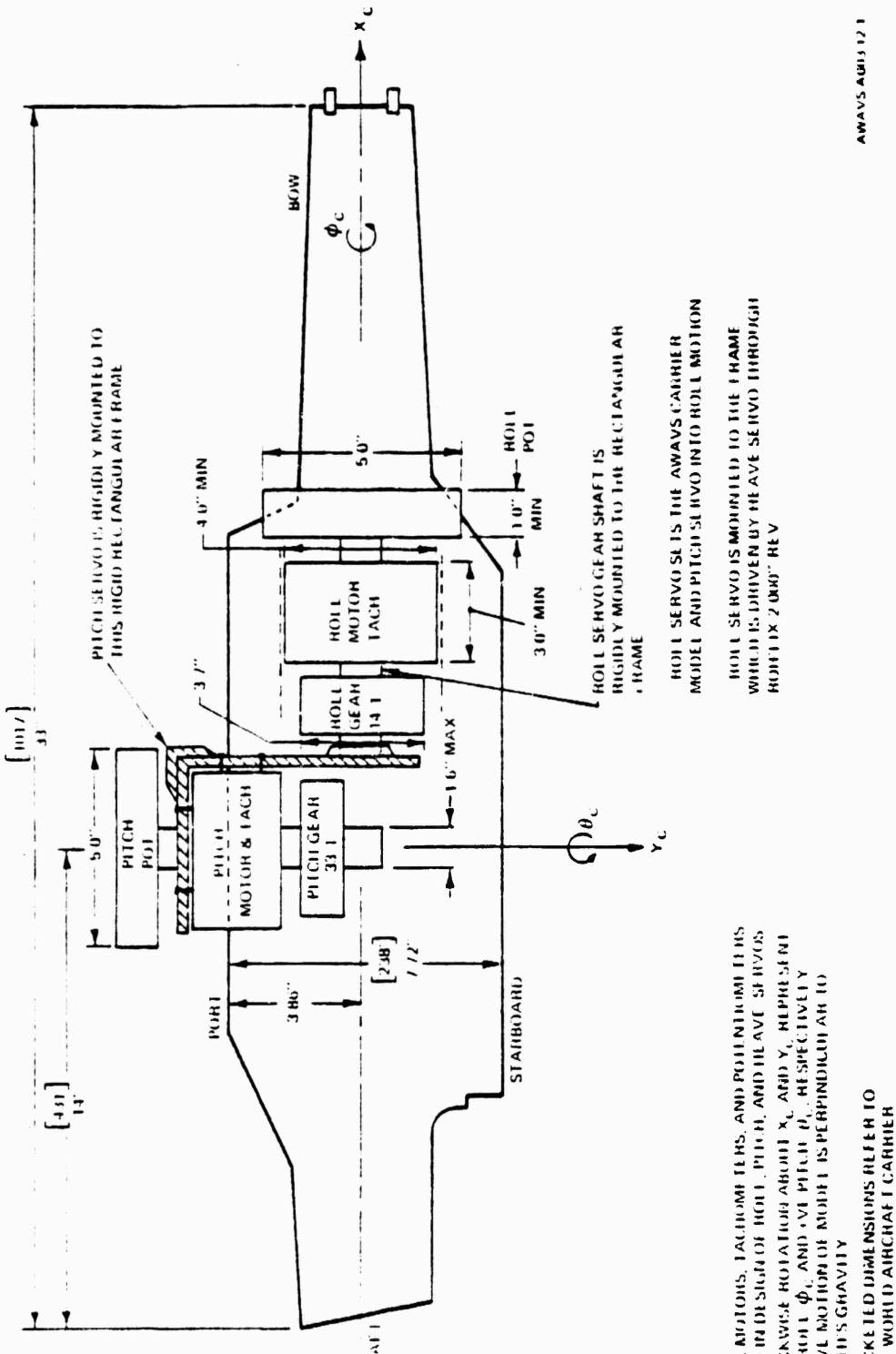

NOTES:
1. SAML MOTORS, TACHOMETERS, AND POTENTIOMETERS USED IN DESIGN OF ROLL, PITCH, AND HEAVE SERVOS
2. CLOCKWISE ROTATION ABOUT X_c AND Y_c REPRESENT +VE ROLL ϕ_c AND +VE PITCH θ_c, RESPECTIVELY
3. HEAVE MOTION OF MODEL IS PERPENDICULAR TO EARTH'S GRAVITY
4. BRACKETED DIMENSIONS REFER TO REAL WORLD AIRCRAFT CARRIER

Figure 12. Physical Setup of Carrier Model Servos (Sheet 1 of 3)

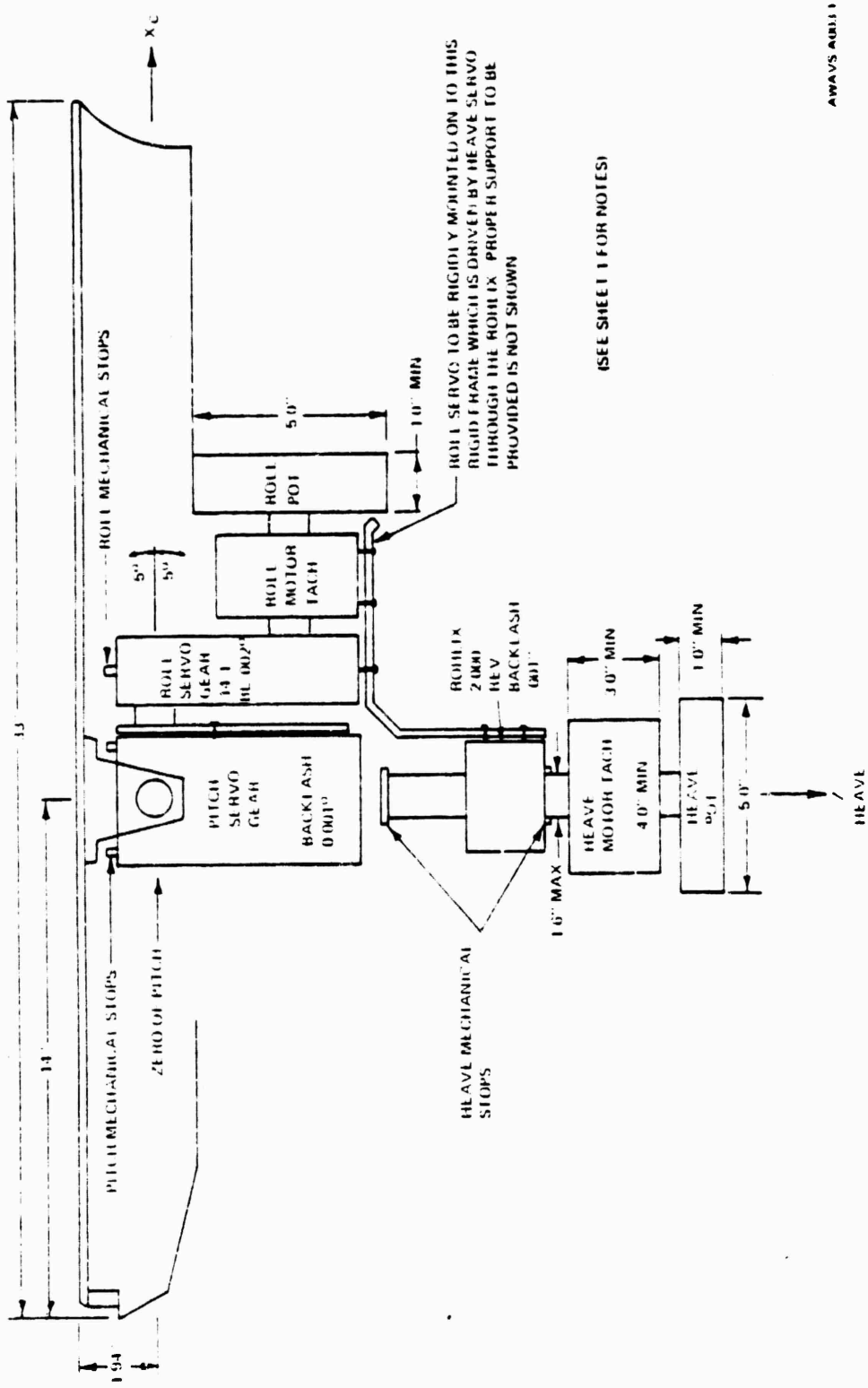

Figure 12. Physical Setup of Carrier Model Servos (Sheet 2 of 3)

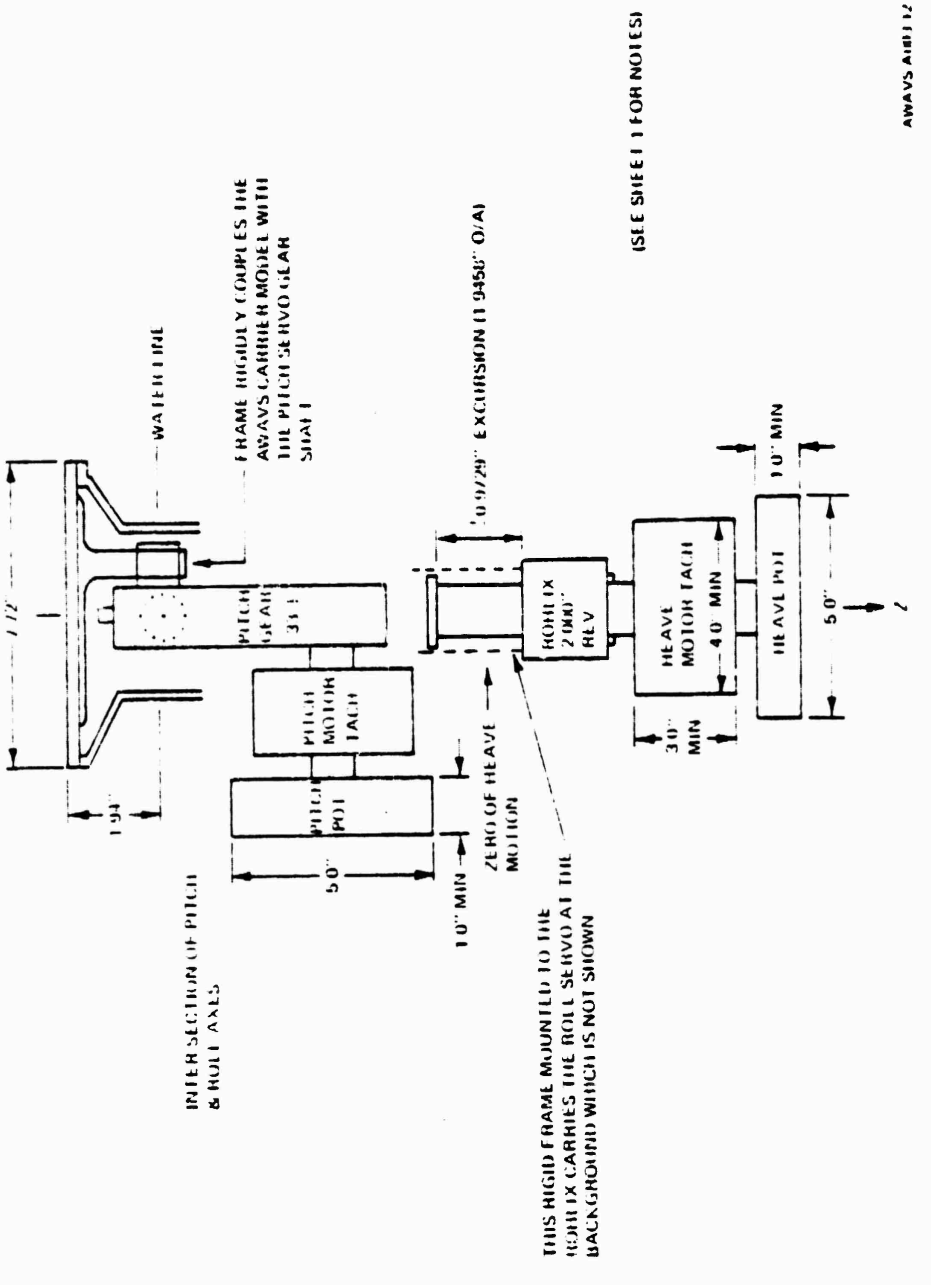

Figure 12. Physical Setup of Carrier Model Servos (Sheet 3 of 3)

3.1.1.4 Carrier Model Motion and Error Analysis. The following paragraphs describe the techniques of servo design, analysis, and evaluation of performance applied to the design of the carrier model servos. Table 3 is a compilation of the carrier model system servos and components. Data common to all three loops is given in paragraphs 3.1.1.4.1 and 3.1.1.4.2, while peculiar data is presented in subsequent hardware oriented paragraphs on individual servos. Criteria established for design of carrier model servos during the AWAVS design analysis were as follows:

a. Input Commands. Servos will operate with input commands formulated as listed in Table 3. Each servo will provide for two sources of input command signals — one source from the computer interface, the other source from the test panels switching between sources will be relay controlled.

b. Minimization of Abrupt Nonlinearities. Components and mechanisms of the above mentioned subsystems servos have been designed to achieve the required smoothness in output motion response. Servo component selections are identified for each servo under the hardware subsystem descriptions. Mechanisms have been developed to eliminate or minimize backlash in gearing, by use of precision gearing, by antibacklash gearing.

c. Feedback Techniques. Feedback components (potentiometer and tachometer) are identified for each servo in the hardware subsystem descriptions of this report. (See Table 3.)

d. Travel Stops and Limit Switches. Travel limit switches will be provided on each noncontinuous servo. Contact with any limit switch will remove power amplifier current to the motor of that servo only in the direction of the approached travel limit. Travel past the limit switches will be controlled by soft mechanical stops with over travel. The stops will safely control deceleration based on the momentum produced by the maximum velocity of the total moving inertia at the instant contact is made with the stop.

e. Lockouts. Removable mechanical lockouts will be incorporated on all servos providing a means of securing moving mechanisms during handling and shipment. The lockout will also provide a preprecise repeatable calibration reference for position sensor alignment.

3.1.1.4.1 Generalized Performance Data. Following are the techniques used in synthesis of performance oriented parameters (displacements, velocities, and accelerations) associated with the carrier model servomechanism loops. The performance data for each servo is tabulated as part of the individual loop discussion. (See paragraphs 3.1.1.4.3 through 3.1.1.4.5, as applicable.)

TABLE 3. CARRIER MODEL SERVOS

SERVO	INERTIA TORQUE ($T_a = J_T \alpha_L$)	DISTURBANCE TORQUE (T_D)	FRICTION TORQUE (T_F)
Heave Z_{CM}	$0.5_{oz\ in\ sec^2}$ x 1.2 rad/sec^2	1 lb-ft	0.07 lb ft
Roll ϕ_{CM}	$0.02_{oz\ in\ sec^2}$ x 0.04 rad/sec^2	0.1 lb-ft	0.07 lb ft
Pitch θ_{CM}	$0.02_{oz\ in\ sec^2}$ x 0.04 rad/sec^2	0.3 lb-ft	0.07 lb ft

Component Data: (Common to all servos)

DC Torquer - Tachometer

Inland TT-2947 (21V x 6 Amp); Singer #2003837-01

T_p = 2.0 lb ft T_G = 1.4 v/rad/sec K_r = 0.3 lb ft/amp

W_{nL} = 45 rad/sec

Feedback Potentiometer

CIC 505; Singer #1003839-01

Conformity = 0.01% Impedance = 5K

Power Amplifier

Inland EM1802; Singer #1003911-03

200 watts at 20 volts

Compensation Buffers

Singer #2061496-01 and 2061498-01

a. Static Accuracy. Accurate line-of-sight placement of the projected image on the projection screen is a critical requirement. To achieve the required projector servo positioning accuracy, the following techniques will be applied to servos of the visual system:

- An integrator incorporated in the forward path of each servo is incorporated which acts to reduce the error signal to virtually zero during static positioning. It also makes the positioning accuracy of the servo independent of output torque thresholds or gravity loads on the output of the servo.

- A unity voltage follower immediately following each feedback pot wiper output signal is physically located as near to the potentiometer as practical. The extremely high input impedance of this voltage follower serves to virtually eliminate errors due to potentiometer loading.

With the application of the techniques described above, remaining static positioning errors occur almost entirely from two sources:gearing errors (between the feedback pot shaft and the applicable controlled output of the servo), and feedback potentiometer linearity (or conformity) errors. Gearing errors are classified by two clearly identifiable components:

- Transmission Error. The variation in the transmission ratio of a gear pair or train from the ideal nominal value, caused by the net sum of individual gear position errors and installation runout errors. This error is single valued and repeatable and combines with the potentiometer linearity error.

- Backlash Error. The total lost motion for a gear pair or train caused by all contributors, such as thinned teeth, enlarged center distance and runout of rotating parts. Backlash error is multivalued and is therefore not a specific repeatable error value. Therefore backlash in gearing is the only significant error in the determination of static repeatability accuracy.

Feedback potentiometer linearity (or conformity) error is the primary accuracy specification of a particular potentiometer assembly. The maximum permitted linearity error will be defined by procurement specifications for each potentiometer assembly used on AWAVS visual system.

Table 3 lists the potentiometer selections and conformity for each servo of the carrier model system. A root-sum-square method is used in combining maximum allowable gearing errors with potentiometer errors. Feedback potentiometer errors listed in Table 3 are the maximum positioning error of the servo based on the potentiometer linearity (or conformity) specification. For the noncontinuous servos, this is directly related by the specified pot linearity and the gearing ratio which determines the percentage of the full potentiometer travel which occurs over the full servo travel.

b. Static Repeatability. As indicated in the discussions of gearing errors and based on the application of the servo design techniques, backlash in gearing is the only significant error source in the determination of static repeatability. As anti-backlash gearing is utilized in each servo, the static repeatability error should be small.

c. Static Compliance. Incorporation of integral control in each servo renders the closed loop dc sensitivity of each servo output displacement to disturbance torques or forces applied at the servo output, to be virtually infinite. This means that the servos are capable of resisting any externally applied output torque or force up to the peak motor torque, without having to hold a corresponding error in position. The result is a static servo compliance which is virtually infinite.

d. Dynamic Range. The capability of the visual system servos to smoothly control the movement of the projected image over a wide range of velocities is a critical requirement. The dynamic range defines the ratio of the largest to the smallest velocity which the servo can control. The maximum velocity for each servo is defined by the motion envelope in the AWAVS detailed servo specifications. Each servo will be judged to have satisfactory smoothness by direct visual observation of the image projected onto the screen at the minimum velocity specified by the applicable performance specification. Verifying smoothness using a test criterion based on monitoring the tachometer signal may not be valid because of large high frequency content in the signal, which is not related to the actual observable smoothness of the projected image. It is valid only if the ripple, high frequency content etc. of the tachometer are taken into account.

e. Frequency Response. A critical requirement in achieving an accurate representation of the external visual scene is synchronization of all servos involved in projecting the scene. This requires that the servos have the same dynamic response as well as the same degree of smoothness. To accurately control the synchronization of the visual system servos, the dynamic response is specified to accurately match (within 20%) an ideal second order system with a damping ratio ζ and natural frequency ω_n chosen for optimum performance.

f. System Type. Based on the specification of dynamic response i.e., stringent tolerance of 0.1% of maximum velocity in high velocity tracking, servo system type should be decided. Optimum choice of bandwidth, stability damping ratio, percentage overshoot, velocity tracking error and other parameters depends mostly on system type. The analysis of the type 1 servos is portrayed in the Bode plots presented with the individual servo loop discussions. The figures indicate the phase margin, bandwidth, damping ratio and velocity error constant. Limitations are also indicated.

In order for a system to reproduce the squarewave at its output, the system would have to have infinite bandwidth. Associated with infinite bandwidth is zero rise time and zero delay time. There is no analytic expression that even approximately relates the two for systems of arbitrary order. In reality a system having large bandwidth is welcomed if the input signal is free from noise. A system with a large bandwidth, is a measure of accuracy for all time and might be called the measure of dynamic accuracy.

The traditional well-established analytic results of system classification and error constants are presented in Figure 13 for stable type 0, type 1 and type 2 unity feedback systems.

g. Compensation Cards. The general compensation card has the capability to properly shape the feedback and forward path signals. The design philosophy of all noncontinuous servos is established to be the same. The components in the compensation card differ because of difference in controlled load and hardware of different servos.

h. The Inherent Zeros and Poles Generated By Servo Components. The values of pertinent parameters of motor, tachometer, power amplifier, and follow-up potentiometer are included in the hardware sheets. The tachometer generates an inherent zero ω_L which contributes to phase-lead and is adjustable for stability as a function of cross-over frequency which determines the bandwidth. The motor-impedance coupled with the mechanical inertia generates a pole ω_{MJ} contributing to a phase lag. The electrical time constant of the motor and amplifier generate two other poles ω_E & ω_A contributing to phase lag.

The system will be stable if the phase margin, ϕ_{PM}, which is a good measure of system stability, is at least 40°. Proper electronic shaping is necessary by utilizing the general compensation card which can generate two free integrators in the forward path, thus transforming an inherent type 1 stable system into type 2 or type 3 stable systems and rendering the velocity error constant to almost infinity, tracking error to almost zero.

3.1.1.4.2 Carrier Model Servo Block Diagram. The noncontinuous position servo block diagram given in Figure 14 is representative of the roll, pitch and heave servo loops. The transfer function for unity gain servos, also shown in Figure 14, is the mathematical expression of the block diagram. Definitions of the terms used in the transfer function and block diagrams are provided in the foregoing servo analysis discussions, while quantitative values are given in subsequent individual hardware discussions.

3.1.1.4.3 Design Analysis of Carrier Model Roll Servo ($\ddot{\phi}_{CM}$). The performance specification of Carrier Model Roll Servo (ϕ_{CM}) is given in Table 4.

INPUT	UNIT STEP		UNIT RAMP		UNIT PARABOLA	
SYSTEM TYPE	K_p POSITION ERROR CONSTANT	STEADY STATE ERROR	K_v VELOCITY ERROR CONSTANT	STEADY STATE ERROR	K_A ACCELERATION ERROR CONSTANT	STEADY STATE ERROR
TYPE 0	$\frac{KB_1(0)}{B_2(0)}$	$\frac{1}{1+K_p}$	0	∞	0	∞
TYPE 1	∞	0	$\frac{KB_1(0)}{B_2(0)}$	$\frac{1}{K_v}$	0	∞
TYPE 2	∞	0	∞	0	$\frac{KB_1(0)}{B_2(0)}$	$\frac{1}{K_A}$

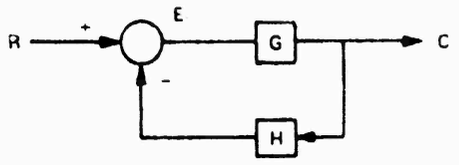

The following notation is used:

The open-loop transfer function for the class of canonical feedback system defined by the foregoing block diagram is given by:

$$GH = \frac{Ks^a \prod_{i=1}^{m-a} (s + z_i)}{s^\ell \prod_{i=1}^{m-a-1} (s + p_i)} = \frac{KB_1(s)}{s^\ell B_2(s)}$$

where, K is a constant, $-Z_i$ and $-P_i$ are nonzero finite zeros and poles of GH respectively and ℓ is equal to or greater than zero.

UNIT PARABOLA	
K_A ERATION RROR STANT	STEADY STATE ERROR
0	∞
0	∞
$KB_1(0)$ / $B_2(0)$	$\frac{1}{K_A}$

defined

$\frac{(s)}{B_2(s)}$

GH respectively

POSITION ERROR CONSTANT (K_p)

This constant is a measure of the steady state error between the input and the output, when the input is a unit-stepfunction

$$K_p = \lim_{s \to 0} G(s) = \lim_{s \to 0} \frac{KB_1(s)}{s^{\ell} B_2(s)} = \begin{cases} \frac{KB_1(0)}{B_2(0)} & \ell = 0 \\ \infty & \ell > 0 \end{cases}$$

The steady state error of a stable type ℓ unity feedback system for a unit step input is

$$e(\infty) = \lim_{t \to \infty} e(t) = \frac{1}{1 + K_p}$$

VELOCITY ERROR CONSTANT (K_v)

This constant is a measure of the steady state error between the input and the output, when the input is a unit-ramp function.

$$K_v = \lim_{s \to 0} sG(s) = \lim_{s \to 0} \frac{KB_1(s)}{s^{\ell-1} B_2(s)} = \begin{cases} 0 & \ell = 0 \\ \frac{KB_1(0)}{B_2(0)} & \ell = 1 \\ \infty & \ell > 1 \end{cases}$$

The steady state error of a stable type ℓ unity feedback system for a unit-ramp function is

$$e(\infty) = \lim_{t \to \infty} e(t) = \frac{1}{K_v}$$

ACCELERATION ERROR CONSTANT (K_A)

This constant is a measure of the steady state error between the input and the output, when the input is a unit-parabolic function

$$K_A = \lim_{s \to 0} s^2 G(s) = \lim_{s \to 0} \frac{KB_1(s)}{s^{\ell-2} B_2(s)} = \begin{cases} 0 & \ell = 0,1 \\ \frac{KB_1(0)}{B_2(0)} & \ell = 2 \\ \infty & \ell > 1 \end{cases}$$

The steady state error of a stable type ℓ unity feedback system for a unit-parabolic function is

$$e(\infty) = \lim_{t \to \infty} e(t) = \frac{1}{K_A}$$

AWAVS-A003-13

Figure 13. Unity Feedback Systems, Classification and Error Constants

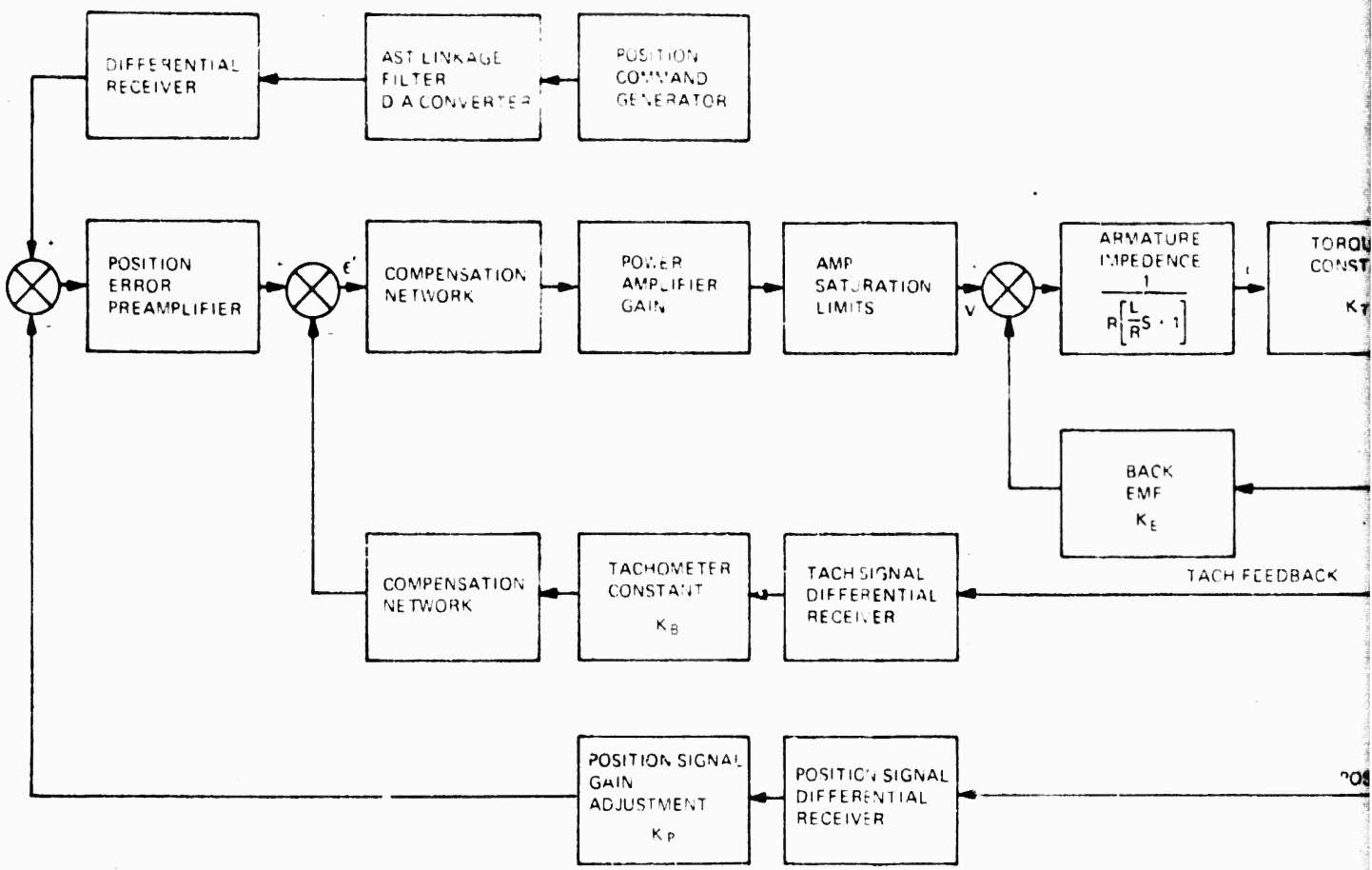

TRANSFER FUNCTION

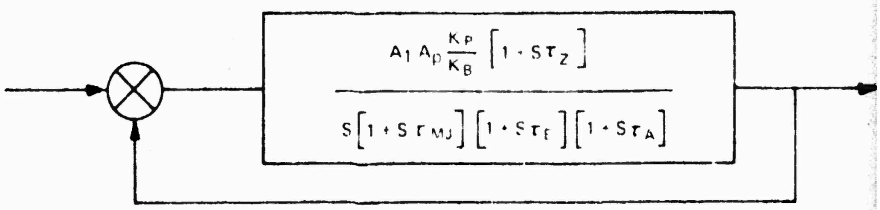

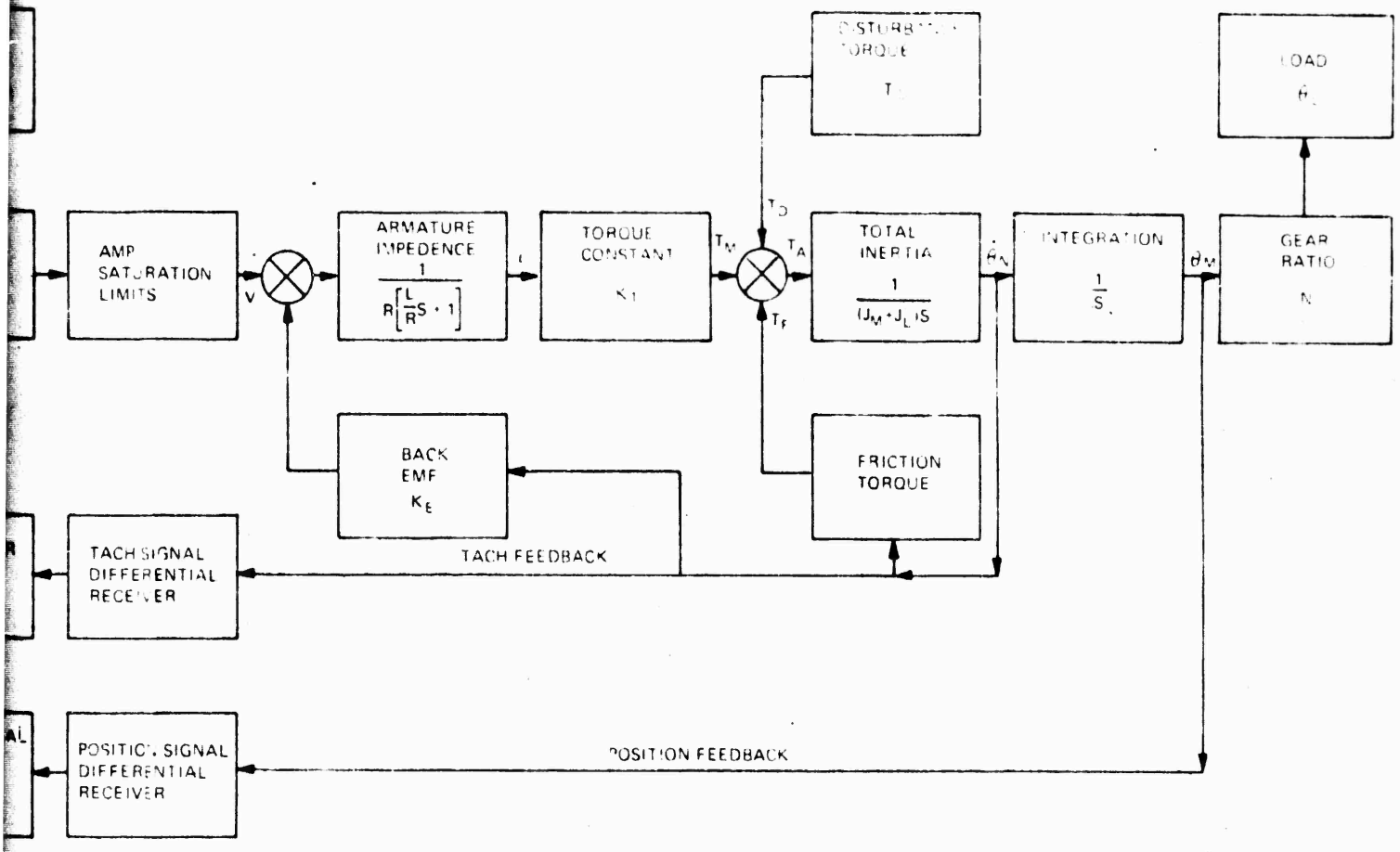

TRANSFER FUNCTION

$$\frac{A_1 A_p \frac{K_P}{K_B}\left[1+S\tau_Z\right]}{S\left[1+S\tau_{MJ}\right]\left[1+S\tau_E\right]\left[1+S\tau_A\right]}$$

AWAVS A003 14

Figure 14. Noncontinuous Position Servos, Block Diagram and Transfer Function

TABLE 4 . 'CARRIER MODEL ROLL SERVO PERFORMANCE

1.	Excursion	±12°
2.	Velocity (Maximum)	4.7°/sec
3.	Acceleration	1.85°/sec^2
4.	Static Accuracy	±5 arc min
5.	Linearity	±5 arc min
6.	Repeatability	±5 arc min
7.	Resolution	±5 arc min
8.	Dynamic Range	500:1
9.	Tracking Accuracy at Velocity (High)	0.6°
	Velocity (Low)	0.3°
10.	Period of Oscillation	16 sec

The carrier model roll servo (Φ_{CM}) is synthesized as follows to meet the performance specification parameters 1 through 9:

1. The mechanical sketch indicates a possible excursion of ±12° for the assembly.

2. Dc torque motor is capable of no load speed of 5156°/sec, and tachometer has a maximum operating speed of 5156°/sec.

3. The dc torquer can generate a peak torque of 2 lb-ft. The estimated inertia of roll assembly is 0.5 oz in sec^2. The possible acceleration limit is approximately 10^6°/sec^2. There is ample allowance for estimated disturbing torque of 1 lb-ft.

4. As described in paragraph 3.1.1.4.1, the static position error for this noncontinuous position servo emanates from the conformity specification of the position feedback potentiometer. The static position error could, at most, be ±1 arc min. The best available potentiometer is used for position transducer as a means of protecting the probe.

5. The principle of the linear servo is to drive the control element by amplifying the actuating signal error. All components of this system are linear, and the linearity of position transducer potentiometer is specified to ±1 arc min.

6. With proper initial calibration to meet the static error requirement as stated above, any position error beyond that specified as conformity of the potentiometer, ±1 arc min, will be reduced to zero because of integral control. Steady state repeatability, in this type of control system, cannot be greater than the steady-state position error.

7. In order to meet the resolution requirement of ±5 arc min, the position transducer potentiometer of infinite resolution is chosen. A digital command signal from the computer is converted to an analog signal by a 12-bit D/A converter, the command signal resolution being less than an arc min when referenced to the carrier model roll motion.

8. The dynamic range, the ratio of maximum velocity to minimum velocity, of 500:1 can be met by the choice of a high quality dc motor and tachometer, by minimizing friction, and by direct driving or by using anti-backlash gears of low gear ratio. In this case, the carrier model roll assembly is driven through anti-backlash gear (14:1) by the motor-tachometer potentiometer system. The noise level is kept to the minimum.

9. The reduced transfer function indicates that this servo is designed to be of type 1 system. As shown in the general analysis, the velocity error coefficient is finite. This implies that the servo follows ramp input of the form t'u(f) with finite steady-state error. With a bandwidth around 18 Hz, with a phase margin of 78°, the velocity error constant is approximately 75 with a tracking accuracy less than 0.1° when referenced to the roll motion of model board, well below what is specified.

The stability analysis is illustrated on the roll servo frequency-gain plot, Figure 15. The criteria used for stability are as follows:

- To keep the phase margin greater than 40°
- To shape the slope of the frequency-gain curve to 20 dB/decade at and around the decade crossover frequency
- To reduce the gain sharply at high frequencies.

Inherent zeros and poles plotted on the frequency-gain curve are defined in Table 5. The phase margin ϕ_{PM} should be at least 40° for the system to be relatively stable. Phase margin is defined as

$$\phi_{PM} = 180 - \sum \text{phase lags and leads in the system.}$$

Phase lags: Integral control ($\frac{1}{s}$): 90°
Mechanical time constant (τ_{MJ}): 83°
Electrical time constant (τ_C): 14°
Power Amplifier time constant: (τ_A): 1°

Phase leads: Tachometer Zero (τ_Z): 85°

Net contribution: 102°

Phase margin: $\phi_{PM} = 180° - 102° = 78°$

This insures excellent stability. However, the compensation card has several adjustable features which if necessary can be used to shape the signal. In fact, τ_{MJ} is estimated and τ_Z is adjustable by tachometer gain adjustment.

TABLE 5. INHERENT ZEROS & POLES FOR CARRIER MODEL ROLL SERVO

ω_L	Zero	Tachometer & Pot	$\frac{K_B}{K_G}$	14 rad/sec
ω_{MJ}	Pole 1	Motor & Load	$\frac{K_T K_B}{RJ}$	15 rad/sec
ω_E	Pole 2	Motor	$\frac{L}{R}$	455 rad/sec
ω_A	Pole 3	Power Amplifier	Bandwidth	6000 rad/sec

3.1.1.4.4 Design Analysis of Carrier Model Pitch Servo (θ_{CM}). The performance specification of carrier model pitch servo (θ_{CM}) is given in Table 6.

The carrier model pitch servo (θ_{CM}) is synthesized as follows to meet the performance specification parameters 1 through 9:

1. The mechanical sketch indicates a possible excursion of ±5° for the pitch assembly.

2. Dc torque motor is capable of no load speed of 5156°/sec, and tachometer has a maximum operating speed of 5156°/sec.

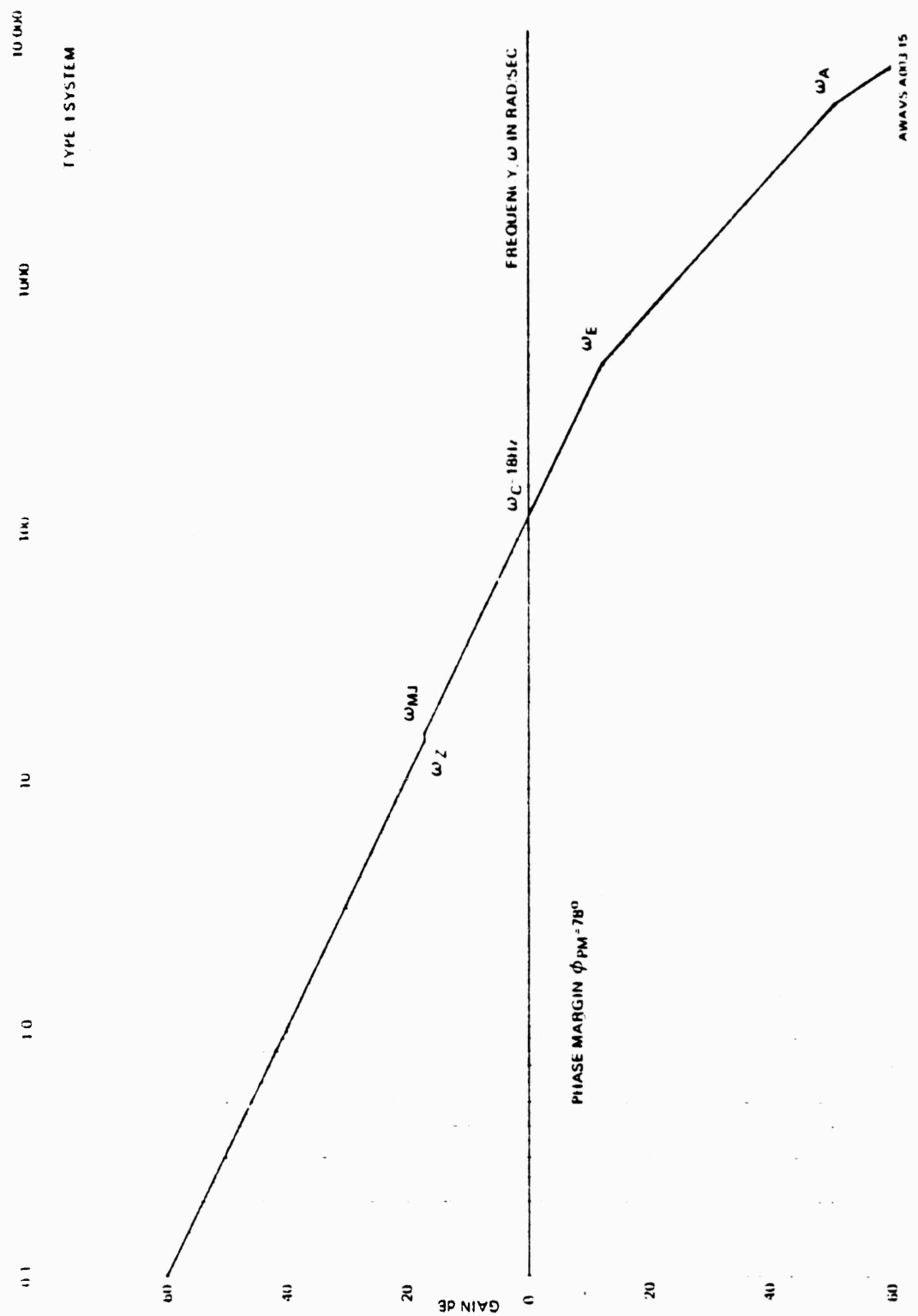

Figure 15. Frequency-Gain Plot for Carrier Model Roll Servo

TABLE 6. CARRIER MODEL PITCH SERVO PERFORMANCE

1.	Excursion	±5°
2.	Velocity (Maximum)	3.14°/sec
3.	Acceleration	1.98°/sec^2
4.	Static Accuracy	±5 arc min
5.	Linearity	±5 arc min
6.	Reapeatability	±5 arc min
7.	Resolution	±5 arc min
8.	Dynamic Range	500:1
9.	Tracking Accuracy at Velocity (High) Velocity (Low)	 0.6° 0.3°
10.	Period of Oscillation	10 sec

3. The dc torquer can generate a peak torque of 2-lb ft. The estimated inertia of pitch assembly is 0.5 oz in sec^2. The possible acceleration limit is 10^6°/sec^2. There is ample allowance for estimated disturbing torque of 1-lb ft.

4. As described in paragraph 3.1.1.4.1, the static position error for this noncontinuous position servo emanates from the conformity specification of the position feedback potentiometer. The static position error will be less than an arc min when referenced to pitch motion of the carrier model. The best available feedback potentiometer is used to obtain this accuracy in order to control the motion of probe and to provide probe protection.

5. The principle of the linear servo is to drive the control element by amplifying the actuating signal error. All components of this system are linear, and the linearity of position transducer potentiometer is specified to ±1 arc min.

6. With proper initial calibration to meet the static error requirement as stated above, any position error beyond that specified as conformity of the potentiometer, ±1 arc min, will be reduced to zero because of integral control. Steady-state repeatability in this type of control system, cannot be greater than the steady-state position error.

7. In order to meet the resolution requirement of ± 5 arc min, the position transducer potentiometer of infinite resolution is chosen.A digital command signal from the computer is converted to an analog signal by a 12-bit D/A converter, the command signal resolution being less than an arc min when referenced to the carrier model pitch motion.

8. The dynamic range, the ratio of maximum velocity to minimum velocity of 500:1 can be met by the choice of a high quality dc motor and tachometer, by minimizing friction and by direct driving or by using anti-backlash gears of low gear ratio. In this case, the pitch assembly is driven by the motor-trachometer potentiometer system by 33:1 anti-backlash gear.

9. The reduced transfer function indicates that this servo is designed to be of type 1 system. As shown in the general analysis, the velocity error coefficient is finite. This implies that the servo follows ramp input of the form t'u(f) with finite steady steady-state error. With a bandwidth of 17 Hz, and phase margin of 74°, the velocity error constant is approximately 75 with tracking error less than 0.1° when referenced to the pitch motion of model board.

The stability analysis is illustrated on the pitch servo frequency-gain plot, Figure 16. The criteria used for stability are as follows:

- To keep the phase margin greater than 40°
- To shape the slope of the frequency-gain curve to 20 dB/decade at and around the decade crossover frequency
- To reduce the gain sharply at high frequencies.

Inherent zeros and poles plotted on the frequency-gain curve are defined in Table 7. The phase margin ϕ_{PM} should be at least 40° for the system to be relatively stable. Phase margin is defined as

$$\phi_{PM} = 180 - \sum \text{phase lags and leads in the system.}$$

Phase lags:	Integral control $(\frac{1}{s})$:	90°
	Mechanical time constant (τ_{MJ}):	84°
	Electrical time constant (τ_C):	13°
	Power Amplifier time constant (τ_A):	1°
Phase leads:	Tachometer zero (τ_Z):	-84°
Net contribution:		104.0

Phase margin: $\phi_{PM} = 180° - 104 = 76°$

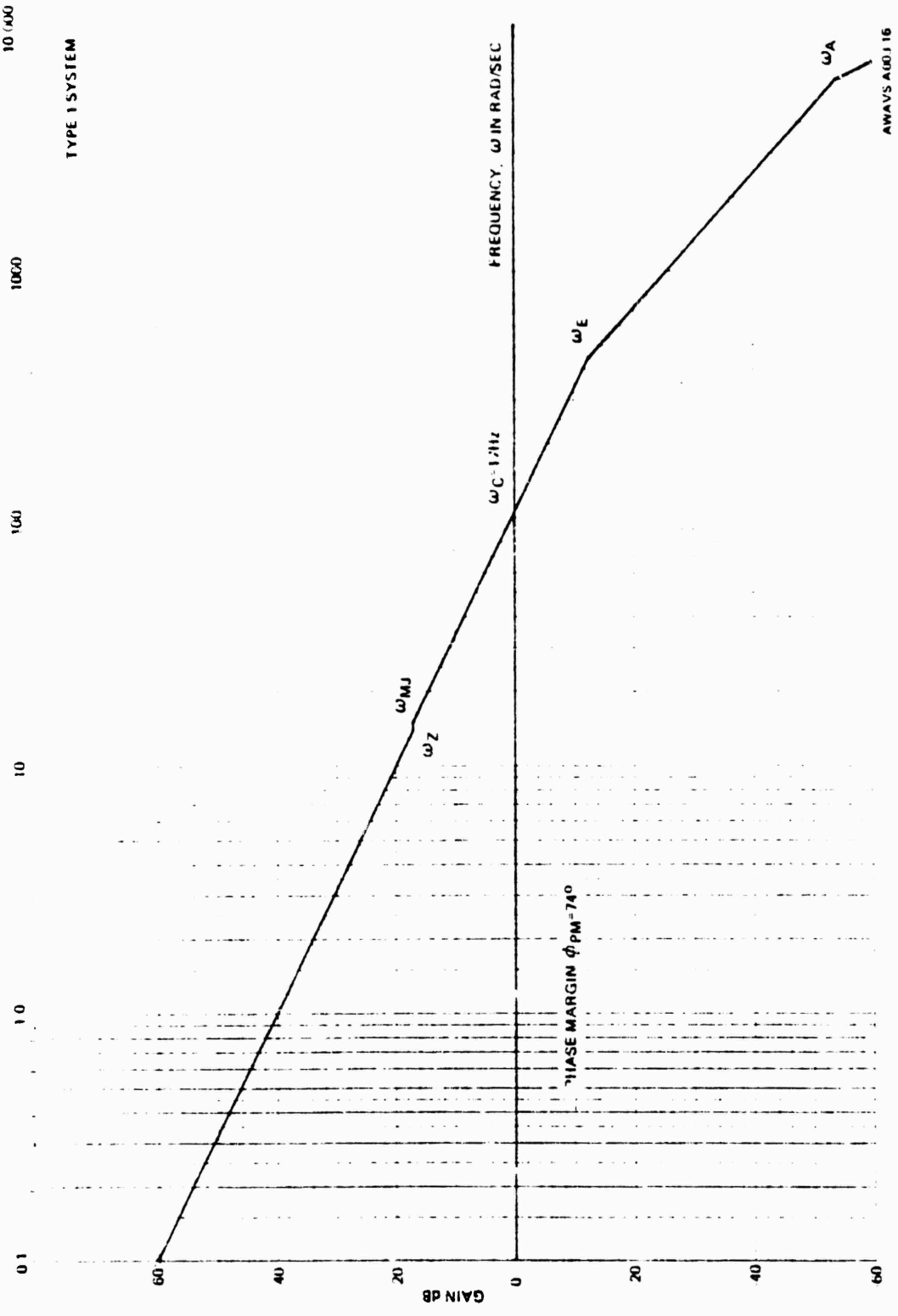

Figure 16. Frequency-Gain Plot For Carrier Model Pitch Servo

This insures excellent stability. However,the compensation card has several adjustable features which if necessary can be used to shape the signal. In fact, τ_{MJ} is estimated and τ_Z is adjustable by tachometer gain adjustment.

TABLE 7. INHERENT ZEROS & POLES FOR CARRIER MODEL PITCH SERVO

ω_L	Zero	Tachometer & Pot	$\frac{K_P}{K_G}$	13.6.rad/sec
ω_{MJ}	Pole 1	Motor & Load	$\frac{K_T K_B}{RJ}$	14.8 rad/sec
ω_E	Pole 2	Motor	$\frac{L}{R}$	455 rad/sec
ω_A	Pole 3	Power Amplifier	Bandwidth	6000 rad/sec

3.1.1.4.5 Design Analysis of Carrier Model Heave Servo (Z_{CM}). The performance specification of carrier model heave servo (Z_{CM}) is given in Table 8.

TABLE 8. CARRIER MODEL HEAVE SERVO PERFORMANCE

1.	Excursion	±0.973"
2.	Velocity (Maximum)	0.61"/sec
3.	Acceleration	0.38"/sec^2
4.	Static Accuracy	±5 mils
5.	Linearity	±5 mils
6.	Repeatability	±5 mils
7.	Resolution	±5 mils
8.	Dynamic Range	500:1
9.	Tracking accuracy at velocity (High) velocity (Low)	 0.1" 0.05"
10.	Period of Oscillation	10 sec

The carrier model heave servo (H_{MRDL}) is synthesized as follows to meet the performance specification parameters 1 through 9:

1. The mechanical sketch indicates a possible excursion of ±973" for the heave assembly.

2. Dc torque motor is capable of no load speed of 1275°/sec ,and tachometer has a maximum operating speed of 1555°/sec.

3. The dc torquer can generate a peak torque of 10 lb-ft. The estimated inertia of azimuth assembly is 6 oz in sec^2. The possible acceleration limit is 10^6°/sec^2. There is ample allowance for disturbing torque of 1-lb ft.

4. As described in paragraph 3.1.1.4.1, the static position error for this noncontinuous position servo emanates from the conformily specification of the position feedback potentiometer. The static position error could, at most, be ±2 mils.

5. The principle of the linear servo is to drive the control element by amplifying the actuating signal error. All components of this system are linear,and the linearity of position transducer potentiometer is specified to ±1 arc min.

6. With proper initial calibration to meet the static error requirement as stated above, any position error beyond that specified as conformity of the potentiometer, ±1 arc min,will be reduced to zero because of integral control. Steady-state repeatability in this type of control system cannot be greater than the steady-state position error.

7. In order to meet the resolution requirement of ±5 mils, the position transducer potentiometer of infinite resolution is chosen. A digital command signal from the computer is converted to an analog signal by a 12-bit D/A converter, the command signal resolution being less than one mil when referenced to carrier heave motion.

8. The dynamic range, the ratio of maximum velocity to minimum velocity, of 500:1 can be met by the choice of a high quality dc motor and tachometer, by minimizing friction,and by direct driving or by using anti-backlash gears of low gear ratio. In this case, the heave assembly is driven directly by the motor-tachometer potentiometer system through rack and pinion arrangement.

9. The reduced transfer function indicates that this servo is designed to be of type 1 system. As shown in the analysis, the velocity error coefficient is finite. This implies that the servo follows ramp input of the form t'u(f) with finite steady-state error. With a bandwidth of 18 Hz, and phase margin of 74°, the velocity error constant is approximately 78 with a tracking error of 0.7°,which translates to less than a mil in heave motion.

The stability analysis is shown on the frequency-gain plot (See Figure 17.) The criteria used for stability are: to keep the phase margin more than 40°, shape the slope of the gain-frequency curve at and around (a decade) crossover frequency to be 20 db/decade, and reduce gain sharply at high frequencies. Inherent zeros and poles plotted on Figure 17 are defined in Table 9. The phase margin Φ_{PM} should be at least 40° for the system to be relatively stable. Phase margin is defined as

$$\Phi_{PM} = 180 - \sum \text{Phase lags and leads in the system}$$

Phase lags:	Integral control $(\frac{1}{s})$:	90°
	Mechanical time constant (τ_{MJ}):	83°
	Electrical time constant (τ_C):	13°
	Power Amplifier time constant (τ_A):	1°
Phase leads:	Tachometer zero (τ_Z):	-81°
Net contribution :		106.0

Phase margin: $\Phi_{PM} = 180° - 106 = 74°$

This insures excellent stability. However, the compensation card has several adjustable features which if necessary can be used to shape the signal. In fact, τ_{MJ} is estimated and τ_Z is adjustable by tachometer gain adjustment.

TABLE 9. INHERENT ZEROS & POLES FOR CARRIER MODEL HEAVE SERVO

ω_L	Zero	Tachometer & Pot	$\frac{K_P}{K_G}$	1.2 rad/sec
ω_{MJ}	Pole 1	Motor & Load	$\frac{K_T K_B}{RJ}$	16 rad/sec
ω_E	Pole 2	Motor	$\frac{L}{R}$	455 rad/sec
ω_A	Pole 3	Power Amplifier	Bandwidth	6000 rad/sec

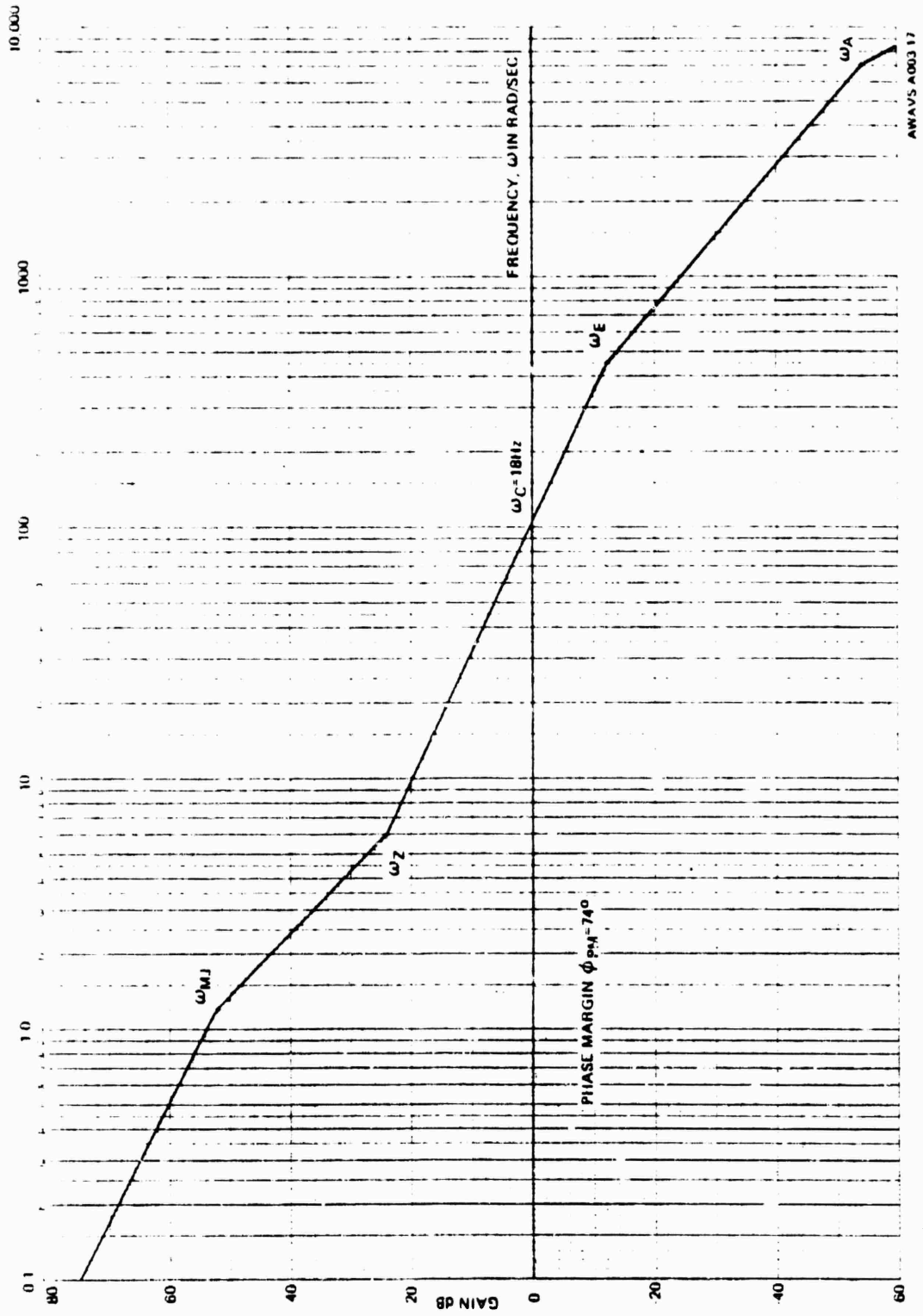

Figure 17. Frequency-Gain Plot For Carrier Model Heave Servo

3.1.1.5 Model Support Structure. The model support structure is constructed with sufficient rigidity to adequately support the several elements of the model board and maintain model alignment during operation. The model support structure consists of five trussed frames bolted to the floor of the facility and linked horizontally by a series of steel angle beams. Lateral stiffness is obtained from the installation of diagonal ties bolted between truss frames. Of the bays thus formed, two are employed to attach and support the model board assembly, the extreme right-hand bay being clear for installation of the double-bay interface cabinet and for gantry maintenance purposes. Spanning the top of the truss frames is the upper X-axis guide rail and its associated mounting structure.

The basic structural element is a plane truss fabricated from welded square structural steel tubing. A series of square steel plates welded to the front vertical face provides for attachment of the horizontal angles spanning each truss and also for model panel corner bolt-down points. A similar plate welded at the center of the linking horizontal member also furnishes a bolting point approximately in the center of upper and lower edges of the model panel. Oversize holes and large washers at these points allow for liberal adjustment of individual model panels.

3.1.1.6 Maintenance Panel Interface. Manual operation of the carrier lights and carrier model servos for test purposes is made possible through a link with the gantry maintenance panel. (See Figure 43.) For manual operation, the SYS CONT key switch on the gantry maintenance panel must be set to TEST. The DROP LINE LIGHT INTEN and DECKEDGE LIGHT INTEN potentiometers each control a dc drive voltage to the respective set of carrier lights. The LIGHT BOX INTENSITY potentiometer controls the voltage drive for the two light boxes which supply illumination for runway edge, runway athwartships, and runway centerline lights. The STROBE RATE potentiometer controls the voltage drive to the carrier strobe servo which, in turn, varies speed of the motor responsible for the runway centerline strobe simulation. The MODEL BOARD CONTROL STROBE switch is on alternate action pushbutton device that controls the on/off function of the runway centerline strobe simulation.

The CARRIER SERVOS MANUAL CONTROL device provide a means of manually operating the carrier servos and controlling direction of travel as well as velocity. A similar group of three controls governs the operation of each servo (pitch, roll, and heave). The RUN/STOP switches are alternate action pushbutton devices to start and stop their respective servos. Each RUN/STOP pushbutton lights to indicate its selected position. The velocity control knob sets the direction of travel as well as the velocity of the servo. Velocity is zero when the control is centered and increases as it is moved toward either extreme. A limit indicator device lights to indicate when its respective servo has been driven to an end limit condition (UP or DOWN for PITCH and HEAVE: CW or CCW for ROLL).

3.1.2 Target Model Illumination. The function of the model illumination subsystem is to illuminate the carrier model and wake so that the probe has sufficient signal for adequate pickup. Primary illumination is from the light bank assembly which is located behind the gantry tower and aimed at the model board. Fill-in lighting is provided by nine No. 2 reflector photoflood lamps mounted on the Z-axis assembly. These eliminate the shadow of the gantry tower on the model board. Subsequent paragraphs provide a subsystem description and block diagram. Paragraph 3.1.2.1 describes the analysis used in determination of the final design, while paragraph 3.1.2.2 gives configuration information on the lamp bank assembly.

A block diagram of the primary target illumination subsystem is given in Figure 18. As shown, primary power is provided by the facility three phase 277/480 V supply to the power control circuitry on the light bank assembly. Time-of-day simulation (day, dusk, night) is normally controlled from the Experimenter/Operator Station via the linkage. For maintenance purposes, however, manual control is possible from the maintenance panel located in the gantry cabinet.

Day is simulated by having all 32 lamps on; dusk by extinguishing 16, leaving alternate lamps on; and night by turning all lamps off. If the system is changed from day to night and then immediately back to day, it will be 19 minutes before full daylight level is achieved. When this sequence of lamps on to lamps off and then immediately back to lamps on (i.e., day-night-day, day-night-dusk, dusk-night-day, dusk-night-dusk; or day-dusk-day) is performed, a timer keeps the voltage from being reapplied for 10 minutes after the initial turnoff. This is to prevent wear on the lamp and also to slightly shorten the reignition time since the starter arc would reappear after five minutes if voltage were reapplied immediately, and the heat from this arc would keep the lamp pressure up which would, in turn, lengthen main arc reignition time.

The lamp fixture is a wide-angle NEMA 6 fixture with a beam spread of 110.5° horizontal by 105.8° vertical. This wide-angle distribution (Figure 19) was chosen in order to avoid any hot spots when half the lamps were turned off for dusk. The fixture itself is composed of a parabolic shaped reflector formed from high purity reflector grade aluminum. In addition, there is a clear thermal shock and impact resistant front glass which is gasketed in a stainless steel hinged door frame. This front glass protects the lamp from external damage and is designed to contain lamp explosions. In addition, this glass helps absorb ultraviolet light from the lamp.

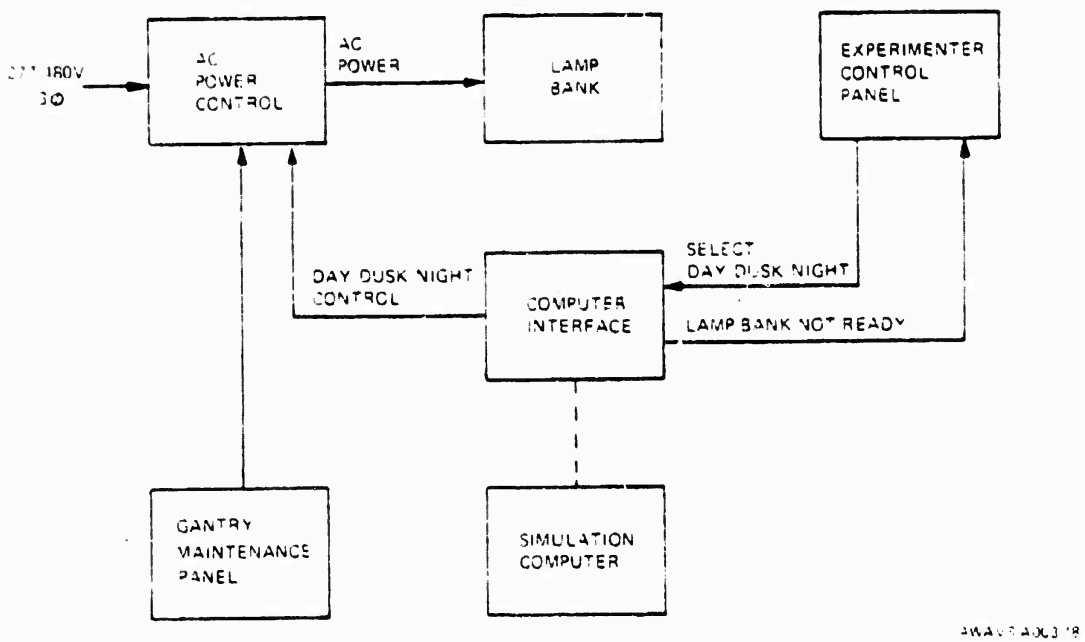

Figure 18. Target Model Illumination, Block Diagram

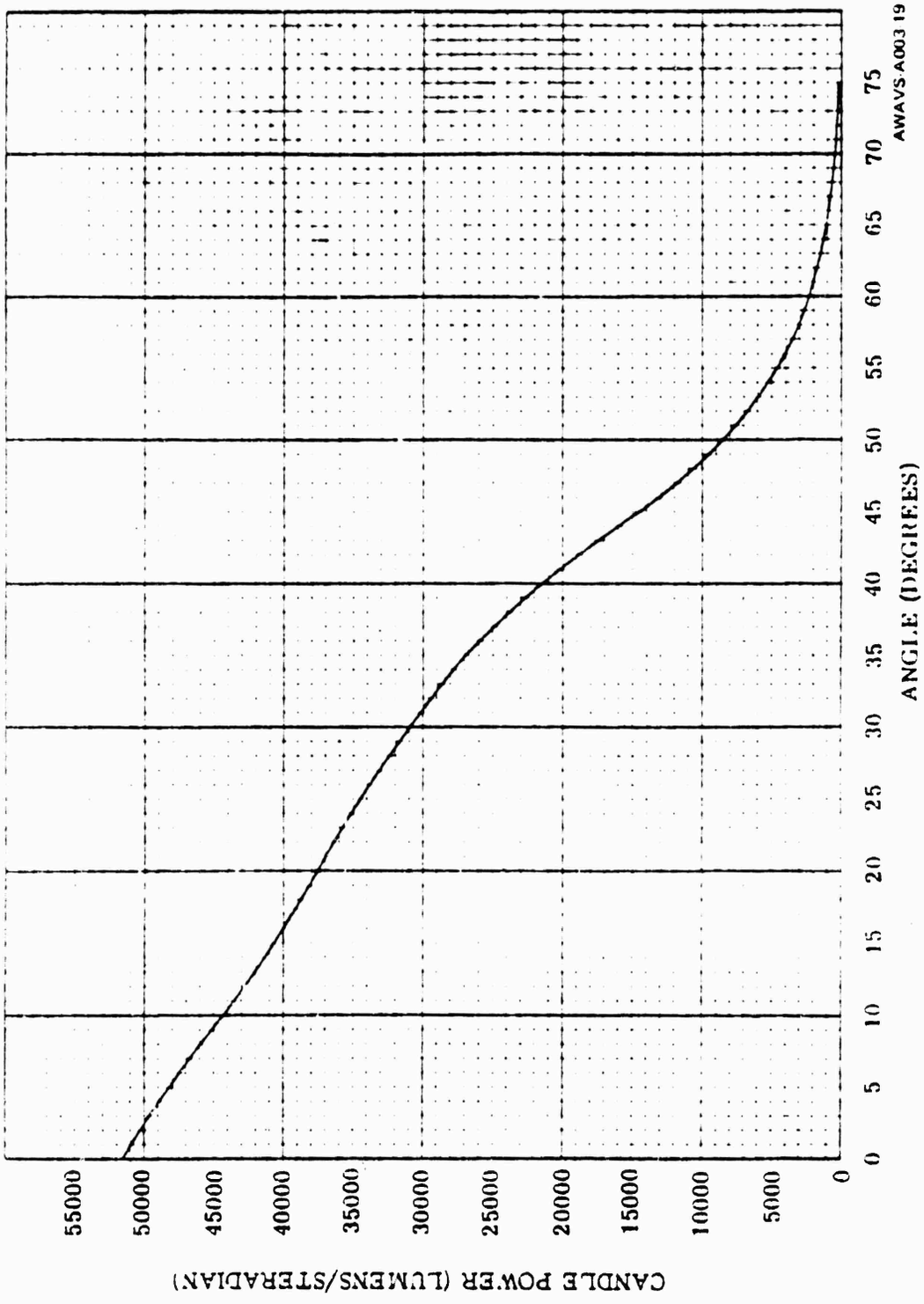

Figure 19. NEMA 6 Fixture Beamspread

The ballasts for the lamps are constant wattage autotransformers (CWA) which require a 277 VAC input. Each ballast lamp combination draws approximately 4.1 amperes and therefore requires approximately 1135.7 volt-amperes. Each ballast-lamp combination draws 1080 watts indicating the ballast is efficient (80 watts loss) and has a high power factor. The starting current for these ballasts does not exceed the running current and they permit only a 10% change in lamp watts for a 10% change in input voltage. The output waveform from these ballasts is of the lead-peaked type which is needed for reliable starting of the metal halide lamps.

The lamps supplied with the system are 1000-watt Sylvania Metalarc lamps, model number M1000/BU-HOR. These lamps are made to operate in any burning position from base vertical up to base horizontal. In the horizontal position (or within 60° of horizontal) they must be operated only in totally enclosed fixtures because of an infrequent occasion in which the lamps fail by explosion in this position. Figure 20 shows the construction of a typical lamp.

The inner tube is a quartz arc tube containing argon gas and mercury plus thorium iodide, sodium iodide, and scandium iodide. The ends of the arc tube have a heat retention coating that raises the temperature of the ends during operation, thus assuring adequate evaporation of the metal iodides. In addition to the two main electrodes there is a starting electrode which eliminates the need for a high starting voltage. This starting electrode is close enough to one of the main electrodes that the normal initial voltage output of the ballast will cause an arc to strike between the two. As the ions produced by this starting arc circulate to the space between the two main electrodes the main arc strikes. When enough heat builds up in this main arc the bi-metal switch shorts the starting electrode to the adjacent main electrode and stops the starting arc. Normal warmup time to full brightness is five minutes. If the power is interrupted it will be approximately 14 minutes before the lamp will reignite. This is because the pressure in the arc tube has to drop before reignition will occur. Also, the bi-metal swtich has to open but this occurs long before the pressure drops sufficiently. After reignition the standard warmup time (five minutes) applies.

3.1.2.1 Model Illumination Analysis. Since it is only necessary to illuminate the carrier model and painted wake as opposed to the entire 24 square foot model board, the number of lamps in the lamp bank assembly has been reduced to 32. All lights are pointed straight ahead rather than being directed toward the carrier model. This fact and the unused light mounting facilities around the perimeter of the light bank assembly allow for future expansion of the lighting system, as required by the specification, to illuminate the whole 24 square foot model board.

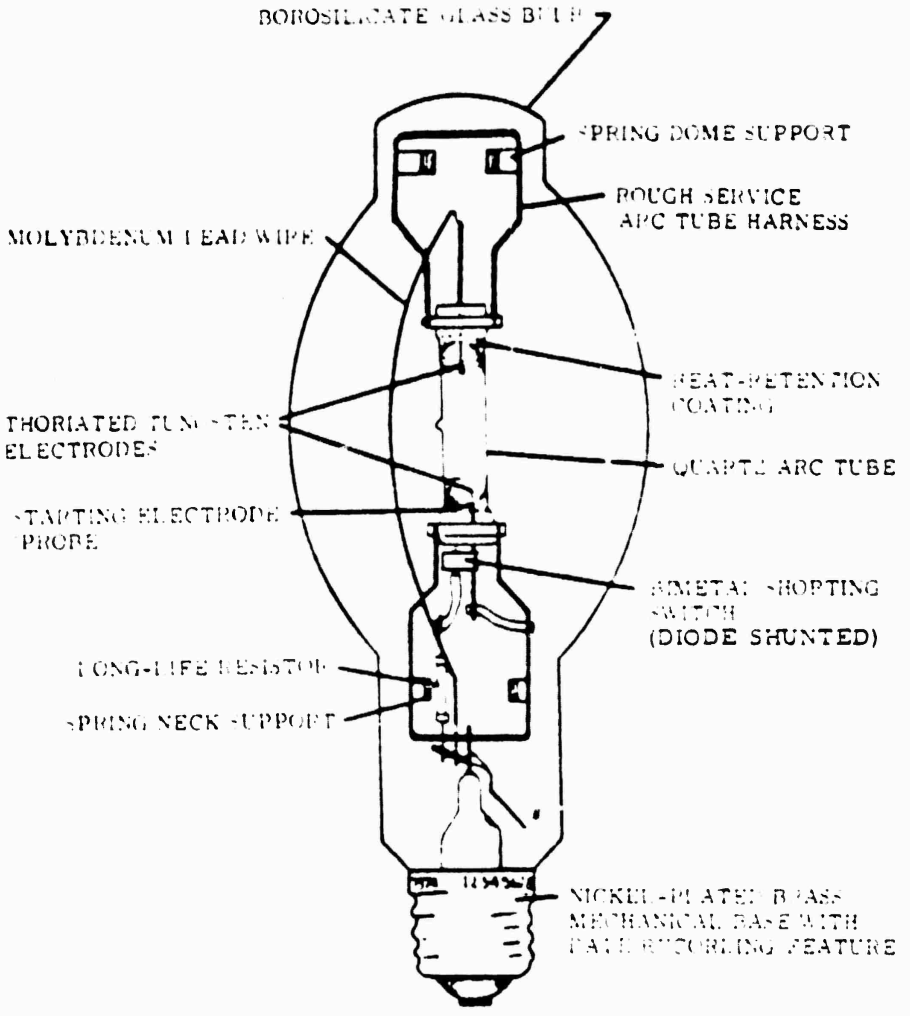

NOTE

THIS FIGURE SHOWS CONSTRUCTION OF A 400-WATT, BASE-UP BURNING METALARC LAMP. THE 100-WATT LAMP IS SIMILAR EXCEPT FOR THE ADDITION OF A DIODE ACROSS THE BIMETAL SWITCH.

AWAVS A003-20

Figure 20. Metalarc Lamp Construction

The f/number of the probe is 39.97 and remains constant with zoom. The probe transmission is 32%. This accounts for the loss of light going to the camera, due to the presence of the spectrally selective beamsplitter, that must be inserted between the probe and the camera to provide light for the FLOLS position sensing detector. Part of the light coming from the probe will be split off from the camera bundle with this spectrally selective beamplitter, and then will be sent through a narrow bandpass filter before going onto the position detector. Because of insufficient information at this time as to the spectral and absorption characteristics of the beamsplitter and bypass filter and as to the requirements of the position detector, it cannot be determined at this time exactly how much the position detector will affect the lighting requirements. However, it is estimated that the detector will increase the lighting requirements by no more than a factor of two. To compute the new illumination required on the carrier model, the following formula is used:

$$I_m = \frac{4 I_i N^2 F}{R T M}$$

Where:

- I_m = Illumination required on the carrier model
- I_i = Illumination required on the camera tube faceplate = 0.074 foot candles for a highlight signal current of 0.75 μa at an 825 television line rate
- N = f/No. = 39.97
- F = Estimated factor to account for light loss due to the beamsplitter needed for the position detector = 2
- R = Average highlight reflectance of the carrier model = 0.60
- T = Probe transmission = 0.32
- M = Maintenance factor to allow for lamp and camera tube aging = 0.8

Using these numbers, the carrier initial illumination requirement (I_m) is 6160 foot-candles.

$$I_m(13,y,z) = \sum_{i=1}^{n} \frac{c(\theta_i) \times \cos \theta_i}{R_i^2}$$

Where: $I_m(13,y,z)$ = Total illumination on the model (in foot-candles) at the point P with coordinates (13,y,z). The 13 is the approximate x value for all points on the model; i.e., the model is 13 feet from the lighting board and parallel to it. The lighting board is the same size as the model board.

θ_i = Angle between the normal to the i^{th} lamp and the line from the i^{th} lamp to the point P

$c(\theta_i)$ = Candlepower (lumens/steradian) of the fixture as a function of angle

R_i = Distance from the i^{th} lamp to the point P in feet

n = Number of lamps on the lighting board

These variables are shown in Figure 21.

From this program, it was determined that 32 1000-watt metal halide lamps in fixtures with a NEMA-5 distribution will provide sufficient illumination. These lights will be arranged in an 8 x 4 matrix with a 2-foot horizontal by 4-foot vertical spacing. These 32 lights will uniformaly illuminate only the carrier and and its wake, and these 32 lights will be the only ones supplied by Singer-SPD with the system. If the lighting were expanded in the future to illuminate the whole 24 ft x 24 ft model board, an additional 50 lights (same type) would be required for a total of 82 lights in the lighting bank. Figure 22 shows the configuration of both the initial lighting system (32 lights) and the expanded system (82 lights).

Figure 22 also shows illumination levels for both the initial and expanded systems. In the expanded system, the illumination at the corner point would be only 30% of the highest illumination point on the model. However, these calculations do not take into account the contributions from any reflectorized scene extenders that could be added for future expansion. Also, at a point 2 feet up and 1 foot over from the corner, the illumination would be already up to 50% even without scene extenders. The highest illumination point in the expanded system would be 7850 foot-candles.

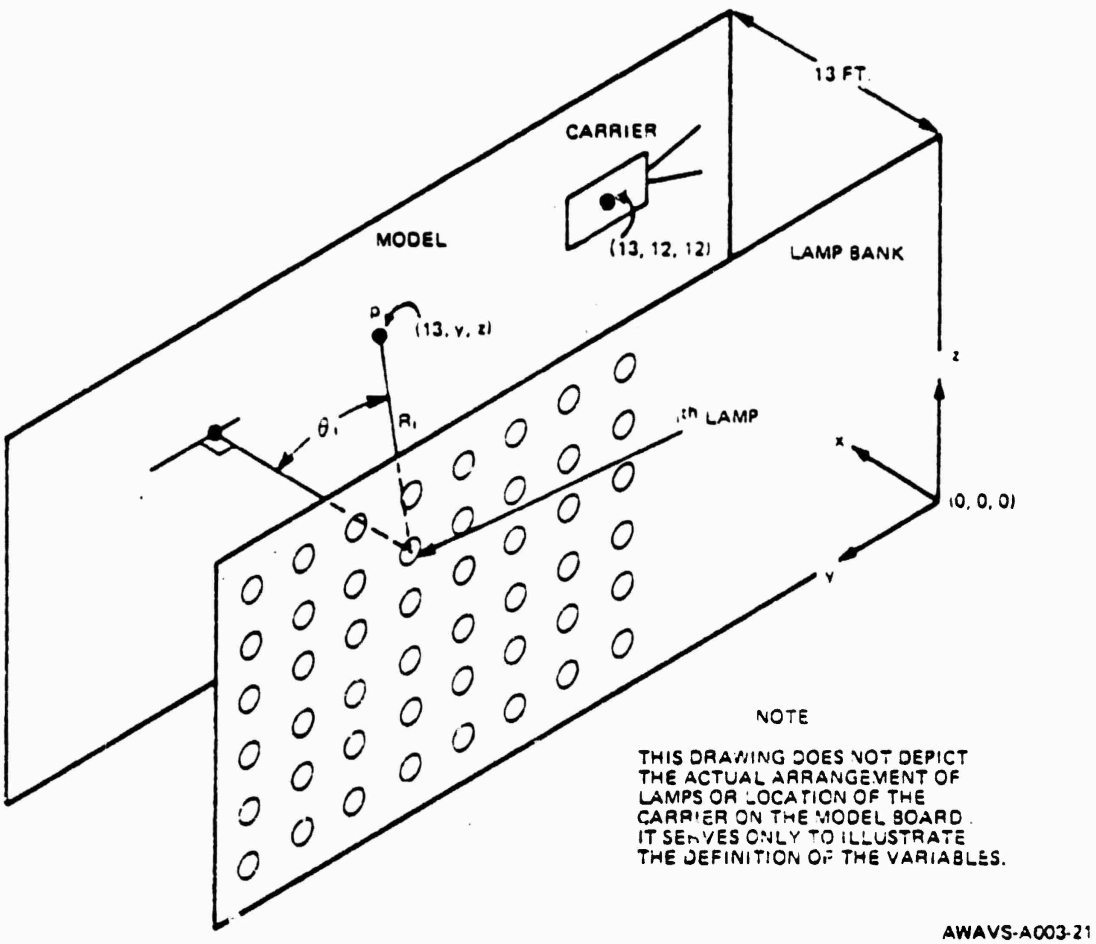

Figure 21. Definition of Variables for Illumination Program

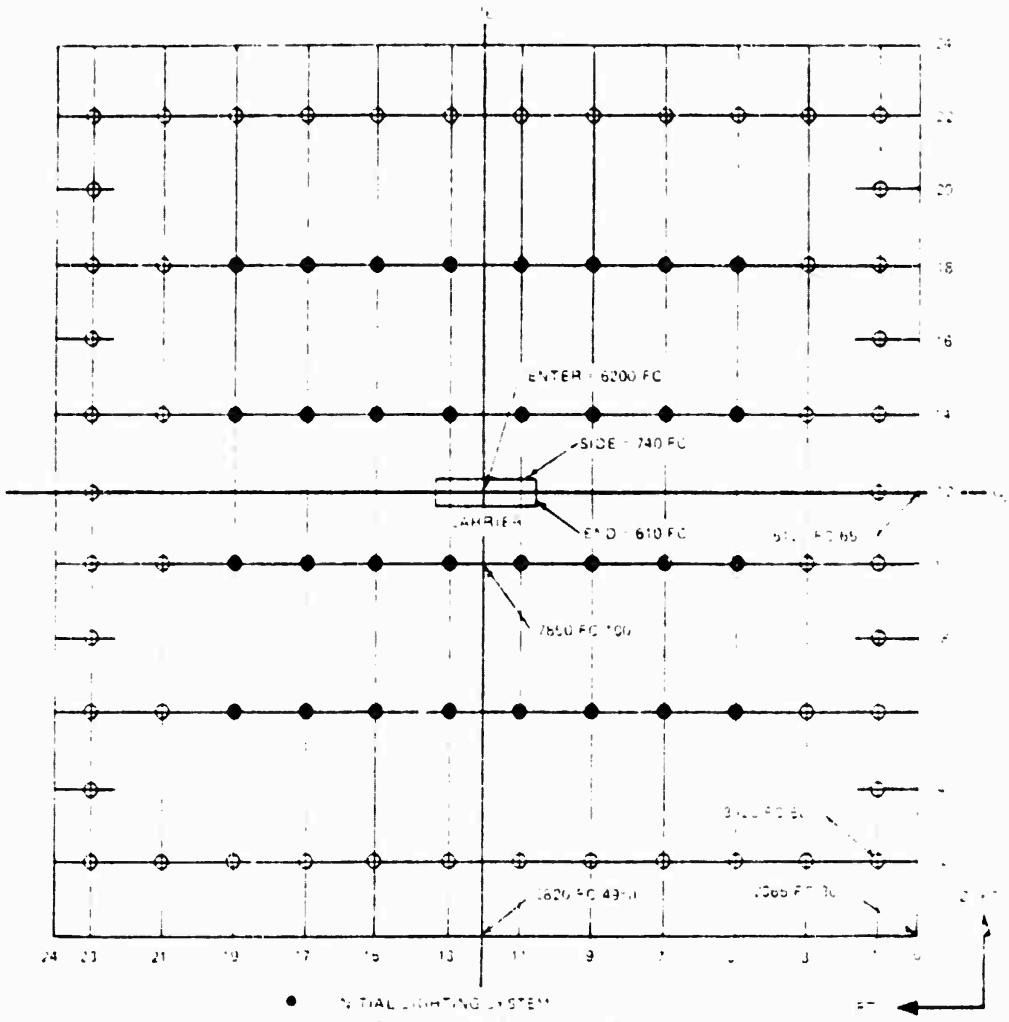

● INITIAL LIGHTING SYSTEM

+ LIGHTS ADDED FOR EXPANDED SYSTEM

NOTES

1. NUMBERS IN PARENTHESES INDICATE ILLUMINATION LEVEL AT INDICATED POINT AFTER EXTRA LIGHTS HAVE BEEN ADDED FOR THE EXPANDED SYSTEM. THE PERCENTAGE INDICATES THE PERCENTAGE OF HIGHEST ILLUMINATION LEVEL SHOWN.
2. NUMBERS WITHOUT PARENTHESES LABELED CENTER, SIDE, AND END INDICATE ILLUMINATION WITH INITIAL SYSTEM BEFORE IT IS EXPANDED.
3. ALL INDICATED ILLUMINATION LEVELS DO NOT TAKE INTO ACCOUNT CONTRIBUTIONS FROM REFLECTION OFF SCENE EXTENDERS WHICH COULD BE ADDED BY NTEC IN THE FUTURE.
4. ALL ILLUMINATION LEVELS ARE WITH NEW LAMPS. THE LAMPS DECREASE IN LIGHT OUTPUT WITH AGE.

AWAVS A005.22

Figure 22. Illumination Levels

In the initial lighting system, the illumination at the center of the carrier model will be approximately 6200 foot-candles with a negligible fall off to the corners of the carrier. This illumination level and the levels discussed below are with new lamps. The initial illumination on the sides of the carrier will be 610 foot-candles on the two short sides (ends), and 740 foot-candles on the two long sides. If the sides of the ship were painted a normal battleship gray of approximately 19.5% reflectance, this means that only 119 foot-lamberts would come off the short side. If the average highlight of 60% were located at the center of the ship, then 3720 foot-lamberts would be reflected at this point. This would mean a contrast ratio of 3720:119 ≈ 31:1, and the blacks would be too black for reliable scene keying in the visual display. In order to avoid this problem, the sides of the ship have been painted with a 90% white so that the short side reflects 549 foot-lamberts, yielding a contrast ratio of 3720:549 ≈ 6.8:1 from the carrier model.

This contrast ratio must be raised to a power equal to the target camera/projector system gamma in order to calculate the contrast ratio on the display screen. At this point, a final determination has not been made as to what this system gamma will be. Therefore, in order to continue the carrier model analysis, an assumption of the final system gamma will have to be made. It will be assumed that the system gamma will be 1.35.

3.1.2.2 Light Bank Assembly. The light bank assembly provides a rigid mounting for the 32 Metalarc lamps used to provide the required level of illumination of the surface of the carrier model. It also provides mounting facilities for the lamp ballasts and incorporates cable raceways to distribute power throughout the structure.

A modular, building-block approach is utilized to yield the straightforward, cost-effective assembly. Each modular structural element of the assembly provides the means to mount the required number of lamps and their associated ballast units, together with the necessary power distribution cable conduit. The structural elements are bolted to each other and to the facility floor to form an assembly 56 feet long by 26 feet, nine inches in height. An electrical junction box positioned at one end of the structure and distribution conduit laid horizontally within the assembled structure furnishes power to each modular element. Relays in the junction box distribute the 440 volt, 3 phase dc input to two circuits of 16 lamps each. With both circuits on, daytime is simulated. With only one circuit on, dusk is simulated. Simulation of night is accomplished by turning all lamps off. Figure 23 is a diagram of the light bank assembly designating lamp usage for day and dusk simulation.

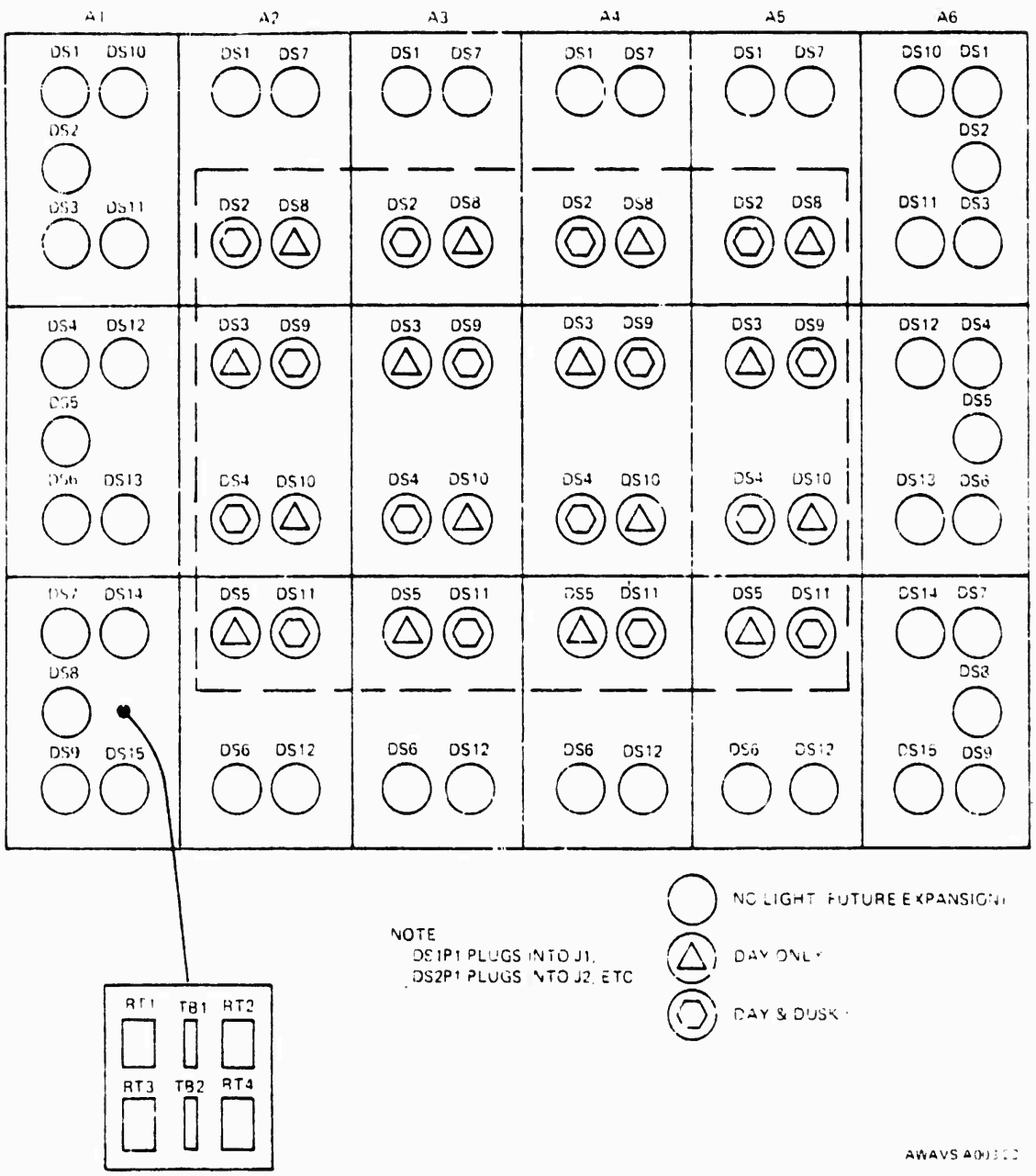

Figure 23. Light Bank Assembly, Layout Diagram

The modular structural element, shown in detail in SPD Drawing 2044520 is a welded steel space frame of triangular prismatic configuration. The three vertical members form the vertices of the traingular cross section and are of square structural steel tubing. all horizontal struts are of structural steel angle and floor mounting brackets are welded to the base of the vertical members.

Individual lamp assemblies are supplied in a U-shaped bracket bolted rigidly to either front side of the central main vertical member. Electrical conduit, furnished with outlets at each lamp level, is attached to both rear faces of this member and serves to connect each lamp with its appropriate ballast unit at the base. These units are mounted to heavy gauge panels attached to each rear face of the lowest bay.

The front face of the structure, four feet in width, is covered almost in its entirety with light gauge reflector panels (three per module) through which each lamp projects a sufficient distance to allow for hinging of the front transparent cover when replacing lamp elements.

3.1.2.3 Maintenance Panel Interface. The LT BANK CONT devices on the gantry cabinet test panel, Figure 43, may be used to operate the light bank when performing maintenance. For this type of operation, the SYS CONT key switch on the test panel must be set to TEST. The DAY/DUSK/NIGHT control selects whether all, half, or none (respectively) of the lamps should be lit when the ENABLE button is depressed. The ENABLE pushbutton switch is a momentary contact device which sets the lamp bank for the time-of-day simulation selected by the DAY/DUSK/NIGHT control. This configuration permits the high switching currents to run through the test panel for the shortest possible length of time.

3.1.3 Optical Probe System. The optical probe system is the servo-operated camera pick-up for the target image generator. As shown in the block diagram, Figure 24, it encompasses the optical probe, a laser light source, and a closed-loop probe position system known as the FLOLS tracker. The loop consists of the FLOLS tracker optics and electronics, the computer linkage which is part of the VTFS, and the optical probe signal interface, electronics, and probe drive servos. In simple terms, the tracker optics separates the laser image from the carrier and wake image and relays the laser image to the tracker electronics. The electronics form the X and Y correction terms used to modify the computer commands for probe positioning. The signal interface transforms the digital output from the computer into an analog drive signal which is used by the probe electronics to form the five dc motion commands for the servos. Stability is enhanced by a position feedback signal to the computer from each servo. The probe can also be operated manually from the gantry cabinet maintenance panel.

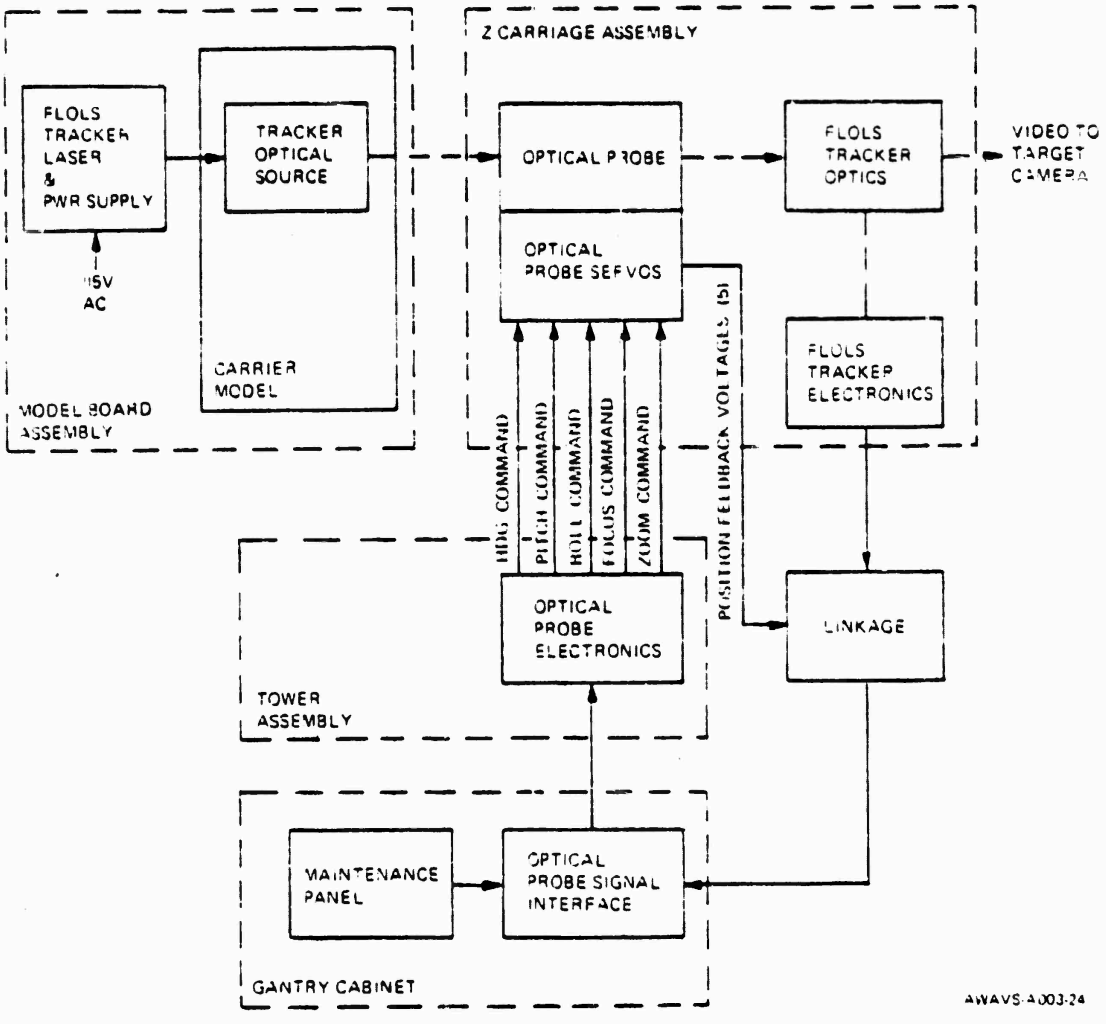

Figure 24. Optical Probe System, Block Diagram

3.1.3.1 Target Optical Probe. The 60° zoom probe is designed and manufactured by the Farrand Optical Co., is a dynamic type, and views a fully illuminated three-dimensional aircraft carrier. It is part of a high resolution television camera visual system. It simulates all possible flight path approaches to and landings on the carrier. All associated cables and electronic chassis are provided to process signals received from the computer and drive the servos to commanded positions.

Figure 25 is an optical schematic of the probe assembly. It is comprised of a complete optical system, which corrects and transfers the slant range view to a focal plane with the entire field of view in focus. All aircraft attitude changes are achieved in the probe by servos that receive commands from a computer. The final image format produced by the probe corresponds to 31.3 mm dia = 60° field of view at a 1-to-1 magnification. However, with the zoom lens feature incorporated into the optical system, the image format is maintained but the magnification can be increased 4:1 = 16.4° FOV.

Figure 26 shows the mechanical configuration of the optical probe. The probe is a compact and totally enclosed unit weighing 100 lbs. All components are housed in a 10 x 10-inch cross section with an overall length of 54.265 inches from the flange mounting surface to its lowest point. The length from the flange mounting surface to the pitch axis (horizon) is 54.107 in. The difference of these two dimensions permits the pitch axis to be placed 0.158 inches (4 mm) above the model. The probe is canterlever mounted to the gantry structure, and has been structurally designed for a maximum deflection at the pitch end of 0.002 inches.

There are three main gimbal axes (pitch, roll and heading) which simulate the three degrees of freedom of the aircraft. They are servo driven and respond to resolver signals. To maintain proper focus, a servo driven focussing lens is positioned as a function of range as determined by the user from computer inputs. A servo driven zoom lens is incorporated into the system. It is located before the re-imaging lens assembly and provides the zoom capability of 1:1 to 4:1 changing the true field coverage of the camera from 60° to 16.4°. This servo also responds to computer inputs. A simple servo driven iris diaphragm is incorporated into the system. This servo is comprised of a motor and potentiometer. The drive electronics for this servo are not provided in the Farrand supplied chassis.

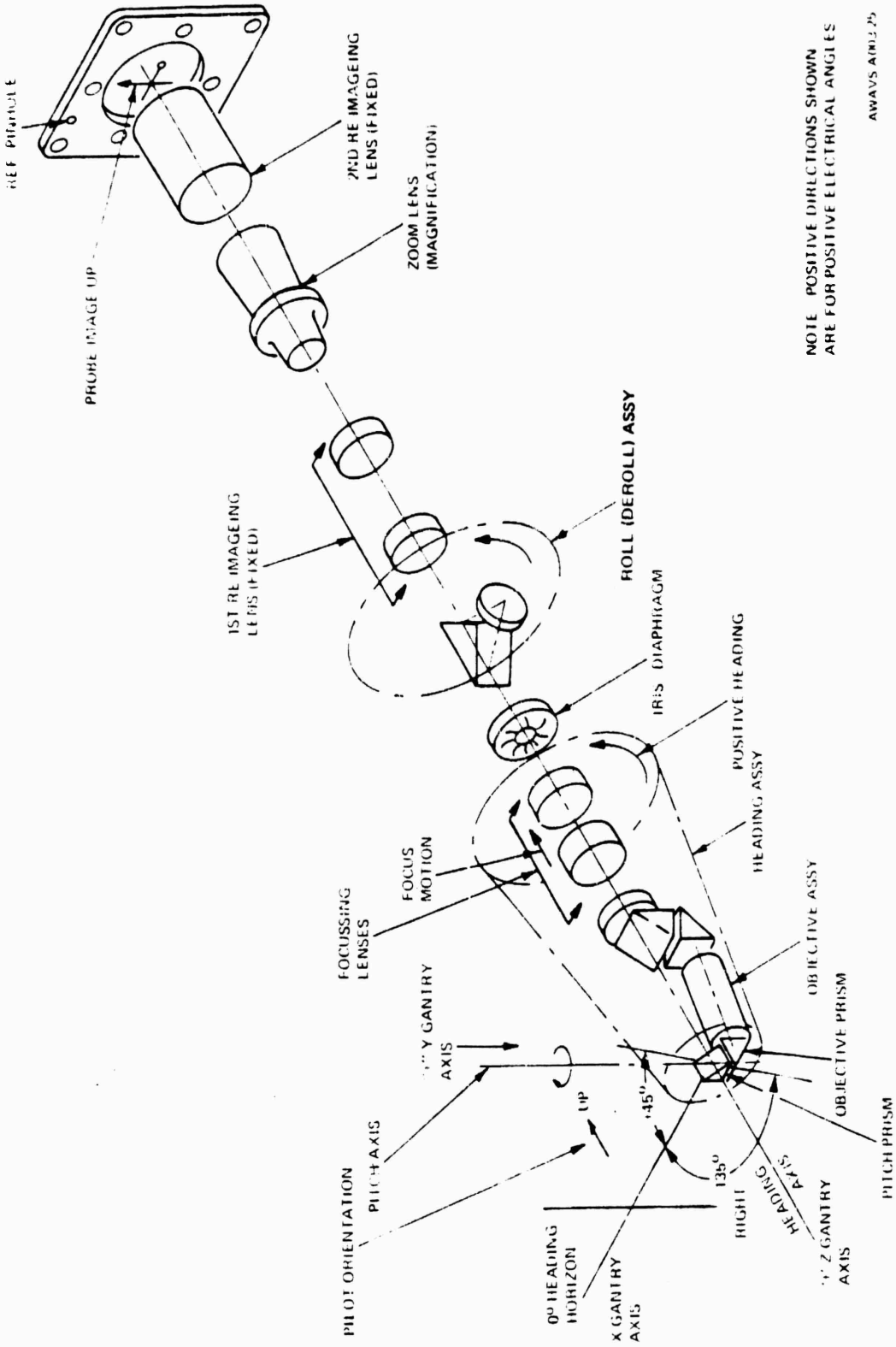

Figure 25. Probe Optical Schematic

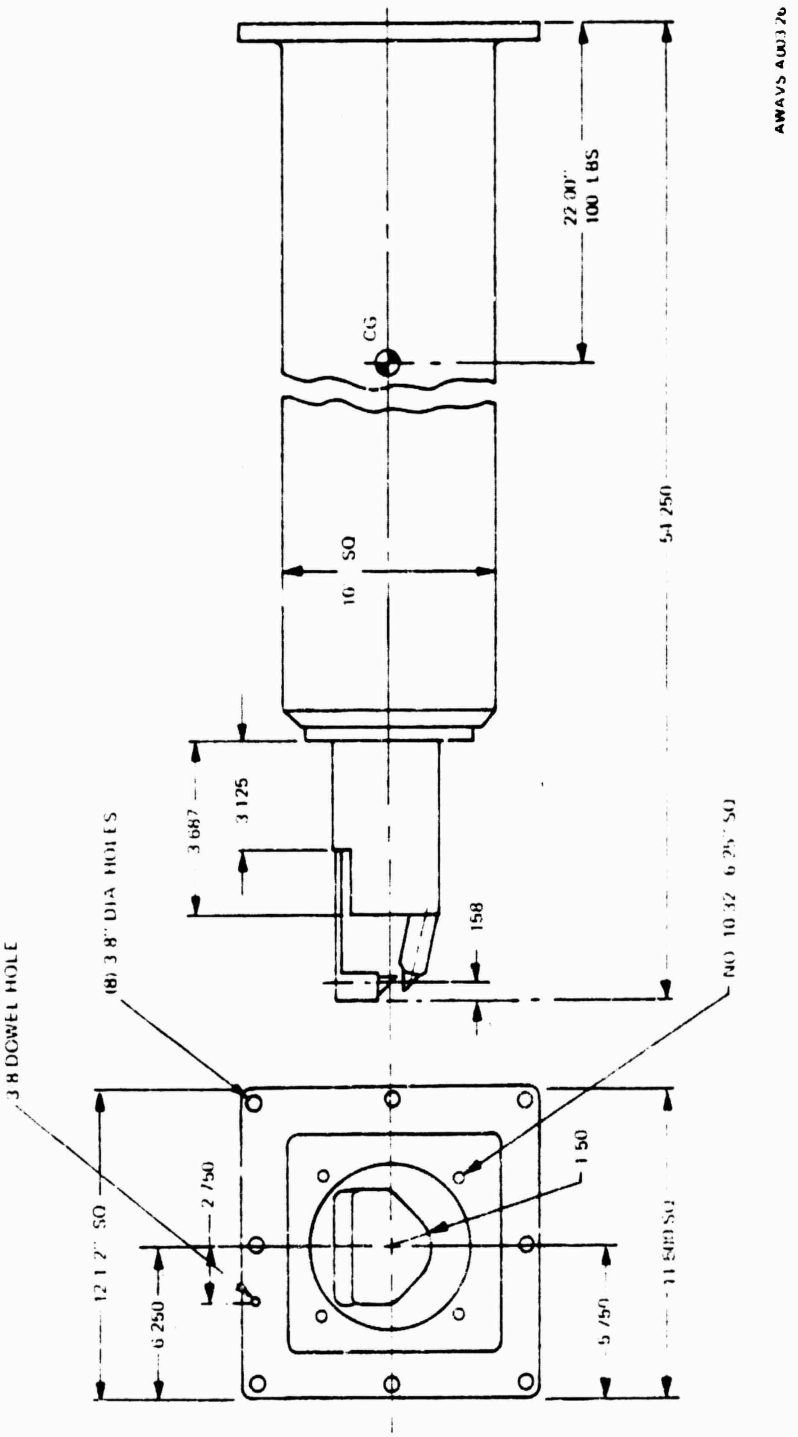

Figure 26. Probe Mechanical Configuration

The roll and heading drives are continuous in rotation, with resolvers geared to 4x LOS. The focus, zoom, pitch and iris diaphragm drives are limited in motion and contained within their limits by switches and mechanical stops. All servo drives except the iris and pitch drives are geared to a 1-speed potentiometer and dial, which indicates the position of the driven optical element. The window ports to observe the dials are located in the cover assembly with cover lids to shut out ambient light. The pitch dial is located at the heading end of the probe and can be observed through an open port, located in the front cover.

The power and signal inputs to the probe, crash sensors and blower are transmitted by means of four connectors (J1, J2, J3 and J4) located on the bottom side of the probe. Optical specifications of the probe are given in Table 10.

TABLE 10. OPTICAL PROBE CHARACTERISTICS

CHARACTERISTICS	VALUE
Transmission	40%
Pupil (entrance)	.7mm to 2.8
Geometric Transformation	±2%F Sin θ Mapping
Field of View	60° to 16.4 Circular
Clearance	4mm from pitch axis (at zero pitch)
Focal Plane	31.3mm
Focal Length	30mm to 240mm

3.1.3.2 FLOLS Tracker Loop Description. The function of the FLOLS tracking loop is to direct the probe's central axis at the point of interest (the FLOLS of the carrier) when the FLOLS is visible. This tracking assures that the FLOLS image and the carrier image register properly on the screen. The carrier image and the FLOLS image are combined optically in the projection system, with the FLOLS at a fixed point on the projector optics. The carrier image can be moved by moving the probe.

The FLOLS tracker system (Figure 27) consists of a laser beam originating at the FLOLS mounting position on the carrier model a and aimed at the probe. The laser beam is optically separated from the carrier image, and directed towards a two-dimensional self-scanned optical sensor array consisting of 2500 silicon photo diodes in a 50 x 50 array which is attached to the probe. A correction signal is obtained from the FLOLS tracker and is used to modify the computation of desired probe azimuth and elevation which is based on gantry axis components of the FLOLS reference point. The correction signal consists of the location of the laser beam on the self-scanned array. The FLOLS tracking system drives the probe such that the laser beam is at the center element of the array. The FLOLS tracker optics and laser light source is described in greater detail in paragraph 3.1.3.3 which follows.

3.1.3.3 FLOLS Tracker Optics. An optical schematic of the FLOLS laser and tracker system is given in Figure 28. The 5mw He Ne laser is relayed via an optical fiber (0.03" dia) to the carrier model. The fiber dispenses the laser light into a 4°V x 90°H cone. Both the laser signal and carrier signal enter the probe. Optical filters separate the laser signal from the background. The laser signal is imaged on a detector array that supplies information to the probe pitch and heading servos to correct pointing errors.

Elements of the FLOLS tracker optics which separate and relay the laser and carrier imagery are as follows:

a. Trimming Filter. A wide band filter that when used at a 45° angle of incidence transmits a 200° HBW centered about 6328°A. Its transmittance in this band is near 80%. Also, it reflects the remaining portion of the video spectrum. The front surface of the filter is used to eliminate any ghosts at the vidicon.

b. Spike Filter. Reduces the 300° band to 30° HBW to increase the signal-to-noise ratio. It has 50% transmittance at 6328°A.

c. Blow-up Lens. Provides the detector array with the necessary field-of-view. It is located at the probe's principle plane at 1:1 zoom.

d. Detector Array. Senses the laser signal.

e. Blocking Filter. Rejects any 6328°A light that may cause a bright spot at the vidicon. It transmits the visible spectrum from 4000 to 6100°A at an average of 80%.

f. Mirror. Directs light to the television camera.

3.1.3.4 FLOLS Tracker Analysis. The analysis which follows is subdivided into detector resolution, laser light calculation, and detector sensitivity discussions. The analysis is then summarized along with presentation of a tabular compilation of all tracking errors.

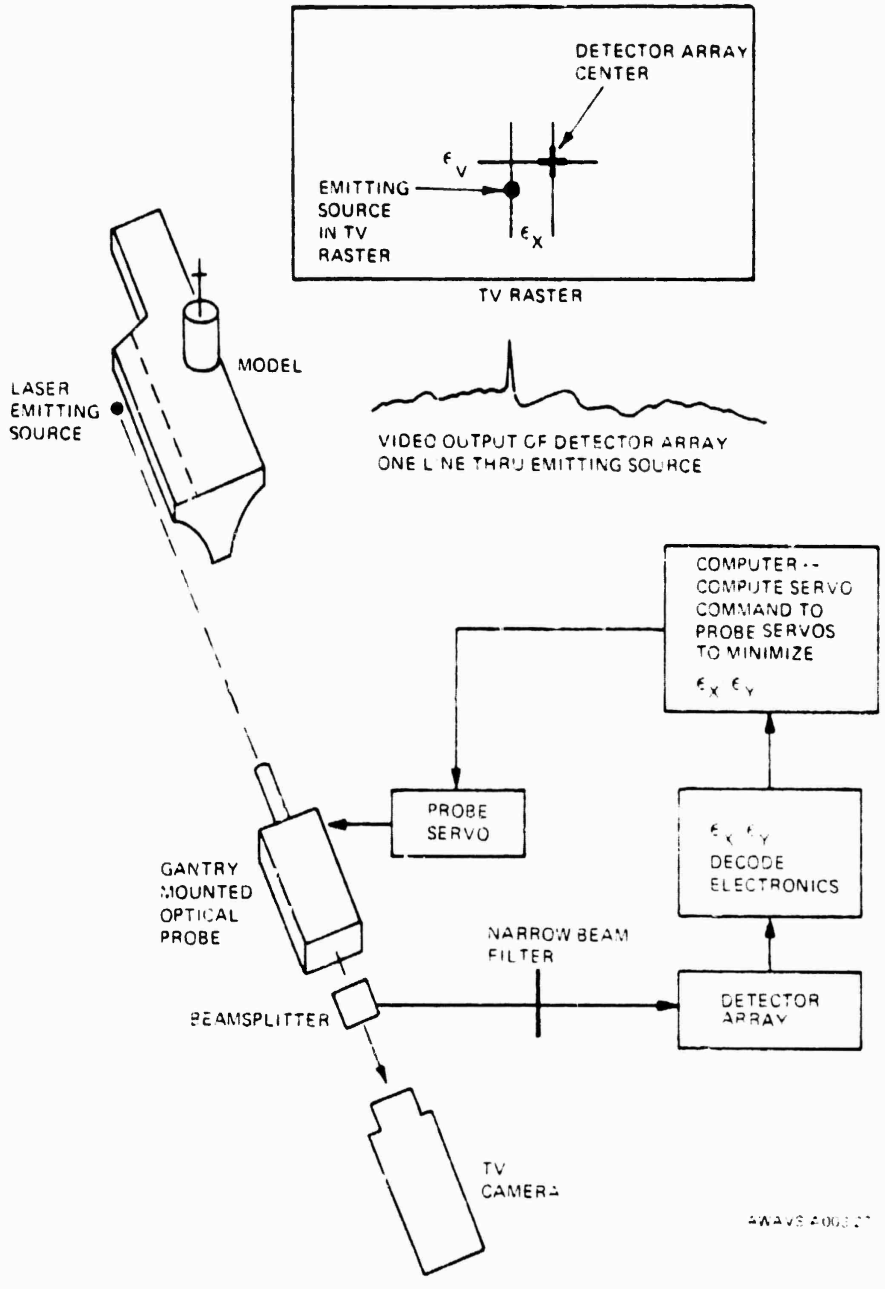

Figure 27. Probe Pointing System, Block Diagram

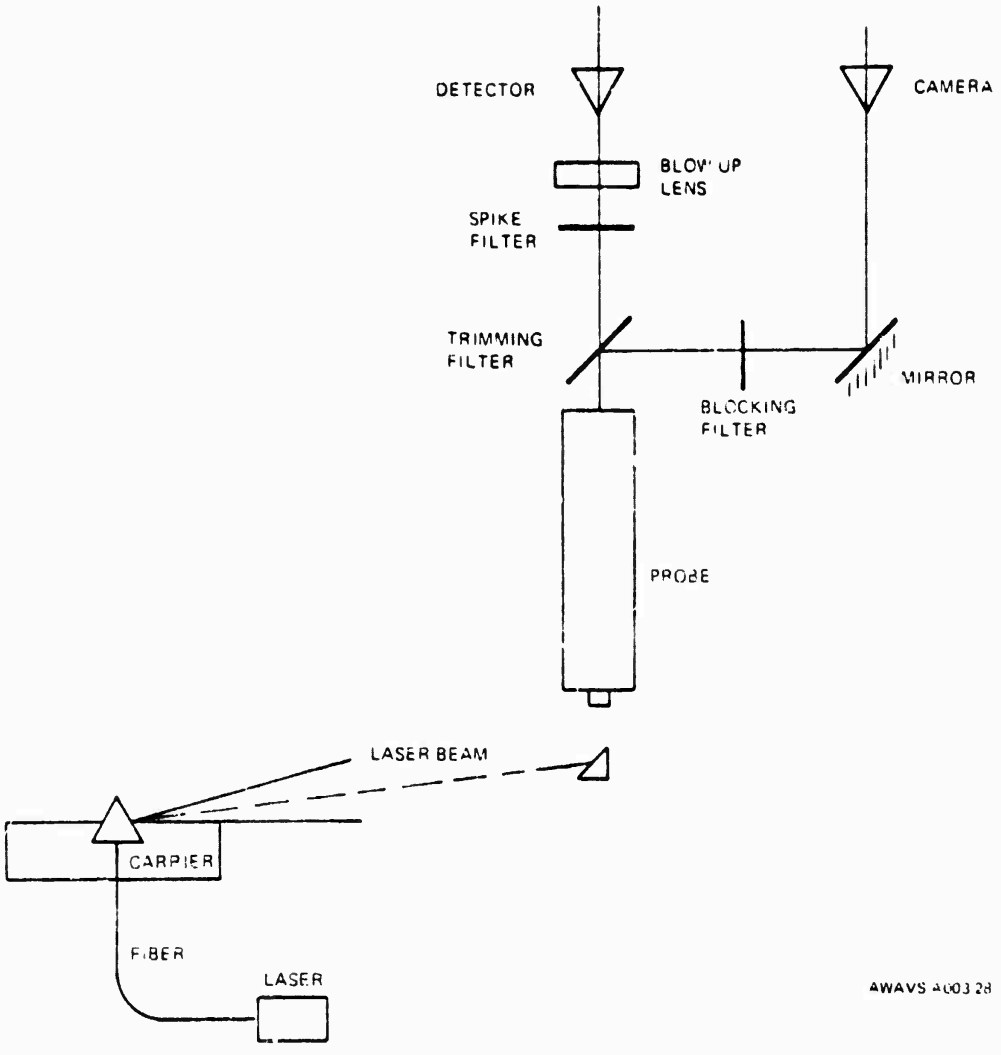

Figure 28. FLOLS Laser and Tracker, Optical Schematic Diagram

3.1.3.4.1 Detector Resolution Analysis.

Blow-up lens EFL = -38.1 nm

Probe EFL @Z_R 1:1 = 31.5

Tracker leg power = $\phi_p + \phi_{BL}$

$$= \frac{1}{31.5} - \frac{1}{38.1} = 0.0055$$

$EFL_{Tracker}$ = 182 nm

$$\text{Tracker field of view} = \frac{\frac{\text{Detector Size}}{2}}{EFL_{Tracker}}$$

$$= \frac{0.1 \text{ in}}{7.16 \text{ in}} = 0.0139 \text{ rad}$$

$$= \pm 48 \text{ min}$$

$$\text{Resolution} = \frac{\text{FOV}}{\text{Number of Elements in Array}}$$

$$= \frac{\pm 48 \text{ min}}{\pm 25 \text{ elements}}$$

$$= \pm 2 \text{ min/element}$$

Obviously, as the probe power increases, then so does the EFL of the tracker. The effect of probe power changes on resolution is shown in Table 11.

The output of the 5mw laser is focused via a 5x microscope objective into the flat fiber end. This objective has a 30mm EFL that ensures a small input cone angle into the fiber and reduces the number of interval reflections, thus increasing transmission.

3.1.3.4.2 Laser Light Calculation. All the laser energy enters the fiber except for insertion losses and fiber transmission. Fiber exit details are illustrated in Figure 29. At the exit of the fiber we have a bundle of 0.762mm diameter impinging upon a cylinderical lens surface (detail A, Figure 29).

TABLE 11. PROBE POWER vs DETECTOR RESOLUTION

PROBE POWER	PROBE EFL (mm)	TRACKER EFL (mm)	±TRACKER FOV(min)	TRACKER DETECTOR RESOLUTION (min)/element)
1:1	31.5	182	48	±2
2:1	63	364	24	1
3:1	94.5	546	16	0.6667
4:1	126	728	12	0.5

The full horizontal direction will not exit from the fiber as some rays are striking the surface at heights, h, such that the critical angle for total internal reflection is exceeded.

$$h = \frac{r}{n} = \frac{0.381}{1.52} = 0.25 \text{ mm}$$

Thus, the maximum width of the laser bundle that can exit is 0.5 mm. In the vertical direction the surface is a plane, thus the full 0.762 height is usable. The emergent rays are therefore bounded in the vertical direction by the fiber diameter and in the horizontal direction by the maximum width at which refraction can occur (detail B, Figure 29). The shaded areas represent the zones lost due to total internal reflection.

At the exit face, because of mixing within the fiber length, we can assume a uniform intensity distribution. Therefore, the ratio of usable area to total area represents that fraction of the laser light exiting from the fiber. This area ratio is 0.77 (detail C, Figure 29).

The combined entering and exit losses are

$$0.9 \times 0.77 \times 0.8 = 0.55$$

Where:

0.9 = insertion transmission

0.8 = fiber transmission

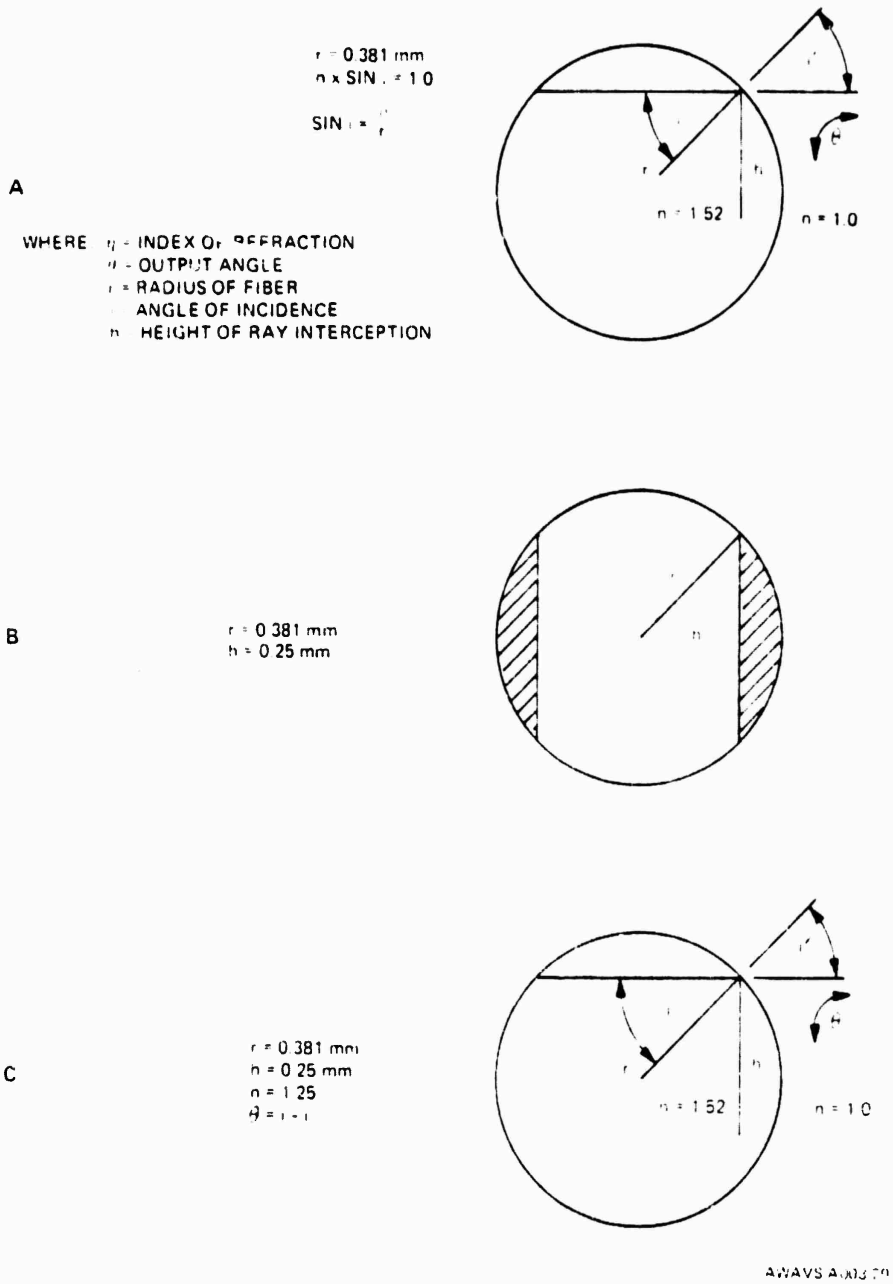

Figure 29 . FLOLS Laser Fiber Exit Details

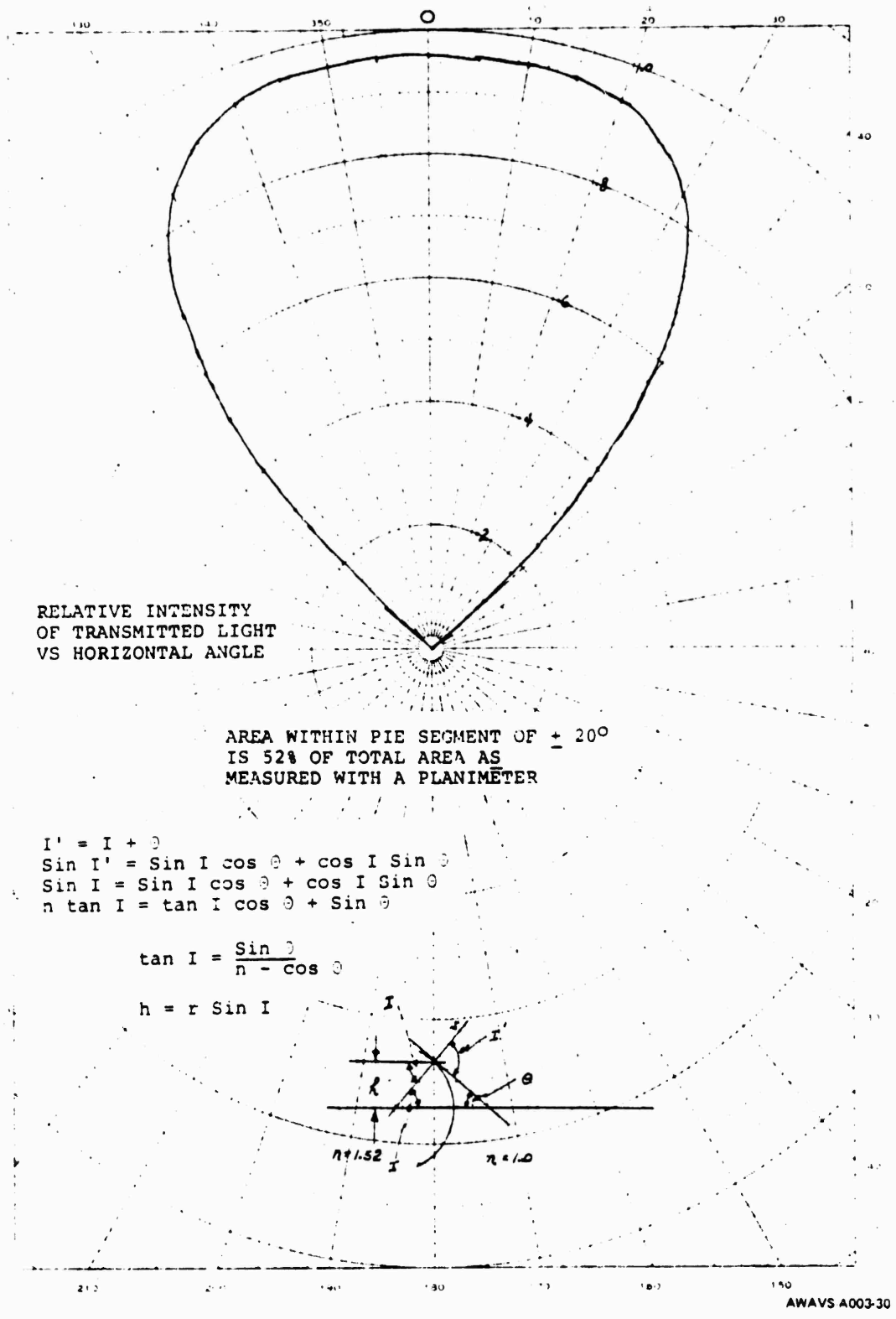

Figure 30. FLOLS Laser Relative Intensity Plot

Because the rays are incident at varying heights, the angles i, i', and θ are a function of the height h, radius r, and refractive index η. The varying angles of incidence result in varying transmittances according to Fernel's laws of reflection. When the incident angle equals the critical angle, the reflection is 100%, therefore, the transmitted intensity must go to zero. Figure 30 is a plot of the relative intensity of the transmitted lights vs the output angle θ. This plot shows that 100% of the transmitted light is within a horizontal angle of ±48.86°. Since we do not turn on the FLOLS until the aircraft is within a horizontal angle of ±20°, that portion beyond the ±20° segments represent that fraction of the laser light lost. Hence, when computing the energy received by the detector, this area ratio must be considered to get the power/sr within the required zone.

The laser beam, because of the power of the exit face of the fiber and mixing within the fiber length, is confined within a ±2° vertical spread and ±48.86° horizontal spread. (See Figure 31.)

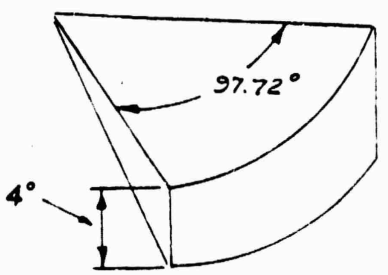

Figure 31 . FLOLS Laser Vertical and Horizontal Beamspread

The solid angle represented by the laser beam upon exiting from the fiber is as follows:

$$4\ \pi \sin 2^\circ \quad \frac{97.72}{360} = 0.119 \text{ sr}$$

j_o = Laser flux in watts out of fiber

K_s = Fiber output in $\frac{\text{watts}}{\text{sr}} = \frac{J_o}{0.119} = 8.4\ J_o$

J_o = (5 x 10^{-3} watts) x (Transmission Losses)

J_o = 5 x 10^{-3} watts x .55

J_o = 2.75 x 10^{-3} watts

K_s = 2.31 x 10^{-2} $\frac{\text{watts}}{\text{sr}}$

But with the 20° horizontal by 2° vertical field of view, corresponding to 0.0487 sr, there exists 52% of the output. Output is uniform within this region by 3%. Thus:

$$K_{s'_{FOV}} = \frac{J_o \times 0.52}{0.0487 \text{ sr}} = \frac{(2.75 \times 10^{-3} \text{ watts})}{0.0487} \quad (0.52)$$

$$= 2.9 \times 10^{-2} \text{ watts/sr}$$

3.1.3.4.3 Detector Sensitivity Analysis. When an object is so small that its image is a diffraction pattern (Airy disk), then techniques that apply to extended sources (for radiometric calculations) cannot be used. Calculation to determine if this is true is shown below.

Diameter (D) of central maximum of airy disk is:

$$D = \frac{(2)\ (0.61)\ (2)}{N' \sin U'}$$

$$D = (1.22)\ (2)\ f\#$$

where,

$$f\# = \frac{1}{2 \sin U'}$$

f# in tracker path is:

$$f\# \cong \frac{EFL}{\text{Clear Aperture}} = \frac{184 \text{ mm}}{2.65 \text{ mm}}$$

$$f\# = 70$$

or,

$$D = (1.22)\ (6328 \times 10^{-10} \text{ mm})\ (70)$$

$$= 5.4 \times 10^{-2} \text{mm}$$

The paraxial magnification (m) predicts that the size of the fiber should be:

$$m = \frac{s'}{s} = \frac{184}{3353} = 0.055$$

Now, size at the tracker is:

$$h = m \times h = 0.055 \times 0.5 \text{ mm}$$

$$= 0.04125 \cong 2.75 \times 10^{-2} \text{ mm}$$

where,

h = 0.5 mm fiber illuminated portion

Since the Airy size is greater than the paraxial approximation, the irradiance at the central pattern of the disk or detector is given by:

$$H_o = 3.5\ (P) \left(\frac{NA}{2}\right)^2 T^*$$

where,

P = Flux intercepted by the probe

NA = Numerical aperture

τ = Wavelength

T = System transmittance

The power (P) intercepted by the probe is:

P = Radiant intensity of laser fiber (Solid angle subtended from probe entrance pupil to fiber)

Or,

Radiant Intensity = watts/sr = 2.9×10^{-2} watts/sr

$$\text{Solid Angle} = \frac{\text{Area of probe entrance pupil}}{\text{Distance}}$$

$$= \frac{(\frac{2.65}{2})\ \pi}{(3353)^2}$$

$$P = (2.9 \times 10^{-2} \text{ watts/sr})\ (4.9 \times 10^{-7} \text{ sr})$$

$$P = 1.42 \times 10^{-8} \text{ watts}$$

Then, transmittance is calculated as:

T = (Filter #1) (Filter #2) (Probe Transmittance)

T = (0.8) (0.5) (0.3) = 0.12

$$NA = \frac{1}{2(f\#)} = \frac{1}{2(70)} = \frac{1}{140} = 0.007$$

$$H_o = (3.5)(1.42 \times 10^{-5})(0.12)\ (\frac{0.007}{6328 \times 10^{-8}})^2$$

$$= 7.3 \times 10^{-5} \text{ watts/cm}^2$$

$$H_o \cong 73\ \mu\text{W/cm}^2$$

Table 12 gives the specifications of the 50 x 50 detector array, while Figure 32 shows the sensitivity and spectral response. The detector electronics scan the array at a rate of 30X per second. Thus, in terms of the data presented:

$$\text{Exposure} = (73\ \mu W/cm^2)\ \frac{1}{30}\ \text{sec}$$

$$= 2.4\ \mu W\ \text{sec}/cm^2$$

Since the spot underfills a diode, H_o must be multiplied by the ratio of the spot-to-diode area.

$$\text{Exposure} = 2.4\ \mu W\ \text{sec}/cm^2\ (\frac{3.5}{8})$$

$$= 1.05\ \mu W\ \text{sec}/cm^2$$

This is sufficient for detection if the signal is centered on one element. The area of one element of the detector 8×10^{-6} sq. inches. The area of the Airy disk or detector is:

$$\text{Area} = [(\frac{5.4 \times 10^{-2}\ mm}{2})(\frac{1\ in.}{25.4\ mm})]^2\ \pi$$

$$= 3.5 \times 10^{-6}\ in^2 \quad \text{or,} \quad 3.5\ mils^2$$

The signal is greater if the signal is centered on a diode, and all the energy is accepted.

There are 2500 diodes on the detector in a 50 x 50 array. Individual diode sensing area is 8 sq mils. Spacing between rows and columns of the array is 4 mils. If we assume that the diodes are square, then the dead spacing between diodes is:

$$4 - \sqrt{8} = 1.17\ \text{mils} = 0.029\ \text{mm} \cong 0.03\ \text{mm}$$

The diamter of the Airy disk is 0.054 mm.

TABLE 12. FLOLS TRACKER DETECTOR SPECIFICATION

ELECTRICAL CHARACTERISTICS (25°C)
(Voltages with respect to common)

	Min	Typ	Max	Units
Video Output Line Bias		-5	-8	Volts
Supply Voltage V_{DD}	-11	-12	-13	Volts
Clock Pulse Amplitude	-11	-12	-13	Volts
Start Pulse Amplitude	-7.5	-10	-13	Volts
Start Pulse Width	1/f*1		*2	Sec
End of line/frame output resistance		5		K ohms
End of line output pulse width		2/f*1		Sec
Video line capacitance (at -5 volts)		150		pf
Diode Sample Rate	$5x10^4$		$5x10^8$	Hz
Frame Rate	20		2000	Hz
Power Dissipation (DC)		10		m watt

ELECTRO-OPTICAL CHARACTERISTICS (25°C)

Photodiode sensitivity*3		250		pA/ft-cd
		5		pA/μwatt/cm²
Uniformity of sensitivity*3*4		±10		%
Saturation Exposure		$3x10^{-3}$		ft-cd sec
		.15		(μwatt/cm²)sec
Saturation charge (at -5 volts)		0.75		pcoul

MECHANICAL CHARACTERISTICS

Number of diodes		2500		
Number of rows and columns		50		
Spacing (row and column)		4		Mils
Diode sensing area		8		Mils*2
Package size (16 pin DIP)		0.6x0.8		Inch

ABSOLUTE MAXIMUM RATING

Voltage with respect to common	0		-20	Volts
Storage temperature	-55		+85	°C
Temperature under bias	-55		+85	°C

NOTES:
- *1 diode sample rate
- *2 self-starting beyond 34/f for 32x32 or 52/f for 50x50
- *3 2870 K tungsten source
- *4 Neglects first and last elements of each line

DETAIL A

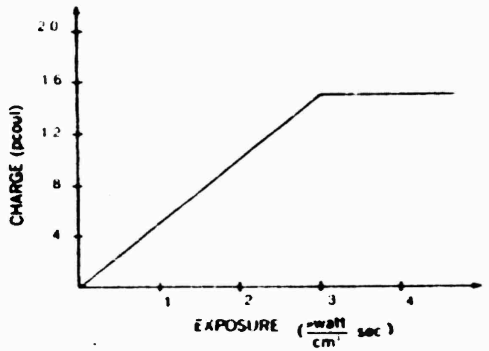

CHARGE OUTPUT PER CELL VERSUS EXPOSURE WHERE EXPOSURE EQUALS LIGHT INTENSITY TIMES FRAME TIME.

DEATIL B

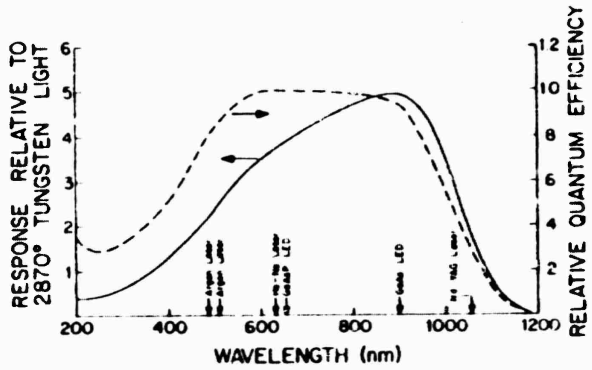

TYPICAL SPECTRAL RESPONSE AND QUANTUM EFFICIENCY

The RA-50x50A operates in the frame storage mode. This means that each diode integrates photocurrent for an entire frame time and empties the integrated charge onto the video line when it is sampled once each frame time. The sensitivity of each diode is, therefore, over 2500 times the sensitivity of an individual diode of equal size operated in the photoconductive mode. The output of each diode (below saturation) is proportional to the light intensity times the frame time and can be specified in terms of charge out per unit of exposure. A plot of output versus exposure is shown in detail A. Spectral response is typical of high quality diffused silicon photodiodes covering the range from 0.4 to 1.1μ and peaking at 0.9μ . Typical spectral response and quantum efficiency curves are shown in detail B.

AWAVS-A003-32

Figure 32. Sensitivity and Spectral Response of FLOLS Tracker Detector

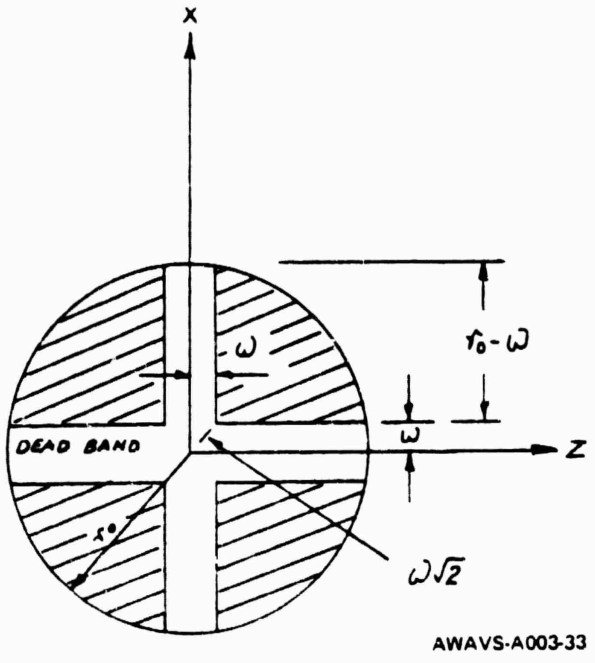

Figure 33. Detector Diffraction Spot

Figure 33 illustrates a small portion of the detector where the diffraction spot may lie. This chosen orientation illustrates the worst possible case, the spot centered on a dead band between four sensors of the 50 x 50 array. The following calculation provides its results in watt sec/cm^2 on the portion of the detector labeled "A".

$$r_o = .027$$

r_o = radius of diffraction spot

$$w \cong .015\text{mm}$$

$$x^2 + z^2 = r_o^2$$

$$z = \sqrt{r_o^2 - x^2}$$

$$A = \int_{\omega}^{\sqrt{r_o^2 - \omega^2}}$$

$$A = \tfrac{1}{2}\left[x\sqrt{r_o^2 - x^2} + r_o^2 \sin^{-1}\frac{(x)}{r_o}\right]\Bigg|_{\omega}^{\sqrt{r_o^2 - \omega^2}}$$

$$A = \frac{r_o^2}{2}\left[\sin^{-1}\left(\frac{\sqrt{r_o^2 - \omega^2)}}{r_o}\right) - \sin^{-1}\frac{(\omega)}{r_o}\right]$$

To check if $\omega = 0$.

$$A = \left(\frac{r_o^2}{2}\right)\left(\frac{\pi}{2}\right) = \frac{\pi r_o^2}{4} = \tfrac{1}{4} \text{ area of circle correct}$$

$$A = 1.43 \times 10^{-4} \text{ mm}^2$$

The diffraction spot's energy is distributed as a Bessel function of the spot's radius. The energy density can be assumed to lie in a cone as illustrated in Figure 34, where h_o is found as follows:

Maximum volume of cone = 0.838 units (Energy in central maximum of Airy pattern)

$$= \frac{(\text{Area of spot})\ h_o}{3}$$

$$=> h_o = \frac{(0.838)3}{\pi(0.027)^2} = 121.9678$$

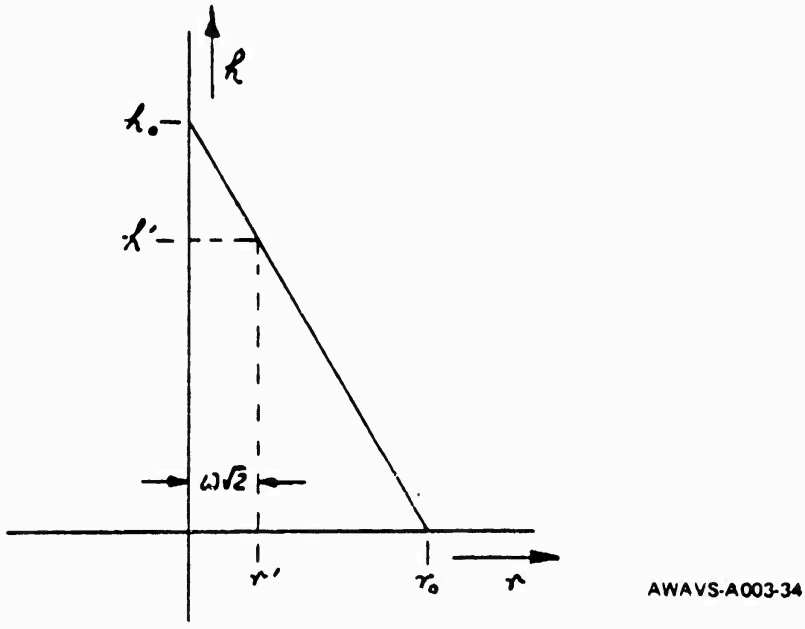

Figure 34 Energy Density Calculation

Now, we need the portion of the cone that falls on A. The equation for the line joining h_o and r_o B:

$$h' = -\left(\frac{h_o}{r_o}\right) r' + h_o$$

where,

$$r' = \omega\sqrt{2}$$

$$h' = 26.14$$

Now, the volume of the cone about "A" is:

$$V = \frac{A}{3} h' = \frac{(1.43 \times 10^{-4} \text{ mm})(26.14 \text{ mm})}{3} = 1.25 \times 10^{-3}$$

Therefore, 1.25×10^{-3} of the total energy accepted by the probe illuminates area "A" on the detector.

Intercepted power (P_o) is calculated as:

$$P_o = 1.47 \times 10^{-8} \text{ watts}$$

Detector power (total energy at the detector) is:

$$P' = (P)(T)(\text{Portion of energy falling on "A"})$$

$$= (1.47 \times 10^{-8})(0.12)(1.25 \times 10^{-3})$$

$$= 2.21 \times 10^{-6} \ \mu W$$

Now,

$$H = \frac{2.21 \times 10^{-6} \ \mu W}{5.16 \times 10^{-5} \ cm^2}$$

(5.16×10^{-5} cm^2 is the area of one diode)

$$H = 4.28 \times 10^{-2} \ \mu W/cm^2$$

Thus,

$$\text{Exposure} = 4.28 \times 10^{-2}\left(\frac{1}{30} \text{ sec}\right)$$

$$= 1.43 \times 10^{-3} \ W \text{ sec}/cm^2$$

3.1.3.4.4 Summary. The laser spot will provide an adequate detectable signal when centered on a diode. When it is between four adjacent diodes, it is doubtful it will light any.

The output of the fiber is speckled due to rough surfaces on insertion and numerous reflections in the fiber. The fiber is vibrated via a fan behind the modelboard. This changes the angles of incidence within the fiber and produces a uniform output. Thus the speckle pattern is time averaged over the field of view.

Shown in Table 13 are the open and closed loop tracking errors as a function of range. The only tracking error not closed in the loop is the camera roster drift.

TABLE 13. FLOLS TRACKER ERRORS VS.

RANGE	WIDTH OF CARRIER ON CAMERA RASTER (MM)	CAMERA RASTER DRIFT (MM)	OUTPUT ERROR DUE TO CAMERA RASTER DRIFT (% CARR WIDTH)	ANGLE FOR 5% OF CARRIER WIDTH (ARC MIN)	PROBE ZOOM	ARRAY FOV ± ARC MIN	ARRAY RESO-LUTION ± ARC MIN	TOTAL OPEN LOOP ERROR (% CARRIER WIDTH)	CLO LOO ERR (% CAR WID
5 nm	1.75	.075	4.28	10.6	1.07	45	1.8	32	4.
4 nm	2.60	.075	2.88	10.6	1.6	30	1.2	32	2.
3 nm	3.48	.075	2.15	10.6	2.14	22.5	.9	32	2.
2 nm	5.23	.075	1.43	10.6	3.21	15	6	32	1.
10,000 ft	6.35	.075	1.18	10.6	3.9	12.3	.492	32	1.
9,120 ft	6.35	.075	1.18	10.6	3.9	12.3	.492	32	1.
7,600 ft	6.35	.075	1.18	10.6	3.9	12.3	.492	32	1.
6,080 ft	6.35	.075	1.18	10.6	3.9	12.3	.492	32	1.
5,840 ft	6.35	.075	1.18	10.6	3.9	12.3	.492	32	1.
3,900 ft	6.35	.075	1.18	10.6	3.5	13.7	.548	28	1.
2,300 ft	6.35	.075	1.18	18.3	2.3	20.9	.836	18	1.
1,000 ft	6.35	.075	1.18	42.0	1.0	48	1.92	8	1.

13. FLOLS TRACKER ERRORS VS. SIMULATED RANGE

ARRAY RESOLUTION ± ARC MIN	TOTAL OPEN LOOP ERROR (% CARRIER WIDTH)	CLOSED LOOP ERROR (% CARRIER WIDTH)	OUTPUT ERROR DUE TO ARRAY RESOLUTION (IN % OF CARRIER WIDTH	OUTPUT ERROR DUE TO PROBE STATIC ERRORS (IN % CARR WIDTH)		OUTPUT ERROR DUE TO GANTRY STATIC ERR (% CARR WIDTH)	OUTPUT ERROR DUE TO ZOOM WANDER (% CARR WIDTH)	OUTPUT ERROR DUE TO PROBE PITCH TRACKING (% CARR WIDTH)	OUTPUT ERROR DUE TO PROBE HEADING TRACKING (% CARR WIDTH)
				REPEAT ABILITY	ACCURACY				
1.8	32	4.36	.85	2.36	21.2	0.22	2.8	14.2	28.4
1.2	32	2.94	.57	2.36	21.2	0.22	1.9	14.2	28.4
.9	32	2.19	.43	2.36	21.2	0.22	1.4	14.2	28.4
6	32	1.46	.28	2.36	21.2	0.22	0.95	14.2	28.4
.492	32	1.2	.23	2.36	21.2	0.22	0.78	14.2	28.4
.492	32	1.2	.23	2.36	21.2	0.22	0.78	14.2	28.4
.492	32	1.2	.23	2.36	21.2	0.22	0.78	14.2	28.4
.492	32	1.2	.23	2.36	21.2	0.22	0.78	14.2	28.4
.492	32	1.2	.23	2.36	21.2	0.22	0.78	14.2	28.4
.548	28	1.2	.26	2.1	18.9	0.22	0.78	12.6	25.2
.836	18	1.2	.23	1.3	11.7	0.22	0.78	8	16
1.92	8	1.2	.23	.58	5.22	0.22	0.78	3.5	7

Errors Which Were Negligible

1) Raster Computer
2) FLOLS Zoom Wander

AWAVS-A003-124

3.1.3.5 Probe Electronics and Servos. The function of the electronics is to provide for computer operated, high accuracy servo systems which are capable of controlling the opto-mechanical assemblies; and which, when subject to full magnitude steps of position, stabilize at the command position within their specified limits of velocity and acceleration. Performance characteristics for servo loops are given in Table 14.

In order to satisfy these requirements, two major areas of design were investigated. These are system design and configuration design and are discussed in the following paragraphs. Controls and indicators for the probe servo electronics are described in paragraph 3.1.3.5.3.

3.1.3.5.1 System Design. Although the performance characteristics specified in Table 14 include data for the zoom-focus mechanisms, the data required parametric conversion so that the actual mechanism design could be completed.

The data for velocity and acceleration was developed in accordance with the aircraft dynamic profile. The accuracy requirements were based on the optical performance characteristics.

In accordance with the specification, all servos are dc. Two of the basic problems of dc servos are low frequency noise and drift. In order to minimize these problems, particular attention has been paid to shielding and the use of low drift operational amplifiers in the sensitive sections of the servo. In addition, the input analog signals must be transmitted over considerable distance between the computer interface and the probe assembly. Hence, line receivers have been utilized in the form of differential inputs with high common mode rejection ratios to maintain the integrity of the signals. Further, in order to increase the system accuracy and provide for increased reliability, the dc sine-cosine potentiometers have been replaced with resolvers. However, a unique Farrand signal conditioning card acts as a buffer between the computer dc sine-cosine signals and the dc error sent back to the chassis, and makes the resolver interface to the computer and chassis appear unchanged. Investigation utilizing the specification for accuracy dictated the need for multi-speed feedback elements.

Due to the limited amount of mechanical space in the probe, it became necessary to place the mechanical limit stops reasonably close to the electrical limit switches (for pitch, focus, tilt). In some cases, the distance was not sufficient to allow the motor drive assembly to coast to a stop before hitting the limit stops. Hence, circuitry was included to reverse the direction of the motor (apply reverse power) to increase the deceleration rate so that at the time the mechanism contacted the stop, the total kenetic energy, and therefore impact force, was insignificant.

In general two types of accuracy specifications have been designed for. They are static accuracy and dynamic accuracy. The previous discussion has dealt primarily with the static accuracy requirements. The dynamic accuracy requirements are generally specified in terms of a velocity constant (Kv), which defines the lag error allowed under steady-state velocity conditions. The required velocity constant for roll, pitch, and heading servos are easily met by a type 1 servo system. However, for the zoom and focus servos, the following error must be very small and hence the velocity constant very high. Farrands approach to the problem has been to utilize type 2 servos as outlined in the analytic support data. Static and dynamic servo performance for the probe system is summarized in Table 15.

3.1.3.5.2 Configuration Design. The design philosophy has been to provide for ease of maintenance, simplicity in provisioning, and high reliability. In order to accomplish this task, a single servo control chassis has been designed which houses the electronics for all five axes.

The electronics for each axis is contained on a single plug-in printed circuit card with the exception of the power amplifier, the signal processing card, and buffer cards. All printed circuit cards are identical for ease of manufacturing. However, each card assumes its peculiar functional identity at assembly. Each card assembly is keyed to prevent accidental placement in the wrong position. All integrated circuits and most passive components are plug-in dip packages for ease of replacement and trouble shooting. Easily accessible test points are located on the top of each card assembly. Except for the power interface, which is connected by a terminal board, all input from the computer interface signals terminate on connectors and are therefore easily removed. All input power is routed through alternate action pushbutton switches and fused at the front panel, thereby enabling easy trouble shooting procedures. In the event that the focus, tilt, or pitch servos are driven to their electrical limits, lights are provided on the front panel indicating which axis and which limit is activated.

The signal processing printed circuit card is located at the probe assembly. All integrated cicuits and most passive elements are plug-in dip packages for ease of assembly.

In addition a buffer card is located in the probe for each axis for transmitting the signal from the one-speed transducer with a minimum increase in noise level.

TABLE 14. OPTICAL PROBE SERVO CHARACTERISTICS

SERVO	UPPER BOUND VELOCITY	LOWER BOUND VELOCITY	VELOCITY ERROR	ACCELERATION	POSITION SENSITIVITY	POSITION REPEATABILITY
Roll	90°/sec	4 $\overset{\frown}{\text{min}}$/sec	1.5°	75°/sec^2	1 $\overset{\frown}{\text{min}}$	±5 $\overset{\frown}{\text{min}}$
Pitch	30°/sec	4 $\overset{\frown}{\text{min}}$/sec	0.5°	30°/sec^2	1 $\overset{\frown}{\text{min}}$	±5 $\overset{\frown}{\text{min}}$
Heading	60°/sec	4 $\overset{\frown}{\text{min}}$/sec	1.0°	45°/sec^2	1 $\overset{\frown}{\text{min}}$	±5 $\overset{\frown}{\text{min}}$
Focus	160°/sec*			2000°/sec^2	1 $\overset{\frown}{\text{min}}$	±1 $\overset{\frown}{\text{min}}$
Zoom	22.5°/sec**			47°/sec^2	27 $\overset{\frown}{\text{min}}$	±27 $\overset{\frown}{\text{min}}$

Notes:

* At sector gear
** At ring gear

TABLE 15. OPTICAL PROBE SERVO PERFORMANCE

SERVO PERFORMANCE (STATIC)		
	Range	Repeatability
Pitch	+45° - 135°	5 $\overset{\frown}{\text{min}}$
Heading	Continuous	5 $\overset{\frown}{\text{min}}$
Roll	Continuous	5 $\overset{\frown}{\text{min}}$
Zoom	1:1 to 4:1	2% Zoom Range
Focus	"0" to .630 in.	.0005 in.
Iris	.158 to 1.260 in. dia	5% of Dia

SERVO PERFORMANCE (DYNAMIC)		
	Velocity	Acceleration
Pitch	30°/sec	30°/sec^2
Heading	60°/sec	45°/sec^2
Roll	180°/sec	150°/sec^2
Zoom (Rotation of Ring Gear)	22°/sec	46"/sec^2
Focus (Rotation of Sector Gear)	160°/sec	2000°/sec^2

It should be noted that an additional advantage of the resolver over a linear pot is that for a given maximum reference voltage (±10 volts) the resolver has a higher voltage gradient, and therefore a higher signal to noise ratio. In addition, drifts of the reference voltage do not affect accuracy if the drift is common for both the sine and cosine sections, because the system operates on the ratio of the two signals. (Multispeed is defined here as indicating that the feedback element rotates more than one degree for each degree of rotation of a one-speed shaft.) Although space was at a premium in the mechanical assembly, it was possible to incorporate one-speed elements (dc potentiometers) in the space envelop specified in the specification. Hence, the problem of ambiguity of position is a reality. The ambiguity of position occurs when the feedback element has more than one stable position for a given input command. As an example, the heading axis utilizes a four-speed sin-cos potentiometer. Hence, the mechanism is stable at 0,90,180 and 270 degrees when the input command is zero degrees. This problem was solved and the ambiguity eliminated by utilizing of the one-speed potentiometers. The information from these devices are sent to the computer for quadrant synchronization.

3.1.3.5.3 Probe Electronics Control Panel. This panel is actually the face of the probe servo electronics drawer. (See Figure 35.) It contains seven ON/OFF rocker switches — one for each servo channel and two for primary dc power. The servo channels switches each control application of the +28V servo B+, while the other two switches are in the output circuits of the +5V and ±15V power supplies. In series with each switch, and located beneath it, is the fuse for that circuit (two for the ±15V power supply; one positive, one negative). Also on the panel are six LIMITS lamps, which light to indicate that the probe PITCH, FOCUS, or ZOOM servo has reached, and is presently at, one of its extreme limits (UP or DOWN for PITCH; NEAR or FAR for FOCUS and ZOOM).

3.1.3.6 Maintenance Panel Interface. A capability for manual operation of all six probe servos is provided from the gantry maintenance panel, Figure 43, when its SYS CONT key switch is in the TEST position. Five individual sine-cosine potentiometers supply the two dc drive voltages (position commands) required for positioning of each of the ROLL, PITCH, HEADING, FOCUS and ZOOM servos. Velocity for each of the foregoing is constant, and the probe stops when the position described by the applicable potentiometers is reached. A sixth potentiometer supplies the dc drive command to operate the IRIS servo. Unlike normal computer controlled operation, no feedback voltages are required since the source of each command is uncalibrated, and the probe is positioned by observation.

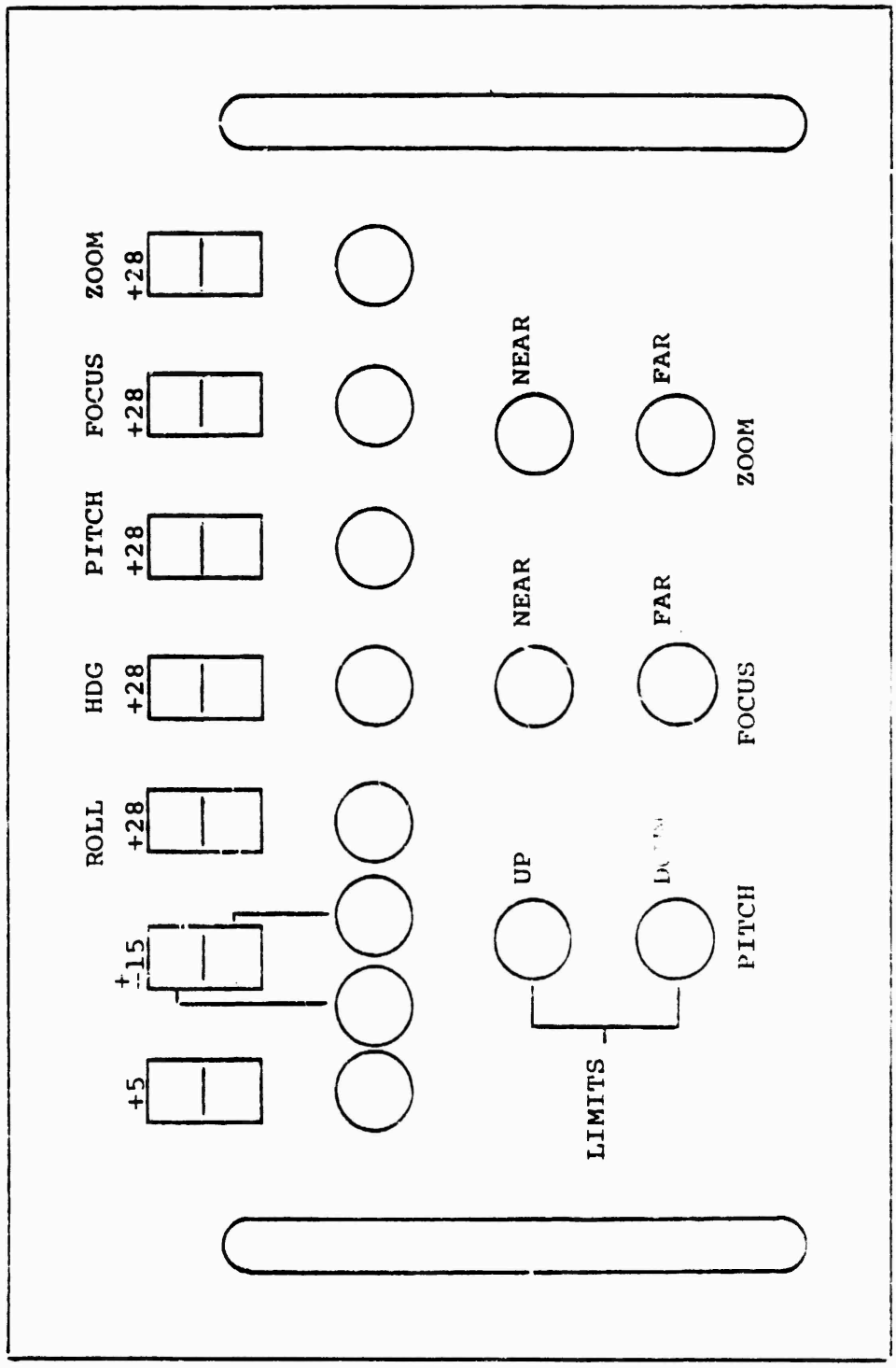

Figure 35. Pedestal Servo Electronics Control Panel

3.1.4 Target Television Camera Subsystem. The target television camera (TIG camera) and its associated control, video processing, and monitoring circuits are shown in the target television camera subsystem block diagram, Figure 36. Dashed lines surrounding functional blocks illustrate physical locations of hardware within major cabinet assemblies. Horizontal and vertical timing signals are developed by the master timing generator which is part of the background system. (See paragraph 3.7.) The test video and control signal sometimes used by the special effects generator are also generated within the background system, however, they are initiated in the SKI electronics drawer. (See paragraph 3.6.) Secondary power supplies for the TIG camera are also mounted on the gantry tower assembly. The EOS monitor and its interface circuitry is remotely located at the Experimentor/Operator Station.

The target image video from the camera head is amplified and processed in the camera electronics card bin. Video processing is comprised of retrace blanking and dc restoration. The target video is then routed to the BIG electronics cabinet and the special effect generator. At this point visibility effects are added to the video signal, or test video signals can be switched into the video chain for test and alignment. The output of the special effects generator is routed to the image enhancer in the TIG cabinet where boost is selectively added to the signal. The image enhancer drives the EOS monitor with one output and the TIG TV monitor with the other. The video is looped through the TIG TV monitor and terminated at the target projecter interface. The linkage provides computer control to the dynamic-analog raster computer (DARC), FOV blanking generator and special effects generator, as required. The DARC shapes the vidicon raster to compensate for an apparent loss of true perspective due to target projector pointing. The camera shading and FOV blanking generators reduce undesirable side effects inherent within vidicon camera systems. A camera control unit routes high voltage from the TIG camera HVPS to the vidicon and provides a means for adjustment of these voltages to compensate for the peculiarities of individual vidicons.

The EOS and TIG television monitors are conventional 17-inch black-and-white broadcast monitors, except for the addition of circuitry which allows switching between two picture size patterns. The waveform monitor is a Tektronix Model 465 oscilloscope, whose function is solely as an item of maintenance equipment. The scope and both video monitors are provided with external horizontal and vertical drives from the master timing generator.

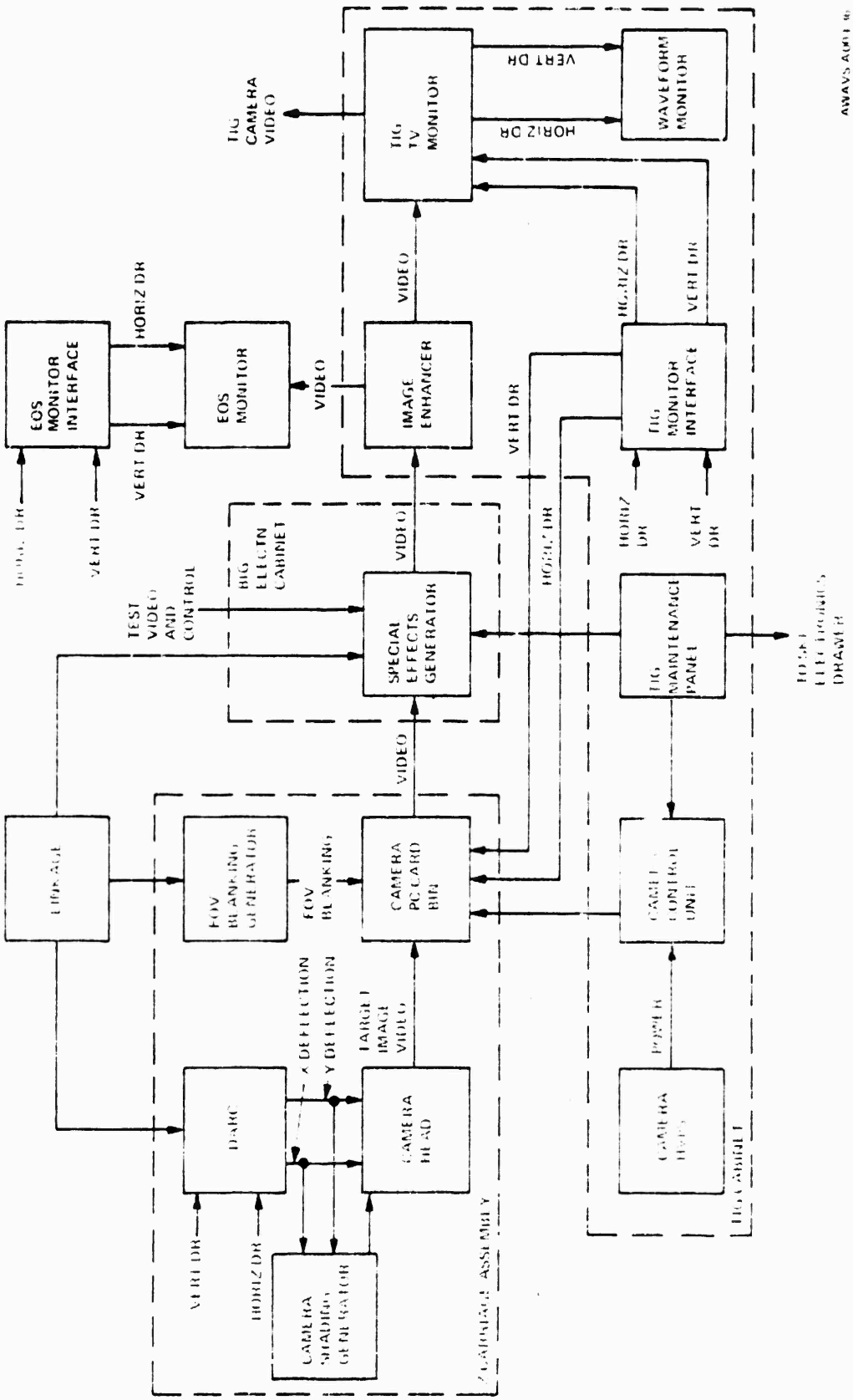

Figure 36. Target Television Camera System, Block Diagram

The target camera system has the capability of operating at three different horizontal scan rates: 525, 825 and 1025 lines. The camera head setup is accomplished by remote control from a line rate switch on the TIG maintenance panel. The TIG DARC is set up for various line rates by the installation of the proper waveform generator printed circuit card set (Singer Dwg No. 2044151). The image enhancer is equipped with a line rate select switch that places the video boost for optimum crispness.

3.1.4.1 Target Image Generation. The target image camera employs the Westinghouse intensified WX3-13836/WX5168 2-inch vidicon, because its superior resolving power and sensitivity provide optimum performance in a very critical area. The target image generator employs dynamic raster shaping at the camera raster to compensate for system distortions, resulting from the target projector pointing.

Six areas of camera performance related to dynamic raster shaping are discussed in paragraphs 3.1.4.1.1 through 3.1.4.1.6. They are: camera video flashing, camera lag characteristics, camera modulation transfer function, target efficiency, shading, and interline interference.

3.1.4.1.1 Camera Video Flashing. Figure 37 illustrates computer output plots which show the required raster shaping at the target image camera. The axes are scaled in millimeters on the vidicon surface. The following conditions were assumed in deriving these rasters. The normal eyepoint is located 15 inches below and 6 inches forward of the 10 ft radius spherical screen center. The target image projector exit pupil is located at a point described by $x = -(4 + 3.5 \sin \theta)$; $y = 3.5 \cos \theta$; $z = -10$ in the screen axis frame: where the dimensions are in inches, and θ is the projector axis azimuth angle. This system configuration is referred to as the 3.5 right-offset configuration. That is, the projector axis frame is 3.5 inches offset to the right of the observer axis frame, when the two frames are parallel. Further, the nominal raster format is defined for the projector pointing at the 0° aximuth -0° elevation, as seen by an observer. Section 3 of the AWAVS Design Analysis Report established that for this nominal condition, the required field of view must be overscanned. The raster plots take the recommended 10% horizontal overscan of the field of view into account. Each plot includes the specified 40° by 60° target image field of view and shows a plot of every 45th active horizontal scan line.

As the target projector pointing angle changes, the raster size, shape and rotation vary. Within the range of +80° to -120° azimuth and +50° to -30° elevation angle, as seen by the observer, the raster varies +7.8 to -20.2 per cent of the vertical raster height along the horizontal axis and +4.4 to -11.4 per cent of vertical height along the vertical axis. Each time the camera raster writes on a new area of the vidicon surface, an area flashing effect will occur. This flashing or jump in the video brightness is a result of the energy storage characteristics of the vidicon photo surface. A special technique used to reduce or eliminate this flashing effect is overscanning of the required field of view.

The major flashing effects occur because the camera raster size changes and scan lines move from discharged to undischarged areas of the photo surface as a function of target projector pointing. It is possible to eliminate these flashing effects in the projected field of view if the required field of view were overscanned by the raster. The overscanning has to be great enough such that the minimum raster size fills the required field of view. The effectiveness of this approach is limited by system resolution. The resolution within the required field of view is determined by how much the maximum raster size overscans the required field of view. Under these operating conditions, the camera video will be blanked when the raster exceeds the required field of view, but the vidicon electron beam would be allowed to discharge the photo surface outside the field of view area. For the AWAVS application, the extent of field-of-view overscan is limited by the performance of the light valve TV projector. With an 825-line scan, the required 700 TV lines horizontal by 500 TV lines vertical resolution is met at the nominal projector pointing angle over the required field of view resulting in a 10-percent horizontal overscan. Thus Figure 37, sheet 7, which represents the minimum raster size under these conditions, demonstrates that the total, required field of view has not been met. Under these conditions the unscanned areas within the required field of view will bloom or flash as the raster size expands into the unscanned areas. In order to eliminate this effect, the field-of-view blanking function is further decreased as required by the projector pointing function on a dynamic basis. This system function provides the full field of view to the observer at all times, except when the projector pointing an angle reduces the raster size below the size of the field of view, and for a fixed time (less than 3 seconds) following this reduced field-of-view condition. Thus, as the raster size increases, the flashing effect within the field of view is blanked out. Preliminary calculation indicates that this reducing blanking will occur at elevation angles greater than 30° and the minimum observer field of view will be 51.3° horizontal by 40° vertical. Thus, the requirements of dynamic raster shaping present difficult but manageable problems for the AWAVS camera design.

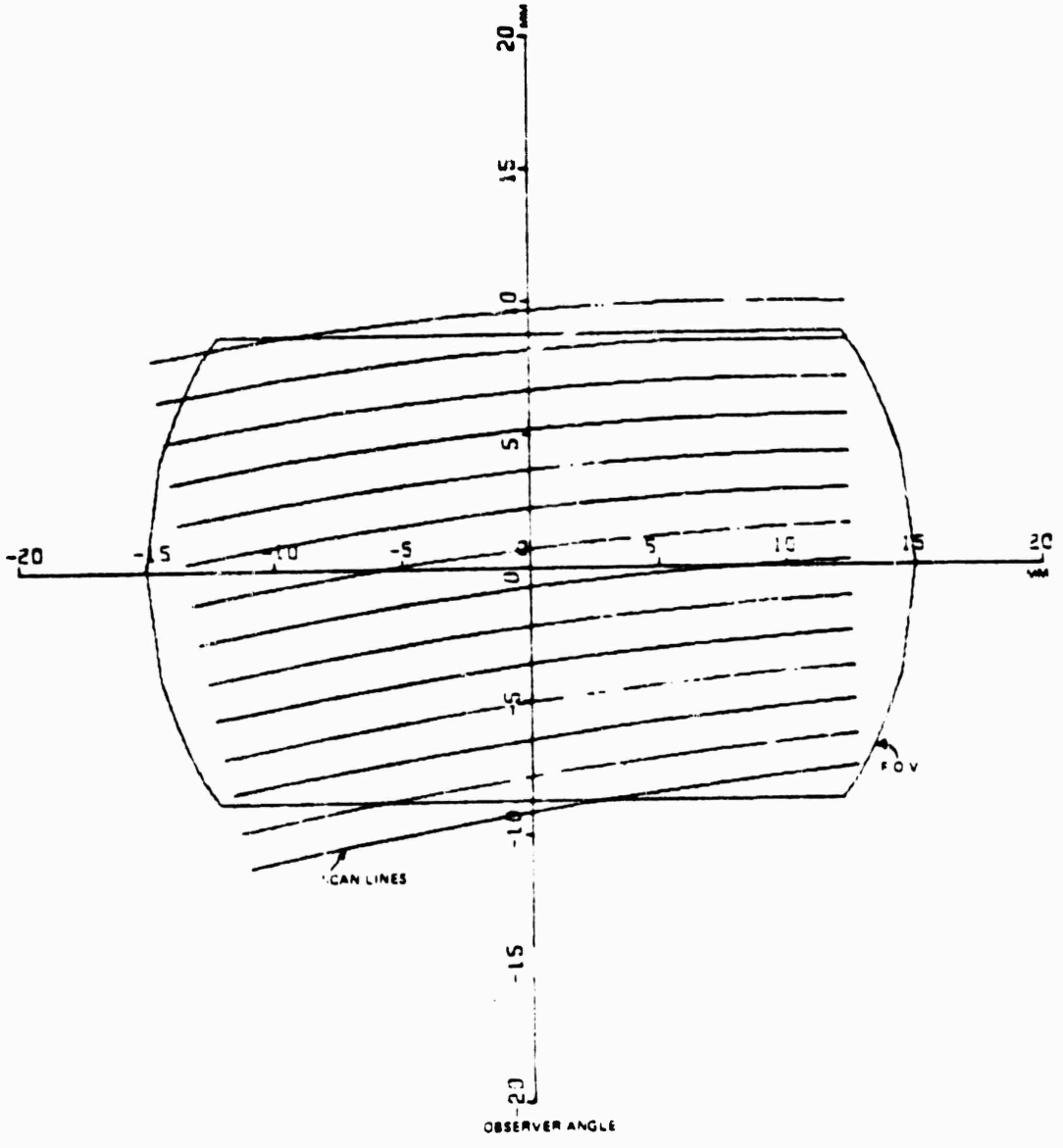

Figure 37. Camera Raster Plots (Sheet 1 of 8)

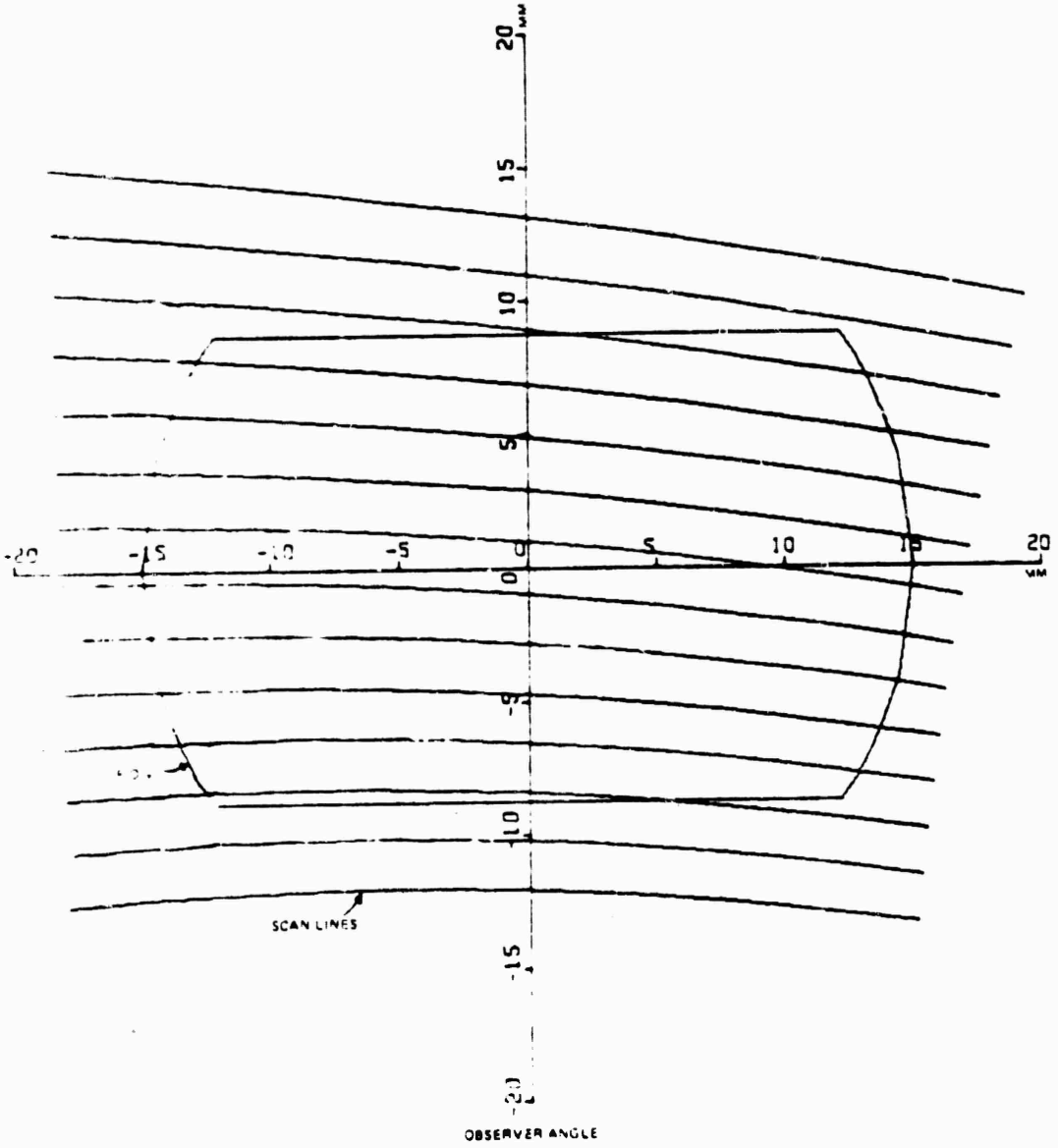

AZIMUTH=30. ELEVATION=-30. -

AWAVS-A003-37.2

Figure 37. Camera Raster Plots (Sheet 2 of 8)

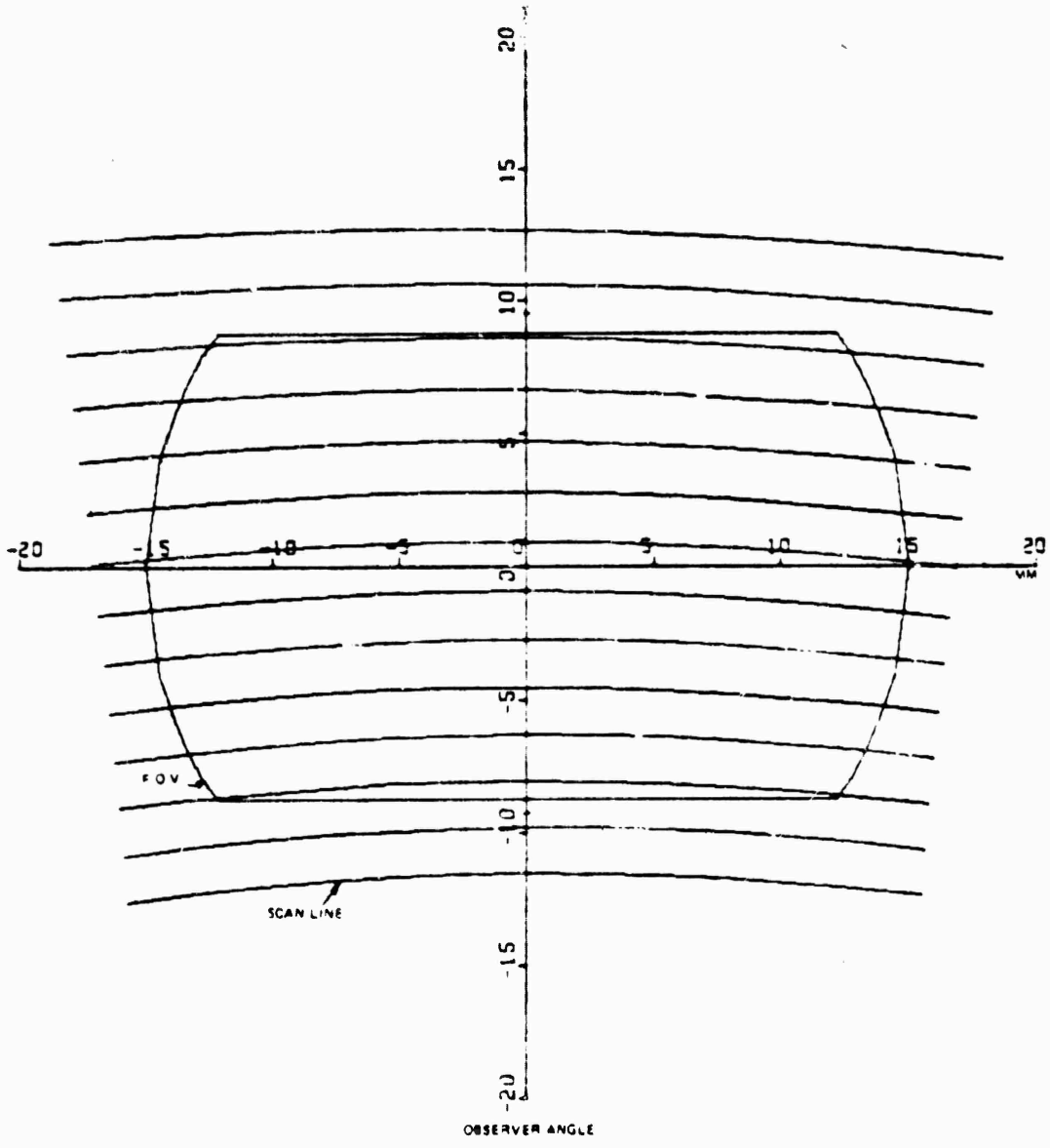

Figure 37. Camera Raster Plots (Sheet 3 of 8)

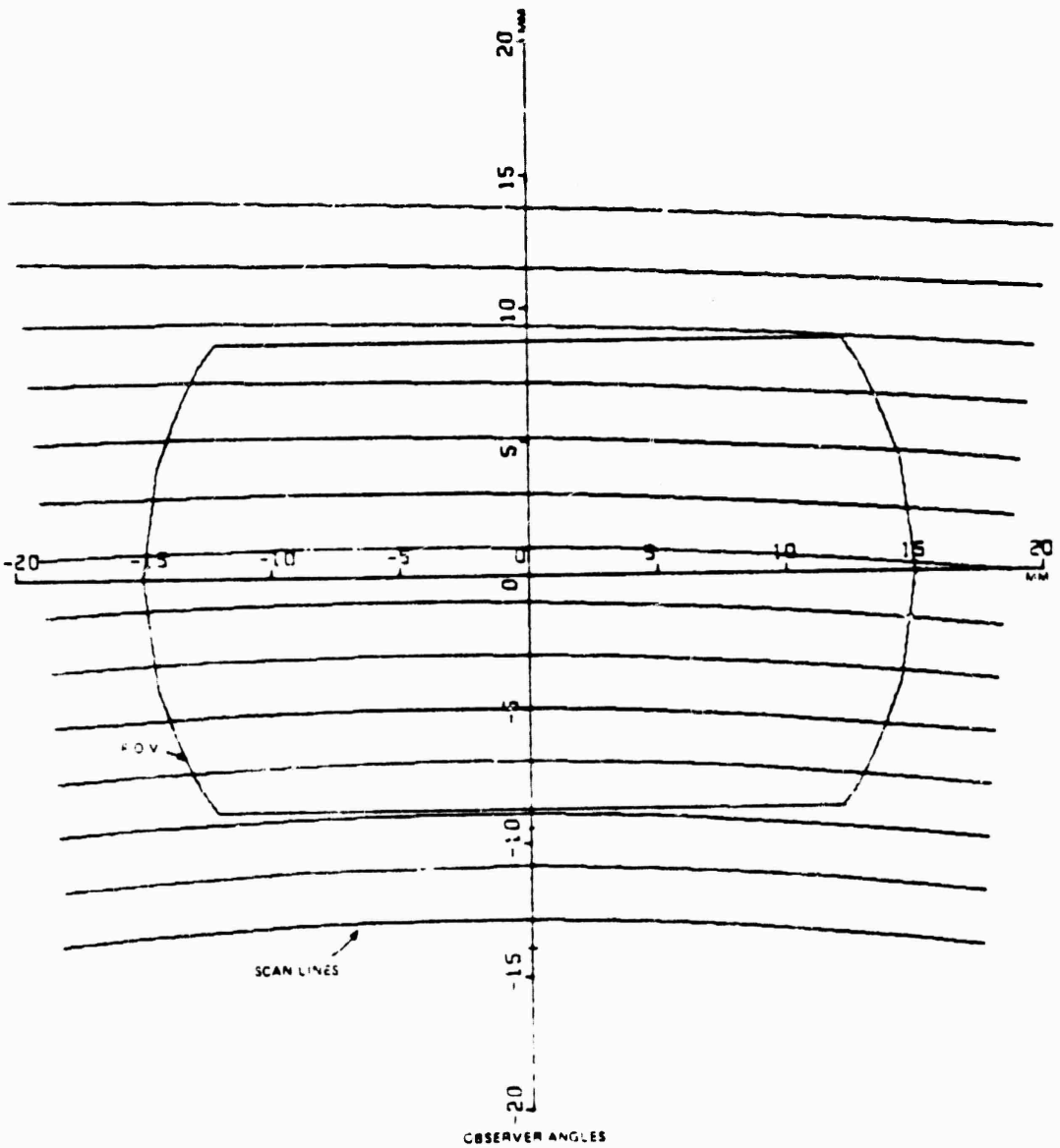

Figure 37. Camera Raster Plots (Sheet 4 of 8)

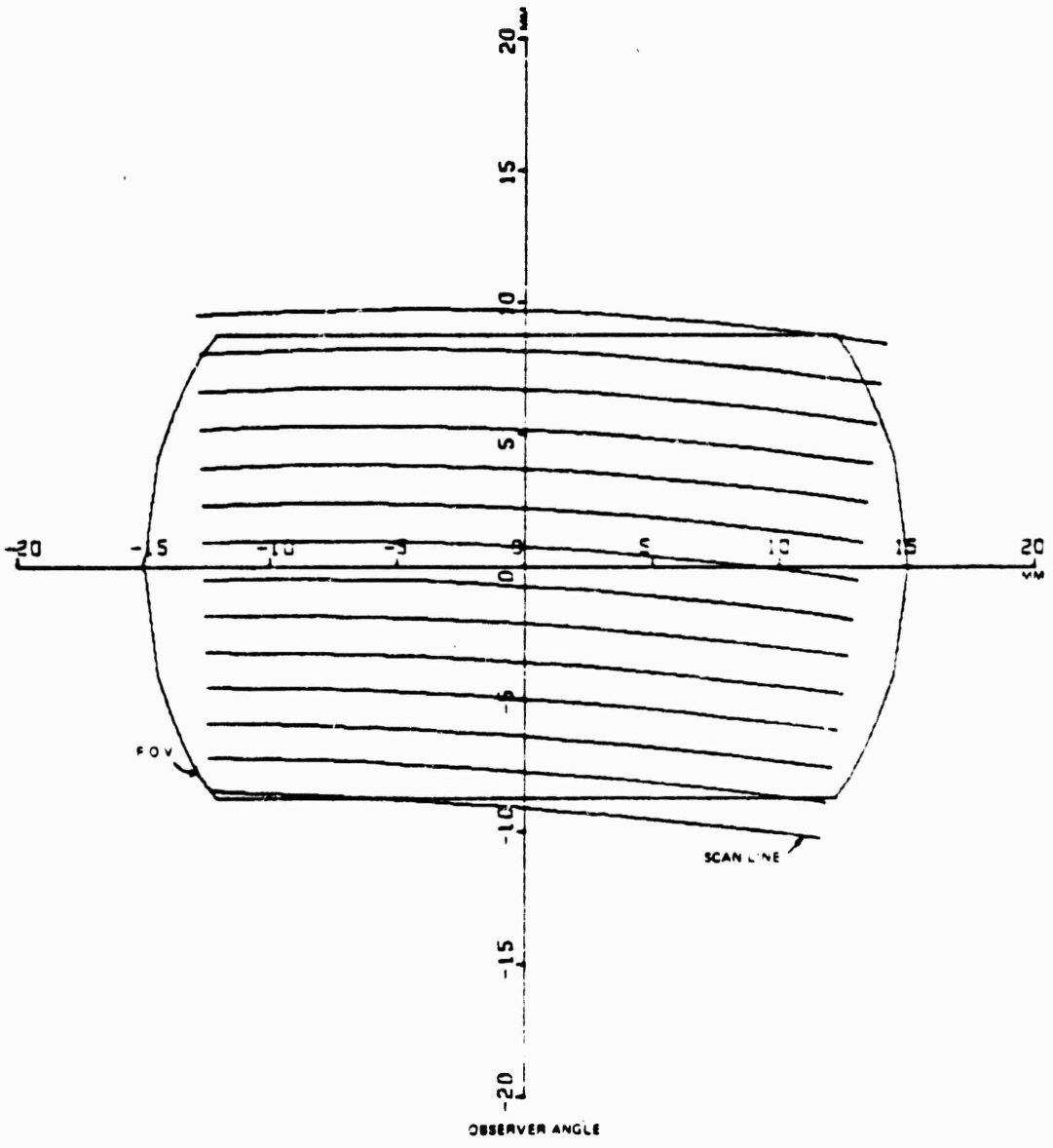

AZIMUTH=-80. ELEVATION=50.

AWAVS-A003-07.5

Figure 37. Camera Raster Plots (Sheet 5 of 8)

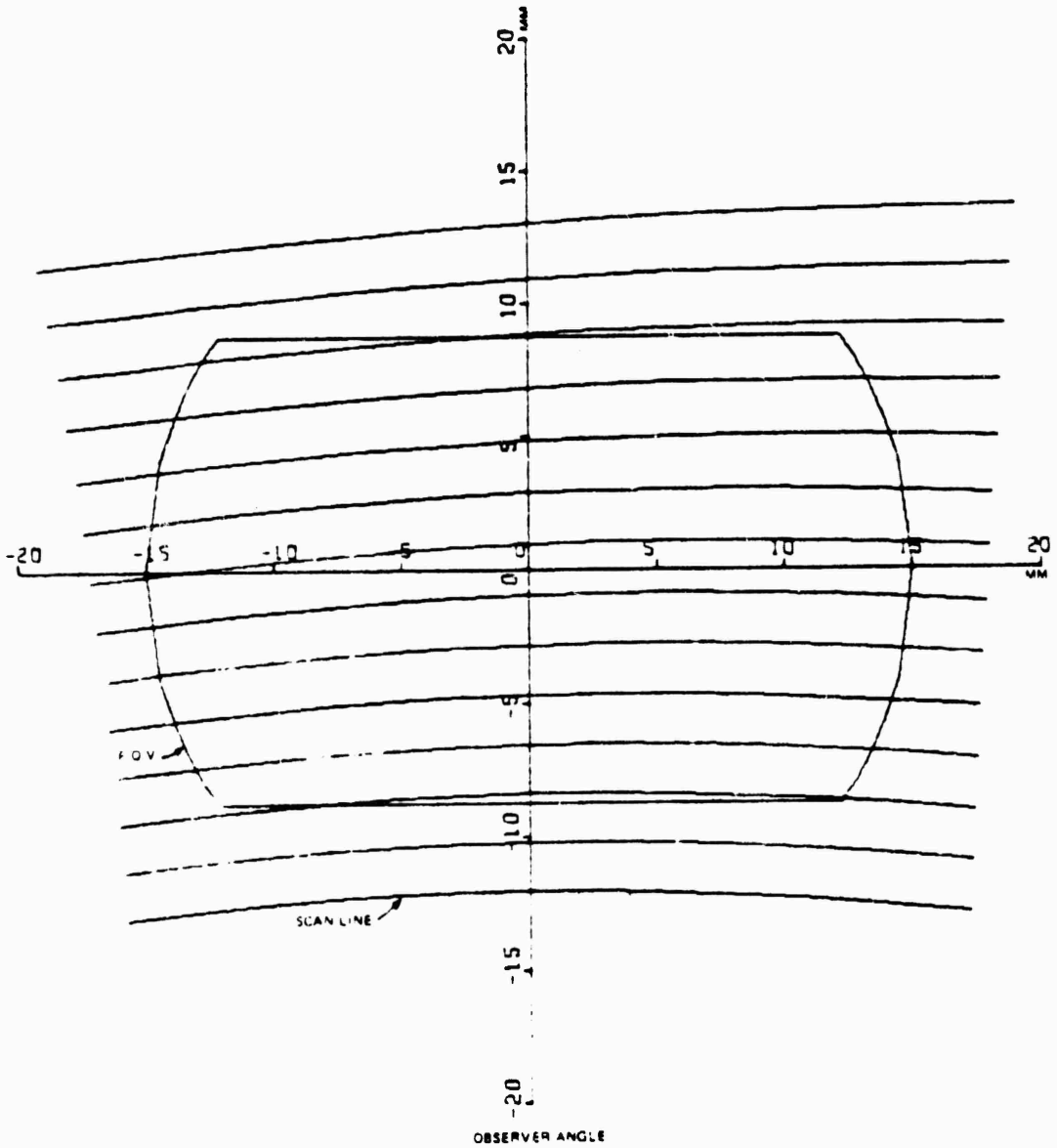

Figure 37. Camera Raster Plots (Sheet 6 of 8)

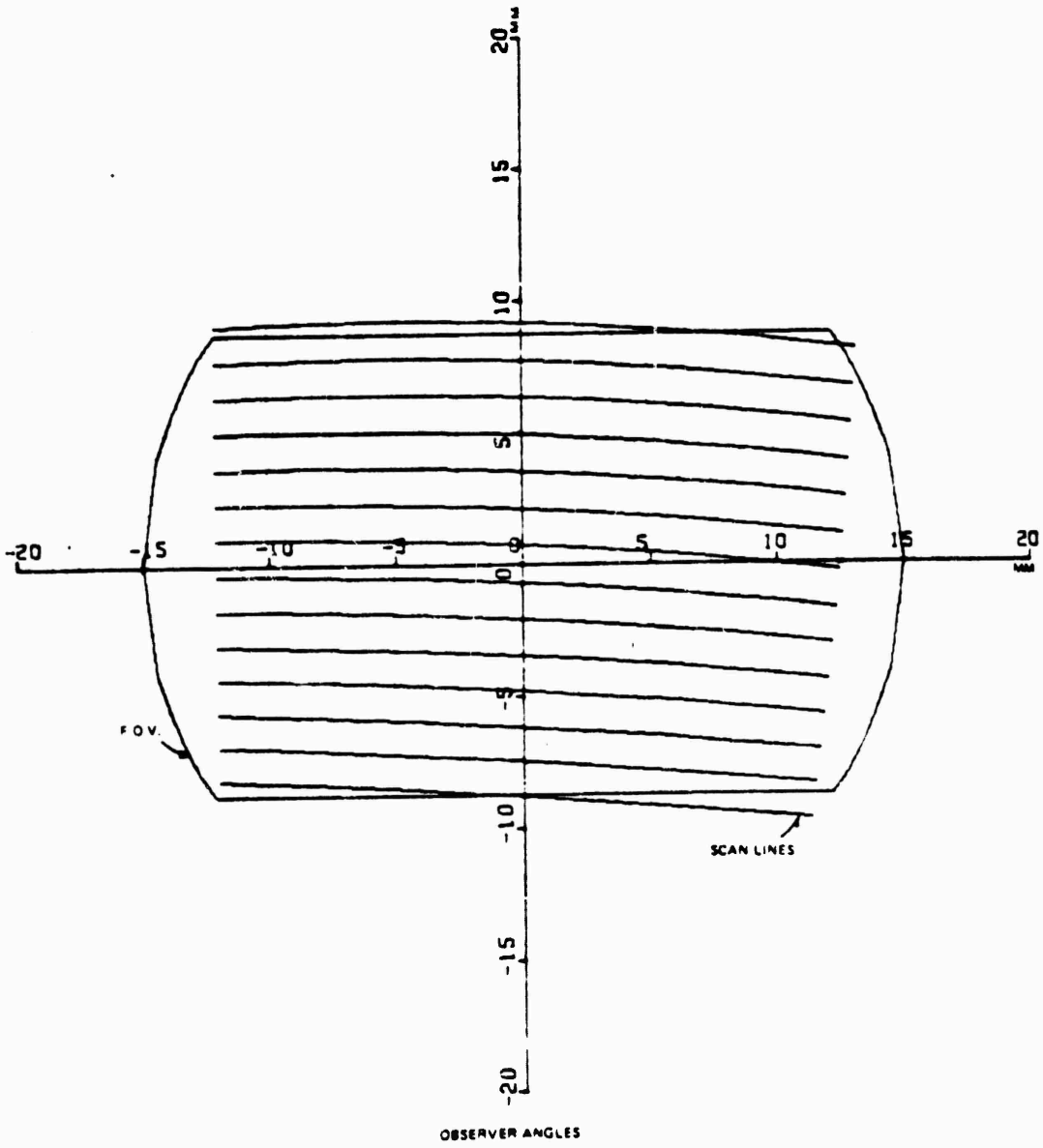

Figure 37. Camera Raster Plots (Sheet 7 of 8)

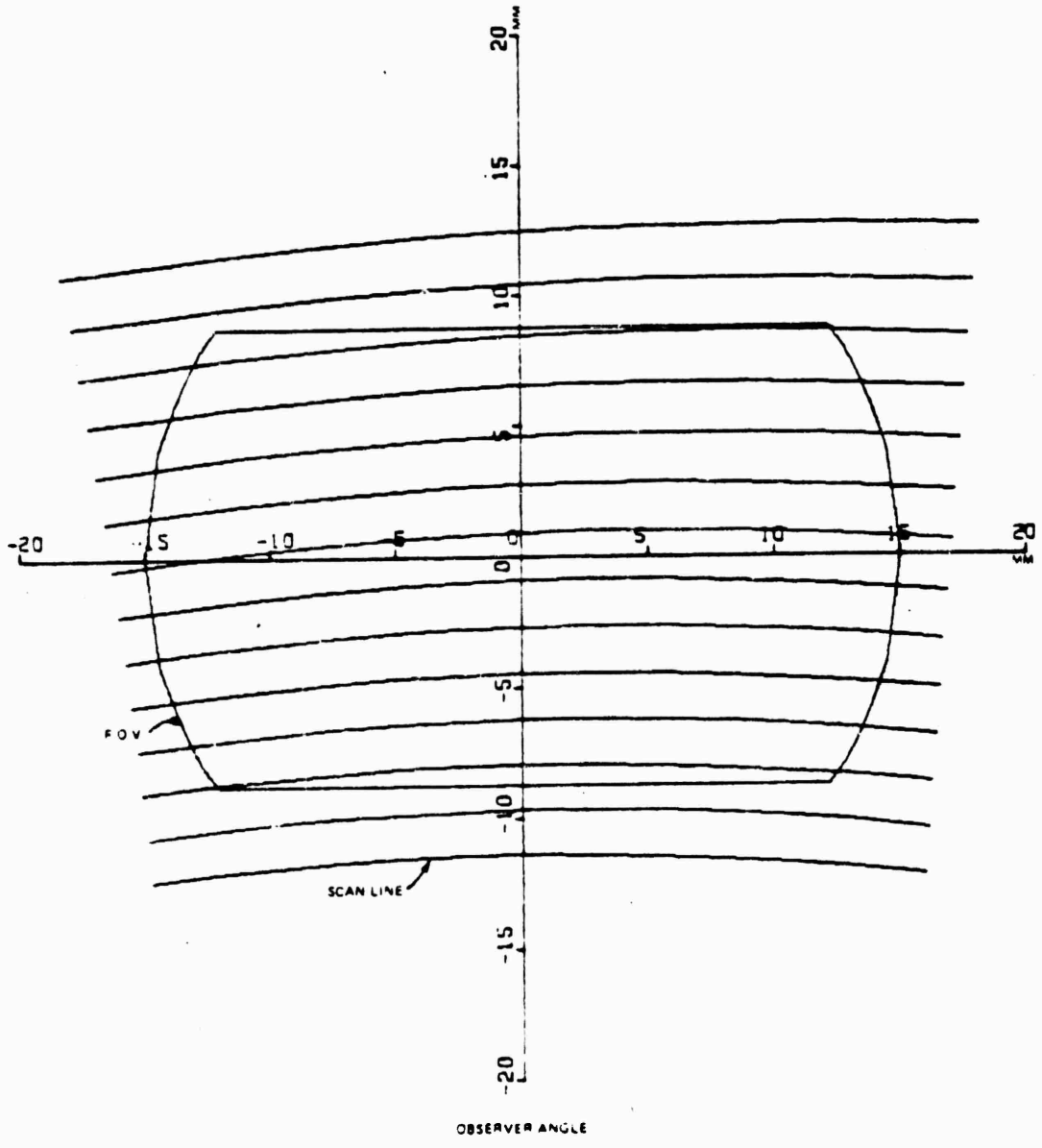

Figure 37. Camera Raster Plots (Sheet 8 of 8)

An FOV blanking circuit card provides a combination of circular and rectilinear blanking to provide the FOV shape shown in Figure 37. Design is incorporated so that this shape may be changed in size, under control of an analog output from the linkage. The dynamic FOV is thus implemented and controlled by computer when the foregoing need arises.

Due to the circular sides of the FOV shape, the FOV blanking circuit causes considerable "ringing" when used in conjunction with the processor module of the original "Hi-Res" illuminance camera. For AWAVS application, a different processor design is used which gives clean results with FOV blanking insertion. The video processor design as used with the AOI camera on the SAAC program is satisfactory for application in this TIG camera. A minor change is performed on this SAAC processor card so that the variable line rates may be used. This card has other advantages such as remote control of video gain and pedestal, and a gamma control that may be set to unity for normal, or to some other value if ever required.

Because FOV blanking is introduced to the output video from the TIG camera, vidicon blanking itself is rectilinear and must be bracketed by the video FOV blanking. The horizontal and vertical drives are simply differentially received, summed, buffered, and sent on to the vidicon blanking and decoupling card for vidicon blanking. The width of the drive is adequate for vidicon beam blanking. Vidicon sweep-fail protection is also introduced at this point.

3.1.4.1.2 Camera Lag Characteristics. A discussion of camera performance is not complete without consideration of the lag characteristics. The intensified 2-inch vidicon lag is specified at 25 percent, 50 milliseconds after removal of a peak white illumination. Since numerical values of lag provide little insight into its effect in picture quality, the following discussion has been prepared.

It is difficult to state what constitutes an acceptable level of lag performance, since the effects of lag are so subjective. However, as a practical matter it will be assumed that the 1-inch plumbicons used in commercial broadcast color cameras provide acceptable lag performance, since they are consistent with the latest state-of-the-art, and provide subjectively useful performance when one considers the applications from an image-motion standpoint; (i.e., the tracking of moving racing cars or a thrown baseball, representing motion rates as high as 50°/sec.).

The plumbicon decay to 5% after 50 milliseconds with motion rates of 50 degrees per second provides a level of performance that is subjectively acceptable.

In the case of the F4E #18 visual system, decay to 25% after 50 milliseconds with motion rates of 120 degrees per second are encountered. This causes a loss of image contrast which is dependent on the image tube residual signal level and the nature of the image being viewed. For example, when moving over medium or low contrast portions of the terrain model, the effect of lag causing image blur will be barely perceptible compared to moving over high contrast airfield lighting during night conditions. In the former case, the residual signal from the luminance channel remaining from previous TV fields will be masked by the chrominance information, and only small detail information is lost. In the latter case, where bright lights will be surrounded by a black background, the residual signals from the luminance channels will be more apparent, and some blurring of these lights will be visible.

In the AWAVS application, the camera is an area of interest (AOI) presentation, as opposed to being locked to the aircraft body axis as in the F4E camera model system. In AWAVS, the maximum motion rates anticipated are 34 degrees per second which are much smaller than motion rates found in F-4E No. 18. This 34°/sec converts to an image motion of 0.495 mm in 50 milliseconds on the vidicon surface. This motion is equivalent to 10.4 TV lines. In comparison to the commercial TV 1" plumbicon, the 50°/sec reduces to a motion of 0.275 mm in 50 milliseconds. This motion is equivalent to 8.7 TV lines. Thus the AWAVS lag characteristics are reasonable when compared to the best broadcast conditions.

3.1.4.1.3 Camera MTF. The camera raster plots contain the information required to specify the camera modulation transfer function. At the time of the AWAVS design analysis report, the best estimate of the camera raster format was a linear 5:8 aspect TV raster. The actual raster density function is contained in the raster plots which show the nominal resolution is 11.5 lp/mm horizontal. Variation between 10.8 to 15.3 lp/mm horizontal occurs due to the raster computer shaping. Figure 38 gives the camera modulation transfer function as a function of television lines. There are three curves presented which represent three conditions. The first curve represents a 1:1 aspect ratio where TV lines per picture height equal TV lines per picture width. The two other curves represent a standard 3:4 aspect ratio. One curve represents TV lines per picture width. The right-hand vertical scale is expression in lp/mm. Thus, knowing lp/mm MTF can be read directly from the left-hand vertical scale. The normal MTF is 0.77 horizontal while variations between 0.79 to 0.64 occur at the raster center due to the raster computer shaping.

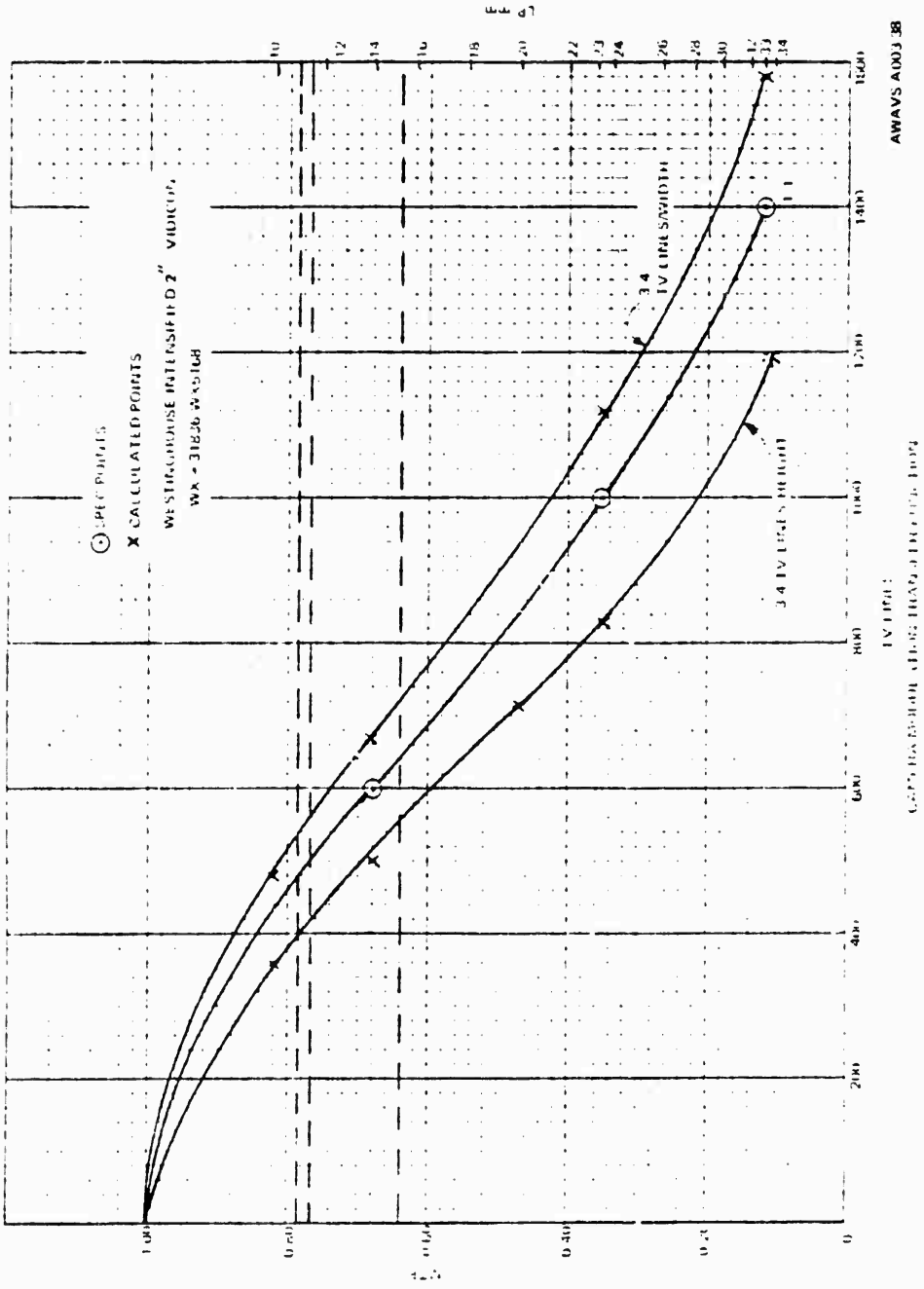

Figure 38. TIG Camera Modulation Transfer Function

3.1.4.1.4 Target Efficiency. Vidicons have the characteristic such that target signal current is a function of illumination, target voltage, and scan velocity. In conventional fixed-raster application, the scan velocity variable becomes immaterial. In the AWAVS application, however, the raster (thus scan velocity) is always changing, as a result of target projector pointing changes (Figure 37). This means that target current, and therefore video level, would vary according to target projector pointing, and would be most undesirable. This effect is eliminated by using an "auto-target" circuit. The auto-target circuit detects peak white video, integrates this level over the entire FOV period, and compares it against a fixed reference. When this peak white video deviates from the desired video reference level, an error is created which is amplified and applied to the target voltage in such a way as to maintain a constant peak white level. This correction, however, does not function for illumination changes due to target attitude and zoom, because the vidicon target photo surface is a selenium compound. A computer-controlled variable probe iris and servo must be employed in the target camera probe optics to correct for illumination variations, and the auto-target only handles the raster effects.

3.1.4.1.5 Shading. The "portholing" characteristic of vidicons results in undesirable shading in the displayed video from center to the edges. With raster shaping, the shading takes on irregular shapes which detract from target video information. This is more undesirable than the circular pattern of shading in the case of linear rasters. A circuit card is used in this AWAVS application to minimize the shading due to "portholing" and thus eliminate the undesirable shading patterns in the projected target image. The shading signal card generates a pair of parabolic waveforms; one which describes a horizontal rate, and the other a vertical rate. These are controlled in amplitude and summed together. The video amplifier system contains a module with an FET mixing stage, which linearly controls video gain from a control signal. This control signal is the sum of the parabolic waveforms. Thus, the video gain is varied in a 2-dimensional parabolic function and the "portholing" shading is thus compensated for.

3.1.4.1.6 Interline Interference. This not bothersome unless the raster is dynamically changing as it does in AWAVS. An erase field would help to eliminate this problem, but is not used in AWAVS due to deflection bandwidth limitations in the projector. An aid in minimizing this problem to acceptable levels is a "hard" cutoff of the vidicon beam during retrace blanking. The vidicon blanking circuit of the Hi-Res camera system is insufficient to do this. A blanking pulse of 100V or more is required for the purpose. A new blanking and decoupling card is used in this AWAVS application. The vidicon cathode blanking driver circuit is of a cascade design so that the blanking will swing over 100 volts with a switching time no greater than 50 nanoseconds.

3.1.4.2 Dynamic Analog Raster Computer. Camera complex raster shaping at the target television camera is required for proper image mapping on the system display screen. Corrections for both the camera and projector lens systems, and for the off-axis position of the target projector relative to the display screen must be incorporated. All raster shaping will occur in the target camera. Raster shaping cannot be applied at the target projector, due to the inflexibility of the light value raster format. Horizontal and vertical deflection waveforms are generated by a dynamic analog raster computer (DARC) and applied to linear deflection amplifiers driving a low-inductance yoke. A relatively wide-band linear amplifier with a small signal (non-slew-rate-limited) bandwidth of at least 10 times the horizontal scan frequency is required for the horizontal deflection field to maintain a faithful reproduction of the camera raster computer waveform.

The function of a DARC is to generate complex V_X and V_Y waveforms which are used to control the trajectory of election beams in the camera. Figure 39 outlines the general equation for generating these waveforms (V_X and V_Y), and illustrates a general block diagram to implement the equations.

Waveform coefficients are the so-called "mapping coefficients" and are uniquely determined for given azimuth and elevation coordinates of field of view. That is, for a given target projector azimuth and elevation, a unique set of values is input from the simulator system digital computer, and these coefficients in turn scale their various corresponding waveforms.

The DARC waveform generator forms a variety of shapes from horizontal and vertical triggers by successive analog integration. Digital coefficients operate on these waveforms through MDAC's (multiplying digital-to-analog converters). The results are summed to form composite V_X and V_Y waveforms. There is a practical limit to the number of waveform terms, imposed by the error terms in the analog integration process.

3.1.4.3 Television Camera Head. The high resolution camera head is a modular assembly, stiff and simple, with strong design emphasis on providing only necessary adjustment motions and eliminating excess or redundant motions. The main components attached to the front plate of the Z-carriage are the optical probe (cantilever mounted), the beamsplitter mount, and the front mount of the luminance camera.

The case of the luminance camera is a 6-inch square tubular shape composed of a U-shaped cover and a fourth side consisting of a semi-fixed front cover and a service cover. The longer service cover may be removed at any time without loss of alignment and is on the bottom of the luminance camera when installed, but on the top side when bench tested. The cover allows access to the coils, coil connections, vidicon socket, and associated printed circuit cards.

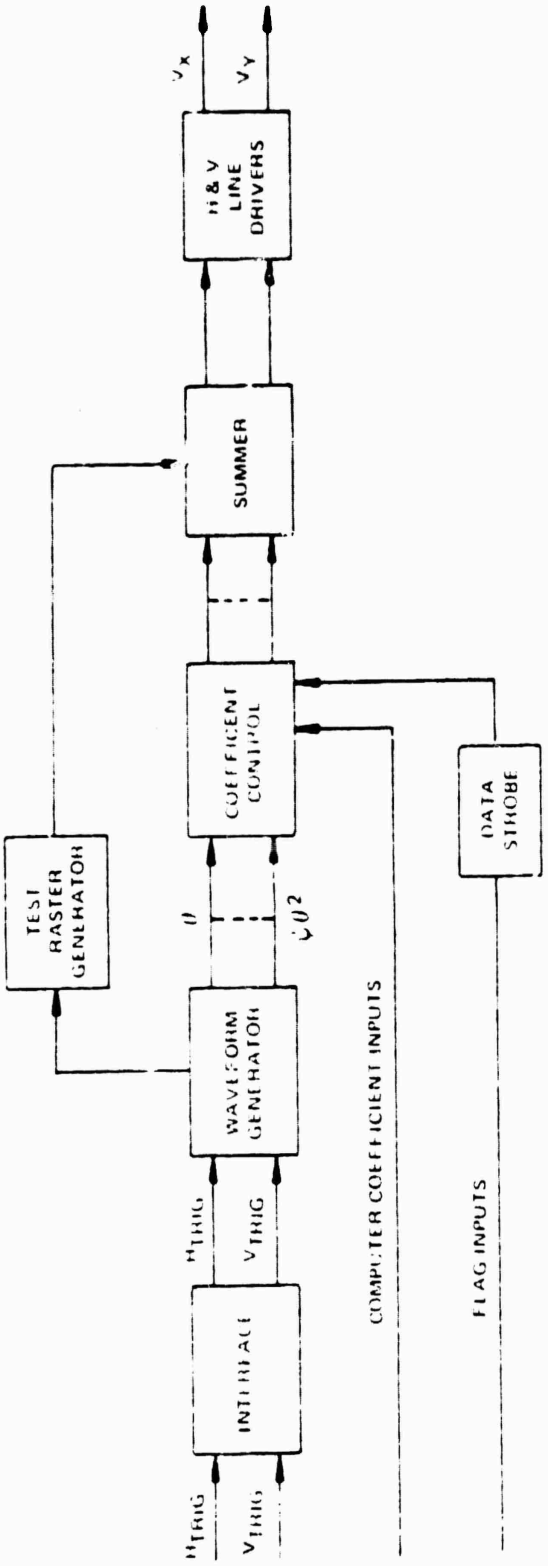

Figure 39. TIG Camera Dynamic Analog Raster Computer, Block Diagram

The intensifier-vidicon assembly is mounted in a 4-inch diameter, 4-inch long split sleeve at the input end and cantilevered back through the deflection and focus coils to the vidicon socket. The 16-inch length of the intensifier and the input face of the vidicon requires a non-redundant type of mounting. There are four adjusting screws located near the intensifier face plate which push the vidicon against a ring of springs $\pm$0.2 inch axially into or out of the deflection and focus coil assembly for optimizing corner resolution. The deflection coil assembly may be moved laterally $\pm$0.05 inch at either end relative to the cantilevered vidicon. These two motions enable optimum positioning of the coils in relation to the actual electronic axis of the vidicon, both for tilts and translations in the X and Y planes. Additionally, the deflection coil (inner coil) may be rotated about the vidicon axis in excess of 10° by screw adjustment to accurately align the luminance camera raster. The vidicon is aligned in azimuth about the tube axis by a keyed plate between the vidicon base and the vidicon socket. The keyed plate is spring loaded, compressing the vidicon into the intensifier with approximately four pounds of force.

3.1.4.4 Camera PC Card Bin. A 10 x 13-inch card bin is located on the camera head to the right of the luminance camera. The bin swings out and is comprised of two layers: the first layer (top) contains eight printed circuit cards and a fan-cooled heat sink; the second layer contains two power supplies (+18V and -18V). It includes circuitry for retrace and FOV blanking, control of vidicon beam scanning parameters, and gain and buffering of the target video signal.

3.1.4.5 TIG Camera Control Unit. The camera control unit (CCU) accepts the high voltage from the camera HVPS and generates the vidicon beam voltages which are applied to the camera PC card bin. Figure 40 shows the CCU front panel. Functions of the ON-OFF switch, power indicator lamp and power fuse are self-explanatory. The BEAM, TARGET, and FOCUS controls adjust the beam current, target voltage, and beam focus, respectively, to match characteristics of individual vidicons. The GAIN control adjusts the overall gain of the video output to the special effects generator, while the PEDESTAL adjustment is for control of the TIG camera video pedestal (blanking depth).

3.1.4.6 Target Special Effects Generator. As discussed later in paragraph 3.4.3 (Background Special Effects) the relationship between video output, camera video and cloud function may be expressed as:

$$e_0 = G\, e_1 + (1-G)\, e_2$$

where,

e_1 = camera video
e_0 = video output of SEG
e_2 = cloud function
G = gain function

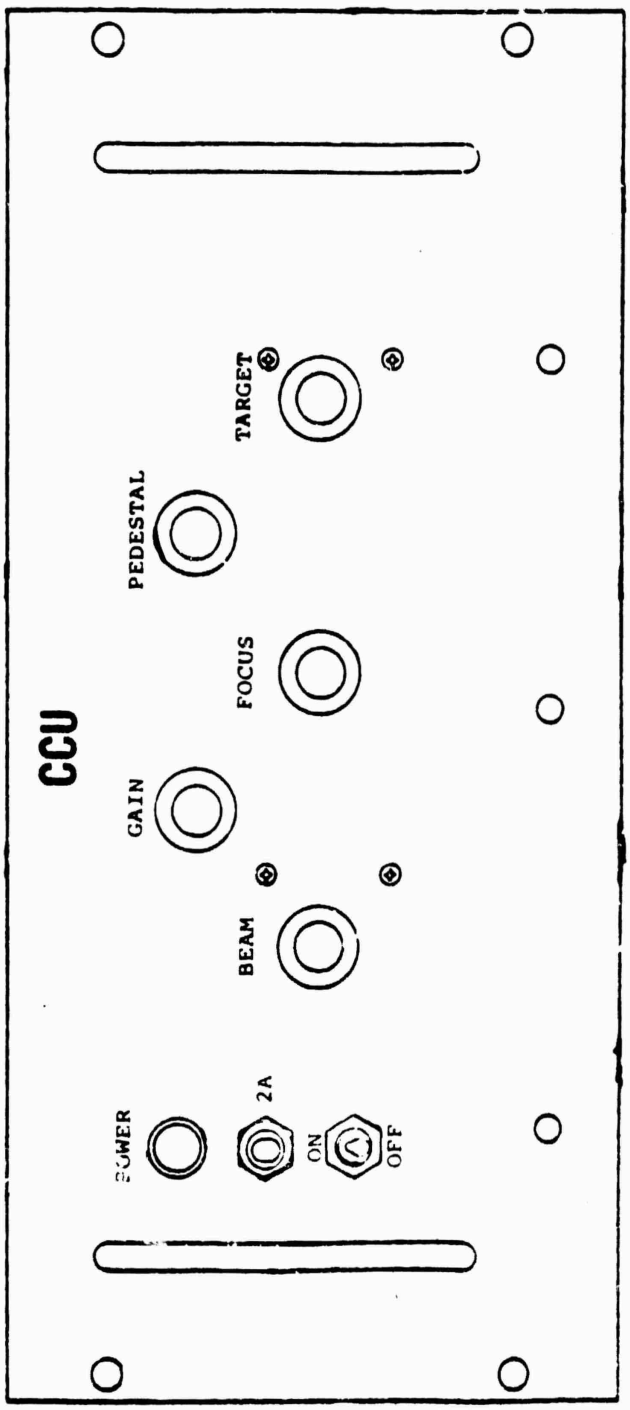

Figure 40. TIG Camera Control Unit, Front Panel

G may be expressed as:

$$G = e - \frac{KR}{RVR}$$

where,

K = constant for scale factor
R = slant range
RVR = runway visibility range

For the target image, the slant range to the camera may be assumed to be constant for any point on the carrier for fog insertion. This has the effect of uniform fog density over the carrier. Referring to the first equation, above, the output may be considered to be composed of two parts. The first part ($G\ e_1$) is done on the target special effects card, where G is under computer control. This is the portion which fades in and out target video. The second portion of the equation is $(1-G)\ e_2$. This is the change in white level by fading in and out cloud level. This portion is done by the background special effects generator. (See paragraph 3.4.3.)

The target special effects generator is physically located on one circuit card housed in the BIG special effects generator card bin. This design is for convenience of accessibility to the dc power supplies and test pattern generator.

3.1.4.7 Image Enhancer. The image enhancer processes the TIG video output from the special effects generator, and provides two isolated outputs for the enhanced video - one to the target projection system (via a loop through the TIG video monitor) and the second to the Experimenter/Operator Station for monitoring only. The image enhancer is purchased according to SPD Drawing 1002782 with specifications as listed in Table 16. The enhancer provides horizontal image enhancement by modulating the video amplitude as a sinusoidal function of frequency while maintaining a linear phase shift. The amplitude of the transfer function is essentially as follows:

$$1 + E_m\ (1 - \cos \omega\ t_d)$$

where,

E_m = one half of the maximum (adjustable) peaking amount

ω = radian frequency = $2 \pi f$

t_d = delay time introduced by the delay line used in the correction circuit

The peak frequency (f_p) is chosen to be approximately 16 MHz, where

$$\cos \omega_p\ t_d = -1$$

or

$$\omega_p t_d = \pi$$

and the delay time required $= \frac{\pi}{\omega_p} = \frac{1}{2 f_p} = \frac{1 \text{ sec}}{2 \times 16 \times 10^6} = 31.2$ nanoseconds. A miniature coaxial cable is used for the time delay; and the delay time can be optimized by trimming the cable length if necessary. Peaking amount is set to be 2 times ($E_m = \frac{1}{2}$) and camera gamma correction is adjusted for unity.

The image enhancer has a coring circuit which introduces a knee to the transfer curve for the detail signal. It attenuates any signals below a threshold level and transmits that above. The threshold level (coring amount) is adjustable and will be set during integration of the visual system. The coring circuit, while improving the signal-to-noise ratio of the enhancer, also results in removing any picture detail that falls below the threshold. Consequently, for the enhanced picture with excessive coring, large transitions will be enhanced while fine details will tend to get lost resulting in cartoon-like images with sharp outlines but no texture in between. Proper use of the coring circuit will be tested during system integration.

The front panel controls and indicators for the image enhancer are illustrated in Figure 41. Functions of the ON-OFF switch, POWER indicator light and fuse are self-explanatory. The DETAIL GAIN control is a potentiometer for controlling the degree of enhancement added to the target video signal. LINE RATE SELECT is a 3-position switch that provides the most visually satisfying image for the selected line seam rate (525, 825, or 1025). With the PROCESS/BYPASS switch in PROCESS position, the video signal is being acted upon by the image enhancer, and the amber PROCESS INDICATOR lamp is lit. When in the BYPASS position, the input video signal is routed directly to the output connector, and the light is off. The INPUT and OUTPUT front panel connectors are for test only, and are connected directly to the VID IN and VID OUT connectors on the chassis rear apron.

TABLE 16. VIDEO IMAGE ENHANCER SPECIFICATIONS

Input Impedance	75 ohms
Output	Dual output, 74 ohms
Output Isolation	-40 db minimum
Input and Output Video Standard	0.7 volts peak-to-peak; non-composite
Vertical Field Rate	60 Hz
Horizontal Line Rate	1021
Frequency Response	±1/2 dB 60 Hz to 30 MHz
Peaking Frequency:	
@ 525 line scan rate	8 MHz 500 kHz
@ 825 line scan rate	12.5 MHz 500 kHz
@ 1025 line scan rate	16 MHz 500 kHz
Peaking Amount	0 to 12 dB continuously variable
Coring	Coring shall be available with an internal control for coring amount
Low Frequency Tilt	Less than 1% with standard window pattern
Front Panel Controls	Power on/off, bypass/process switch, detail gain
Video Connectors	BNC type
Dimensions	19" wide, 1-3/4" high, 10" deep suitable for rack amount
AC Input	105 - 130 volts, 48 to 63 Hz, 20 watts

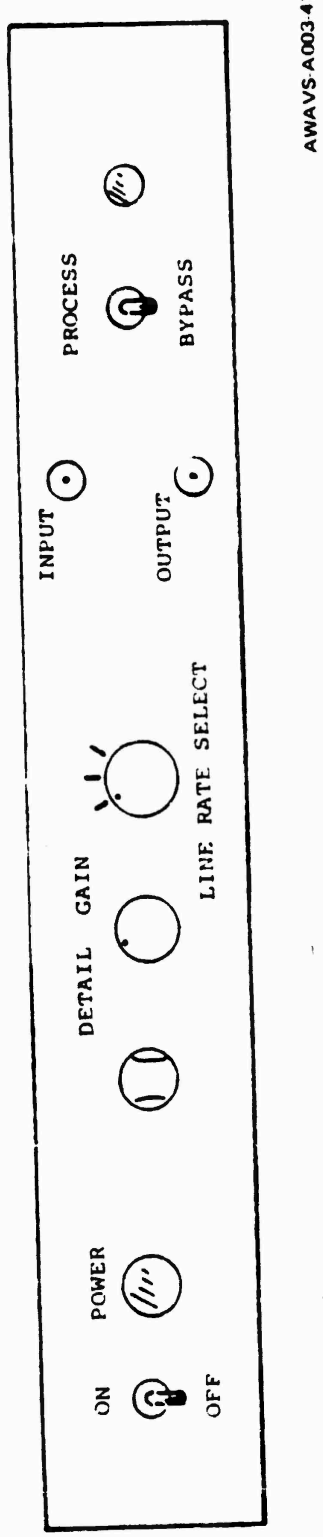

Figure 41. Video Image Enhancer, Front Panel

3.1.4.8 TIG Maintenance Panel. The TIG cabinet maintenance panel, Figure 42, is used to select the scanning line rate and external sweep source for the TIG television camera. The LINE RATE SELECT switch is a 3-position toggle switch that allows for selection of 525, 825, or 1025 line horizontal scan rates. A second 3-position toggle switch placarded CAMERA SWEEP SELECTOR is used to select the the source of X- and Y-deflection signals used by the vidicon. In the computer position, deflection signals are supplied from the target DARC; these are shaped to correct for perspective and mapping errors. In the LINEAR position, a conventional sweep is applied directly from the master timing generator, bypassing the DARC. The DARC TEST position applies a specially shaped sweep for maintenance and alignment purposes only. The TIG/SKI POWER MAINT switch is an alternate action pushbutton device used to interrupt application of dc power to both the TIG cabinet and the SKI electronics drawer of the BIG electronics cabinet. It is light green under normal conditions and red when power is interrupted for maintenance.

3.1.5 Gantry System. The optical probe, monochromatic camera, associated optical elements, and electronic devices are rigidly mounted to the Z-axis carriage, the motion of which is normal (perpendicular) to the model plane. The Z-axis carriage assembly is secured at three places to the Y-axis carriage assembly through the medium of self-aligning linear ball bushings and precision guide shafts. The Z-axis drive motor and shaft are mounted to the Y carriage and effect translation of the Z-carriage by means of a Roh'lix linear actuator fastened thereto. The Y axis carriage is attached to the tower in similar fashion and is also driven the height of the tower through the medium of a Roh'lix linear actuator translating along the drive shaft attached to the tower.

The tower is mounted to a trolley assembly having two wheel supports on the precision steel X-guide rail. The X-guide rail is mounted solidly to a steel I-beam assembly which, in turn, is bolted and grouted to the facility floor. Static equilibrium is obtained through an extension to the upper part of the tower toward the upper X-guide rail attached to the top of the model support structure which incorporates guide rollers in contact with the rail. One trolley wheel forms an integral part of the X-drive assembly, and tower motion is imparted thorugh friction between the wheel a and the lower X-axis guide rail. Rotary optical encoders, together with rack and pinion action in all three axes, provide for position feedback.

Limit switches and operating ramps are provided in all three axes to slow down and stop their respective drive motors. The X and Y axes are also furnished with hydraulic shock absorbing devices capable of dissipating the maximum kinetic energy that can be acquired in either axis. A hard mechanical stop is furnished on the Z carriage to prevent probe contact with the surface of the carrier when it is in the level position.

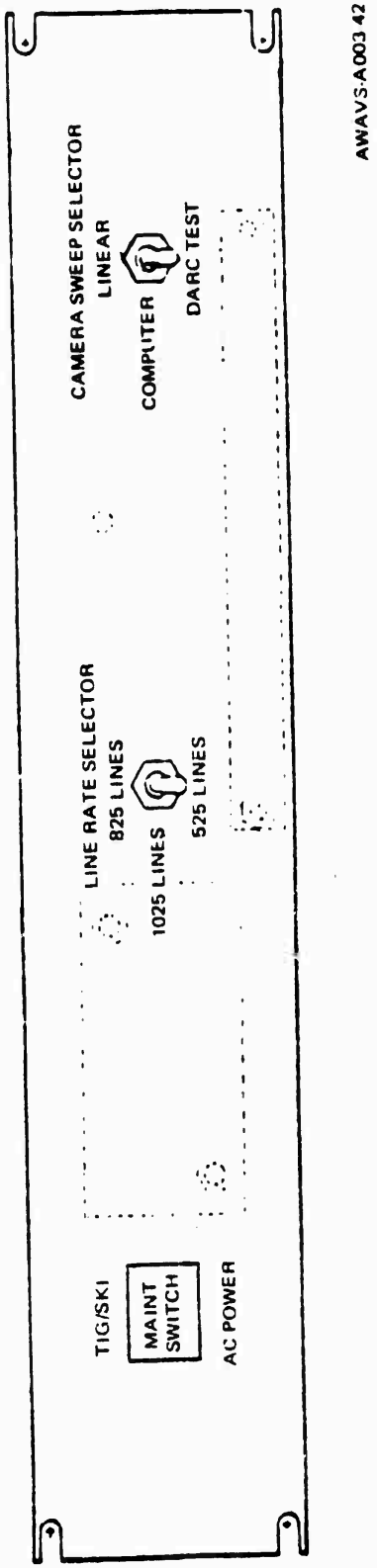

Figure 42. TIG Cabinet Maintenance Panel

3.1.5.1 Gantry Cabinet. The gantry cabinet contains the gantry drive control electronics, encoder position readout (LED) display, and the gantry maintenance panel. The gantry drive control electronics are predicated on providing the operator with the ability to select between computer and manual control of the gantry servo system. Complete isolation between control units is provided.

3.1.5.2 Maintenance Panel. The maintenance control panel provides for substitution of manual control for computer control of all servos and model lighting subsystems. These will be under the control of maintenance personnel.

The gantry maintenance panel (placarded TEST PANEL) is illustrated in Figure 43. Controls directly relating to gantry operation carry the major placarding of GANTRY POSITION READOUT, AXIS OVER-SPEED TEST, SYS CONT, and GANTRY AXIS RATE. These,along with the MAINT and GANTRY FREEZE pushbuttons which control dc power application, are discussed herein. Other groups of controls are covered along with the systems or subsystems with which they interface or control. These controls and their paragraph references within this report are as follows:

Light bank controls	para 3.1.2.3
Carrier model lights	para 3.1.1.6
Optical probe servos	para 3.1.3.6
Carrier model servos	para 3.1.1.6

The MAINT switch at the top of the panel is an alternate action device that interrupts ac power to the gantry cabinet when depressed. It is lit green under normal operating conditions and red when depressed for maintenance. When activated, the MAINT switch actually opens the gantry cabinet circuit breaker in the VTFS power distribution cabinet, and prevents it from being reset. The GANTRY FREEZE switch functions in a similar manner to stop all motion along the X, Y and Z axes. The X, Y and Z POSN GANTRY POSITION READOUT displays each consist of 16 light emitting diodes, arranged to provide a straight binary readout relative to gantry position along its respective axis. Lights are labeled in powers of two to provide for simple decimal conversion.

The AXIS OVSP TEST group is comprised of one momentary contact 2-position, center-off toggle switch, one OVSP indicator light for each axis, and a single RESET momentary pushbutton. When an overspeed condition is sensed by the overspeed pc card relative to one axis, the applicable OVSP indicator lights and motion of all three servos is frozen. Each toggle switch can be used to simulate an overspeed condition in either direction (+ or -) for test purposes. Momentarily depressing the RESET button resets all three servos to normal operation.

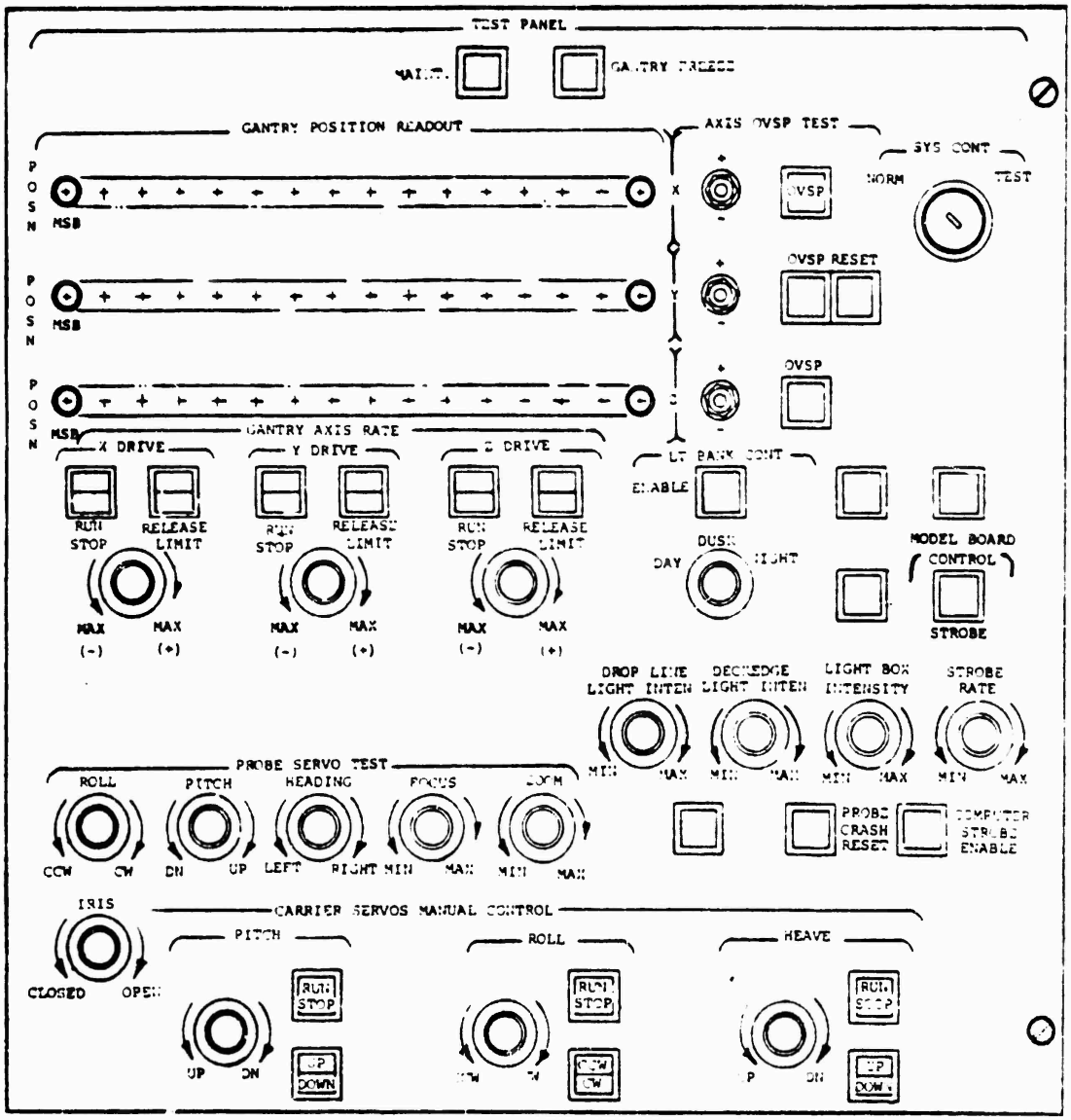

AWAVS-A003-43

Figure 43. Gantry Cabinet Test Panel

The GANTRY AXIS RATE group provides the controls to start, stop, and modify the velocity and direction of each servo. An identical group of three controls governs operation of each servo. The RUN/STOP switch is an alternate action pushbutton device to start and stop the servo. The pushbutton lights to indicate the selected position. The velocity control knob establishes the direction of travel (+ or -) and the velocity for each axis. Velocity increases as the control is moved towards either extreme and is zero when the control is centered. The positive (+) direction for each servo is:

X-axis	toward the right
Y-axis	upwards
Z-axis	away from model board

The RELEASE/LIMIT switch is a momentary device which indicates that the servo has reached the end of its travel by lighting of the LI LIMIT segment. When this occurs, the gantry enters a freeze state. The velocity control is then reset to the opposite position, and with the RUN/STOP switch at RUN, the RELEASE/LIMIT switch is depressed. The LIMIT light is extinguished and the RELEASE light comes on.

A key-lock device labeled SYS CONT allows maintenance personnel to control mode of operation. By inserting the key into the lock and turning the lock from the NORM to the TEST position, the visual system is taken off-line from the computer, allowing maintenance procedures to be performed.

3.1.5.3 Tower Cabinet. The tower cabinet contains the gantry servo amplifiers, the optical probe electronics, and dc power supplies for the servos, probe, and TIG television camera. Probe electronics and power supplies are discussed with their appropriate subsystem block diagrams, while the gantry servo amplifiers are covered in the following text.

3.1.5.4 Gantry Servo System. The function of the gantry servo system is to drive the probe around the model in accordance with the simulated location of the aircraft. The gantry servo system drives the gantry in three translational degrees of freedom. The servo system designs are primarily directed toward providing smooth, precise control over a wide range of velocities. The servos track the flight profile of the aircraft within the computation rate of the flight equations to an accuracy consistent with motion and instrumentation. The three translational degrees of freedom - X, Y and Z axes - correspond to the model horizontal length, vertical height and horizontal depth (i.e., aircraft altitude, the dimension perpendicular to the model surface). The gantry servo system transports the gantry mounted probe and television camera over the model at the scaled position, velocity, and acceleration of the simulated aircraft.

For smooth operation, the basic servo loop is an analog velocity servo. To remove errors of integration and to provide increased accuracy at very low velocities, an additional high-gain position loop is closed through the computer. Wide dynamic range dc tachometers and direct drive dc torque motors are used to achieve smooth, jitter-free wide dynamic range operation. The effects of back-lash and drive train compliance are eliminated by mounting the motors and tachometers close together on the same shaft, and driving the load directly without intervening gear trains. The drive torque on all axes is transmitted by friction drives. The X-axis drive torque is transmitted by a wheel machined as part of the motor hub. This wheel supports one-half of the weight of the gantry structure and rides on a hardened steel rail of circular cross section. Drive torque in the Y and Z axes is transmitted by a Roh'lix drive assembly.

Operating ranges and inertia loads vary from axis to axis; therefore the compensation electronics and drive ratios will be different for different axes. High-performance motor/tachometer combinations are used to drive the Y and Z Roh'lix units, and a special high-torque motor has been developed to meet X-axis requirements. All servo designs are based on a design concept utilizing a velocity drive command from the computer, direct tachometer feedback, and shaft encoder position sensing.

The block diagram of a typical gantry servo is shown in Figure 44. The gantry servos can be operated under computer control or manually from the gantry cabinet. In the manual mode, the servo differentially receives a velocity command from the gantry cabinet, which passes through the compensation and summing electronics, power amplifier and run relay to drive the dc torque motor. The commanded velocity is maintained by feeding the dc tachometer voltage back into the compensation and summing electronics and summing it with the command input signal. The resulting difference, or error, signal from this summation is amplified and increases or decreases the motor velocity and tachometer output voltage to reduce the error signal to a minimum. Thus the gantry velocity is maintained at the commanded velocity.

In the operational mode each servo is driven from the computer. The computer generates gantry velocity drive signals from the flight equations. These signals are converted from digital-to-analog form in the Y-carriage subcontroller. The basic servo loop operation is identical to that in the manual mode. In addition, gantry present position information is monitored by position shaft encoders and sent back to the computer. The computer compares the actual gantry position with the computed position and modified the velocity command to remove any errors of integration.

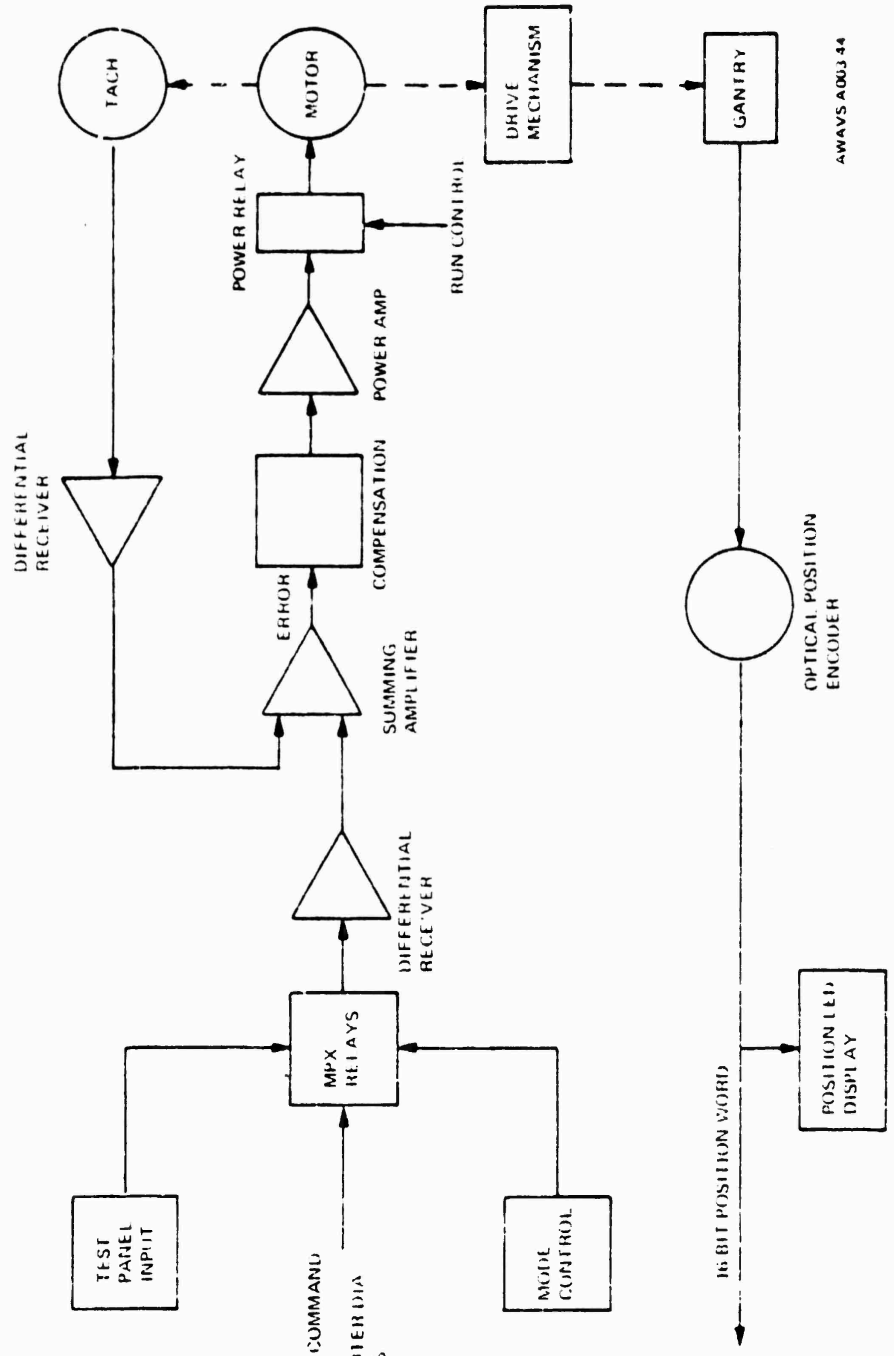

Figure 44. Typical Gantry Servo (X, Y, or Z) Signal Flow Diagram

The position encoder is a 32-turn optical encoder unit. In each of the three axes of gantry travel the encoder is driven by a pinion gear which is spring-loaded against a stationary rack mounted on the servo support member. (See Figure 45.) For example, the X-axis encoder is mounted on the gantry tolley and the rack is attached to the gantry rail support structure.

The 16-bit data word is directly transmitted to the computer. The data word is also buffered and used to drive position display read-out lights on the gantry cabinet maintenance panel.

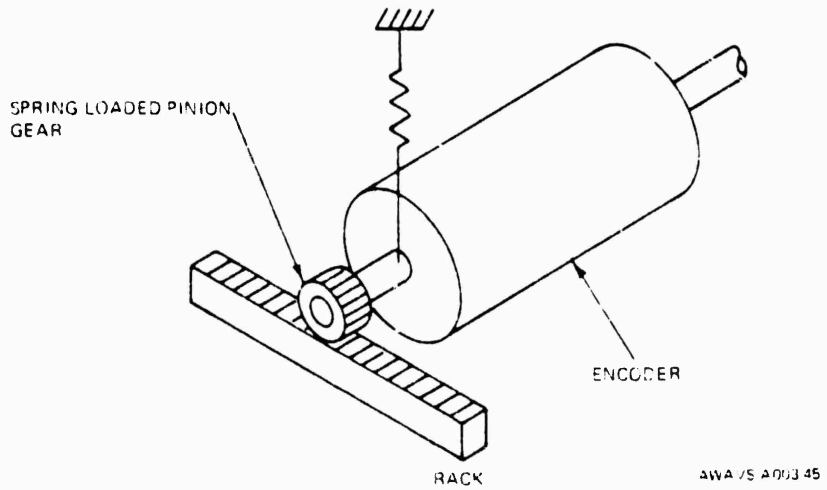

Figure 45. Position Feedback Encoder Mounting

3.1.5.5 Gantry Servo Analysis. Tables 17 and 18 describe the performance specifications and maximum allowable tracking errors, respectively, for the gantry X, Y and Z axes. The analysis given in the following paragraphs was performed to verify these parameters.

TABLE 17. GANTRY SERVO PERFORMANCE PARAMETERS

Axis	Range	Velocity	Acceleration	Resolution	Linearity
X	±11 ft	2.186 ft/sec	0.348 ft/sec^2	0.0015 ft	0.05%
Y	±11 ft	2.186 ft/sec	0.348 ft/sec^2	0.0015 ft	0.05%
Z	±2.7 ft	0.274 ft/sec	0.261 ft/sec^2	0.0015 ft	0.05%

TABLE 18. GANTRY SERVO TRACKING ERRORS

Axis	High Speed Tracking Error	Low Speed Tracking Error
X	0.1% at 90% velocity	0.05% at 10% velocity
Y	0.1% at 90% velocity	0.05% at 10% velocity
Z	0.1% at 90% velocity	0.05% at 10% velocity

3.1.5.5.1 X-Axis Acceleration and Velocity Analysis. A 30 lb-ft motor is used to meet the acceleration requirement. The motor mounting hub is formed into a 3.6 inch diameter wheel which rides the X-axis drive rail. The significant forces to overcome in accelerating the gantry are gantry inertia, gantry friction, and the force required to pull the cable tow assembly. The gantry weight is approximately 7600 lb, and a friction force of 34 lb is expected. The maximum cable tow force will be approximately 21 lb peak. The resulting peak acceleration at stall, assuming a worst-case motor torque of 28 lb-ft, is calculated as follows:

$$\text{Force} = \frac{\text{torque}}{\text{wheel radius}} = \frac{28 \text{ lb-ft}}{0.15 \text{ ft}} = 187 \text{ lb}$$

187 lb	motor force
- 55 lb	cable tow and gantry friction
132 lb	force available for acceleration

$$A = \frac{F}{M} = \frac{132 \text{ lb } (32.2) \text{ ft/sec}^2}{7600 \text{ lb}} = 0.56 \text{ ft/sec}^2 \ (6.4 \text{ G})$$

Essential to meeting the 500:1 velocity requirement is the selection of a wid dynamic range tachometer. The voltage gradient for the tachometer is 0.6 volts per radian per second. The tachometer rotates at 12.17 radians per second at the maximum operating speed of 0.826 ft/sec and outputs 117 volts. At the minimum speed of 0.00365 ft/sec, the tachometer rotates at 0.0243 rad/sec and outputs approximately 234 millivolts. This voltage is much greater than the minimum usable tachometer signal and good performance over the 500:1 range is easily achieved.

3.1.5.5.2 Y-Axis Acceleration and Velocity Analysis. The Y-axis tachometer is nominally rated for a 200-volt output at 40 rad/sec. A 4-inch Roh'lix lead was chosen for the Y-drive assembly to maximize the voltage output at low speeds without resulting in destructive voltages at high speeds. The Y-axis tachometer has a voltage gradient of 5 volts per radian per second which results in a voltage output of 344 millivolts at the minimum speed of 0.0688 rad/sec and 172.1 volts at 34.42 rad/sec, the maximum operating speed. Friction loading on the motor is as follows:

Y-carriage, counterweight and bearings	0.7 lb-ft
Motor and tachometer brush and bearings	0.3 lb-ft
Roh'lix drive	1.6 lb-ft
	2.6 lb-ft

With the power amplifiers used, the torque output of the Y-motor at stall is typically 6 lb-ft. Taking the effect of friction into consideration, the motor has 3.4 lb-ft available for acceleration. Y-axis gantry acceleration is calculated as follows:

Total weight of Y-carriage and counterweight = 2200 lb

Shaft inertia reflected through Roh'lix drive = 1445 lb

$$\text{Force delivered to load} = \frac{2\pi \text{ torque}}{\text{Lead}}$$

$$F = \frac{2\pi\ (3.4)\ \text{lb-ft}}{0.333\ \text{ft}} = 64.1\ \text{lb}$$

$$A = \frac{F}{M} = \frac{64.1\ \text{lb}\ (32.2)\ \text{ft/sec}^2}{(2200 + 1445)} = 0.57\ \text{ft/sec}^2 = (6.5\ G)$$

Thus the Y-axis drive will deliver well in excess of the required 0.348 ft/sec peak acceleration at stall.

3.1.5.5.3 Z-Axis Acceleration and Velocity Analysis. For smooth operation at low velocities and to avoid the cogging problems of small motor drives, the same motor used on the Y-drive assembly is used on the Z-drive assembly. The tachometer voltage gradient is 10.5 volts per radian per second. The Roh'lix lead of 1-3/16 inches was selected to drive the tachometer near its maximum rated output at maximum operating speed. This lead results in a maximum motor/tachometer operating speed of 17.45 rad/sec at 0.274 ft/sec linear velocity with a corresponding tachometer output voltage of 183 volts. At the minimum speed of 0.000548 ft/sec, the Roh'lix drive shaft is rotating at 0.0349 rad/sec and the tachometer output is 366 millivolts.

Since the driven load is lower for the Z gantry servo than for the Y servo, the peak acceleration at stall is well in excess of the required 0.261 ft/sec^2. The expected acceleration is approximately 1.0 ft/sec^2 or 11 G.

3.1.5.5.4 Excursion. The gantry servo system is designed to have minimum excursions of 22ft 1 in. in the X direction (longitudinal), 22.1 in. in the Y direction (lateral), and 2.7 feet in the Z direction (altitude).

For safety considerations, stop switches are provided near the end of each axis of travel. This allows sufficient time for the gantry to decelerate to a safe stop. Shock absorbers are provided at each end of the X and Y axis travel which are capable of absorbing the full gantry inertia. An adjustable mechanical stop is provided to prevent contact with the carrier when it is at its level position. Slow switches are provided to limit the gantry velocity near the end of the excursion when in the test mode of operation.

3.1.5.5.5 Gantry Position Resolution. The X-axis optical encoder is geared to a full count in 281.49 in. The encoders used are 16 bits for a full count of 65,536 for 32 turns. The resulting resolution is 0.004295 inches/bit or 0.000358 ft (0.0016% of excursion). The Y-axis encoder is identical to that used on the X-axis. The encoder is geared to a full count in 91.1062 inches resulting in a resolution of 0.00139 inches/bit or 0.000158 ft (0.0059% of excursion).

3.1.5.5.6 Gantry Position Accuracy (Linearity). Experience with similar gantry systems indicates that the X and Y servos will be able to position within 0.0086 in and the Z servo within 0.0028 in. The optical encoder rack error for the X and Y axes is 0.026 inches maximum and the Z axis error is 0.0027 inches maximum. The total worst case errors are 0.0346 inches (0.013% of excursion) and 0.0055 inches (0.017% of excursion), respectively. Since the carrier deck is used for the encoder reference, the worst case errors over the carrier deck are considerably less because rack errors are small.

3.1.5.5.7 Gantry Tracking Error. Measured dynamic position errors of similar servo systems indicate that the X and Y servos typically will track the computer commanded position within 0.02 inches with a constant velocity command and the Z-axis servo will track within 0.006 inches. Therefore no problems will be encountered in meeting the high and low speed tracking errors specified.

NOTE: 0.05% error for X and Y corresponds to 0.132 inches and 0.016 inches for Z.

3.1.5.5.8 Servo Compensation. Analysis of the three servo axes is identical in principle to that of the Y axis, so only the Y axis is discussed in detail.

The Y-axis frequency response was compensated using a minor loop technique. The Y axis is described as follows:

The combined Y-axis load inertia reflected to the motor is:

$$J_{Total} = J_{Shaft} + J_{Motor} + J_{Tach} + J_{Hub} + J_{Carriage}$$

$$= 0.113 + 0.013 + 0.0075 + 0.0085 + 0.174$$

$$= 0.316 \text{ lb-ft/sec}^2$$

Motor Viscous Damping = D = 0.282 lb-ft/rad/sec

$$\omega_{Mech} = \frac{D}{J} + \frac{0.282}{0.316} = 0.895 \text{ rad/sec}$$

The motor electrical corner frequency is:

$$\omega_{ME} = 580 \text{ rad/sec}$$

Using an open loop dc gain of 70 dB, the uncompensated open loop response of the Y-axis servo system is shown as A_{m_Y} on Figure 46. (Final circuit gains are somewhat higher to compensate for the effects of friction on motor/tachometer gains.)

The uncompensated Y-axis servo loop transfer function block diagram is shown in Figure 47. Since the frequency response curve shows a -12 dB/octave slope at gain crossover, the servo system will not be stable and compensation will be required. Minor loop compensation was selected because of its superior ability to reduce the effects of external load disturbances compared to series equalizer techniques. Minor loop compensation also tends to linearize functions within the loop and thus compensate for parameter variations. The system viscous damping is dependent on the motor resistance, back EMF and torque constant which can vary as much as ±10%. Changes in the mechanical time constant, which is dependent upon system friction, will affect the minor loop only and not the major loop.

The desired corrected open-loop response is the Am_C curve of Figure 46. Bandwidth has beer. reduced to 32 rad/sec (approximately 5 Hz), and the rate of gain decrease is 6 dB per octave over a rang range in excess of two octaves each side of gain crossover. This insures a well-damped, stable system.

3.1.5.6 Gantry Tower. The gantry structure is designed with sufficient strength to minimize deflection of structural elements caused by changing loads. The gantry structure supports tower assembly, trolley, associated electronics, and drive systems. The gantry possesses the capability of translating the center line of the optical probe to within six inches of the model board edge. However, excursion safety limit devices restrict free probe centerline excursion within a distance of 14 inches from the model board edge. The gantry has the capability to translate the probe 24 inches from the model board runway surface in an axial direction normal thereto. A hard mechanical stop is provided to prevent probe contact with the model surface when over the aircraft carrier.

3.1.5.6.1 Z-Carriage Structure. The Z-carriage structure is an aluminum alloy weldment whose construction is based on a heavy rectangular tube (6 x 3 x 3/16 inch) acting to resist torsional loads. An upper horizontal rail and two vertical stiles are welded and braced to the torsion member and form the basic framework to which machined pads are welded to mount the Z-axis guide bearings. A heavy plate welded and gusseted to one end of the framework is precisely machined to end mount the optical probe assembly; the camera mounting plate is welded and gusseted to the torsion member approximately midway along its length; means for monochromatic camera mounting are provided in the front gusset of the camera mount and the rear surface of the probe mounting plate.

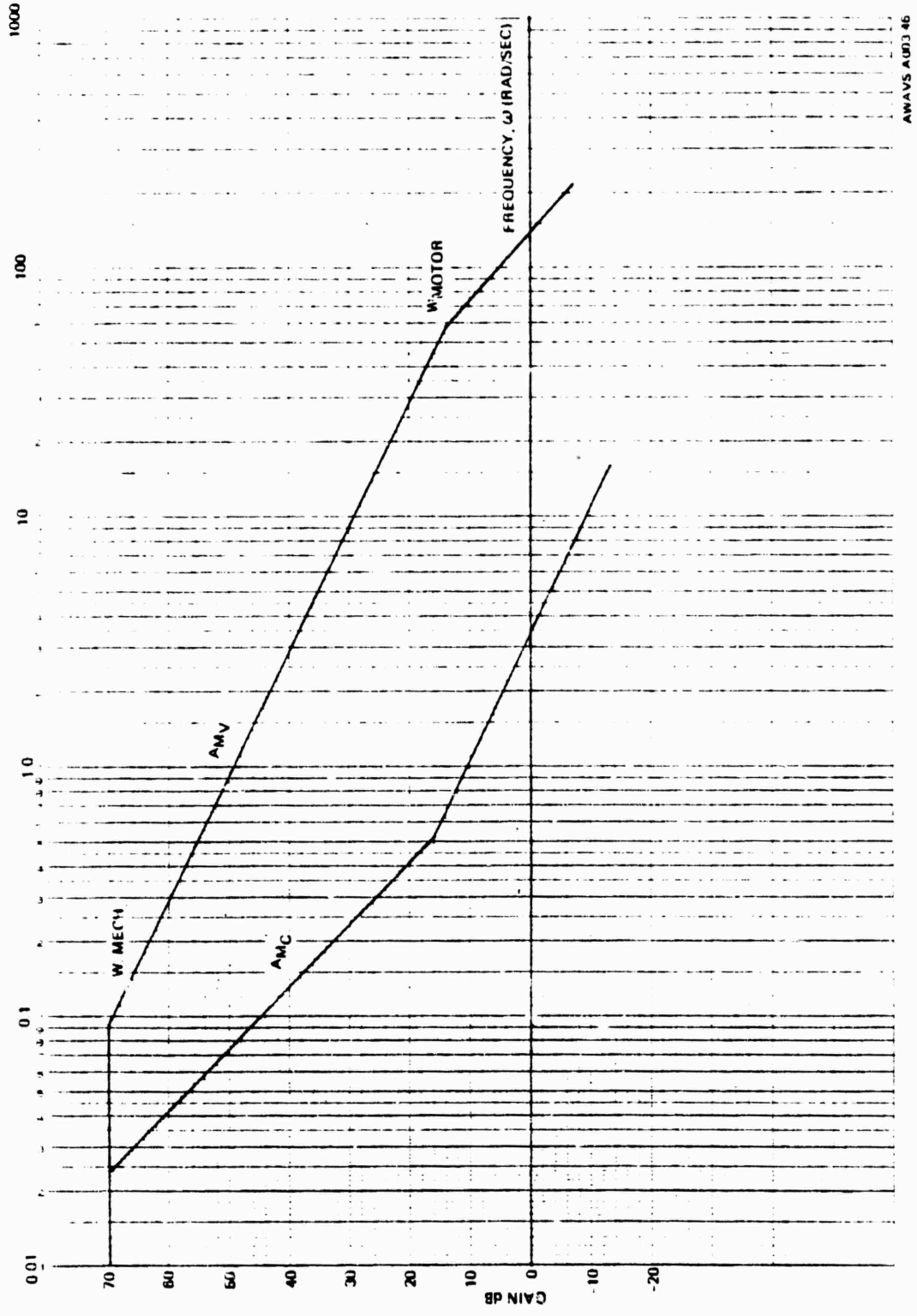

Figure 46. Frequency-Gain Plot For Gantry Y-Axis Servo

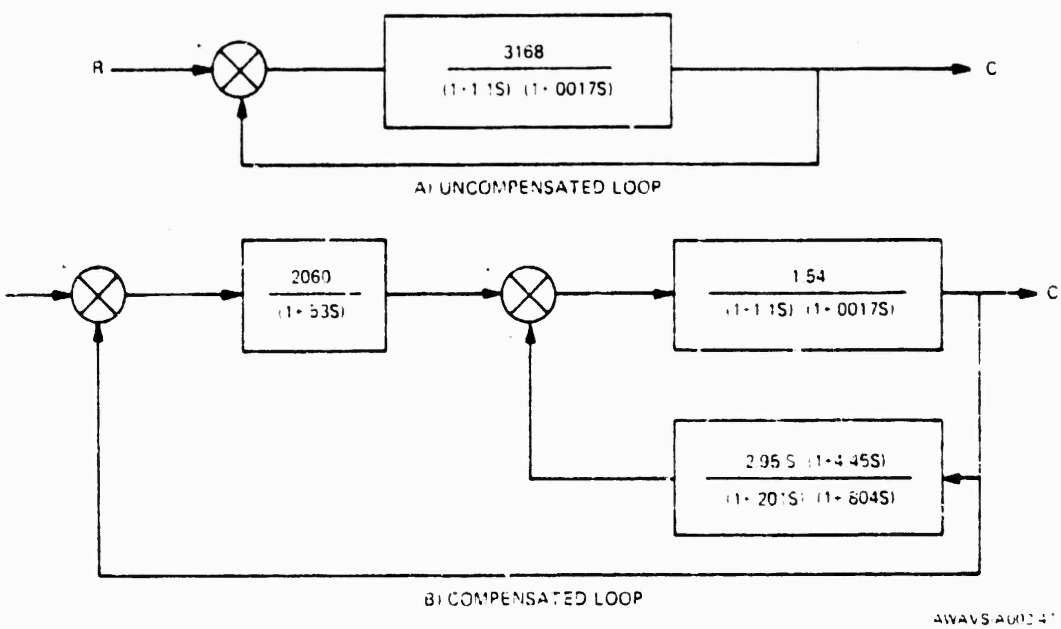

Figure 47. Gantry Y-Axis Servo, Transfer Function Diagram

Location for the probe image magnification elements is provided through two rectangular plates welded at an angle to the torsion member between the camera and probe mounting plates. The assembly is fabricated from 6061 and 6063 aluminum alloy and heat treated to the -T6 condition prior to machining to relieve stress and obtain optimum material properties.

3.1.5.6.2 Y-Carriage Structure. Rectangular structural steel tubing, 3 x 2 x 1/8 inch is welded into a plane trussed framework forming the basic Y-carriage structure. Mounting pads are welded to the framework and machined to locate and attach the Z-guide rail support brackets, the Y-axis guide bearings, Z-axis drive motor and shaft support housing, Y- and Z-axis feedback encoder assemblies, Z-axis travel limit switch assemblies and the Y-axis Roh'lix linear actuator. The framework is stress-relieved after the welding and prior to machining for maximum dimensional stability.

3.1.5.6.3 Tower Structure. The tower is fabricated in the shape of a rectangular prismatic space frame of welded structural steel square and rectangular tubing, 26 feet, 10 inches in height, five feet breadth and two feet, six inches width. Each bay of the structure is diagonally or 'K'-braced to yield maximum stiffness for minimum weight. An open section in the bottom bay is left clear for installation of rack-mounted electronic equipment. The major vertical members (5 x 3 x 3/16 inch) are furnished with pads welded at intervals along their length for attachment of the Y-axis guide rail supports.

3.1.5.6.4 X-Axis Carriage (Trolley) Structure. The function of the trolley is to provide a rigid base upon which the tower structure is mounted. It incorporates provision for mounting and aligning the two wheels through the medium of which the trolley translates along the X-guide rail. The structure comprises two 8 x 3 inch x 18.7 lb/ft structural steel channels spaced ten inches apart, to which are welded the flat, gusseted plates on which the tower is bolted. Also spanning this gap at each end is the wheel attachment structure, a channel stiffener at the center, and on the underside, structural steel angles for the attachment of the X-shaft round-way bearings.

3.1.5.6.5 X-Rail Assembly. Total length of the X-axis guide rail is 32 feet consisting of two sections, each of which is two inches in diameter and 16 feet long. The rail sections are manufactured from ground 1060 steel case hardened to 58-63 Rockwell C. Offset at the joints is reduced to a minimum by the use of a one-inch diameter, four-inch long steel dowel pin, force-fitted in one end of the rail and a close push fit at the other. The guide rail is supported throughout its length from structural steel I-beam 8 x 4 inch x 18.4 pounds per foot which is bolted and grouted to the facility floor after initial levelment. The guide rail is supported from the structural beam at equal pitches of thirty-one inches throughout its length by waymounts adjustable horizontally and vertically. After straightness of the rail has been established by optical alignment means, the space between waymounts, the underside of the guide rail and top of the I-beam is filled with high-strength grout using a special dam facility. Support structures are installed at each end of the installed guide rail to carry the motion limiting hydraulic shock absorbers. The I-beam has the feedback rack assembly attached to it and ramps for the actuation of the X-axis travel limit switches, Figure 48.

3.1.5.6.6 Upper Guide Roller Assembly. This structure is an extension to the upper part of the tower toward the model board and functions to hold the guide rollers in contact with the upper X-axis guide rail to maintain coplanarity of tower X-axis excursion with the model plane. Assembly is constituted of square steel tubing welded to form a braced twin triangle stiffened on both side edges by a trussed beam. The bearing housings are bolted to the front face of the support structure at two locations and the rollers are adjustable within the housings to facilitate alignment of the tower structure.

3.1.5.6.7 X-Axis Drive Assembly. Motive power is furnished by a dc torque motor of 30 lb-ft capacity, and is installed in combination with a tachometer/generator to yield velocity feedback data. The rotors of both torque motor and tachometer are clamped directly to the driving wheel hub which rotates with respect to a fixed axle shaft through the medium of preloaded duplexed angular contact and cylindrical roller bearings. The roller bearing is of a type that has the inner race abutment removed on one side to allow for differential movement of shaft and hub in response to thermal influences. The drive casing is a three-element assembly consisting of a central shell to house the torque motor and tachometer stator assemblies, bolted to end covers supporting the ends of the axle shaft, and providing the means to mount the drive assembly to the trolley structure. The wheel hub is fabricated from AISI 8620, a case hardened nickel-chromium-molybdenum alloy steel, the axle shaft from 303 stainless steel, and the casing from 356 aluminum alloy castings.

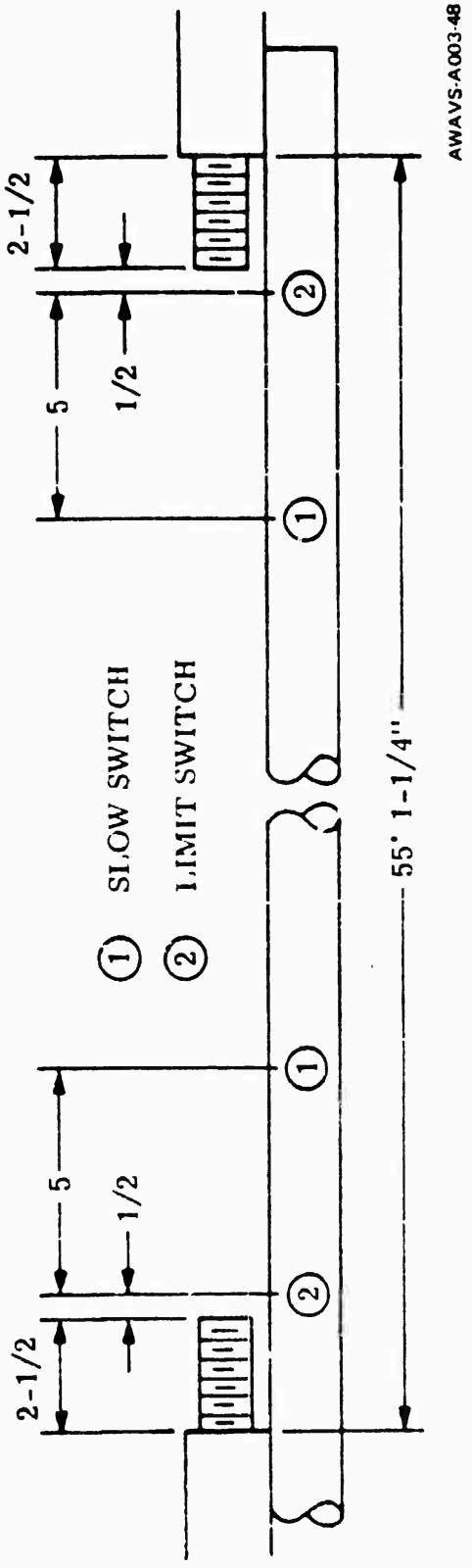

Figure 48. X-Axis Limit Switch Configuration

3.1.5.6.8 Y- and Z-Axis Drive Assemblies. An 8 lb-ft capacity dc torque motor and tachometer/generator provide motive power for both Y and Z-translation axes. A common assembly is employed in both cases modified only by the mounting plate and the external profile of the motor stub shaft. The stub shaft is supported from the housing assembly by preloaded duplexed angular contact and Conrad deep groove ball bearings. The hub on which motor and tachometer rotors are mounted is clamped directly to the drive motor stub shaft. The three-element housing assembly consists of an end plate mounting the duplex angular contact bearings, a central body locating the motor and tachometer stators in the correct relationship with their respective rotors, and the motor mounting plate, also housing the Conrad ball bearings. The mounting plate is attached to the supporting structure by four bolts clamping through fine-pitch adjustment bolts to facilitate drive axis alignment. The drive shaft is fabricated from 303 stainless steel as is the hub to which torquer and tachometer rotors are mounted. The housing elements are constructed from 2024-T4 and 6061-T5 aluminum alloys.

3.1.5.6.9 Counterweight Installation. The entire weight of the assembled Y- and Z-carriages is counter balanced by an equivalent weight in cast lead ingots, retained within a carrier framework fabricated from structural steel. Vertical edges of the frame are of steel angle welded to a 'VEE' configuration constrained to move in a vertical path between a pair of steel guide rails bolted to the side of the tower. The 'VEE' faces in contact with the guide rails are lined with nylon strip to reduce the effects of friction. A 3/8 inch diameter steel cable attached to the counterweight frame is run to the top of the tower where it passes through two sheave assemblies bolted thereto and to a clevis bolt attachment built into the Y-carriage assembly. This point is located to reduce the carriage moment and thus the friction due to load imposed on the Y-guide rails to an acceptable minimum.

3.1.5.6.10 Y-Drive Installation. The Y-drive shaft is a composite assembly of four elements, the stub shaft forming part of the Y-drive motor mounted at the top of the tower, two hollow tubular lengths extending the range of Y-carriage motion, and the lower stub shaft, guided in the lower shaft bearing housing. The two tubular sections are joined with a threaded adaptor having locating registers fitting closely in the bore of each section to control eccentricity of mating shafts within tolerable limits. Both stub ends are machined with registers and threads fitting accurately into the ends of the tubular section assembly. The lower shaft bearing is a steel weldment bolted to the tower base and incorporates a pair of self-aligning ball bearings at a pitch that offers rigid lateral support to the lower end of the drive shaft. The shaft has an outside diameter of 3.0 inches and an unsupported length between upper and lower bearing assemblies of 310 inches.

3.2 FLOLS Simulation

The FLOLS must be simulated in such a way that when viewed from the cockpit, the lights appear in the correct position and attitude with respect to the carrier and present the correct size, color, and configuration for all altitudes and ranges. The FLOLS image is inserted into the target image, via an optical coupling of a scaled FLOLS model into the target projection path. This method provides the best compromise of performance, complexity, and flexibility.

3.2.1 Simulation Method. Figure 49 is a simplified illustration of the selected method of composite image generation for the target and the FLOLS. To achieve high brightness and de-emphasize the tracking requirements, a separate FLOLS image generator with high intensity light sources (xenon arc lamps) is optically coupled into the path of the target projector. The FLOLS image generator consists of a scaled model (about 40:1) of the FLOLS array with the necessary optics for imaging and motion to project a high intensity image at the target zoom. The model board is fixed with respect to the target projector, thus eliminating errors due to differences between the target projector and the FLOLS projector. Central to this approach is the reduction in the size of the servos from those required to move a whole projector to instrument size servos where higher accuracies are easier to obtain.

The FLOLS and the carrier bundles are combined at the beamsplitter and projected as a composite image.

The FLOLS range simulation is done completely with the FLOLS zoom. Range simulation of the FLOLS is determined by the relative powers of the FLOLS zoom and the target projection zoom. The projection zoom operates in conjunction with the probe zoom to provide a carrier image of proper angular subtent. In order to obtain maximum resolution as quickly as possible for the carrier image, the projection lens zoom relative power remains at a minimum for long simulated ranges while the probe zoom operates until the carrier subtends its maximum size on the vidicon. At this position, the probe zoom has reached its maximum power. Further changes in the simulated range are now made by the projection zoom until the simulated range where the probe begins to move. The total power in the target projection system is the product of the probe and display zoom relative powers. At the position where the probe begins to move, the probe zoom relative power is decreased while the projection zoom power continues to increase. At all times, the product of their relative powers equals the ratio of the probe range to the simulated range.

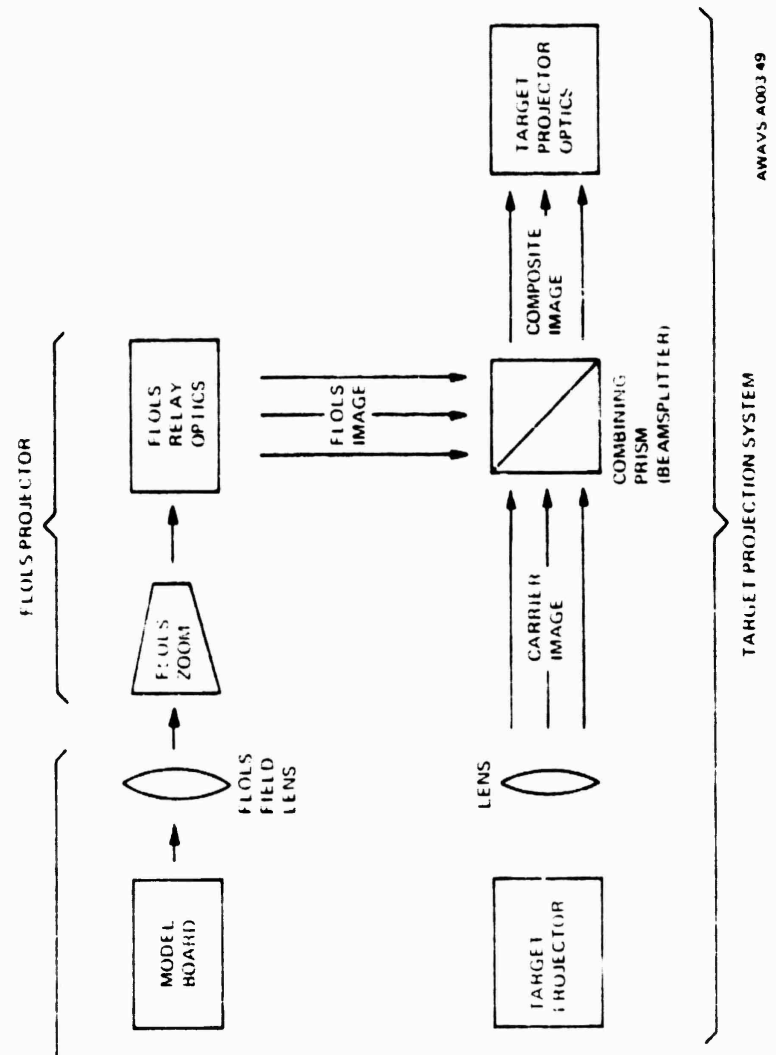

Figure 49. FLOLS Composite Image Generation, Simplified Block Diagram

The FLOLS image must change in size down to the limit of 500 ft. where the simulated FLOLS image is no longer useful. Since the FLOLS zoom is used in conjunction with the projection zoom to display the FLOLS image, the product of their relative powers must equal the ratio of 500 ft. to the simulated range. This ratio divided by the projection zoom power equals the relative FLOLS zoom power. Table 19 shows the relationship between the relative zoom powers over a range from 6 nmi to 500 ft.

The FLOLS are on whenever the pilot is within the meatball field of view. This occupies a 40°H x 1-1/2°V cone, referenced about the basic glideslope angle. When he is not within this cone, the FLOLS zoom iris servo is closed thus extinguishing the lights. The zoom is operated at f/12 to f/15 thus just a few degrees rotation of the zoom iris barrel will extinguish the lights.

3.2.2 FLOLS Image Generator. The individual FLOLS lights are each modeled by a fiber and lens. The fiber conducts the light from an arc lamp and shutter system to a model board which appears just like the FLOLS system. Each lens on the model collimates the output end of its fiber and is cut to the size and shape of the particular FLOLS light. All the individual lights on the FLOLS are collimated and have their axis parallel to the system axis. This is so that when the zoom lens is at its greatest focal length the FLOLS field lens images or decollimates the pupil of the zoom through the fiber end and projects all onto the same surface. The size of this image is sufficiently large, so that there is no vignetting when the zoom is at its shortest focal length. Therefore, the luminosity of the FLOLS image is constant over the zoom range.

Configuration details of the FLOLS model board are given in paragraph 3.2.2.1, with a block diagram discussion in paragraph 3.2.2.2. An analysis of the optics involved in FLOLS image generation is provided in paragraph 3.2.2.3.

TABLE 19. RELATIVE ZOOM POWERS FOR FLOLS SIMULATION

Simulated Range Ft	Probe Range Ft	Relative Power Probe Zoom	Relative Power Display Zoom	Relative Power FLOLS Zoom
36480	4070	1.1157	0.1	0.137
24320	4070	1.6735	0.1	0.206
18240	4070	2.2315	0.1	0.274
12160	4070	3.3470	0.1	0.411
10000	4070	4.07	0.1	0.5
9120	4070	4.07	0.10965	0.5
7600	4070	4.07	0.13158	0.5
6080	4070	4.07	0.16447	0.5
5840	4070	4.07	0.17123	0.5
4070	3627.5	3.6275	0.24570	0.5
2300	2300	2.30	0.43478	0.5
1000	1000	1.0	1.0	0.5
500	500	1.0	1.0	1.0

3.2.2.1 FLOLS Model Board. A 2 x 6 inch model board is the primary imaging device for the FLOLS simulation. It is comprised of 32 fixed lenses backed up by appropriately colored filters to simulate the datum, wave-off, auxiliary wave-off and cut lights, and one movable lens to simulate the FLOLS meatball. Figure 50 shows the physical configuration of the model board. The vertical position of the meatball with respect to the datum lights defines the pilot's orientation relative to the glideslope. (On the actual carrier the meatball is positioned approximately 150 feet behind the datum lights, and the vertical orientation of the observer gives the impression of a movable meatball.) At its lowest level, a chopper with a red filter is imposed in front of the meatball to simulate the danger zone. Meatball motion is under software control. A detailed discussion of the meatball servo is provided as part of paragraph 3.2.6. The model board also contains a shutter to simulate on/off operation of the auxiliary wave-off lights. This shutter is normally controlled from the EOS.

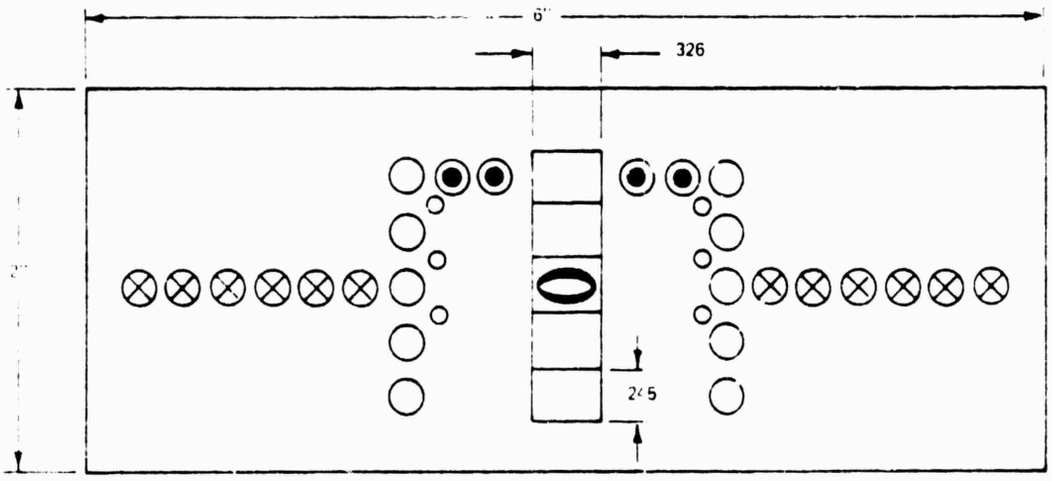

LEGEND

SYMBOL	LIGHT DESIGNATION	COLOR	QUANTITY
⊗	DATUM	GREEN	12
○	WAVE OFF	RED	6
◉	CUT	GREEN	2
○	AUX WAVE OFF	RED	6
⬭	MEATBALL	YELLOW (BOTTOM POSITION RED)	1

AWAVS A00250

Figure 50. FLOLS Model Board Configuration

3.2.2.2 Functional Description. Figure 51 is a block diagram of the FLOLS image generator showing the basic optical paths and control interface, while Figure 52 shows the optical details of the image generator assembly. Illumination for the model board originates in two lamphouses, each of which contains an arc lamp, two f/7 condensers, and two decollimating lenses. The condensers collect the flux from the arc lamps, while the decollimating lenses control arc imaging onto the fiber bundles. A separate power supply strikes the arc and provides operating power to each lamphouse. Lamphouses are blower cooled. Decollimated light from the lamphouses is directed toward four cold mirrors, whose function is to filter out the infrared and bend the light to the fiber bundles (via the pupil lenses). Five pupil lenses (collimage condensers) are used to give even illumination over groups of fiber optics for specific functions.

Light from one lamphouse is distributed by two pupil lenses to 18 fibers for simulation of the datum and auxiliary wave-off lights. Each of these lenses collimates light for six datum and three auxiliary wave-off lights. The datum lights glow continuously whenever the FLOLS is on, while the auxiliary wave-off lights are under control of a shutter on the model board. The shutter is operable either from the EOS, via the linkage or from the cockpit electronics test panel.

Light from the second lamphouse is aimed via the cold mirrors at pupil lenses for the meatball, cut, and wave-off lights. Meatball simulation is achieved by a moving lens and single fiber driven up and down the model board, thus giving smooth continuous changes in glideslope angles. The lens has an oval shape to give the light its proper outline. When at its lowest level, the fibers light path intersects a chopper with a red filter to simulate the low condition. The meatball servo is normally under software control, via the linkage. A detailed discussion of the meatball servo is included in paragraph 3.2.6. The cut and waveoff lights are actuated by a 2-position driven mirror at the lamphouse. Since the waveoff and cut condition never occur simulatneously, the mirror locates the arc's image at the cut, wave-off, or off-condition as required. Collimated light from one of the pupil lenses is routed via four fibers to simulate cut lights, while ten fibers from another pupil lens direct light for wave-off. All fibers terminate at the model board, which contains the lenses and filters for the simulated lights described above, as well as the auxiliary wave-off shutter and the meatball servo. The optical pattern from the model board is then directed toward the FLOLS projection system via the FLOLS field lens, whose function it is to decollimate the light from each of the fiber exit pupils.

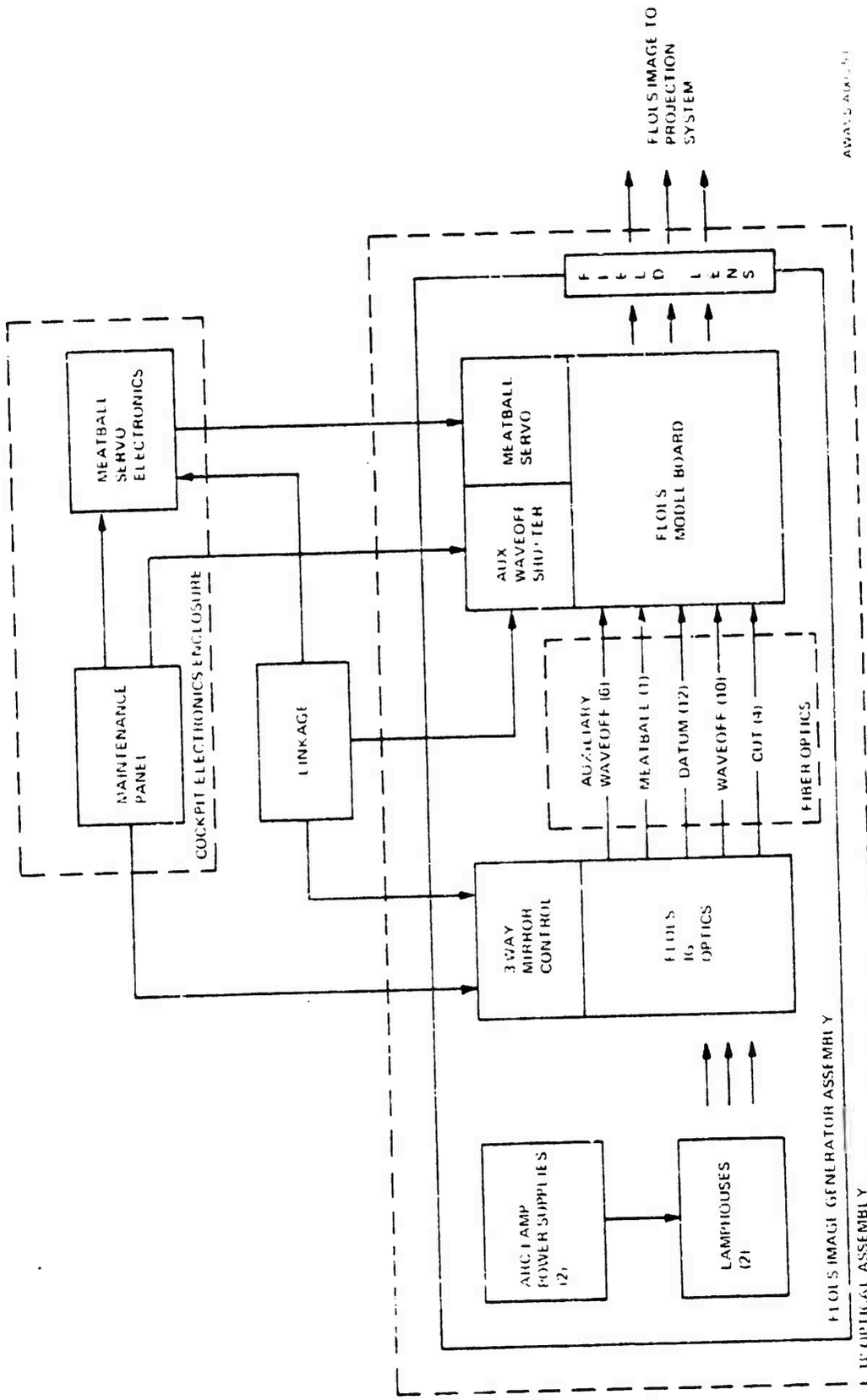

Figure 51. FLOLS Image Generator, Block Diagram

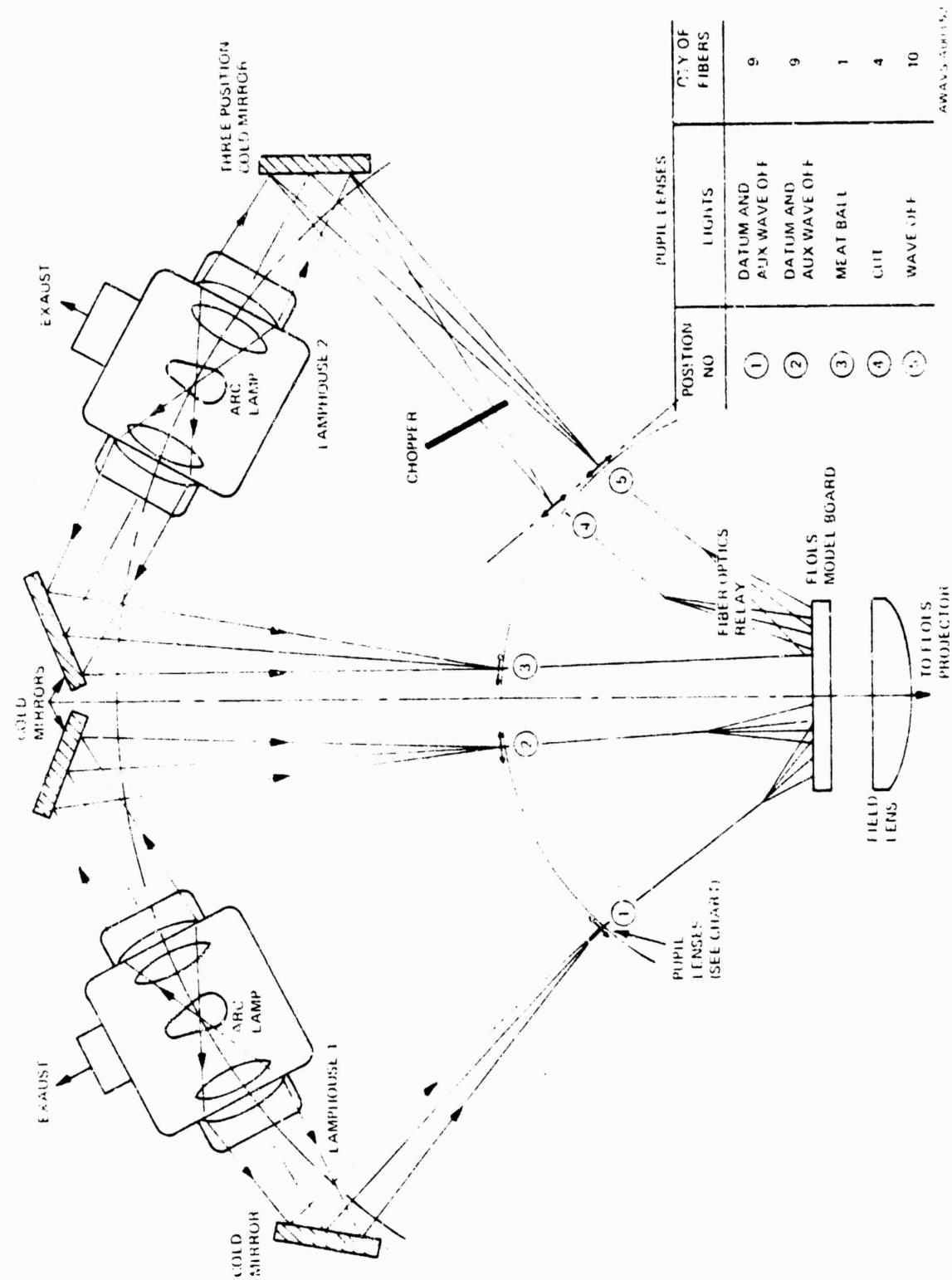

Figure 52. FLOLS Image Generator, Optical Diagram

3.2.2.3 Image Generator Optics. The following is the analysis used to establish the optical design for the FLOLS image generator beginning with the light requirements and continuing through the FLOLS field lens to the zoom entrance pupil (first element of FLOLS projector). Figure 53 presents the optical schematic for the image generator, but for simplification has been limited to coverage of a single light path. The f/0.7 condenser collimates the arc. The decollimator then images the arc on a fiber bundle. The size of the imaged arc is:

$$h' = m \cdot h$$

where,

$$m = \frac{f_{(decollimator)}}{f_{(condenser)}} = \frac{463.3 \text{ mm}}{50 \text{ mm}}$$

$$h = \text{arc bright spot} = 0.3 \text{ mm}$$

Thus:

$$h' = \frac{(0.3)(463.3)}{50} = 2.78 \text{ mm}$$

There are five bundles to illuminate. The maximum number of fibers in a bundle are 10 of 0.015 inch/dia. The size of this bundle is 1.5mm diameter. Thus, the imaged arc on the bundle overfills it, which provides a tolerance, for adjustment.

The vertical input 1/2 cone to the fiber is:

$$u' = \tan^{-1} \left(\frac{\tan (u)}{m}\right)$$

where,

$$u = 30°$$

Therefore,

$$u' = 3.5°$$

The pupil lens collimates the condenser pupil that is 500 mm away. This provides the same acceptance cone to all field points. Thus, the EFL of the pupil lens is 500 mm.

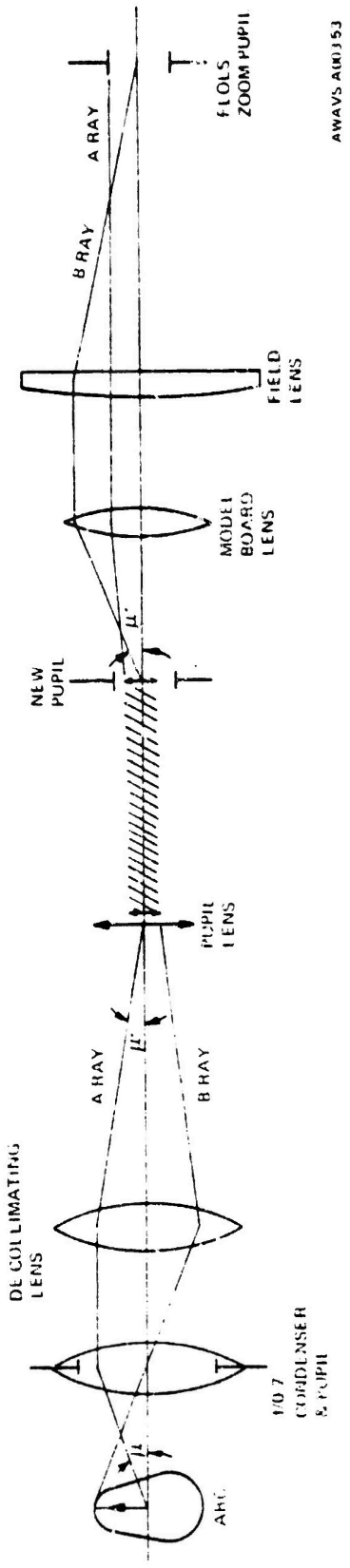

Figure 53. FLOLS Image Generator, Singe-Path Optical Schematic

The arc's image is relayed through the fiber optics to the FLOLS model board. The model board lens collimates the fiber end and then the FLOLS field lens images the arc's image to the FLOLS zoom pupil. Diameters and effective focal lengths for these lenses are given in Table 20.

TABLE 20. FLOLS FIELD AND MODEL BOARD LENS CHARACTERISTICS

LENS	DIAMETER	EFL
Meatball	8.3mm	64mm
Aux Wave-off Wave-off Cut Datum	4.5mm	32mm
Field Lens	153mm	1090mm

The output bundle of 7° just over fills each lens thus ensuring illumination of the clear aperture.

The field lens relays the fiber end to the zoom pupil. The size of the fiber end at the zoom pupil is:

$$\left(\frac{\text{EFL of Field Lens}}{\text{EFL of Model Board Lens}}\right)(\text{Dia of fiber}) = \text{Fiber Image Size}$$

Thus:

$$\text{Meatball fiber} = \left(\frac{1090\text{mm}}{64\text{mm}}\right)(0.03\text{ in.}) = 12.9\text{ mm}$$

$$\text{Other fibers} = \left(\frac{1090\text{mm}}{32\text{mm}}\right)(0.015\text{ in.}) = 12.9\text{ mm}$$

Therefore, if the zoom entrance pupil is 10mm or less, there should be no vignetting through zoom. The zoom pupil subtends a 3.8° half angle from the model board; then at the zoom's lay EFL (120mm) the FLOLS is at its maximum size. As it zooms, the pupil moves forward and gets smaller, and the image brightness remains a constant. (The zoom is stopped down to f/12.)

The zoom lens is located approximately 27.5 inches from the field lens so the fibers are imaged at the zoom pupil when at 120mm focal length.

3.2.3 FLOLS Projector. The FLOLS projector relays the model board image to the point where it is combined with the target image, and provides correct orientation of the FLOLS with respect to the target optical axis and the aircraft roll axis. It also contains a zoom lens, which is the primary element for FLOLS range simulation, and two optical irises — one for on/off simulation and the other for FLOLS intensity control.

Figure 54 is a block diagram showing the FLOLS projector and its related electronics, while Figure 55 is an optical schematic of the FLOLS projector. The linkage sends commands to the FLOLS servo electronics which, in turn, form the dc drive commands for the servos. There are six servos: zoom, zoom iris, roll, X-displacement, Y-displacement, and iris. For test purposes servos can be manually positioned from the cockpit enclosure test panel. For an in-depth discussion of FLOLS servo technique as well as individual analyses of each servo, refer to paragraph 3.2.6.

3.2.3.1 Zoom and Zoom Iris. The zoom lens controls the size of the FLOLS image. The lens is identical to the zoom lens used in the target projector, and is further described therein. Since the lens is primarily intended for use in three-color systems, a color correction prism is used to correct the back focus as required for a monochromatic system.

The zoom iris servo can close the iris in the zoom lens to no opening. This is used to shut off the FLOLS light when the aircraft is out of range, thus avoiding frequent restarting of the arc lamps.

The zoom lens subtends 7.6° to the FLOLS model board. The maximum size of the FLOLS in the zoom image plane is:

$$h = f \tan \theta$$

where,

$$f = 120\text{mm}$$
$$\theta = 3.8°$$

Therefore:

$$h = (120\text{mm}) \tan 3.8°$$
$$h = 8\text{mm}$$

or,

$$\phi = 16\text{mm}$$

When the zoom is set at 12mm EFL,

$$h = (12\text{mm}) \tan 3.8°$$
$$h = 0.8\text{mm}$$

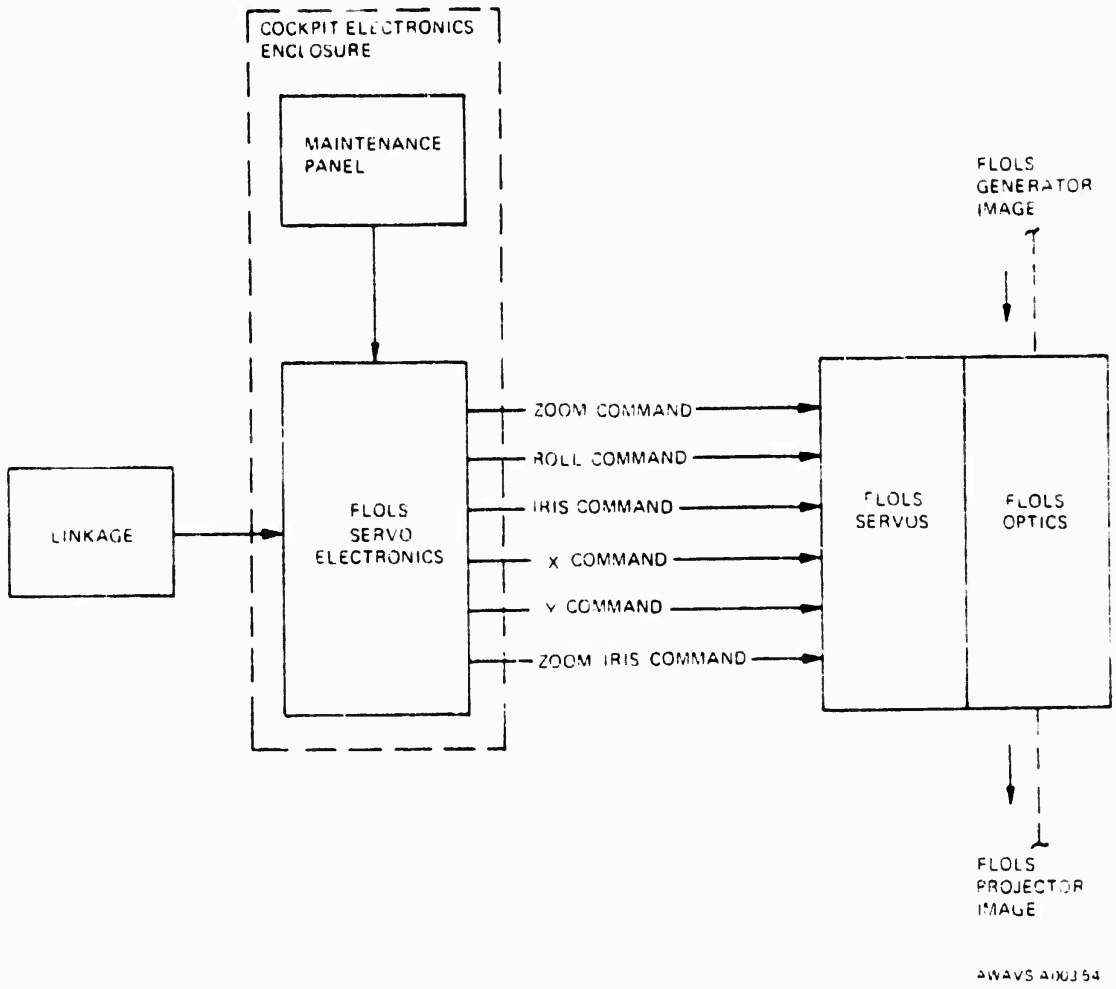

Figure 54. FLOLS Projection Subsystem, Block Diagram

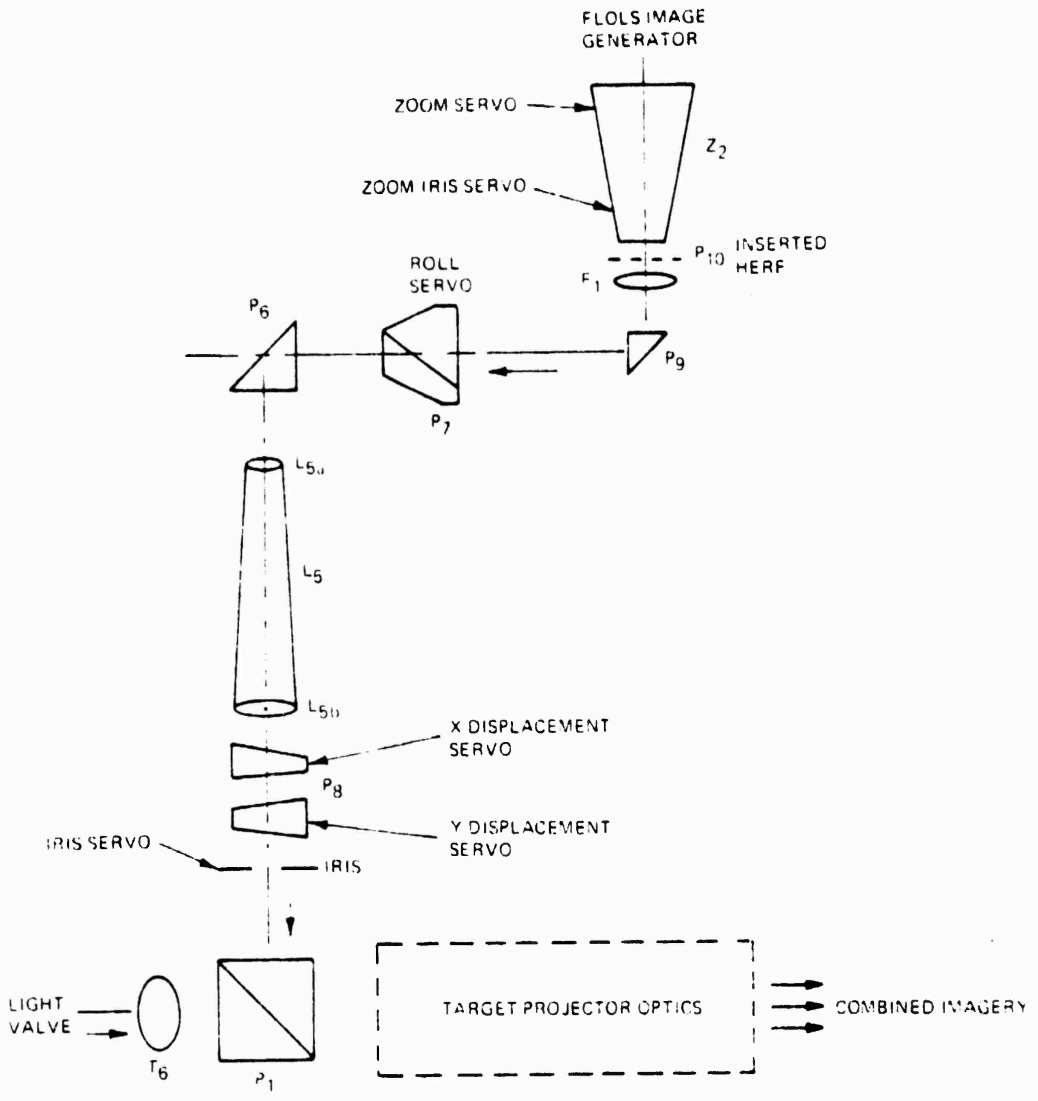

IRIS	VARIES THE FLOLS BRIGHTNESS
P_8, PITCH WEDGES	TRANSLATE THE FLOLS IMAGE IN X Y ORTHOGANOL TO THE TARGET OPTICAL AXIS
L_5 (L_{5A} L_{5B}) TELEPHOTO LENS	COLLIMATES THE FLOLS IMAGE
L_6, RIGHT ANGLE PRISM	RE DIRECTS FLOLS OPTICAL PATH
P_7, PECHAN PRISM	PROVIDES AIRCRAFT ROLL TO THE FLOLS
P_9, PRISM	RE DIRECTS LIGHT PATH
F_1, LENS	FIELD LENS
Z_2, ZOOM	CANNON PV 10 x 129 ZOOM LENS 10 : 1 RANGE

AWAVS 8003 53

Figure 55. FLOLS Projector, Optical Schematic

3.2.3.2 Roll and Relay Optics. The FLOLS projection optics relay this image (at the proper size) to the target optics. Magnification of the FLOLS, including target optics, is:

$$\frac{60°}{16mm} = \frac{2.37°}{Xmm}$$

where, 2.37° is the maximum angular subtent of the FLOLS at 500 feet. (From 500 feet to touchdown, no further size change in FLOLS is provided.) Solving the equation:

$$X = 0.632mm$$

or a demagnification of 16/0.637, 25.3.

Therefore, the finite f/# relayed back to the FLOLS zoom is:

$$\text{Target f/\# (max)} = 1.88$$

Since magnification through FLOLS = 25.3, then f/# at FLOLS zoom is:

$$(1.88)(25.3) = 47.56$$

A field lens relays the zoom image to the roll (pechan) prism. The roll servo provides the FLOLS with aircraft roll, which is synchronized with probe roll. Two prisms at either side of the roll prism merely redirect the light path, and a telephoto lens collimates the FLOLS image and provides the necessary magnification.

3.2.3.3 Pitch Wedges. The pitch X- and Y-displacement (pitch wedges) servos move the FLOLS image from the center of the target field as the probe point of interest varies from the FLOLS carrier position to the aircraft roll axis. The correct location of the FLOLS image is calculated by software, and the servos move the pitch wedges to position the image correctly in the target field of view.

Figure 56 is an optical schematic of the pitch wedges. The input from the FLOLS projector is shown at the right along the optical axis. The angle (ζ) represents the output deviations from the prisms. Terms ν_1 and ν_2 are the angular rotations of the wedges to produc some defined (ζ) as represented by Equation 1. When the prisms are in the null position; $\nu_1 - 0°$, $\nu_2 = + 180°$, $\zeta = 0$. (Keep in mind (ζ) is the magnitude of deviation not the direction.)

Maximum field displayed = 67.38°
Maximum field FLOLS subtends at 500' = 2.367°
Maximum output field of T6 (representing 60°) = 8.9°

= Maximum deviation required by pitch wedges;

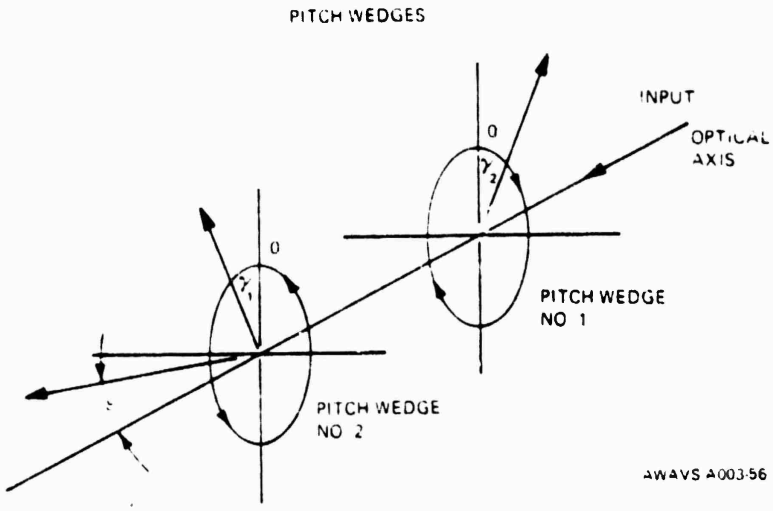

Figure 56. Pitch Wedges, Optical Schematic

$$\frac{2.67°}{67.38°} \times 8.9 + 8.9 = 9.21°$$

8.9° = maximum semi field angle of T6.

33.69° = maximum half angle out of TIP zoom.

8.9 = 33.69 relating to wedge

$$= 3.79 \frac{\text{Target°}}{\text{FLOLS°}}$$

The equation that represents the deviation magnitude by the pitch wedges is;

$$\text{(deviation)} = r_0 \quad (2 + 2 \cos (\gamma_1 - \gamma_2)^{\frac{1}{2}} \qquad (1)$$

r_0 = 5.49°; maximum deviation each pitch wedges can introduce alone.

γ_1, γ_2; (gamma) rotation of pitch wedges

The magnitude of each pitch wedge's deviation is a constant independent of γ, and can be represented as a vector; as shown below.

$$\bar{r}_1 = r_0 (\cos \gamma_1 \bar{I} + \sin \gamma_1 \bar{j}) \quad (2)$$

$$\bar{r}_2 = r_0 (\cos \gamma_2 \bar{I} + \sin \gamma_2 \bar{j}) \quad (3)$$

When $\gamma_1 = \gamma_2$, the deviation introduced by the wedges is a maximum, and when $r_1 = (180° + \gamma_2)$ no deviation occurs. Also, the direction of the resultant vector is the addition of $\bar{r}_1 + \bar{r}_2$, and the magnitude is represented by equation 1. Thus, these relationships can describe the placement of the FLOLS anywhere in the target FOV by introducing the zoom of the TIP.

This is achieved simply by proper choice in r_0' dependent on zoom.

Where $r_0' = 2 r_0 \beta Z_{TIP}$

= when Z_{TIP} = 1 the wedge deviation is related to the maximum TIP FOV

when Z_{TIP} = 0.1 the wedge deviation is related to minimum TIP FOV

To summarize:

$$\text{Deviation } \zeta' = r_0' (2 + 2 \cos (\gamma_1 - \gamma_2))^{\frac{1}{2}}$$

$$\text{Direction } \bar{r}_3 = r_0' (\cos \gamma_1 + \cos \gamma_2) \bar{I} + (\sin \gamma_1 + \sin \gamma_2) \bar{j}$$

or the direction cosines are:

$$\cos \alpha = \left[\frac{\cos \gamma_1 + \cos \gamma_2}{\zeta'} \right] r_0'$$

$$\cos \beta = \left[\frac{\sin \gamma_1 + \sin \gamma_2}{\zeta'} \right] r_0'$$

Thus knowing ζ' and the direction cosines, $\bar{r}_1$ and $\bar{r}_2$ can be solved for resulting in the proper rotation of the wedges.

3.2.3.4 Iris Servo. The iris servo controls the intensity of the FLOLS image entering the beamsplitter. Its setting is manually controlled from the EOS via the linkage. There is no software control of this servo.

3.2.4 FLOLS Luminance. The brightness calculations are carried out from the arc source to the screen. Figure 53 shows the schematic used in the calculation.

Assumptions:

All optical systems obey the brightness formula or the sine condition is obeyed and the system is completely aplanatic.

P= total flux intercepted by the condenser system.

Figure 57 is the lamp specification. The lamp output lumens are 12,000. It radiates into a solid angle of 60°V x 360°H. And the condenser accepts = solid of 60°V x 92°H;

$$\text{Thus } \frac{12{,}000 \text{ lumens}}{6.6 \text{ str}} = \frac{(x) \text{ lumens}}{1.7 \text{ str}}$$

$x = P = 3090$ lumens.

Attenuation of flux to the screen is as follows:

(1) FLOLS path transmittance

(2) Portion of imaged arc accepted by fiber

(3) Light vignetted by FLOLS zoom pupil from image generator

(4) f/# mismatch due to FLOLS zoom and relayed target zoom f/# back to FLOLS zoom.

FLOLS path transmittion is shown in Table 20.

The area of the imaged fiber is:

$$(0.3 \times 0.3)\text{mm}^2 \times (9.26)^2 = 7.7\text{mm}^2$$

where 9.26 is the magnification

The fiber area is $\pi r^2 = (0.381)^2 = 0.46 \text{ mm}^2$

$$T_2 = \left(\frac{0.46}{7.7}\right) = 0.06$$

DIMENSIONS COLD	
Overall Length	4-7/8 ± 1/32 in.
Distance from top of cathode ferrule to cathode tip.	1.700 ± .010 in.
Outside diameter of bulb	25 mm max.
Diameter of ferrules...anode	.798 ± .002 in.
cathode	.873 ± .002 in.
Arc length..... ..cold	.035 ± .005 in.
hot	.025 ± .005 in.
OPERATING POSITION: Anode up, within 30° cone from lamp axis.	

OPERATING DATA	
Open circuit voltage	70 volts min.
Lamp operating voltage	14-20 volts
Current	30 nom. amps.
Rated power consumption	500 watts
Ignition voltage	20-30 kilovolts
Luminous flux	12,000 lumens
Intensity	2000 candles
Average brightness....40010	3500 cds/mm^2
Effective area..... .15 x .15	.3 x .3 mm
Average rated life	300 hrs.
COOLING. The lamps should be cooled with an axial flow of about 300 c.f.m. More or less may be used depending upon the temperature of the seals (marked A) which should not exceed 200°C.	

AUXILIARY EQUIPMENT: Power System Hanovia 27301.

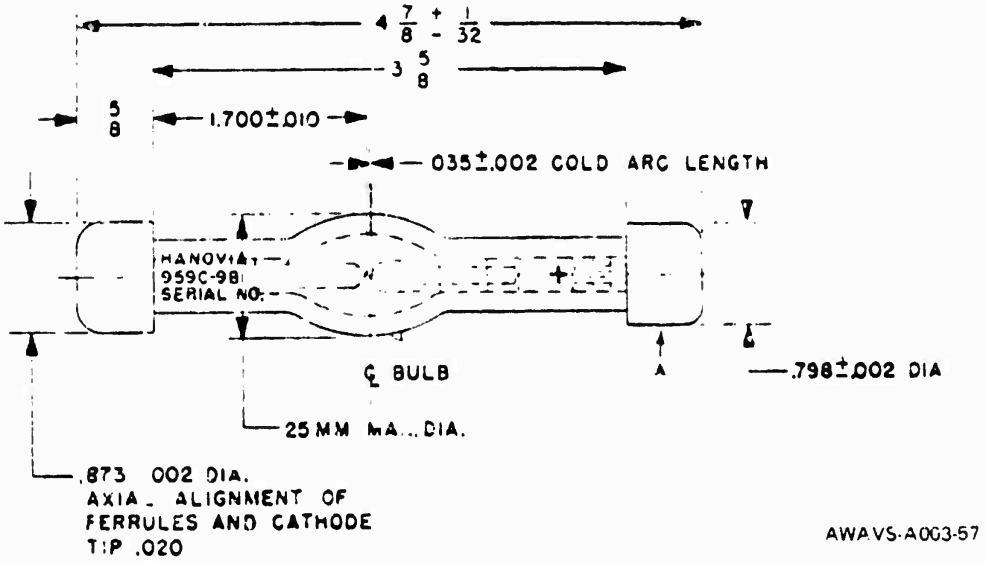

Figure 57. Conrad-Hanovia Lamp Specification

TABLE 21. FLOLS LIGHT PATH TRANSMITTANCE

Cold mirror	= .80	
Condenser	= .75	
De-Collimator	= .95	
Fiber insertion	= .80	
Fiber transmittance	= .85	(fiber length 10")
Model board lens	= .95	
Field lens	= .95	
Pupil lens	= .95	
FLOLS zoom	= .70	
FLOLS projection Optics	= .70	
Beam Splitter	= .10	
Target Optics	= .45	
Target Zoom	= .70	
Total Transmittance	= 5.1×10^{-3}	= T_1

The mismatch of f/# transmittance is:

$$\frac{\text{f\# of FLOLS zoom}}{\text{Relayed target f/\# back to FLOLS zoom}} = \left(\frac{12}{47.6}\right)^2 = 0.063 = T_3$$

The light transmitted by the FLOLS zoom is the ratio of the angles squared from the fiber to collimator and from field lens to zoom pupil

$$\theta_1 = \arctan\left(\frac{0.381 \text{ [meatball fiber radius]}}{64\text{mm [EFL of meatball lens]}}\right)$$

$$\theta_2 = \arctan\left(\frac{5\text{mm [radius of FLOLS Entrance Pupil]}}{1090\text{mm [EFL of Field Lens]}}\right)$$

$$\theta_1 = 0.341$$

$$\theta_2 = 0.263$$

$$T_4 = \left(\frac{0.263}{0.341}\right)^2 = 0.59$$

Now the estimated power to the screen is:

$$P^1 = P \times T_1 \times T_2 \times T_3 \times T_4$$

$$P^1 = (3090 \text{ lumens})\ (5.1 \times 10^{-3})(0.06)(0.59)(0.063)$$

$$P^1 = 3.51 \times 10^{-2} \text{ lumens}$$

Meatball's target area on the screen is 24×10^{-4} ft^2 and the screen gain is 2.5

Therefore the brightness of the meatball is:

$$B = \frac{P^1 * 3}{24 \times 10^{-4}\ ft^2} \cong 36 \text{ ft lamberts}$$

The brightness is 6 times brighter than the target.

3.2.5 FLOLS Resolution. The bases used for the FLOLS limiting resolution is when the separation between the center meatball and adjacent datum lights subtend 1 arc minute to the pilot. This range implies the size of the FLOLS at the target image plane.

Separation:

Datum Meatball

←4.25' →

S = R
θ = 1 arc min = 0.0003 rad
S = 4.25'
→ $R = \frac{4.25}{0.0003} = 14{,}000'$

According to the zoom tables:

$$\text{FLOLS zoom} = \frac{500'}{14{,}000} \qquad \frac{1}{1} \text{ target zoom}$$

Now the size of the FLOLS at the target zoom image plane is:

$$\frac{\text{(Maximum FLOLS size at FLOLS zoom)}}{\text{(Demagnification of FLOLS and Target Optics)}} \cdot \text{(FLOLS Zoom Ratio)} = D$$

$$D = \left(\frac{16mm}{28}\right)\ (0.36) = 0.21mm$$

Now the resolution requirement of the system is:

$$\frac{\frac{20.67'}{4.25'}\ lp}{0.21mm} = 23\ lp/mm$$

where 20.67 ft is the total real world width of the FLOLS.

This is 700 TV lines at the target zoom image plane. The FLOLS optics and target optics are near diffraction limited at f/50, thus the system limiting resolution is:

$$\frac{1}{\lambda}\ \frac{1}{f\#} = \frac{1800}{50} = 36\ \text{lp/mm}$$

The on axis MTF of the target zoom at (f/20) 23-lp/mm is near 90% and so is the FLOLS zoom. Thus, the resolution of the FLOLS is met.

3.2.6 FLOLS Simulation System Motion and Error Analysis. The following paragraphs describe the techniques of servo design, analysis, and evaluation of performance applied to the design of the FLOLS servos. Coverage is provided herein for both the FLOLS image generator (FIG) and FLOLS projector (sometimes referred to as FLOLS image transformation, FIT) servos. The FIG servo is the FLOLS meatball. Six FIT servos include FLOLS zoom, zoom iris, roll, X- and Y-displacement, and iris servos. Tables 21 through 23 provide identification, torque ratings, and component make-up for the FLOLS servos. Data of a general nature common to all seven loops is given in paragraphs 3.2.6.1 and 3.2.6.2, while peculiar data for each servo is presented in subsequent hardware oriented paragraphs. Portions of the carrier mode servo analysis (para 3.1.1.4) are referenced in the generalized discussions where data is identical. Criteria established for design of FLOLS motion servos during the AWAVS design analysis were as follows:

a. Input Commands. Servos will operate with input commands formulated as listed in Table 21 according to two types — continuous and noncontinuous. Each servo will provide for two sources of input command signals — one source from the computer interface, the other source from the test console. Switching between sources will be relay controlled.

b. Minimization of Abrupt Nonlinearities. Components and mechanisms of the above mentioned subsystem servos have been designed to achieve the required smoothness in output motion response. Servo component selections are identified for each servo under the hardware subsystem descriptions. Mechanisms have been developed to eliminate or minimize backlash in gearing by use of precision gearing, and by antibacklash gearing.

c. Feedback Techniques. Feedback components (potentiometer and tachometer) for each servo in the hardware subsystem descriptions of this report. (See Table 23.)

d. Travel Stops and Limit Switches. Travel limit switches will be provided on each noncontinuous servo except for the zoom and zoom iris. (See paragraph 3.3.2.3.) Contact with any limit switch will remove power amplifier current to the motor of that servo only in the direction of the approached travel limit. Travel past the limit switches will be controlled by soft mechanical stops with over travel. The stops will safely control deceleration based on the momentum produced by the maximum velocity of the total moving inertia at the instant contact is made with the stop.

TABLE 22. FLOLS SERVO IDENTIFICATION

SUB-SYSTEM	SERVO NAME	SYMBOL	INPUT TYPE	SYSTEM TYPE	CONTROLLED ELEMENTS
FLOLS Image Generator (FIG)	Meat-ball	H_{MRDL}	Non-Continuous	Type 1	Fibre Optical Unit Rectilinear Motion
FLOLS Image Transformation (FIT)	Zoom	Z_{FIT}	Non-Continuous	Type 1	FLOLS zoom lens barrel rotation
	Zoom-Iris	I_{ZFIT}	Non-Continuous	Type 1	Iris in the FLOLS zoom
	Iris	I_{FIT}	Non-Continuous	Type 1	Independent Iris - Rotation
	Roll	Φ_{FIT}	Continuous	Type 2	Roll Prism Unit - Continuous Rotation
	X Displacement	$\Delta\theta_X$	Continuous	Type 1	Pitch Wedge Unit - Continuous Rotation
	Y Displacement	$\Delta\theta_Y$	Continuous	Type 1	Pitch Wedge Unit - Continuous Rotation

TABLE 23. FLOLS SERVO INPUT TORQUES

SERVO NAME	INERTIA TORQUE ($T_a = J_T \alpha_L$)	DISTURBANCE TORQUE (T_D)	FRICTION TORQUE (T_F)
Meatball	$0.02_{\frac{oz\ in.sec^2}{}} \times 300\ rad/sec^2$	1 oz in.	3 oz in.
Iris	$0.01_{\frac{oz\ in.sec^2}{}} \times 10\ rad/sec^2$		4 oz in.
Roll	$2.0_{\frac{oz\ in.sec^2}{}} \times 10.5\ rad/sec^2$		3 oz in.
X-Displacement	$0.04_{\frac{oz\ in.sec^2}{}} \times 10.5\ rad/sec^2$		3 oz in.
Y-Displacement	$0.04_{\frac{oz\ in.sec^2}{}} \times 10.5\ rad/sec^2$		3 oz in.

TABLE 24. FLOLS SERVO COMPONENTS

SERVO	DC TORQUER-TACHOMETER	POTENTIOMETER	POWER AMPLIFIER	COMPENSATION BUFFER
Meatball	Inland TT 1403-A (19V x 4.6A) Singer 1004204-01 T_P=79 oz in T_G=0.2V/rad/sec K_T=16.6 oz in/amp W_{NL}=158 rad/sec	CIC 111 Singer 658016 Linearity 0.5% Impedance 1K	Inland EM 1802 Singer 1003911-03 200 Watt at 20V	Singer 2061496-01 and 2061498-01
Zoom	Escap 28 G112190254	Helipot 17366	Stanl Research Labs LEN Control 217	
Zoom Iris	Escap 16 M11 207C	Spectro 140-0-0103	Same as zoom servo	None
Iris	Same as Meatball	CIC 175 Singer 518005 Conformity 0.1% Impedance 5K	Same as Meatball	Same as Meatball
Roll	Same as Meatball	CIC 306 Singer 1004205-01 Conformity 0.05% Sin-Cos Pot 10K	Same as Meatball	Same as Meatball
X-Displacement	Same as Meatball	Same as Roll	Same as Meatball	Same as Meatball
Y-Displacement	Same as Meatball	Same as Roll	Same as Meatball	Same as Meatball

e. Lockouts. Removable mechanical lockouts will be incorporated on all continuous and noncontinuous servos, providing a means of securing moving mechanisms during handling and shipment. The lockout will also provide a precise repeatable calibration reference for position sensor alignment.

3.2.6.1 Generalized Performance Data. Following are the techniques used in synthesis of performance oriented parameters (displacements, velocities, accelerations, etc.) associated with the FLOLS servos. Quantitative performance data for each servo is tabulated as part of the individual hardware loop discussion. (See paragraphs 3.2.6.2 through 3.2.6.9, as applicable.)

a. Static Accuracy. Accurate line-of-sight placement of the projected image on the projection screen is a critical requirement. To achieve the required projector servo positioning accuracy, the following techniques are applied to servos of the visual system:

1. An integrator incorporated in the forward path of each servo acts to reduce the error signal to virtually zero during static positioning. It also makes the positioning accuracy of the servo independent of output torque thresholds or gravity loads on the output of the servo.

2. A unity voltage follower, immediately following each feedback pot wiper output signal, is physically located as near to the potentiometer as practical. The extremely high input impedance of this voltage follower serves to virtually eliminate errors due to potentiometer loading.

3. The method by which the position error signal is generated in the continuous sine/cosine servos depends first upon exciting the sine/cosine feedback pots with the computer generated sine/cosine commands; and secondly, upon summing the output wiper voltages of the sine/cosine feedback pots. The overall positioning accuracy of these servos depends, in part, on retaining the accuracy of the computed sine/cosine command up to the point where the excitation signals are applied to sine/cosine pots; also, upon the accuracy of the summation of the sine/cosine feedback pot wiper voltages. For this reason, precision resistors are used in these critical functions.

With the application of the techniques described above, remaining static positioning errors occur almost entirely from two sources: gearing errors (between feedback pot shaft and applicable controlled output of servo), and feedback potentiometer linearity or conformity errors.

Gearing errors are classified by two clearly identifiable components:

1. Transmission Error. The variation in the transmission ratio of a gear pair or train from the ideal nominal value, caused by the net sum of individual gear position errors and installation runout errors. This error is single valued and repeatable and combines with the potentiometer linearity error.

2. Backlash Error. The total lost motion for a gear pair or train caused by all contributors, such as thinned teeth, enlarged center distance, and runout of rotating parts. Backlash error is multivalued and is therefore not a specific repeatable error value. Therefore backlash in gearing is the only significant error in the determination of static repeatability accuracy.

Feedback potentiometer linearity (or conformity) error is the primary accuracy specification of a particular potentiometer assembly. The maximum permitted linearity error will be defined by procurement specifications for each potentiometer assembly used on AWAVS visual system.

Table 23 lists the potentiometer selections and static accuracy analysis summary for each servo of the visual system. A root-sum-square method is used in combining maximum allowable gearing errors with potentiometer errors. Feedback potentiometer errors listed in Table 23 are the maximum positioning error of the servo based on the potentiometer linearity (or conformity) specification. For the noncontinuous servos, this is directly related to the specified pot linearity and the gearing ratio, which determines the percentage of the full potentiometer travel that occurs over the full servo travel.

For the continuous servos which use sine/cosine feedback potentiometers, the relationship between the potentiometer conformity specification and the corresponding servo positioning error is based on the analytical derivation given in Figure 58.

b. Static Repeatability. As indicated in the discussion of gearing errors and based on the application of the servo design techniques, backlash in gearing is the only significant error source in the determination of static repeatability. As antibacklash gearing is utilized in each servo, the static repeatability error should be zero.

c. Static Compliance. Incorporation of integral control in each servo renders the closed loop dc sensitivity of each servo output displacement to disturbance torques or forces applied at the servo output virtually to infinity. This means that the servos are capable of resisting any externally applied output torque or force up to the peak motor torque, without having to hold a corresponding error in position. The result is a static servo compliance which is virtually infinite.

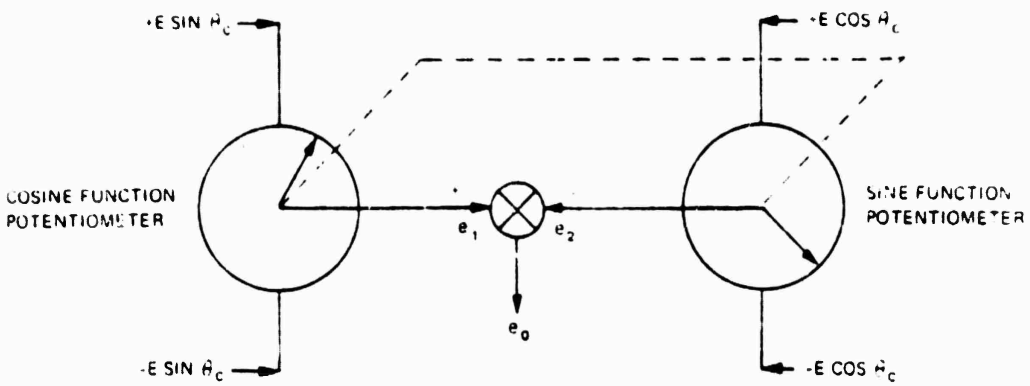

Where

- I = voltage scaling of the sine cosine functions of θ_c (10 volts)
- θ_c = commanded angle (radians)
- θ_f = Potentiometer shaft position angle (radians)
- e_1 = voltage output of cosine function potentiometer (volts)
- e_2 = voltage output of sine function potentiometer (volts)
- C = independent conformity of sine or cosine potentiometer expressed as a percentage of the full potentiometer excitation voltage

$$e_1 = I \sin\theta_c \cos\theta_f \pm 2I\left(\frac{C}{100}\right)\sin\theta_c$$

$$e_2 = I \cos\theta_c \sin\theta_f \pm 2I\left(\frac{C}{100}\right)\cos\theta_c$$

The true integration in the forward part of the servo loop will provide infinite dc open loop gain thereby making $e_1 - e_2 = 0$

Then

$$I \sin\theta_c \cos\theta_f \pm 2I\left(\frac{C}{100}\right)\sin\theta_c - I \cos\theta_c \sin\theta_f \pm 2I\left(\frac{C}{100}\right)\cos\theta_c = 0$$

$$\pm 0.02C \sin\theta_f \pm 0.02 \cos\theta_c = \sin\theta_c \cos\theta_f - \sin\theta_f \cos\theta_c$$
$$= \sin(\theta_c - \theta_f)$$
$$= (\theta_c - \theta_f) \text{ for small errors}$$

The servo position error due to the sine cosine feedback potentiometers is

$$\varepsilon = \left\{\theta_c - \theta_f\right\} = \pm 0.02C \sin\theta_c \pm 0.02C \cos\theta_c$$

The worst case error occurs at $\frac{d\varepsilon}{d\theta_c} = 0$

$$\frac{d\varepsilon}{d\theta_c} 0 = \pm 0.02C\dot{\theta}_c \cos\theta_c \pm 0.02C\dot{\theta}_c \sin\theta_c$$

$$\theta\Big|_{\text{worst case}} = \frac{\pi}{4} = \frac{3\pi}{4}$$

Then

$$\varepsilon_{\text{worst case}} = \frac{\sqrt{2}}{100} C = \frac{\sqrt{2}}{100} C \text{ radians}$$

For C = 0.0 worst case error = 0.04 = 0.04 degrees = ± 4.8 arcmin

AWAVS A003-58

Figure 58. Relationship Between Sine-Cosine Feedback Pot Conformity and Servo Positioning Error

d. Dynamic Range. The capability of the FLOLS simulation system servos to smoothly control the movement of the projected image over a wide range of velocities, is a critical requirement. The dynamic range defines the ratio of the largest to the smallest velocity which the servo can control. The maximum velocity for each servo is defined by the motion envelope in the AWAVS detailed servo specifications. Each servo will be judged to have satisfactory smoothness by direct visual observation of the image projected onto the screen at the minimum velocity specified by the applicable performance specification. Verifying smoothness using a test criterion based on monitoring the tachometer signal may not be valid because of large high frequency content in the signal which is not related to the actual observable smoothness of the projected image. It is valid only if the ripple, high frequency content, etc., of the tach are taken into account.

e. Frequency Response. A critical requirement in achieving an accurate representation of the external visual scene is synchronization of all servos involved in projecting the scene. This requires that the servos have the same dynamic response as well as the same degree of smoothness. To accurately control the synchronization of the visual system servos, the dynamic response is specified to accurately match (within 20%) an ideal second order system with a damping ratio, ζ, and natural frequency ω_n chosen for optimum performance.

The descriptions of the synthesis techniques which follow have been developed to achieve the specified servo dynamic response. Because of the two methods of providing input command signals to servos of the visual system — continuous servos with position inputs and noncontinuous servos with position inputs — two different synthesis approaches are used to achieve the required accuracy in setting the dynamic response. The distinction between continuous versus noncontinuous servos is important because the technique of handling sine/cosine position information precludes the use of compensating networks in both the input and feedback signal paths of the continuous servos.

f. System Type. Based on the specification of dynamic response (stringent tolerance of 0.1% of maximum velocity in high velocity tracking) servo system type has been decided. Optimum choice of bandwidth, stability damping ratio, percentage overshoot, velocity tracking error, and other parameters depends mostly on system type. The analysis of the type 1 servos is portrayed as a set of Bode plots presented as part of the individual servo loop discussions. The curves indicate the phase margin, bandwidth, damping ratio and velocity error constant. Limitations are also indicated.

In order for a system to reproduce the squarewave at its output, the system would have to have infinite bandwidth. Associated with infinite bandwidth is zero rise time and zero delay time. There is no analytic expression that even approximately relates the two for systems of arbitrary order. In reality, a system having large bandwidth is welcomed if the input signal is free from noise. A system with a large bandwidth can follow inputs with little error, and may be considered accurate, not only in its final value, but for all time. Speed of response, directly related to bandwidth, is a measure of accuracy for all time, and might be called the measure of dynamic accuracy.

The traditional well established analytic results of system classification and error constants for stable type 0, type 1 and type 2 unity feedback systems is shown in Figure 13. Based on the theory presented therein, the performance requirements given in Tables 21 and 22, and the analysis of servos as type 1 systems, the more critical FLOLS roll servo (ϕ_{FIT}) is designed as a type 2 system and the remaining servos as type 1 systems.

g. Generalities. The general compensation card has the capability to properly shape the feedback and forward path signals. The design philosophy of all noncontinuous servos is established to be the same. The components in the compensation card differ because of difference in controlled load and hardware of different servos. Similarly, same design philosophy is established for all continuous servos. Continuous servos need one more actuating signal generator card which is exactly the same for all of them. Table 23 shows the hardware components. The torquer-tachometers, power amplifiers, and buffers are common for all FLOLS servos manufactured by Singer.

h. Inherent Zeros and Poles Generated By Servo Components. The values of pertinent parameters of motor, tachometer, power amplifier, and follow-up potentiometer are included in hardware discussions. The tachometer generates an inherent zero which contributes to phase lead and is adjustable for stability as a function of cross-over frequency which determines the bandwidth. The motor impedance coupled with the mechanical inertia generates a pole contributing to a phase lag. The electrical time constant of the motor and amplifier generate two other poles contributing to phase lag.

The system will be stable if the phase margin, ϕ_{PM} which is a good measure of system stability, is at least 40°. Proper electronic shaping is necessary by utilizing the general compensation card which can generate two free integrators in the forward path, thus transforming an inherent type 1 stable system into type 2 or type 3 stable systems, and rendering the velocity error constant to almost infinity, and tracking error to almost zero.

3.2.6.2 FLOLS Motion Systems Servo Block Diagrams. The noncontinuous position servo block diagram given in Figure 14 is representative of the meatball, and iris servos. A continuous position servo block diagram, representative of the roll and X- and Y-displacement, servos is given in Figure 59. Transfer functions provided on each diagram are the mathematical expressions for the respective loops. Definitions of terms used in the transfer function equations and block diagrams are presented in the foregoing generalized servo discussions. Quantitative values are given in the individual servo hardware discussions, which follow.

The block diagrams of the zoom and zoom iris servos are not only far less complex than the others, but are also peculiar to these loops. Not being common to several servos as the continuous and noncontinuous loops covered herein, they are presented with their hardware discussions in paragraphs 3.2.6.4 and 3.2.6.5, respectively.

3.2.6.3 Design Analysis of FLOLS Meatball Servo. The performance specification of meatball servo [H_{MRDL} Height of meatball relative to datum lights] is given in Table 24.

TABLE 25. FLOLS MEATBALL SERVO PERFORMANCE

1. Excursion	±0.5 in.
2. Velocity (maximum)	10 in./sec
3. Acceleration	10 in./sec^2
4. Static Accuracy	±10 mils
5. Linearity	±10 mils
6. Repeatability	±10 mils
7. Resolution	±10 mils
8. Dynamic Range	100:1
9. Tracking Accuracy at velocity (high) velocity (low)	 1% max velocity 0.5% max velocity

The meatball servo [H_{MRDL}] is synthesized as follows to meet the performance specification parameters 1 through 9:

1. The mechanical sketch indicates a possible excursion of ±0.5in for the meatball assembly.

2. The dc torque motor is capable of a no load speed of 9000°/sec and the tachometer has a maximum operating speed of 9750°/sec.

3. The dc torquer can generate a peak torque of 79 oz in. The estimated inertia of meatball assembly is 0.02 oz in sec^2. The possible acceleration limit is 400in/sec^2. There is ample allowance for friction and disturbing torque of 0.4 oz in.

4. As described in paragraph 3.2.6.1, the static position error for this noncontinuous position servo emanates from the conformity specification of the position feedback potentiometer. The static position error could be ±10 mils.

5. The principle of the linear servo is to drive the control element by amplifying the actuating signal error. All components of this system are linear, and the linearity of the position transducer, potentiometer is specified to ±10 mils.

6. With proper initial calibration to meet the static error requirement as stated above, any position error beyond that specified as conformity of the potentiometer ±10 mils will be reduced to zero, because of integral control. Steady-state repeatability in this type of control system, cannot be greater than the steady-state position error.

7. In order to meet the resolution requirement of ±10 mils, a linear potentiometer of infinite resolution is chosen as the position transducer. The digital command signal from the computer is converted to an analog signal by a 12-bit D/A converter, the command signal resolution being 6 arc min, corresponding to 1 mil.

8. The dynamic range, the 100:1 ratio of maximum velocity to minimum velocity can be met by the choice of a high quality dc motor and tachometer, by minimizing friction, and by direct driving or by using anti-backlash gears of low gear ratio. In this case, the meatball assembly is driven through a Roh'lix of 4 rev/inch by the motor-tachometer. A one-inch rectilinear potentiometer is used as feedback position transducer.

9. The reduced transfer function indicates that this servo is designed as a type 1 system. As shown in the analysis, the velocity error coefficient is finite. This implies that the servo follows a ramp input of the form t'u(f) with finite steady state error. The velocity error constant is approximately 72, with tracking error ±4 mils, which is well below the required tracking accuracy.

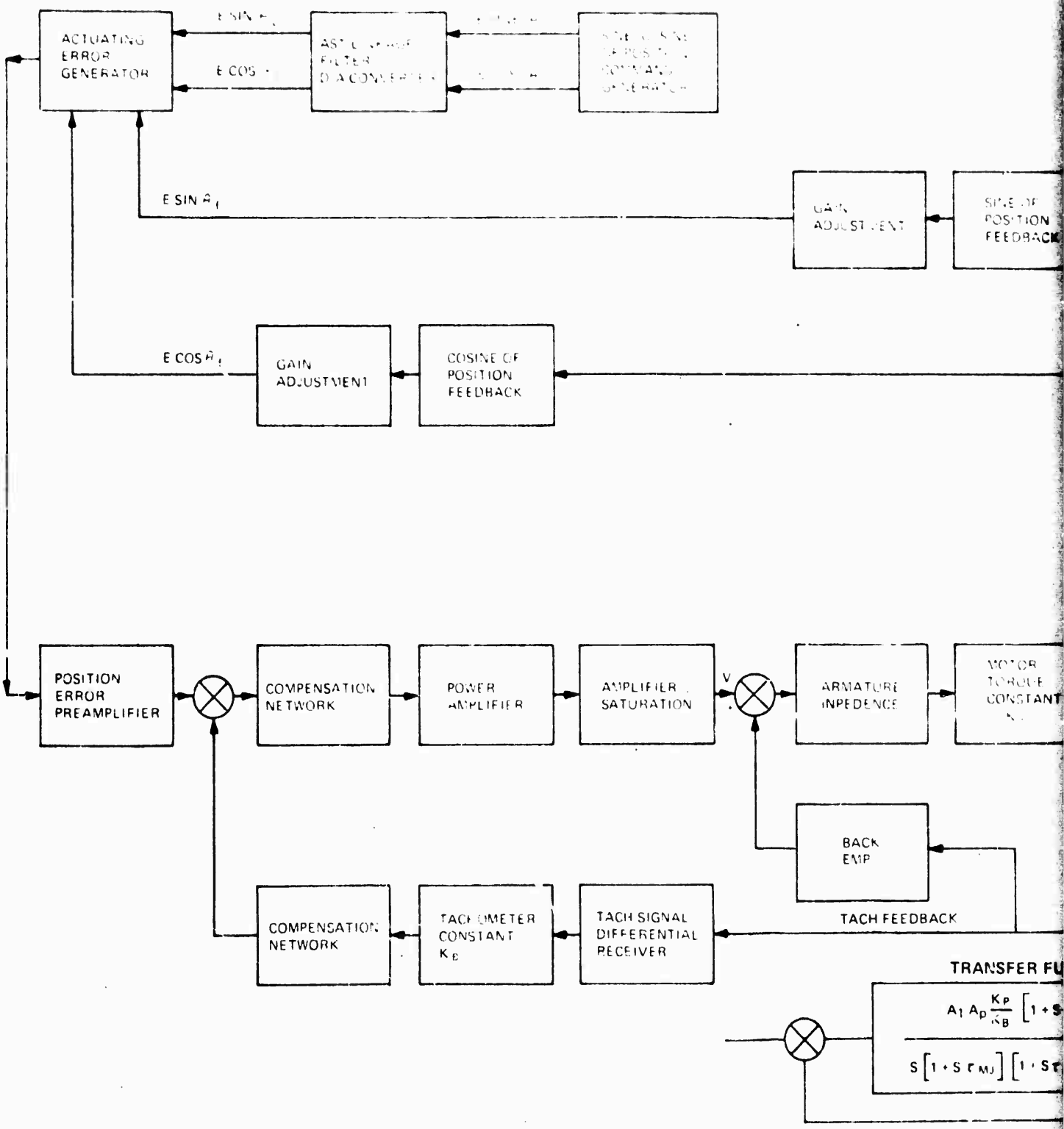
ACTUATING ERROR GENERATOR
E SIN
E COS
FILTER
D/A CONVERTER
E SIN A_1
GAIN ADJUSTMENT
SINE OF POSITION FEEDBACK
E COS A_1
GAIN ADJUSTMENT
COSINE OF POSITION FEEDBACK
POSITION ERROR PREAMPLIFIER
COMPENSATION NETWORK
POWER AMPLIFIER
AMPLIFIER SATURATION
V
ARMATURE IMPEDENCE
MOTOR TORQUE CONSTANT
BACK EMF
TACH FEEDBACK
COMPENSATION NETWORK
TACHOMETER CONSTANT K_B
TACH SIGNAL DIFFERENTIAL RECEIVER
TRANSFER FU
$A_1 A_p \frac{K_P}{K_B} \left[1 + S$
$S\left[1 + S\tau_{MJ}\right]\left[1 + S\tau$

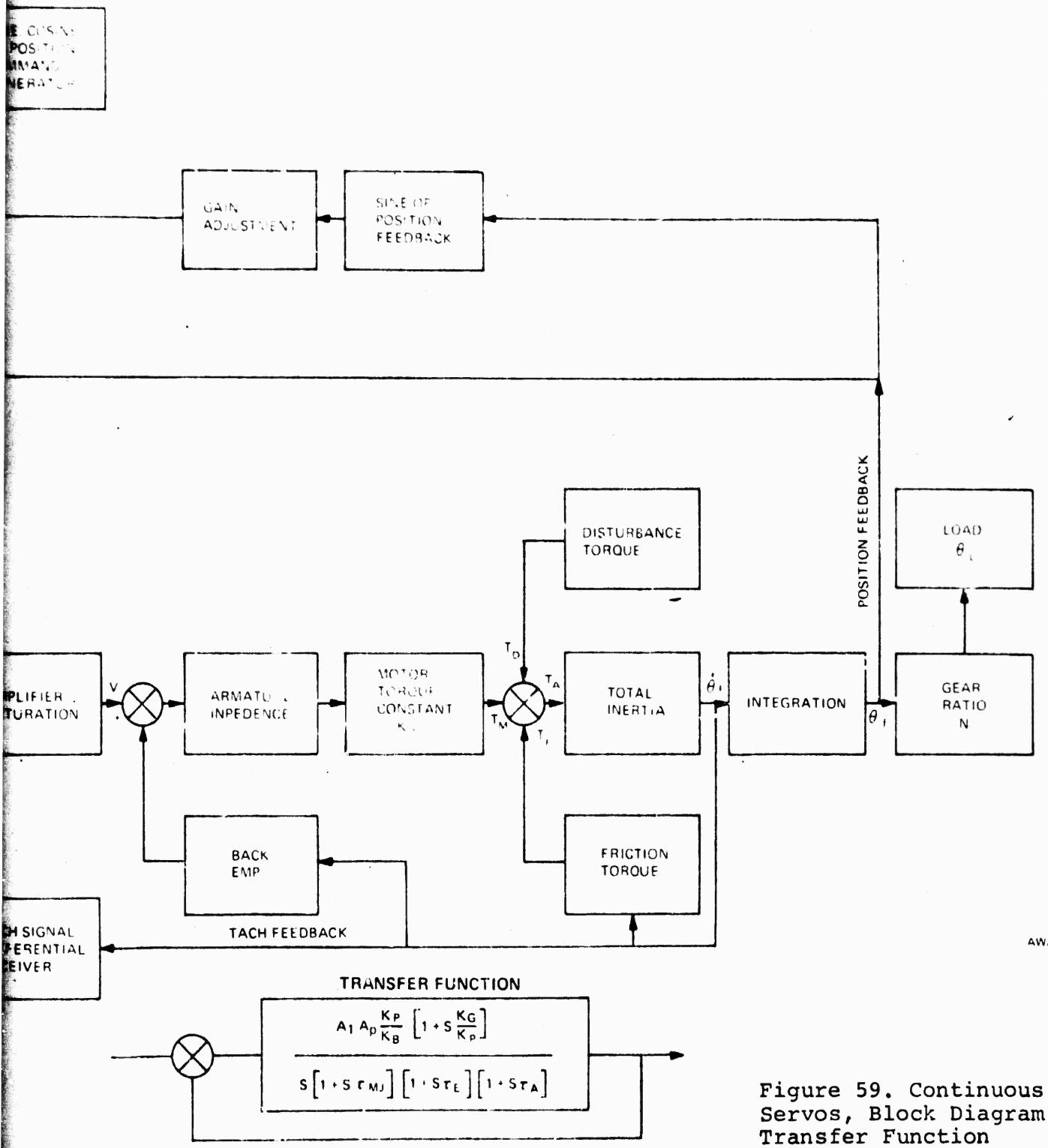

TRANSFER FUNCTION

$$\frac{A_1 A_p \frac{K_P}{K_B}\left[1 + S\frac{K_G}{K_P}\right]}{S\left[1 + S\tau_{MJ}\right]\left[1 + S\tau_E\right]\left[1 + S\tau_A\right]}$$

Figure 59. Continuous Position Servos, Block Diagram and Transfer Function

The stability analysis is illustrated on the frequency-gain plot, Figure 60. The criteria used for stability are as follows:

- To keep the phase margin greater than 40°.
- To shape the slope of the frequency-gain curve to 20 dB/decade at a decade around the crossover frequency.
- To reduce the gain sharply at high frequencies.

Inherent zeros and poles plotted on the frequency-gain curve are defined in Table 25. The phase margin ϕ_{PM} should be at least 40° for the system to be relatively stable. Phase margin is defined as:

$$\phi_{PM} = 180 - \sum \text{phase lags and leads in the system}$$

Phase lags:	Integral control	$[\frac{1}{S}]$	: 90°
	Mechanical time constant	$[\tau_{MJ}]$	: 85°
	Electrical time constant	$[\tau_e]$	: 5°
	Power amplifier time constant	$[\tau_A]$	: 1°
Phase leads:	Tachometer zero	$[\tau_Z]$	:-85°
Net contribution			: 96°

Phase margin: $\phi_{PM} = 180° - 96° = 84°$

This insures excellent stability. However, the compensation card has several adjustable features which, if necessary, can be used to shape the signal. In fact, τ_{MJ} is estimated and τ_Z is adjustable.

TABLE 26. INHERENT ZEROS AND POLES FOR FLOLS MEATBALL SERVO

ω_L	Zero	Tachometer and Pot	$\frac{K_P}{K_G}$	10 rad/sec
ω_{MJ}	Pole 1	Motor and Load	$\frac{K_T K_B}{RJ}$	10 rad/sec
ω_E	Pole 2	Motor	$\frac{L}{R}$	1500 rad/sec
ω_A	Pole 3	Power Amplifier	Bandwidth	6000 rad/sec

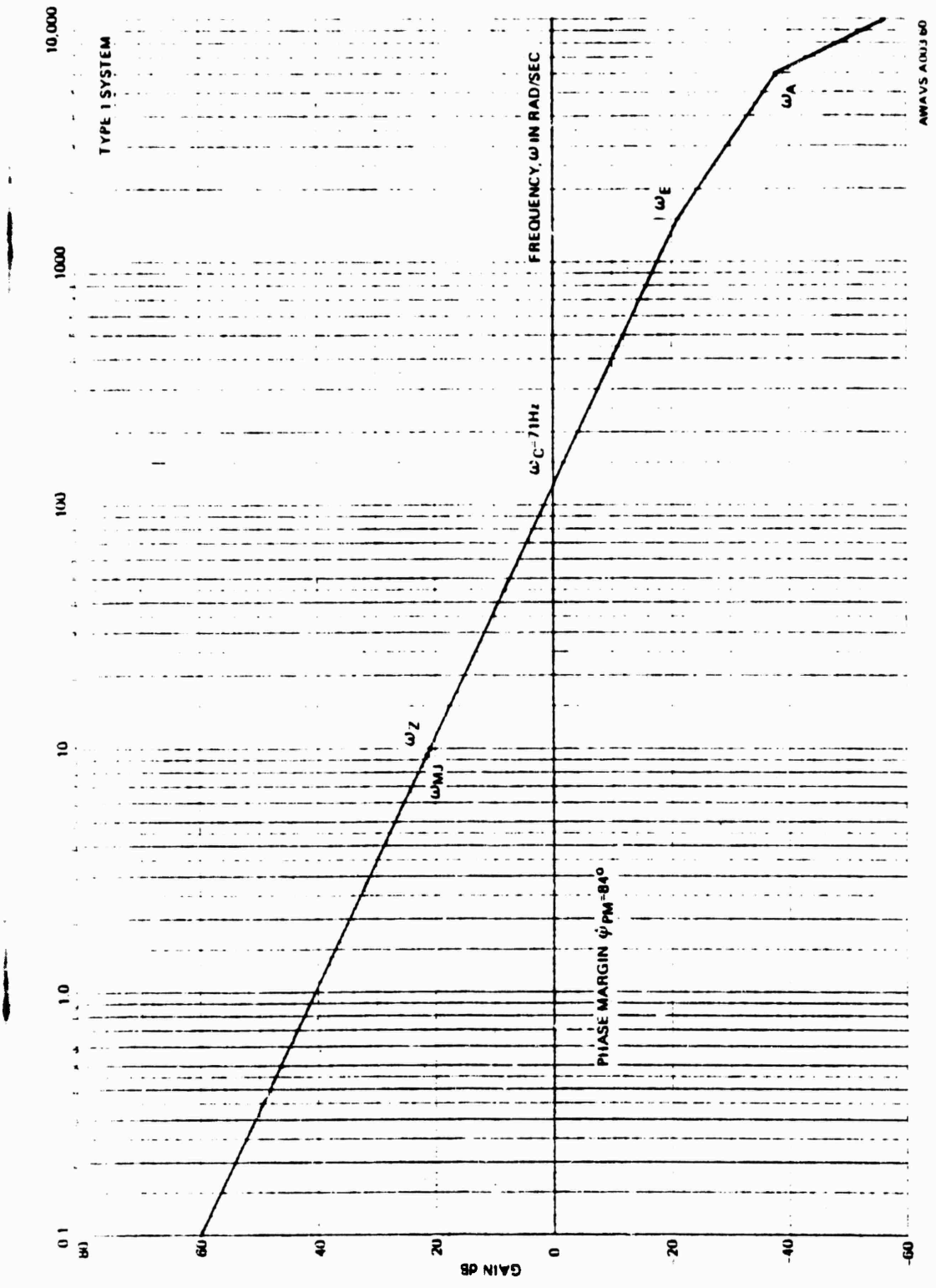

Figure 60. Frequency-Gain Plot for FLOLS Meatball Servo

3.2.6.4 Design Analysis of FLOLS Zoom Servo. The performance specification for the zoom servo [Z_{FIT}] is given in Table 26.

TABLE 27. FLOLS ZOOM SERVO PERFORMANCE

1.	Excursion	187°
2.	Velocity [maximum]	60°/sec
3.	Acceleration	30°/sec^2
4.	Static Accuracy	±10 arc min
5.	Linearity	±0.1% max excursion
6.	Repeatability	±10 arc min
7.	Resolution	±0.05% max excursion
8.	Dynamic Range	500:1
9.	Tracking Accuracy at Velocity (high)	0.5% max velocity
	Velocity (low)	0.1% max velocity

The zoom servo has been designed by Stahl Research Laboratories to drive the zoom mechanism smoothly over a wide dynamic range. The zoom lens is driven by a precision miniature direct current servo motor through a gear train and friction clutch as shown in the block diagram, Figure 61. All circuitry for the zoom servo including the power amplifier output stage and the compensation and summing electronics, is contained on one circuit board mounted in a small housing directly on the lens assembly. The zoom servo utilizes tachometer velocity feedback for loop stabilization, with a supplementary followup potentiometer position feedback signal. The zoom lens driven by the servo is a Cannon PV10 X 12 specially modified for the servo drive application. Both the lens and servo are identical to those used in the target projection optical system.

The command signal for the zoom servo is ±10V dc analog. It is received differentially so as to reject any accompanying noise.

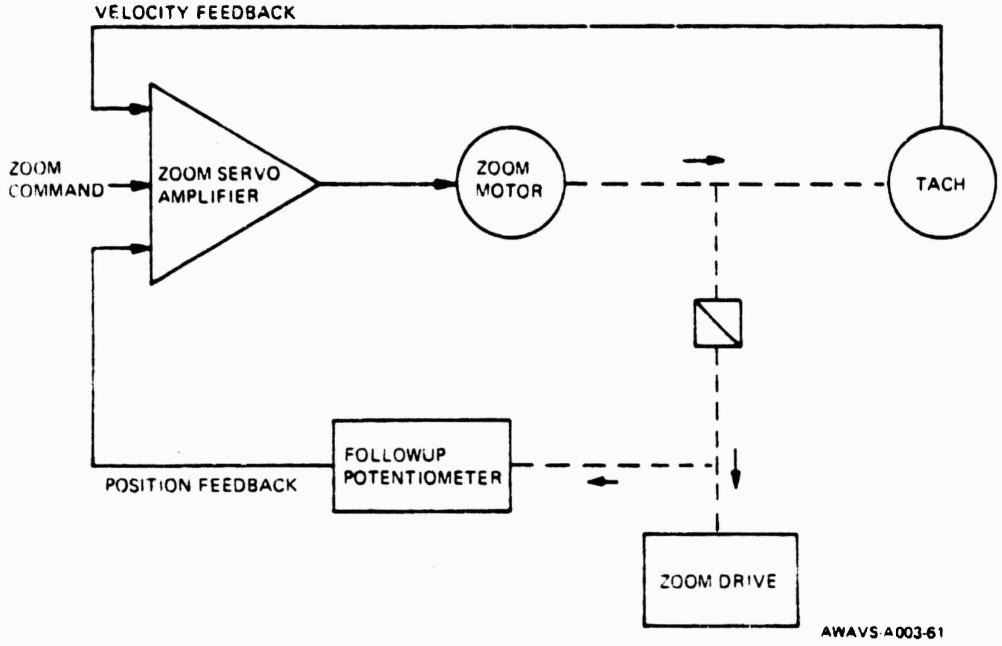

Figure 61. FLOLS Zoom Servo, Block Diagram

3.2.6.5 Design Analysis of FLOLS Zoom Iris Servo. The performance specification for the zoom iris servo (I_{ZFIT}) is given in Table 27.

TABLE 28. FLOLS ZOOM IRIS SERVO PERFORMANCE

Excursion	120°
Accuracy	±5%

The zoom iris servo has been specially designed by Stahl Research Laboratories to drive the zoom iris mechanism smoothly over a wide dynamic range. The iris is driven by a precision miniature direct current servo motor through a gear train and friction clutch. All the circuitry for the servo, including the power amplifier output stage and the compensation and summing electronics, is contained on two individual circuit boards (one of which also contains the zoom circuitry) mounted in a housing on the lens assembly. The iris servo uses forward path lead/lag circuitry to ensure stable, low overshoot performance.

Zoom iris servos for the FLOLS and target projector zoom lenses are identical. A differentially received analog input signal drives the servo. Input signals differ in magnitude, however, since the FLOLS zoom iris is driven to a maximum aperture of f/12 to f/15, while the target projection iris is driven to the maximum aperture of the Cannon PV 10 x 12 lens. On the FLOLS zoom iris servo, the iris is used only as an on-off shutter. Using the relatively small aperture, only a 1/4 turn of the control ring is necessary for the iris to be driven from its maximum aperture to fully closed.

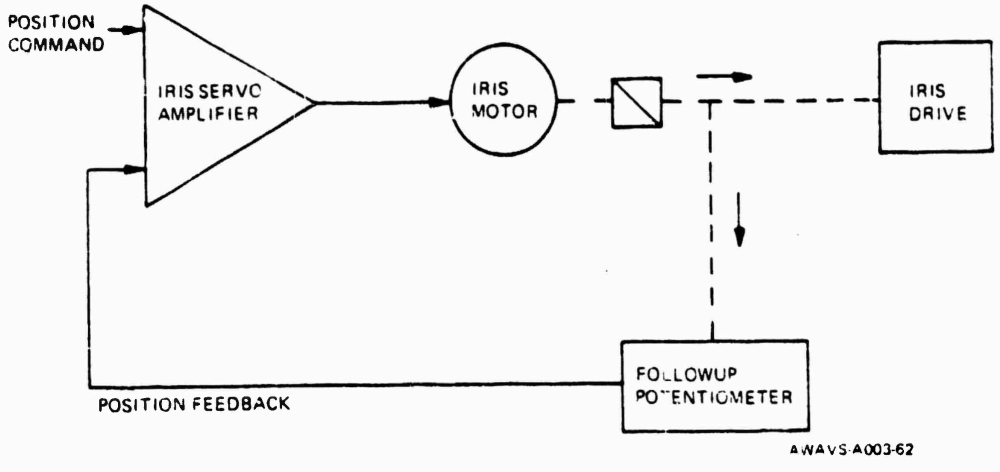

Figure 62. FLOLS Zoom Iris Servo, Block Diagram

3.2.6.6 Design Analysis of FLOLS Iris Servo [I_{FIT}]. The performance specification of iris servo is given in Table 28.

TABLE 29. FLOLS IRIS SERVO PERFORMANCE

1.	Excursion	±40°
2.	Velocity [Maximum]	360°/sec
3.	Acceleration	600°/sec^2
4.	Static Accuracy	±30 arc min
5.	Linearity	±30 arc min
6.	Repeatability	±30 arc min
7.	Resolution	±30 arc min
8.	Dynamic Range	100:1
9.	Tracking Accuracy at Velocity (high)	2%
	Velocity (low)	1%

The FLOLS iris servo is synthesized as follows to meet the performance specification parameters 1 through 9:

1. The mechanical sketch indicates a possible excursion of ±40° for the azimuth assembly.

2. The dc torque motor is capable of a no load speed of 9000°/sec and the tachometer has a maximum operating speed of 9750°/sec.

3. The dc torque can generate a peak torque of 79 oz in. The estimated inertia of iris assembly is 0.01 oz in sec^2. The possible acceleration limit is 106°/sec^2. There is ample allowance for friction and disturbing torque of 6 oz in.

4. As described in paragraph 3.2.6.1, the static position error for this noncontinuous position servo emanates from the conformity specification of the position feedback potentiometer. The static position error could be ±30 arc min.

5. The principle of the linear servo is to drive the control element by amplifying the actuating signal error. All components of this system are linear and the linearity of position transducer potentiometer, is specified to ±30 arc min.

6. With proper initial calibration to meet the static error requirement as stated above, any position error beyond that specified as conformity of the potentiometer ±30 arc min will be reduced to zero, because of integral control. Steady-state repeatability in this type of control system, cannot be greater than the steady-state position error.

7. In order to meet the resolution requirement of ±30 arc min, a potentiometer of infinite resolution is chosen as the position transducer. The digital command signal from the computer is converted to an analog signal by a 12-bit D/A converter, the command signal resolution being ±6 arc min.

8. The dynamic range, the 100:1 ratio of maximum velocity to minimum velocity, can be met by the choice of a high quality dc motor and tachometer, by minimizing friction, and by direct driving or by using anti-backlash gears of low gear ratio. In this case, the iris assembly is driven by a gear ratio of 2:1 by the motor-tachometer potentiometer system.

9. The reduced transfer function indicates that this servo is designed as a type 1 system. As shown in the analysis, the velocity error coefficient is finite. This implies that the servo follows a ramp input of the form t'u(t) with finite steady-state error. Velocity error constant is approximately 50. Error at maximum speed would be about 11°. Thus the tracking accuracy of the specification is met.

The stability analysis is indicated on the frequency-gain plot, Figure 63. The criteria used for stability are as follows:

- To keep the phase margin greater than 40°.

- To shape the slope of the frequency-gain curve to 20 dB per decade at and around the decade crossover frequency.

- To reduce the gain sharply at high frequencies.

Inherent zeros and poles plotted on the frequency-gain curve are defined in Table 29. The phase margin ϕ_{PM} should be at least 40° for the system to be relatively stable. Phase margin is defined as

ϕ_{PM} = 180 - $\sum$ phase lags and leads in the system.

Phase lags:	Integral control	$[\frac{1}{S}]$	:90°
	Mechanical time constant	$[\tau_{MJ}]$	:87°
	Electrical time constant	$[\tau_e]$	:25°
	Power amplifier time constant	$[\tau_A]$	:05°
Phase leads:	Tachometer zero	$[\tau_Z]$	:-70°
Net contribution:			:110

Phase margin : ϕ_{PM} = 180° - 110 = 70°

This insures excellent stability. However, the compensation card has several adjustable features which, if necessary, can be used to shape the signal. In fact τ_{MJ} is estimated and τ_Z, is adjustable.

TABLE 30. INHERENT ZEROS AND POLES FOR FLOLS IRIS SERVO

ω_L	Zero	Tachometer and Pot	$\frac{K_P}{K_G}$	26 rad/sec
ω_{MJ}	Pole 1	Motor and Load	$\frac{K_T K_B}{RJ}$	5 rad/sec
ω_E	Pole 2	Motor	$\frac{L}{R}$	1500 rad/sec
ω_A	Pole 3	Power Amplifier	Bandwidth	6000 rad/sec

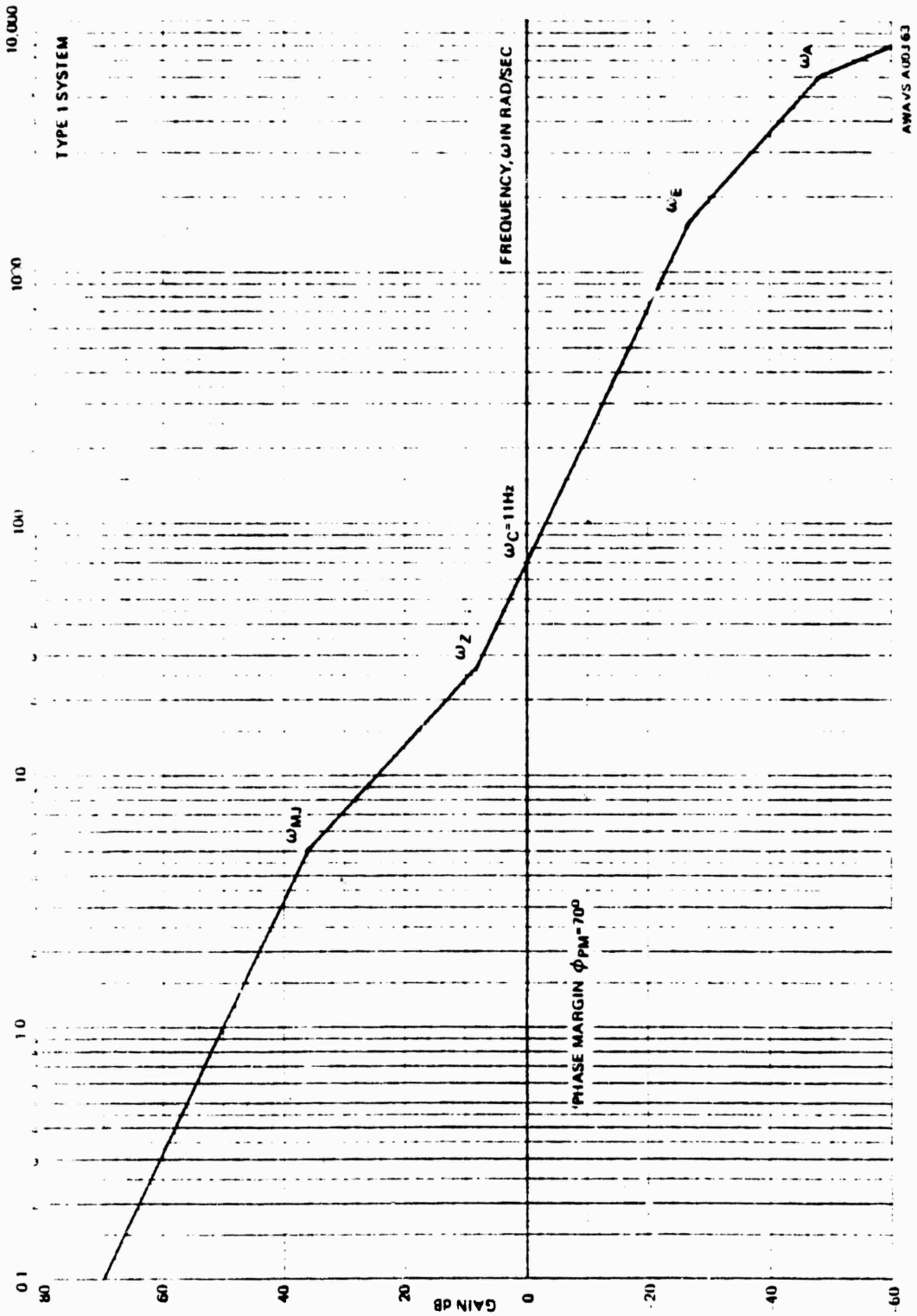

Figure 63. Frequency-Gain Plot for FLOLS Iris Servo

3.2.6.7 Design Analysis of FLOLS Roll Servo. The performance specification of roll servo [φ_{FIT}] is given in Table 30.

TABLE 31. FLOLS ROLL SERVO PERFORMANCE

1.	Excursion	360°
2.	Velocity [Maximum]	360°/sec
3.	Acceleration	600°/sec^2
4.	Static Accuracy	20 arc min
5.	Linearity	0.05% max excursion
6.	Repeatability	20 arc min
7.	Resolution	0.01% max excursion
8.	Dynamic Range	1000:1
9.	Tracking Accuracy at Velocity (high)	0.1% max velocity
	Velocity (low)	0.05% max velocity

The FLOLS roll servo is synthesized as follows to meet the performance specification parameters 1 through 9:

1. The roll servo is designed for continuous rotation of 360°. The position transducer is constructed as a pair of sine-cosine potentiometers. The error signal,which is amplified to drive the dc motor, is generated by exciting the sine-cosine potentiometers as described in the foregoing paragraph on general servo considerations. The system is stabilized for smooth performance by both tachometer feedback and electronic signal shaping.

2. The dc torquer tachometer is capable of no a no load speed of 9000°/sec.

3. The dc torquer can generate a peak torque of 79 oz in. The estimated inertia of the roll assembly is 2 oz in sec^2, and the possible acceleration limit 2000°/sec^2.

4. As described in paragraph 3.2.6 1, the static position error for the continuous servo emanates from the conformity specification of the sine-cosine potentiometers. The maximum possible static error could be ±5 arc min.

5. The principle of the continuous servo is to drive the control element by amplifying the error signal, which is generated by exciting the sine-cosine potentiometers. The linearity is specified to ±0.05%.

6. With the initial calibration to meet the static error requirement, any steady-state position error beyond that specified as conformity of potentiometers ±5 arc min will be reduced to zero, because of integral control. Steady-state repeatability, in this type of control system, cannot be greater than the steady-state position error.

7. In order to meet the resolution requirement of ±0.01% of maximum excursion, potentiometers of infinite resolution are chosen. The digital command signal from the computer is converted to an analog signal by a 14-bit D/A converter, the command resolution being 1.3 arc min.

8. The dynamic range, the 1000:1 ratio of maximum velocity to minimum velocity, can be met by the choice of high quality dc motor and tachometer, by minimizing friction, and by direct driving or by using anti-backlash gears of low gear ratio. In this case, the roll assembly is driven by the motor-tachometer potentiometer system through a 2:1 antibacklash gear.

9. The reduced transfer function indicates that this servo is designed as a type 2 system. As shown in the analysis, the velocity error coefficient is ∞. This implies that the servo follows a ramp input of the form $t'u(t)$ with zero steady state error. Therefore the tracking accuracy of the specification is met.

The stability analysis is indicated on the frequency-gain plot, Figure 64. The criteria used for stability are as follows:

- To keep the phase margin greater than 40°.
- To shape the slope of the frequency-gain curve to 20 dB per decade at and around the decade crossover frequency.
- To reduce the gain sharply at high frequencies.

Inherent zeros and poles plotted on the frequency-gain curve are defined in Table 31. The phase margin ϕ_{PM} should be at least 40° for the system to be relatively stable. Phase margin is defined as:

ϕ_{PM} = 180 - $\sum$ phase lags and leads in the system

Phase lags:	Integral control	$[\frac{1}{S}]$	: 180°
	Mechanical time constant	$[\tau_{MJ}]$	: 88°
	Electrical time constant	$[\tau_e]$	: 3°
	Power amplifier time constant	$[\tau_A]$	: 1°
Phase leads:	Tachometer zero	$[\tau_Z]$	: -81°
	Electronic zero	$[\tau_I]$	: -88°
Net contribution:			: 103

Phase margin: ϕ_{PM} = 180° - 103 = 77°

This insures excellent stability. However, the compensation card has several adjustable features which if necessary can be used to shape the signal. In fact, τ_{MJ} is estimated and τ_Z and τ_I are adjustable.

TABLE 32. INHERENT ZEROS AND POLES FOR FLOLS ROLL SERVO

ω_L	Zero	Tachometer and Pot	$\frac{K_P}{K_G}$	10.5 rad/sec
ω_{MJ}	Pole 1	Motor and Load	$\frac{K_T K_B}{RJ}$	97 rad/sec
ω_E	Pole 2	Motor	$\frac{L}{R}$	1500 rad/sec
ω_A	Pole 3	Power Amplifier	Bandwidth	6000 rad/sec

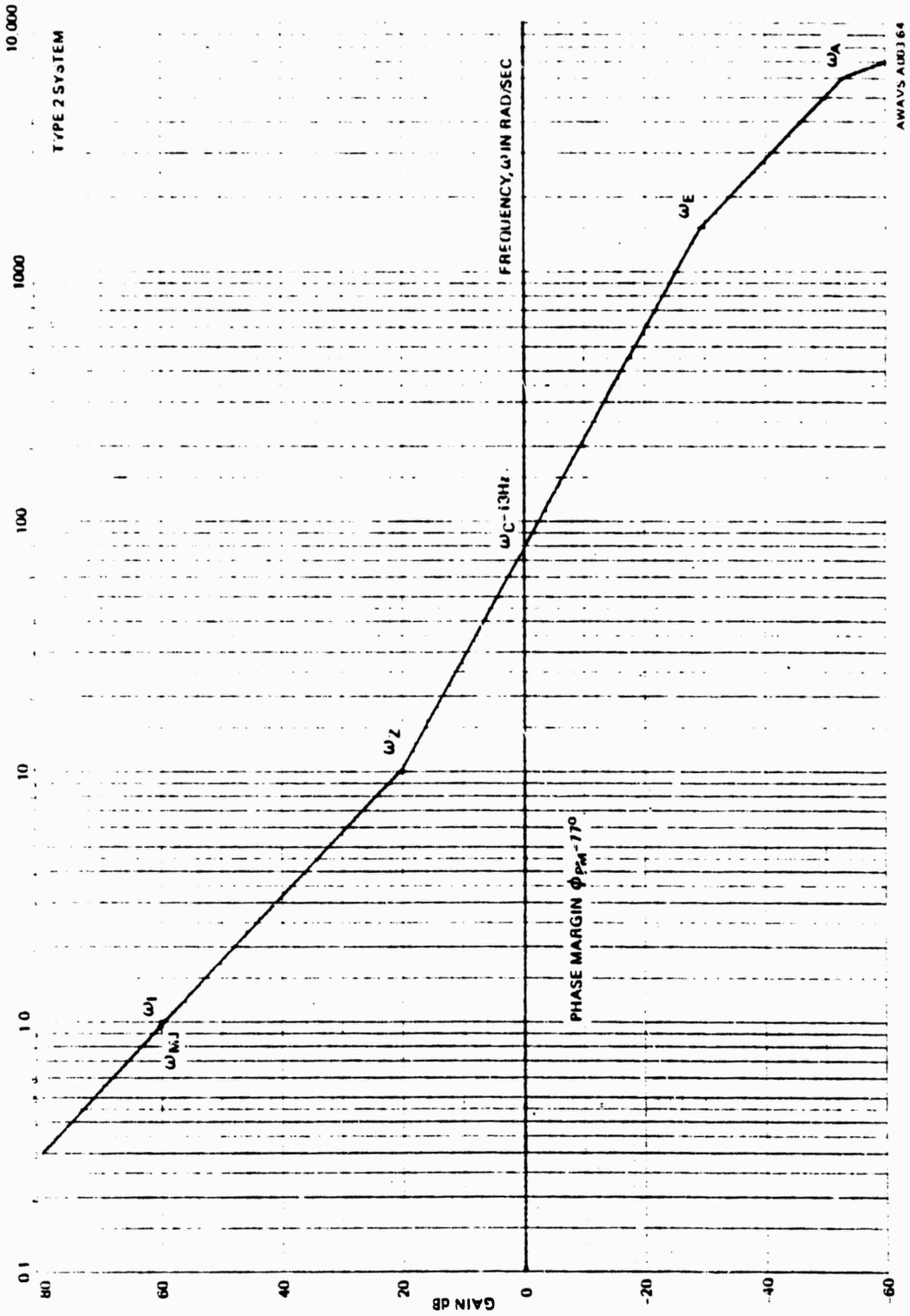

Figure 64. Frequency-Gain Plot for FLOLS Roll Servo

3.2.6.8 Design Analysis of X- and Y-Displacement (Pitch Wedge) Servos. The performance specification of X- and Y-displacement pitch wedge servos [$\Delta\theta_X$, $\Delta\theta_Y$] is given in Table 32.

TABLE 33. FLOLS PITCH WEDGE SERVO PERFORMANCE

1.	Excursion	360°
2.	Velocity [Maximum]	360°/sec
3.	Acceleration	360°/sec^2
4.	Static Accuracy	±20 arc min
5.	Linearity	±0.05% max excursion
6.	Repeatability	±20 arc min
7.	Resolution	±0.01% max excursion
8.	Dynamic Range	200:1
9.	Tracking Accuracy at Velocity (high)	0.1% max velocity
	Velocity (low)	0.05% max velocity

The pitch wedge servos are synthesized as follows to meet the performance specification parameters 1 through 9:

1. The pitch wedge servos are designed for continuous rotation of 360°. The position transducer is constructed as a paired sine-cosine potentiometer. The error signal, which is amplified to drive the dc motor, is generated by exciting the sine-cosine potentiometers as described in the foregoing paragraph on general servo considerations. The system is stabilized for smooth performance by both tachometer feedback and electronic signal shaping.

2. The dc torquer tachometer is capable of a no load speed of 9000°/sec.

3. The dc torquer can generate a peak torque of 79 oz in. The estimated inertia of either pitch wedge assembly is 0.04 oz in sec^2 and the possible acceleration limit is 104°/sec^2.

4. As described in paragraph 3.2.6.1, the static position error for the continuous servo emanates from the conformity specification of the sine-cosine potentiometers. The maximum static error could be ±5 arc min.

5. The principle of the continuous servo is to drive the control element by amplifying the error signal, which is generated by exciting the sine-cosine potentiometers. The linearity is specified to ±0.5%.

6. With the initial calibration to meet the static error requirement, any steady-state position error beyond that specified as conformity of potentiometers ±5 arc min will be reduced to zero, because of integral control. Steady-state repeatability in this type of control system cannot be greater than the steady-state position error.

7. In order to meet the resolution requirement of ±0.01% of maximum excursion, potentiometers of infinite resolution are chosen. The digital command signal from the computer is converted to an analog signal by a 14-bit D/A converter, the command resolution being ±1.3 arc min.

8. The dynamic range, the 200:1 ratio of maximum velocity to minimum velocity, can be met by the choice of a high quality dc motor and tachometer, by minimizing friction, and by direct driving or by using anti-backlash gears of low gear ratio. In this case, the pitch wedge assembly is driven by the motor-tachometer potentiometer system through 1:1 antibacklash gearing.

9. The reduced transfer function indicates that this servo is designed as a type 1 system. As shown in the analysis, the velocity error coefficient is finite. This implies that the servo follows a ramp input of the form $t'u(t)$ with finite steady-state error. Therefore the velocity error constant is approximately 130 resulting in a tracking error of less than 0.1%.

The stability analysis is indicated on the frequency-gain plot, Figure 65. The criteria used for stability are as follows:

- To keep the phase margin greater than 40°.
- To shape the slope of the frequency-gain curve to 20 dB per decade at and around the deacde crossover frequency.
- To reduce the gain sharply at high frequencies.

Inherent zeros and poles plotted on the frequency-gain curve are defined in Table 33. The phase margin ϕ_{PM} should be at least 40° for the system to be relatively stable. Phase margin is defined as

$$\phi_{PM} = 180 - \sum \text{phase lags and leads in the system}$$

Phase lags:	Integral control	$[\frac{1}{S}]$	: 90°
	Mechanical time constant	$[\tau_{MJ}]$	: 88°
	Electrical time constant	$[\tau_e]$	: 75°
	Power amplifier time constant	$[\tau_A]$	: 2°
Phase leads:	Tachometer zero	$[\tau_Z]$	: -82°
Net contribution:			: 106

Phase margin: $\phi_{PM} = 180° - 106° = 74°$

This insures excellent stability. However, the compensation card has several adjustable features which if necessary can be used to shape the signal. In fact, τ_{MJ} is estimated and τ_Z is adjustable.

TABLE 34. INHERENT ZEROS AND POLES FOR FLOLS PITCH WEDGE SERVOS

ω_L	Zero	Tachometer and Pot	$\frac{K_P}{K_G}$	24 rad/sec
ω_{MJ}	Pole 1	Motor and Load	$\frac{K_T K_B}{RJ}$	4.5 rad/sec
ω_E	Pole 2	Motor	$\frac{L}{R}$	1500 rad/sec
ω_A	Pole 3	Power Amplifier	Bandwidth	6000 rad/sec

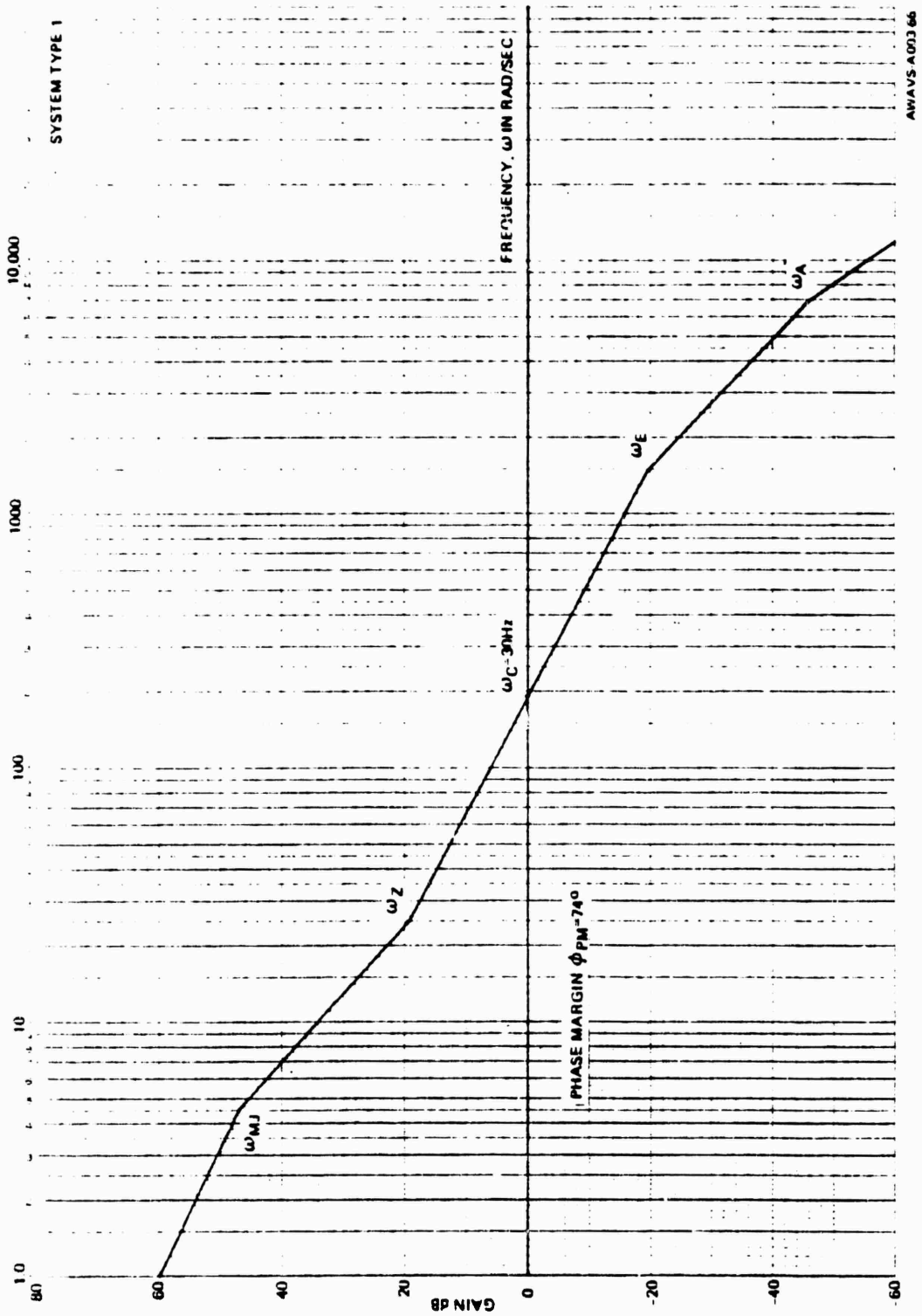

Figure 65. Frequency-Gain Plot for FLOLS Pitch Wedge Servos

3.2.7 Maintenance Panel Interface. For test purposes, manual operation of the FLOLS lights and servos is possible from controls on the cockpit electronics test panel. (See Figure 66.) This is a dual purpose maintenance panel used for manual control of both the FLOLS and the target projection equipment. Only the FLOLS related controls are discussed herein; refer to paragraphs 3.3.5 and 3.6.4 for the remaining coverage. In order for any of the FLOLS SERVOS or TARGET PROJECTION SERVOS MANUAL CONTROLs on the cockpit electronics test panel to be brought on-line, the key switch must be set to the TEST position. The MISCELLANEOUS controls operate independently of the key switch.

Five FLOLS lighting and six FLOLS servo functions are controllable from the cockpit electronics test panel. The CUT, WAVEOFF, and AUX WAVEOFF pushbutton switches are alternate action devices. When depressed, the normal control line from the EOS (via the linkage) is opened and the indicated FLOLS lights are turned on. These switches control the lights only — not the choppers. The chopper devices which simulate the waveoff and red meatball strobe effects are controlled by the WAVEOFF and RED MEATBALL STROBE (RUN/STOP) pushbuttons on the MISCELLANEOUS segment of the test panel. All of the alternate action swithces mentioned above light to indicate their present position.

Manual operating controls are provided for all FLOLS servos except the zoom iris. The special manual control function for the zoom iris is not necessary since it is only used as an on/off device and is manually operable to that extent from the EOS. The control knobs for the other six servos provide velocity and directional control when the respective RUN/STOP buttons are pressed. The ROLL, P WEDGE X, and P WEDGE Y controls operate continuous servos, and, therefore, have no limit indicators. The MEATBALL and IRIS servo controls are provided with indicators which light when a limit of travel has been reached. The ZOOM control, although operating a non-continuous type servo, is not provided with a limit indicator since the zoom servo is fitted with a slip clutch that allows the servo to overrun its limits without damage.

3.3 Target Projection System

The target projection system is the portion of the visual system whose function is to display the carrier, wake, and FLOLS to the pilot within the required field of view. Figure 67 is the system block diagram. The target projector electronic interface relays the TIG video and sync to the light valve projector. The projector optically synthesizes the target image (carrier and wake) and inserts it into the target optical chain. Within this chain the carrier and FLOLS images are merged and projected on the screen. The carrier image brightness and contrast can be controlled from the target projector remote control unit. The linkage relays commands to the target projector servos to display the image in the correct size and position. The servos can be manually operated from the maintenance panel, located in the cockpit enclosure, for test purposes.

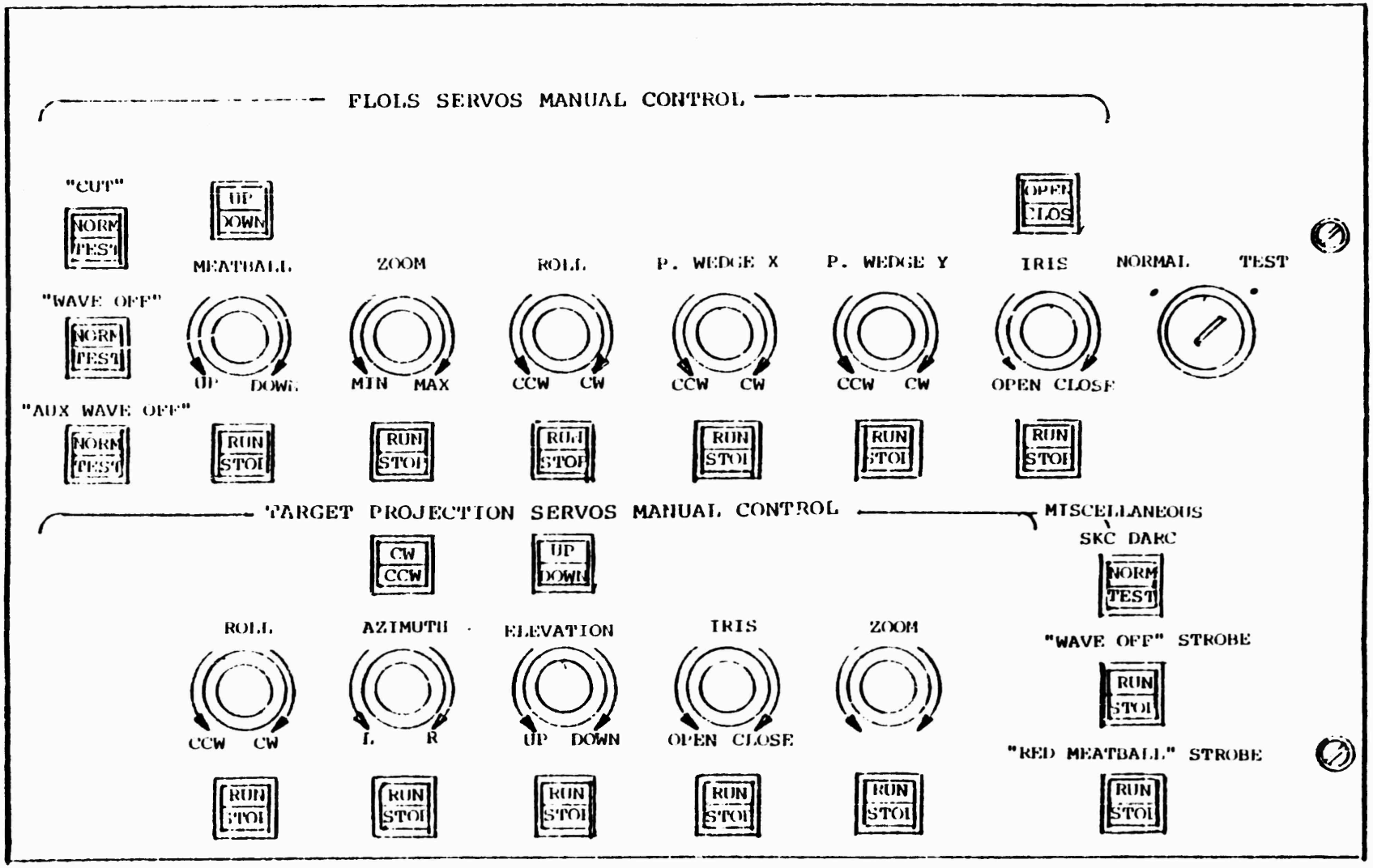

Figure 66. Cockpit Enclosure Test Panel

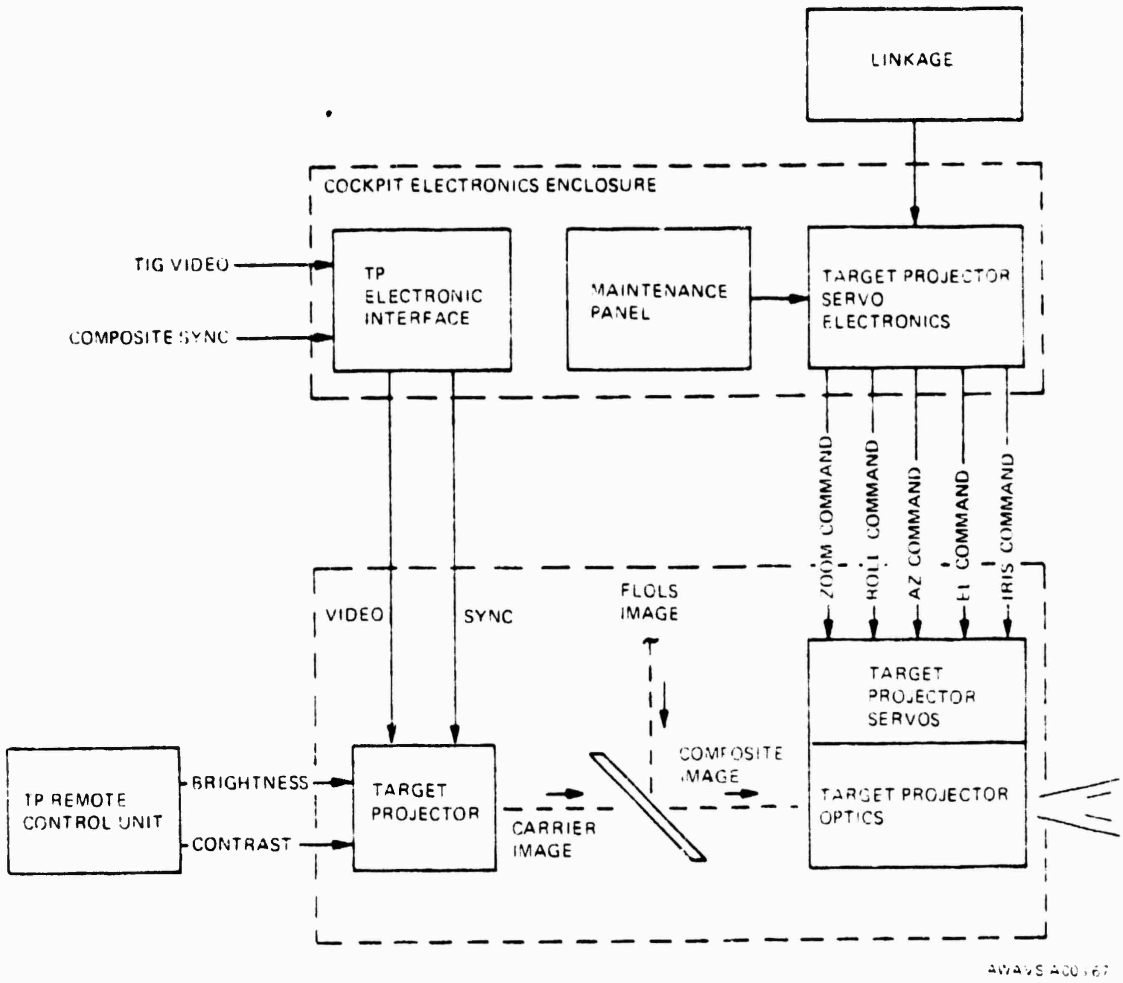

Figure 67. Target Projection System, Block Diagram

3.3.1 Target TV Projector. Except for a difference in optics, the General Electric PJ7150 light valve projector used in this capacity is identical to the background TV projector. (See paragraph 3.5.6 for details.) The projection lens (T_6 in paragraph 3.3.2.1) used on the target projector is the lens supplied by GE, whereas its counterpart (T_6M) used with the background projector has been modified for compliance with resolution requirements. The remote control units for the target and background projectors are also identical.

3.3.2 Target Projector Optics. The target projector optics performs the dual function of combining the FLOLS and target projector images and relaying them to the display screen. An optical schematic is provided in Figure 68. For discussion purposes, the optics is divided into the combining optics, relay optics, and zoom lens.

3.3.2.1 Combining Optics. The combining optics is comprised of imaging lens T_6 and beamsplitter P_1. The T_6 lens collimates the light valve projector raster plane and presents it to the straight through axis of the beamsplitter. The beamsplitter is actually used in reverse as a combining prism. With the FLOLS projector image focused on the reflective axis of the beamsplitter, the two images are superimposed at the proper brightness ratios.

3.3.2.2 Relay Optics. The seven elements linking the superimposed target raster and FLOLS image to the zoom lens from the relay optics. The first three elements (L_2, P_2, and F_2) are fixed-mounted to the motion platform, while the remaining elements, along with the zoom lens, are mounted on a two-degree-of-freedom gimbal assembly. Decollimating lens L_2 images the target at an internal field stop to clean the raster. The roll prism (P_2) is servo driven to compensate for the roll introduced by target projector pointing of the gimbal assembly. Lens F_2 relays the roll compensated image to prism P_5, which redirects the light path into the gimbal assembly. Lens L_{4C} relays the image along the azimuth (yaw) axis, and prism P_4 redirects it along the elevation (pitch) axis, via field lens L_{4B}, to prism P_3. The last prism not only redirects the light path to the zoom lens, but also provides the necessary compensation for monochromatic use of the color-corrected zoom lens.

The T_6 lens has a image diagonal of 1". This is relayed to the zoom's format of 0.69". The paraxial magnification is 0.63. Also, the T_6 lens is an f/3 lens, thus the zoom is accepting approximately an f/2 cone.

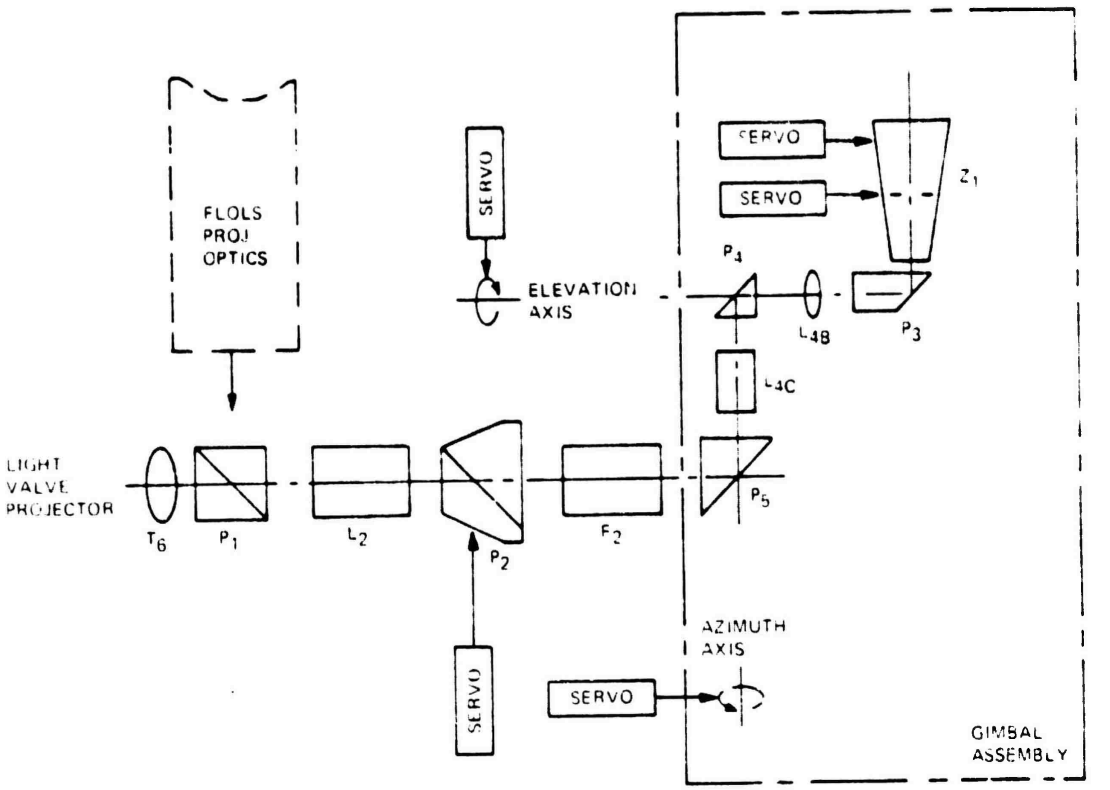

LEGEND

T_6 LENS (P O PROJECTOR)

P_1 BEAM SPLITTER PRISM

L_2 DECOLLIMATING LENS

P_2 PECHAN (ROLL) PRISM

F_2 RELAY LENS

P_5 RIGHT ANGLE PRISM

L_{4C} RELAY LENS

P_4 RIGHT ANGLE PRISM

L_{4B} FIELD LENS

P_3 PRISM

Z_1 ZOOM LENS

AWAVS 4203 68

Figure 68. Target Projector Optics, Block Diagram

3.3.2.3 Zoom Lens. The zoom lens is essentially the projection lens for the target projection system. Its zoom range is 10:1 (12 to 120mm) and its maximum aperature is f/2. At greater focal lengths, however, (over 68mm) the maximum aperture is reduced. The zoom iris is therefore servo driven to maintian a constant aperture while zooming, thus providing a consistent level of screen illumination. Since the zoom lens (Canon model PV 10x12B) is designed primarily for use in three-color TV systems, a correction element is required to improve clarity in the present monochromatic system. This correction element is incorporated into the design of prism P_3 in the target projector optics. The identical zoom lens is used in the FLOLS simulation as the ranging device. In the FLOLS system, however, the servo driven iris is used as a shutter for on/off simulation only. Complete specifications for the zoom lens are given in Table 34.

Both the zoom and iris mechanisms are equipped with slip-clutch friction drives. These allow the servo motors to continue running without damage after the internal components have reached their travel limits.

3.3.2.4 Screen Illumination. The f/# of the zoom lens is f/2.0. Its image diagonal is 16mm. The f/# of the light valve T_6 lens is f/3.0, and a format diagonal of 25.4 mm => magnification to zoom image plane:

$$M = \frac{16}{25.4} = 0.6299$$

f/# reduction: f/3.0 x 0.6299 = 1.8897

Now the light lost due to vignetting (T_1) is the ratio of the f/# squared:

$$T_1 = \left(\frac{1.8897}{2}\right) = 0.893$$

The transmittance of the target optics is;

Zcom	= 0.70	T_2 (product of combined transmittance)
Target Optical	= 0.537	
Beamsplitter	= 0.8	
Pechan	= 0.95	
Prisms	$= (0.95)^3$	= 0.245
T_2	= 245	

TABLE 35. CANON TV ZOOM LENS PV10x12B SPECIFICATIONS

Parameter	Valve
Focal length	12- 120mm
Maximum relative aperture	1:2.0 (12-68mm) 1:3.1 (at 120mm)
Zoom ratio	1:10
Lens construction	17 Components 23 Elements
Wavelength range for color correction	400-700mμ
Image format covered	12.8mm x 9.6mm dia. 16.0mm
Minimum object distance from front vertex	0.45m
Angular field of view	Wide 55.4° x 43.0° dia. 66.5° Tele 6.0° x 4.5° dia. 7.5°
Object dimension at minimum object distance	Wide 56.9cm x 42.7cm dia.71.2cm Tele 5.1cm x 3.8cm dia.6.3cm
Clear aperture of front glass	68.0mmφ
Clear aperture of rear glass	30.6mmφ
Overall length (from front vertex to focal plane)	300.43mm (in air)
Back focal distance (in air)	59.36mm
Glass compensation	72.6mm
Distance from focal plane to exit pupil	-187.2mm

The light valve projector has 1000 lumens output and the screen gain is 2.5.

Thus the screen luminance (B) is

$$B = \left(\frac{1000 \text{ lumens}}{73 \text{ sq-ft}}\right) (.245)\ (.893)\ (2.5) = 7.5 \text{ ft-lamberts}$$

Thus, even if the screen should become reduced with the 6 foot lambert, highlight brightness will be achievable.

This result for brightness to the pilot is realistic because the zoom exit pupil and the pilot are nearly conjugate inside the dome.

3.3.3 Projected Image Resolution. The target system resolution is comprised of the cascaded transfer function of four components. There are:

a) Optical Probe

b) Target Camera

c) Light Valve Projector

d) Projector Optics

Table 35 presents the basis for the modulation transfer function (MTF) extimates.

TABLE 36. BASIS OF TARGET MTF ESTIMATES

Component	Basis of MTF Estimates
Optical Probe	Measured On Axis Data
Target Camera	Westinghouse Data
Light Valve Projector	G. E. Data
Projector Optics	Lens Design Data

3.3.3.1 Target Resolution Summary. Figure 69 illustrates the estimated target system resolution. Sheet 1 is in units of ℓ_p/mm where 700 TV lines is equivalent to:

$$(700 \text{ TV lines})\ (\tfrac{1}{2}\ell_p/\text{line})\ \left(\frac{1}{25.4\text{mm}}\right) = 13.78\ \ell_p/\text{mm}$$ @ light valve

$$(700 \text{ TV lines})\ (\tfrac{1}{2}\ell_p/\text{line})\ \left(\frac{1}{313\text{mm}}\right) = 11.18\ \ell_p/\text{mm}$$ @ Camera @ Probe

$$(700 \text{ TV lines})\ (\tfrac{1}{2}\ell_p/\text{line})\ \left(\frac{1}{16\text{mm}}\right) = 21.86\ \ell_p/\text{mm}$$ @ Target Zoom

The estimated projected system resolution at 700 TV lines is ~ 9% MTF. Sheet 2 shows that when both probe and target optics represent 60°, 700 TV lines is 0.097 cycles/min a 10.3 min/cycle or 5.15 min/line. Therefore, at maximum field there is 5.15 min resolution horizontally.

As zoom decreases angular resolution improves drastically — sheet 3 illustrates this. The probe at 10,000 ft is at 4:1, or a maximum angular field of 15° horizontal. The target is at 10:1 or 6° horizontal field. For this reason the 700 TV line limit is different for the probe and target systems. Again, the 700 TV line horizontal limit is approximately 9% as expected, but the angular resolution to the pilot is near 1 cycle/min. Thus at 10,000 ft, the angular resolution is 10x better than at 1000 ft.

3.3.3.2 Criteria For Curves.

1) Probe MTF is averaged measured data.

2) Target optics is from computer generated data ACCOS V.

3) G.E. light valve and camera.

If the limiting resolution is known for a system (5%) MTF then using a Gaussian approximation the MTF can be found for any frequency.

Example: G.E. light valve limiting resolution = 1300 TV lines

Or 1300 TV lines or

$$1300 \text{ lines} \times \tfrac{1}{2}\ \ell_p/\text{line} \times \frac{1}{27.99\text{mm}} = 23.26\ \ell_p/\text{mm}$$

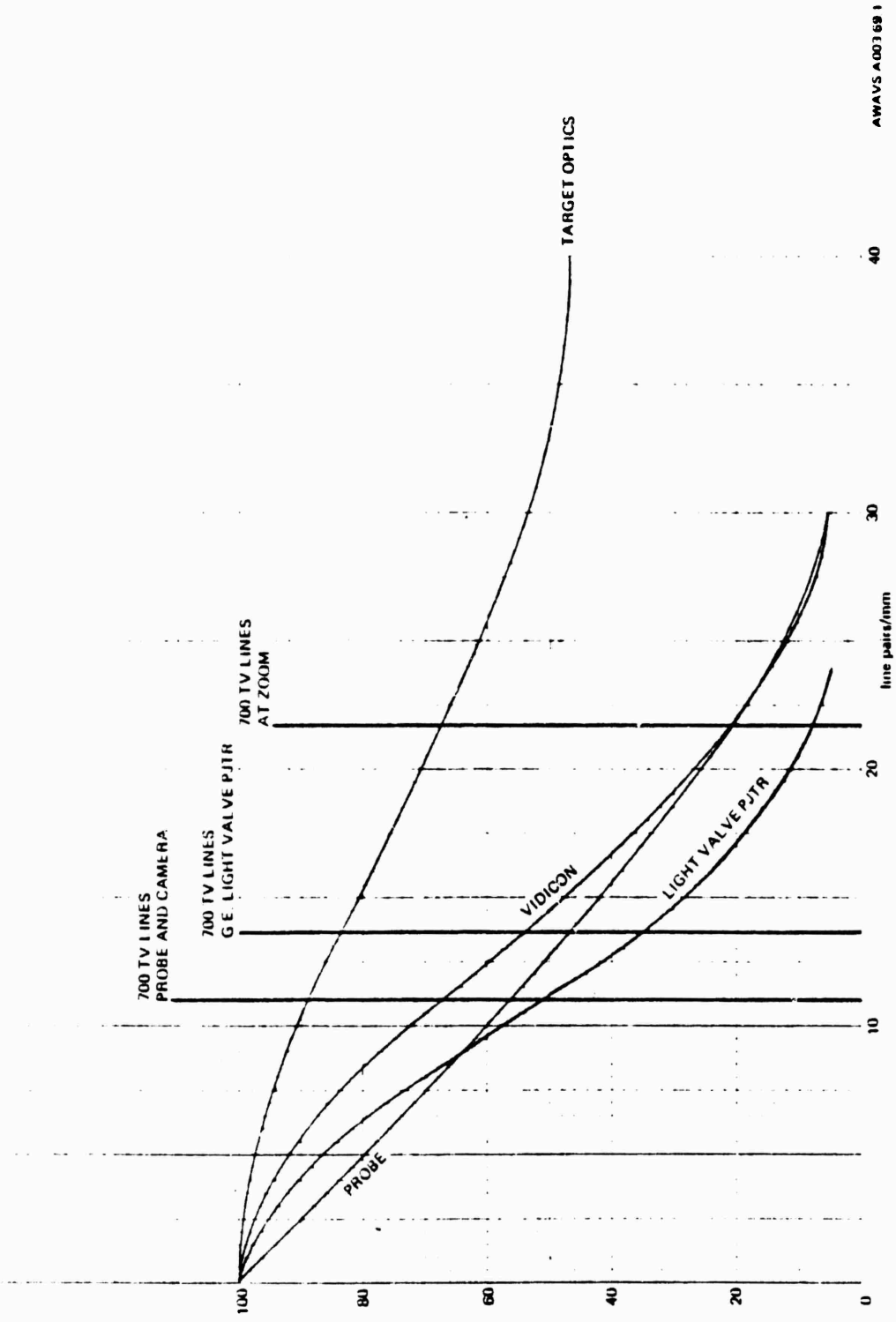

Figure 69. Estimated Target System Resolution (Sheet 1 of 3)

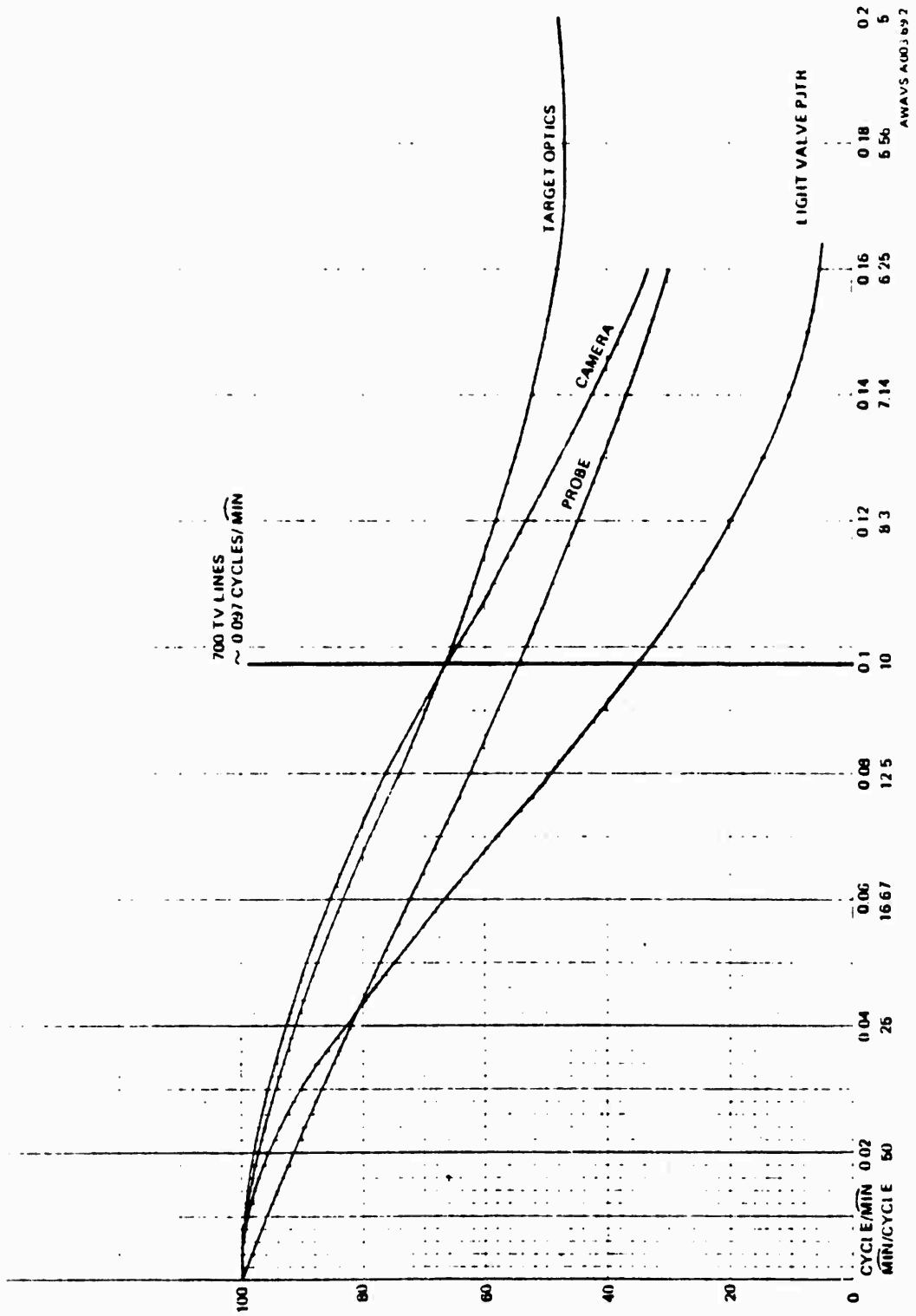

Figure 69. Estimated Target System Resolution (Sheet 2 of 3)

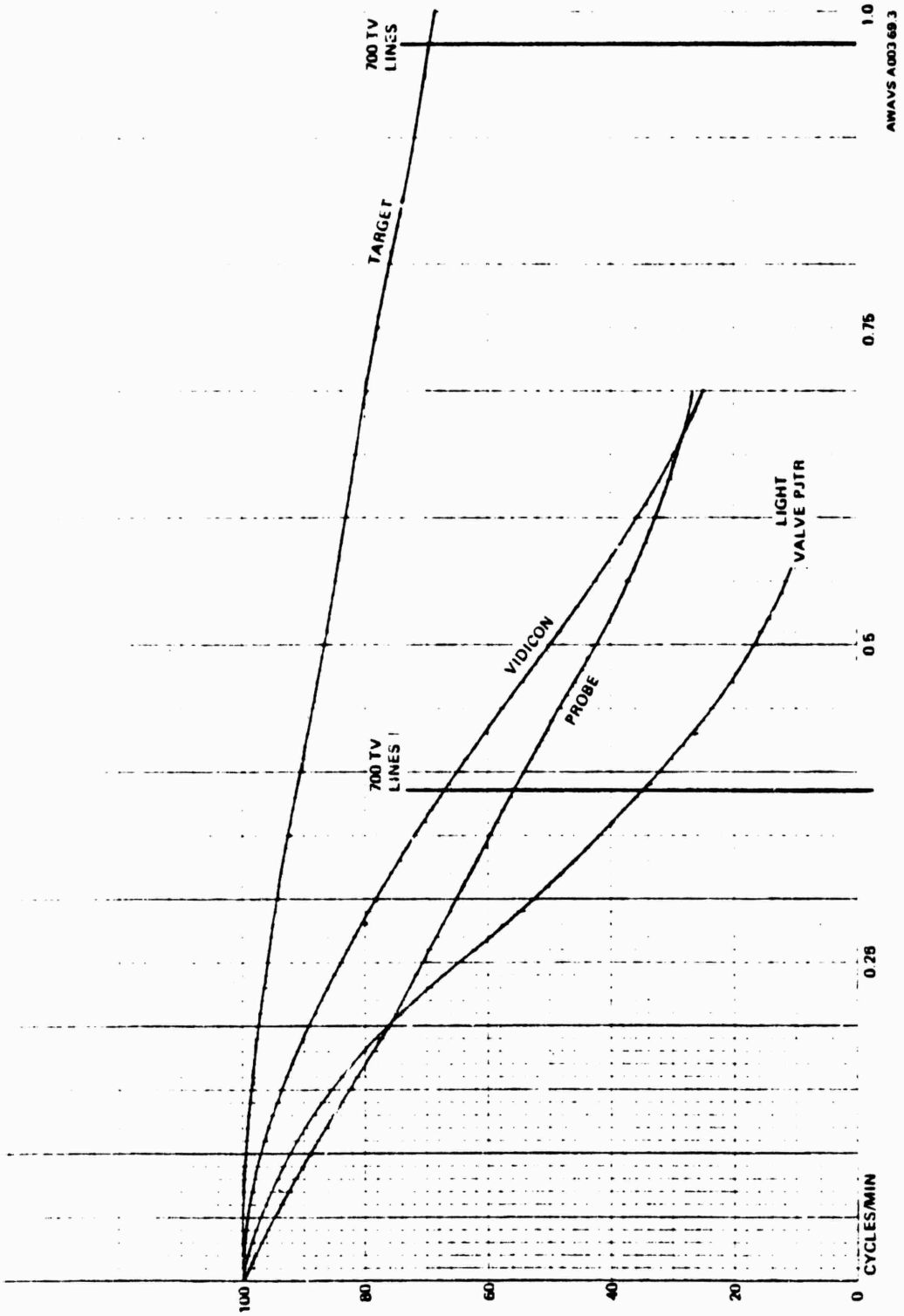

Figure 69. Estimated Target System Resolution (Sheet 3 of 3)

$$MTF = \exp\left(\frac{\omega^2 \delta^2}{2}\right)$$

where $\omega = 2\pi f$; $f = \frac{\text{cycles}}{\text{length}}$

if MTF (limiting) = 0.05

$$\delta^2 = 0.0002809$$

$$\Rightarrow \text{MTF @ 20 } \ell_p/\text{mm} = 10.8\%$$

For camera 1980 lines, limiting resolution is over 33mm or 30 ℓ_p/mm.

3.3.4 Target Projector Gimbal Assembly. The primary function of the gimbal assembly is to aim the zoom lens, and thus the target image, at its appropriate point on the display screen. The target image excursion is +95°/-1[illegible] horizontally (azimuth axis) and +65°/-55°vertically (elevation axis). The elevation assembly houses the zoom lens and is pivoted on the azimuth assembly providing a two degree-of-freedom pointing system. As shown in Figure 63, the zoom lens and optical elements P_3, F_2, and L_{4B} pivot with the elevation assembly while P_4 and L_{4C} rotate with the azimuth assembly. Element P_5 is fixed mounted to the gimbal assembly frame. The azimuth and elevation servos are fully described in paragraph 3.3.5.

3.3.5 Target Projection System Motion and Error Analysis. The following paragraphs describe the technique of servo design, analysis, and evaluation of performance applied in design of the target projection servos. The five target projector servos are: roll, zoom, zoom-iris, azimuth, and elevation. Tables 36, 37, and 38 provide identification, torque readings, and component data for the target projectot servos. Portions of the carrier model (paragraph 3.1.1.4) and FLOLS (paragraph 3.2.6) servo analyses are referenced in the generalized discussion, where data is identical. The target projector zoom and zoom iris servos are identical to the zoom and zoom-iris servos used in the FLOLS system and are therefore covered by reference only except for their inclusion in tabular material herein. Data of a general nature common to the five target projector servos is given in paragraphs 3.3.5.1 and 3.3.5.2, with peculiar data for each servo given in subsequent individualized hardware oriented paragraphs.

Criteria established during the AWAVS design analysis for design of the target projector servos were as follows:

a. Input Commands. Servos will operate with input commands formulated as listed in Table 36 according to two types — continuous and non-continuous. Each servo will provide for two sources of input command signals — one source from the computer interface, the other source from the test console. Switching between sources will be relay controlled.

b. Minimization of Abrupt Nonlinearities. Components and mechanisms of the above mentioned subsystems servos have been designed to achieve the required smoothness in output motion response. Servo component selections are identified for each servo under the hardware subsystem descriptions. Mechanisms have been developed to eliminate or minimize backlash in gearing, by use of precision gearing, and by antibacklash gearing.

c. Feedback Techniques. Feedback components (potentiometer and and tachometer) are identified for each servo in the hardware subsystem descriptions of this report. (See Table 38.)

TABLE 37 TARGET PROJECTOR SERVO IDENTIFICATION

SERVO	SYMBOL	INPUT	SYSTEM	CONTROLLED ELEMENTS
ROLL	Φ_{TIP}	Continuous	Type 2	Roll Prism Unit - Continuous Rotation
ZOOM	Z_{TIP}	Non-Continuous	Type 1	Target Image Zoom Lens Barrel Motion
ZOOM-IRIS	I_{ZTIP}	Non-Continuous	Type 1	I_{TIS} In The Target Image Zoom
AZIMUTH	Ψ_{TIP}	Non-Continuous	Type 2	Azimuth Unit Carrying Elevation Assembly - Rotational Motion
ELEVATION	Θ_{TIP}	Non-Continuous	Type 2	Elevation Unit Carrying Target Image Zoom - Rotational Motion

TABLE 38 TARGET PROJECTOR SERVO INPUT TORQUES

SERVO	INERTIA TORQUE (T_a J_T α_L)	DISTURBANCE TORQUE (T_D)	FRICTION TORQUE (T_F)
ROLL	3.0 oz in sec^2 x 10.5 rad/sec^2		3 oz in

TABLE 39 TARGET PROJECTOR SERVO COMPONENTS

SERVO SERVO	DC TORQUER-TACHOMETER	POTENTIOMETER	POWER AMPLIFIER	COMPENSATION BUFFER
ROLL	Inland TT 1403-A (19V x 4.6A) Singer 1004204-01 T_P = 79 oz in T_G = 0.2 v/rad/sec K_T = 16.6 oz in/amp W_{NL} = 158 rad/sec	CIC 306 Singer 1004205-01 Conformity 0.05% sin-cos pot 10K	Inland EM 1802 Singer 1003911-03 200 watt at 20v	Singer 2061496-01 & 2061498-01
ZOOM	Escap 28 G11 2192054	Helipot 17366	Stahl Research Labs LEN CONTROL 217	None
ZOOM IRIS	Escap 16 M11#2076	Spectro 140-0-0-103	Same as zoom servo	
AZIMUTH	Inland TT 4404-A (20.7V x 14.8A) Singer 1004167 T_P = 10 lb ft T_G = 2.45 v/rad/sec K_T = 0.67 lb ft/amp W_{NL} = 22 rad/sec	CIC 305 Singer 437523-04 Conformity 0.02% Impedance 5K	Inland EM 1803 Singer 1003911-01 300 watt at 20v	Same as roll servo
ELEVATION	Inland TT 4405-A (21V x 10.5A) Singer 1004168 T_P = 4.5 lb ft T_G = 2.45 v/rad/sec K_T = 0.43 lb ft/amp W_{NL} = 36 rad/sec	CIC 305 Singer 1004170-01 Conformity 0.025% Impedance 10K	Same as azimuth servo	Same as roll servo

d. Travel Stops and Limit Switches. Travel limit switches will be provided on each noncontinuous servo except the zoom and iris. (See paragraph 3.3.2.3.) Contact with any limit switch will remove power amplifier current to the motor of that servo only in the direction of the approached travel limit. Travel past the limit switches will be controlled by soft mechanical stops with over travel. The stops will safely control deceleration based on the momentum produced by the maximum velocity of the total moving inertia at the instant contact is made with the stop.

e. Lockouts. Removable mechanical lockouts will be incorporated on all continuous and noncontinuous servos, providing a means of securing moving mechanisms during handling and shipment. The lockout will also provide a precise repeatable calibration reference for position sensor alignment.

3.3.5.1 Generalized Performance Data. Following are the techniques used in synthesis of performance oriented parameters (displacements, velocities, decellerations, etc.) associated with the target projection servos. Quantitive performance data for each servo is tabulated as part of the individual hardware loop discussion. (See paragraphs 3.3.5.3 through 3.3.5.7, as applicable.)

a. Static Accuracy. Accurate line-of-sight placement of the projected image on the projection screen is a critical requirement. To achieve the required projector servo positioning accuracy, the following techniques are applied to target projection system servos:

1. An integrator incorporated in the forward path of each servo acts to reduce the error signal to virtually zero during static positioning. It also makes the positioning accuracy of the servo independent of output torque thresholds or gravity loads on the output of the servo.

2. A unity voltage follower, immediately following each feedback pot wiper output signal, is physically located as near to the potentiometer as practical. The extremely high input impedence of this voltage follower serves to virtually eliminate errors due to potentiometer loading.

3. The method by which the position error signal is generated in the continuous sine/cosine servos depends first upon exciting the sine/cosine feedback pots with the computer generated sine/cosine commands; and secondly, upon summing the output wiper voltages of the sine/cosine feedback pots. The overall positioning accuracy of these servos depends, in part, on retaining the accuracy of the computed sine/cosine command up to the point where the excitation signals are applied to sine/cosine pots, and also upon the accuracy of the summation of the sine/cosine feedback pot wiper voltages. For this reason, precision resistors are used in these critical functions.

With the application of the techniques described above, remaining static positioning errors occur almost entirely from two sources: gearing errors (between feedback pot shaft and applicable controlled output of servo), and feedback potentiometer linearity or conformity errors.

Gearing errors are classified by two clearly identifiable components:

1. Transmission Error. The variation in the transmission ratio of a gear pair or train from the ideal nominal value, caused by the net sum of individual gear position errors and installation turnout errors. This error is single-valued and repeatable and combines with the potentiometer linearity error.

2. Backlash Error. The total lost motion for a gear pair or train caused by all contributors, such as thinned teeth, enlarged center distance, and runout of rotating parts. Backlash error is multivalued and is therefore not a specific repeatable error value. Therefore backlash in gearing is the only significant error in the determination of static repeatability accuracy.

Feedback potentiometer linearity (or conformity) error is the primary accuracy specification of a particular potentiometer assembly. The maximum permitted linearity error will be defined by procurement specifications for each potentiometer assembly used on the AWAVS visual system.

Table 38 lists the potentiometer selections and static accuracy analysis summary for each servo of the visual system. A root-sum-square method is used in combining maximum allowable gearing errors with potentiometer errors. Feedback potentiometer errors listed in Table 38 are the maximum positioning error of the servo based on the potentiometer linearity (or conformity) specification. For the noncontinuous servos, this is directly related by the specified pot linearity and the gearing ratio, which determines the percentage of the full potentiometer travel that occurs over the full servo travel.

For the continuous servos which use sine/cosine feedback potentiometers, the relationship between the potentiometer conformity specification and the corresponding servo positioning error is based on the analytical derivation given in Figure 58. (Refer to FLOLS servo discussion.)

b. Static Repeatability. As indicated in the discussion of grading errors and based on the application of the servo design techniques, backlash in gearing is the only significant error source in the determination of static repeatability. As anti-backlash gearing is utilized in each servo, the static repeatability error should be zero.

c. Static Compliance. Incorporation of integral control in each servo renders the closed loop dc sensitivity of each servo output virtually to infinity. This means that the servos are capable of resisting any externally applied output torque or force up to the peak motor torque, without having to hold a corresponding error in position. The result is a static servo compliance which is virtually infinite.

d. Dynamic Range. The capability of the target projection system servos to smoothly control the movement of the projected image over a wide range of velocities, is a critical requirement. The dynamic range defines the ratio of the largest to the smallest velocity which the servo can control. The maximum velocity for each servo is defined by the motion envelope in the AWAVS detailed servo specifications. Each servo will be judged to have satisfactory smoothness by direct visual observation of the image projected onto the screen at the minimum velocity specified by the applicable performance specification. Verifying smoothness using a test criterion based on monitoring the tachometer signal may not be valid because of large high frequency content in the signal which is not related to the actual observable smoothness of the projected image. It is valid only if the ripple, high-frequency content, etc. of the tach are taken into account.

e. Frequency Response. A critical requirement in achieving an accurate representation of the external visual scene is synchronization of all servos involved in projecting the scene. This requires that the servos have the same dynamic response as well as the same degree of smoothness. To accurately control the synchronization of the visual system servos, the dynamic response is specified to accurately match (within 20%) an ideal second order system with a damping ratio ζ and natural frequency ω_n chosen for optimum performance.

The descriptions of the synthesis techniques which follow have been developed to achieve the specified servo dynamic response. Because of the two methods of providing input command signals to servos of the visual system — continuous servos with position inputs and noncontinuous servos with position inputs — two different synthesis approaches are used to achieve the required accuracy in setting the dynamic response. The distinction between continuous versus noncontinuous servos is important because the technique of handling sine/cosine position information precludes the use of compensating networks in both the input and feedback signal paths of the continuous servos.

f. System Type. Based on the specification of dynamic response (stringent tolerance of 0.1% of maximum velocity in high velocity tracking) servo system type has been decided. Optimum choice of bandwidth, stability damping ratio, percentage overshoot, velocity tracking error, and other parameters depends mostly on system type. The analysis of the Type 1 servos is portrayed as a set of Bode plots presented as part of the individual servo loop discussions. The curves indicate the phase margin, bandwidth, damping ratio and velocity error constant. Limitations are also indicated.

In order for a system to reproduce the square wave at its output, the system would have to have infinite bandwidth. Associated with infinite bandwidth is zero rise time and zero delay time. There is no analytic expression that even approximately relates the two for systems of arbitrary order. In reality a system having large bandwidth is welcomed if the input signal is free from noise. A system with a large bandwidth can follow inputs with little error; and may be considered accurate, not only in its final value, but for all time. Speed of response, directly related to bandwidth, is a measure of accuracy for all time and might be called the measure of dynamic accuracy.

The traditional well-established analytic results of system classification and error constants for stable type 0, Type 1 and Type 2 unity feedback systems is given in Figure 13. (Refer to carrier model servo discussion.) Based on the theory presented therein, the performance requirements given in Tables 36 and 37, and the analysis of servos as Type 1 systems, the more critical FLOLS roll servo (ϕ_{FIT}) is designed as a Type 2 system and the rendering servos as Type 1 systems.

g. Generalities. The general compensation card has the capability to properly shape the feedback and forwardpath signals. The design philosophy of all noncontinuous servos is established to be the same. The components in the compensation card differ because of difference in controlled load and hardware of different servos. Similarly, same design philosophy is established for all continuous servos. Continuous servos need one more actuating signal generator card, which is exactly the same for all of them. Table 38 shows the hardware components.

h. Inherent Zeros and Poles Generated By Servo Components. The values of pertinent parameters of motor, tachometer, power amplifier, the follow-up potentiometer are included in the hardware discussions. The tachometer generates an inherent zero which contributes to phase-lead and is adjustable for stability as a function of cross-over frequency which determines the bandwidth. The motor impedence coupled with the mechanical inertia generates a pole contributing to a phase lag. The electrical time constant of the motor and amplifier generate two other poles contributing to phase lag.

The system will be stable if the phase margin, ϕ_{GPM}, which is a good measure of system stability, is at least 40°. Proper electronic shaping is accomplished utilizing the general compensation card which can generate two free integrators in the forward path, thus transforming an inherent type 1 stable system into type 2 or type 3 stable systems, and rendering the velocity error constant to almost infinity and the tracking error to almost zero.

3.3.5.2 Target Projection System Servo Block Diagrams. The noncontinuous position servo block diagram given in Figure 14 is representative of the azimuth and elevation servos, while the continuous position servo block diagram shown in Figure 59 describes the roll servo. The zoom and zoom-iris noncontinuous servo block diagrams are presented in Figures 61 and 62, respectively, along with the FLOLS zoom and zoom iris servos which are identical. Transfer functions provided on each block diagram are the mathematical expressions for their respective loops. Definitions of terms used in block diagrams and transfer function equations are presented in paragraph 3.3.5.1, with peculiar quantitive values given in the individual hardware discussions which follow.

3.3.5.3 Design Analysis of Target Projector Roll Servo. The performance specification of roll servo [ϕ_{TIP}] is given in Table 39.

TABLE 40 TARGET PROJECTOR ROLL SERVO PERFORMANCE

1.	Excursion	360°
2.	Velocity (Maximum)	310°/sec
3.	Acceleration	600°/sec^2
4.	Static Accuracy	± 20 arc min
5.	Linearity	0.05% max excursion
6.	Repeatability	± 20 arc min
7.	Resolution	± 0.01% max excursion
8.	Dynamic Range	1000:1
9.	Tracking Accuracy at Velocity (High)	0.1% max velocity
	Velocity (Low)	0.05% max velocity

The target projector roll servo is synthesized as follows to meet the performance specification parameters 1 through 9:

1. The roll servo is designed for continuous rotation of 360°. The position transducer is a pair of sine-cosine potentiometers. The error signal, which is amplified to drive the dc motor, is generated by exciting the sine-cosine potentiometers as described in the foregoing paragraph on general servo considerations. The system is stabilized for smooth performance by both tachometer feedback and electronic signal shaping.

2. The dc torquer tachometer is capable of a no load speed of 9000°/sec.

3. The dc torquer can generate a peak torque of 79 oz in. The estimated inertia of roll assembly is 3 oz in sec^2 and the possible acceleration limit 1500°/sec^2.

4. As described in paragraph 3.3.5.1, the static position error for the continuous servo emanates from the conformity specification of the sine-cosine potentiometers. The maximum possible static error could be ±5 arc min.

5. The principle of the continuous servo is to drive the control element by amplifying the error signal, which is generated by exciting the sine-cosine potentiometers. The linearity is specified to ±0.05%.

6. With the initial calibration to meet the static error requirement, any steady state position error beyond that specified as conformity of potentiometers ±5 arc min will be reduced to zero, because of integral control. Steady state repeatability, in this type of control system, cannot be greater than the steady state position error.

7. In order to meet the resolution requirement of ±0.01% of maximum excursion, potentiometers of infinite resolution are chosen. The digital command signal from computer is converted to an analog signal by a 14-bit D/A converter, the command resolution being ±1.3 arc min.

8. The dynamic range, the 1000:1 ratio of maximum velocity to minimum velocity, can be met by the choice of a high quantity dc motor and tachometer, by minimizing friction and by direct driving or by using anti-backlash gears of low gear ratio. In this case, the roll assembly is driven by the motor-tachometer portentiometer system through 2:1 anti-backlash gearing.

9. The reduced transfer function indicates that this servo is designed to be of type 2 system. As shown in the analysis, the velocity error coefficient is ∞. This implies that the servo follows ramp input of the form t'u(T) with zero steady state error. Therefore the tracking accuracy of the specification is met.

The stability analysis is indicated on the frequency-gain plot, Figure 70. The criteria used for stability are as follows:

- To keep the phase margin greater than 40
- To shape the slope of the frequency-gain curve to 20 db per decade at and around the decade crossover frequency
- To reduce the gain sharply at high frequencies.

Inherent zeros and poles plotted on the frequency-gain curve are defined in Table 40. The phase margin ϕ_{PM} should be at least 40° for the system to be relatively stable. Phase margin is defined as:

$$\phi_{PM} = 180 - \sum \text{Phase lags and leads in the system.}$$

Phase lags:	Integral Control	$[\frac{1}{S}]$	: 180°
	Mechanical time constant	$[\tau_{MJ}]$	: 89°
	Electrical time constant	$[\tau_e]$	: 3°
	Power amplifier time constant	$[\tau_A]$	: 1°
Phase leads:	Tachometer zero	$[\tau_Z]$	: -88°
	Electronic zero	$[\tau_I]$	: -89°
Net contribution:			: 96°

Phase margin: $\phi_{PM} = 180° - 96° = 84°$

This insures excellent stability. However, the compensation card has several adjustable features which if necessary can be used to shape the signal. In fact, τ_{MJ} is estimated and τ_Z and τ_I are adjustable.

TABLE 41. INHERENT ZEROS AND POLES FOR TARGET PROJECTOR ROLL SERVO

ω_L	Zero	Tachometer & Pot	$\frac{K_D}{KG}$	5.8 rad/sec
ω_{MJ}	Pole 1	Motor & Load	$\frac{K_T K_B}{RJ}$	0.72 rad/sec
ω_E	Pole 2	Motor	$\frac{L}{R}$	1500 rad/sec
ω_A	Pole 3	Power Amplifier	Bandwidth	6000 rad/sec

3.3.5.4 Design Analysis of Target Projector Zoom Servo [Z_{TIP}] This servo is identical to the FLOLS projector zoom servo. Refer to paragraph 3.2.6.4 for a complete analysis.

3.3.5.5 Design Analysis of Target Projector Zoom-Iris Servo [I_{ZTIP}]. Except for its intended use (brightness control as opposed to on/off sheltering) the target projector zoom-iris servo is identical to the FLOLS projector zoom-iris servo. Refer to paragraph 3.2.6.5 for a complete analysis.

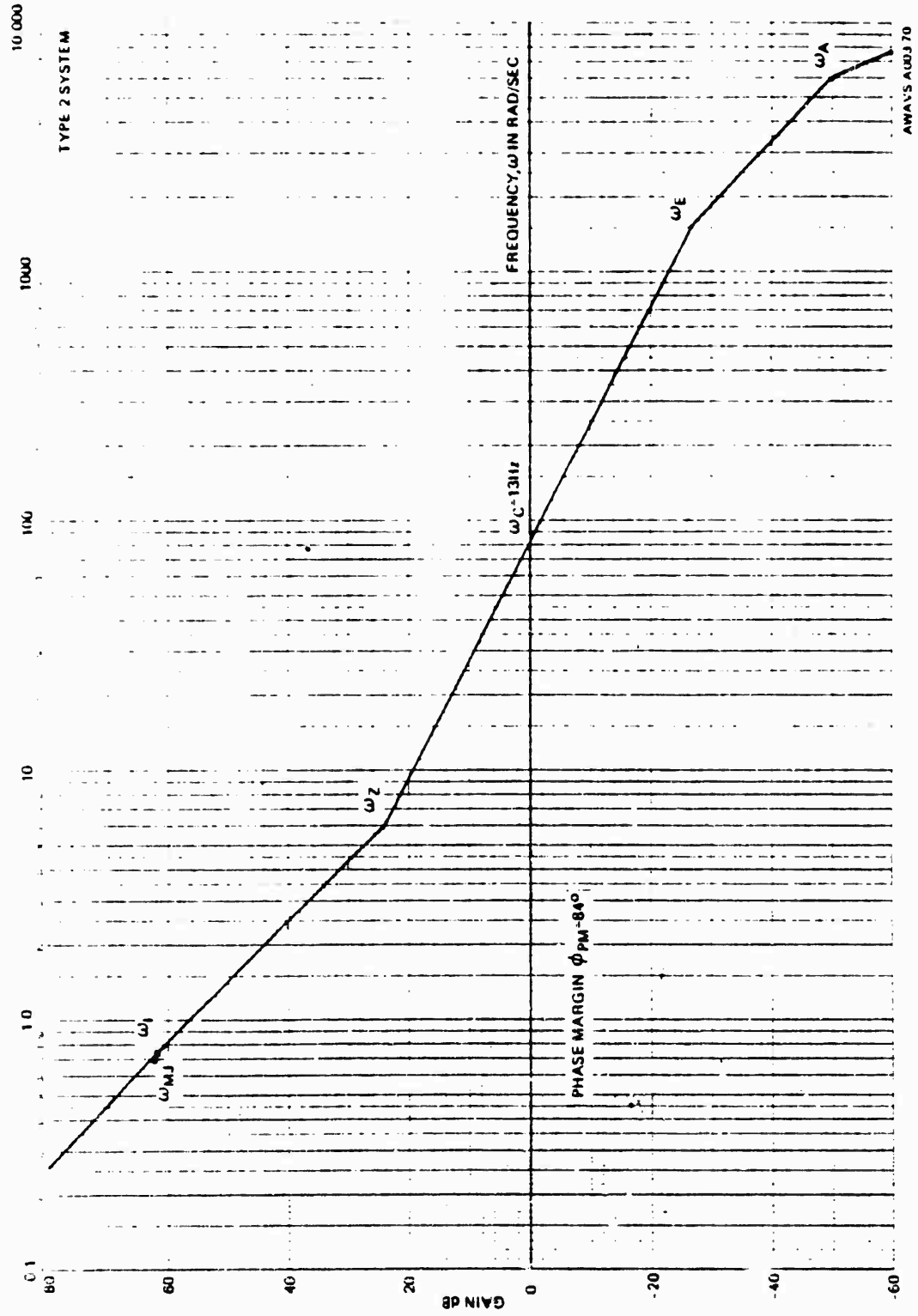

Figure 70. Frequency-Gain Plot For Target Projector Roll Servo

3.3.5.6 Design Analysis of Azimuth Servo. The performance specification of Azimuth Servo [ψ_{TIP}] given in Table 41.

TABLE 42. TARGET PROJECTOR AZIMUTH SERVO PERFORMANCE

1.	Excursion	±150°
2.	Velocity Maximum	300°/sec
3.	Acceleration maximum	900°/sec^2
4.	Static Accuracy	±10 arc min
5.	Linearity	±0.05% max excursion
6.	Repeatability	±10 arc min
7.	Resolution	±0.0 1% max excursion
8.	Dynamic Range	1000:1
9.	Tracking Accuracy At Velocity (High)	0.1% max velocity
	Velocity (Low)	0.05% max velocity

1. The mechanical sketch indicates a possible excursion of ±160° for the azimuth assembly.

2. The dc torque motor is capable of a no load speed of 1275°/sec and the tachometer has a max operating speed of 1555°/sec.

3. The dc torque can generate a peak torque of 10 lb ft. The extimated inertia of azimuth assembly is 0.35 lb ft sec^2. The possible acceleration limit is 1635°/sec^2. There is ample allowance for friction and disturbing torque of 0.2 lb ft.

4. As described in paragraph 3.3.5.1, the static position error for this noncontinuous position servo emanates from the conformity specification of the position feedback potentiometer. The static position error could be ±2 arc min.

5. The principle of the linear servo is to drive the control element by amplifying the actuating signal error. All components of this system are linear and the linearity of position transducer potentiometer, is specified to ±2 arc min.

6. With proper initial calibration to meet the static error requirement as stated above, any position error beyond that specified as conformity of the potentiometer ±2 arc min, will be reduced to zero, because of integral control. Steady state repeatability, in this type of control system, cannot be greater than the steady state position error.

7. In order to meet the resolution requirement of ±0.01% of maximum excursion (±1.8 arc min), an infinite resolution position transducer potentiometer is chosen. The digital command signal from the computer is converted to an analog signal by a 14-bit D/A converter, the command signal resolution being ±1.08 arc min.

8. The dynamic range, the 1000:1 ratio of maximum velocity to minimum velocity, can be met by the choice of a high quality dc motor and tachometer, by minimizing friction, and by direct driving or by using anti-backlash gears of low gear ratio. In this case, the azimuth assembly is driven directly by the motor-tachometer potentiometer system. The system noise level is kept as slow as possible.

9. The reduced transfer function indicates that this servo is designed as a type 2 system. As shown in the analysis, the velocity error coefficient is ∞. This implies that the servo follows ramp input of the form t'u(t) with zero steady state error. Therefore the tracking accuracy of the specification is met.

The stability analysis is indicated on the frequency-gain plot, Figure 71. The criteria used for stability are as follows:

- To keep the phase margin greater than 40°
- To shape the slope of the frequency-gain curve to 20 db per decade at and around the decade crossover frequency.
- To reduce the gain sharply at high frequencies.

Inherent zeros and poles plotted on the frequency-gain curve are defined in Table 42.

The phase margin ϕ_{PM} should be at least 40° for the system to be relatively stable. Phase margin is defined as:

$$\phi_{PM} = 180 - \sum \text{Phase lags and leads in the system.}$$

Phase lags:	Integral control	$[\frac{1}{S}]$	: 180°
	Mechanical time constant	$[\tau_{MJ}]$	: 89°
	Electrical time constant	$[\tau_e]$	: 12°
	Power amplifier time constant	$[\tau_A]$	: 1°
Phase leads:	Tachometer zero	$[\tau_Z]$	: -85°
	Electronic zero	$[\tau_I]$	: -89°
Net contribution:			: 102°

Phase margin: $\phi_{PM} = 180° - 102 = 78°$

This insures excellent stability. However, the compensation card has several adjustable features which, if necessary, can be used to shape the signal. In fact, τ_Z and τ_I are adjustable.

TABLE 43. INHERENT ZEROS AND POLES FOR TARGET PROJECTOR ROLL SERVO

ω_L	Zero	Tachometer & Pot	$\frac{Kp}{KG}$	9 rad/sec
ω_{MJ}	Pole 1	Motor & Load	$\frac{K_T K_B}{RJ}$	0.9 rad/sec
ω_E	Pole 2	Motor	$\frac{L}{R}$	454 rad/sec
ω_A	Pole 3	Power Amplifier	Bandwidth	6000 rad/sec

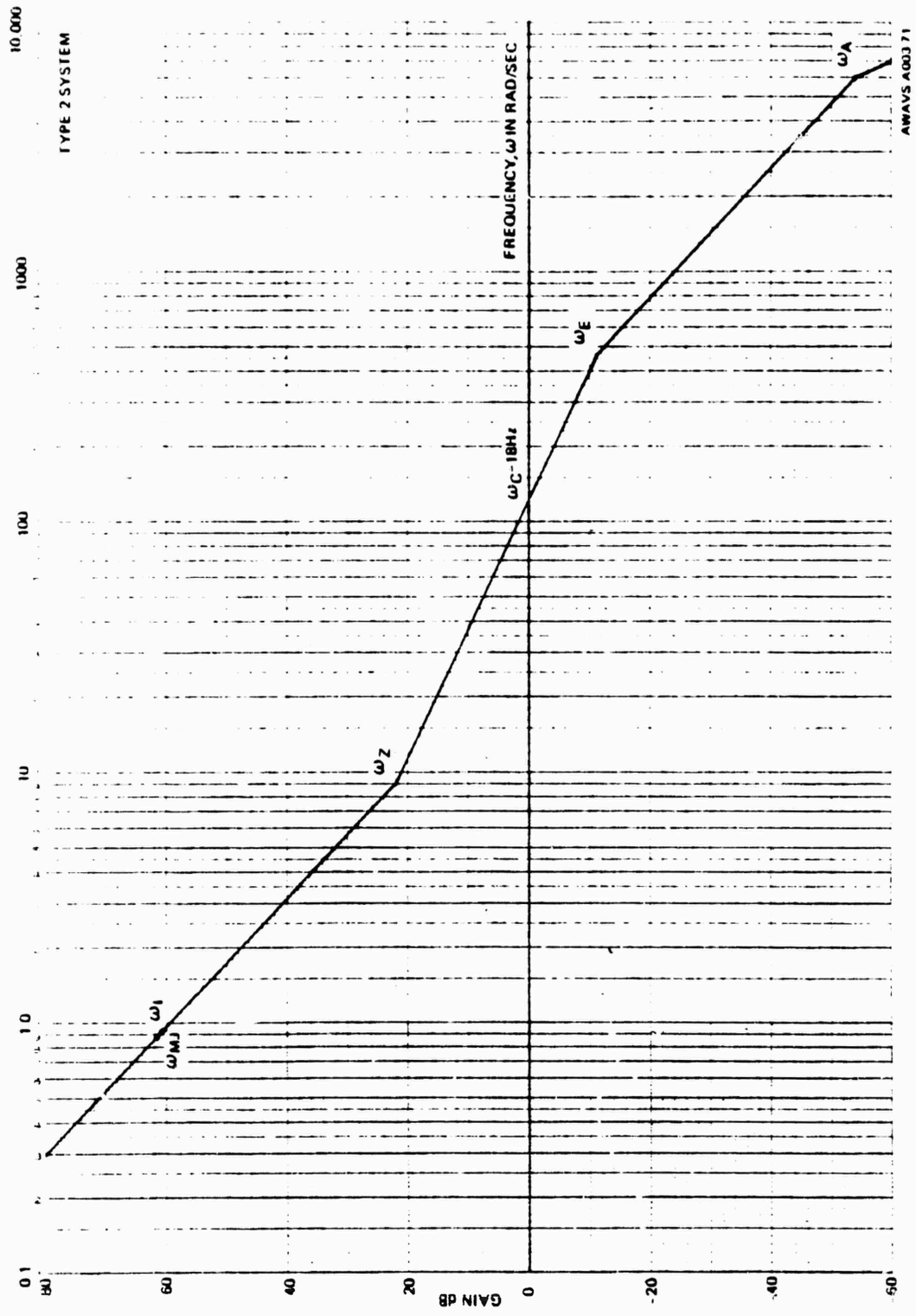

Figure 71. Frequency-Gain Plot For Target Projector Azimuth Servo

3.3.5.7 Design Analysis of Elevation Servo. The performance specification of Elevation Servo [θ_{TIP}] given in Table 43.

TABLE 44. TARGET PROJECTOR ELEVATION SERVO PERFORMANCE

1.	Excursion	+80 -60
2.	Velocity (Maximum)	360°/sec
3.	Acceleration	600°/sec^2
4.	Static Accuracy	±10 arc min
5.	Linearity	±0.05% max excursion
6.	Repeatability	±10 arc min
7.	Resolution	±0.01% max excursion
8.	Dynamic Range	1000:1
9.	Tracking Accuracy at Velocity (High)	0.1% max velocity
	Velocity (Low)	0.05% max velocity

The target projector elevation servo is synthesized as follows to meet the performance specification, parameters 1 through 9:

1. The mechanical sketch indicates a possible excursion of +80°, -60° for the elevation assembly.

2. The dc torque motor is capable of a no load speed of 1555° and the tachometer has a maximum operating speed of 1555°.

3. The dc torquer can generate a peak torque of 4.5 lb ft. The estimated inertia of azimuth assembly is 0.16 lb ft sec^2. The possible acceleration limit is 1600°/sec^2. There is ample allowance for friction and disturbing torque of 0.2 lb ft.

4. As described in paragraph 3.3.5.1, the static position error for this noncontinuous position servo emanates from the conformity specification of the position feedback potentiometer. The static position error could, at most, be ±2 arc min.

5. The principle of the linear servo is to drive the control element by amplifying the actuating signal error. All components of this system are linear, and the linearity of position transducer potentiometer, is specified to ±2 arc min.

6. With proper initial calibration to meet the static error requirement as stated above, any position error beyond that specified as conformity of the potentiometer ±2 arc min will be reduced to zero, because of integral control. Steady-state repeatability in this type of control system, cannot be greater than the steady state position error.

7. In order to meet the resolution requirement of 0.01% of maximum excursion (±1.8 arc min), a potentiometer of infinite resolution is chosen as the position transducer. The digital command signal from the computer is converted to an analog signal by a 14-bit D/A converter, the command signal resolution being ±1.08 arc min.

8. The dynamic range, the 1000:1 ratio of maximum velocity to minimum velocity, can be met by the choice of a high quality dc motor and tachometer, by minimizing friction and by direct driving or by using anti-backlash gears of low gear ratio. In this case, the azimuth assembly is driven directly by the motor-tachometer potentiometer system.

9. The reduced transfer function indicates that this servo is designed to be of type 2 system. As shown in the analysis, the velocity error coefficient is ∞. This implies that the servo follows ramp input of the form t'u(t) with zero steady state error. Therefore, the tracking accuracy of the specification is met.

The stability analysis is indicated on the frequency-gain plot, Figure 72. The criteria used for stability are as follows:

- To keep the phase margin greater than 40°.
- To shape the slope of the frequency-gain curve to 20 dB per decade at and around the decade crossover frequency.
- To reduce the gain sharply at high frequencies.

Inherent zeros and poles plotted on the frequency-gain curve are defined in Table 44. The phase margin ϕ_{PM} should be at least 40° for the system to be relatively stable. Phase margin is defined as:

$$\phi_{PM} = 180 - \sum \text{phase lags and leads in the system.}$$

Phase lags of:	Integral control	$[\frac{1}{S^2}]$	: 180°
	Mechanical time contant	$[\tau_{MJ}]$	: 89°
	Electrical time constant	$[\tau_e]$	: 5.5°
	Power amplifier time constant	$[\tau_A]$	: 1°
Phase leads of:	Tachometer zero	$[\tau_Z]$	: -77°
	Electronic zero	$[\tau_I]$	: -89°
Net contribution			: 109.6°

Phase margin: $\phi_{PM} = 180° - 109.6° = 70.4°$

This insures excellent stability. However, the compensation card has several adjustable features which, if necessary, can be used to shape the signal. In fact, τ_{MJ} is estimated and τ_Z, τ_I are adjustable.

TABLE 45. INHERENT ZEROS AND POLES FOR TARGET PROJECTOR ELEVATION SERVO

ω_L	Zero	Tachometer and Pot	$\frac{K_P}{K_G}$	15 rad/sec to 5 rad/sec
ω_{MJ}	Pole 1	Motor and Load	$\frac{K_T K_B}{RJ}$	0.78 rad/sec
ω_E	Pole 2	Motor	$\frac{L}{R}$	625 rad/sec
ω_A	Pole 3	Power amplifier	Bandwidth	6000 rad/sec

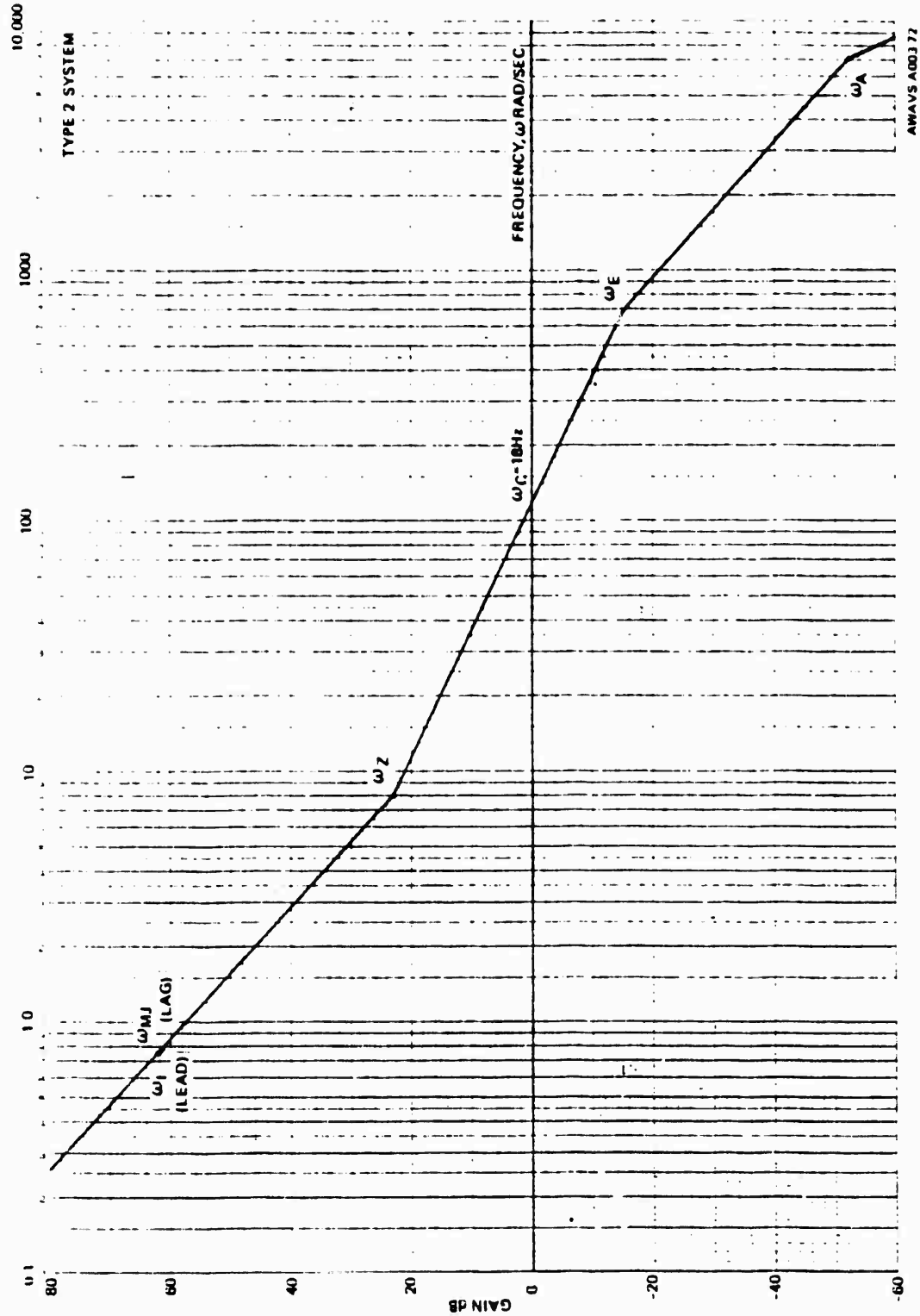

Figure 72. Frequency-Gain Plot For Target Projector Elevation Servo

3.3.6 Maintenance Panel Interface. Five of the six target projection servos may be manually driven from the cockpit electronics test panel. (See Figure 66.) The NORMAL/TEST key switch on the test panel must be in the TEST position for this purpose. Each of the five servos (ROLL, AZIMUTH, ELEVATION, IRIS and ZOOM) are operated by depressing an alternate action RUN/STOP pushbutton switch, which lights to indicate its present position when the key switch is in the TEST mode. A potentiometer control for each servo determines both the direction and velocity when the pushbutton is set at RUN. Velocity is always zero when the control is centered. The three precision noncontinuous servos (AZIMUTH, ELEVATION, and IRIS) are provided with limit indicators, which light to indicate when the servo has reached one extreme limit of travel. The ZOOM servo, while noncontinuous, has no limit indicator since the lens zoom mechanism is fitted with a slip clutch friction drive. The zoom iris servo, which is not operable from the test panel, is internally operated to maintain a constant aperture while zooming. When the key switch is in the NORMAL mode, all servo commands come from the linkage.

3.3.7 Target Projector Remote Control Unit. This component contains the controls and indicators which effect the quality and aesthetics of the projected video image (contrast, brightness, etc) as well as the normal video selectors (on/off, sync select channel, etc). Units for the target and background projectors are identical. Descriptions of individual controls are provided along with the background projector discussion. (Refer to paragraph 3.5.6.)

3.4 Background Image Generator

The background image is comprised of sky, horizon, seamerge and seascape imagery. The background image generator produces the seascape or wave imagery from a film plate employing standard flying spot scanner (FSS) techniques. The seascape image will appear in proper perspective for aircraft altitude, heading, velocity and altitude. This is accomplished by properly shaping the FSS sweep inputs to dynamically follow the aircraft attitude, altitude, velocity and heading parameters and the static perspective required by optical distortions, mapping and projection/screen geometry consideration.

The background image generator is capable of producing the required image perspective for all aircraft attitude and heading. Because of hardware limitations, the seascape visual cues for velocity are limited to 400 knots (max) along the CRT deflection axis within an altitude range from 40 ft to 760 ft. Outside these limits, no further visual cue will be generated in the seascape imagery. The raster reset method used to provide the velocity cue does have the advantage of an unlimited gaming area. Figure 73 is a block diagram of the background image generator. The three primary blocks in the image generation chain, as shown in the diagram, are the dynamic analog raster computer (DARC), the seascape generator, and the background special effects generator (SEG).

The background DARC receives display timing information from the system synchronous pulse generator and aircraft attitude information from the AWAVS digital computer (part of linkage). Artificial timing and attitude data may be input via the BIG/WIG maintenance panel for destined alignment purposes, bypassing the linkage. Two sets of outputs are provided by the DARC. The instantaneous direction cosines (k_{LOSO}, ℓ_{LOSO}, m_{LOSO}), with respect to the observer frame of the background image projector television presentations, are supplied to the special effects generator and the FSS sweep input waveforms (X deflections and Y deflections) are supplied to the flying spot scanner. The flying spot scanner converts the film imagery, with the proper perspective, into video time base information for display by the background projector.

The seascape video is fed to the special effects generator where, under computer control via the linkage, the clouds, horizon, seamerge and visibility range information is added to seascape video to create the composite background video scene. The background video is sent to the scene keyed insetting system where the "hole" is blanked in the background scene for insetting of the target image.

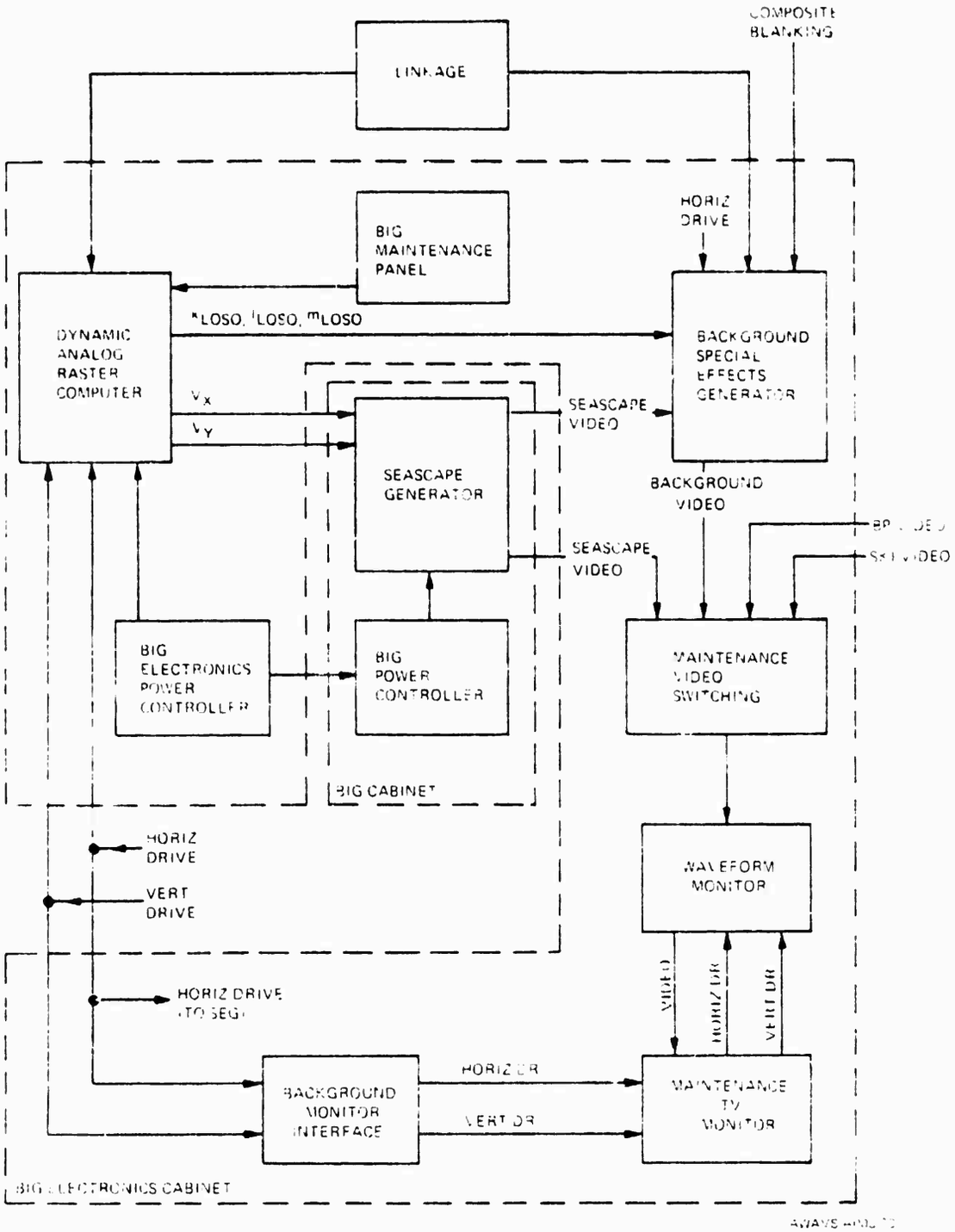

Figure 73. Background Image Generator, Block Diagram

Although not actually a part of the image generation circuitry, BIG monitoring and video switching is covered herein due to its physical location with respect to BIG equipment. Video and waveform monitors in the BIG electronics cabinet sample selected visual inputs from either the seascape generator, special effects generator, background TV projector, or scene keying camera. Switching controls are physically located on the BIG/WIG maintenance panel. (See paragraph 3.4.4.) The video monitor is a conventional 17-inch black and white broadcast monitor manufactured by Conrac. It is identical to the TIG and EOS monitors. The waveform monitor is a Tektronix model 465 oscilloscope used solely as test equipment. The power controllers in the BIG and BIG electronics cabinets sequence dc power on and off to prevent damage to the CRT in the flying spot scanner. Power controllers also contain additional CRT protection circuitry. External sync, in the form of horizontal and vertical drives and composite blanking, for all BIG components including monitoring equipment, is supplied from the master timing generator.

3.4.1 Background Dynamic Analog Raster Computer. A functional block diagram of the background DARC is shown in Figure 74. The vertical and horizontal drive pulses are input to the waveform generator, which produces the linear waveforms ψ and θ by integration. Thus ψ and θ are linear ramp signals representing the fast and slow time functions. (Since V_X or V_Y may be either fast or slow; that is, representative of the display fast sweep and the display slow sweep, the terms horizontal or vertical are only relative.) The ψ linear ramp circuitry is independent of the horizontal drive frequency over a sufficient range to permit operation of the FSS DARC at all scan rates from 525 to 1025 lines.

All other waveforms (ψ^2, $\theta\psi$, etc) are generated using analog multipliers, as opposed to successive integrations, thus eliminating the dependency of scan line frequency. The output of the waveform generator is fed to the direction cosine generator where the observer instantaneous line of sight vectors k_{LOSO}, ℓ_{LOSO}, and m_{LOSO} are produced. Two separate cosine generators are required to cover the observer FOV's for background projector position 1 (-120° and +90° azimuth) and position 2 (-80° and +80° azimuth). The output of the direction cosine generator is weighted and summed by four-quadrant multiplying D/A converters and summing amplifiers in the matrix transformation section in response to computer coefficients from the linkage.

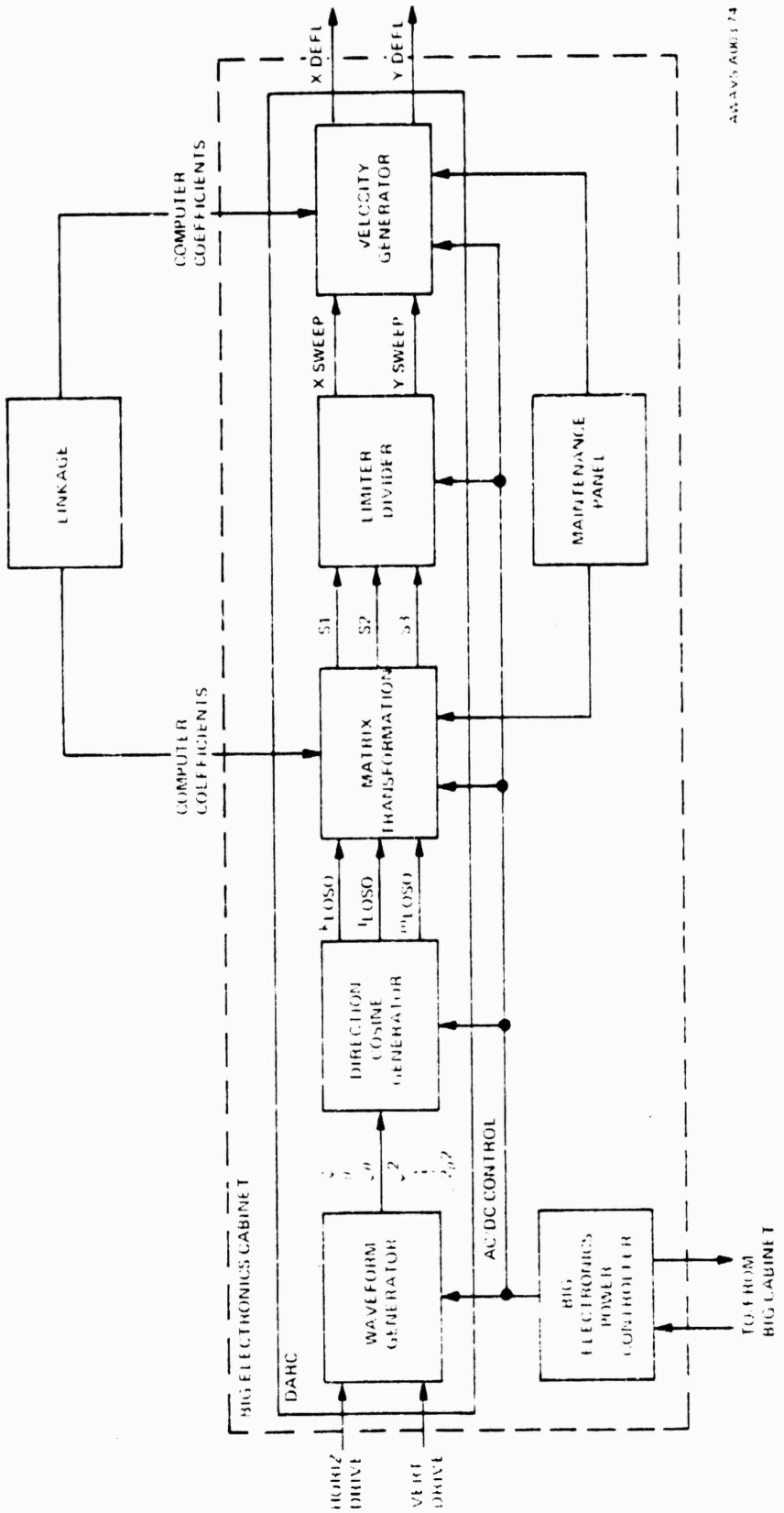

Figure 74. Background DARC, Block Diagram

Following the matrix transformation, the signals are amplitude limited and with proper division and X_s and Y_s drive signals are produced to be applied to the velocity generator. X_s and Y_s produce a sub raster on the FSS of the proper size and shape to which the velocity generator adds a low frequency position signal that creates the aircraft velocity cue in response to velocity command from the digital computer. Further, the velocity generator digitally creates the raster reset operational mode in conjunction with the 2X2 seascape film image plate to provide continuous motion over an unlimited sea plane. The deflection signals are amplitude and frequency limited and scaled at the output of the velocity generator, thus eliminating overscan problems in the FSS.

3.4.2 Seascape Generator. The seascape generator is located in a single-bay electronics cabinet designated the BIG cabinet. The principle components are the high resolution display generator, the seascape image film plate, an optical coupler and the video processor. These are clamped together to form a single assembly. The BIG power controller circuitry in the same cabinet provides the CRT blanking which disables the CRT until all sweeps and deflections are available. Figure 75 is a block diagram of the seascape generator. Details of the major components, as well as the simulation technology, are given in the following paragraphs.

3.4.2.1 High Resolution Display System. The seascape generator display system is a high precision system featuring high resolution, ultra high linearity, wide bandwidth and fast settling time. The system consists of four separate assemblies, which when integrated, provide a high resolution light source for the AWAVS flying spot scanner image generation. The assemblies are the deflection amplifier assembly, the CRT assembly, the bias supply/blanking amplifier assembly and the control electronic assembly. The following is a general description of these assemblies. These, plus any additional or alternate components necessary to provide a functional system, shall be provided.

3.4.2.1.1 Deflection Amplifier Assembly. The deflection amplifier assembly (LPN 1003344-01) is a CELCO model RDA-1260 60 volt, 12 amp X-Y deflection amplifier with regulated quadrupower supplies. Input power to the assembly is standard 105-125 VAC 60 Hz line voltage. The deflection yoke connections are made via a rear panel MS style connector. The linear X-Y drive input signals are applied to the rear panel BNC type connectors. Y damping, X damping, Y centering and X centering controls are available on the front panel along with test points on the "X Deflection," "Y Deflection" inputs and the "X Deflection Current" and "Y Deflection Current" inputs.

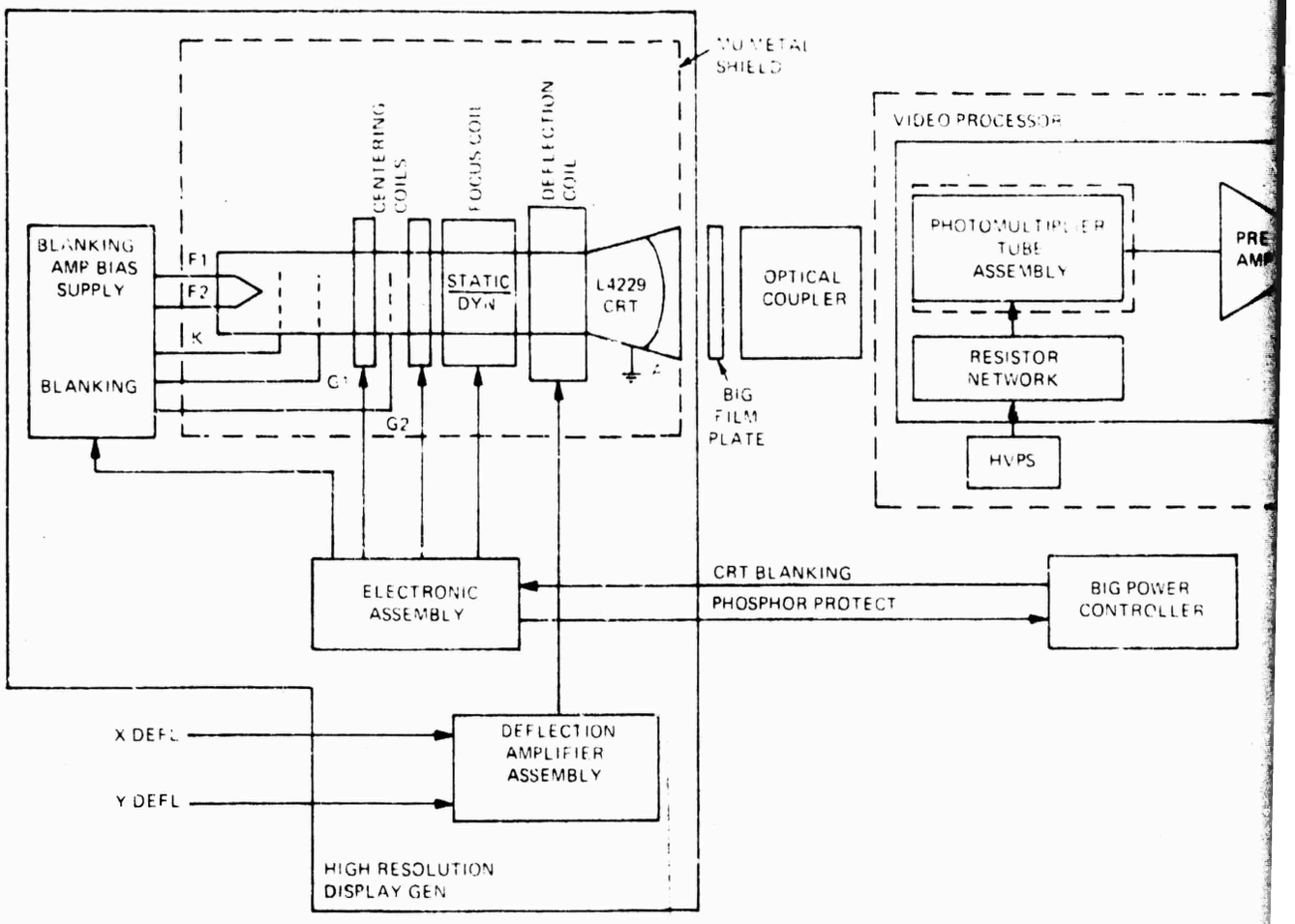
MU METAL SHIELD
CENTERING COILS
FOCUS COIL
DEFLECTION COIL
BLANKING AMP BIAS SUPPLY
F1
F2
K
BLANKING
G1
G2
STATIC
DYN
L4229 CRT
OPTICAL COUPLER
BIG FILM PLATE
VIDEO PROCESSOR
PHOTOMULTIPLIER TUBE ASSEMBLY
RESISTOR NETWORK
HVPS
ELECTRONIC ASSEMBLY
CRT BLANKING
PHOSPHOR PROTECT
BIG POWER CONTROLLER
X DEFL
Y DEFL
DEFLECTION AMPLIFIER ASSEMBLY
HIGH RESOLUTION DISPLAY GEN

2

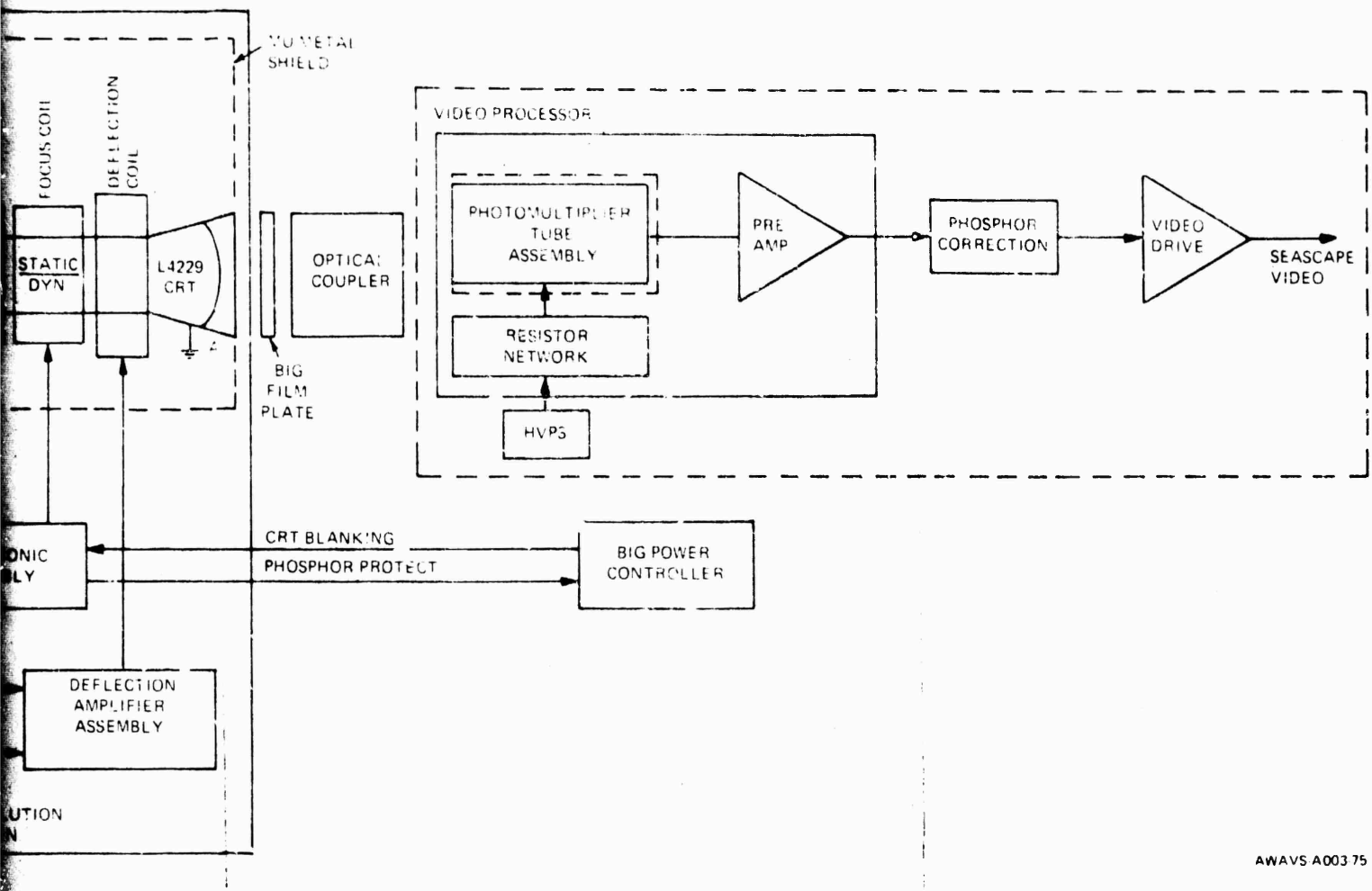

Figure 75. Seascape Generator, Block Diagram

3.4.2.1.2 CRT Assembly. The CRT assembly will include the CELCO assemblies listed in Table 45.

TABLE 46. CRT ASSEMBLY COMPONENTS

QTY	SINGER P/N	CELCO P/N	DESCRIPTION
1	1003340-01	B5M10-2	Shield, Magnetic
2	1003341-01	KC403-S320	Coil, Centering
1	1003342-01	HD428S660	Special coil, deflection
1	1003343-01	HFL334-379/620	Coil, Focus
1	1003349-01	C1-22	Positioner mount - CRT and coil
1	1003337-01	PIR	Micropositioner, deflection coil
1	1003338-01	PI	Micropositioner, focus coil
2	1003339-01	FI	Micropositioner, coil holder

This assembly will also include the Litton Industries, Inc. L4229-01/LP201 fiber-optic faceplate CRT. This CRT will mount in the assembly in such a manner which allows direct surface contact between the fiber-optic faceplate and the five-inch diameter film plate in the final FSS assembly. All components of the CRT assembly will be locked into position, after alignment, such that operation will be possible in both the horizontal and vertical (tube face-up) positions. For alignment purpose, a special mechanical adjustment feature will be incorporated into the standard CELCO micro-positioner assembly. The fiber-optic faceplate on the CRT has a precision spherical radius ground on the inside surface which is designed to match the deflection radius of the deflection yoke. This feature eliminates the need for electronic correction of geometric distortions associated with a flat-faced CRT. In order to take advantage of the spherical radius, a precision adjustment along the electron beam trajectory must be incorporated into the deflection coil micropositioner assembly. A total adjustment range of ±1/32 inch with a resolution of 0.001 inch is required. This will allow an accurate alignment of the deflection coil deflection center with the faceplate center along with the conventional yaw, pitch, and roll adjustments of the deflection coil micropositioner. The total micropositioner-CRT assembly will be enclosed in the magnetic shield housing with all connections to this assembly made through the rear panel.

3.4.2.1.3 Bias Supply/Blanking Amplifier. The Bias Supply/Blanking Amplifier assembly (LPN 1003326-01) is a Computer Power Systems model 1411/1695. This unit supplies all bias voltage for operation of the CRT. In this configuration, the CRT anode is operated at ground potential because of the fiber-optic faceplate. The electron gun assembly is operated at -20KV potential. This assembly provides a means of blanking the CRT with standard TTL input levels.

3.4.2.1.4 Control Electronic Assembly. The control electronic assembly is mounted along side the FSS on the FSS assembly. This assembly provides the static focus and centering coil current drives, the dynamic focus amplifier, and the phosphor protection modules. Assemblies to be included are listed in Table 46.

TABLE 47. CONTROL ELECTRONIC ASSEMBLY COMPONENTS

QTY	SINGER P/N	CELCO P/N	DESCRIPTION
1	1003345-01	FA100	Amplifier, dynamic focus
1	1003346-01	PR5-2	Power supply, precision, reference
2	1003347-01	CR100	Regulator, current
1	1003348-01	SR1000A	Regulator current
1	2061546-01	-	Phosphor protection

All connections to this assembly will be made via connections at the rear panel of the assembly.

3.4.2.1.5 High Resolution Display System Performance. The desired performance of the high resolution display system is outlined in Table 47.

3.4.2.2 Seascape Film Plate. The seascape film plate, Figure 76, contains four, identical seascape images obtained from a high precision step and repeat printing process. The patterns will be overlapped in order to smoothly integrate the wave pattern in the area of the film junctions. The picture area to be scanned is 3,775 feet per side of each seascape image. The film is half the size used in the original system; but due to the superior optical efficiency of the fiberoptic faceplate over the CRT compared to the efficiency of a lens which was required for the FSS system, the beam current can be reduced, and spot size will therefore also be half the size. Thus, the criteria for the resultant television picture quality is the same as analyzed in Section 5 of the AWAVS Design Analysis Report. No deviation is expected from the MTF curves and signal-to-noise derived from the original system, except for a slightly improved SNR of 3 dB due to the increased optical efficiency. It should be clearly understood that the raster reset is concerned only with the seascape image background. Any abnormalties present due to offset jitter or MTF response, if present, would not be a part of the target or target inset.

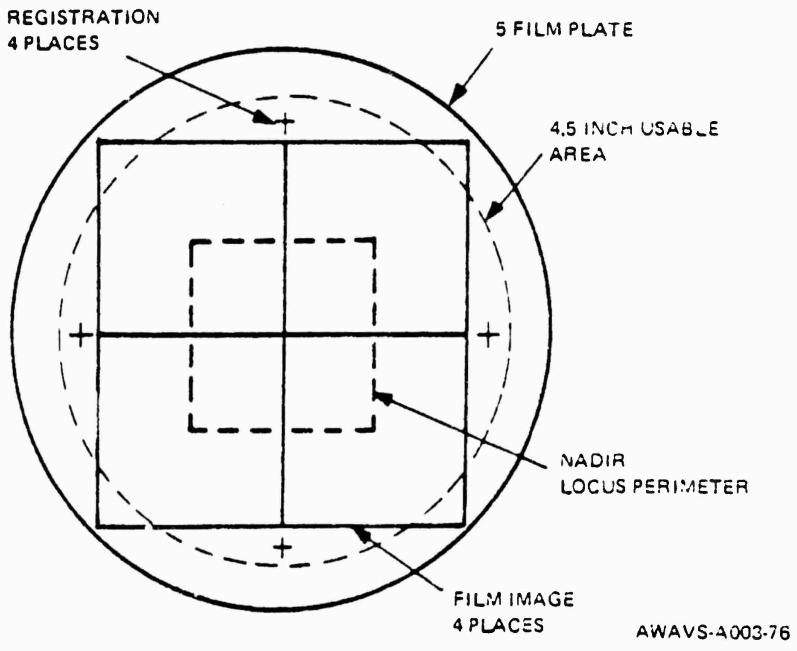

Figure 76. BIG Film Plate

TABLE 48. HIGH RESOLUTION DISPLAY SYSTEM PERFORMANCE

PARAMETER	COMMENTS	RESOLUTION
Spot Size	Half amplitude at 1 μamp current	0.0010 inch at center 0.0011 inch at edge
Spot Settling Time	Over the useful screen diameter	To 1% of final position 1.4 sec. max. To 0.1% of final position 9 sec. max.
Deflection Bandwidth	300 ma p-p with 25 μH yoke	DC to 1.4 MHZ @ 1.4 MHZ/min
Spot Drift		0.02% of useful screen diameter after 30 min.
Spot Jitter		0.001% of useful screen diameter
Linearity	Max. dev. from ideal location with respect to useful screen diameter	0.02% inside centered 1" radius circle 0.04% over remainder of useful screen area
Repeatability		±0.05% of useful screen diameter
Deflection Signal Input		Amplitude +6 volts (signal plus DC) impedance 1000 ohms (min.)
Blanking Signal Input		Blank level +0.5V; Unblank level +2V Impedance TTL (approx. 2K) Rise/fall time 100μsec. (max.)
Phosphor Protection	Protects the phosphor from damage due to loss of sweep. This circuit will protect the CRT from damage due to system failures, i.e., loss of sweep input, loss of input power supplies, open deflection coil, or excessive CRT beam current.	

The film plate will contain registration marks on the outer edge of the picture for alignment purposes. The film plate will not include the nadir locus perimeter outline included in the figure as a broken line. This is an invisible boundary which, when intersected by the aircraft nadir, will cause a raster reset to an identical image pattern on one of the other three film images. The reset will be controlled by hardware and will occur during the flying spot scanner vertical retrace period. It is therefore possible to fly over a seascape of unbounded size and almost unlimited velocity range.

3.4.2.3 Optical Coupler. The purpose of the optical coupler is to relay the light from the photographic plate to the photomultiplier.

The whole optical system consists of the photographic plate and optical coupler. The flying spot scanner has a fiber optics faceplate and is in contact with the photograph.

The fiber optics faceplate relays the spot image from the phosphor surface to the exit face of the FSS. The transparency is placed with the emulsion side in intimate contact with its exit face. An oil film is used to fill the gap. The oil reduces the divergence and growth in spot size. It also reduces surface caused light losses. In addition, many surface defects, which would appear in the image, will disappear.

The optics coupler works by total internal reflection. The light diverging from a spot strikes the cylindrical surface of the coupler. The angle is greater than the critical angle for the glass and it reflects totally.

The length of the coupler is such that the edge point of the FSS image will have its extreme ray arriving at the opposite side of the photomultiplier. This is shown in Figure 77. This insures that each point in the image illuminates the whole photomultiplier active surface. This is necessary because the photomultiplier surface does not have uniform responsivity.

The large photocathode on the photomultiplier will keep the vergence of the rays the same. Since the photomultiplier response falls off rapidly with increasing angle from its peak, the response will be higher. The use of a smaller photomultiplier would mean that the vergence of the incident energy would be increased to condense the pupil on the smaller area and hence lower response would result.

The coupler is interfaced with oil to the photograph read side and photomultiplier face.

The size of the coupler can be calculated from the requirement to have the extreme ray of the edge image point strike the opposite side of the photomultiplier tube. Figure 72 shows the geometry for the calculation. Figures 78 and 79 show details of the flying spot scanner and photomultiplier tube.

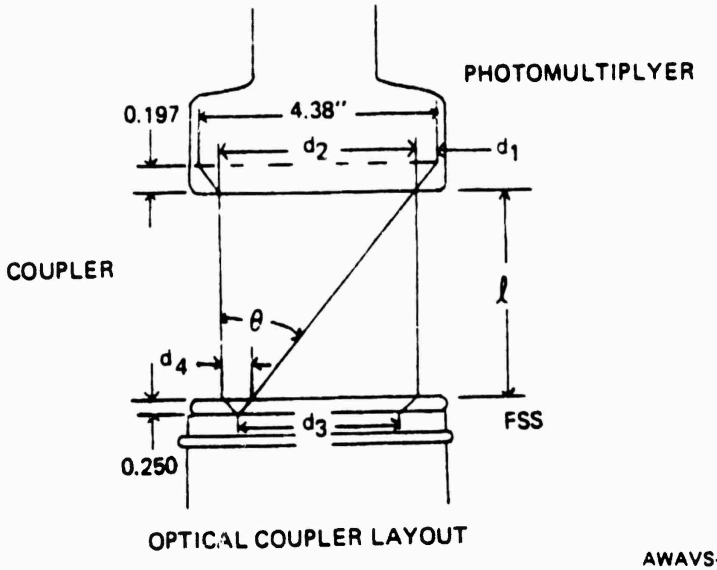

Figure 77. Optical Coupler Layout

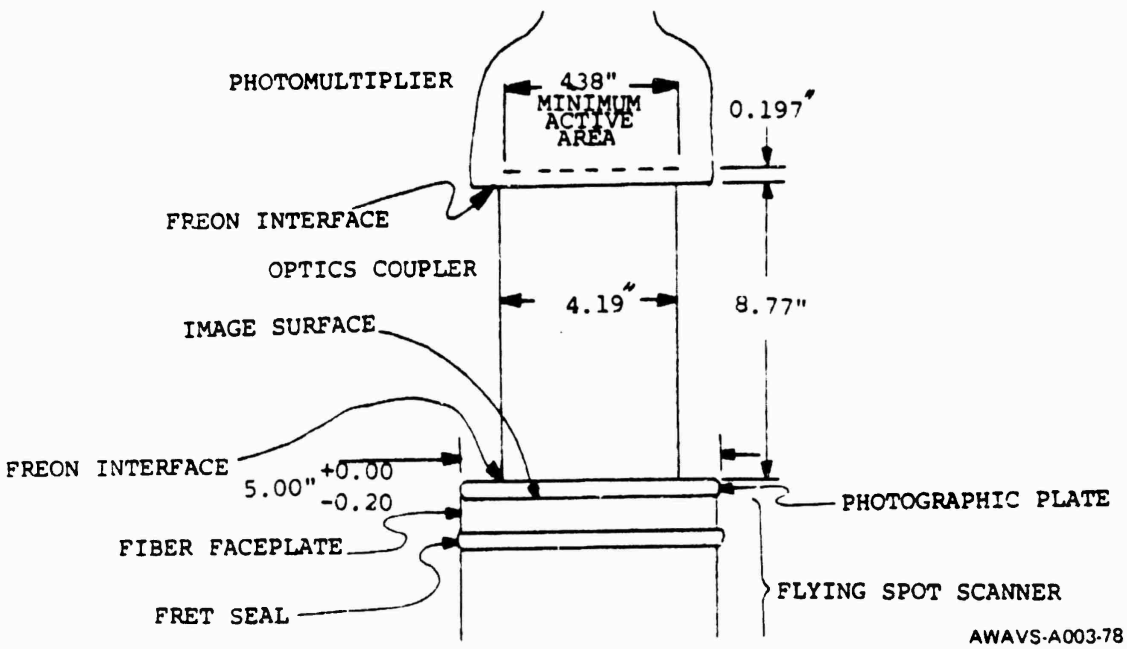

Figure 78. Seascape Generator Optical System

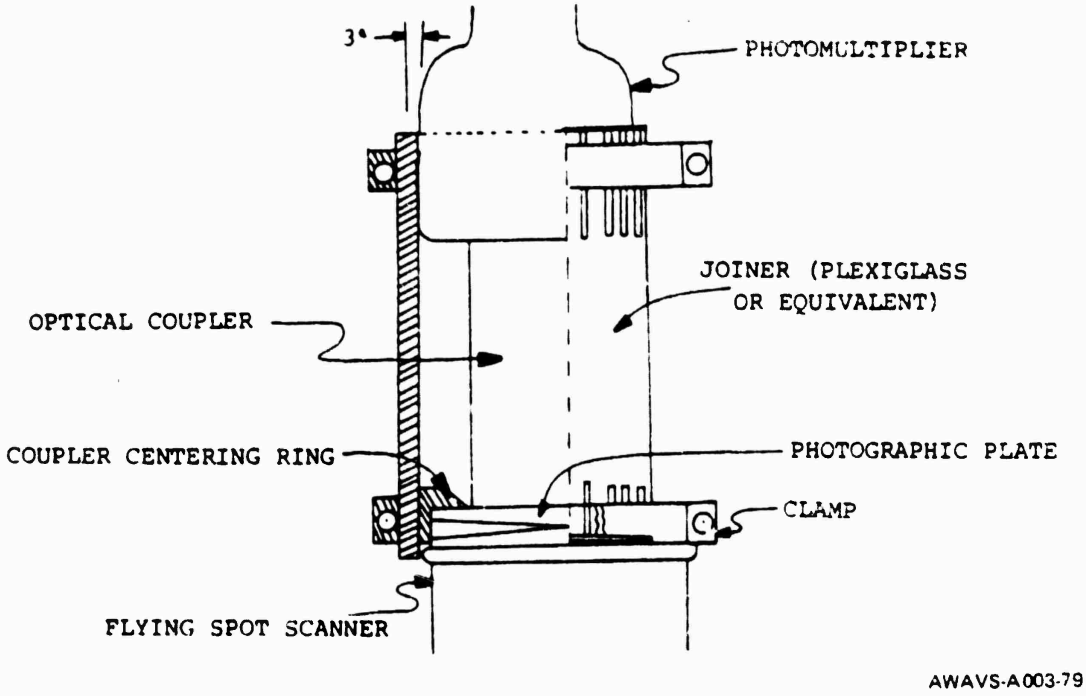

Figure 79. Joining Device For Seascape Generator

The numerical aperture of the radiance from the flying spot scanner is 0.66. The index of the glass bottle of the photomultiplier, a coupler and photographic plate, is about 1.52. This gives a vergence of (n.a.)/n. = sin θ:

$$\theta = \sin^{-1} \frac{0.66}{1.52} = 25.8 \qquad (\theta \text{ is the half angle.})$$

The size of the minimum active photomultiplier area is 4.38 inches. With the above divergence, the size of the coupler is:

$$d_2 = 4.38 - 2d_1 = 4.38 - 2\ (197)\tan 25.8 = 4.19"$$

The size of the active area of the photographic plate and flying spot scanner is d_3. It is calculated below.

$$d_3 = 4.19 - 2\ (0.250)\ \tan 25.8 = 3.95"$$

The length of the coupler "L" can be calculated:

$$L = (d_2 - d_4)/\tan \theta = (4.190 - 2 \times 0.250/\tan 25.8)\ \tan 25.8 = 8.17"$$

The flatness requirement can be calculated from the vergence and permitted spot size growth. The growth can be 0.0002 maximum or ±0.0001.

With no fluid medium, the angular vergence is:

$$\theta = \sin^{-1} 0.66 = 41.3°$$

The permitted 0.0002" spot growth would be reached in a distance of

$$d = \frac{0.0001}{\tan 41.3°} = 0.00014 \text{ over } 5"$$

or 0.000023 over 1"

It is over five inches because the photograph covers the FSS surface. This requires the use of Kodak "Micro Flat" glass whose flatness is 0.00002" Kodak Ultra Flat, 0.0005"/in. is not adequate because it permits a worst-case spot growth of

$$2 \times 5" \times (0.0005"/\text{in.}) \tan (41.3°) = 0.0044$$

which is 20 x the permitted 0.0002". (Refer to Figure 80 for Glass Plate Specifications.)

Figure 79 shows the assembly of the optical coupler; while Figures 81 and 82 show the dimensions of the photographic plate and optical coupler respectively. Figure 83 is the specification sheet for coupler glass.

Figure 79 shows the selected method of assembly for the components. The coupler centering ring is used to center the coupler and the photographic plate on the flying spot scanner. It is split so that when the clamp is tightened it will tighten on the components it is centering. It is important to have as little area as possible contacting the side of the optical coupler because this causes a loss of light. Therefore, the contact is along a relatively sharp edge.

The coupler centering ring and joiner have a spherical mating surface so that misalignment of any part will not cause strain or a breaking of the interface oil film when the system is clamped. The uniformity of the oil film thickness is particularly important for the emulsion-faceplate interface because of defocusing.

The signal level out of the photomultiplier can now be calculated.

GLASS FOR PLATES

• The glass on which sensitized emulsions are coated is often of considerable importance in scientific work. Photographic glass has yet to be surpassed as a base for photographic emulsion in critical applications where dimensional stability is paramount.

DIMENSIONAL STABILITY OF GLASS

• Glass has even greater dimensional stability than the famous steel-gage blocks used for standardized measurements. Kodak glass has a *humidity coefficient of zero* and a thermal coefficient of only 0.00000045 inch per inch per degree Fahrenheit. In this respect, Kodak glass is roughly three times as stable as aluminum and is superior to hardened steel.

The high-strength "soda-lime" glass used for Kodak plates is carefully selected with special attention to other physical characteristics as well. Flatness, size, and thickness considerations are thoroughly screened to suit customer needs for the specific job involved.

Standard thickness specifications are given in the Data Sheets.

FLATNESS SPECIFICATIONS

• Except for 0.250-inch thick plates, photographic glass is flat drawn and fire polished. The sheet is characterized by its brilliant surface. Marked improvements in the drawing of sheet glass have produced a sheet with a very minimum of surface wave.

EMULSION-COATED PLATES WITH THE FOLLOWING GLASS SPECIFICATIONS CAN BE SUPPLIED ON SPECIAL ORDER ONLY:

Selected Flat Glass

0.001 in. /in. in. — Selected flat glass can be supplied in sizes 11" x 14" and smaller, and in thicknesses of 0.030 to 0.130 inch, inclusive. This glass is inspected to meet a flatness tolerance of 0.001 inch per linear inch.

Ultra Flat Glass

0.0005 in. /in. in. — Ultra flat glass is selected to a higher degree of flatness and can be supplied in thicknesses of 0.060 to 0.250 inch, inclusive. Each sheet is inspected on optical instruments to a flatness tolerance of 0.0005 inch per linear inch.

Micro Flat Glass

0.00002 in. /in. in. — Micro flat glass is available in sizes no smaller than 4 x 4 inches and no larger than 10 x 10 inches and in the 0.250-inch thickness only in order to provide maximum stability. The front and back surfaces of these plates possess an extremely high degree of parallelism. The front surface of micro flat glass, on which the emulsion is coated, does not depart by more than 0.00002 inch per linear inch from a true plane and will meet the most critical requirements of the integrated photographic systems. The precisely flat surfaces of micro flat glass are exceeded only by the plane surfaces of high-grade optical flats.

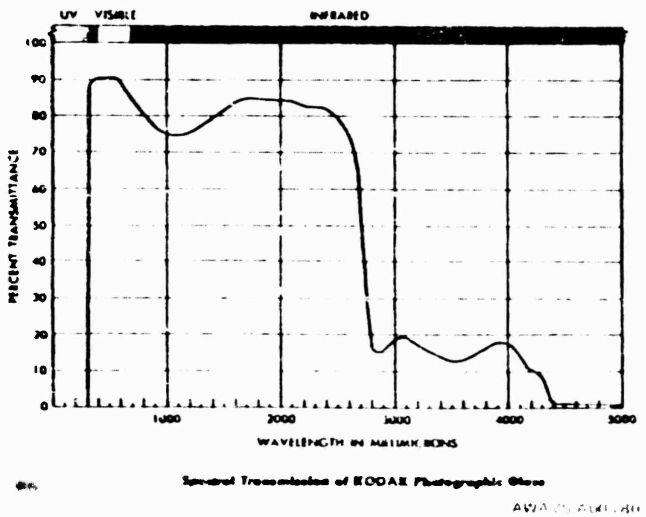

Spectral Transmission of KODAK Photographic Glass

Figure 80. Glass Plate Specification Sheet

$\sum$ = 743 Relative Integrated Emittance

$\sum = 0.354 \frac{\text{Amps}}{\text{Watt Output}}$ Relative Signal Output

$8.17 \times 25.4 \div 10 = 20.75$ Calculation of Exponential

Integrated Emittance $0.006 \frac{\text{Watt (Output)}}{\text{Watt (Input)}}$

$\times$ 0.02 watts input = 0.0012 watts (Output)

$7.48K = 0.0012$ watts (output) $K = 0.000160$ watts

$0.S - 0.554 \times 0.000160 = 0.0000887 = 0.0887$ ma

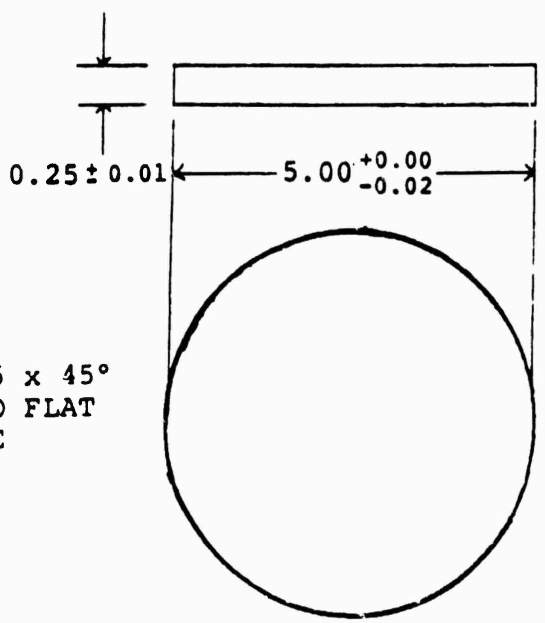

BRAKE SHARP EDGES .015 x 45°
MATERIAL: KODAK MICRO FLAT GLASS PLATE

AWAVS-A003-81

Figure 81. Photographic Plate Dimensions

Figure 83 shows the spectral transmission of the glass used in the coupler per 10mm length. This data is entered in Table 48, columns 1, 2 and 3 show the spectral transmission of the whole coupler.

Figures 84 and 85 contain the phosphor data. The relative spectral emittance shown on Figure 84 is entered in column 4 of Table 48. The integration of the relative spectral emittance is equivalent to the energy output of the FSS. The energy output is proportional to the beam power. The constant of proportionality is 0.006 watts radiance/watts electrical. The planned power is 20* kilovolts at 1 microamp or 0.02 watts electrical. The output emittance is 0.02 × 0.006 = 0.00012 watts emittance.

The constant which converts the relative spectral emittance to absolute can be calculated. The integration of the emittance is 7.48 which is equivalent to 0.00012 watts emittance. The constant for conversion is 0.00012/7.40 = 0.000160.

The photomultiplier response is shown in Figure 86 and this data is listed on column 5 of Table 48. Column 6 shows the product of these factors. The integrated relative signal output is 0.554 amps/watt output. The signal is 0.554 × 0.000160 - 0.0000887 or 88.7 microamps.

3.4.2.4 Video Processor. The input to the video processor is the light flux coupled onto the photomultiplier cathode via the optical coupler. The photocathode current is amplified in the phototube dynode structure which is biased via the resistor network and variable high voltage power supply. Varying the power supply output around 800 volts will allow an optimum signal-to-noise ratio operating point at the anode output of the phototube. The anode signal current is buffered and amplified by the preamplifier. The output of the preamplifier will drive the phosphor correction filter network. This filter will accent the high frequency detail of the input signal and thus make up for rolloff in the response of the CRT phosphor and the photomultiplier dynamic response to high frequency changes in the input. The AWAVS design analysis called for a 20-MH frequency response at a desired signal-to-noise ratio of at least 37 dB. The filter output will be used to drive the wide bandwidth video line driver which provides the current required to drive the image generator output "seascape video." The output is routed to both the special effects generator and BIG monitoring equipment.

3.4.2.5 BIG Power Controller. The function of the background power controller is to sequence the dc power applied to the high resolution system on and off in such a manner to prevent damage to the CRT. In addition, phosphor protection circuits protect the system from excessive CRT beam current and loss of sweep signals. These circuits are found in both the BIG cabinet and the BIG electronics cabinet.

*Re: Litton communication

TABLE 49. SPECTRAL TRANSMISSION OF OPTICAL COUPLER

WAVE LENGTH	GLASS USED IN COUPLER /10 mm	OF WHOLE COUPLER	RELATIVE SPECTRAL EMITTANCE	PHOTO-MULTIPLIER RESPONSE	PRODUCT OF FACTORS
370	0.991	0.829	0.08	0.072	0.00477
380	0.991	0.829	0.48	0.075	0.0298
390	0.994	0.883	0.81	0.078	0.0558
400	0.995	0.9012	0.99	0.079	0.0705
410	0.995*	0.90122	0.98	0.082	0.0724
420	0.995	0.9012	0.93	0.084	0.0704
430	0.995*	0.9012	0.84	0.087	0.0659
440	0.995	0.9012	0.68	0.088	0.05393
450	0.995*	0.9012	0.47	0.088	0.03727
460	0.996	0.9202	0.41	0.087	0.03782
470	0.996*	0.9202	0.29	0.084	0.02242
480	0.997	0.9396	0.21	0.082	0.01618
490	0.997*	0.9396	0.15	0.079	0.01113
500	0.997	0.9396	0.09	0.075	0.00634
510	0.997*	0.9396	0.05	0.070	0.00329
520	0.997*	0.9396	0.01	0.066	0.00062
530	0.998*	0.9593	0.01	0.060	0.0005756
540	0.998*	0.9593	0.00	0.055	0.0
550	0.998	0.9593	0.00	0.048	0.0

*These numbers interpolated.

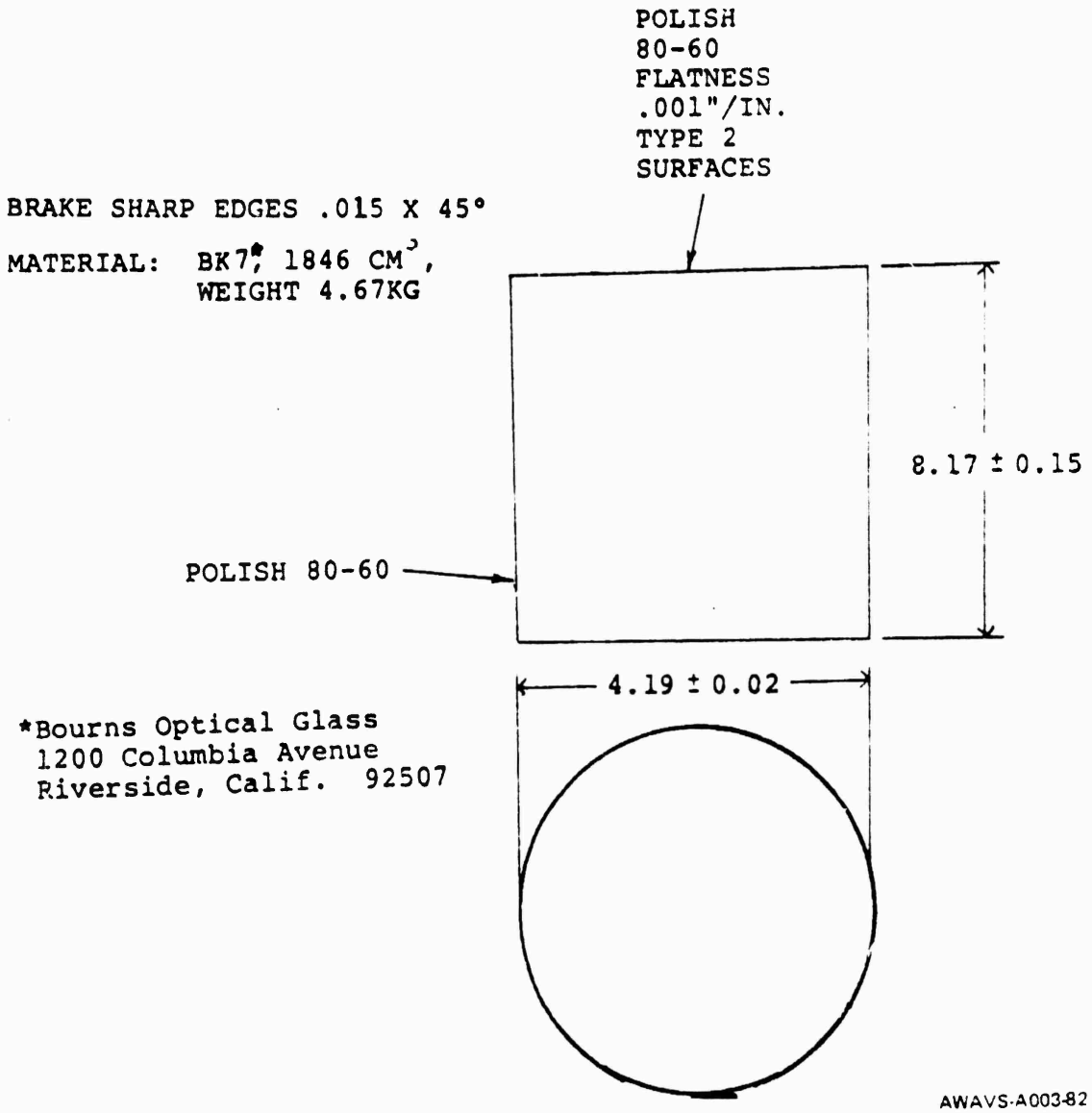

Figure 82. Optical Coupler Dimensions

Refractive Index		$\frac{n_d - 1}{n_F - n_C}$ =		Dispersion	
	n_d 1.51633		ν_d 64.15	$n_F - n_C$	0.008049
	n_e 1.51825		ν_e 63.93	$n_{F'} - n_{C'}$	0.008106

Refractive Indices λ(nm)		Relative Partial Dispersions				Internal Transmittance	
n_t (1014.0)	1.50687	$\frac{n_C - n_t}{n_F - n_C}$ 0.8676	$\frac{n_C - n_A}{n_F - n_C}$ 0.3582	$\frac{n_d - n_C}{n_F - n_C}$ 0.3075	$\frac{n_e - n_C}{n_F - n_C}$ 0.5462	λ(nm)	τ_i 10mm
$n_{A'}$ (768.2)	1.51097	$\frac{n_g - n_d}{n_F - n_C}$ 1.2275	$\frac{n_g - n_F}{n_F - n_C}$ 0.5350	$\frac{n_h - n_g}{n_F - n_C}$ 0.4414	$\frac{n_i - n_g}{n_F - n_C}$ 1.1878	280	
n_h (706.5)	1.51243					290	.08
n_C (656.3)	1.51385	$\frac{n_{C'} - n_t}{n_{F'} - n_{C'}}$ 0.9103	$\frac{n_e - n_{C'}}{n_{F'} - n_{C'}}$ 0.4935	$\frac{n_{F'} - n_e}{n_{F'} - n_{C'}}$ 0.5065	$\frac{n_i - n_{F'}}{n_{F'} - n_{C'}}$ 1.6548	300	.30
						310	.57
$n_{C'}$ (643.8)	1.51425					320	.77
		Deviation of Relative Partial Dispersion $\Delta\theta$ from "Normal"				330	.88
n_D (589.3)	1.51626	$\Delta\theta_{C,t} = \Delta\frac{n_C - n_t}{n_F - n_C}$ 0.0200	$\Delta\theta_{C,A'} = \Delta\frac{n_C - n_{A'}}{n_F - n_C}$ 0.0047	$\Delta\theta_{g,d} = \Delta\frac{n_g - n_d}{n_F - n_C}$ −0.0037	$\Delta\theta_{g,F} = \Delta\frac{n_g - n_F}{n_F - n_C}$ −0.0024	340	.938
					$\Delta\theta_{i,g} = \Delta\frac{n_i - n_g}{n_F - n_C}$ 0.001	350	.968
n_d (587.6)	1.51633					360	.987
		Other Properties				370	.991
n_e (546.1)	1.51825	Specific Gravity g/cm³ 2.53		Water Resistance 3		380	.991
		Coloring 33/29		Acid Resistance (Powder) 0		390	.994
n_F (486.1)	1.52190	Bubble Quality Group 1		Acid Resistance (Surface) 1		400	.995
						420	.995
$n_{F'}$ (480.0)	1.52236	Knoop Hardness Group 6		Weathering Resistance a		440	.995
n_g (435.8)	1.52621	Abrasion 95		Transformation Temperature T_g (°C) 565		460	.996
						480	.997
$n_{e'}$ (434.0)	1.52639	Young's Modulus K_g - Wt./mm² 7980		Yield Point A_t (°C) 624		500	.997
		Rigidity Modulus K_g - Wt./mm² 3300		Softening Point S_p (°C) 715		550	.998
n_h (404.7)	1.52976	Poisson's Ratio 0.207		Expansion Coefficient $\alpha \times 10^7$/°C (−30° to 70°C) 74		600	.998
					(100° to 300°C) 86	650	.998
n_i (365.0)	1.53577	Remarks —				700	.998

Constants of Dispersion Formula					
A_0	A_1	A_2	A_3	A_4	A_5
2.2697655	−9.6395197·10⁻³	1.1025458·10⁻²	7.9465126·10⁻³	1.0120957·10⁻³	4.4096694·10⁻⁴

AWAVS A003-82

Figure 83. Optical Coupler Specification Sheet

LP201 phosphor is a fast decay, blue-violet emitting phosphor suitable for scanning applications. In many respects it is similar to P16, however, this new phosphor has certain inherent advantages over P16. They are:

1. This phosphor has a blue emissive color, which is more suitable for optical design than the ultraviolet emission of P16.
2. The initial efficiency of this phosphor is approximately the same as P16, but it ages at a much slower rate, so the net effect is higher useful efficiency.
3. Decay times are relatively constant with respect to electron beam aging and are approximately equal to the best P16 can do after it has been heavily aged.
4. This phosphor does not possess the long decay low level phosphorescence of P16.

LP201 is also useful as a direct replacement for P37. In this case its much higher efficiency and inherent lack of property change due to current saturation make it clearly superior for scanning applications.

COMPARISON CHART

Phosphor	LP201	P16	P37
Color 10% Peak 10%	370 nm 400 nm 500 nm	360 nm 390 nm 440 nm	380 nm 430 nm 480 nm
Relative Screen Efficiencies, New	1x	1x	<0.1x
Aged to 1 C/cm²	.75x	.5x	—
Aging, C/cm² to ½ Output	>10	0.1 to 1	—
Relative Decay Time, New	1x	2x to 5x	2x
Aged	1x	1x	—
Phosphorescence	Slight	3%	—
Current Sensitivity	Slight	Slight	—

Figure 84. LP201 Phosphor Specification Sheet

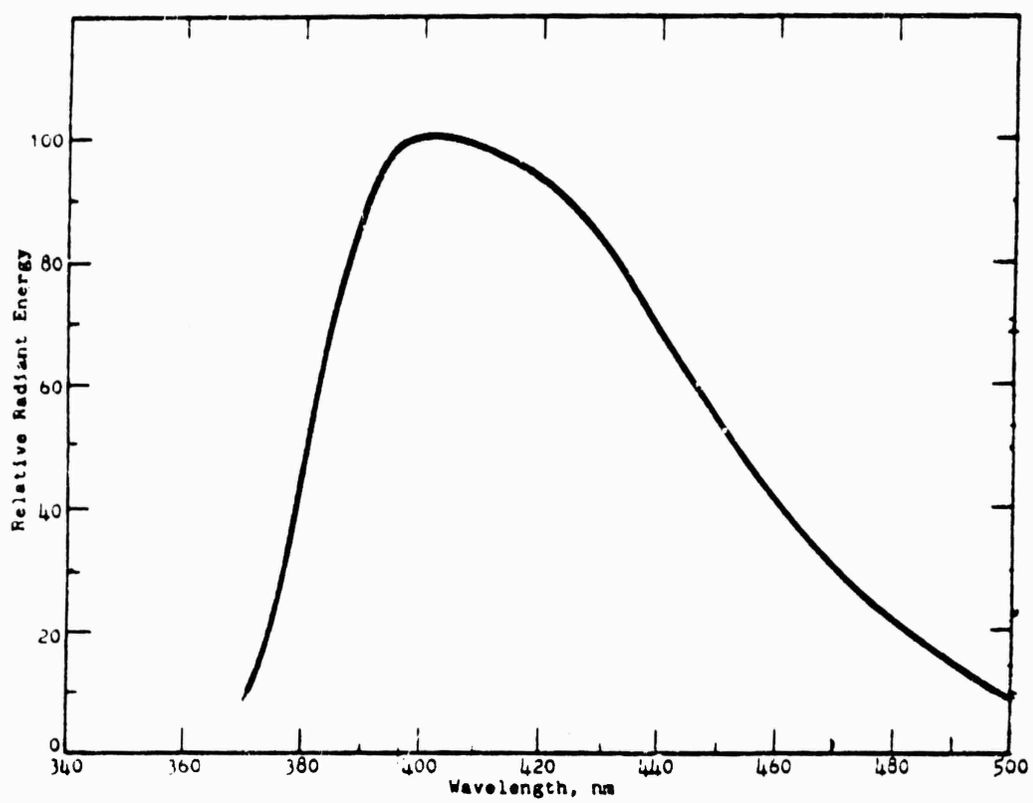

Note 1: The information presented here is from tests of representative tubes. This chart is intended to give comparative qualitative data only.

Note 2: Ratio of actual energy efficiencies (not relative visual brightness) as measured on an aluminized screen at 20 KV.

Note 3: Based on decay to 10% of a 0.1 us pulse at low current density.

Note 4: Based on published data.

Note 5: Depends upon phosphor manufacturer and lot.

Note 6: Light output of P37 was too low for complete testing.

Note 7: Extrapolation of data taken to ~ 1 C/cm^2 indicates this figure to be approximately 100 C/cm^2.

AW3V3 A.00385

Figure 85. Phosphor Tentative Spectral Energy Distribution

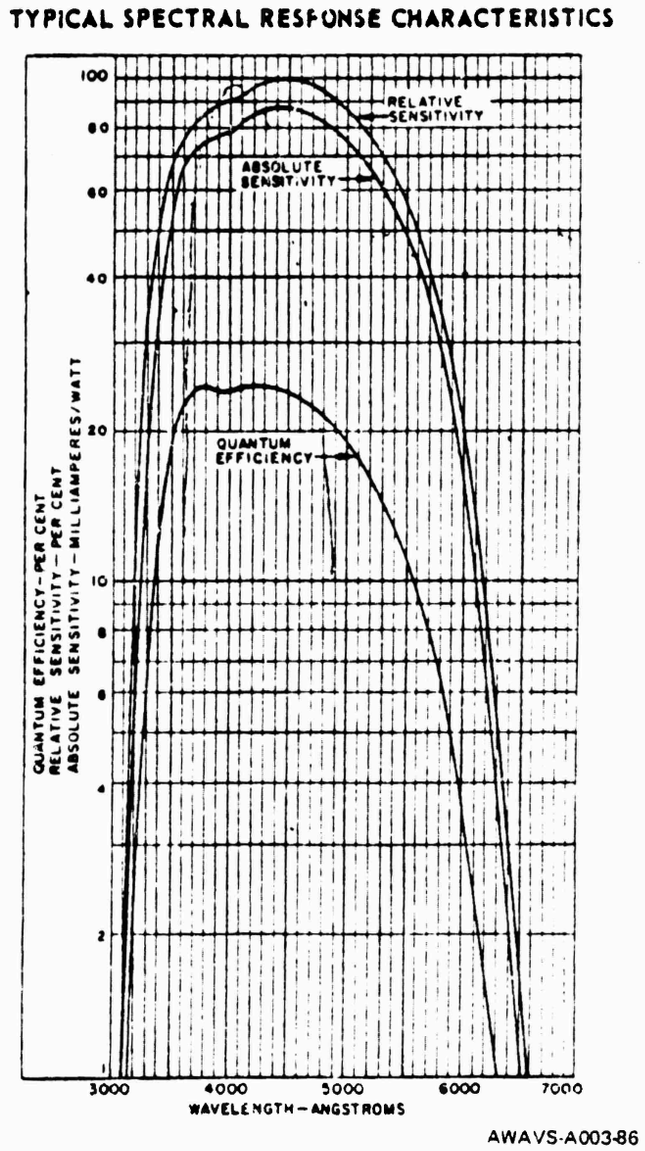

Figure 86. Photo Spectral Energy Response

3.4.3 Background Special Effects Generator. The function of the special effects generator (SEG) is to combine video signals from all sources, and produce a composite video signal for delivery to the projector. In the background SEG, the seascape film plate image must be extended from the limit of film plate generation out to the horizon. It must then provide a horizon, and synthetically generate and add to the video scene fog (or haze), cloud, and sky shades. The special effects generator card bin physically houses circuitry for both the background and target generators. The target SEG, consisting of only one circuit card is located herein solely for the convenience of dc power availability. The following paragraphs are devoted to the background SEG only. Refer to paragraph 3.1.4.6 for the target SEG description.

Seamerge shading fills in the sea between the film plate image and the horizon, providing a gradual transition to the selected film plate seascape image. The transition to a definable seascape imagery varies as a function of the depression angle below the horizon, eventually becoming all seascape film plate video and continuing to the bottom of the projected scene. The horizon itself is formed by the relatively hard transition between the cloud level and the remainder of the video scene. Synthetically generated video is employed to simulate the remaining functions, as follows:

a. Clouds - a separately adjustable uniform level that fills in the above-the-horizon scene during below-the-clouds flight simulation, or the below-the-horizon scene during above-the-clouds flight. A constant cloud level fills the picture during simulated in-clouds flight.

b. Sky - a separately adjustable uniform level that replaces the composite seascape/seamerge video during above-the-clouds flight simulation.

c. Fog on haze - a gradual mix of composite seascape/seamerge video to cloud level varying as a function of RVR/H (visibility range/altitude).

When below clouds, the upper portion of the picture is cloud shade down to the horizon. Moving below the horizon, the component of cloud shade is decreased as the range to the point on the simulated sea plane decreases, and there is a complementary increase in the seascape video component of the scene. (This simulates fog on haze.) In clouds, a constant cloud shade fills the entire picture. Above clouds, a cloud shade fills the portion of the scene below the horizon. The component of cloud shade decreases with increasing angle above the horizon, and sky shade is complementarily mixed in. This gives a "scud above clouds" effect.

Figure 87 is a block diagram of the background SEG. The seascape video from the seascape image generator is combined with the seamerge video under control of the seamerge line. The seamerge line controls the point where seamerge starts to replace seascape film plate video. The combined seascape/seamerge output of the mixer is applied to a summing amplifier which provides facilities for adding a synthetically generated carrier wake (WIG video). The synthetic wake is not, however, used in the present design. The MC1545 video mixer combines the internally generated cloud level with either seascape/seamerge video for below clouds flight, or an internally generated sky level for above clouds flight. This mixer is controlled by the fog function signal. (See paragraph 3.4.3.1.) The adjustable gain amplifier varies the gain of the composite video signal as a function of ambient light, thereby matching the scene brightness of the target system governed by the light bank illumination. The background dusk condition is simulated by attenuation of the overall video signal. For night simulation, however, the seascape/seamerge or sky video is set to zero while the cloud shade is severely attenuated, providing a visible horizon. The composite video is buffered by a line driver before being output to the background projector.

3.4.3.1 Fog Function Generation. The desired relationship between video output, camera video seascape/seamerge), and cloud function is:

$$e_0 = Ge_1 + (1-G)\, e_2 \qquad (1)$$

where,

e_1 = Camera video

e_0 = Video output of SEG

e_2 = Cloud function

G = Gain function

G may be defined by:

$$G = e^{-K/X} \qquad (2)$$

where K establishes the scale factor, and

$$X = \frac{RVR}{R} = \frac{RVR}{H} = \cos \theta$$

In defining X,

RVR = Runway visibility range

H = Height above sealevel

R = Slant range

θ = Angle between local vertical and instantaneous line of sight

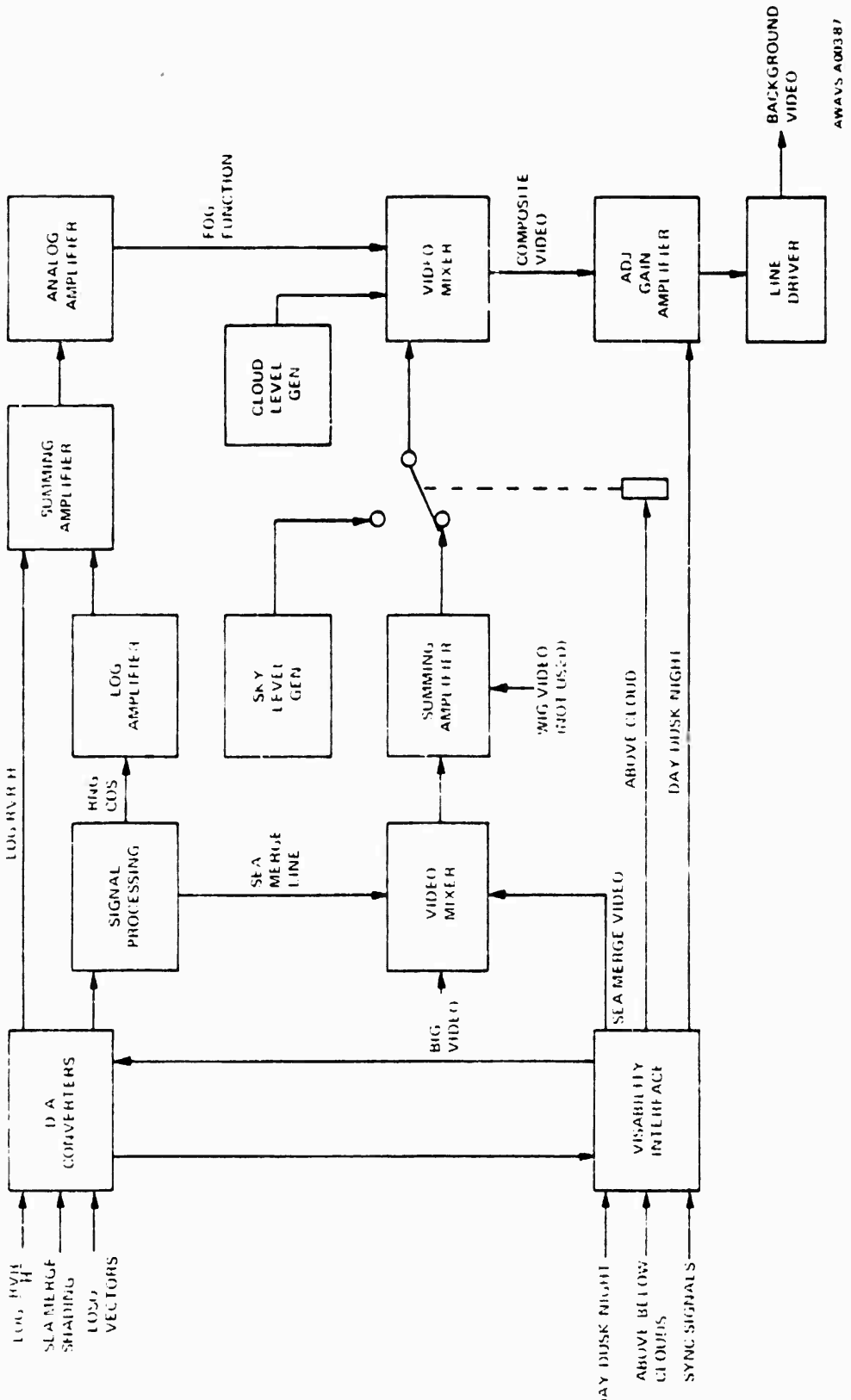

Figure 87. Background SEG, Block Diagram

Figure 88 shows the transfer function of the MC1545 video mixer. Over the range of G from -70 dB to 0 dB,

$$V_c = 0.2 \log G + 0.7 \quad (3)$$

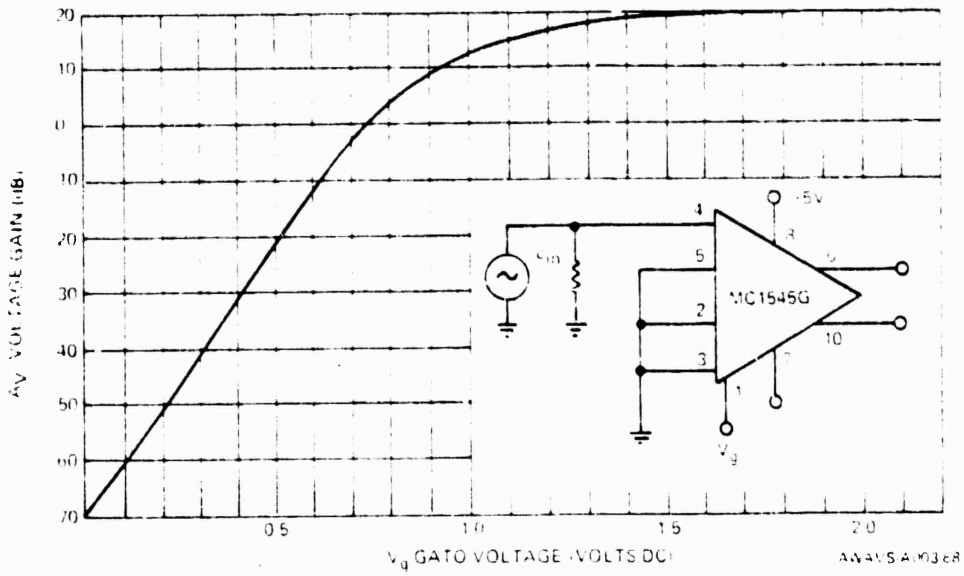

Figure 88. MC1545 Mixer, Transfer Function

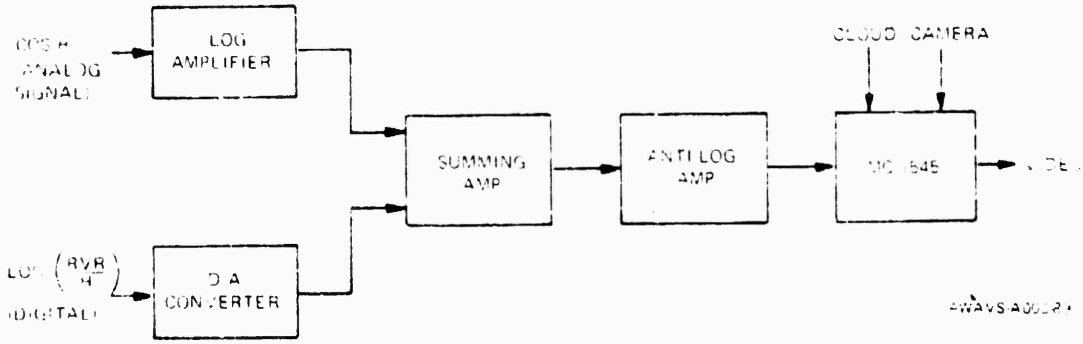

Figure 89. Fog Function Generation, Simplified Block Diagram

The desired system is represented as

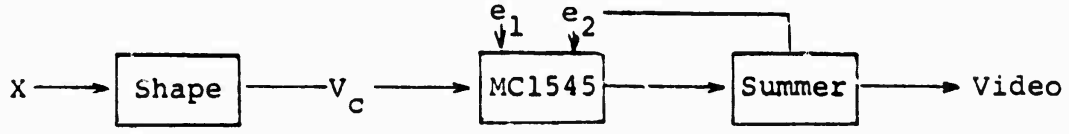

with a desired gain of $G = e^{-K/X}$ for the MC1545 mixer.

Substituting equation (2) into equation (3), we have

$$V_c = 0.2 \log (e^{-K/X}) + 0.7$$

$$= \frac{(0.2)K}{X} \log e + 0.7$$

$$= \frac{0.869K}{X} + 0.7 \qquad (4)$$

Equation (4) gives the desired shaping function. (See Figure 89 (1))
Equation (1) may be rewritten

$$e_0 = G(e_1 - e_2) + e_2 \qquad (5)$$

Since the MC1545 has a differential input, it can be used for the calculation of $e_1 - e_2$, giving

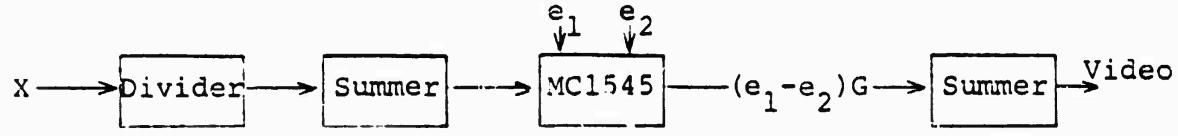

Thus, a circuit can be built which provides the exact function, and is both easily adjustable and mathematically predictable.

Figure 89 is a simplified presentation of the fog function portion of the overall SEG block diagram. It shows the actual implementation of the foregoing equations using the following relationship of H/RVR cos ϑ to drive the MC1545.

$$\frac{H}{RVR \cos \vartheta} = \text{antilog} \left(-\ln \frac{(\cos \vartheta)\ RVR}{H}\right)$$

$$= \text{antilog} \left(\ln \frac{H}{RVR \cos \vartheta}\right)$$

3.4.3.2 Visibility Interface and Controls. The visibility interface block of the background SEG block diagram (Figure 87) contains the switching and level potentiometers for manual override of visibility effects normally controlled by the computer. It also processes and distributes to other blocks the sync signals, consisting of horizontal drive and composite video blanking, from the master timing generator. The day/dusk/night and above/below clouds signals are discretes originating at the EOS and delivered via the linkage. The remaining input signals are received in digital form by the D/A converters, and converted to analog before transmission to the visibility interface circuits.

Maintenance controls on the background SEG are illustrated in Figure 90. Overall control is governed by the MASTER switch which selects between normal program control in the CMPTR position, manual control of individual functions from the SEG in the MAINT position, and OFF. In the OFF position, seascape video is passed through the SEG unaltered. Each of the remaining controls has a CMPTR position, which selects normal program control for that particular function when the MASTER switch is set at MAINT. The A/B CLOUD control is a selector switch providing a simulated static ABOVE or BELOW clouds scene as alternates to computer controlled video. Similarly, the time of day selector provides DAY, DUSK, or NIGHT ambient lighting as alternates, to the condition selected at the EOS. The other four controls are each comprised of CMPTR/MAINT toggle switch, and a rotary control (switch or potentiometer) which is switched into the circuit when the toggle switch is in MAINT. The PITCH & ROLL rotary switch selects one of four static aircraft rolls. The ALTITUDE rotary switch selects one of four fixed aircraft altitudes. At the maximum altitude, the seascape film plate image is totally replaced by seamerge shading. The manual controls for SEAMERGE SHADING and RVR/H are potentiometers which provide a dc level variable from MINimum to MAXimum effect for each function.

3.4.4 BIG/WIG Maintenance Panel. This maintenance panel provides a capability for manual override of programmed events for both the BIG and BIG electronics cabinets. (The BIG cabinet contains the seascape generator, while the BIG electronics cabinet houses the DARC, SEG, monitoring equipment and ancillary electronics.) The panel also includes video switching for the waveform and TV monitoring and provides for the eventual inclusion of maintenance functions for a synthetic wake image generator (WIG) cabinet. The BIG/WIG maintenance panel is illustrated in Figure 91. Maintenance controls are grouped into three functions: video switching, sweep selection, and power sequencing. The first two are grouped under the overall placarded designation of TEST.

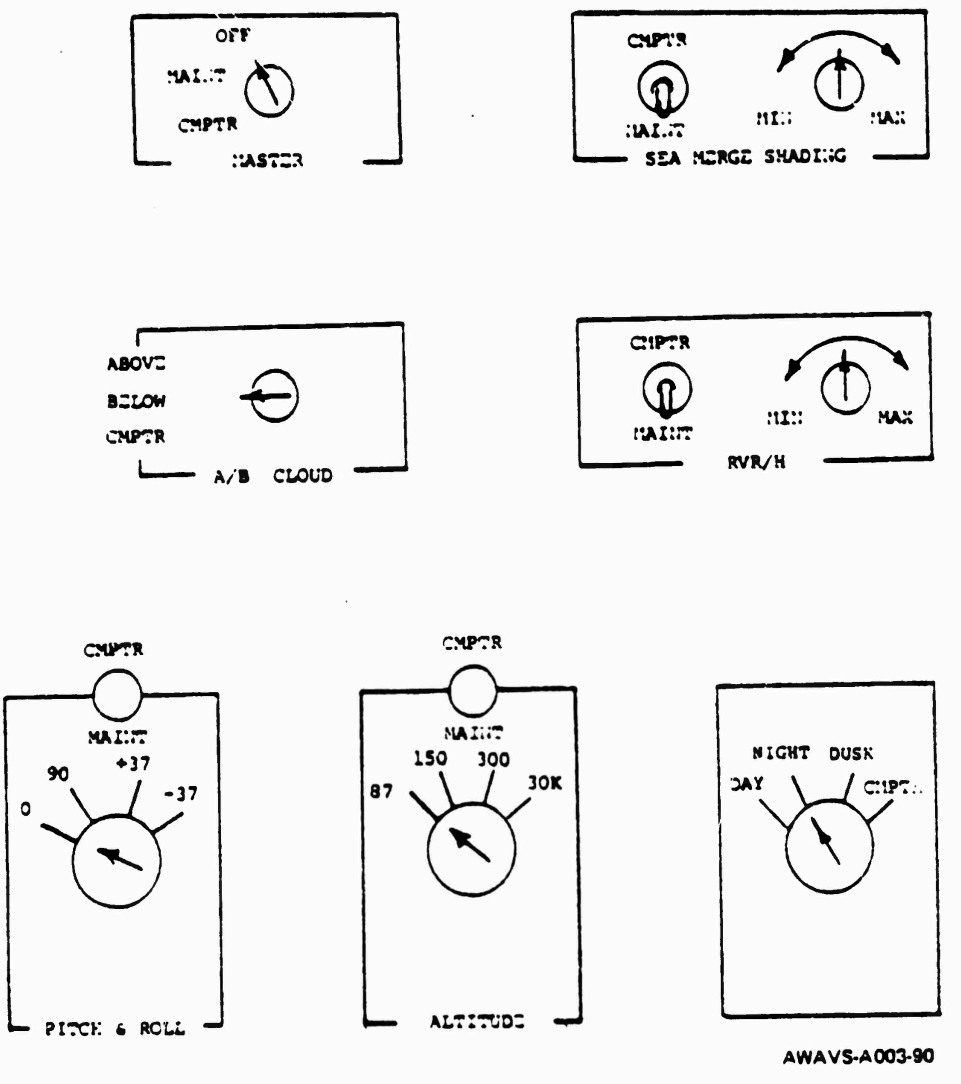

Figure 90. BIG Special Effects Generator, Maintenance Controls

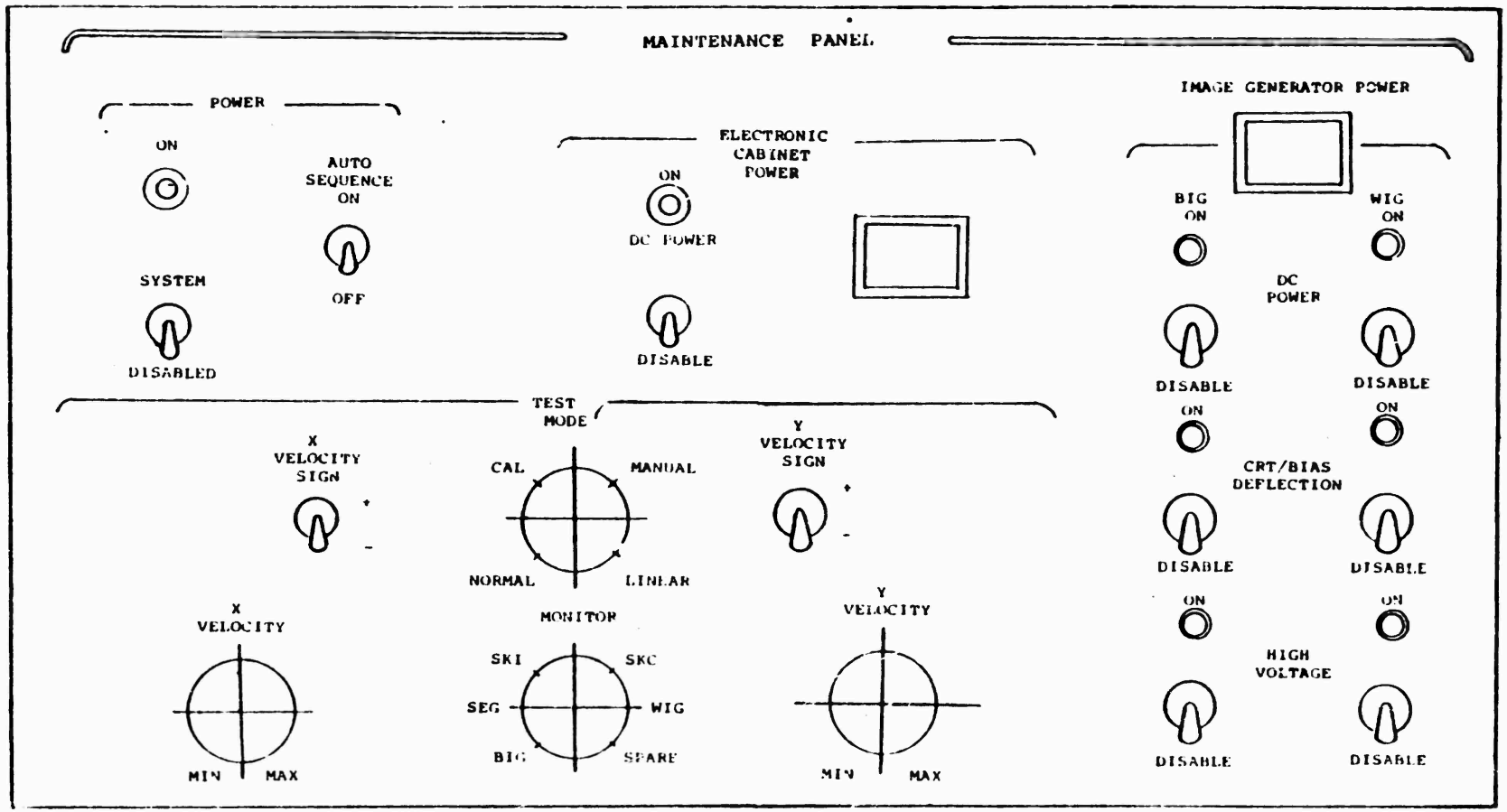

Figure 91. BIG/WIG Maintenance Panel

The TV MONITOR switch is a six-position rotary switch that directs video from several sources to the waveform and TV monitors. In the BIG position, seascape film plate video only is selected. In the SEG position, the composite video output of the background special effects generator is selected. This consists of either seascape/seamerge, horizon, and cloud level with fog on haze; or sky, horizon, and cloud level. The SKI position (scene keyed insetting) selects the input signal to the background projector (actually sampled at the output of the target insertion electronics). This is the composite background scene with the "hole" blanked for target insertion. The SKC position selects the scene keying camera image, which is essentially the target outline defining the "hole." The last two video signals are fully described in the target insetting system discussion (paragraph 3.6). The SPARE and WIG positions are not used.

The sweep selection group is comprised of five controls which govern the X- and Y-velocity outputs of the DARC. The MODE switch selects one of four sweeps affecting the raster pattern (mapping) of the projected image. The NORMAL position is for full computerized operation. The CAL position is for projection of a seascape image as viewed from a fixed aircraft position, and is used for system calibration. In the LINEAR position, a linear sweep (typical of normal CRT television) is generated by the DARC for set-up purposes. The MANUAL position allows maintenance personnel to "fly" the aircraft at a constant altitude, using the four X- and Y-velocity controls on the maintenance panel. The SIGN toggle switches select the polarity of the X- and Y-velocity commands (sweeps) in MANUAL mode, while the two potentiometers control the respective signal magnitudes.

Two alternate action pushbutton switches control interruption of ac power for maintenance purposes. The ELECTRONIC CABINET POWER MAINT SWITCH controls the BIG electronics cabinet power input and the IMAGE GENERATOR POWER MAIN switch controls the BIG cabinet power. The latter is designed for concurrent control of WIG cabinet power, if added in future design. The switches light red to indicate maintenance in progress or green to indicate normal operation. When activated, the MAINT switch causes its respective circuit breaker in the VTFS power distribution cabinet to open. The circuit breaker can then not be reset until the MAINT switch is deactivated.

The remaining toggle switches control the sequential application or removal of dc power by the BIG power controllers. The AUTO SEQUENCE toggle switch is a 3-position momentary contact/center off device that initiates the BIG startup sequence when depressed towards ON and the shutdown sequence when depressed toward OFF. Individual DISABLED toggle switches inhibit indicated application of dc power. When one group of voltages is disabled, all subsequent action ceases. Indicator lights for each group light to indicate that the respective step of the startup sequence has been completed, or extinguish to indicate that the shutdown step has been initiated. The SYSTEM DISABLED toggle switch is actually the power on-off switch for the BIG electronics cabinet. When the switch is on the upper position, the POWER/ON indicator will light only if +28V dc and 110V ac inputs to the BIG electronics cabinet are available. The lit indicator designates that the AUTO SEQUENCE switch may be operated to energize or deenergize the BIG circuitry.

3.5 Background Projection System

The background projection system is comprised of the scene keying electronics (SKE), the background projection equipment, and the scene keying camera (SKC) subsystem. The system is essentially a closed loop which has the dual function of projecting the BIG image and blanking out a hole in the background scene for projection of the target image. In describing the target insetting philosophy, the roles of the target projector and display screen therefore also warrant consideration. The projection equipment (described later) consists of the light valve projector with its related interface and control circuitry, and Singer modified optics. The basic projector with its remote control unit is identical to the target projector described in paragraph 3.3.1.

Figure 92 illustrates in block diagram form the components used to implement the projected scene keying technique. The background projector displays a blue-green seascaped sky and clouds on the screen. The target projector displays a gray aircraft carrier on the screen. The SKC looks at the identical area of the screen as the background projector. However, because the background projector contains a red-stop optical filter and the SKC contains a red-pass optical filter, only the target image can be seen by the SKC. The SKE processes the SKC video and blanks the background image where the target image appears. Blanking assures the background image does not appear superimposed over the target image. This superimposition would create an effect of sea waves on the deck of the carrier.

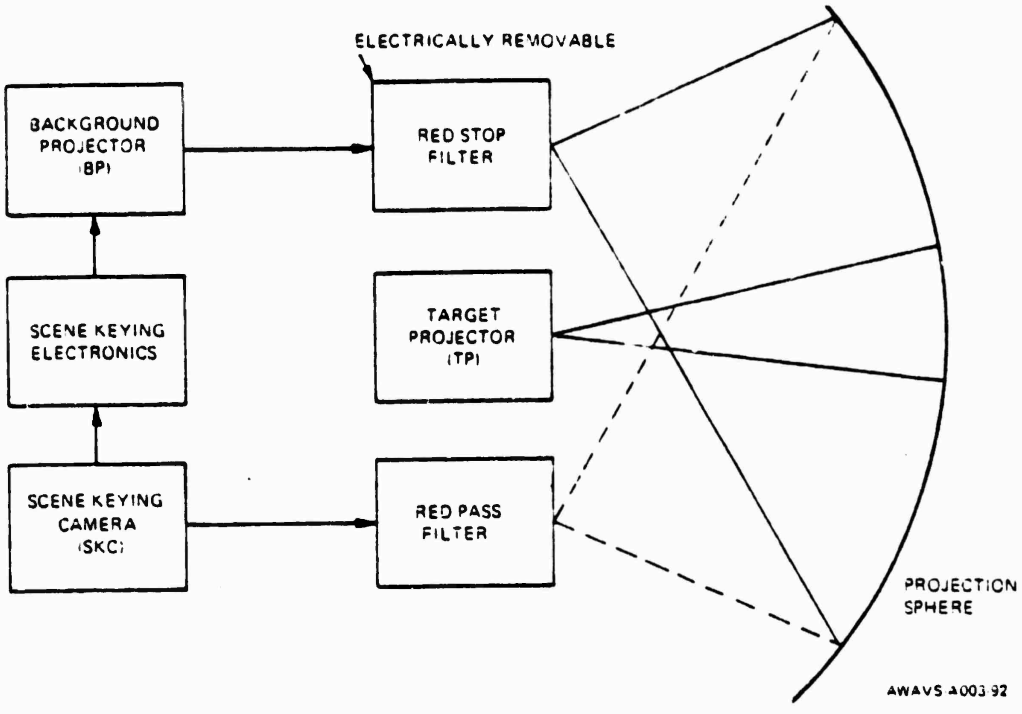

Figure 92. Projected Scene Keying Technique, Block Diagram

The camera has a conjugate raster to the background projector. Each point which is scanned in the projector is projected to the screen by a lens. The light reflects from the screen to the key camera. The lens on this camera is identical to the lens on the background projector so that with a small alignment of the camera raster, the point which is projected is simultaneously scanned by the camera. To synchronize the camera and projector rasters, a raster calibration is performed whenever the visual system is turned on. The red-stop filter used to spectrally code the background is automatically removed from the optical path when the raster calibration mode is entered.

The discussion which follows is subdivided into principles of operation, an analysis of the design requirements, and hardware block diagrams with descriptive accompanying discussions. The analysis is centered around detection of the projected target by the scene keying camera under varying conditions.

3.5.1 Projected Scene Keying Principles. The following paragraphs describe the operational modes and related scene keying functions of the projected scene keying technique. These are presented first in order to develop an understanding of the analysis which follows later.

3.5.1.1 Raster Calibration Mode. Tracking of SKC and background projector scan lines is achieved by software modification of scene keying DARC coefficients. These coefficient changes result in changes in SKC raster shape to achieve scan line tracking. The software receives information about SKC raster shape, by placing a pattern on the projector and measuring where it appears on the SKC. The white diamond shown in detail A of Figure 93 appears on the display sphere from the background projector. The SKC with the same field of view, has a video output representation of the SKC raster calibration pattern on the display sphere. The SKC video output can be processed to make positional measurements in the background projector field of view.

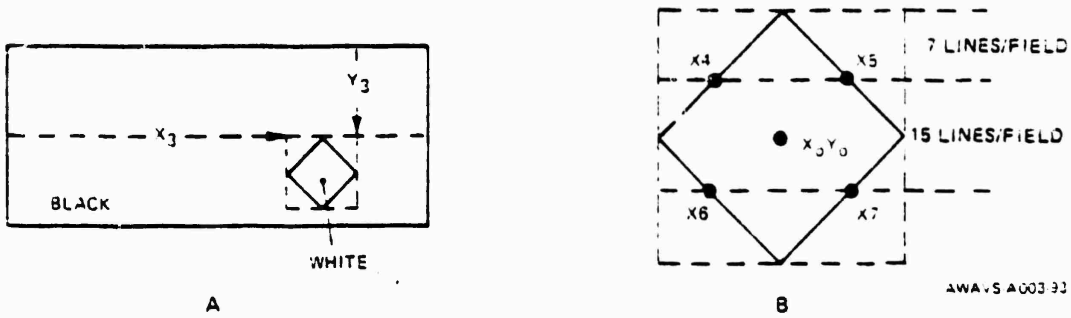

Figure 93. Raster Calibration Pattern

Communications between the software and the hardware is done by an "X-Y" coordinate system. The X coordinate is 1452 elements for all line rates. The Y coordinate is the scene line number in one field. The Y coordinate varies with line rate. The scene of the X coordinate is 1 to 1452 increasing from left to right. The Y coordinate is the number of active lines per field (243 for 525 line rate, 383 for 825 line rate, and 475 for 1025 line rate) increasing from top to bottom.

The hardware positions the raster calibration pattern in the odd field of the background projector as specified by X3, Y3. The video output of the SKC is detected in the odd field raster as follows. The starting point (X_3, Y_3) for the raster calibration pattern is contained in the linkage analog outputs JVCORX and JVCORY respectively. In order for the SKC to see the background projector raster, the red-stop filter (Figure 92) must be removed. The linkage lamp driver output LVBIPFIN removes the filter and places the raster calibration pattern on the background projector. The target projector must be off to avoid the SKE detecting target video during raster calibration. The SKE counts seven lines in one field from (X_3, Y_3), and sends the points X_4 and X_5 to the linkage. An additional 15 lines are counted, and X_6 and X_7 are sent to the linkage. X_4, X_5, X_6 and X_7 are the linkage inputs called JVSKLCX4, 5, 6 and 7.

Since the background projector and SKC rasters are not necessarily coincident yet, the diamond defined by X_4, X_5, X_6 and X_7 may represent a diamond at an arbitrary angle. However, the points can be used to define X_0, Y_0, the center of the diamond (B, Figure 3) with redundancy. The redundancy can be used by the software to assure that the information received is correct. If it is not correct, the software can have the raster calibration pattern repositioned in the same place again. Knowing X_0, Y_0 at a sufficient number of points on the SKC raster, the software can establist a correspondence between each X_0, Y_0 on the SKC and background projector.

3.5.1.2 Normal Insetting Operations. Normal insetting operation is provide by enabling the linkage discrete output called LVSKCOFF. In this mode, the background projector is blanked where the target image is found. In response to either the LVLBDAY or LVLBDUSK signal, the threshold for blanking is set at the 8th shade of gray for day conditions and the 5th shade of gray for dusk conditions. For night conditions insetting is disabled. In order to avoid blanking the background image in response to noise where there is no target image, the blanking is enabled only around the carrier, in response to the linkage digital called JVCARRX1, X2, Y1, and Y2. These signals designate the corners of a rectangle which is parallel to the scan lines and circumscribes the carrier. The rectangle is illustrated in Figure 94.

The shade of gray to which the background video is blanked is a function of the desired RVR, and forms one component of the target visability technique. It is defined by AVBNKLVL, a linkage analog output called "SKC BLANKING LEVEL". Blanking to a black level is done for greatest visability, while a white level is used for zero visability. Computer controlled blanking levels are used for restricted visability between zero and eleven. The blanking of the background image is not a sharp transition, but rather a fade function. The fade will make the background to target image transition appear smooth.

In the raster calibration mode only black and white detection is required; therefore, the threshold for detection can be set midway between black and white. In the normal operating mode, the 8th gray shade must be detected during day conditions. During night conditions scene keying is disabled.

Under normal operating levels, due to system noise and low signal levels, detection becomes difficult. For a uniform brightness target image, the video output of the SKC will be a nonuniform height. The nonuniformity varies as the target projector is moved in the background field of view due to SKC tube and lens shading, and the fact that the brightness to the observer is constant, but to the SKC varies due to its different location. The target projector itself has light falloff across its own field of view, which gives nonuniform video level for an intended flat field.

The detection reference level is adjusted to compensate for the foregoing shading effects in order to blank the BP at the desired shade of gray.

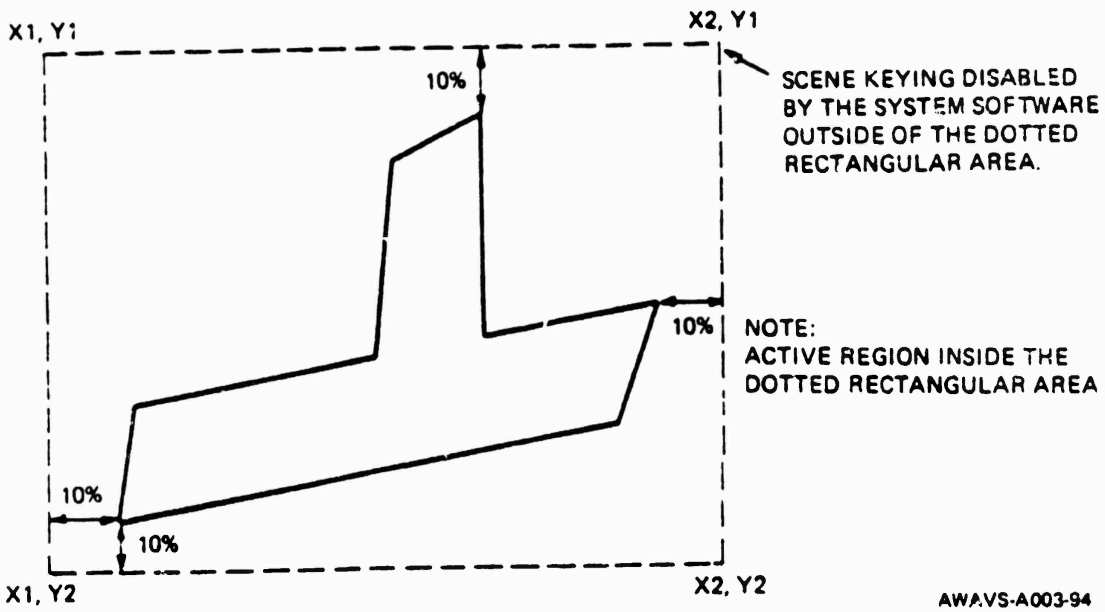

Figure 94. Scene Keying Active Region

3.5.1.3 Miscellaneous Functions. The BP and TP LINE RATE digital inputs to linkage (LVTIPLR1, LVTIPLR2, LVBIPLR1, and LVBIPLR2) from the SKE provide target and background projector line rate information to the software. Line rate information is used to decode position on the screen. The linkage discrete inputs called LVNORMBV and LVNORMTV provide information to the software when target and background projectors are in a test mode. The software uses this information to turn on the SERVO IN MAINT light on the EOS.

The linkage discrete output called LVSTROBS is used to phase lock the visual system to the computer iteration rate. The visual system updates information once per frame during vertical blanking. Phase locking assures that the linkage is not updating information while the visual system is updating registers.

Test patterns for the background and target projectors are provided to set up and test operation of the system. The patterns provided are crosshatch, burst, gray shade, and flat field. Cross hatch is used for system timing adjustments and linearity measurements. Burst patterns are used for resolution capability checks. Gray shade patterns check contrast ratios of projectors. Flat field patterns are used for calibration of shading compensation and observing system shading effects.

3.5.2 Scene Keying Image Detection Analysis. The precision with which the projected scene keying technique is implemented is dependent upon the capability of the system to accurately detect the projected target image. Scene keying detection must occur in the raster calibration mode and for day and dusk conditions in the normal mode. Detection is done by an analog comparator which operates on a variable reference level supplied by the shading compensation generator.

In establishing the comparator levels, the following factors must be considered.

a. Mode - Day, dusk or raster calibration.

b. Isocon noise.

c. Bleedthrough from the background projector to the scene keying camera.

d. System shading effects.

Before analyzing these requirements, however, it is first necessary to establish the signal level at the video output of the scene keying camera. SKC video levels are discussed in paragraph 3.5.2.1.

3.5.2.1 SKC Video Output Signal Level. The following equations were used to determine the highlight values of foot-lamberts and isocon anode current of the keying camera. Since the gamma of the isocon tube is not unity for all incident light levels, the tube characteristic curves must be used to determine the true anode current for levels above the knee (4 μa).

$$\sum_{n=1}^{n=31} \frac{L_{(n)} * T_{(n)} * V_{(n)} * 680 * G * S1}{A1 * 10^6}$$

= Foot-lamberts from target projector on screen = 6

$$\sum_{n=1}^{n=31} \frac{L_{(n)} * T_{(n)} * B_{(n)} * I_{(n)} * Fl_{(n)} * S1}{A1 * 4 * M^2 * 1000}$$

= Total anode current in a out of keying camera

$$\sum_{n=1}^{n=31} \frac{L_{(n)} * C_{(n)} * V_{(n)} * F2_{(n)} * 680 * G * S2}{A2 * 10^6}$$

= Foot-lamberts from background projector on screen = 6

$$\sum_{n=1}^{n=31} \frac{L_{(n)} * C_{(n)} * Fl_{(n)} * F2_{(n)} * B_{(n)} * S2 * I_{(n)}}{A2 * 4 * M^2 * 1000}$$

= Total bleed through anode current of the keying camera in μa from background image

Gains were adjusted on the target and background brightness such that 6 foot-lamberts brightness levels were obtained.

where:

$L_{(n)}$	=	Lamp spectral characteristics in μwatts/10nm/ lumen in the nth wavelength interval
$T_{(n)}$	=	Transmission of the target projection system in the nth wavelength interval
A1	=	Area of projected scene by target projector in ft^2 = 73
$B_{(n)}$	=	Transmission of the keying camera lens in the nth wavelength interval
$I_{(n)}$	=	Isocon response in na/μw/ft^2 in the nth wavelength interval
$J_{(n)}$	=	Signal current with no filter in na/10nm per input lumen in the nth wavelength interval
G	=	Gain of screen
S1	=	Total lumens entering target projection optics = 1000
M	=	f/# of keying camera lens = 3
$F1_{(n)}$	=	Keying camera blocking filter transmission in the nth wavelength interval
$C_{(n)}$	=	Background projection lens transmission in the nth wavelength interval
A_2	=	Background scene area in ft^2 = 345
$F2_{(n)}$	=	Background projector blocking filter transmission in the nth wavelength interval
S2	=	Total lumens entering background projection optics = 1000
n	=	nth 10nm wavelength interval starting with n = 1 at 400nm and ending with n = 31 at 700nm (i.e., n = 1 corresponds to the interval 395nm to 405nm)
680	=	Conversion constant from watts to lumens at a wavelength of 550nm only
$V_{(n)}$	=	Relative visibility of light to the human eye in nth wavelength interval

With the key camera filters, the signal current for the carrier highlight is 7 μa, considering all losses. The corresponding bleedthrough current is 0.59 μa.

3.5.2.2 Mode. In the raster calibration mode, black and white video levels are encountered with no intermediate levels. Under day conditions, peak brightness of the detected image occurs and the eighth shade of gray can be detected. In dusk conditions, half the brightness levels of day conditions allow detection of the fifth shade of gray.

3.5.2.3 Isocon Noise. If the detection level is not chosen properly, detection may happen on noise instead of the eighth gray shade. This false detection may occur due to noise causing the video level to reach the detection level.

The noise level $N_{(s)}$ can be determined from the equation

$$N_{(s)} = \frac{S}{(S/N)\ peak}$$

where the S/N is the signal to noise ratio. This ratio is found from charts supplied by RCA which are shown in Figures 95 and 96. Figure 96 shows typical S/N as a function of faceplate illuminance from flux levels within a given scene.

The carrie will have a 13.75:1 contrast ratio. Therefore, the smallest ignal is $(\frac{1}{13.75}) \times (8.94 \times 10^{-3}$ ft-candles) or 1.29 μa. The 7 μa is the maximum current previously calculated. The eighth gray shade corresponds on Figure 96 to a faceplate illumination of 6.5×10^{-4} lumens/ft . Then by using Figure 96 where one finds the S/N_0 can be transformed to the 16-MHz bandwidth by the equation below:

$$(S/N)_{dB} = (S/N_0)_{dB} + 20 \log \left(\frac{BW_0}{BW}\right)^{\frac{1}{2}}$$

$$(S/N)_{dB} = 25 + 20 \log \frac{(4.2)^{\frac{1}{2}}}{16}$$

$$= 23 - 5.8$$

$$= 19.2$$

the value for the peak signal to peak noise can be found from the equation:

$$(S/N)_{peak} = 1/6 \text{ antilog } (S/N)_{dB}/20$$

$$= 1/6 \text{ antilog } (19.2/20$$

$$= 1.52$$

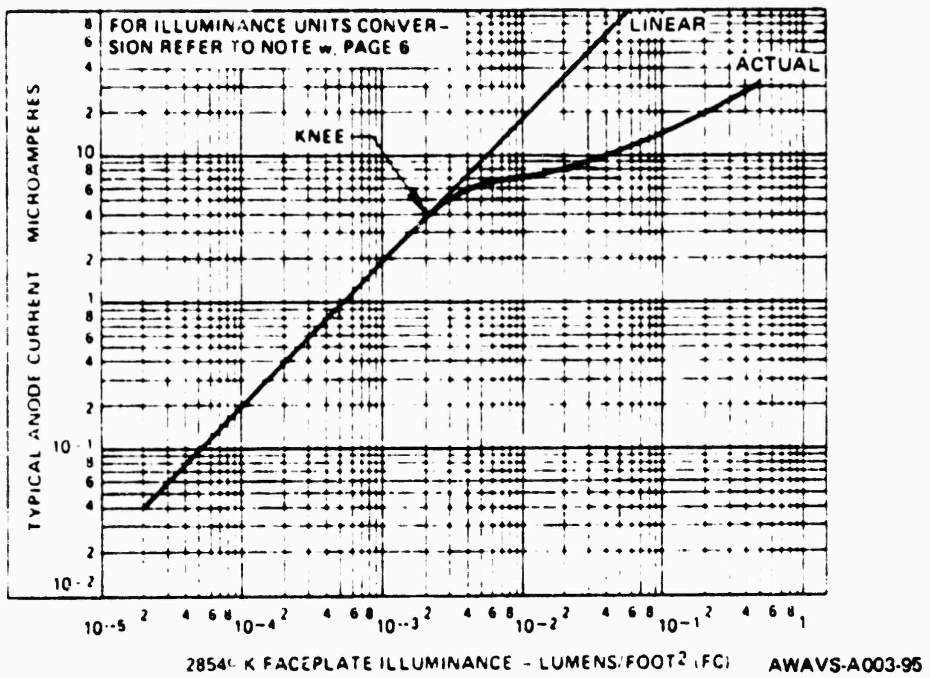

Figure 95. Typical Isocon Transfer Characteristic

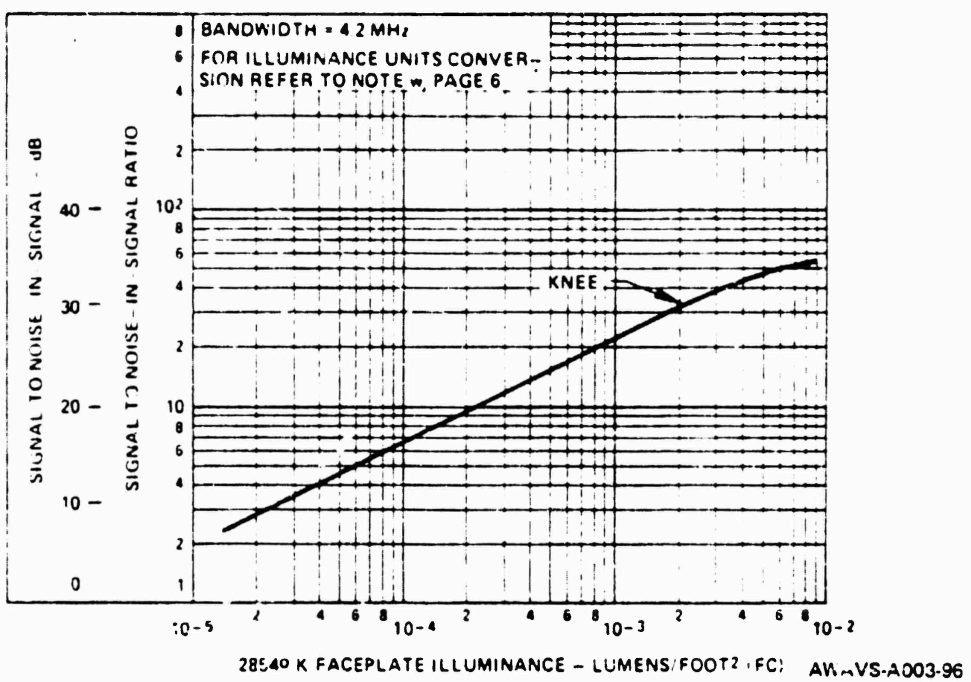

Figure 96. Typical Isocon Signal-to-Noise Ratio

3.5.2.4 Bleedthrough. The S/N for the bleedthrough is similarly determined, for a 6 foot-lambert background brightness. For it, the equivalent faceplate illumination is 3.1×10^{-4}. This produces a value of 23 for S/N with a bandwidth of 4.2 MHz. The (S/N_0) is factored to a 16-MHZ bandwidth as before.

$$(S/N)_{db} = 21 + 20 \log \left(\frac{4.2}{16}\right)^{\frac{1}{2}}$$

The value of the peak signal to peak noise is found to be:

$$(S/N)_{peak} = 1/6 \text{ (antilog } 15.2/20)$$

$$= 0.96$$

For the carrier signal, the noise is:

$$N(S_C) = \frac{1.29}{1.52} = 0.85$$

For the bleedthrough signal, the noise is:

$$N(S_B) = \frac{0.59}{0.96(2)} = 0.307$$

For dusk conditions the minimum carrier signal is at the 5th grey shade. Therefore, the carrier signal is

$$(8.94 \times 10^{-3})/4.5\ (0.5) = 9.9 \times 10^{-4} \text{ ft/cdls}$$

$$= >1.97 \text{ µa}$$

At 16 MH 27 - 5.8 = 21.2

$$(S/N)_{peak} = 1/6 \text{ antilog } \left(\frac{21.2}{20}\right)$$

$$= 1.91$$

Now $N(SC) = \frac{1.95}{1.91} = 1.02$

The bleedthrough signal is 0.295 µa. The signal-to-noise is 18dB.

Converted to 16-MH it is 18 = 5.8 = 12.2

The peak signal to peak noise is:

$$(S/N)_{peak} = 1/6 \text{ antilog } \left(\frac{17.2}{20}\right) = 0.679$$

Since both this and the background will be used as the noise level, then

$$\text{Dusk } N(S_C) = 1.02$$

$$\text{Dusk } N(S_B) = \frac{0.295}{2(0.679)} = 0.217$$

3.5.2.5 System Shading Effects. Table 49 is a collection of shading data taken from either a specification of the component or a vendor's best approximation at this point. Shading means % functional transmission decrease around the edge of the raster plane compared to the center of the raster. Therefore, the detection level must change as a function of position in the FOV. The screen components have negligible shading because the SKC and background projector are both located near screen center.

TABLE 50. SHADING DATA ASSOCIATED WITH SCENE KEYING

Component	Shading (%)	Approx.Shading Function
Light Valve and Lens	50%	$f_1 = ax^2 + b$
SKC Lens	50%	$f_2 = cx^2 + d$
SKC	Negligible	
Display Screen	Negligible	(because both SKC and background projector are located near screen center)
x = position variable; a,b,c,d = constants.		

3.5.2.6 Detection Comparator Reference Levels. A summary of isocon noise, shading and projector bleedthrough is given in Table 60. All factors are in terms of isocon current. Figure 97 graphically defines the comparator input and reference signal levels and errors.

TABLE 51. SUMMARY OF COMPARATOR LEVELS

Parameter	Day	Dusk
Bleedthrough	0.59 μa	0.295 μa
Black Level Noise	0.307 μa	0.217 μa
Detection Gray Shade	1.29 μa	1.97 μa
Detection Gray Sgade Noise	0.85 μa	1.02 μa
Shading Max	75%	75%

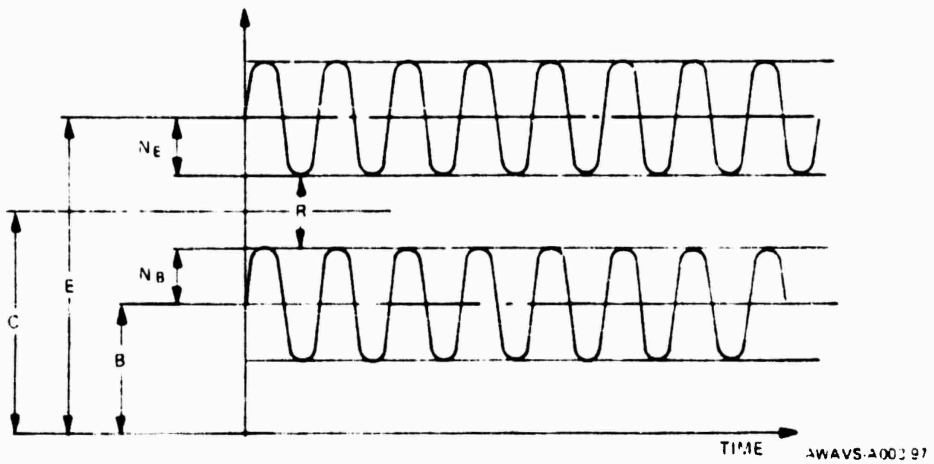

C = Comparator Setting
E = Eight gray shade average current
N_E = Noise associated with E (peak)
B^E = Average value of bleedthrough plus lag
N_E = Noise associated with B (peak)
R^E = Allowable error for shading compensation simulation

Figure 97. Comparator Reference Levels

The equation for the comparator setting shown in Figure 97 is:

$$C = \frac{(E - N_E) - (B + N_B)}{2} + (B + N_B)$$

$$= \frac{E - N_E + B + N_B}{2}$$

$$\text{DAY: } C = \frac{1.29 - \frac{0.85}{2} + 0.59 + \frac{0.307}{2}}{2} = 0.804\ \mu a$$

$$\text{DUSK: } C = \frac{1.97 - \frac{1.02}{2} + 0.295 + \frac{0.217}{2}}{2} = 0.932\ \mu a$$

Accuracy of shading compensation (% of full scale) is calculated as follows:

$$\frac{R}{2E} = \frac{-(B + N_B/2) + (E - N_E/2)}{2E}$$

$$\text{DAY:} \quad = \frac{1.29 - \frac{0.85}{2} - 0.59 - \frac{0.307}{2}}{2(1.29)} = 6.4\%$$

$$\text{DUSK:} \quad = \frac{1.97 - \frac{1.02}{2} - 0.295 - \frac{0.217}{2}}{2(1.97)} = 26.8\%$$

3.5.3 Target Insetting Error Analysis. The total insetting error is a function of the following factors:

a. System spread function - The gausian distribution of the camera beam causes the error in detecting to be a function of the brightness of the image detected. A brighter image will be detected sooner than a darker image.

b. System short term changes - these are changes which occur over the course of one mission (approximately fifteen minutes).

3.5.3.1 System Spread Function. An analysis of the scene keying camera indicates that the spread function is based on a limitation of television response to 1000 TV lines (per picture height); a lens response at the center of 24 line pairs/mm (ℓ_p/mm) vertically by 40 ℓ_p/mm horizontally; and a reduction off axis to 12 ℓ_p/mm vertically by 20 ℓ_p/mm horizontally. These specifications are based upon a 3 × 4 aspect ratio in a 25.4 × 19.1mm faceplate.

The spread function is found as follows: (Horizontal on axis)

$$\text{Camera Resolution (5\%) (Limiting)} = \frac{\frac{4}{3} \text{ 1000 lines}}{160 \times 60 \text{ min}} = 0.139 \frac{\text{line}}{\text{min}}$$

$$\text{Lens Resolution (5\%)} = \frac{80 \text{ lines}}{\text{mm}} \times \frac{25.4\text{mm}}{160 \times 60 \text{ min}} = 0.212 \frac{\text{line}}{\text{min}}$$

Assuming that both the camera and the lens have Guassian spread function (impulse response) of the following form the system limiting resolution can now be calculated.

$$G(x) = e^{-x^2/2\delta_2}$$

where

$$\delta = \frac{\uparrow}{2\sqrt{2}}$$

$\uparrow$ = the full width of the spread function at 63% of peak

The Fourier transform of the impulse response is the MTF or

$$G(w) = e^{-\frac{(\omega^2\delta^2)}{2}}$$

where

$\omega = 2\pi f$

f = cycles/length

For a combined system MTF of 5% (limiting resolution) the individual MTF's are multiplied together, or

$$e^{\frac{-\omega^2\delta_s^2}{2}} = e^{\frac{-\omega^2\delta_1^2}{2}} \quad e^{\frac{-\omega^2\delta_2^2}{2}} = 0.05$$

Taking the natural log of both sides,

$$\frac{\omega^2}{2}(\delta_1 + \delta_2^2) = 3$$

$$f_L^2 = \frac{6}{(2\pi)^2} \cdot \left(\frac{1}{\delta_1^2} + \frac{1}{\delta_2^2}\right) \quad 1$$

f_L = Limiting system frequency

Considering each component at 5% resolution,

$$0.05 = e^{\frac{-\omega_1^2\delta_1^2}{2}}$$

$$3 = \frac{\omega_1^2\ \delta_1^2}{2}$$

$$\delta_1^2 = \frac{6}{(2\pi f_1)^2}$$

Similarly, $\delta_2^2 = \frac{6}{(2\pi f_2)^2}$

Substituting $\delta_1 + \delta_2$ into 1,

$$f_L = \frac{1}{\frac{1}{f_1^2} + \frac{1}{f_2^2}} = \frac{(f_1 f_2)^2}{f_2^2 + f_1^2}$$

$$f_L = \frac{f_1 f_2}{\sqrt{f_1^2 + f_2^2}}$$

The camera and lens limiting resolution is

$$f_L = \frac{(0.139)(0.212)}{\sqrt{(0.139)^2 + (0.212)^2}} = 0.115 \ \frac{\text{lines}}{\widehat{\text{min}}}$$

To find the value of $\uparrow$ at the limiting resolution,

$$G(\omega) = e^{\frac{-\omega^2 \delta^2}{2}} \qquad \delta = \frac{\uparrow}{2\sqrt{2}}$$

or

$$\frac{-\uparrow^2 \omega^2}{16}$$

$$G(\omega) = e \qquad \text{at } G(\omega) = 0.05$$

$$0.05 = e^{\frac{-\uparrow^2 \omega^2}{16}}$$

$$3 = \frac{\tau^2 \omega^2}{16} \quad \frac{\tau^2 (2\pi)^2 f_L^2}{16}$$

$$f_L = \frac{48}{(2\pi)^2} \frac{L}{\pi^2}$$

$$f_L = \underline{1.103}$$

Now

$$\tau = \frac{1.103}{.116} = 9.5 \ \widehat{\text{min}}$$

The impulse response for the target image and system resolution is found similarly (on axis) for the GE projector.

$$\frac{4}{3}\,\frac{(900 \text{ lines})}{160 \times 60 \text{ min}} = 0.125 \frac{\text{lines}}{\text{min}}$$

The lens is the same for the cameras, or

$$0.212 \frac{\text{line}}{\text{min}}$$

$$f_L = \frac{(0.212)(0.125)}{\sqrt{(0.212)^2 + (0.125)^2}} = 0.108 \frac{\text{lines}}{\text{min}}$$

$$\tau = \frac{1.103}{.108} = 10.2 \text{ min}$$

Since the τ's of both the projection and camera systems are independent, the system τ can be RSS.

$$\tau = \sqrt{(10.2)^2 + (9.5)^2}$$

$$\tau = 13.9 \text{ min}$$

The horizontal corner resolution is

Camera: $$\frac{850 \text{ lines} \times \frac{4}{3}}{160 \times 60 \text{ min}} = 0.118 \frac{\text{lines}}{\text{min}}$$

Lens: $$\frac{40 \frac{\text{lines}}{\text{min}} \times 25.4 \text{ min}}{160 \times 60 \text{ min}} = 0.106 \frac{\text{lines}}{\text{min}}$$

$$f_L = 0.0788 \frac{\text{lines}}{\text{min}}$$

$$\tau = 14.0 \text{ min}$$

Projector: $$\frac{\frac{4}{3} \times 700 \text{ lines}}{160 \times 60 \text{ min}} = 0.0972 \frac{\text{lines}}{\text{min}}$$

Lens: $0.106 \frac{\text{lines}}{\text{min}}$

$f_{L_2} = 0.0716 \frac{\text{lines}}{\text{min}}$

$\tau = 15.4$ min

$\tau_L = 20.8$ min

3.5.3.1.1 Horizontal Detection Error. Parameters of allowable horizontal detection errors are as follows (See Figure 98):

For centers:

EIGHTH GRAY SCALE DETECTION (See Figure 98, detail A.)

Detection occurs at 0.8 / 1.29 = 0.62
or $x = 0.31\gamma = 0.31 / 2\sqrt{2} = 1.5 \overset{\frown}{\text{min}}$ (center)

WHITE LEVEL DETECTION (See Figure 98 detail B.)

Detection occurs at 0.8 / 7 = 0.114
or $1.21\gamma = 1.39\tau / 2\ 2 = 5.9 \overset{\frown}{\text{min}}$ (center)

TOTAL ERROR 5.9 + 1.5 = 7.4 $\overset{\frown}{\text{min}}$ (center)

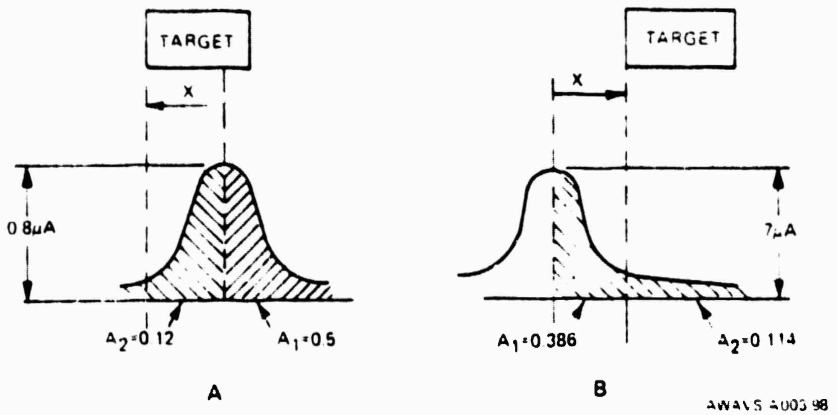

Figure 98. Horizontal Detection Error

For corners:

EIGHTH GRAY SCALE DETECTION

$x_{8th} = .31\gamma = 2.28 \overset{\frown}{min}$

WHITE LEVEL DETECTION

$x_{white} = 1.21\gamma = 8.89 \overset{\frown}{min}$

TOTAL ERROR : $2.28 + 8.89 = 11.17 \overset{\frown}{min}$

3.5.3.1.3 Error Summary for Spread Function.

Error	Center	Corners
Vertical	$+7, -0 \overset{\frown}{min}$	$\pm 7 \overset{\frown}{min}$
Horizontal	$+1.5, -5.9 \overset{\frown}{min}$	$\pm 2.3, -8.9$

3.5.3.1.2 Vertical Deflection Error. The vertical error differs from the horizontal in that the error is quantized because of the line spacing.

$$MTF_S(\omega) = MTF_1(\omega)\ MTF_L(\omega)$$

where

$$MTF_1(\omega) = e^{\frac{-\omega^2\delta_1^2}{2}}$$

$$MTF_1(\omega) = e^{\frac{-\omega^2\delta_L^2}{2}}$$

δ_1 is due to camera

δ_2 is due to lens

$$\text{Now } g(x) = e^{\frac{-x^2}{2(\delta^2 + \delta_2^2)}}$$

where

$x = Ky$

K is an integer 1,2,3,4.....

and y = line spacing $\widehat{min}$

The vertical line spacing in $\widehat{min}$ is

$$\frac{90 \times 60}{766}\ \widehat{min}\ \text{lines} = 7\ \widehat{min}$$

$$\delta_1^2 + \delta_2^2 = \frac{\tau_1^2}{8} + \frac{\tau_2^2}{8}$$

$$= \frac{1}{8} \left[\uparrow_1^2 + \uparrow_2^2 \right]$$

$$= \frac{1}{8} \left[(10.2)^2 + (9.5)^2 \right]$$

$$\delta_1^2 + \delta_2^2 = 24.28 \widehat{\text{min}}$$

Now, for centers:

$$x = K\ 7 \widehat{\text{min}}$$

normalized for tables

$$x = \frac{K\ 7 \widehat{\text{min}}}{\sqrt{\delta_1^2 + \delta_2^2}} = \frac{K\ 7 \widehat{\text{min}}}{\sqrt{24 \widehat{\text{min}}}} = \quad (1.43)$$

NOTE: Refer to paragraph 3.5.3.4 for an analysis of the following image detection process.

EIGHTH GRAY SCALE DETECTION: (See Figure 99, detail A.)

Detection at 0.623

Image detected at $1.43 = 7 \widehat{\text{min}}$

WHITE LEVEL DETECTION: (See Figure 99, detail B.)

Detection occurs at 0.8 / 7 = 0.114 (This occurs for x = 0.)

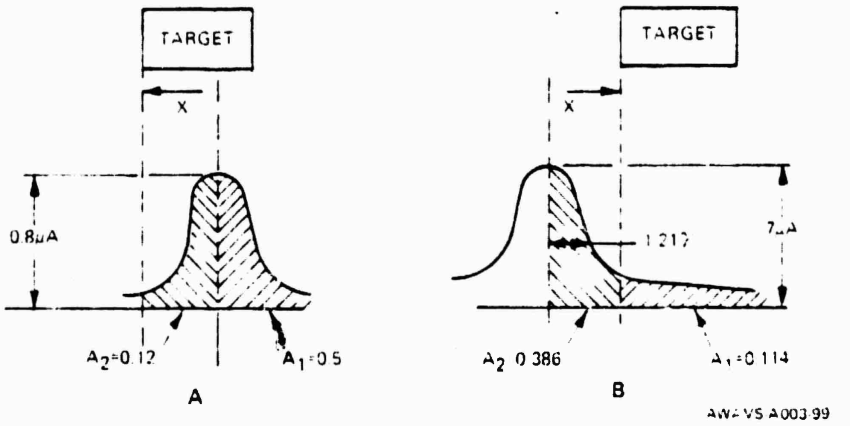

Figure 99. Vertical Detection Error

TOTAL VERTICAL ERROR: $= 7 \widehat{\text{min}}$ (centers)

For corners: $\gamma_1^2 + \gamma_2^2 = \frac{1}{8} \ 20.8^2 = 54.08$

$$x = K \frac{7}{\sqrt{54.08}} = \frac{7}{7.35} K = .952K$$

EIGHTH GRAY SHADE DETECTION

Image detected at $.952\gamma = 7 \widehat{\text{min}}$

WHITE LEVEL DETECTION

$-0.952\gamma = 7 \widehat{\text{min}}$

error $= 14 \widehat{\text{min}}$

3.5.3.2 System Short-Term Changes. Short-term changes occuring over the course of one simulated mission (approximately 15 minutes) are as follows:

a) Scene Keying Camera - Deflection stability 0.1% pict 0.1% pict height = 0.14% pict = ±13.5 min

b) Scene Keying Electronics - accuracy of detection is one element out of 1452 = ±6.6 min (horizontal). Vertical error does not exist.

c) Alignment errors - errors that are left after calibration is performed = ±6 min center; ±12 min corners.

3.5.3.3 Target Insetting Error Summary. A summary of all errors discussed in the foregoing paragraphs is given in Table 51.

TABLE 52. SCENE KEYING ERROR SUMMARY

Error	Center	Corners
Vertical Spread	+7, -0	±7
Horizontal Spread	+1.5, -5.9	+2.3, -8.9
SKC drift	±13.5	±13.5
SK Electronics	±6.6 horizontal only	±6.6 horiz
Alignment Errors	±6	±12
Worst-case error	Horiz + 27.6, -32	+34.4, -41
Worst-case error	Vert +26.5, -19.5	±39.1

3.5.3.4 Calculation Method for Error Due to Spread Function. The comparator detects the image when a certain fixed current is exceeded. The beam current, as seen by the comparator, is the area under the curve of the product of the beam current distribution times the target image (Figure 100 shaded area). The function to be integrated is: (all values are normalized).

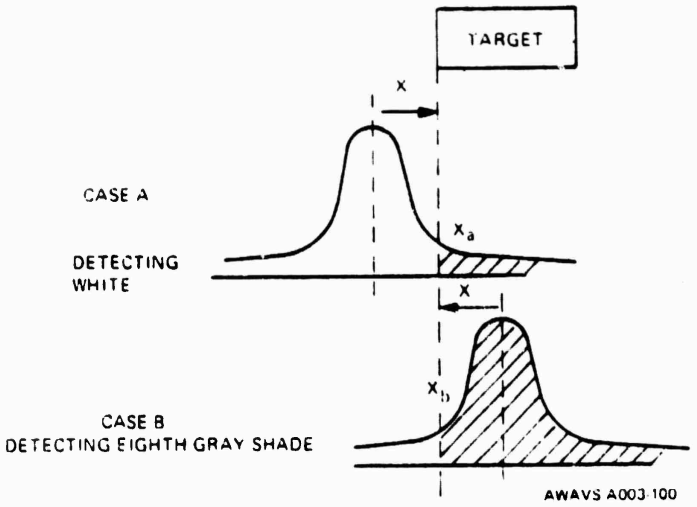

Figure 100. Spread Function Error Calculation

Case A

$$\int_{+Xa}^{\infty} e^{\frac{-X^2}{2\gamma 2}}\, dX = \int_{0}^{\infty} e^{\frac{-X^2}{2\gamma 2}}\, dX - \int_{0}^{Xa} e^{\frac{-X^2}{2\gamma 2}}\, dX$$

$$= \tfrac{1}{2}\int_{-\infty}^{\infty} e^{\frac{-X^2}{2\gamma 2}}\, dX - \tfrac{1}{2}\int_{-Xa}^{Xa} e^{\frac{-X^2}{2\gamma 2}}\, dX$$

$$= \tfrac{1}{2}\int_{\infty}^{\infty} e^{\frac{-t^2}{2}}\, dt - \tfrac{1}{2}\int_{\frac{-Xa}{\gamma}}^{\frac{Xa}{\gamma}} e^{\frac{-t^2}{2}}\, dt$$

$$t = \frac{X}{\gamma} \qquad y = \frac{Xa}{\gamma}$$

Case B

$$\int_{-X_b}^{\infty} e^{\frac{-X^2}{2\gamma^2}}\,dX = \tfrac{1}{2}\int_{-X_b}^{X_b} e^{\frac{-X^2}{2\gamma^2}}\,dX + \tfrac{1}{2}\int_{-\infty}^{\infty} e^{\frac{X^2}{2\gamma^2}}\,dX$$

$$= \tfrac{1}{2}\int_{\frac{-X_b}{\gamma}}^{\frac{X_b}{\gamma}} e^{\frac{-t^2}{2}}\,dt + \tfrac{1}{2}\int_{-\infty}^{\infty} e^{\frac{-t^2}{2}}\,dt$$

$$t = \frac{X}{\gamma} \qquad y = \frac{X_b}{\gamma}$$

Using the normal probability integral $\frac{1}{\sqrt{2\pi}}\int_{-a}^{+a} e^{-t^2/2}\,dt$ (*)

Case A

$$A = \tfrac{1}{2}\left[1 - \int_{\frac{-Xa}{\gamma}}^{\frac{Xa}{\gamma}} e^{\frac{-t^2}{2}}\,dt\right] \qquad (1)$$

Case B

$$A = \tfrac{1}{2}\left(\int_{\frac{-X_b}{\gamma}}^{\frac{X_b}{\gamma}} e^{\frac{-t^2}{2}}\,dt + 1\right) \qquad (2)$$

To find detection point I_C = comparator setting

I_E = Eighth gray shade current I_W = white current

Case B and A

$$\frac{I_C}{I_e} = A$$

look up A and find corresponding y

---

*"Introduction to Mathematical Statics"; HOEL, page 315

3.5.4 Scene Keying Electronics. Under normal operating conditions, the scene keying electronics accepts background video from the background image generator, blanks the hole for insertion of the target in response to SKC video, and redrives the video for transmission to the background projector. It also responds variations in target intensity due to screen position and time of day, and produces one component of the target visibility effect. In the raster calibration mode, the scene keying electronics generates the diamond pattern for projection by the background projector and measures where it appears when photographed by the SKC. Auxilliary functions include generation of test patterns for both the target and background projectors, and generation of test mode discretes.

Figure 101 is a block diagram of the scene keying electronics. All components are contained in the SKI electronics drawer assembly located in the BIG electronics cabinet. This drawer also contains a portion of the master timing generator discussed in paragraph 3.6. Operating controls for the scene keying electronics are located on the front panel of the drawer assembly. Timing for the SKI electronics eminates from the self-contained master clock which also supplies the sync generator.

3.5.4.1 SKI Blanking Generator. The blanking generator differentially receives background video which contains both the film plate imagery and the special effects video. A feather circuit switches between background video and the SKI blanking level under controlled switching from 50 to 150 nsec. The switching function is:

$$E_o = tB + (1-t)\ S$$

where

E_o = Output of feather circuit

t = Scaled time (switches from 0 to 1 in τ nsec)

B = Background video

S = SKI blanking level

τ = Control adjustable from 50-150 nsec

This function allows a controlled switch from the background video which gradually fades out to a predetermined blanking level which gradually fades in. The blanking level, which forms a component of the target visability effect, is black for unlimited visability gradually blending toward white for zero visibility.

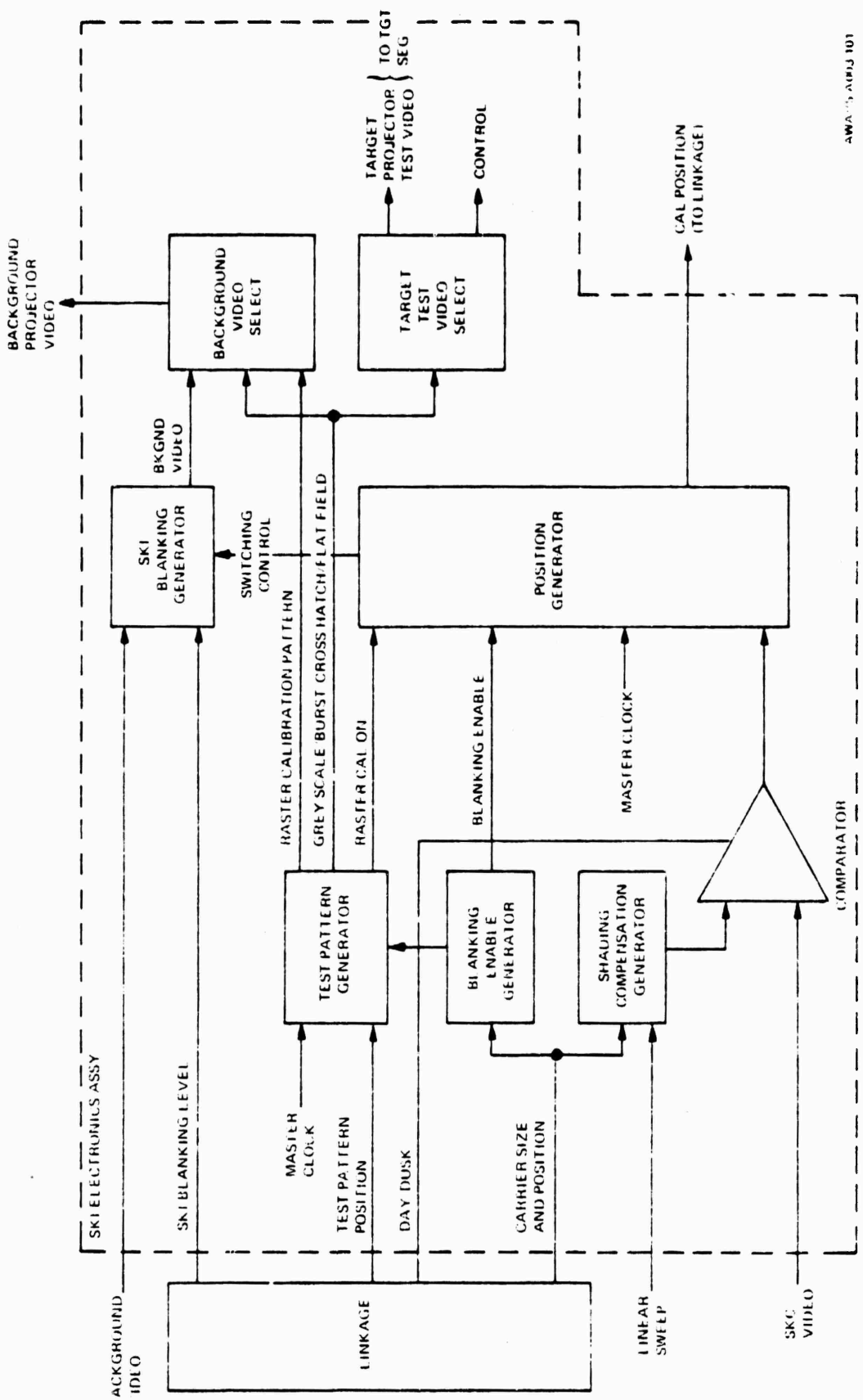

Figure 101. Scene Keying Electronics, Block Diagram

3.5.4.2 Signal Detection. Detection of the target carrier image is accomplished by the comparator, which differentially receives the keying camera video and determines whether or not it is greater than the reference. The DAY DUSK signal from the linkage sets the detection threshold at the appropriate shade of gray: 8th for day and 5th for dusk. (During simulated night operations, the blanking level input to the SKI blanking generator disables the blanking function.)

The shading compensation generator varies the reference level to compensate for errors produced by position of the carrier image on the display screen and falloff of signal intensity as sensed by the image isocon in the SKC. The target position error is caused by the fact that the target projector is not located at the optical center of the spherical screen. Thus, as the target is moved about the screen and the distance between the target projector lens pupil and the screen changes, so does the projected image intensity. The CARRIER SIZE AND POSITION signals from the linkage supply the shading compensation generator with necessary data to correct for this effect. Image intensity falloff at the SKC is a parabolic function of the LINEAR SWEEP. The input signal is provided directly from the function generator within the BIG DARC. (NOTE: Although LINEAR SWEEP should logically originate at the SKC DARC, the BIG DARC has been used as the source due to its physical presence in the same cabinet as the SKI electronics. This manipulation is feasible since the static signals from both DARC function generators are identical.) A proportional boost in the reference level is provided towards either extreme of the sweep.

3.5.4.3 Blanking Enable and Position Generators. During normal operation, the CARRIER SIZE AND POSITION signals from the linkage, buffered by the blanking enable generator, define the corners of the active rectangle pictured in Figure 94. Whenever the swept output from the comparator comes within the active rectangle, the switching control signal is provided by the position generator. This signal is the enable for the SKI blanking generator. The secondary output from the blanking enable generator is a safety signal which disables the raster calibration circuitry in the test pattern generator when the linkage is supplying carrier size and position data. In the raster calibration mode, the position generator stores the position of the detected points of the raster cal pattern senses by the SKC. The RASTER CAL ON signal informs the position generator of the current mode of operation.

3.5.4.4 Test Pattern Generator. The test pattern generator produces five patterns of test video. The raster calibration pattern is for projection by the background projector only during the raster calibration mode. A thorough discussion is given in paragraph 3.5.1.1. The pattern is illustrated in Figure 93. The four remaining test patterns are for use by either projection system. They are illustrated in Figure 102. A description of each follows:

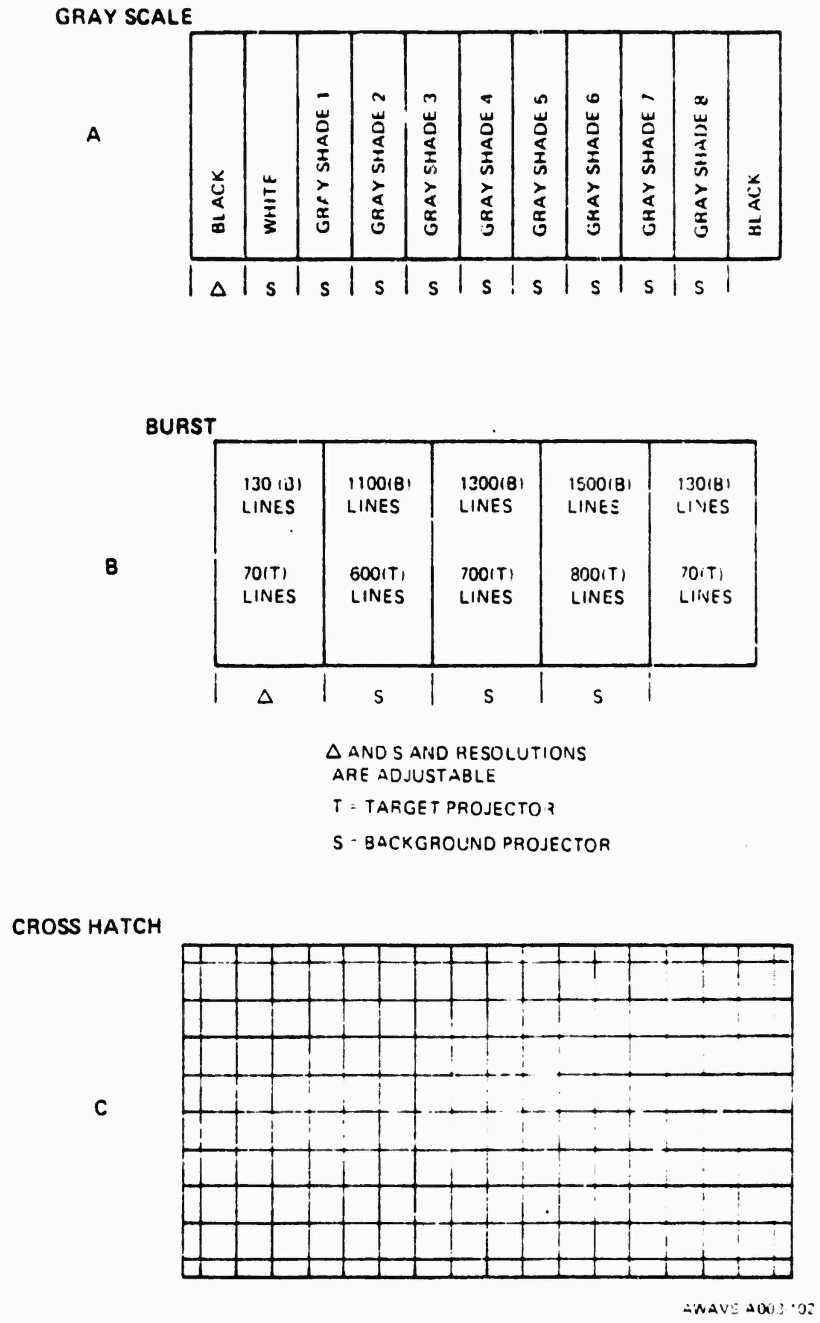

Figure 102. Video Test Patterns

a. Gray Scale (A, Figure 102). Gray scale is used to test the system contrast dynamic range. Black, white and 8 intermediate gray shades are provided. The width of the shades are adjustable as shown in the illustration.

b. Burst (B, Figure 102). The burst pattern is used to test system resolution. Resolutions of 130, 1100, 1300 and 1500 lines/picture width are provided for the background projection system (spec is 1300 lines). Resolutions of 70, 600, 700, 800 lines/picture width are provided for the target projection system (spec is 700 lines). The number of lines resolution and the widths of the resolution bands are adjustable.

c. Cross Hatch (C, Figure 102). The crosshatch pattern is used to adjust system delays, so that start of video corresponds to start of blanking, and for linearity measurements. Sixteen boxes by eight boxes are provided corresponding to ten degree increments.

d. Flat Field. The flat field pattern is used to check uniformity of brightness across the field of view. The flat field pattern actually appears as a conventional TV raster with a uniform shade of gray. Therefore, no illustration is provided. The shade of gray is programmable, but the 8th shade is normally used.

3.5.4.5 Video Switching. Switching of normal video, calibration pattern, or test patterns is accomplished by two rotary switches on the SKI electronics drawer front panel (See Figure 103). The BACKGROUND PROJECTOR MODE switch can be used to select either NORMAL VIDEO (SKI blanked background video) or any of the five test patterns from the test pattern generator. The output of the BACKGROUND PROJECTOR MODE switch is called BP video, and is routed to the background projector via the BP electronic interface.

The TARGET PROJECTOR MODE switch is identical to its background counterpart, except for the omission of the CAL PATT position. The NORMAL VIDEO position, however, essentially functions as an "off" position for the test pattern output to the target projector since target video is not routed through this circuitry. The target test video from the mode switch goes directly to the target special effects generator, where it is ORed with the target TV camera video. A control signal from the TARGET PROJECTOR MODE switch provides the appropriate enable for the decision as to which source is to be selected.

Output discretes from both the BACKGROUND and TARGET either PROJECTOR MODE switches inform the linkage that the respective projection system is or is not in NORMAL VIDEO. The linkage uses these discretes to light the SERVOS IN MANUAL indicator on the EOS VISUAL subpanel.

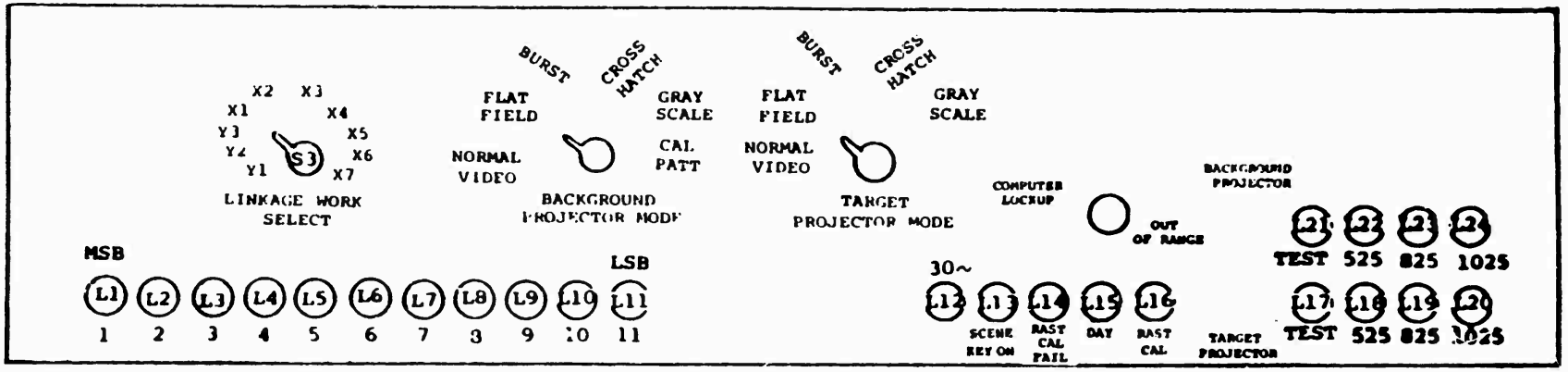

Figure 103. SKI Electronics Drawer Assembly, Front Panel

3.5.4.6 Linkage Signal Monitoring. The LINKAGE WORD SELECT rotary switch on the SKI electronics drawer front panel is used to select one of nine linkage words input to the SKI electronics. The 11-bit words are displayed on the LED lights immediately below the switch, in a straight binary configuration (1=on; 0=off). While the iteration rate is too fast to be visibly useful, the indicators are useful during maintenance when the computer is frozen. The remaining LED indicators are for use during normal operation. The TARGET and BACKGROUND PROJECTOR indicators each consist of an identical four light array. The TEST indicators light to indicate if the respective projection equipment is in a test mode. One of the three line rate indicators (525, 825 or 1025) is always lit indicating the selected line scan rate. It is noteworthy that all the lights on this panel are interpreting signals received from linkage rather than merely indicating internal switch settings. Whenever the simulator is operating, either the RAST CAL or SCENE KEY ON light should be lit (the other off) to indicate a raster calibration or normal operating mode. If RAST CAL FAIL lights during a raster calibration procedure, then the points acquired were not valid. The DAY indicator is on during simulated daylight conditions and off during dusk or night conditions. The 30~ and COMPUTER LOCKUP OUT OF RANGE lights are used as part of the master timing circuitry. (See paragraph 3.6.)

3.5.5 Background Projection Equipment. The background projection equipment consists of the light valve projector (supplied with remote control unit), the BP electronic interface, and the background projector optics. The projector and its optics are mounted atop the lower structural section of the cockpit electronics enclosure, and are part of an assembly referred to as the BP optical assembly. The background projector is hard mounted to the structure. The remote control unit supplied as part of the projector is housed in the cockpit electronics enclosure beneath the target projector. It is accessible from the rear, but may be removed from its location and carried into the cockpit while still connected to the projector.

A block diagram of the background projection equipment is given in Figure 104. The BP electronic interface relays the background video from the SKI electronics and composite sync from master timing to the projector. At this point, background video is the background SEG composite signal with the "hole" blanked for target insertion. The background projector transforms the electronic signal into a projected image. The wide angle optics display the image on the spherical screen with the required -40°/+50° vertical by $\pm 80^{\circ}$ horizontal field of view, and add the spectral coding required for projected scene keying. When in the raster calibration mode, a signal from the linkage removes the coding filter so that the

test pattern from the background projector may be seen by the keying camera. The quality and aesthetics of the projected image may be altered by operating and alignment controls on the BP remote control unit.

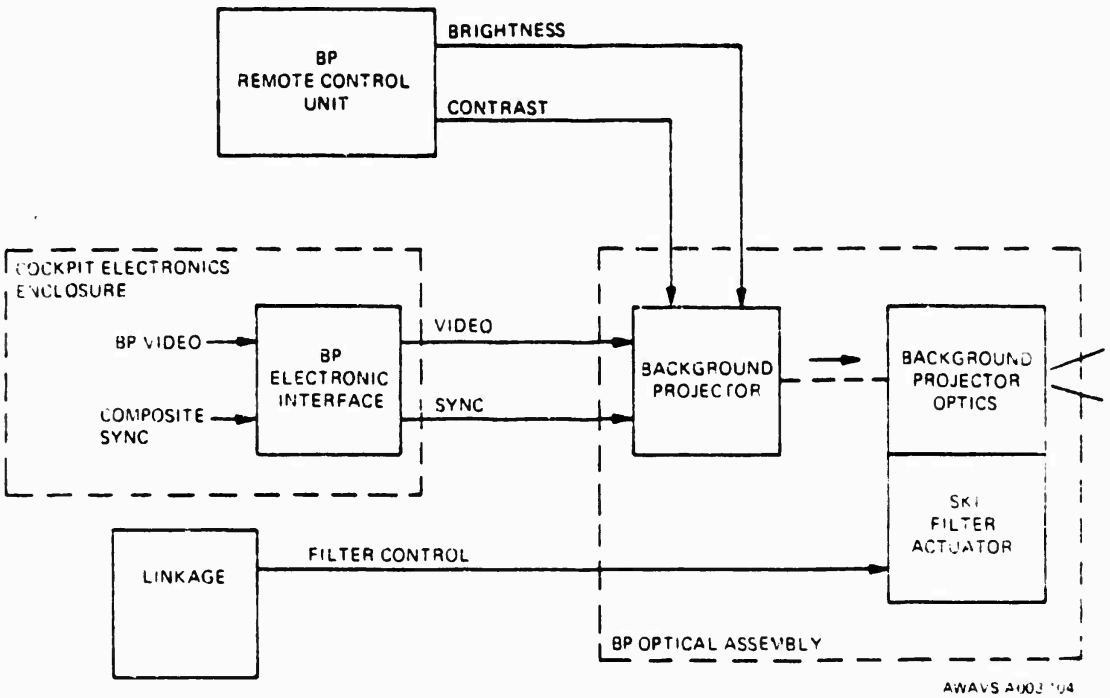

Figure 104. Background Projection Equipment, Block Diagram

3.5.5.1 Background TV Projector. The projector chosen is a General Electric PJ7150 light valve projector because of its high brightness output, practical size, and compatibility with the motion system requirements. Except for the differences in optics, the background and target projectors are identical. The specifications for the projector are as follows:

a. Light Output. Modulated light output of 1250 lumens is typical. (Minimum 1000 lumens). At brightness values up to rated level, picture remains sharp and in focus with simultaneous high contrast, brightness and resolution. These output ratings may be sustained on a 100% duty cycle basis.

b. Contrast Ratio. The large area contrast ratio is typically 100 to 1 (minimum 75 to 1) when measured under specified operating conditions in negligible ambient light.

c. Resolution. When operating from wide-band video signals, the horizontal resolution capability is a minimum of 800 TV lines per picture height.

d. Picture Geometry. Overall geometric distortion of the projected image is less than 2% with standard projection lens.

e. Video.

1) Input Circuits. BNC connectors are provided for two composite video inputs and one external sync input. All inputs are 75-ohm unbalanced and can be switch selected for either 75 ohm termination or loop-through operation.

2) Input Level. Composite video: -0.75 p-p min to 1.5V p-p max. Non-composite video: 0.5V p-p min to 1.5V p-p max. All inputs are ac connected. Maximum dc bias $\pm$10 volts.

f. Synchronization.

1) Scanning circuits: 1025/825/525 lines, 60 fields, 2:1 interlace.

2) Synchronization can be derived from the composite video signal or can be provided by an external sync signal of nominally 4V p-p.

g. Input Power.

1) Line Voltage. The nominal input voltage is 117 volts $\pm$10% 60 Hz.

2) Line Power. The total power input to the projector is approximately 1200 watts at 117V, 60-Hz input.

h. Operation.

1) Controls. Operation and gray scale controls are mounted in a removable module at the rear of the projector. The control unit is removable to allow control from remote locations at separations of up to 200 feet, but is supplied with a 30 ft long cable.

2) Switches with illuminated status indication:

Standby/Operate
Video/Black
Video Select: Comp 1/Comp 2

3) Operator Controls:

Brightness Peaking
Contrast

4) Set-up Controls:

Trap in/out
Sync in/out (internal/external)
Video drive and background

5) Test Points. The equipment is provided with test points and a built-in test meter to monitor circuit operation and to facilitate maintenance.

6) Elapsed Time Meter. A time-meter system is incorporated to show cumulative operating time of the light valve.

7) Provision is made for a standby mode of operation. Standby time does not register on the elapsed-time meter and is not counted as operating time for the light valve warranty.

8) X-Ray Radiation. There is no X-ray radiation (7.2KV anode voltage).

i. Mechanical.

1) Size/Weight. The projector system consists of one assembly. The weight of the projector is 130 pounds. Overall dimensions are: 22 inches high by 17 inches wide by 30.5 inches long.

2) Construction. Modular construction is used and components are readily accessible for replacement. All modules use solid state electron devices, with the exception of the 7.2KV shunt regulator tube.

3) Finish. The projector is supplied with a painted finish.

j. Environmental.

1) Temperature.

Operating: 10°C to 35°C
Storage: 0°C to 50°C

2) Pitch. The projector will operate with static pitch values from -15° to +25°. Satisfactory operation is maintained with cyclical pitch and roll variations of ±45°.

3) Magnetic Fields. Specified performance may be attained in a static magnetic field of any direction up to a magnitude of 1 gauss.

3.5.5.2 Background Projector Remote Control. The remote control unit is a hand held control box for the G.E. light valve projector. It contains both set up and normal operating controls. A 30-foot umbilical cable which connects the remote control box to the projector, allows the control box be removed from its housing in the cockpit electronics enclosure and used to adjust the projector from an operator viewable position inside the cockpit. The remote control units for both the target and background projectors are identical. Both are normally housed side-by-side, at the rear of the cockpit electronics enclosure, beneath the target projector. The front panel of a typical projector remote control box is illustrated in Figure 105. Controls on the upper half of the panel (TRAP, VIDEO, SYNC, DRIVE, and BACKGROUND) are essentially alignment controls for use by maintenance personnel only, while those on the lower half are for normal operation and setup.

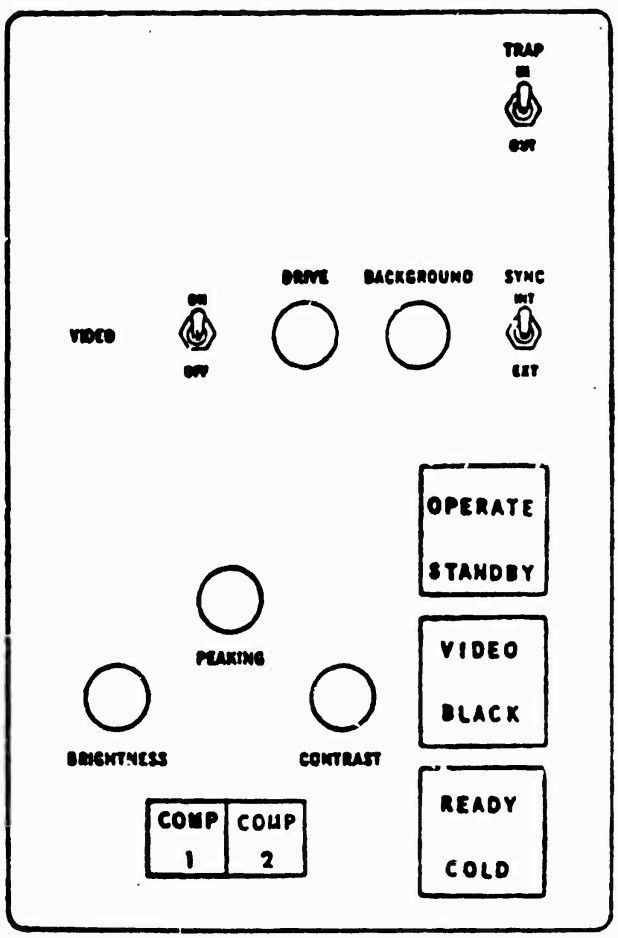

AWAVS 003-105

Figure 105. Light Valve Projector Remote Control

A hinged flap covers the setup controls and switches. The TRAP switch is always set to OUT. The SYNC switch is normally set to EXT, but INT sync is available for test only. The VIDEO switch controls application of video information to the projector optics, following the point at which all video processing has been accomplished. The DRIVE and BACKGROUND potentiometers are the course (preset) picture adjustments which govern video gain (contrast) and dc level (raster brightness).

The function of the CONTRAST and BRIGHTNESS is the same as for normal television. Varying the PEAKING control increases the apparent sharpness of the picture by altering the white level. The OPERATE/STANDBY switch is an alternate action device which lights to indicate the selected position. An internally adjustable circuit provides a nominal 45-second delay in application of all dc voltages. The READY/COLD indicator lights to show the operational status of the light valve projector. Approximately 45 minutes is required to bring the light valve up to operating temperature from a cold start. The COMP 1/COMP 2 switch selects which of two channels of composite video input to the projector is to be displayed. In AWAVS, only one channel (COMP 1) is used. The VIDEO/BLACK control is an alternate action illuminating switch that controls the application of the selected video signal to the video processing circuits. In the BLACK position no video is applied. This differs from the VIDEO ON/OFF switch (above) which controls output of processed video, thus exercising the projector circuitry.

3.5.5.3 Background Projector Optics. Comprising the optical train of the background projector are the modified projector lens, the blue-green optical filter for spectral coding, and the anamorphic wide-angle attachment. Figure 106 is a block diagram of the projector optics.

3.5.5.3.1 Projection Lens. The projection lens normally supplied with the light valve projector has been modified by altering the front end in order to meet a new diffraction specification limited at 700 TV lines. This lens, designated as the T_6 in the target projector optics where it is used as supplied by G.E., has been reidentified as T_6M in its modified version. The T_6 and T_6M projection lenses are the only difference between the background and target TV projectors. The focal length of either lens is 81 mm and the aperture is f/3.

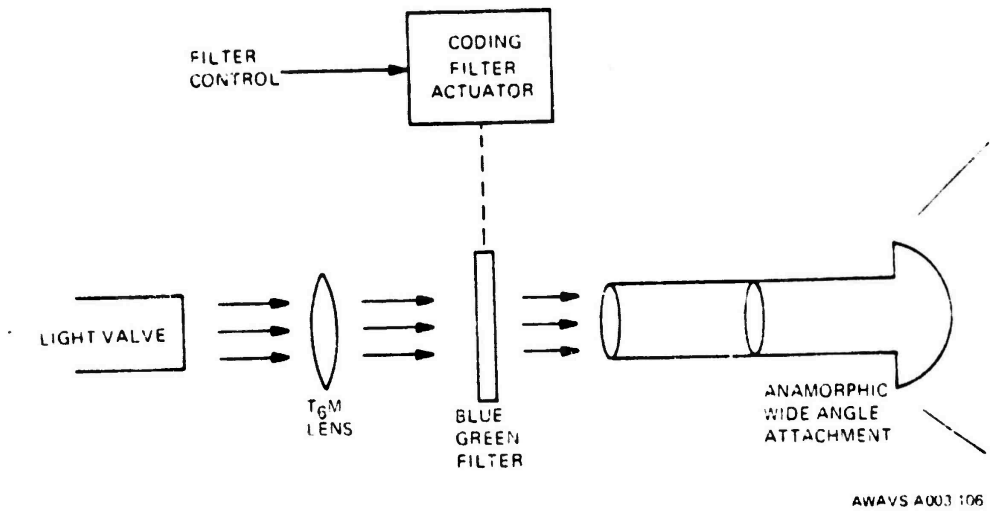

Figure 106. Background Projector Optics, Block Diagram

3.5.5.3.2 Spectral Coding Filter. The blue-green optical filter is inserted in a 7/8 inch air space between the T_6M projection lens and the wide-angle attachment. Since the filter is in collimated light, it has no measurable effect on optical performance other than spectral coding. The filter removes red light from the background image displayed on the screen. Since the keying camera filters out blue-green light, admitting only the red, it does not see the background and responds only to the white light target carrier. In the raster calibration mode (paragraph 3.5.1.1), however, the keying camera must be able to photograph the diamond pattern from the background projector. Therefore, when in that mode, a signal from the linkage operates an actuator, which removes the filter from the optical path and replaces it by a glass of the same size and refractive index.

3.5.5.3.3 Wide Angle Attachment. The wide-angle attachment is an anamorphic lens (exhibits different power in two orthogonal medians) which accepts collimated light from the projector, and displays it on the screen covering a 90° vertical by 160° horizontal field of view as illustrated in Figure 107. The exit pupil of the background projector wide-angle attachment is located at the center of curvature of the spherical screen. The attachment is approximately 35 inches long and has a maximum diameter (at the front element) of 8.8 inches. There are two cylindrical mounting surfaces, each slightly less than two inches in diameter and about 2 inches wide, whose centers are approximately 18 1/2 inches apart. They are located symmetrically around the center of gravity. Optical specifications are given in Table 52. The identical wide-angle attachment is used for both the background projector and scene keying camera.

The wide-angle attachment is comprised of 18 elements with 26 air-to-glass surfaces. Reflection losses with MgFl anti-reflection coatings average approximately 1% per surface. Ignoring absorption losses, transmission is:

$$T_{refl} \times 99^{26} \times 100\% = 77\%$$

The six elements nearest the spectral coding filter relay the collimated output of the T_6M lens to an intermediate image and interchangeable field stop. The purpose of the field stop is to occult light outside the specified format. The remaining 12 elements then project the image onto the screen. The relay is incorporated to increase the length of the system to meet mechanical constraints.

TABLE 53. WIDE ANGLE-ATTACHMENT, OPTICAL SPECIFICATIONS

Field of view	90° by 160° H
Resolution (for T_6M and anamorphic lens set):	
Center of field	24 optical lp/mm vertically 40 optical lp/mm horizontally
Any off axis point	12 optical lp/mm vertically 20 optical lp/mm horizontally
Modulation at red resolution	35% minimum; 50% optimum
Mapping accuracy	Within 30 $\overset{\frown}{\text{min}}$ or 2% of computed angle at any point
Transmission:	
For projection lens	At least 70% of total available lumens of light valve projector
For camera lens	At least 70% between 500 and 700 nm
Uniformity	Within 50% over entire format

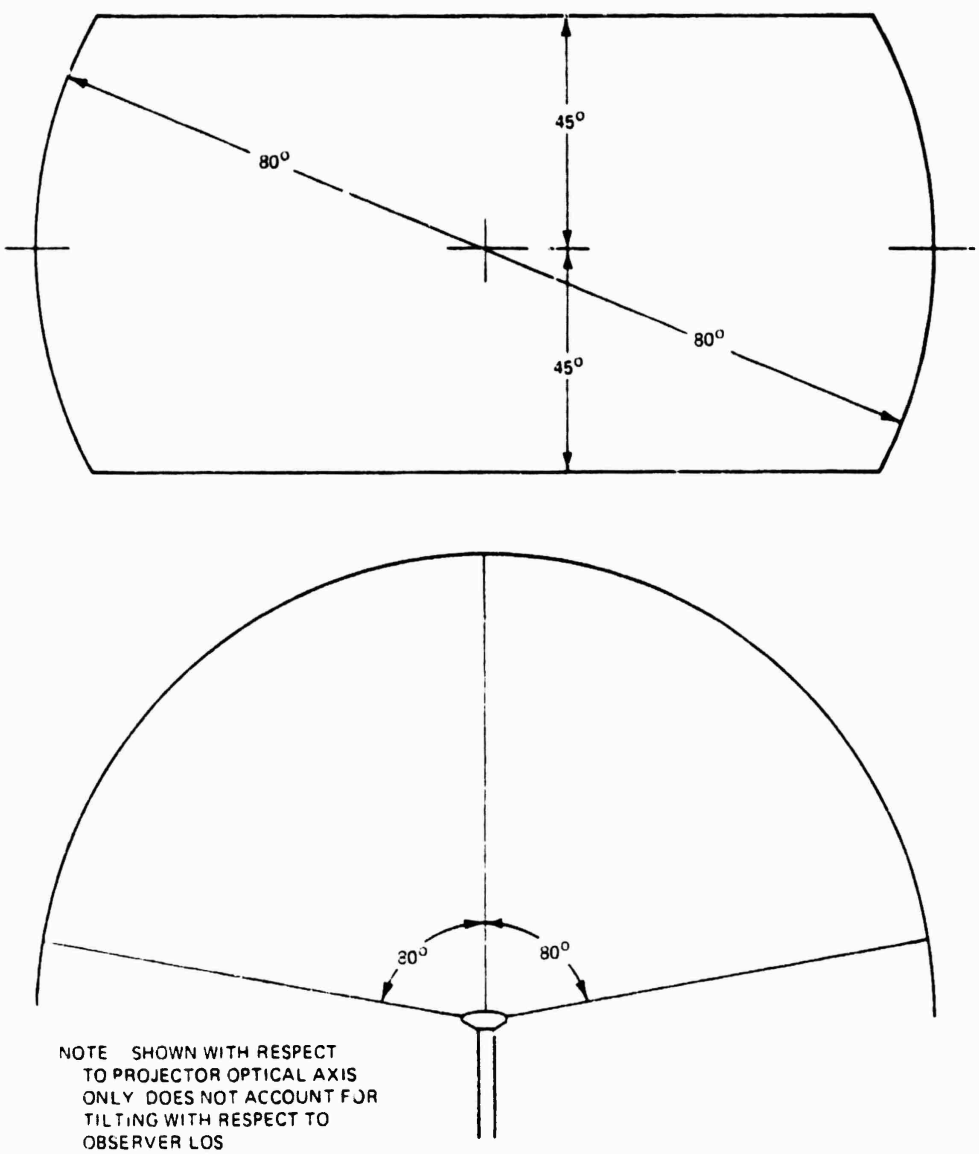

Figure 107. Projected Angular Field of Background Projector

The mapping for the wide-angle attachment is most simply described as a sequence of two transformations. The first transforms the input image plane into a fictitious object plane anamorphically, as follows:

$x' = kx$
$y' = y$
k = anamorphic power
x, y = rectangular coordinates in the input object plane
x', y' = rectangular coordinates in the fictitious object plane

The second transformation is rotationally symmetrical, and shall be as far as reasonably possible, an analytically simple function such as:

$$r' = f \cdot (\theta + C\theta^3 + d\theta^5 + ---)$$

where

$r' = \sqrt{x'^2 + y'^2}$ = radius from center of fictitious object plane

θ = angular distance of an image point on the screen from the lens axis, as measured from the center of the exit pupil for the projection lens or center of the entrance pupil for the camera lens for on-axis imagery

f = proportionally factor

c,d = constants (c minimized; d and following negligible)

The anamorphic power k and the proportionally factor f are adjusted to cause the light valve format (or SKC isocon format) of 0.750 by 1.000 inches to correspond to the field of view, as defined above.

The mapping of the projection and camera lens are matched to within 0.57%.

The existing field of the wide-angle attachment covers the required pilot field of view. The rounding edges of the field are within 30° of azimuth and 15° of elevation. The light valve format used is 1.00 inch horizontal by 0.75 inch vertical, thus reducing vignetting at the fields edge as would exist if the full 1.1 inch horizontal dimension were used. The effective falloff as presented to the scene keying camera at 10% in from the projected edge (assuming full horizontal usage) is 50% of center brightness. Thus, the total fall off read at the scene keying camera, considering the two wide angle lenses, is 0.5 x 0.5 = 0.25 = 25% of center brightness (not including any differences between axial and non axial transmission).

3.5.5.3.4 Screen Illumination. The projected field as illustrated in Figure 106 is near elliptical. Thus, the area coverage on the screen is:

$$\frac{\pi\ (120\text{ in.})^2\ (80)\ (45)}{(144\text{ in.})\ (57.3)^2} = 345\text{ sq. ft.}$$

Additional factors to be considered are:

Background lens axial transmission	= 0.85
Background filter transmission	= 0.5
Screen gain	= 2.5
Light valve projector output	= 1000 - 1500 lumens

For a 1000 lumen projector output, the screen luminance (B) is:

$$B_{1000} = \left(\frac{1000\text{ lumens}}{345\text{ sq. ft.}}\right)\ (0.85)\ (0.5)\ (2.5) = 3.0\text{ ft. lamberts}$$

For 1500 lumens output:

$$B_{1500} = \left(\frac{1500\text{ lumens}}{345\text{ sq. ft.}}\right)\ (0.85)\ (0.5)\ (2.5) = 4.6\text{ ft. lamberts}$$

While 1000 lumens is the nominal output of the light valve projector, tests have indicated that separating the T_6M lens doublet closest to the raster permits extension to 1500 lumens. If not separated, the thermo-plastic adhesive joining the doublet separates and clouds when subjected to the extended output. The T_6M lens is presently being modified to permit the extended output.

3.5.5.4 Projected Image Resolution. The background system resolution is comprised of two components: the combined T_6M and wide angle attachment resolution and the light valve projector resolution. Limiting resolution for the lens combination is:

Axial: 24 lp/mm or 5.89 $\widehat{\text{min}}$/line vertically
40 lp/mm or 4.73 $\widehat{\text{min}}$/line horizontally

Edge: 12 lp/mm or 11.8 $\widehat{\text{min}}$/line vertically
20 lp/mm or 9.45 $\widehat{\text{min}}$/line horizontally

Limiting resolution (at center of format) light valve projector:

1100 TV lines or 17.7 $\widehat{\text{min}}$/line horizontally
740 TV lines or 13.0 $\widehat{\text{min}}$/line vertically

The limiting system resolution (r_L) is found using the equation:

$$r_L = \sqrt{r_1^2 + r_2^2}$$

Horizontal and vertical limiting system frequencies are as follows:

Axial: r_L (Horizontal) = 14.27 min/line
r_L (Vertical) = 18.32 min/line

3.5.6 Scene Keying Camera Subsystem. The primary components of the scene keying camera subsystem are the scene keying camera (SKC) the SKC optics, the camera control unit (CCU), and the dynamic analog raster computer (DARC). A block diagram of the camera subsystem is given in Figure 108. Dashed lines surrounding functional entities indicate hardware placement. Basically, the SKC is aimed at the same area of the display screen as the background projector, and uses the same wide-angle optics as the projector (except for the filter). By virtue of its optical filtration, the camera photographs only the white light aircraft carrier. Vertical and horizontal deflection sweeps for the camera are developed by the DARC. All other electronics for camera operation and video processing, including dc power supplies and alignment and operating controls, are housed in the CCU. The primary output of the CCU is the SKI VIDEO used by the SKI electronics assembly to blank the "hole" in the background video. A secondary output is provided for video and waveform monitoring. The scene keying camera subsystem uses fixed and variable (Ø4) phase horizontal drives as well as vertical drive and composite blanking from master timing. Refer to paragraph 3.6 for a complete description of those signals.

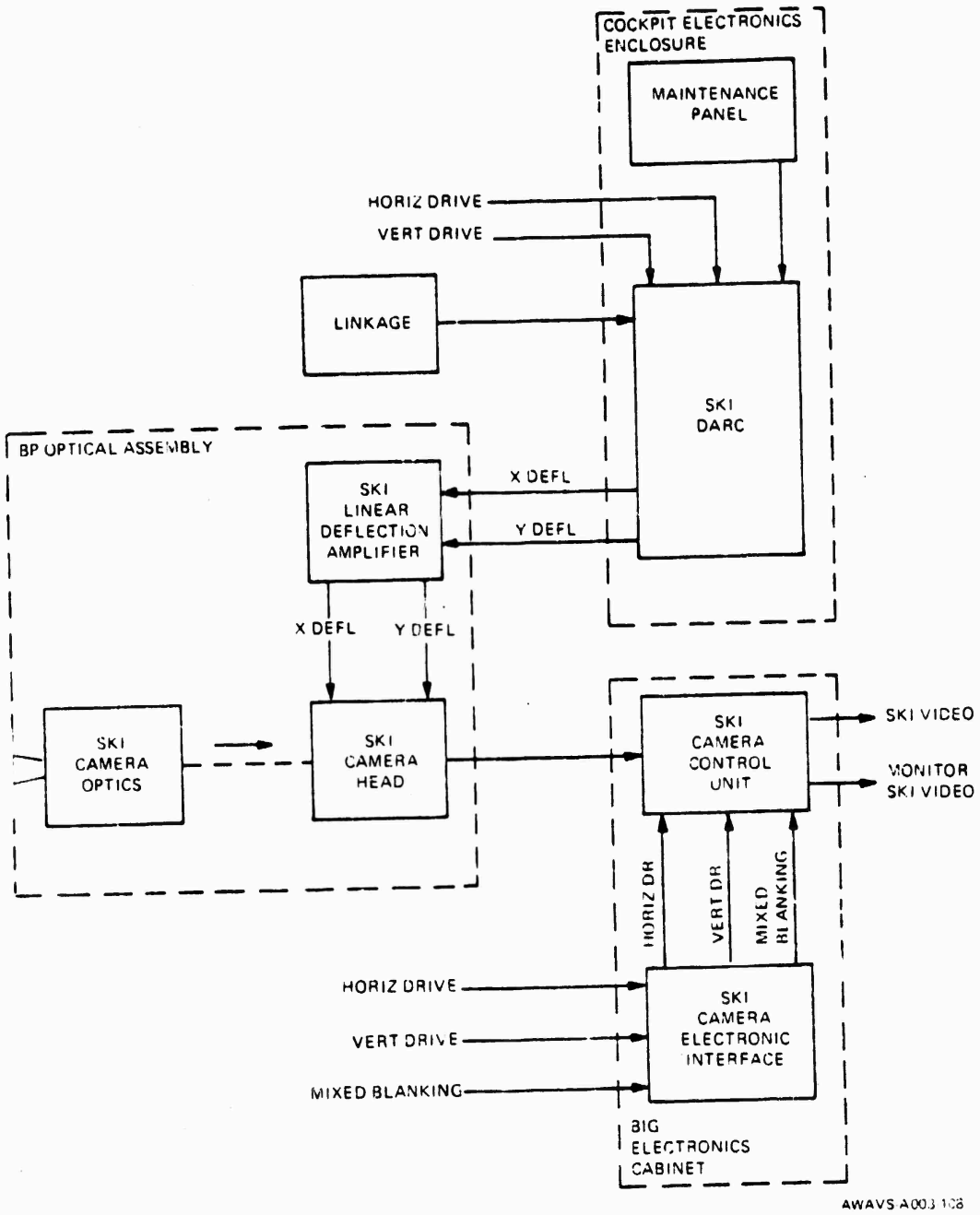

Figure 108. Scene Keying Camera Subsystem, Block Diagram

3.5.6.1 SKC Optics. The approach taken in design of the optics for the scene keying camera was to duplicate the optics for the background projector, since the camera is photographing the identical projected image from nearly the same position. To further facilitate this duplicity, the isocon image format of the camera is identical to the output format of the light valve projector (0.750 by 1.000 inches).

A block diagram of the SKC optics is given in Figure 109. The T_6M lens and the wide-angle anamorphic attachment are identical to those of the background projector. The only difference between the two systems is the optical filter, which in the case of the camera optics is red pass (blue-green blocking). Also, the camera filter is fixed, as removal is not required for raster calibration.

The SKC lens pupil (part of wide-angle attachment) is laterally offset 14 inches from the background projector exit pupil, then tilted back 1.5 degrees in azimuth to cover the same field of view.

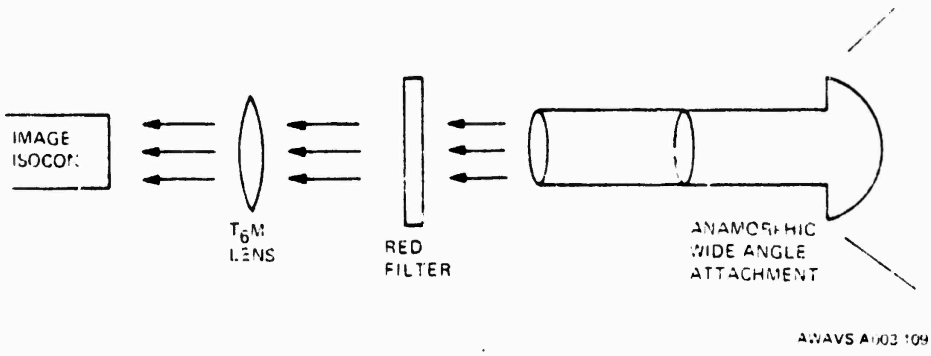

Figure 109. SKC Optics, Block Diagram

3.5.6.2 Scene Keying DARC. As previously stated, the scene keying camera raster is synchronized with the background projector raster so that the point on the display screen being projected is simultaneously scanned by the camera. The keying camera DARC is used to modify the camera scan lines so that they coincide with background projector mapping. The tracking is initially acheived during the raster calibration mode, with the DARC providing the horizontal and vertical deflection camera sweeps under control of the linkage. Details of the process are given in paragraph 3.5.1.1. In order that the DARC may be used to provide camera sweeps for testing the SKC, artificial and unsynchronized inputs may be provided from the cockpit enclosure test panel. (See Figure 66.) When the SKC DARC button is pressed, the artificial cues are substituted for the computer generated scanning cues. The SKC DARC switch is an alternate action device with a split lens indicator button, which lights to indicate either NORMAL or TEST. It is not necessary to operate the key switch on the test panel for this purpose.

3.5.6.3 Scene Keying Camera Head. The TV camera head houses an image isocon, the linear deflection amplifiers and the video preamp. The camera head is an off-the-shelf Model ISO-3 Video Standard TV Camera (marketed by Sierra Scientific Corporation, Mountain View, California) except for a modification of the internal deflection circuitry. Since the camera uses a preshaped raster supplied by the DARC for tracking of the background projector scan lines, the resonant deflection amplifier, and consequently the isocon yoke assembly, normally supplied in the camera had to be replaced by linear devices. The isocon image format is 0.750 by 1.000 inches, which is identified to the object format of the background light valve projector. The RCA type 4807A image isocon is a ruggedized fiber optic faceplate television camera tube designed for high-resolution, low-light level TV systems. Figure 110 is an extract from the RCA data sheet on the isocon. Electrical specifications for the camera are included in Table 53.

General Data

Direct Interelectrode Capacitance

- Anode to all other electrodes (output capacitance)
  - Potted .... 24 pF
  - Non-Potted (including tube base) .... 12 pF

Target-to-Mesh Spacing (Nominal) .... 0.02 in (0.5 mm)

Spectral Response (See Figure 10) .... Modified S-20

Photocathode, Semitransparent

- Material .... Na-K-Cs-Sb (Multialkali)

Useful Size of Image

- Maximum target diagonal .... 1.4 in (35 mm)
- Maximum photocathode diagonal .... 1.4 in (35 mm)

Note: The size of the optical image focused on the photocathode should be adjusted so its maximum diagonal does not exceed the specified value. The corresponding electron image on the target should have a size such that [illegible] of the rectangle just touch the target ring.

Orientation: Proper orientation is obtained when the vertical scan is [illegible] parallel to the plane [illegible] through the center of the [illegible] and the index [illegible] at the shoulder base. The horizontal [illegible] can should [illegible] at the corner of the raster between the [illegible] lead [illegible] and [illegible] of the shoulder base. See RCA AJ2206 [illegible] assembly bulletin for proper tube-yoke orientation.

Image Surface

- Material .... Dark-Clad Fiber-Optics
- Pitch (nominal center-to-center spacing) .... 6 μm
- Flatness .... Within 0.5 μm

Focusing Method .... Magnetic

Deflection Method .... Magnetic

Shoulder Base .... Annular [illegible] leads (See Dimensional Outline)

End Base (AJ2? 4507A) .... Semiflex [illegible] potted in silicone rubber. See Dimensional Outline

Associated Scanning and Focusing Coil Assembly .... RCA Type AJ2206 or Equivalent

Operating and Storage Position .... Any

Weight (Approx.) .... 1.5 lbs (.620 kg)

Maximum and Minimum Ratings, Absolute-Maximum Values

Voltages are with respect to thermionic cathode unless otherwise specified. All ratings are maximum unless otherwise stated.

Faceplate:

- Irradiance .... 25 W/m² (watts/square meter)
- Illuminance .... 50 lm/ft² (fc); 500 lm/m² (lux)

Temperature

- Any part of bulb .... 65 °C

Temperature Difference

- Between target section and any part of bulb hotter than target section .... 5 °C

Heater, for Unipotential Thermionic Cathode

- AC or DC current (pin No 1 and pin No 20 or lead No 16 and 17) .... 0.63 A; 0.57 min. A

Peak Heater-Cathode Voltage

- Heater negative with respect to cathode .... 125 V
- Heater positive with respect to cathode .... 10 V

Photocathode Voltage (E_{pc}) .... −1000 V

Grid-No.6 Voltage (E_{g6}) .... −750 V

Target Voltage (E_t)

- Positive value .... 10 V
- Negative value .... 10 V

Grid-No.5 (Field-Mesh) Voltage (E_{g5}) .... 600 V

Grid-No.4 Voltage (E_{g4}) .... 600 V

Grid-No.3 Voltage (E_{g3}) .... 600 V

Grid-No.2 Voltage (E_{g2}) .... 450 V

Grid-No.1 Voltage (E_{g1}) .... −150 to −40 V

Steering-Plate Voltages

- Plate SX_1 (E_{sx1}) .... 600 V
- Plate SX_2 (E_{sx2}) .... 600 V

Misalignment-Plate Voltages

- Plate SY_1 (E_{sy1}) .... 600 V
- Plate SY_2 (E_{sy2}) .... 600 V

Anode Voltage (E_b) .... 1800 V

Voltage Between Adjacent Dynodes .... 600 V

Typical Operating Values

Regulation of power supply and divider network circuitry should be such that the operating values specified below are held within the limits shown.

Heater Current	±5	%
Focus Coil Current (The values of currents to [illegible] requirements [illegible] in the data sheet [illegible] the magnetic component, e.g., AJ2206)	±0.3	%
Grid No.4 Voltage (As adjusted)	±0.2	%
Other DC Voltages (Fixed or as adjusted)	±1.0	%
Beam Blanking Pulse Voltage	+50 / −0	%

Voltages are with respect to thermionic cathode unless otherwise specified. For circuit design purposes, nominal [illegible] currents are 10 μA or less, including leakage, except where otherwise noted.

Heater for Unipotential Cathode (Between Pins 1 and 20)		
Current	0.6	A
Voltage (nominal for current of 0.6 A)	6.3	V
Photocathode Voltage (Image focus)	−300 to −650	V
Grid No.6 Voltage (Accelerator — approximately [illegible] of cathode voltage)	−370 to −410	V
Target Voltage	3.5	V
Grid No.5 (Field mesh) Voltage	E_{g4} + 12	V
Grid-No.4 Voltage	400 to 440	V
Grid-No.3 Voltage (Max. output)	E_{g4} + 120	V
Grid-No.2 Voltage	400	V
Current	200	μA
Grid-No.1 Voltage for Picture Cutoff	−120 to −60	V

AWAVS A[illegible]

Figure 110. RCA Type 4807A Image Isocon, Data Sheet (Sheet 1 of 2)

Typical Operating Values (Cont'd)

Steering Plate Difference Voltage (Center voltage same value as grid No.4)			
$E_{sx1} - E_{sx2}$	0 to +60	max.	V
Misalignment Plate Difference Voltage (Center voltage same value as grid No.4)			
$E_{sy1} - E_{sy2}$	0 to +60	max.	V
Dynode No.1 Voltage	375		V
Dynode No.2 Voltage	700		V
Dynode No.3 Voltage[D]	750 to 1050		V
Dynode No.4 Voltage	1350		V
Dynode No.5 Voltage[D]	1650		V
Anode Voltage	1700		V
Current	25		μA
Target Temperature Range	30 to 50		°C
Beam Blanking Voltage (Applied to grid No.1)			
Peak-to-peak	30		V
Field Strength at Center of Focusing Coil (Approx.)	70		G

Performance Characteristics Range Values

With conditions shown under Typical Operating Values, picture highlights at 2×10^{-5} lm/ft² on the photocathode, 525 lines/scanning, interlaced 2:1, frame time 1/30 second, and 1.4" photocathode diagonal with 4 × 3 aspect ratio.

	Min.	Typ.	Max.	
Photocathode Radiant Sensitivity at 440 nanometers	–	50	–	mA/W
Photocathode Luminous Response to 2854° K tungsten source[A]	130 2.6	140 3.2	–	μA/lm mA/W, 2854° K
Signal Output Current (Peak to peak)	3	5	–	μA
Photocathode Illuminance at 2354° K required to reach "Knee" of Transfer Characteristic	–	.001	.002	lm/ft²
Photocathode Irradiance at 440 nanometers Required to Reach "Knee" of Transfer Characteristic	–	–	5.7×10^{-5}	W/m²
Signal-To-Noise Ratio				
Signal to noise-in-signal for highlights	26	30	–	dB
Highlight signal-to-dark current noise	40	43	–	dB
Amplitude Response (Contrast transfer) at 300 TV Lines Per Picture Height (Percent of response to large-area black to large-area white transition)	70	80	–	%
Limiting Resolution:				
At center of picture	1000	1100	–	TV Line
At corner of picture	350	900	–	TV Line
Geometric Distortion	–	1	–	%

	Min.	Typ.	Max.	
Lag (Percent of Initial Signal Output Current 1/20 Second After Illuminance is Removed	–	–	2% at 2×10^{-3}	lx
	–	–	10% at 8×10^{-4}	lx
Shading (Uniformity)				
Black level				
Variation of output current with tube capped (Percent of maximum highlight signal)				
	–	2	5	%
	–	1	2	%
Shading (Uniformity)				
White level				
Variation of highlight signal (Percent of maximum highlight signal)				
	–	15	30	%
	–	12	15	%

Typical Spectral Response

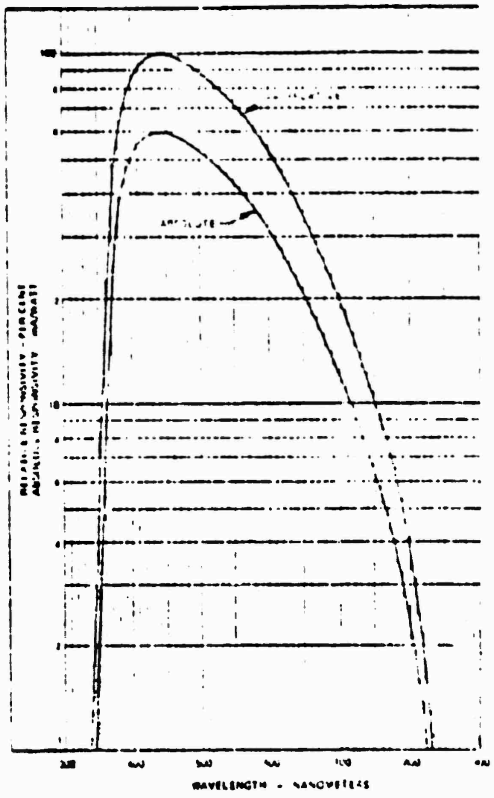

AWAVS-A003110.2

Figure 110. RCA Type 4807A Image Isocon, Data Sheet (Sheet 2 of 2)

TABLE 54. SKC/CCU ELECTRICAL SPECIFICATIONS

Power Requirement	105-130V dc, 60 Hz, 1Ø
Scan Rates	525, 825 and 1025 lines/ frame with 3:4 aspect ratio, 2:interlace, and 30 frames/ second at each rate
Output Video Waveform	One 75-ohm source terminated 0.7 volt peak-to-peak across 75 ohms, noncomposite. White positive
Synchronization	Ext horiz and vert drive and composite blanking per EIA RS 343-A.
Resolution:	
Horizontal MTF at 525 lines	Center - 5% at 1000 TV lines/ picture height Corner - 5% at 850 TV lines/ picture height
Vertical at 525 lines	Center - 375 TV lines/picture height Corner - 300 TV lines/picture height
Vertical at 825 lines	Center - 550 TV lines/picture height Corner - 450 TV lines/picture height
Vertical at 1025 lines	Center - 650 TV lines/picture height Corner - 500 TV lines/picture height
Video Bandwidth	Flat within 1 dB to 27 MHz and -3 dB (max) at 30 MHz; and sufficient to meet resolution requirements, above.
Sensitivity and S/N Ratio	Equal to or better than those of the image isocon, with no gamma or image enhancement. In black portion of signal, preamp generated noise shall be at least 1/5 isocon generated noise.

TABLE 54. SKC/CCU ELECTRICAL SPECIFICATIONS (CONTINUED)

Gray Scale Rendition	10 shades of gray
Transmission Cable Distances:	
Camera Head to CCU	250 ft.
CCU to Monitor Display	250 ft.
Geometric Distortion	±0.5% within a circle dia equal to picture height; ±1% elsewhere
Scan Failure Protection	Isocon image tube protected against horizontal or vertical sweep failure of any nature
Ringing or Spurious Signals	None perceptible in displayed picture
Gamma Correction	Adjustable from 0.4 to 1.0
Deflection Amplifiers	Linear type (with compatible yoke) capable of scanning entire useable area of image isocon. For use with externally supplied H and V sweep signals

The overall dimensions of the camera head, excluding the wide-angle attachment, are 8.03 inches high by 9.22 inches wide by 32 inches long. Removal of a U-shaped cover permits access to all interior components except the isocon and the deflection amplifier circuit boards. A shield covering the circuit boards has access holes for the centering adjustments (± 15% horizontal and vertical). The T_6M lens and optical filter are housed within the camera head, and become accessible by removal of the U-shaped cover. A circular flange at the front of the camera housing forms the rear mounting surface for the wide-angle attachment. A 90 mm dia threaded hole with a 1 mm thread pitch is provided in the isocon housing for mounting the T_6M lens. The camera head is hard mounted to the cockpit electronics structure by four 1/4-20 bolts into threaded holes in the underside of the housing on 11.25 by 4.80 inch centers.

3.5.6.4 Camera Control Unit. The camera control unit (CCU) is supplied by Sierra Scientific Corporation as part of the Video Standard Camera package. The CCU receives the horizontal and vertical drive pulses from the sync generator (via the electronic interface) and produces the vertical sweep current and delayed and shaped horizontal drive pulses. The camera electronic interface (not part of CCU) differentially receives and buffers the timing drives and blanking. This is done to avoid tying the signal input returns to the return of the CCU, thus reducing the possibility of ground loops and noise. The CCU has its own master oscillator and sync circuits, which produce the four standard pulse groups and control all timed operation of the camera chain. A self-contained power supply generates dc voltage for operation of internal circuitry as well as the camera head, and a synchronous dc to dc converter generates high voltage for the isocon. The CCU also contains all video processing circuits providing AGC, shading control, polarity selection, blanking insertion, white clipping, gamma correction, and sync adddition functions. Two video outputs are provided from the CCU: one for the video chain, the other for monitoring via the BIG/WIG maintenance panel. Both are 75-ohm outputs from the identical circuit point, but isolated from each other. A delayed clamp output is also provided, plus a go-to-black feature, and a means for inserting a grating signal for linearity measurements.

The front panel of the CCU is shown in Figure 111. The ON/OFF switch on the power supply module controls the ac input, while OPERATE/STANDBY switch on the LED control (shading control) module governs the application of high voltages. The FOCUS, BEAM, and TARGET potentiometers on the camera control module adjust the beam focus, beam current, and target voltage, respectively, to match peculiar characteristics of individual isocons. Front panel test points are provided for these three voltages. The GAIN control on the input video module adjusts the reference voltage for the AGC. The output video module contains three front panel controls. The PEDESTAL control varies the blanking depth; the POL switch selects normal or reverse polarity for the video image; and, the GAMMA control allows variation of the video amp characteristics to suit the particular isocon or to provide black or white stretch for maximum gray scale utilization. Both the input video and output video modules have isolated front panel test jacks to check incoming and outgoing signals, respectively. Test jacks are also provided on the power supply front panel for low voltage checks. Power and OVERHEAT indicators are also provided.

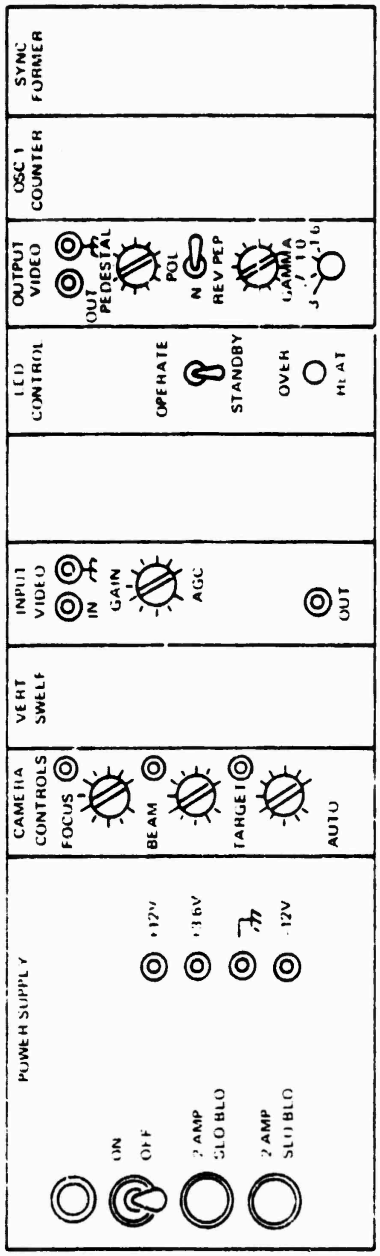

Figure 111. Scene Keying Camera Control Unit, Front Panel

The CCU measures 5.25 inches high by 19 inches wide by 13 inches deep and is designed for standard 19-inch rack mounting. It weighs approximately 20 pounds. It contains eight modules removable from the main frame by loosening captive screws and pulling out. Except for the power supply, each module consists of a front panel, a single circuit card and a rear connector. An extender card is provided for maintenance, and is stored behind the sync former module front panel. Electrical specifications for the camera and control unit package, as supplied by the camera vendor, are given in Table 53.

3.6 Master Timing Generator

The master timing generator provides all system timing signals for AWAVS. Circuitry for generation and development of timing signals is divided between the SKI electronics and sync generator drawers, while amplification and distribution is governed by the sync generator distribution panel. Figure 112 is a block diagram of the master timing generator illustrating development of all AWAVS timing signals. Table 54 is a timing chart showing signal durations, delays, and miscellaneous related parameters for each of the three selectable TV line rates. Table 55 shows the distribution throughout the visual system of signals developed in Figure 112. The three assemblies shown in the block diagram and enumerated above are all located in the BIG electronics cabinet.

3.6.1 High Frequency Timing Generation. The source of all AWAVS timing is a 170.4781 voltage-controlled oscillator (VCO) in the SKI electronics drawer. This frequency is divided down and phase locked to the 30-Hz computer iteration rate, which is controlled by VTFS timing. The phase-lock is done to assure that linkage update occurs only during vertical blanking, thus preventing any disturbances, which might accompany update data, from becoming visable. The VCO output frequency is divided down to a 14.21 MHz source for the sync generator and three high frequency master clocks for SKI electronics timing. The location of high frequency circuitry within the SKI electronics drawer is dictated by the signal usage in the SKI position and test pattern generators.

3.6.2 Line Rate Timing Generation. The TV format used for each line rate is 30 full frames per second with a two-to-one interlace. The 14.21 MHz sync generator main clock is digitally divided to provide the timing for all three line rates. A decoding network for each set of timing signals develops drive, sync, and blanking signals which are applied to the line rate switching circuits. All signals shown at this point are generated and developed simultaneously. Timing signals developed at each line rate include horizontal, vertical, and composite sync; composite blanking; and horizontal and vertical drives.

TABLE 55. AWAVS SYSTEM TIMING

PARAMETER \ LINE RATE	525	825	1025
Frames per Second	30	30	30
Fields per Frame	2	2	2
Horizontal Period	63.492 usec	40.404 usec	32.52 usec
Main System Clock		170.478 MHz	
Scene Key/WIG Main Clock	42.620 MHz	56.826 MHz	28.413 MHz
Horizontal Decoding Elements	1452	1452	1452
Horizontal Blanking	12.38 usec	6.34 usec	6.97 usec
Horizontal Active	51.10 usec	34.07 usec	25.55 usec
Fixed Horizontal Drive Width (No delay from start of blanking)	6.19 usec	3.73 usec	3.73 usec
Horizontal Sync Width	4.72 usec	2.75 usec	2.75 usec
Horizontal Sync Delay (With respect to H drive)	1.48 usec	0.985 usec	0.985 usec
Adjustable Horizontal Drive Width	5 usec	5 usec	5 usec
Resolution of Delay	70 nsec	70 nsec	70 nsec
Vertical Blanking	1206 usec	1173 usec	1203 usec
Active Horizontal Lines	487	766	951
Vertical Sync Width	190.5 usec	121.2 usec	97.56 usec
Vertical Sync Delay (From start of blanking)	190.5 usec	121.2 usec	97.56 usec
Vertical Drive Width (No delay from start of blanking)	603.2 usec	606.1 usec	601.6 usec

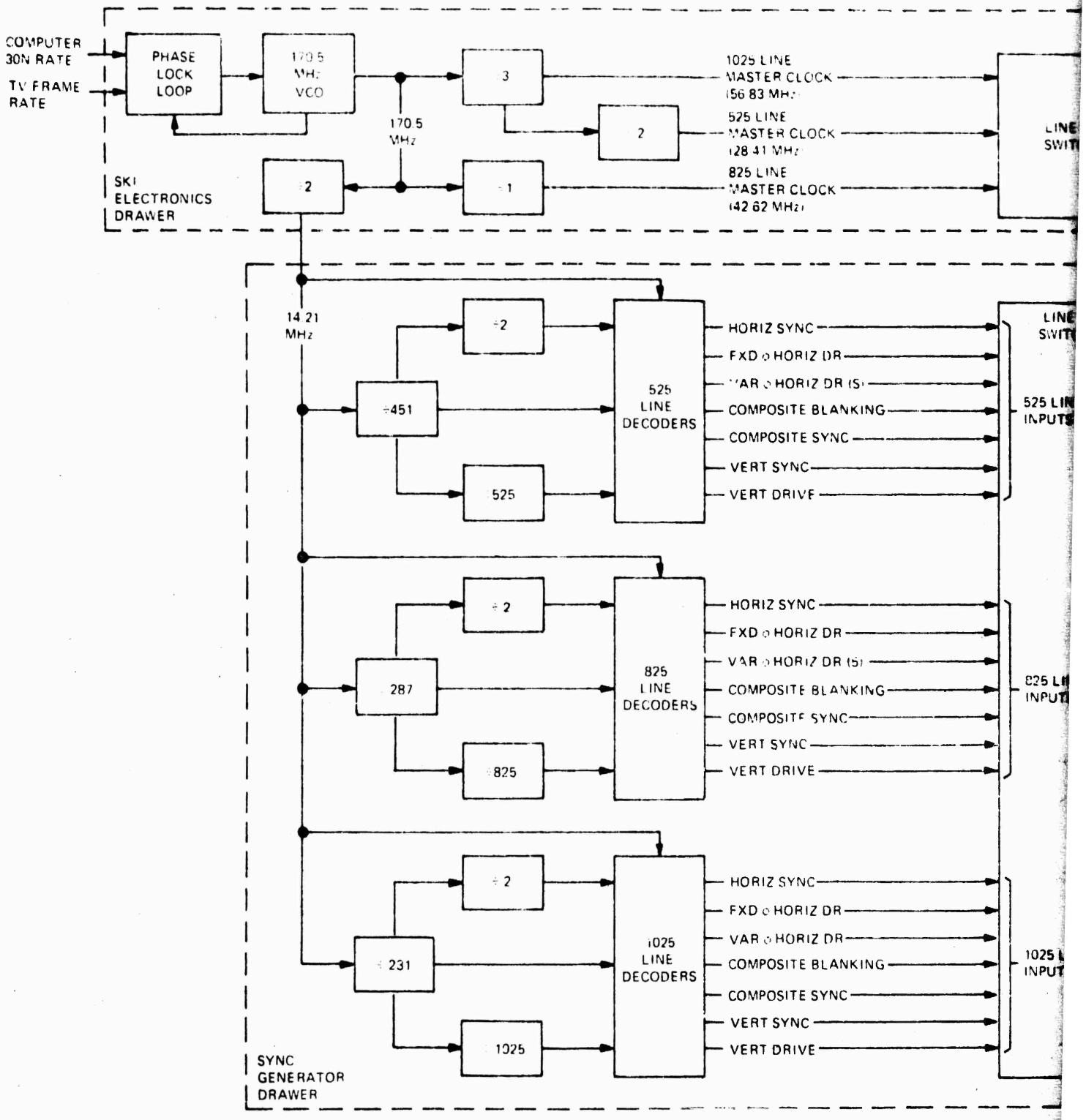
COMPUTER 30N RATE
TV FRAME RATE
PHASE LOCK LOOP
170.5 MHz VCO
170.5 MHz
÷3
÷2
÷2
÷1
1025 LINE MASTER CLOCK (56.83 MHz)
525 LINE MASTER CLOCK (28.41 MHz)
825 LINE MASTER CLOCK (42.62 MHz)
SKI ELECTRONICS DRAWER
14.21 MHz
÷2
÷451
÷525
525 LINE DECODERS
HORIZ SYNC
FXD ◇ HORIZ DR
VAR ◇ HORIZ DR (S)
COMPOSITE BLANKING
COMPOSITE SYNC
VERT SYNC
VERT DRIVE
÷2
÷287
÷825
825 LINE DECODERS
HORIZ SYNC
FXD ◇ HORIZ DR
VAR ◇ HORIZ DR (S)
COMPOSITE BLANKING
COMPOSITE SYNC
VERT SYNC
VERT DRIVE
÷2
÷231
÷1025
1025 LINE DECODERS
HORIZ SYNC
FXD ◇ HORIZ DR
VAR ◇ HORIZ DR
COMPOSITE BLANKING
COMPOSITE SYNC
VERT SYNC
VERT DRIVE
SYNC GENERATOR DRAWER

2

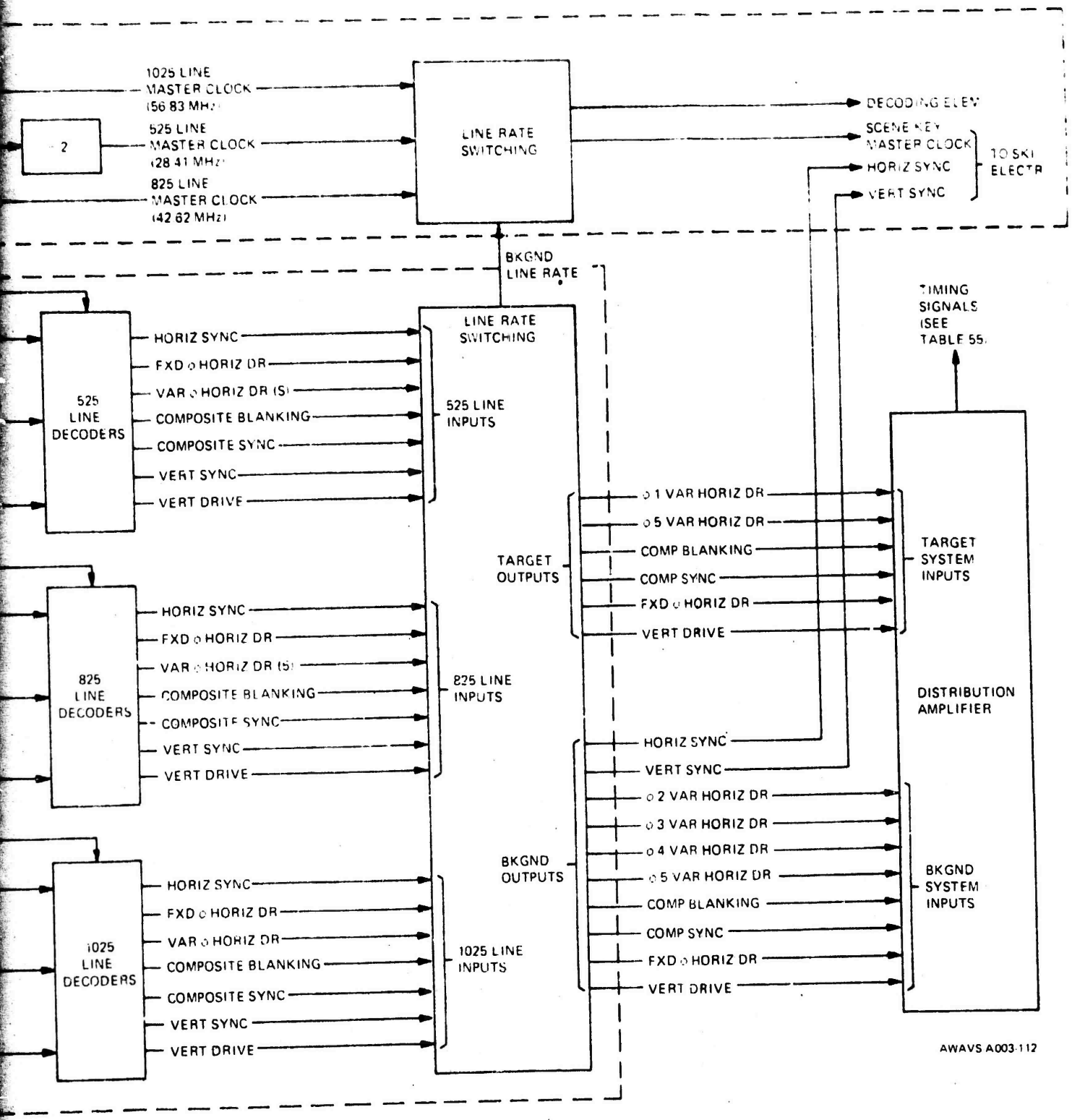

Figure 112. Master Timing Generator, Block Diagram

In addition to the fixed vertical and horizontal drives, the 14.21 MHz main clock is used by each decoder to provide a set of five delayed horizontal drive signals. These are collectively designated "variable phase" horizontal drive, with individual signals called phase 1 through phase 5. Variable phase horizontal drive delays are individually programmable to move AWAVS camera and display deflections in time with respect to video. Each delay is adjusted so that the start of unblank is coincident with the start of video. Delays may be programmed at a digital rate (based on main clock frequency) from zero to five usec.

3.6.3 Line Rate Switching. Within the line rate switching networks in both the SKI electronics and sync generator drawers, groups of line rate timing signals are digitally selected for distribution to the target and background systems. Any of the three available line rates (525, 825, or 1025) may be selected for either the target (TIG) or background (BIG) systems, under control of the TIG and BIG LINE RATE switches on the sync generator front panel (See Figure 113). For experimentation purposes, either the same or different line rates may be selected for both systems.

Digital switching in the sync generator drawer produces one set of timing signals for distribution to each system at its selected line rate. All signals developed within the sync generator are not output to either system. In addition to selecting one of the three high frequency signals as the SKI master clock, the SKI line rate switching provides 1452 decoding elements from the selected clock frequency. These are used for positioning video information at one of 1452 points across the active picture width. Horizontal blanking times have been chosen to permit the use of all points at all line rate with available master clock frequencies.

3.6.4 Timing Signal Distribution. The vertical and horizontal sync individual timing pulses (not composite sync) developed in the sync generator drawer are only used by the SKI electronics and are routed directly there without further amplification. All other system requirements for vertical and horizontal sync extract the timing from the composite sync signal. All remaining timing signals are applied to the sync generation distribution amplifier. This assembly redrives and distributes all input signals to the target and background systems via 75-ohm coaxial (BNC) connectors. Each connector is placarded with the signal identification. Destinations are given in Table 55.

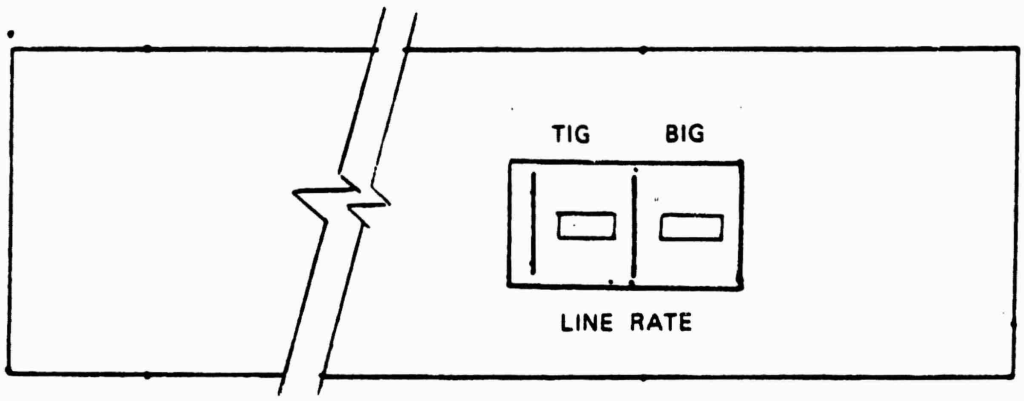

Figure 113. Sync Generator, Front Panel

TABLE 56. TIMING SIGNAL DISTRIBUTION

Signal Identification	Target System Distribution	Background System Distribution
Fixed Phase Horizontal Drive	1. TIG Monitor Interface 2. EOS TV Monitor Interface	1. SKC Electronic Interface 2. Background Monitor Interface 3. Background SEG
Variable Phase Horizontal Drives:		
Phase 1	1. TIG DARC	1. BIG DARC
Phase 2		1. SKC DARC
Phase 3		
Phase 4		
Phase 5	1. Spare No. 1 2. Spare No. 2	1. Spare No. 1 2. Spare No. 2
Vertical Drive	1. TIG Monitor Interface 2. TIG DARC 3. EOS TV Monitor Interface 4. Spare No. 1 5. Spare No. 2	1. SKC Electronic Interface 2. Background Monitor Interface 3. SKC DARC 4. BIG DARC 5. Spare No. 1 6. Spare No. 2
Composite Sync	1. TP Electronic Interface 2. Spare No. 1 3. Spare No. 2	1. BP Electronic Interface 2. Spare No. 1 3. Spare No. 2
Composite Blanking	1. Spare No. 1 2. Spare No. 2	1. SKC Electronic Interface 2. Spare No. 1 3. Spare No. 2

Connectors marked SPARE are connected to unused line drivers. The spare outputs named in Table 55 are marked with the appropriate signal identification. These include two spare outputs for each basic input, with the horizontal drive spares emanating from a spare programmable delay circuit; and, are intended to facilitate future growth. Phase 3 horizontal drive is reserved for the possible addition of an artificial wake image generator (WIG) attachment in the background system.

3.6.5 Phase-Lock Loop Monitoring. Two LED indicators on the front panel of the SKI electronics drawer (Figure 103) monitor linkage signals related to the phase-lock loop, as discussed in paragraph 3.6.1. The 30∿ indicator monitors the 30-Hz computer iteration rate from the linkage to which the VCO is phase-locked. The light flashes on once every five seconds when an accurate 30-Hz rate is detected. The COMPUTER LOCK-UP OUT OF RANGE light is a fault indicator that lights and remains lit in the event the TV frame rate received from the linkage is not coincident with the computer iteration rate. Loss of coincidence indicates a probable loss of phase-lock since the frame rate is developed from the VCO frequency.

3.7 Display System

The display system, as covered in the following paragraphs, encompasses the spherical screen which surrounds the motion platform, the target and background video projectors, and the scene keying camera. The projectors and camera, however, are described only in the area of display geometry, as related to projection of the video image and the viewpoint of the observer. (For a discussion of the electronics, servos, and optics, refer to applicable paragraphs covering the target and background projection systems.)

3.7.1 Projection Geometry. Figures 114 and 115 show the relationship of the FOV's for the projector and camera optics to the 10-foot diameter projection screen. Figure 114 shows elevation angles in respect to either the observers line-of-sight (LOS) in simulated level flight; or to the background projector axis, which is an imaginary line parallel to the observer's LOS. Figure 115, which is a bird's eye view from inside the dome, shows the two positions for the background projector and scene keying camera. Position 1 is the primary position used for simulated carrier landings. Position 2 is the alternate position required by the design specification for future use in other simulation situations such as formation flying and air-to-air combat. Table 56 provides quantitative data for the angles shown in the illustrations.

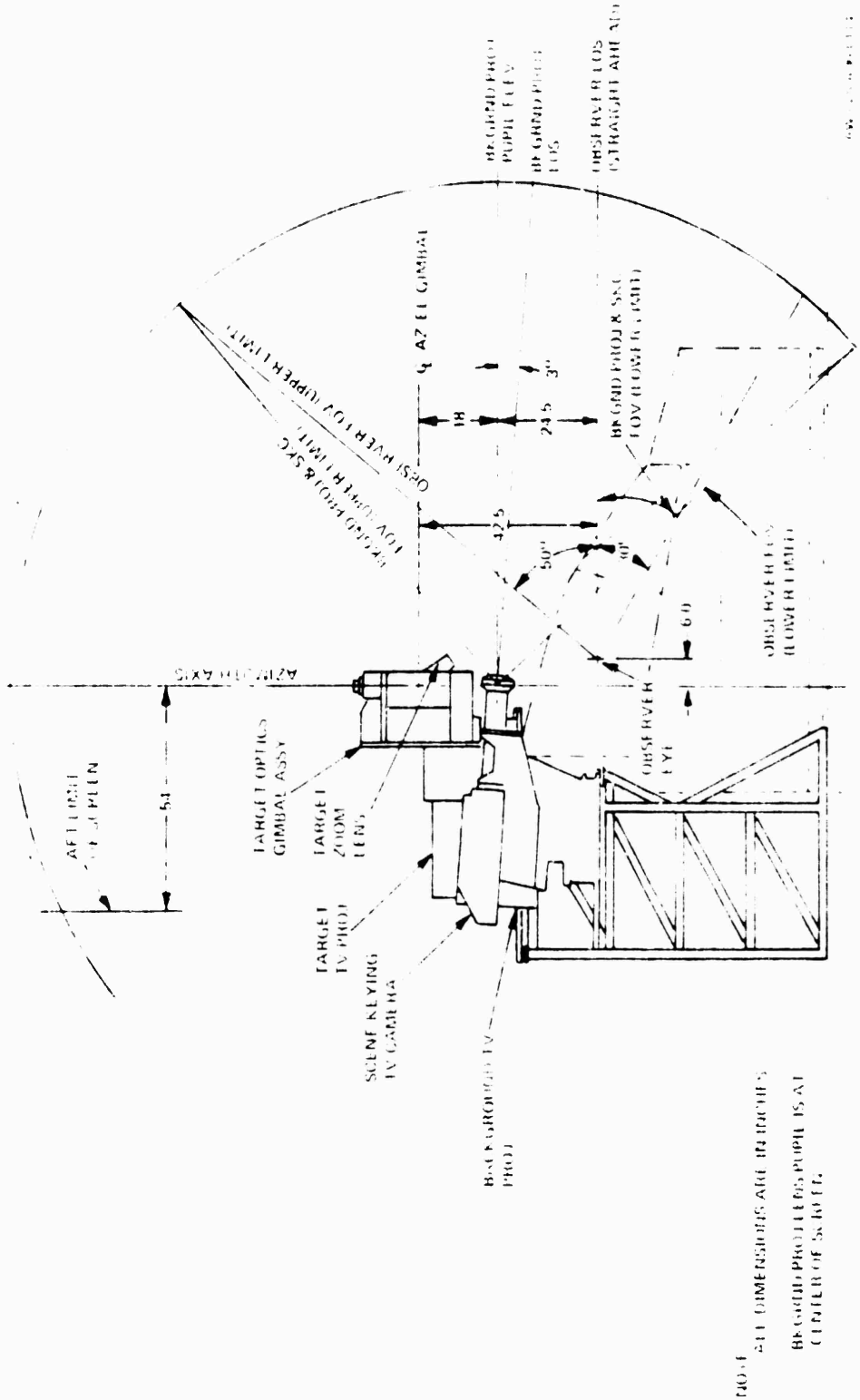

Figure 114. Display System Geometry Elevation Axis

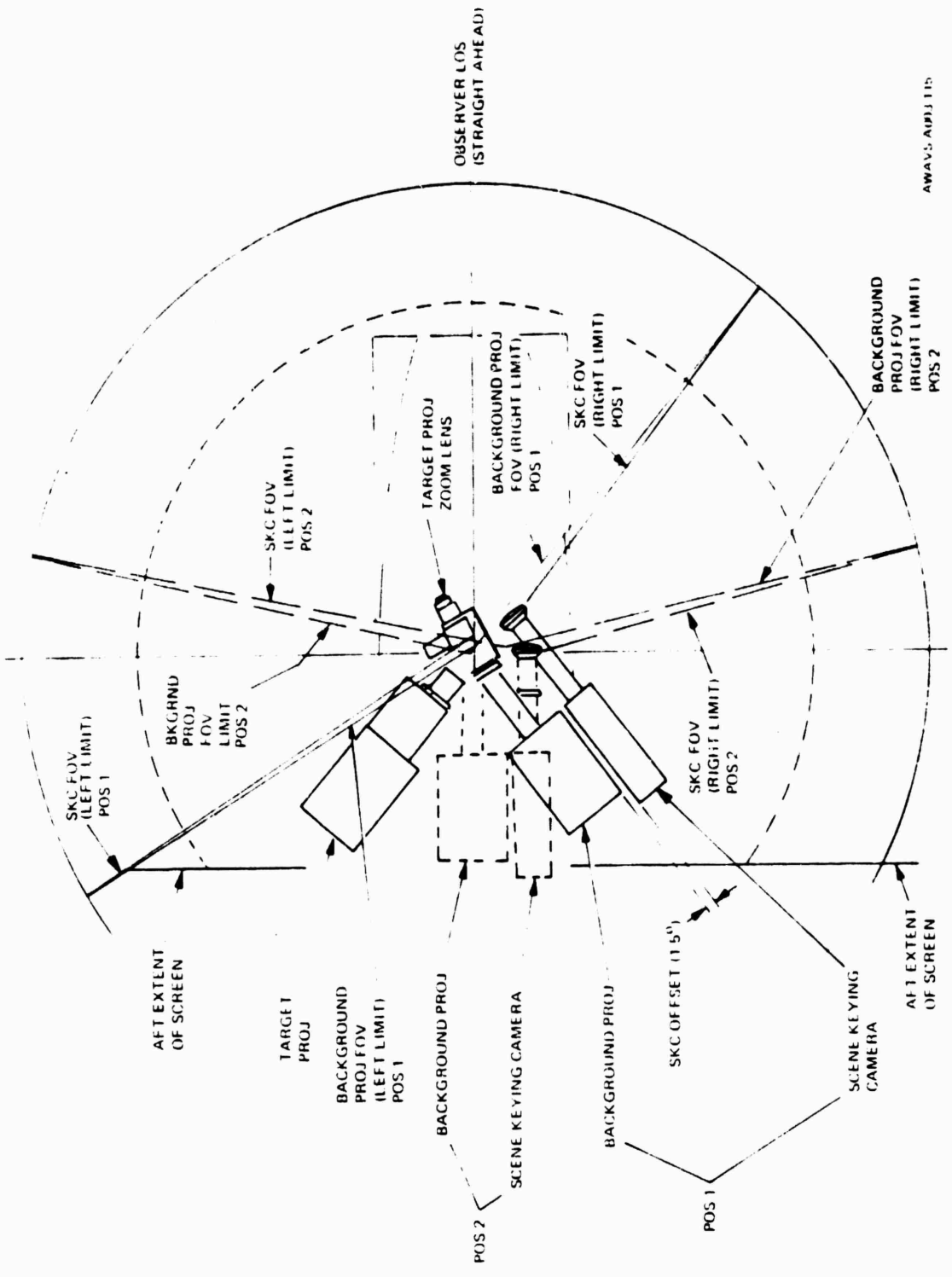

Figure 115. Display System Geometry, Azimuth Axis

Table 57. DISPLAY SYSTEM GEOMETRY

Description	Limits	
	Theoretical	Specification
Background Image System: (with respect to Observer)		
Elevation Upper Limit	+ 55°	+ 50°
Elevation Lower Limit	- 45°	- 30°
Elevation Total FOV	100°	80°
Azimuth Left Limit (Pos 1)	-125°	-120°
Azimuth Right Limit (Pos 1)	+ 45°	+ 40°
Azimuth Total FOV (Pos 1)	170°	160°
Azimuth Left Limit (Pos 2)	- 85°	- 80°
Azimuth Right Limit (Pos 2)	+ 85°	+ 80°
Azimuth Total FOV (Pos 2)	170°	160°
Target Image System: (with respect to Observer)		
Elevation LOS Mapping Upper Limit	+ 50°	Target System Limits Not Specified
Elevation LOS Mapping Lower Limit	- 30°	
Elevation LOS Mapping Total FOV	80°	
Elevation Gimbal Upper Limit	+ 90°	
Elevation Gimbal Lower Limit	- 60°	
Elevation Gimbal Total FOV	150°	
Azimuth LOS Mapping Left Limit	-120°	
Azimuth LOS Mapping Right Limit	+ 80°	
Azimuth LOS Mapping Total FOV	200°	
Azimuth Gimbal Left Limit	-158°	
Azimuth Gimbal Right Limit	+103°	
Azimuth Gimbal Total FOV	262°	

NOTE: Theoritical limits are design goals. It is anticipated that these will be the same as actual limits after test of system.

3.7.2 Display Screen Details. Spherical sections of aluminum are fastened together to form a partial sphere. Once the spherical sections have been bolted together, the seams are filled and sanded to the proper radius prior to painting, so they will not be apparent to the viewer when the visual scene is projected on the screen. The lightweight partial sphere structure is mounted to and supported by a mechanical super structure which is bolted to the motion platform. Where necessary, the motion platform is extended by means of outrigger supports. The screen is rigidly supported so that no movement of the displayed image is observable under normal, simulated, vehicle acceleration cues. The structure is designed to withstand a 4g acceleration.

The outside dimensions of the screen support structure are contained within a diameter no greater than 21 feet. To provide for future extension of the simulated field of view, the spherical display screen provides a minimum unobstructed field of view of 240° (±120°) horizontal and 120° (+90°, -30°) vertical, measured from the pilot's design eye position. The maximum weight of the display screen and supporting structure does not exceed 2,000 pounds, with the weight distributed.

It has been determined in the design analysis study that a gain of 2.5 is adequate to meet the worst case luminance requirements of Specification 212-102, as discussed in the previous paragraphs.

The paint for the display screen is of a resin base with suspended aluminum particles. The panels are cleaned to remove any grease and/or oil deposits, then rinsed and dried. The concave surface is then sprayed with horizontal overlapping strokes; the gain is controlled by the number of coats applied.

3.7.3 Screen Gain. The minimum screen gain is determined by the transmission of the various projectors and the required minimum 6 ft-lambert highlight brightness. The target and FLOLS systems require very low gains to meet the minimum requirements. The target projector would require a gain of only one to meet 6 ft-lamberts minimum of the FLOLS required an even lower gain. With a gain of one, there would be no variation in luminance with either a change in field or viewing position. The background projector however, because of its low transmission requires a screen gain of 2.5 to meet the 6 ft-lambert requirement. For field points within the required field of view, the maximum bend angle between the observers line of sight and the reflected ray is approximately 6^{o}. For any point in the field, the variation with head motion is approximately 2^{o}.

3.8 VTFS Interface

Interface between AWAVS and VTFS systems exists in the areas of linkage, Experimenter/Operator Station (EOS) controls and monitors, and power distribution. Although the linkage, computers and the EOS are actually integral parts of the VTFS, limited coverage herein is provided for the input and output signals to the extent that they affect the visual system. The power distribution system is covered separately in Section V.

3.8.1 Linkage. Linkage circuitry in the visual system consists of one card bin in each cabinet dedicated to interface of AWAVS signals. The cards essentially provide buffering and voltage amplification, and consist primarily of line receiver and line driver circuits. A block diagram of the linkage card bins showing generalized signal distribution is given in Figure 116. More detailed routing data will be found in the linkage input and output listings given in Tables 57 through 60. The tables provide a brief description of each signal, along with the linkage card address and word number, as well as the Singer drawing number and sheet number for the system drawing. Sheet numbers are shown in parenthesis in the drawing number columns. Listings are divided into analog and digital formats as well as inputs and outputs.

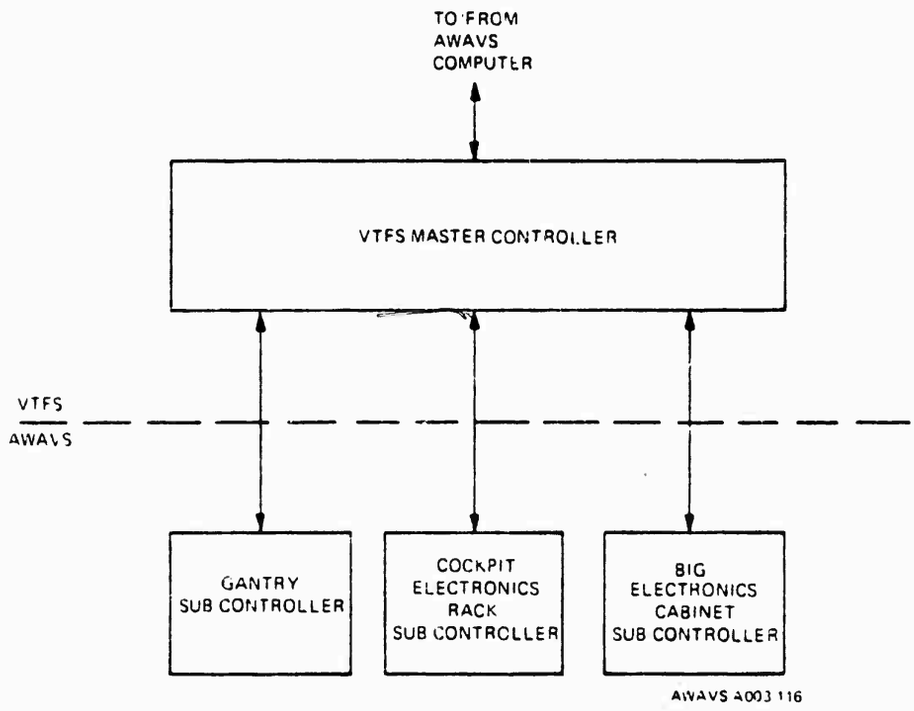

Figure 116. Linkage Block Diagram

TABLE 58. ANALOG INPUTS TO LINKAGE

MNEMONIC	DESCRIPTION	CARD ADDRESS	WORD	DWG & SHEET NUMBER
AVPPITCH	PROBE PITCH FEEDBACK	41	1	2Ø61316(3)
AVPFOCUS	PROBE FOCUS FEEDBACK	41	2	2Ø61316(4)
AVPZOOM	PROBE ZOOM FEEDBACK	41	3	2Ø61316(1)
AVPSINHD	SIN PROBE HEADING FEEDBACK	41	4	2Ø61316(2)
AVPCOSHD	COS PROBE HEADING FEEDBACK	41	5	2Ø61316(2)
AVPSINRL	SIN PROBE ROLL FEEDBACK	41	6	2Ø61316(5)
AVPCOSRL	COS PROBE ROLL FEEDBACK	41	7	2Ø61316(5)

TABLE 59. LINKAGE ANALOG OUTPUTS

MNEMONIC	DESCRIPTION	CARD ADDRESS	WORD	DWG & SHEET NUMBER
AVSTBRT	CARRIER STROBE RATE	24	1	2Ø61325(1)
AVDLINEB	DROP LINE LIGHTS BRIGHTNESS	24	2	2Ø61325(2)
AVRWEDGB	RUNWAY EDGE LIGHTS BRIGHTNESS	24	3	2Ø61325(1)
AVDKEDGB	DECK EDGE LIGHTS BRIGHTNESS	24	4	2Ø61325(2)
AVBNKLVL	SKC BLANKING LEVEL	25	1	2Ø61307
AVXFILMV	BIG FILM PLATE X VELOCITY	25	2	2Ø61304(1)
AVYFILMV	BIG FILM PLATE Y VELOCITY	25	3	2Ø61304(1)
AVTIGOOH	TIG CONTRAST	25	4	2Ø61322(1)
AVCMHEAV	CARRIER MODEL HEAVE	25	5	2Ø61319(1)
AVCMROLL	CARRIER MODEL ROLL	25	6	2Ø61319(2)
AVCMPITC	CARRIER MODEL PITCH	25	7	2Ø61319(3)
AVRWCNTB	RUNWAY C.LINE LIGHTS BRIGHTNESS	25	8	2Ø61325(1)
AVFSINX	SIN X PITCH WEDGE	52	1	2Ø61328(5)
AVFCOSX	COS X PITCH WEDGE	52	2	2Ø61328(5)
AVFSINY	SIN Y PITCH WEDGE	52	3	2Ø61328(6)
AVFCOSY	COS Y PITCH WEDGE	52	4	2Ø61328(6)
AVTIPZON	TARGET PROJ ZOOM DRIVE	52	5	2Ø61329(1)
AVTZMIRS	TARGET PROJ ZOOM IRIS DRIVE	52	6	2Ø61329(2)
AVMEATBL	FLOLS MEATBALL DRIVE	52	7	2Ø61324(1)
AVFLSZOM	FLOLS ZOOM DRIVE	52	8	2Ø61328(1)
AVFLIRIS	FLOLS IRIS DRIVE	53	1	2Ø61328(2)
AVFZMIRS	FLOLS ZOOM IRIS DRIVE	53	2	2Ø61329(2)
AVPIRIS	PROBE IRIS DRIVE	41	1	2Ø61316(6)
AVTIGFOV	TIG FIELD OF VIEW SCALE	41	2	2Ø61320(2)

TABLE 60. DIGITAL INPUTS TO LINKAGE

MNEMONIC	DESCRIPTION	CARD ADDRESS	WORD	BIT	DWG & SHEET NUMBER
JVFLTRKR	TRACKER FEEDBACK	32	Ø		2061323(1)
JVXFEEDB	GANTRY X FEEDBACK	32	1		2061312(4)
JVYFEEDB	GANTRY Y FEEDBACK	32	2		2061313(4)
JVZFEEDB	GANTRY Z FEEDBACK	32	3		2061314(4)
LVNORMBV	BIG VIDEO NORMAL	16	Ø	15	2061Ø7(25)
LVNORMTV	TIG VIDEO NORMAL	16	Ø	14	2061Ø7(26)
LVTIPLR1	TARGET PROJ LINE RATE 1	16	Ø	13	2061Ø7(18)
LVTIPLR2	TARGET PROJ LINE RATE 2	16	Ø	12	2061Ø7(18)
LVBIPLR1	BKGND PROJ LINE RATE 1	16	Ø	11	2061Ø7(18)
LVBIPLR2	BKGND PROJ LINE RATE 2	16	Ø	1Ø	2061Ø7(18)
LVRSTSBY	RASTER GENERATOR STROBE	16	Ø	8	2061315(2)
LVNORMGN	GANTRY IN NORMAL	16	Ø	7	2061317(1)
LVNORMVV	SERVO ELECTN IN NORMAL	16	Ø	6	2061Ø6
LVLGTNOT	LIGHT BANK NOT READY	16	Ø	5	2061318(1)
LVTESTPS	POSITIVE INTEGRATION ARRAY(CONSISTS OF:)	16	2	11	2061332(1)
LVTESTP1	TEST BOX 1 UP	16	2	11	2061332(1)
LVTESTP2	TEST BOX 2 UP	16	2	12	2061332(1)
LVTESTP3	TEST BOX 3 UP	16	2	13	2061332(1)
LVTESTP4	TEST BOX 4 UP	16	2	14	2061332(1)
LVTESTP5	TEST BOX 5 UP	16	2	15	2061332(1)
LVTESTNG	NEGATIVE INTEGRATION ARRAY(CONSISTS OF:)	16	2	6	2061332(1)
LVTESTN1	TEST BOX SW 1 DN	16	2	6	2061332(1)
LVTESTN2	TEST BOX SW 2 DN	16	2	7	2061332(1)
LVTESTN3	TEST BOX SW 3 DN	16	2	8	2061332(1)
LVTESTN4	TEST BOX SW 4 DN	16	2	9	2061332(1)
LVTESTN5	TEST BOX SW 5 DN	16	2	1Ø	2061332(1)
LVTEST6	TEST BOX SW 6 ON	16	2	5	2061332(1)
LVELSTOP	TEST BOX SW 7 ON	16	2	4	2061332(1)
LVINDVUL	TEST BOX SW 8 ON	16	2	3	2061332(1)
LVTEST1Ø	TEST BOX SW 1Ø ON	16	2	2	2061332(1)
LVTESTON	TEST BOX ON	16	2	1	2061332(1)
LVTEST9	ROTARY SWITCH ARRAY (CONSISTS OF:)	16	3	14	2061332(2)
LVTST9Ø1	TEST BOX ROTARY 1	16	3	4	2061332(2)
LVTST9Ø2	TEST BOX ROTARY 2	16	3	5	2061332(2)
LVTST9Ø3	TEST BOX ROTARY 3	16	3	6	2061332(2)
LVTST9Ø4	TEST BOX ROTARY 4	16	3	7	2061332(2)
LVTST9Ø5	TEST BOX ROTARY 5	16	3	8	2061332(2)
LVTST9Ø6	TEST BOX ROTARY 6	16	3	9	2061332(2)
LVTST9Ø7	TEST BOX ROTARY 7	16	3	1Ø	2061332(2)
LVTST9Ø8	TEST BOX ROTARY 8	16	3	11	2061332(2)
LVTST9Ø9	TEST BOX ROTARY 9	16	3	12	2061332(2)
LVTST91Ø	TEST BOX ROTARY 1Ø	16	3	13	2061332(2)
LVTST911	TEST BOX ROTARY 11	16	3	14	2061332(2)
LVTST912	TEST BOX ROTARY 12	16	3	15	2061332(2)

TABLE 60 DIGITAL INPUTS TO LINKAGE (CONTINUED)

MNEMONIC	DESCRIPTION	CARD ADDRESS	WORD	BIT	DWG & SHEET NUMBER
JVSKLOX4	SKC TEST POSITION X4	17	Ø		2Ø613Ø7( )
JVSKLOX5	SKC TEST POSITION X5	17	1		2Ø613Ø7(8)
JVSKLOX6	SKC TEST POSITION X6	17	2		2Ø613Ø7(9)
JVSKLOX7	SKC TEST POSITION X7	17	3		2Ø613Ø7(1Ø)
LVNORMCP	COCKPIT IN NORMAL	48	Ø	15	2Ø61317(2)
LVBIP1	BKGND PROJ IN POSITION 1	4Ø	Ø	14	2Ø6131Ø(1)
LVSKCBAD	SKI DIAMOND BAD	16	Ø	4	2Ø613Ø7
LVSFCIN	DIAMOND POSITION RD9	16	Ø	9	2Ø613Ø7

TABLE 61. LINKAGE DIGITAL OUTPUTS

MNEMONIC	DESCRIPTION	CARD ADDRESS	WORD	BIT	DUMP & SHEET NUMBER
JVXGNVEL	GANTRY X VELOCITY DRIVE	34	Ø		2Ø61312(1)
JVYGNVEL	GANTRY Y VELOCITY DRIVE	34	1		2Ø61313(1)
JVZGNVEL	GANTRY Z VELOCITY DRIVE	34	2		2Ø61314(1)
JVPSINFC	SIN PROBE FOCUS DRIVE	34	3		2Ø61316(4)
JVPSINRL	SIN PROBE ROLL DRIVE	34	4		2Ø61316(5)
JVPCOSRL	COS PROBE ROLL DRIVE	34	5		2Ø61316(5)
JVPSINZM	SIN PROBE ZOOM DRIVE	35	Ø		2Ø61316(1)
JVPCOSZM	COS PROBE ZOOM DRIVE	35	1		2Ø61316(1)
JVPSINHD	SIN PROBE HEADING DRIVE	35	2		2Ø61316(2)
JVPCOSHD	COS PROBE HEADING DRIVE	35	3		2Ø61316(2)
JVPSINPH	SIN PROBE PITCH DRIVE	35	4		2Ø61316(3)
JVPCOSPH	COS PROBE PITCH DRIVE	35	5		2Ø61316(3)
JVTGK26	TIG COEFFICIENT 16	36	Ø		2Ø61321(7)
JVTGK25	TIG COEFFICIENT 15	36	1		2Ø61321(7)
JVTGK27	TIG COEFFICIENT 17	36	2		2Ø61321(7)
JVTGK28	TIG COEFFICIENT 18	36	3		2Ø61321(8)
JVTGK29	TIG COEFFICIENT 19	36	4		2Ø61321(8)
JVTGK21Ø	TIG COEFFICIENT 20	36	5		2Ø61321(8)
JVTGK18	TIG COEFFICIENT 8	37	Ø		2Ø61321(5)
JVTGK19	TIG COEFFICIENT 9	37	1		2Ø61321(5)
JVTGK11Ø	TIG COEFFICIENT 10	37	2		2Ø61321(5)
JVTGK22	TIG COEFFICIENT 12	37	3		2Ø61321(6)
JVTGK23	TIG COEFFICIENT 13	37	4		2Ø61321(6)
JVTGK24	TIG COEFFICIENT 14	37	5		2Ø61321(6)
JVTGK12	TIG COEFFICIENT 2	38	Ø		2Ø61321(2)
JVTGK13	TIG COEFFICIENT 3	38	1		2Ø61321(3)
JVTGK14	TIG COEFFICIENT 4	38	2		2Ø61321(3)
JVTGK15	TIG COEFFICIENT 5	38	3		2Ø61321(4)
JVTGK16	TIG COEFFICIENT 6	38	4		2Ø61321(4)
JVTGK17	TIG COEFFICIENT 7	38	5		2Ø61321(4)
LVSTROBY	Y CARRIAGE DATA STROBE	39	Ø	15	2Ø61315(2)
JVTGK11	TIG COEFFICIENT 1	39	1		2Ø61321(2)
JVPCOSFC	COS PROBE FOCUS DRIVE	39	2		2Ø61316(4)
JVTGK21	TIG COEFFICIENT 11	39	3		2Ø61321(3)
LVSTROBS	VIDEO SYNC	18	Ø	15	2Ø613Ø7(22)
LVSKCOFF	SKC OFF	18	Ø	14	2Ø613Ø7(4)
LVSKICAL	SKC CALIBRATION	18	Ø	12	2Ø613Ø7(4)
LVXVELPS	BIG X POSITION VELOCITY	18	Ø	11	2Ø613Ø4(1)
LVYVELPS	BIG Y POSITION VELOCITY	18	Ø	1Ø	2Ø613Ø4(1)
LVABCLUD	ABOVE CLOUDS	18	Ø	9	2Ø613Ø6(1)
JVCARRX1	SKC CARRIER POSITION X1	18	2		2Ø613Ø7
JVCARRX2	SKC CARRIER POSITION X2	18	3		2Ø613Ø7
JVCARRY1	SKC CARRIER POSITION Y1	18	4		2Ø613Ø7(3)
JVCARRY2	SKC CARRIER POSITION Y2	18	5		2Ø613Ø7(3)
JVBGPI11	BIG ELEMENT 11	19	Ø		2Ø613Ø3(1)

TABLE 61. LINKAGE DIGITAL OUTPUTS (CONTINUED)

MNEMONIC	DESCRIPTION	CARD ADDRESS	WORD	BIT	DWG & SHEET NUMBER
JVBGPI12	BIG ELEMENT 12	19	1		2Ø613Ø3(2)
JVBGPI13	BIG ELEMENT 13	19	2		2Ø613Ø3(4)
JVBGPI21	BIG ELEMENT 21	19	3		2Ø613Ø3(1)
JVBGPI22	BIG ELEMENT 22	19	4		2Ø613Ø3(3)
JVBGPI23	BIG ELEMENT 23	19	5		2Ø613Ø3(4)
JVBGPI31	BIG ELEMENT 31	2Ø	Ø		2Ø613Ø3(2)
JVBGPI32	BIG ELEMENT 32	2Ø	1		2Ø613Ø3(3)
JVBGPI33	BIG ELEMENT 33	2Ø	2		2Ø613Ø3(5)
JVBGPIAA	BIG ELEMENT AA	2Ø	3		2Ø613Ø3(7)
JVCORX	SKC PATTERN X	21	Ø		2Ø613Ø7 4)
JVCORY	SKC PATTERN Y	21	1		2Ø613Ø7(4)
JVNSEAMG	COS SEA MERGE	21	2		2Ø613Ø6
JVBDER31	BODY TO EARTH 31	21	3		2Ø613Ø6
JVBDER32	BODY TO EARTH 32	21	4		2Ø613Ø6
JVBDER33	BODY TO EARTH 33	21	5		2Ø613Ø6
JVMHRIZN	COS HORIZON	22	Ø		2Ø613Ø6
JVHRVR	HORIZON/RVR	22	1		2Ø613Ø5
JVSEASHD	SEA SHADE	22	2		2Ø613Ø6
LVGNTMAL	GANTRY MALFUNCTION(LDO)	23	Ø	15	2Ø61315(2)
LVLBDAY	DAY FOR LIGHT BANK(LDO)	23	Ø	14	2Ø61318(1)
LVLBDUSK	DUSK FOR LIGHT BANK(LDO)	23	Ø	13	2Ø61316(1)
LVLBNITE	NITE FOR LIGHT BANK(LDO)	23	Ø	12	2Ø61318(1)
LVTESTL1	TEST BOX LIGHT 1 (LDO)	23	Ø	11	2Ø61332(2)
LVTESTL2	TEST BOX LIGHT 2 (LDO)	23	Ø	1Ø	2Ø61332(2)
LVSTBOFF	CARRIER LIGHT STROBE(LDO)	23	Ø	9	2Ø61325(1)
LVCUTLGT	FLOLS CUT LIGHT (LDO)	49	Ø	15	2Ø61324(2)
LVWAVLGT	FLOLS WAVEOFF (LDO)	49	Ø	14	2Ø61324(2)
LVAUXLGT	FLOLS AUX WAVEOFF(LDO)	49	Ø	13	2Ø61324(2)
LVBIPFIN	BKGND PROJ FILTER IN(LDO)	49	Ø	12	2Ø61310(1)
JVSKIADS	SKC COEFFICIENT NUMBER	5Ø	Ø		2Ø61308(3)
JVSKIPI	SKC COEFFICIENT BUFFER	5Ø	1		2Ø61308(3)
JVFSINRL	SIN FLOLS ROLL DRIVE	5Ø	2		2Ø61328(3)
JVFCOSRL	COS FLOLS ROLL DRIVE	5Ø	3		2Ø61328(3)
JVTSINRL	SIN TARGET PROJ ROLL DRIVE	5Ø	4		2Ø61329(3)
JVTCOSRL	COS TARGET PROJ ROLL DRIVE	5Ø	5		2Ø61329(5)
LVSTROBC	COCKPIT STROBE	51	Ø	15	2Ø61328(3)
JVTIPELV	TARGET PROJ ELEV DRIVE	51	1		2Ø61329(4)
JVTIPAZT	TARGET PROJ AZM DRIVE	51	2		2Ø61329(3)
LVSKCOUT	DIAMOND STROBE	18	Ø	13	2Ø61307
JVSKTPVC	VERT TP SHAD CT	2Ø	5		
JVSKTPHC	HORZ TP SHAD CT	2Ø	4		
LVSKTPBL	TP TOP ABV CNTR	18	Ø	8	
LVSKTPRT	TP LFT RGT CNTR	18	Ø	7	

The digital listings (Tables 59 and 60) also give the bit number assignment in the digital word for discrete inputs and outputs. The absence of an entry in the BIT column indicates use of the full 16-bit word. The abbreviation (LDO) found in the description column of Table 60 is indicative of a lamp driver output. These signals are of a greater magnitude than the other (logic level) digital signals, and are used to operate incandescent indicators or electromechanical devices.

Connector and pin numbers for each signal, as well as logic levels and analog signal characteristics, are given on the system drawings. These drawings are identified in Tables 57 through 60.

3.8.2 Visual System Controls. This paragraph summarizes the visual system controls and indicators which are found on the Experimenter/Operator Station (EOS). Although part of the VTFS rather than AWAVS, they are included in this report to maintain continuity of the visual system descriptions. The EOS controls and indicators involved are the FLOLS position indicator and those on the VISUAL subpanel. They are illustrated in Figure 117. All communication between these controls and the visual system is via the linkage; there is no direct interface.

The FLOLS BALL WIDTHS meter provides an indication, via linkage signals, of the pilot's elevation with respect to the FLOLS. If the meter registers ZERO, the pilot is exactly on the glide path and the pilot sees the meatball aligned with the datum lights. In response to the foregoing indication the EO operates the WAVE OFF and AUX WAVE OFF pushbuttons. The three FLOLS switch indicators (above two and CUT) are alternate-action pushbutton devices that operate the respective FLOLS lights on the carrier model. The CARRIER DECK LTS and RUNWAY STROBE LTS switch indicators are similar devices which govern operation of all carrier deck lighting except the runway centerline strobe lights. These five devices light when a return signal from the linkage shows that the designated action has occurred. A lit indicator does not merely signify that the button has been pressed.

The DAY/DUSK/NIGHT switch provides the linkage with selection of desired visability. The linkage, in turn, operates the light bank lighting and provides an indication of the selected visability to the special effects generator and the scene keying electronics. After initially extinguishing any lamps in the lampbank, a 15 minute waiting period starts. During this time, a signal from the linkage illuminates the red LT BNK NOT READY indicator.

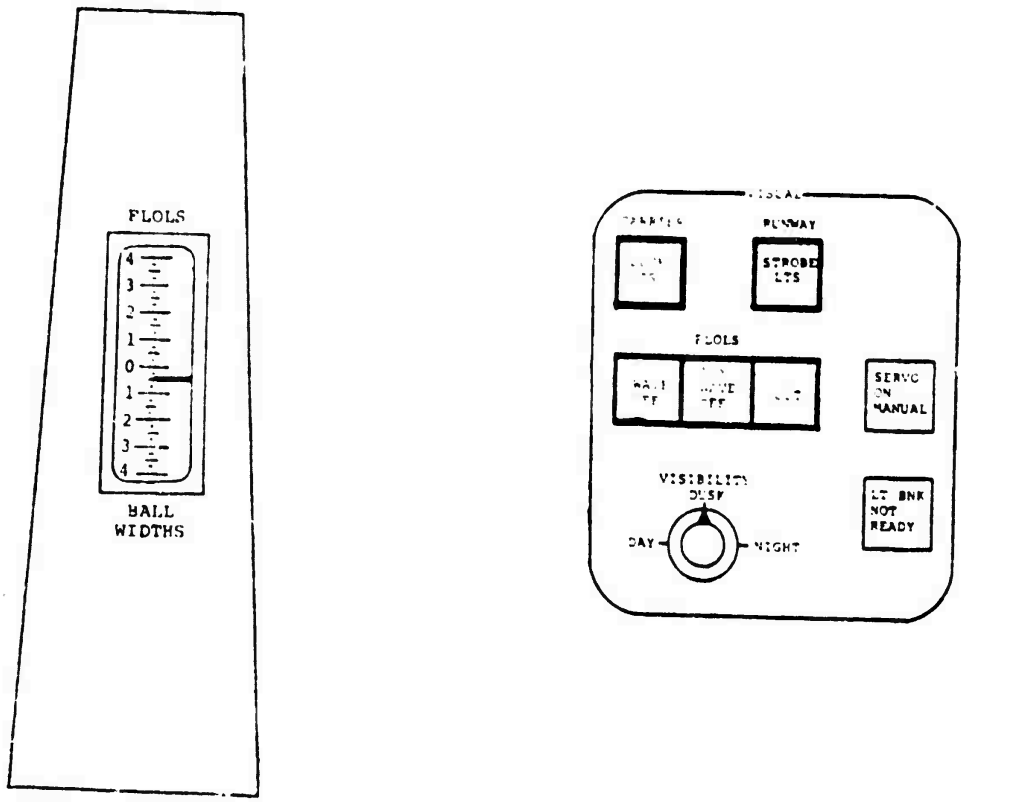

AWAVS-A003-117

Figure 117. EOS Visual Controls and Indicator

The red SERVO ON MANUAL indicator lights on a signal from the linkage when either of the following circumstances occur: (a) any maintenance panel key switch is set to TEST, or (b) the TARGET or BACKGROUND PROJECTOR MODE switch on the SKI electronics drawer is set to any test position (taken off NORMAL VIDEO).

Other control functions affecting operation of the visual system, including selection of operating modes, are accomplished using the input keyboard.

3.8.3 Video Monitoring - The EOS video monitor is physically a part of the EOS, but is functionally an entity of the target television camera system. (See paragraph 3.1.4 and Figure 36.) It is used to monitor target video only, and receives its input video directly from the target image enhancer, without going through the linkage.

SECTION IV

4.0 ENVIRONMENTAL SYSTEM DESIGN

This section provides an outline of the design techniques and implementation methods used in simulation of each environmental effect required by the trainer design specification. The impression of horizon, clouds, and sky is created electronically within the background special effects generator (SEG). The effect of restricted visibility on a scene viewed by the pilot is also simulated in the background SEG, insofar as the overall projected FOV is concerned. The effect of restricted visibility covering the target carrier and wake, however, is a composite of effects governed by both the target and background SEG's along with a controlled blanking level introduced at the SKI electronics. The effect of restricted visibility also affects luminance of the FLOLS image; this is controlled by computer signals to the FLOLS projector. Time of day is primarily evidenced by the ambient light produced by the light bank assembly. Selection of DAY, DUSK, or NIGHT, however, also effects both the background SEG and the SKI electronics.

4.1 Background Special Effects

The following paragraphs describe the environmental effects produced solely by the background special effects generator (SEG). These include signals which when displayed on the projection screen create the impression of cloud, fog, sky, and above-cloud flight. Also covered is the technique of horizon generation and extension of the seascape imagery to the horizon, as well as the generation of signals that control selection of the various effects.

4.1.1 Atmospheric Simulation. Synthetically generated video is used to fill in the background scene between the end of the BIG film plate imagery and the horizon. This fill-in level is known as seamerge video. Seamerge and film plate video are blended together where they merge. Clouds are simulated by a synthetically generated and separately adjustable uniform level. The horizon itself is formed by the relatively hard transition between seamerge shading and cloud level. Sky is simulated by a separately adjustable uniform level that is substituted for the seascape/seamerge image during above clouds flight. When flying above the clouds, a uniform cloud level fills in the picture below the horizon. In clouds, a constant cloud shade fills the entire picture.

4.1.2 Visibility Technique. The effect of restricted visibility on a below clouds scene viewed by the pilot will be to cause a loss of seascape detail and a reduction in contrast by attenuation and back scattering, which is proportional to the pilot-to-object visual range. Thus, the scene displayed in the cockpit will have seascape information at the bottom, and progressing upward across the picture a larger percentage of flat gray tone will be mixed with the terrain information. At the point of maximum visual range, the picture will be made up predominantly of gray and white tones, which will continue to the top of the picture. The mixing in of the gray tone will be smooth from bottom to the horizon so that no abrupt changes in tone take place to create the impression of a window shade effect. Restricted visibility is varied by the addition of cloud shade so as to form a gradual mix of seascape video to cloud level varying as a function of RVR/H (visibility range/attitude).

When below clouds, the upper portion of the picture is cloud shade down to the horizon. Moving below the horizon, the component of cloud shade is decreased as the range to the point on the simulated sea plane decreases, and there is a complementary increase in the seascape video component of the scene. (This simulates fog or haze.) In clouds, a constant cloud shade fills the entire picture. Above clouds, a cloud shade fills the portion of the scene below the horizon. The component of cloud shade decreases with increasing angle above the horizon, and sky shade is complementarily mixed in.

4.1.3 Special Scene Effects. Special effects will be simulated in the following manner:

a. Variable Haze Effects and RVR. The visibility effects simulation will employ an electronic system which operates on the video as a function of visibility range, established by the visibility control at the E/O Station. The range and effects of altitude will be continuously computed according to the instantaneous line of sight.

A close approximation of true atmospheric visibility effects can be acheived by the assumption of a uniformly scattered atmosphere. This assumes a water droplet fog, as contrasted with a smog in which many of the particles are opaque. With a uniformly scattering atmosphere, seascape visual information is attenuated as an exponential function of visual range, and background illuminance (haze) simultaneously increases exponentially towards sky brightness. These effects can be expressed as follows:

$$V_v = V_t e^{-R/R_0} \quad \text{and} \quad V_h = V_s (1 - 3^{-R/R_0})$$

V_V is the visible portion of the seascape reflectance modulation (V_t) and V_h is the haze brightness seen as the portion of sky brightness (V_S) superimposed on the visible portion of the terrain modulation. In these expressions, R_0 is a visibility constant representing a range for 37% of the clear weather visual modulation, and is equivalent of the limited visibility generator. R is the instantaneous range of a point in the scene and is a function of the television raster deflection signal in the implementation. The function e^{-R/R_0} is therefore a mixture of sweep signals representative of the display and aircraft roll and pitch. The analog function then controls a video modulator to obtain the desired video attenuation.

b. Weather Capability. Ceiling effects will be provided by initiating a "white-out" of the visual scene when the ceiling altitude is reached. A variable ceiling control signal, will be compared with the simulated aircraft altitude and will activate the limited visibility generator when the set altitude is reached.

c. Over-the-Clouds Flight. Simulation will be provided for an above-cloud presentation with a featureless white cloud top and a light sky above. The presentation of the horizon line will be controlled by the same system as the normal sky horizon and will respond to the roll and pitch of the aircraft.

d. In-the-Clouds Flight. A condition of "in cloud" will be displayed whenever the aircraft altitude is between "cloud bottom" and "cloud top". The "in cloud" condition will be controlled by the computer. The cloud condition will be an extension of the sky scene to completely cover the display.

4.1.4 Ceiling Ranges. Both cloud base and cloud top altitude levels are entered via the computer input keyboard at the E/O Station. Cloud levels are expressed with respect to mean sea level. Cloud base and cloud top are individually selectable over ranges of zero (mean sea level) to 9900 feet.

4.1.5 Horizon Generation Technique. (See Figure 118.) The technique of generation of the horizon is best understood by considering the technique for computing "R" in the expressions referred to in Paragraph 4.1.3 where R is the magnitude of the range of the instantaneous line of sight from the pilots nominal viewpoint to the horizontal plane of reference BIG film plate as seen in the display image. Under the idealized condition of a flat earth:

$$R = \frac{h}{\cos \lambda}$$

where h = Aircraft altitude above terrain

$\cos \lambda$ = Direction cosine between R and local vertical

In the SEG, the horizon line is artificially placed in the camera generated scene at points in the scene where $\cos \lambda$ becomes identically equal to a specified value (λ = same angle from local vertical with all points when λ is greater than the specified value being replaced by overcast. The accuracy of placement of the horizon in the displayed image is governed by how accurately the combination of visual effects hardware and computer inputs can calculate the correct value of $\cos \lambda$ for any point in the display.

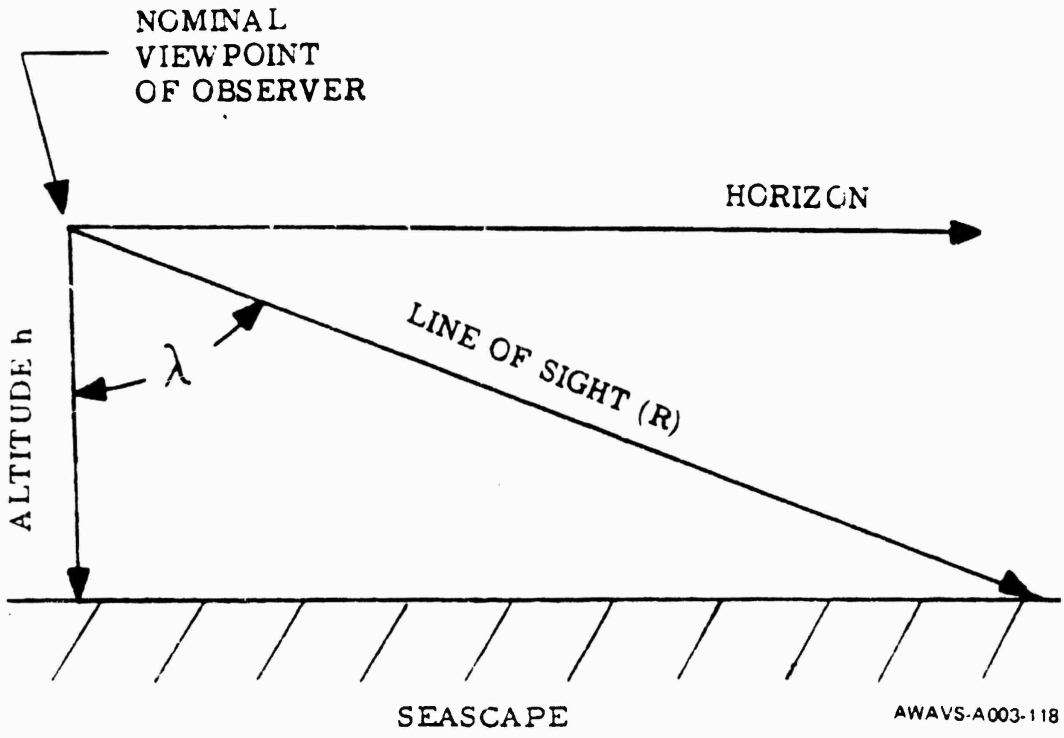

Figure 118. Graphic Representation of Horizon Generation

4.2 Target Visibility Effects

Simulation of environmental effects related to target (carrier and wake) visibility consists of merging a fog level with the target image. This is somewhat simplified by the fact that from the observer's viewpoint in a landing situation, the projected target appears in a two-dimensional plane lacking significant depth. Thus, only a uniform density fog level must be simulated, as opposed to a graduated level varying with slant range and altitude as used in the background visibility situation.

Notwithstanding the foregoing simplification, there still remains three distinct elements involved in implementation of this uniform density fog level. These are illustrated in the simplified block diagram given in Figure 119, and summarized below:

a. Attenuation of TIG camera video signal level in response to a selected RVR.

b. Attenuation of FLOLS optical image intensity in response to a selected RVR.

c. Variance of the blanking pedestal within the SKI electronics (from black for unlimited visibility to white for zero visibility) in response to calculated cloud level.

4.2.1 Target Scene Component. Inasmuch as the TIG video is electronically attenuated to fade in or fade out the carrier and wake before combining with the FLOLS image, the intensity of the FLOLS image must also be controlled at a similar point. Since simulation of the FLOLS is done entirely by electro-optical means, the aperature of the independent FLOLS iris is varied in response to a servo command. The target projection system synthesizes the carrier and wake image from the attenuated video signal, and optically merges it with the FLOLS image before projecting the composite into the blanked "hole" from the background system. Control of both target video and FLOLS luminance is governed by linkage analog outputs.

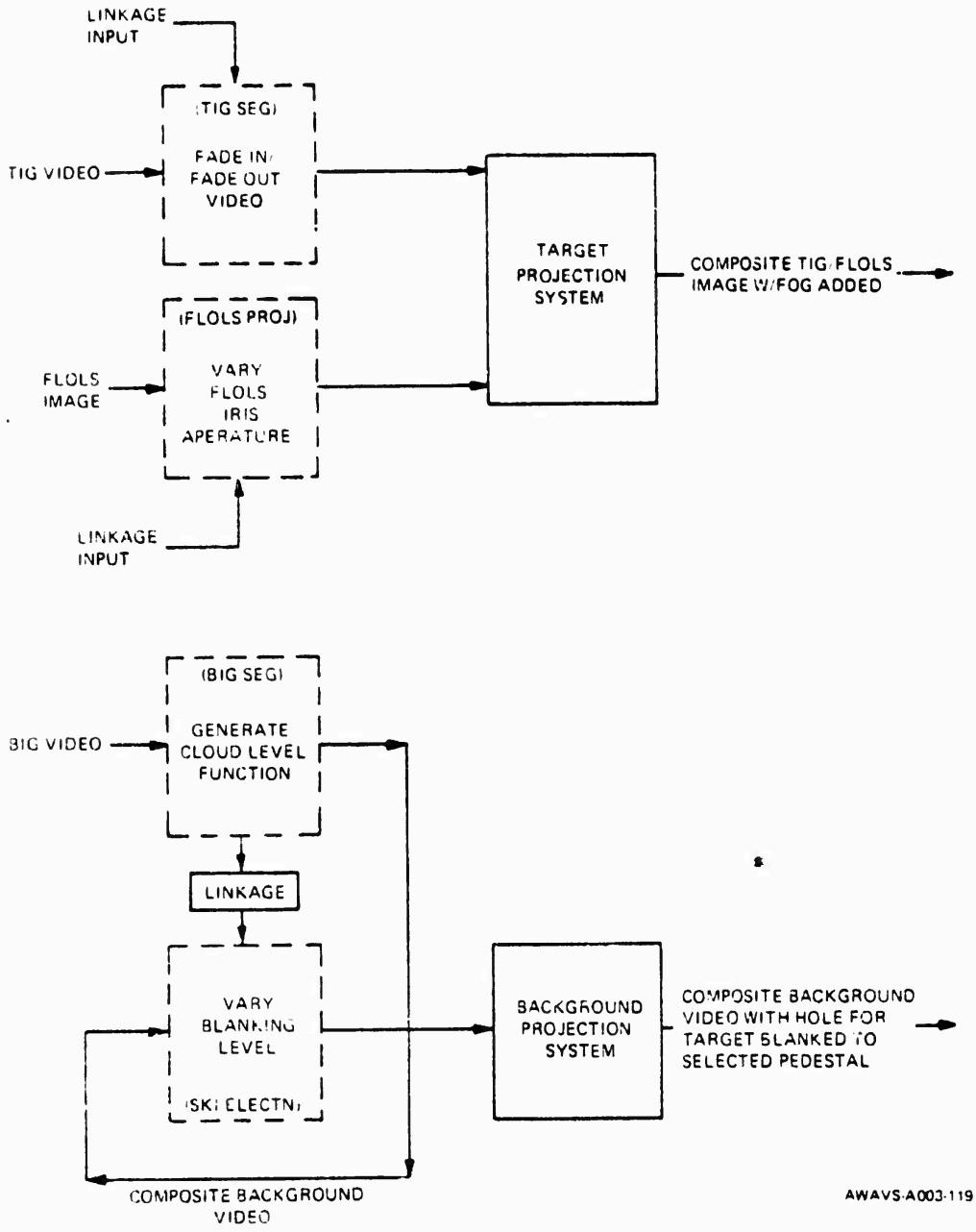

Figure 119. Target Visability Effects, Simplified Block Diagram

4.2.2 Background Scene Component. The "hole" is formed by selective blanking in response to the scene keying camera video. Under conditions of unrestricted visibility a black hole is presented on the screen for keying in the target image. Rather than referencing black for all visibility situations, it has been discovered that superior realism can be effected by controlling the reference level, such that the reference plus the target image gives the desired peak white for zero visibility. Increased visibility occurs by changing the reference (or blanking pedestal) from gray to black. The extent to which the blanking pedestal must be varied is calculated within the background SEG. The SKI blanking level from the background SEG is transmitted to a blanking generator in the SKI electronics drawer. The blanking generator is turned off when the carrier is totally hidden in fog; otherwise, a linkage analog output controls the blanking pedestal.

4.2.3 Composite Target Display. Implementation of the target/background hole composite restricted visibility effect for five selected conditions is outlined in Table 61. The background video referenced therein is actually the cloud level (or blanking pedestal) within the keyed hole projected by the background TV projector.

4.3 Time-of-Day Simulation

Time-of-day is manually selectable at the E/O Station. It can be either DAY, DUSK, or NIGHT. The primary and most obvious effect of time of day selection is the illumination or extinguishing of the 1000-watt incandescent lamps on the lamp bank assembly. These illuminate the carrier model from a position behind the gantry. For daytime simulation all 32 lamps are on. At dusk 16 lamps are on, with 16 alternate lamps off (forming a checker board pattern). To simulate night, all lamps are turned off. Since the incandescent lamps light only the carrier model and wake, they control time-of-day simulation for the target image system only.

Time of day simulation for the background system is effected by electronic means in controlling the gain of an adjustable gain amplifier in the background SEG. The background time of day function varies the gain of individual components of the background video signal as a function of ambient light, thereby matching the scene brightness of the target system as governed by the light bank. No special effects are involved in daylight simulation. The background dusk condition is simulated by attenuating all components of background video. For night simulation either the seascape/seamerge or sky level video (depending upon aircraft orientation to clouds) is set to zero, while cloud shade is only attenuated. This provides a realistic night background with a visible horizon formed by the scene transition to cloud level.

TABLE 62. TARGET VISIBILITY IMPLEMENTATION

Scene Component / Visibility	Carrier Video	Background Video	Scene Keyed Signal	Resulting Target Display
Carrier Hidden in Fog	0 volt amplitude	Constant gray shade	Off	Gray picture with no target image. Scene is background.
Carrier Just Becoming Visible	5% amplitude	Constant gray shade	Not on (computer controlled)	Gray picture with faint white image emerging from gray fog.
Carrier 50% visible	50% amplitude	Scene keyed, but fog reduced only small amount	On (computer controlled)	Carrier more visible; lowered (50%) contrast, with fog becoming less dominant
Carrier 75% Visible	75% amplitude	Fog reduced to 25% by scene keying signal	On (computer controlled)	Carrier 75% visible, with white image; fog providing a 25% contrast reduction level
Carrier Not Obscured by Fog	100% amplitude	Fog reduced to zero by scene keying signal	On (computer controlled)	Carrier inset into background scene.

During simulation of night conditions, as with total fog conditions, the SKI blanking generator (para. 4.2.2) is turned off. Although not apparent to the observer, the selection of dusk or day also affects the SKI electronics, such that the reference level for minimum detection of a carrier photographed by the keying camera must be altered.

SECTION V

5. POWER DISTRIBUTION AND LOAD ANALYSIS

5.1 Facility and VTFS Power Distribution

The facility power distribution provides 480/277 volt and 208/120-volt, three-phase, 60-Hertz power. All primary power for the visual system is controlled and distributed by VTFS circuitry. For a description of 208/120 volt power distribution to the main busses of the VTFS power cabinet (Unit 5), refer to the Visual Technology Flight Simulator (VTFS) Trainer Design Report F002. Details of facility power distribution to the VTFS, including 480/277 volt distribution to the lamp bank power box, are provided in the Aviation Wide-Angle Visual System and Visual Technology Flight Simulator Facilities Report A00K/F003.

5.2 AWAVS 480/277 Volt AC Power Distribution

The model illumination lamp bank assembly consisting of a total of 32 lamp/ballast combinations presents the only AWAVS requirement for 277-volt ac input power. Each lamp/ballast combination draws approximately 4.1 amperes. Lamps are 1000-watt metallic hallide arc lamps. Starting current for ballasts does not exceed running currents. Ballasts permit only a 10% change in lamp wattage for a 10% change in input voltage.

Design of the light bank assembly is based upon similar lighting systems used by Singer on the 2B31 and 2B33 visual systems. Use of the 480/277-volt power requirement results in a current per phase of approximately 46 amperes rather than the almost 110 amperes that would be required from a 208/120 volt system.

A simplified schematic of the light bank power distribution curcuitry is given in Figure 120.

Because of the requirement for operating half the lights for dusk operation, the load is split into two halves by two 150-ampere rating magnetic contactors which are controlled via signals from the gantry cabinet. To further split the load and provide short-circuit protection, the output to the main light bank is divided through two 6-pole, 80-ampere magnetic breakers which provide power to the ballast assemblies for the arc lamps. A third 6-pole, 5-ampere breaker is provided to route power to the gantry power assembly for fill-in lighting. The fill-in lighting is provided to prevent shadowing of the model by the gantry tower structure. The power distribution circuitry is contained within the light bank junction box assembly.

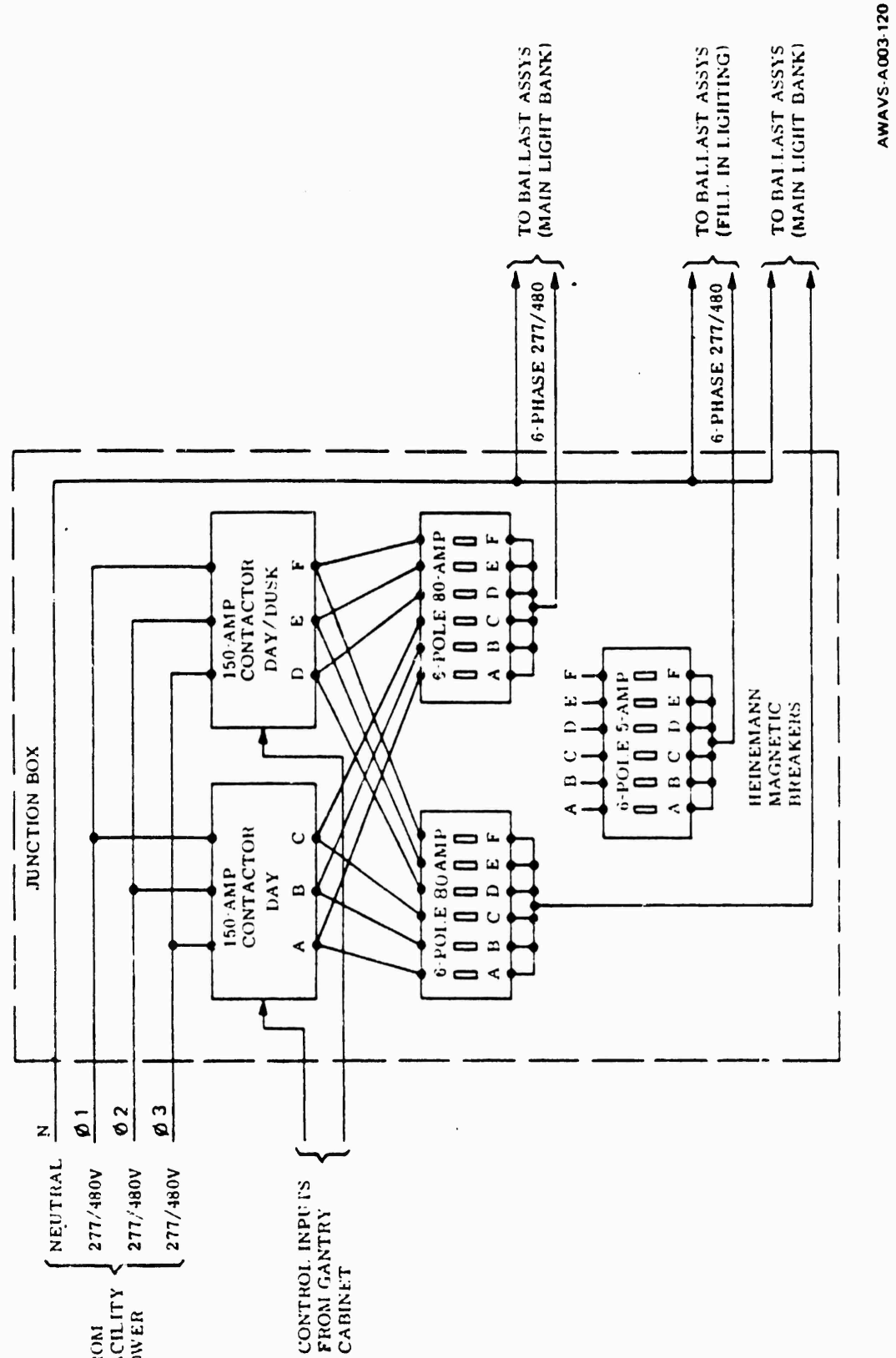

Figure 120. AWAVS 480/277 Volt Power Distribution, Simplified Schematic

5.3 AWAVS 208/120 Volt AC Power Distribution

Distribution of 208/120 volt, 3-phase ac power and 120-volt single-phase power for AWAVS originates at the VTFS main power cabinet. Figure 121 illustrates distribution of this power from the main power busses to the user AWAVS components. This illustration identifies and provides electrical ratings for all circuit breakers and distribution components whether part of AWAVS or VTFS hardware. AWG sizes for all inter-cabinet ac primary power conductors (including neutrals and power grounds) are also included in Figure 121. Names of VTFS power cabinet control circuits (corresponding to switch-light markings on VTFS cabinet 5 front panel) which govern operation of the high-current distribution contactors at the outputs of the main busses are also indicated.

Distribution contactors for all AWAVS outputs except 3-phase power to the cockpit electronics rack are physically located in the VTFS power cabinet. The electronics rack contactor is located within the cockpit electronics structure, along with its analog switch drive and supplementary output circuit breakers for the drive and supplementary output circuit breakers for the FLOLS simulator and target projection subsystems. The control circuits which govern operation of the contactors (see above) are part of the VTFS, and are therefore not described in this report.

Special safety features incorporated in design of the AWAVS power distribution circuitry include maintenance switches, cabinet overheat sensors, and an emergency stop feature. Those interface with the power control circuitry in the VTFS, and are described in the following paragraphs.

5.3.1 Maintenance Switches. There are eight maintenance switches on the AWAVS equipment cabinets - one on each maintenance panel and two on the gantry. Each maintenance switch, when activated, generates an inhibit signal which is sensed by its related power control card in the VTFS power cabinet. Each of the distribution contactors mentioned above is driven from one of these power control cards. When sensed, the inhibit signal will prevent energization of its respective distribution contactor, and thereby prevent distribution of primary power to associated components. A maintenance switch is an alternate action, lighted pushbutton device which lights red when in maintenance and green when not in maintenance.

The relationship between AWAVS switches and VTFS power control circuitry is shown by Table 62. Distribution of utility 120-volt, single-phase power is not affected by the maintenance switches. It is noteworthy that a maintenance switch is strictly a safety device to interrupt ac power and prevent inadvertent reapplication while maintenance is being performed on a particular cabinet or assembly. It does not control the operational mode of the simulator or of any cabinet.

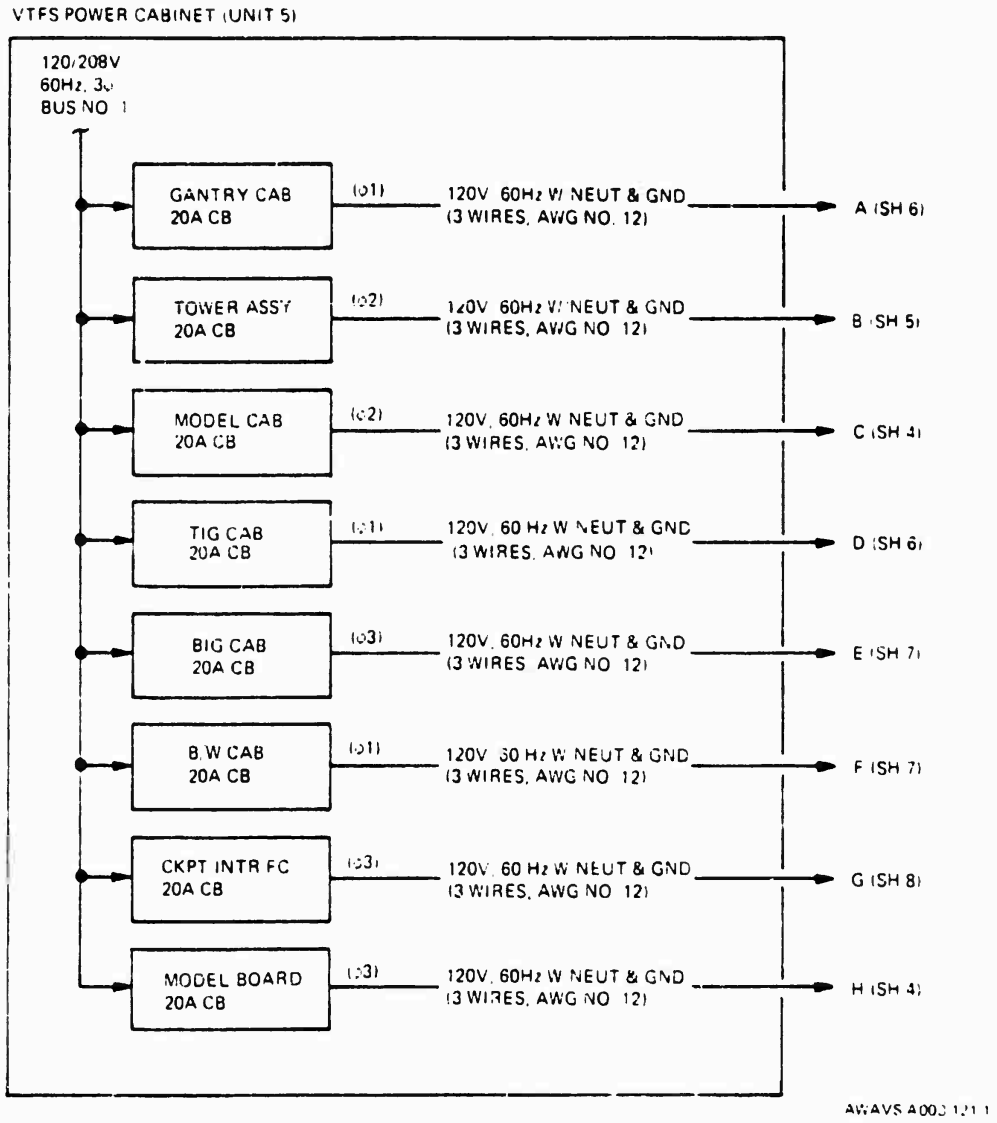

Figure 121. AWAVS 208/120 Volt, 60 Hz Power Distribution Diagram (Sheet 1 of 8)

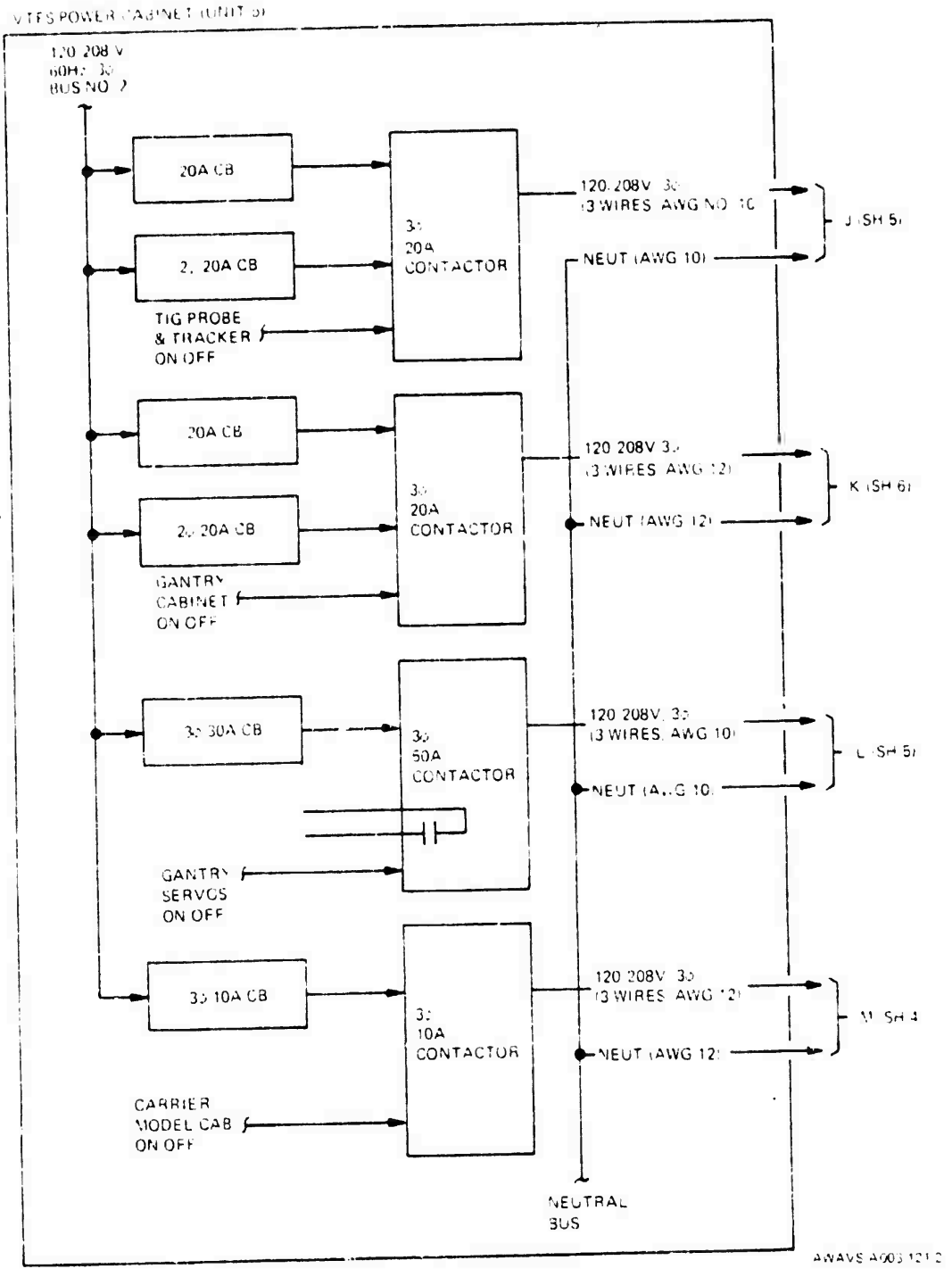

Figure 121. AWAVS 208/120 Volt, 60 Hz Power Distribution Diagram (Sheet 2 of 8)

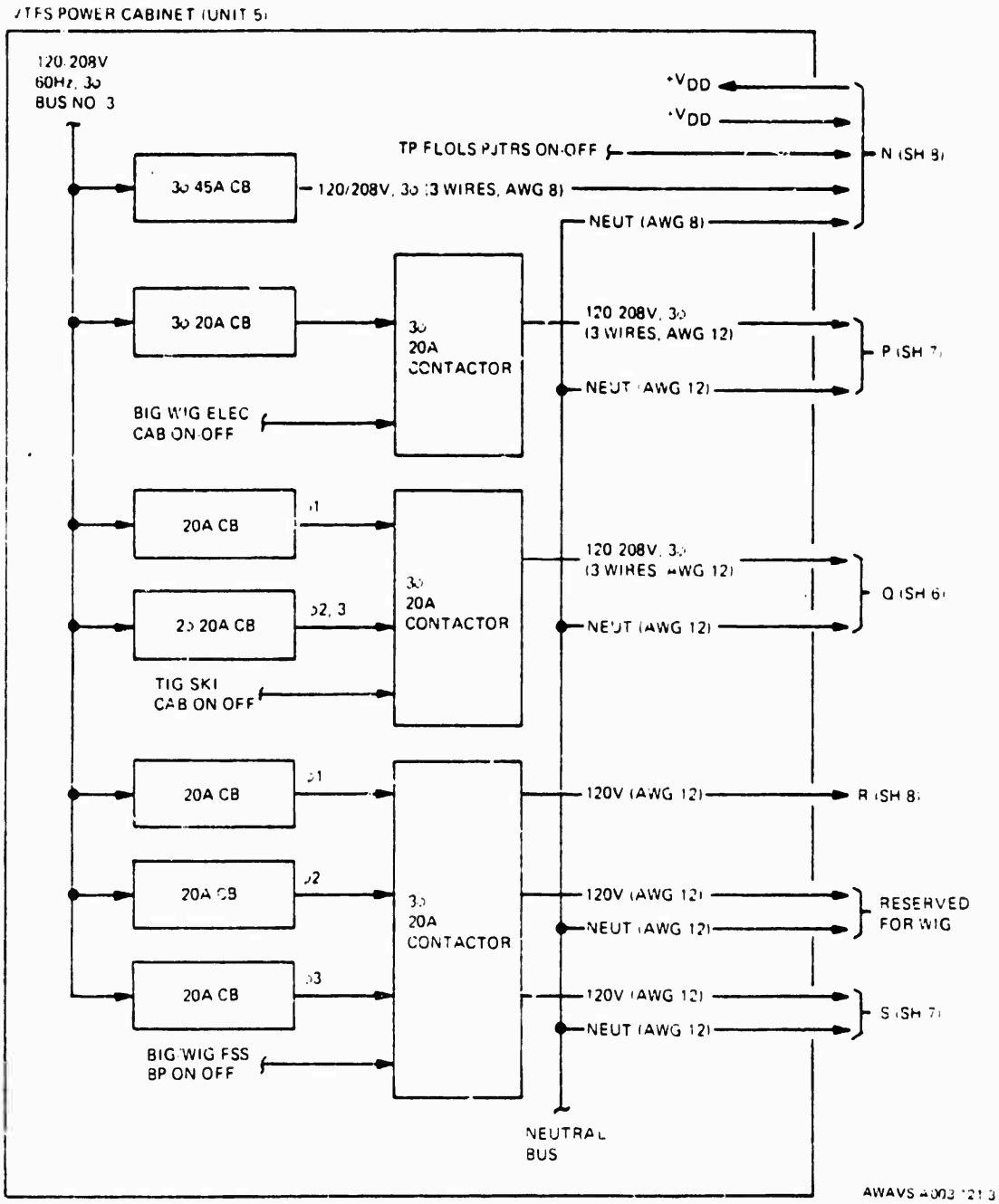

Figure 121. AWAVS 208/120 Volt, 60 Hz Power Distribution Diagram (Sheet 3 of 8)

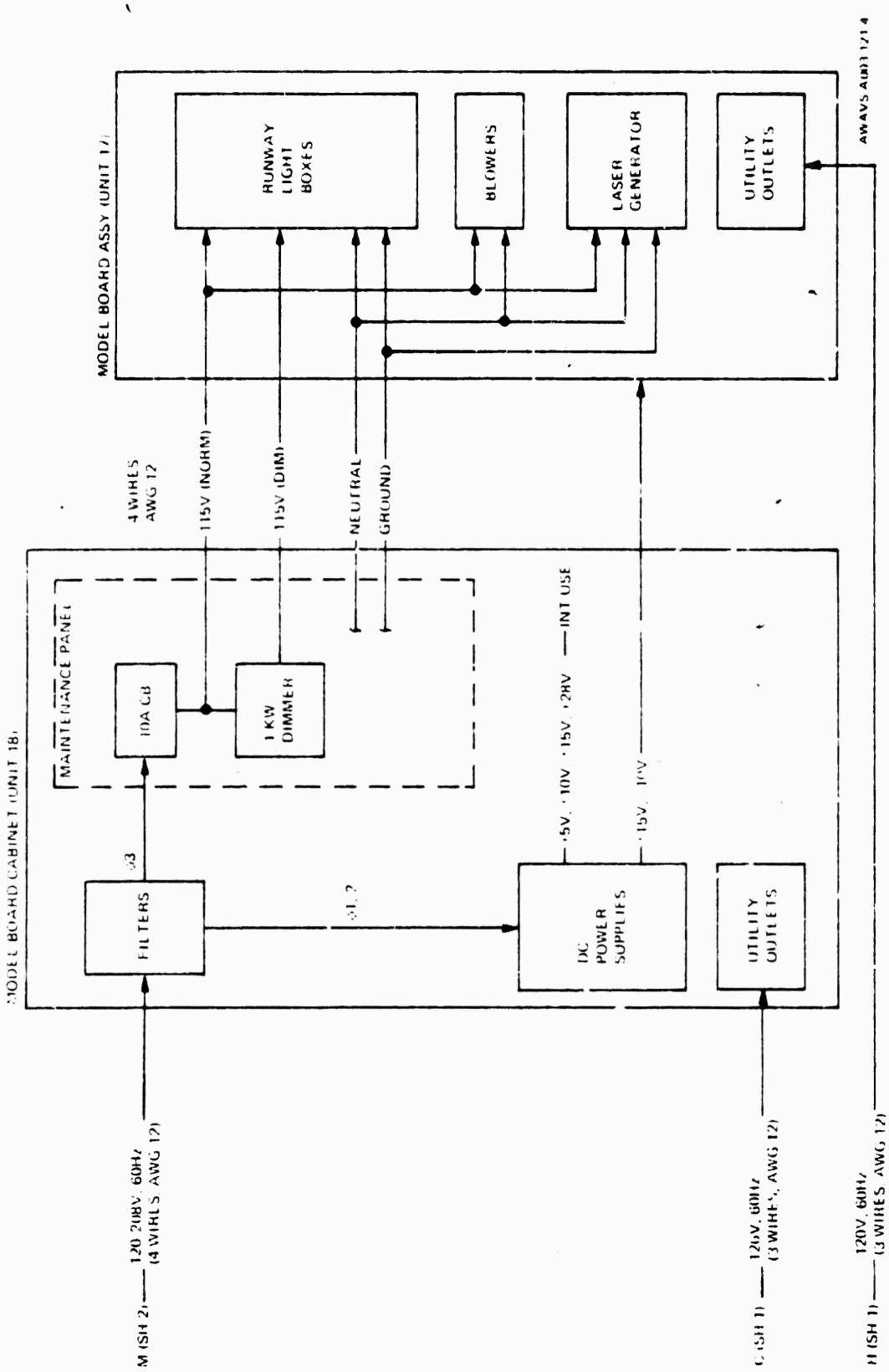

Figure 121. AWAVS 208/120 Volt, 60Hz Power Distribution Diagram (Sheet 4 of 8)

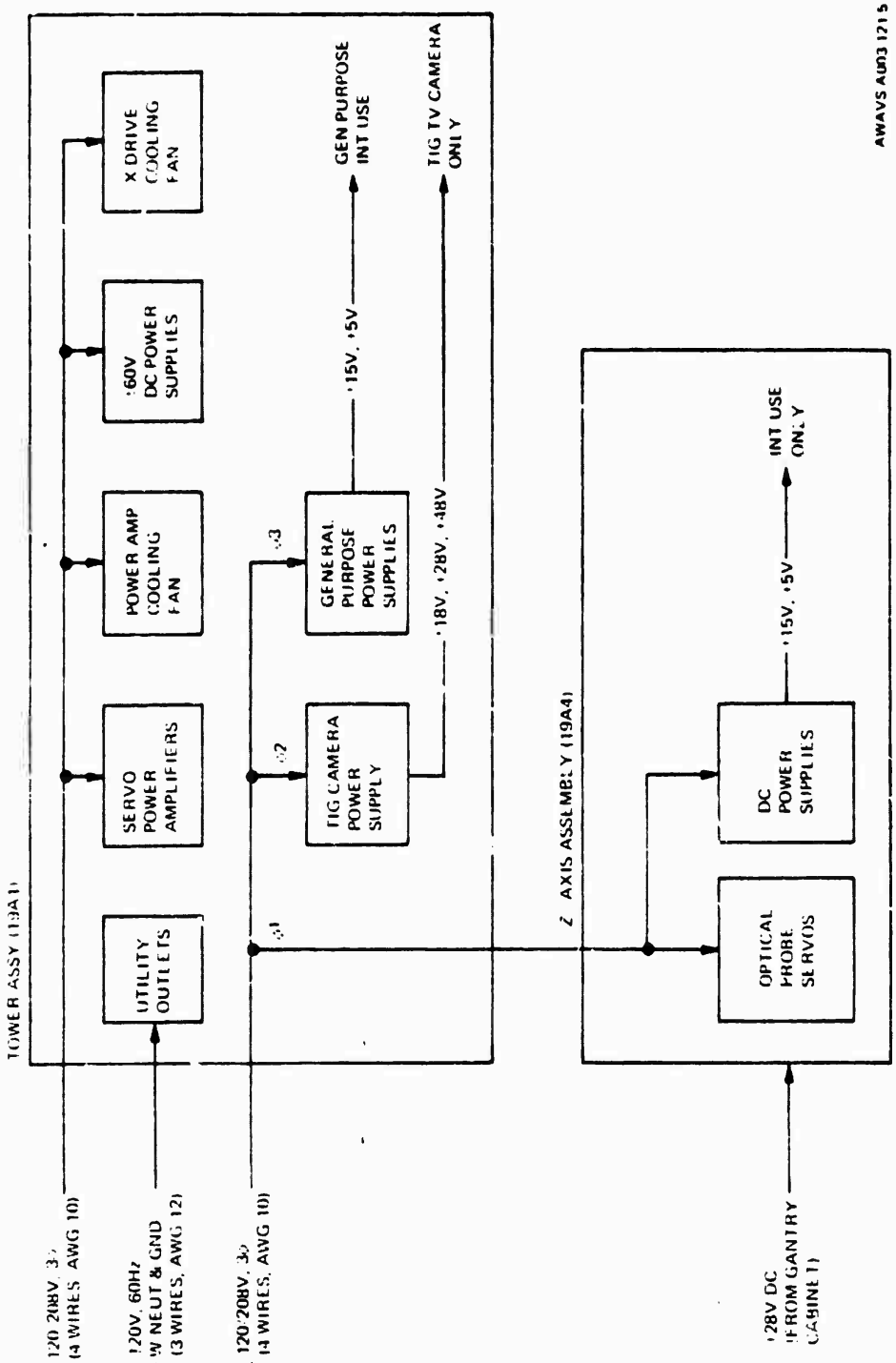

Figure 121. AWAVS 208/120 Volt, 60 Hz Power Distribution Diagram (Sheet 5 of 8)

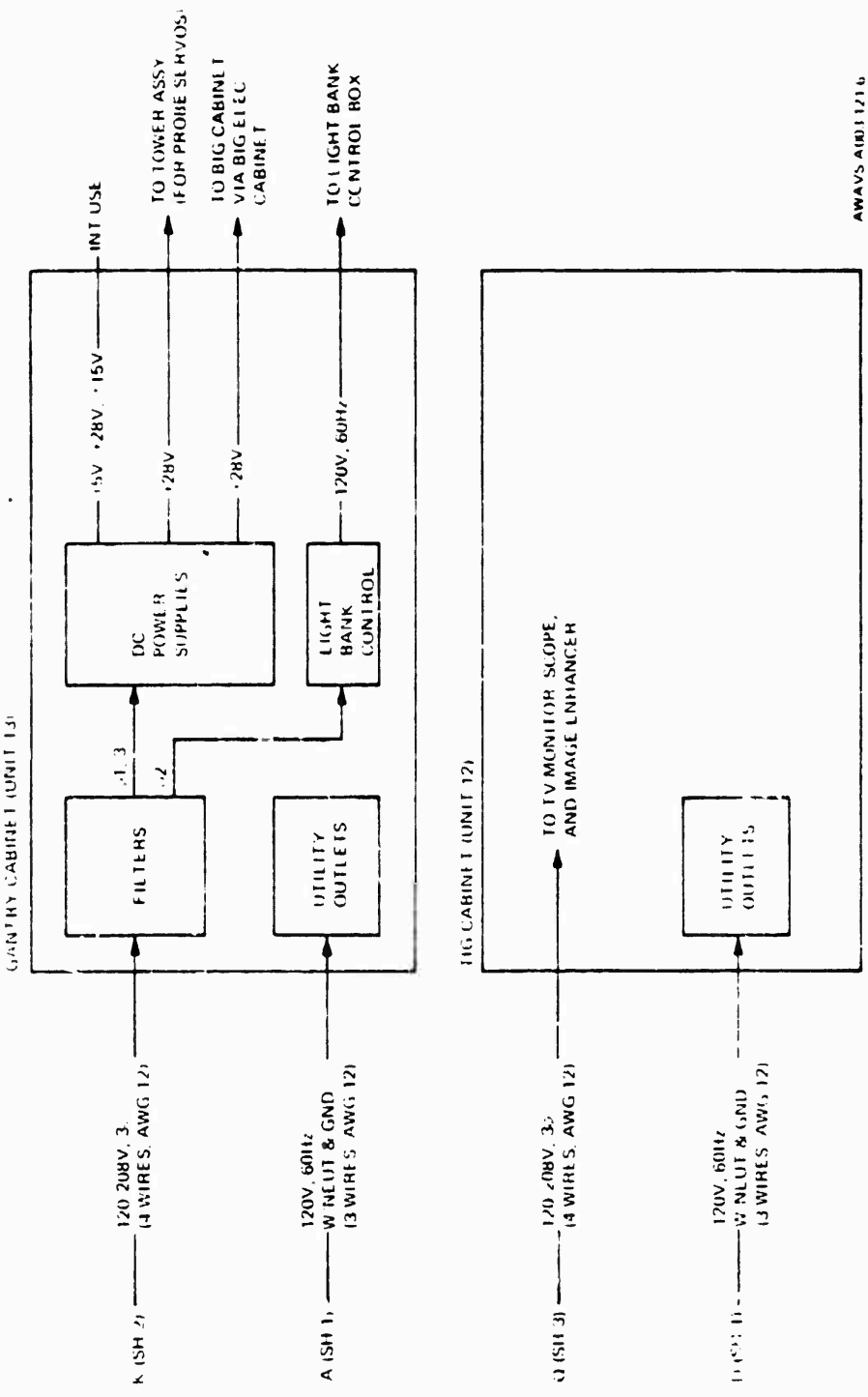

Figure 121. AWAVS 208/120 Volt, 60 Hz Power Distrioution Diagram (Sheet 6 of 8)

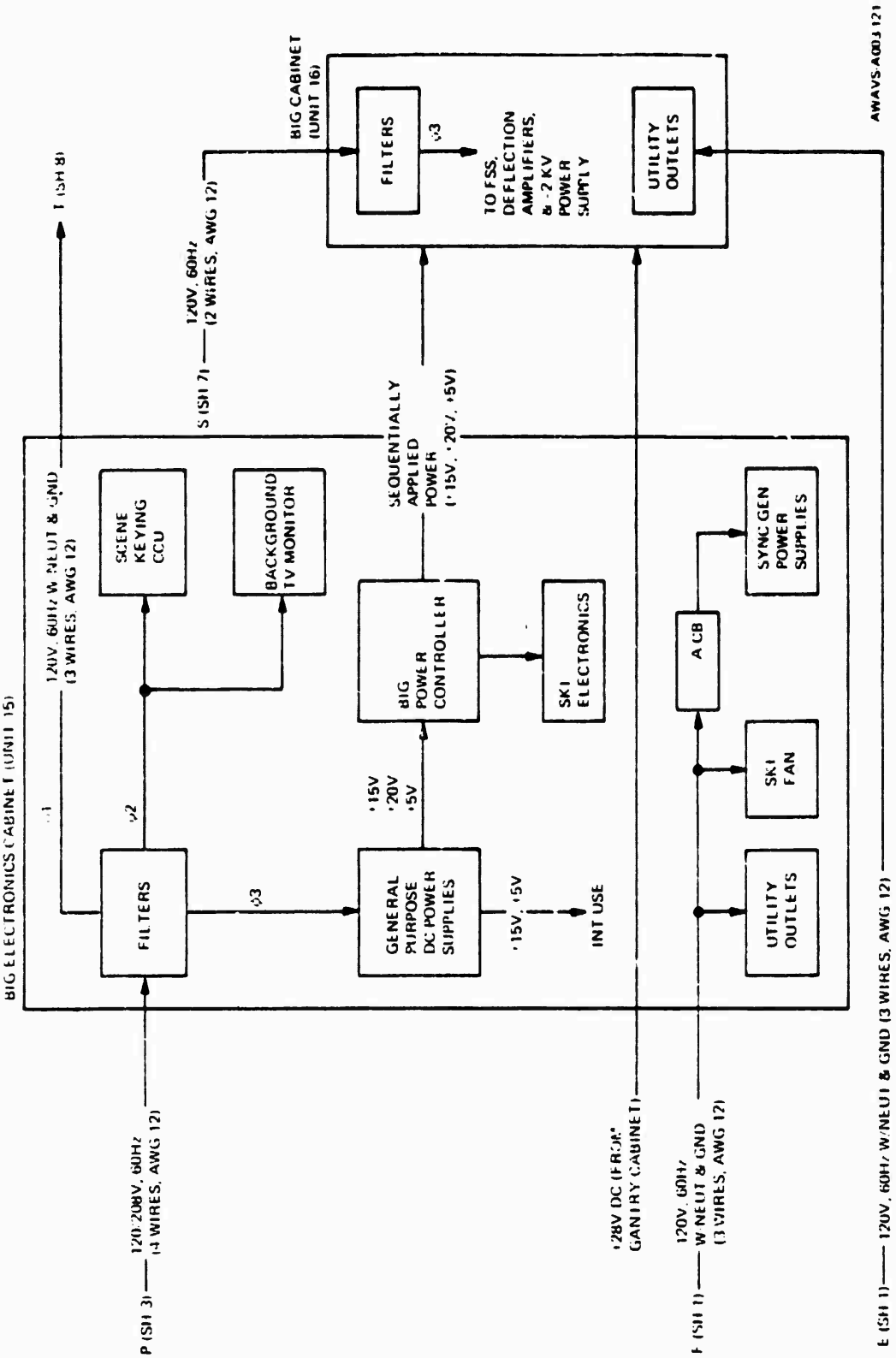

Figure 121. AWAVS 208/120 Volt, 60 Hz Power Distribution Diagram (Sheet 7 of 8)

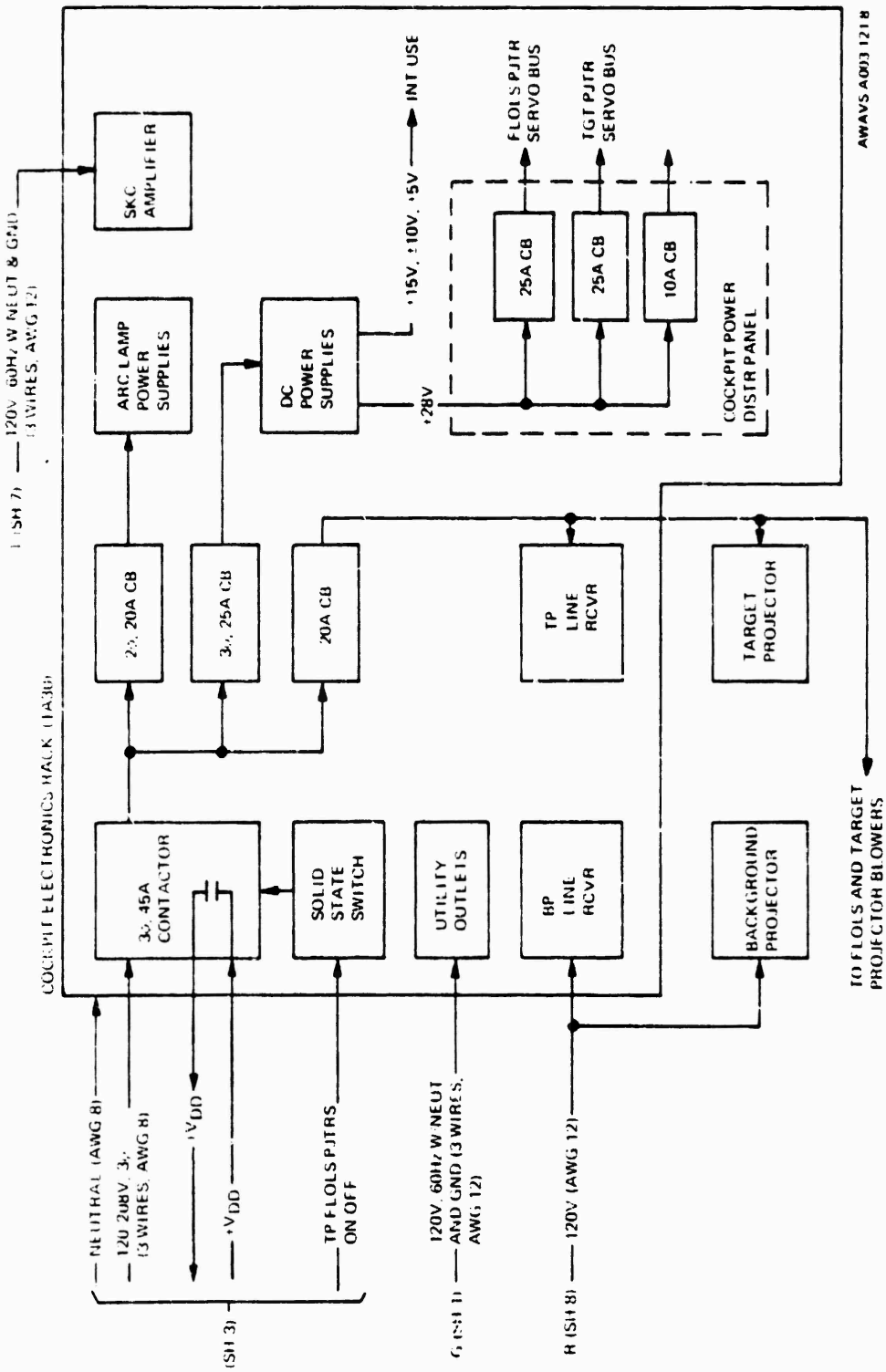

Figure 121. AWAVS 208/120 Volt, 60 Hz Power Distribution Diagram (Sheet 8 of 8)

TABLE 63. AWAVS MAINTENANCE SWITCH APPLICATIONS

Affected VTFS Power Control Circuit	Location of Applicable MAINT SWITCH
TIG PROBE & TRACKER	Gantry Z-Axis Carriage Assy
GANTRY SERVOS	Gantry Tower Assy
GANTRY CABINET	Gantry Cabinet Test Panel
CARRIER MODEL CABINET	Model Board Cabinet Maintenance Control Panel
BIG/WIG ELEC CABINET	BIG/WIG Maintenance Panel (ELECTRONIC CABINET POWER Section)
BIG/WIG FSS BP	BIG/WIG Maintenance Panel (IMAGE GENERATOR POWER Section)
TIG/SKI	TIG Cabinet Maintenance Panel
TP FLOLS	Cockpit Electronics Test Panel

5.3.2 Overheat Sensors. Temperature sensors are located in every AWAVS equipment cabinet, plus the gantry assembly and the cockpit electronics rack. Each temperature sensor is adjustable, and is preset to activate an overheat relay in the VTFS power cabinet in the event of an overtemperature condition. Overheat relays activate shunt trip circuit breakers to remove primary power from the main power busses. An indicator light labled CABINET OVERHEAT located in the general vicinity of each temperature sensor lights to indicate where the overtemperature condition originated. One such indicator is located at the top of each single or double bay electronic equipment cabinet. Indicators are also found on the tower assembly, the Z-axis carriage, and the cockpit electronics enclosure.

5.3.3 Emergency Stop. There are twelve EMERGENCY STOP pushbutton switches distributed throughout the visual system - one next to each CABINET OVERHEAT indicator and one at the top rear of each equipment cabinet. The visual system emergency stop circuitry is tied into that of the VTFS, and causes a complete shutdown of both systems by tripping the main bus circuit breakers. When the emergency stop system has been activated, all main bus circuit breakers must be manually reset to start up both the VTFS and AWAVS.

TABLE 64. DC POWER SUPPLIES

Volts	Current	Mfr. & Model No.
Model Board Cabinet		
+ 5V	6A	Transistor Devices SPS 1868
±10V	1.7A	Transistor Devices SPS 1907
±15V	3A	Transistor Devcies SPS 1863
±28V	28A	LAMDA 282729-126
Gantry Cabinet		
+5V/+28V	16A/22A	LAMDA 282729-113
±15V	9A	LAMDA 282729-114
±28V	28A	LAMDA 282729-126
BIG Electronics Cabinet		
+ 5V	8A	H.P. 62005E
-12V	3A	H.P. 62012C
+20V	6A	Transistor Devices SPS 1925
-20V	6A	Transistor Devices SPS 1925
±15V	20A	Transistor Devices SPS 1865
± 5V	30A	Transistor Devices SPS 1862
- 5V	4A	H.P. 62005C
Cockpit Electronics Enclosure		
+28V	68A	Transistor Devices SPS 1983
±15V	9A	LAMDA 282729-114
± 5V	60A	Transistor Devices SPS 1864
±10V	1A	Transistor Devices SPS 1875
Gantry Tower Assy		
+60V	1A	Transistor Devices SPS 1950
-60V	1A	Transistor Devices SPS 1950
+ 5V	30A	Transistor Devices SPS 1862
±15V	9A	LAMDA 282729-114
±18/±28/+48V	4.5A/3.25A/2.0A	H.P. 62018E/62028E/62948E

5.4 DC Power Distribution

DC power requirements are fulfilled through the use of commercially available power supplies, where possible. These power supplies are all supplied by 120-volt single-phase ac power, and are generally located either in the same electronics cabinet as their load equipment or in the electronics cabinet which services the load equipment. Distribution of ac power to the dc supplies is shown in Figure 121. Power supply outputs and loads are given in Table 63, along with the manufacturer's identification for each unit. The power supplies covered herein do not include special purpose units such as video high-voltage supplies. (These are covered in the individual subsystem descriptions in Section III of this report.)

5.5 Visual System Power-Up Sequencing. (To be supplied.)

5.6 Visual System Power-Down Sequencing. (To be supplied.)

5.7 AC Load Analysis

The model illumination lamp bank assembly, consisting of 32 1000-watt incandescent lamps, presents the total AWAVS requirement for 480/277 volt, 3-phase, 60-Hz power. Calculated per phase current for this requirement is approximately 46 amperes. The projected loads for 208/120 volt, 3-phase, 60-Hz power are summarized in Table 64.

TABLE 65. 208/120 VOLT AC LOAD ANALYSIS

Load Description	Ø1 Current (amps)	Ø2 Current (amps)	Ø3 Current (amps)	Power Factor	Total Power (watts)
Gantry Cabinet DC Supplies	10	12	14	To be Determined	To be Determined
BIG Electronics Cabinet DC Supplies	5	10	5		
TIG Cabinet DC Supplies	8	7	10		
Tower Assembly DC Supplies	30	30	30		
Cockpit Enclosure DC Supplies	20	20	20		
Background TV Projector	-	-	12.5		
Target TV Projector	12.5	-	-		
FLOLS Arc Lamp Supply #1	7.5	7.5	-		
FLOLS Arc Lamp Supply #2	-	7.5	7.5		
Model Board Cabinet	10	10	10		
Model Board Structure	10	-	-		
TIG Camera HVPS	5	-	-		
BIG Flying Spot Scanner HVPS	-	-	15		
TOTALS	118	104	124		

SECTION VI

6.0 ADAPTIVE TRAINING SYSTEM.

(Does not apply.)

SECTION VII

7.0 VISUAL SYSTEM EQUIPMENT DESCRIPTION

The Aviation Wide-Angle Visual System (AWAVS) is an experimental visual system designed for use with the T-2C Operational Flight Trainer (Device 2F101), also known as the Visual Technology Flight Simulator. The AWAVS is being designed and manufactured by the Singer Company, Link Division, Binghamton, NY, under NTEC Contract N61339-75-C-0009. The integrated AWAVS and VTFS systems provide an advance research/training tool for application in the development of future aircraft carrier landing simulation systems, as well as experimentation in development of simulated carrier landing techniques and procedures.

7.1 Functional Description

The AWAVS system presents the pilot with a realistic view of an external scene, normally consisting of a Forrestal class aircraft carrier on a seascape of unlimited expanse, which responds to the simulated operation of an aircraft. The seascape and aircraft carrier images are combined on a single wraparound spherical screen, 20 feet in diameter, with the observer's eye positioned slightly below and six inches forward of the center of the sphere.

The background scene is developed using flying spot scanner techniques to scan film transparencies of seascape, while the target image is developed using a video camera to scan a 370:1 scale model of an aircraft carrier and wake. The two images are simultaneously projected on the screen, with the target inset into the background seascape so that the two images are not superimposed. The target insetting technique used is known as projected scene keying. A three-color FLOLS presentation is simulated using an independent model board, and optically combined with the target aircraft carrier before projection.

Horizon, cloudscape, and limited visibility effects are synthetically generated and used to modify the projected images. Above and in-cloud conditions are also synthetically generated, and time of day may be controlled to simulate daytime, dusk, or night conditions. The carrier model is provided with runway and deck edge lights for simulated night conditions.

7.2 Visual System Reliability and Maintainability

Refer to

7.3 Physical Configuration

Configuration details of both the AWAVS and VTFS systems, including a VTFS/AWAVS Equipment Layout Diagram, are provided in Section VII of the Visual Technology Flight Simulator (VTFS) Trainer Design Report (NAVTRAEQUIPCEN 75-C-0009-9).

7.4 Physical Characteristics

Dimensions and weights of major AWAVS components, as well as power and air conditioning requirements are combined with similar VTFS data and provided in Section VII of the Visual Technology Flight Simulator (VTFS) Trainer Design Report (NAVTRAEQUIPCEN 75-C-0009-9).

7.5 Simulation Performance Characteristics

(Does not apply.)

7.6 Support Equipment Documentation

Refer to Support Equipment List NAVTRAEQUIPCEN 75-C-0009-H003.

NAVTRAEQUIPCEN 75-C-0009-13

DISTRIBUTION LIST

Defense Documentation Center (12)
Cameron Station
Alexandria, Virginia 22314

Commanding Officer (58)
Naval Training Equipment Center
Orlando, Florida 32813

Chief of Naval Edcn & Trng Support (1)
Code N-21
Pensacola, Florida 32508

Chief of Naval Edcn & Training (1)
Code N-331
Pensacola, Florida 32508

Naval Air Systems Command (6)
AIR 340F
Washington, D.C. 20350

Chief of Naval Operations (1)
OP 59
Washington, D.C. 20350

Chief of Naval Material, Navy Dept. (1)
Code 0324
Washington, D.C. 20360

Commander (1)
Naval Air Dev. Ctr. Library (1)
Warminster, Pennsylvania 18974

Chief of Naval Research (1)
ONR 461
800 North Quincy Street
Arlington, Virginia 22217

Chief of Naval Air Training (1)
Training Research Department
NAS Corpus Christi, Texas 78719

Headquarters U.S. Marine Corps (1)
CMS A03C
Washington, D.C. 20380

PM TRADE (4)
Orlando, Florida 32813

AF HRL/ASM (2)
Attn: Mr. Don Gum
Wright Patterson AFB, OH 45433

AF HRL (2)
Attn: Col. J.D. Boren
Williams AFB, AZ 85224

AF ASD/ENE (1)
Attn: Mr. A. Doty
Wright Patterson AFB, OH 45433

Scientific Tech Info Office (1)
NASA
Washington, D.C. 20546

NASA Ames Research Center (1)
Moffett Field, California 94035
Attn: Mr. J. Dusterberry

NASA Langley Research Ctr (1)
Attn: Mr. Kurbjan
Hampton, Virginia 23365

CDR James Goodson, MSC USN (1)
Code L 53
Naval Aerospace Med Rsrch Lab
Pensacola, FL 32512

LCR H.Wayne Kelly (1)
Light Attack Wing 1, NAS
Cecil Field, FL 32215

Dr. Frederick A. Muckler (1)
Navy Personnel R&D Center
San Diego, CA 92153

Mr. James D. Basinger (1)
ASD/ENETV
Wright Patterson AFB, OH 45433

LCDR Patrick M. Curran (1)
Naval Air Development Center
Human Factors Eng Div
Warminster, PA 18974

Mr. James A. Bynum (1)
US Army Rsrch Inst Fld Unit
Fort Rucker, AL 36362